Molecular control of murine ureter development – The function of FGF and BMP4 signaling

Von der Naturwissenschaftlichen Fakultät der

Gottfried Wilhelm Leibniz Universität Hannover

zur Erlangung des Grades
Doktorin der Naturwissenschaften (Dr. rer. nat.)

genehmigte Dissertation
von
Lena Deuper, M.Sc.

2023

Referent: Prof. Dr. rer. nat. Andreas Kispert
Korreferentin: Prof. Dr. rer. nat. Rita Gerardy-Schahn
Korreferent: Prof. Dr. rer. nat. Thomas Hollemann
Tag der Promotion: 22.03.2023

Hannover Medical School

Angefertigt am
Institut für Molekularbiologie
der Medizinischen Hochschule Hannover
unter der Betreuung von
Prof. Dr. rer. nat. Andreas Kispert

Meinen Eltern

Erklärung zur kumulativen Dissertation von Lena Deuper (geboren am 02.01.1993 in Osnabrück)

Diese kumulative Dissertation basiert auf nachfolgenden Veröffentlichungen und unveröffentlichten Manuskripten:

1. Max Meuser*, Lena Deuper*, Carsten Rudat, Nurullah Aydogdu, Hauke Thiesler, Patricia Zarnovican, Herbert Hildebrandt, Mark-Oliver Trowe and Andreas Kispert (2021). “FGFR2 signaling enhances the SHH-BMP4 signaling axis in early ureter development”. *Development* (2022), 149. doi:10.1242/dev.200021
*Contributed equally to this work

2. Lena Deuper, Max Meuser, Hauke Thiesler, Ullrich W. H. Jany, Carsten Rudat, Herbert Hildebrandt, Mark-Oliver Trowe and Andreas Kispert (2021). “Mesenchymal FGFR1 and FGFR2 control patterning of the ureteric mesenchyme by balancing SHH and BMP4 signaling”. *Development* (2022), 149. doi:10.1242/dev.200767

3. Lena Deuper, Nicolas Hense, Tamrat Mamo, Florian Bergmann, Marc-Oliver Trowe and Andreas Kispert “BMP4 signaling regulates expression of signals and transcription factors for coordinated cyto-differentiation in the murine ureter”. Manuscript in preparation.

In **Artikel 1** habe ich die Abbildung 4E und 4F experimentell und graphisch erstellt. Für die Abbildung 4H habe ich das Material gesammelt und die RNA isoliert. Die Abbildungen 5 und 6 sowie die Abbildungen S1, S2, S3, S4, S5, und S6 habe ich experimentell und graphisch erstellt. Das inhaltliche Konzept des Projekts wurde von Andreas Kispert, Max Meuser und mir gemeinsam erstellt. Das Manuskript wurde von Andres Kispert, Max Meuser und mir gemeinsam geschrieben. Das Projekt wurde von Andreas Kispert finanziert.

In **Artikel 2** habe ich alle Abbildungen (mit Ausnahme der Abbildung 7 und Abbildung S1) experimentell und teilweise graphisch erstellt. Für die Abbildungen 4A;B;C;H und Abbildung 5 habe ich das Material gesammelt und die RNA isoliert (mit Ausnahme des Materials für Figure 5A,B *Fgfr1/2cDKO-UE*). Das inhaltliche Konzept des Projekts wurde von Andreas Kispert und

mir gemeinsam erstellt. Das Manuskript wurde von Andres Kispert und mir gemeinsam geschrieben. Das Projekt wurde von Andreas Kispert finanziert.

In **Artikel 3** habe ich die Abbildung 1E;F experimentell und graphisch erstellt. Ich habe die Abbildung 2E;K experimentell und graphisch erstellt. Ich habe das Material für die Abbildung 2G-J gesammelt und die RNA isoliert. Ich habe die Abbildung 3E experimentell und graphisch erstellt. Ich habe die Abbildung 4 experimentell und graphisch erstellt. Ich habe die Abbildung 5B graphisch erstellt und die Statistik durchgeführt. Ich habe Figure 6J experimentell und graphisch erstellt. Die Figure 6E habe ich graphisch erstellt. Ich habe die Abbildungen S1, S2, S3 und S4 experimentell und graphisch erstellt. Das inhaltliche Konzept des Projekts wurde von Andreas Kispert und mir gemeinsam erstellt. Das Manuskript wurde von Andres Kispert und mir gemeinsam geschrieben. Das Projekt wurde von Andreas Kispert finanziert.

Abstract

The ureters are muscular tubes that propel the urine from the renal pelvis to the bladder by unidirectional peristaltic contractions. To fulfill this function the ureters are compartmentalized into an outer mesenchymal wall with layers of fibrocytes in the inner lamina propria (LP) and the outer tunica adventitia (TA) unsheathing smooth muscle cells (SMC), and an inner highly specialized epithelium: the urothelium. The urothelium features a three-layered organization of superficial (S), intermediate (I) and basal (B) cells. The ureteric mesenchyme (UM) as well as the ureteric epithelium (UE) arise from pools of homogeneous, uncommitted precursor cells. Patterning, proliferation and differentiation of these progenitors rely on a very complex interplay of various signaling pathways. SHH and WNT signals from the UE and BMP4 from the UM promote epithelial and mesenchymal proliferation and differentiation. In contrast, retinoic acid (RA) within the UM and the UE inhibits differentiation and promotes precursor proliferation in both compartments. How these signals cooperate with each other and possibly additional as yet unknown signals and how they impinge on various transcription factor (TF) genes to control the development of three different cell types from homogeneous precursor cell populations in two different tissue compartments is poorly understood. Aim of this thesis was to address the function of FGF and BMP4 signaling in this context.

Expression of *Fgfr1* and *Fgfr2* was found in the undifferentiated UE as well as in the surrounding UM. Targeted inactivation of *Fgfr2* in the UE resulted in loss of I and B cells, delayed onset of SMC differentiation and in an inability to form the LP. *Fgfr2* was found to increase SHH and BMP4 signaling to allow differentiation of epithelial cells and to precisely activate SMC differentiation. FGFRs in the mesenchyme act as a molecular sink to fine tune this signaling axis. Targeted ablation of *Fgfr1* and *Fgfr2* delayed the onset of SMC differentiation and led to premature development of the LP. Pharmacological rescue and gain of function experiments showed that increased SHH and BMP4 signaling promote I and B cell as well as SMC differentiation, while increased SHH but decreased BMP4 signaling promotes LP development.

BMP4 signaling was previously described to act on the development of the UE and the UM but the transcriptional targets remained widely unexplored. Genetic and pharmacological inactivation of BMP4 signaling identified TF genes differentially controlling the development of the UM and UE. Molecular inspection unraveled that some of these TF genes were regulated as a consequence of increased RA signaling in *Bmp4* mutant ureters.

This thesis identified FGF signaling as a crucial regulator of signaling networks controlling temporal and spatial differentiation of the murine ureter and increased our knowledge of the molecular function of BMP4 signaling in the context of ureter development.

Keywords: Ureter, differentiation, FGF, BMP4, urothelium, SMC, *lamina propria*

Zusammenfassung

Der Ureter leitet als Teil des harnableitenden Systems durch gerichtete Kontraktionen den Urin aus dem Nierenbecken in die Blase ab. Dazu besitzt der Ureter eine Zellschicht aus glatter Muskulatur, umgeben von Fibroblasten der inneren *Lamina propria* (LP) und der äußeren *Tunica adventitia* (TA). Dieses als Uretermesenchym (UM) bezeichnete Gewebekompartiment umschließt ein hochspezialisiertes Epithel (Urothel, UE), welches aus Schirm (S)-, Intermediär (I)- und Basal (B)-Zellen aufgebaut ist. UE und UM entwickeln sich je aus einer Vorläuferpopulation homogener, undifferenzierter Zellen. Musterungs-, Proliferations- und Differenzierungsprozesse während der murinen Ureterentwicklung basieren auf einer komplexen Interaktion von Signalwegen, die räumlich und zeitlich präzise aufeinander abgestimmt sind. SHH- und WNT-Signale aus dem UE, sowie BMP4-Signale aus dem UM stimulieren die Proliferation und Differenzierung beider Kompartimente. Retinsäure (RA) inhibiert Differenzierung und stimuliert Proliferation, um so ausreichend Vorläuferzellen zu erhalten. Wie genau die einzelnen Signalwege miteinander und mit eventuell noch unbekannten Faktoren kooperieren und wie sie die Expression unterschiedlicher Transkriptionsfaktoren (TF) kontrollieren, um die Entwicklung hochspezialisierter Zelltypen zu ermöglichen, ist bislang nur wenig verstanden. Ziel dieser Arbeit war es, die Funktion des BMP4- und FGF-Signalweges in diesem Kontext zu untersuchen. *Fgfr1* und *Fgfr2* sind im undifferenzierten UE und UM exprimiert. Die Inaktivierung von *Fgfr2* im UE führt zu einem Verlust von I- und B-Zellen sowie der LP und einer verzögerten Differenzierung der glatten Muskulatur. Molekulare Analysen zeigten, dass *Fgfr2* die SHH-BMP4-Signalachse verstärkt und so die Differenzierung fördert. FGF-Rezeptoren im UM agieren als molekulare Modulatoren zur Vermeidung einer Überaktivierung epithelialer Signale. Die Inaktivierung von *Fgfr1* und *Fgfr2* im UM verzögert die Differenzierung der glatten Muskulatur und fördert die Bildung der LP. Weitere pharmakologische Experimente zeigten, dass verstärkte SHH- und BMP4-Signale Muskel-, I- und B-Zelldifferenzierung fördern, während verstärkte SHH-Signale bei gleichzeitiger Reduktion von BMP4-Signalen die Entwicklung der LP fördern.

Die Notwendigkeit des BMP4-Signalwegs für die Entwicklung des murinen Ureters wurde bereits in früheren Studien beschrieben, aber die transkriptionellen Ziele waren in diesem Kontext noch gänzlich unbekannt. Diese Arbeit identifizierte durch genetische und pharmakologische Inhibierung des Signalwegs TF, die spezifisch die Differenzierung des UE und des UM kontrollieren. Die TF werden dabei entweder direkt oder indirekt durch BMP4 reguliert. Indirekte Regulation erfolgt durch gesteigerte RA-Aktivität in Folge eines inaktiven BMP4-Signalwegs.

Diese Arbeit zeigte, dass FGF-Signale als wichtige Regulatoren der Signalnetzwerke agieren, die die murine Ureterentwicklung kontrollieren, und erweiterte unser Wissen im Hinblick auf die transkriptionelle Kontrolle des BMP4-Signalwegs im Kontext der murinen Ureterentwicklung.

Schlagworte: Ureter, Differenzierung, FGF, BMP4, Urothel, glatte Muskulatur, *lamina propria*

Table of contents

Table of abbreviation

ΔN	delta N
µg	Microgram
µM	Micromolar
µm	Micrometer
Acta	Actin alpha 2, smooth muscle
Actg2	Actin, gamma 2, smooth muscle, enteric
Ahr	Aryl-hydrocarbon receptor
Aldh1	Aldehyd dehydrogenase 1
Atoh8	Atonal bHLH transcription factor 8
avg	average
B cells	Basal cells
BAC	Bacterial Artificial Chromosome
Bmp4	Bone morphogenic protein 4
Bmp4cKO	*Tbx18$^{cre/+}$;Bmp4$^{fl/fl}$*
Bmper	BMP-binding endothelial regulator
Bmpr	Bone morphogenic protein receptor
BMS	BMS189453
BrdU	5-Bromo-2'-deoxyuridine
CAKUT	Congenital Anomalies of the Kidney and the Urinary Tract
Car3	Carbonic anhydrase 3
Ckm	Creatine kinase, muscle
CND	Common Nephric Duct
Cnn1	Calponin 1
Col1a2	Collagen, type I, alpha 2
Ctrl	Control
DAPI	4’,6-diamidino-2-phenylindole
Dkk	Dickkopf WNT signaling pathway inhibitor
DMSO	Dimethylsulfoxid
DNA	Deoxyribonucleic Acid
E	Embryonic day
Ecm1	Extracellular matrix protein 1
Egr1	Early growth response 1
Elf3	E74-like factor 3
Elf5	E74-like factor 5
Etv	Ets variant transcription factor
Fbln2	Fibulin 2
Fbxl22	F-box and leucine-rich repeat protein 22
FC	Fold Change
Fgf	Fibroblast growth factor
Fgfr	Fibroblast growth factor receptor
Fgfr1/2cDKO-UE	*Pax2cre/+;Fgfr1$^{fl/+}$;Fgfr2$^{fl/fl}$*
Fgfr1/2cDKO-UM	*Tbx18$^{cre/+}$;Fgfr1$^{fl/fl}$;Fgfr2$^{fl/fl}$*
Fgfr2cKO	*Pax2cre/+;Fgfr1$^{fl/+}$;Fgfr2$^{fl/fl}$*
Fig	Figure
fl	floxed
Fos	FBJ osteosarcoma oncogene

Foxa1	Forkhead box A1
Foxf1	Forkhead box F1
Foxi1	Forkhead box I1
Frs2α	FGFR substrate alpha
Gapdh	Glyceraldehyde-3-phosphate dehydrogenase
Gata	GATA binding protein
Gdnf	Glial-derived neurotrophic factor
Grb2	Growth factor receptor bound 2
Grhl3	Grainyhead like transcription factor 3
Hhip	Hedgehog-interacting protein
Hopx	HOP homeobox
Hoxb8	Homeobox B8
I cells	Intermediate cells
Id	inhibitor of DNA binding
IgG	Immunoglobulin G
Ihh	Indian hedgehog
IM	Intermediate Mesoderm
Irf5	Interferon regulatory factor 5
Ivl	Involucrin
Klf5	Kruppel-like factor 5
Krt	Keratin
Lim1	LIM homeobox protein 1
LP	*Lamina Propria*
MAPK	Mitogen-Activated Protein Kinase
ml	Milliliter
mm	Millimeter
MM	Metanephric Mesenchyme
Msx2	Msh homeobox 2
Myh11	Myosin, heavy polypeptide 11, smooth muscle
Myh6	Myosin, heavy polypeptide 6, cardiac muscle, alpha
Myocd	Myocardin
MyoD	Myogenic Differentiation 1
nd	not defined
ND	Nephric Duct
ng	Nanogram
NOG	NOGGIN
ns	not significant
Ovol1	Ovo like zinc finger 1
P-	Phosphorylated
Pax	Paired box
PBS	Phosphate Buffered Saline
Pcp4l1	Purkinje cell protein 4-like
PCR	Polymerase Chain Reaction
Perp	PERP, TP53 apoptosis effector
Plcg	Phospholipase C gamma
Pparg	Peroxisome proliferator activated receptor gamma
Ppia	Peptidylprolyl isomerase A
Ptch	Patched
RA	Retinoic Acid

Rab27b	RAB27B, member RAS oncogene family
Rarb	Retinoic acid receptor, beta
RNA	Ribonucleic Acid
RT-qPCR	Real-Time quantitative PCR
S cells	Superficial cells
S100a1	S100 calcium binding protein A1
SD	Standard Derivation
Sh2	Src-homology-2
Shh	Sonic hedgehog
SISH	Section *In Situ* Hybridisation
Smad	Small mothers against decapentaplegic homolog
Smad4cKO(UE)	*Pax2cre/+;Smad4$^{fl/fl}$*
Smad4cKO(UM)	*Tbx18$^{cre/+}$;Smad4$^{fl/fl}$*
SMC	Smooth Muscle Cells
Smo	Smoothened
Snai1	Snail family zinc finger 1
Sox9	Sex-determining region Y box 9
Sp5	Trans-acting transcription factor 5
Spry	Sprouty RTK signaling antagonist
STAT	Signal Transducer and Activator of Transcription
Stra6	Stimulated by retinoic acid gene 6
T	Tween 20
TA	*Tunica Adventitia*
Tab	Table
Tagln	Transgelin
Tbx	T-box transcription factor
Tcf24	Transcription factor 24
TF	Transcription Factor
Tgfβ	Transforming growth factor beta
Tnnt2	Troponin T2, cardiac
Trim29	Tripartite motif-containing 29
Trp63	Transformation related protein 63
TSA	Tyramide Signal Amplification
Tshz3	Teashirt zinc finger homeobox 3
UB	Ureteric Bud
UE	Ureteric Epithelium
UM	Ureteric Mesenchyme
Upk	Uroplakin
VUR	Vesicoureteral Reflux
Wnt	Wingless type MMTV integration site

Introduction

The urinary system and its functions

The mammalian urinary or excretory system is a multi-organ entity that maintains the body homeostasis by generating the urine with its metabolic pathway degradation products and by expelling it from the body. The urinary system consists of the paired kidneys and ureters and the unpaired bladder and urethra which each fulfill specific sub-tasks. Within the kidneys, nephrons filter the blood and modify the primary filtrate by secretion and resorption processes, before the resulting urine is transported via the collecting duct system to the renal pelvis. The ureters then transport the urine from the renal pelvis to the bladder by peristaltic contractions. The bladder stores the urine until it is released from the body via the urethra (Wallace, 1998).

Structure and function of the ureter

The ureters present a compartmentalized design with a specialized epithelium, the urothelium, on the inside and an outer mesenchymal wall made of fibromuscular material. The urothelium is stratified with layers of three major cell types (Hicks, 1965). The innermost luminal cells, the so-called umbrella or superficial (S) cells, are large and multinucleated and feature semi-crystalline plugs made of uroplakin (UPK) proteins on their surface. Interconnected by tight junctions they form a physical barrier against the hypertonic urine to protect the underlying tissue (Hicks, 1966, Acharya et al., 2004, Langbein et al., 2002). The second layer consists of one or several rows of intermediate (I) cells that are marked by weak expression of both UPKs as well as the ΔN isoform of the transcription factor TRP63 (ΔNP63). These cells are much smaller than S cells and are mononucleated. The third cell type are basal (B) cells. These cuboidal cells are marked by the combinatorial and strong expression of ΔNP63 and Keratin 5 (KRT5). B cells tether the urothelium to the basement membrane and the mesenchymal wall (Hicks, 1965, Bohnenpoll et al., 2017a).

The mesenchymal wall features a three-layered cellular architecture as well. The innermost layer, the *lamina propria*, is a connective tissue with excessive extracellular matrix with embedded immune and endothelial cells, and nerve endings. It is surrounded by a thick layer of smooth muscle cells (SMCs) which account for the peristaltic activity of the tube. A third layer of fibroelastic material, the *tunica adventitia*, anchors the mesenchymal coat to the dorsal body wall (Hicks, 1965).

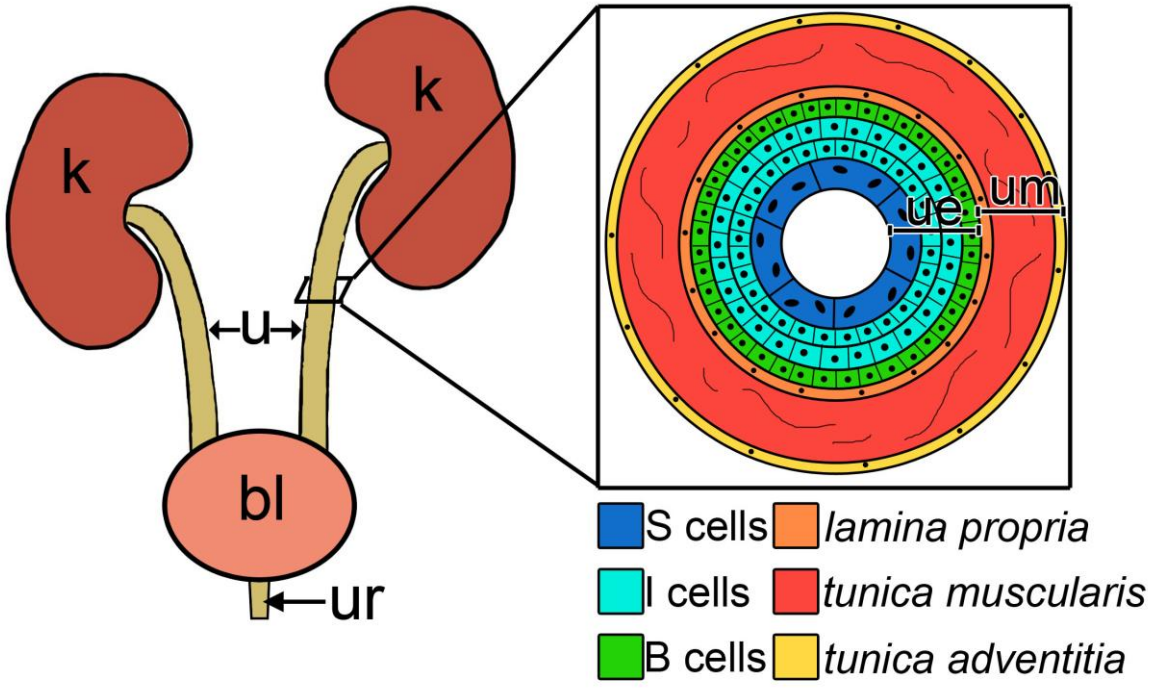

Figure 1: Structure of the urinary system and the ureter.
The urinary system consists of the kidneys (k), the ureters (u), the bladder (bl) and the urethra (ur). The ureters display a three-layered urothelium (ue), consisting of superficial (S), intermediate (I) and basal (B) cells, and a surrounding three-layered mesenchymal wall (um) that is comprised of the *lamina propria*, *tunica muscularis* and the *tunica adventitia*. Idea for graphical design for ureter cross-section adapted from (Bohnenpoll et al., 2017c).

Development of the murine ureter

Although structurally and functionally diverse, ureters arise together with the kidneys from a common mesodermal rudiment, the nephric duct (ND), while the bladder and urethra originate from the cloaca, an ectodermal infolding. The ND forms as an epithelial condensation within the intermediate mesoderm (IM) at the level of the future forelimb bud and elongates posteriorly until it encounters and fuses with the cloacal epithelium (Uetani and Bouchard, 2009, Saxen and Sariola, 1987, Brenner-Anantharam et al., 2007, Tanaka et al., 2010). At E11.5, an epithelial outgrowth emerges from the ND on the level of the hindlimb buds and grows towards an adjacent mesenchymal condensation at the posterior end of the intermediate mesoderm, the metanephric mesenchyme (MM) (Costantini and Kopan, 2010).

The proximal part of the epithelial outgrowth, the ureteric bud (UB) invades the MM and undergoes multiple branching events to generate the collecting duct system of the kidney. The distal stem of the UB which is surrounded by a loosely organized mesenchymal cell population (the ureteric mesenchyme, UM) simply elongates and differentiates into the urothelium of the ureter. The MM which surrounds the proximal tip of the UB, gives rise to nephrons and the renal stroma, respectively, whereas the UM differentiates into SMCs and fibrocytes of the ureter (Costantini and Kopan, 2010, Bohnenpoll and Kispert, 2014). To allow unopposed urine

flow from the kidney to the bladder, the ureters need to be connected to the bladder lumen. At the onset of its development the ureter is connected to the ND by a common end-piece, the common nephric duct (CND), that in turn is fused to the cloacal epithelium. To disconnect ureter and ND from one another the CND is removed by apoptosis until E12.5. The ureter is then displaced from the ND to its final position in the dorsal bladder wall (Uetani and Bouchard, 2009).

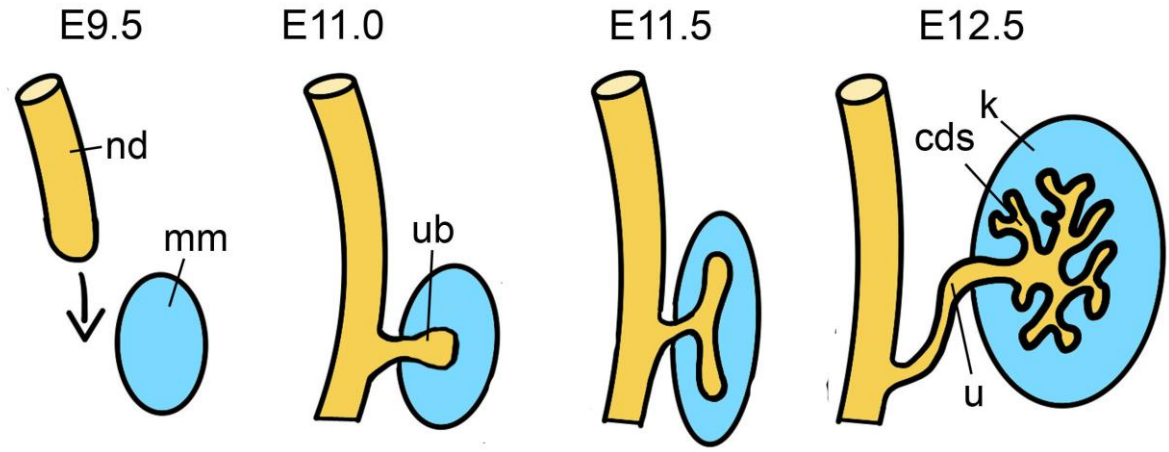

Figure 2: Development of the murine urinary system.
Kidney (k) and ureter (u) derive from the nephric duct (nd) that forms as an epithelial condensation from the intermediate mesoderm at E8.5 on the level of the future forelimb buds and elongates caudally. At E11.0, the ureteric bud (ub) invades the metanephric mesenchyme (mm). The proximal part of the ureteric bud undergoes multiple branching events to form the collecting duct system (cds) of the kidney, while the distal part elongates and forms the ureter. Idea for graphical design adapted from (Costantini and Kopan, 2010).

At E11.5, the ureter is composed of a single layered epithelium and a surrounding population of undifferentiated and loosely arranged *T-box transcription factor 18* positive (*Tbx18*$^{+}$) cells (Bohnenpoll et al., 2017a, Airik et al., 2006). At E12.5, cells from the inner mesenchymal region separate from those of the outer mesenchyme, condense and acquire a rhomboid shape. At E14.5, they start to express *Myocardin* (*Myocd*), the key transcriptional regulator of SMC development (Wang et al., 2003, Bohnenpoll et al., 2017a). Around E16.5, some mesenchymal cells that lie directly underneath the urothelium, switch *Myocd* off and activate *Aldehyd dehydrogenase 1, subfamily A2* (*Aldh1a2*) expression indicating differentiation of *lamina propria* fibrocytes. The other ones maintain *Myocd* expression and activate in a stepwise fashion the expression of SMC structural genes until birth. Parallel to mesenchymal development, the UE starts to express ΔNP63 and initiates a stratification program at E14.5. At E16.5, the luminal layer upregulates expression of UPKs and differentiates into S cells. From E16.5 onwards, the first cells of the urothelial basal cell layer start to express KRT5. The proportion of B cells increases towards the end of embryonic development but even more so after birth until adulthood (Bohnenpoll et al., 2017a, Qasrawi et al., 2022). Due to these highly coordinated cellular

programs a functional, i.e. a sealing and peristaltically active ureter tube, is established shortly after onset of urine production in the fetal kidney at E16.5.

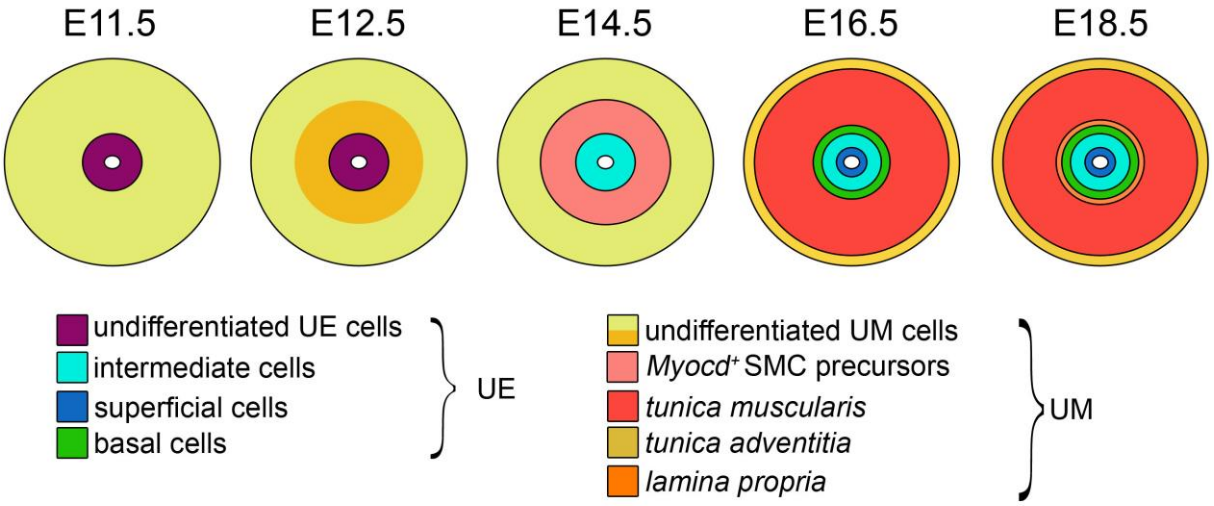

Figure 3: Embryonic cyto-differentiation of the murine ureter.
At E11.5, the urothelium consist of undifferentiated epithelial cells that are surrounded by undifferentiated, loosely organized mesenchymal cells. At E12.5, the inner mesenchyme starts to condense; at E14.5 it switches on *Myocd* expression, defining smooth muscle cell (SMC) precursors. The epithelium expresses ΔNP63 from E14.5 onwards and starts stratification. Between E15.5 and E16.5, various structural SMC genes become upregulated in the SMC layer, while the inner and outer cells of the urothelium differentiate into superficial and basal cells, respectively. At E18.5, the ureter has achieved its typical cyto-architecture consisting of a three-layered epithelium and mesenchyme. UE, ureteric epithelium; UM ureteric mesenchyme. Idea for graphical design adapted from (Bohnenpoll and Kispert, 2014).

Congenital anomalies of the urinary system

Given the complexity of the cellular programs that control the development of the urinary system from multiple tissue rudiments, it is not surprising that Congenital Anomalies of the Kidney and the Urinary Tract (CAKUT) are frequently observed in human newborns. With a frequency of 3 to 6 out of 1000 live births CAKUT phenotypes are responsible for 48% to 59% of kidney disease in children and for 34% to 43% of end stage kidney disease (Postoev et al., 2016, Yosypiv, 2012, Harambat et al., 2012).

Destroyed kidney parenchyma and dilatated ureters as a part of these malformations is a consequence of an inability of the ureter to correctly drain urine from the renal pelvis to the bladder. Increased hydrostatic pressure from accumulated urine leads to dilation of the ureters in the first place and hence, to secondary hydronephrosis. Possible causes for inadequate urine transport are functional or physical obstruction of the ureters. While a functional obstruction describes an insufficiency of the UM to propel urine, due to reduced or absent SMCs, a physical obstruction describes an occlusion of the ureter lumen or of its junctions, due to a disturbed budding process or alterations of distal ureter maturation (Jaslove and Nelson, 2018, Chevalier, 2015, Forbes et al., 2012, Chang et al., 2004, Peters, 1995). Furthermore, increased

hydrostatic pressure leads to dedifferentiation of already existing SMCs and formation of interstitial myofibroblast worsening the condition (Siow et al., 2003, Diamond et al., 1995, Weiss et al., 2019).

Inappropriate development of the urothelium has also been associated with various CAKUT phenotypes. Alterations concerning regulation and expression of p63 or TP63 in mice and men have been associated with bladder exstrophy and impaired mesenchymal development (Wilkins et al., 2012, Ching et al., 2010, Cheng et al., 2006). Furthermore, mutations in different *Upk*s contribute to various CAKUT phenotypes (Jackson et al., 2020). Mutations in almost all *Upk*s result in urothelial hyperplasia. Loss of *Upk2* additionally accounts for an occlusive ureter lumen leading to physical obstruction and secondary hydronephrosis as well as vesicoureteral reflux (VUR) (Jenkins et al., 2006, Kong et al., 2004). Mutations in *Upk1b* result in weak hydronephrosis, that worsens until adulthood, and in very rare cases to duplex kidneys, indicating a role of this gene in the budding process (Carpenter et al., 2016, Carpenter and McHugh, 2017). Loss of *Upk3a* results in a leaky urothelium due to loss of plaque synthesis and VUR (Hu et al., 2000). In humans very rare cases of renal aplasia and dysplastic, multicystic kidneys are associated with *UPK3A* mutations (Jenkins et al., 2005, Schönfelder et al., 2006).

Molecular control of ureter development

Owing to the relevance of CAKUT for human disease, lots of research has been done in recent years to unravel the molecular mechanisms that control the development of a functional ureter from simple tissue rudiments. Mainly due to genetic analysis in the mouse, critical factors for UB formation, distal ureter maturation and ureteric cyto-differentiation have been determined (Airik and Kispert, 2007, Bohnenpoll and Kispert, 2014, Woolf and Davies, 2013). *Paired box 2* (*Pax2)* and *Paired box 8* (*Pax8)* specify the renal fate in the IM. Expression of these transcription factor (TF) genes promotes a mesenchymal to epithelial transition, thereby controlling the formation of the ND (Bouchard et al., 2002). They synergistically induce the expression of TF genes *GATA binding protein 3 (Gata3)* and *LIM homeobox protein 1 (Lim1)* to stimulate proliferation and elongation of the ND towards the cloacal mesenchyme (Grote et al., 2006, Pedersen et al., 2005). UB formation is under the control of MM-derived glial-derived neurotrophic factor (GDNF) and its receptor Ret on the ND. While *Ret* expression occurs along the whole ND, the expression of *Gdnf* is restricted to the MM. As soon as the ND passes the MM, GDNF binds to RET and initiates a local bud outgrowth. Disturbance of the GDNF-RET signaling system leads to several anomalies including kidney agenesis (complete failure of UB induction), duplex systems (induction of more than one UB) or improper distal ureter maturation (to rostral or caudal budding). Distal ureter maturation is additionally controlled by retinoic acid signaling (Costantini and Shakya, 2006, Uetani and Bouchard, 2009).

Cyto-differentiation of the ureter is controlled by a complex interplay of TF genes and signaling systems that act within and between the epithelial and mesenchymal primordium of the ureter. Two TF genes controlling the onset SMC differentiation are Sex-determining region Y box 9 (SOX9) and teashirt zinc finger homeobox 3 (TSHZ3). SOX9 and TSHZ3 synergistically regulate the development of SMCs by controlling the activity of MYOCD (Airik et al., 2010, Caubit et al., 2008, Martin et al., 2013). As already indicated the UM is specified by the expression of *Tbx18* at the begin of its development. TBX18 does not only define ureteric fate, but has also important functions in coordinating and maintaining different signaling pathways in the ureteric cyto-differentiation programs, namely Retinoic acid (RA-), Wingless type MMTV integration site (WNT)-, Sonic Hedgehog (SHH)- and Bone morphogenic protein 4 (BMP4) signaling (Airik et al., 2006, Bohnenpoll et al., 2013).

RA signaling was shown to antagonize cyto-differentiation during early ureter development. The RA synthesizing enzymes *Aldh1a2* and *Aldh1a3* are expressed from E11.5 until E12.5 in the UM and UE, respectively. Receptor and target gene expression occurs both in the UM and UE, showing that RA signaling is active prior to the onset of the stratification and differentiation programs of the ureter. Pharmacological gain- and loss-of-function experiments in ureter explant cultures showed that prolonged RA signaling increased cell proliferation and the proportion of $\Delta NP63^+$ cells in the UE, while KRT5 and UPK expression was reduced. Furthermore, the differentiation of SMCs appeared disturbed under these conditions. Opposing effects were observed when RA signaling was inhibited: proliferation was decreased while differentiation was stimulated (Bohnenpoll et al., 2017a). Up- and downstream of RA signaling *Gata2* controls the onset of SMC development in the UM (Weiss et al., 2019).

Ureteric cyto-differentiation is positively influenced by WNT signaling. *Wnt7b* and *Wnt9b* are expressed in the UE from E11.5 onwards. While *Wnt9b* expression is shut down after E14.5, *Wnt7b* is maintained until E18.5. Expression of the WNT receptor *Frzd1* occurs in the surrounding UM. In early ureter development, at E11.5, expression of the target gene *Axin2* is detected in the UE and UM; after E12.5 until the end of embryonic development, *Axin2* is exclusively expressed the UM, indicating a paracrine mode of WNT signaling. Targeted genetic ablation of the intracellular mediator of the canonical subbranch of WNT signaling, β-Catenin (CTNNB1) in the UM, resulted in a loss of mesenchymal differentiation and SMC formation as well as reduced epithelial differentiation leading to hydroureter formation and hydronephrosis at birth (Trowe et al., 2012). Two important mediators of WNT signaling are the T-box transcription factors TBX2 and TBX3. Embryos with genetic inactivation of *Tbx2* and *Tbx3* in the UM show reduced SMC differentiation and invasion of extracellular matrix components. TBX2/3 mediate the patterning of the UM by repressing BMP4 and WNT antagonists (*Bmper* and *Dkk* and *Shisa*, respectively), to maintain WNT and BMP4 signaling (Aydoğdu et al., 2018).

Of utmost relevance for ureteric cyto-differentiation is the SHH signal. *Shh* is expressed in the UE from E11.5 onwards (Yu et al., 2002, Bohnenpoll et al., 2017c, Haraguchi et al., 2012). SHH binds to its receptor Patched1 (PTCH1) in the UM, thereby activating Smoothened (SMO)-dependent signaling (Murone et al., 1999, Stone et al., 1996). Inactivation of *Shh* in early ureter development leads to hydroureter formation at birth due to a complete failure of epithelial and mesenchymal differentiation (Yu et al., 2002, Bohnenpoll et al., 2017c). SHH also accounts for proliferation in the epithelium and inner mesenchyme and dampens apoptosis in the outer region of the UM. The differentiation potential of SHH is mediated by the transcription factor Forkhead box F1 (FOXF1) in the UM. FOXF1 controls the expression of the SMC regulator *Myocd* but also of *Bmp4* in the UM, which in turn controls epithelial and mesenchymal differentiation (Bohnenpoll et al., 2017c).

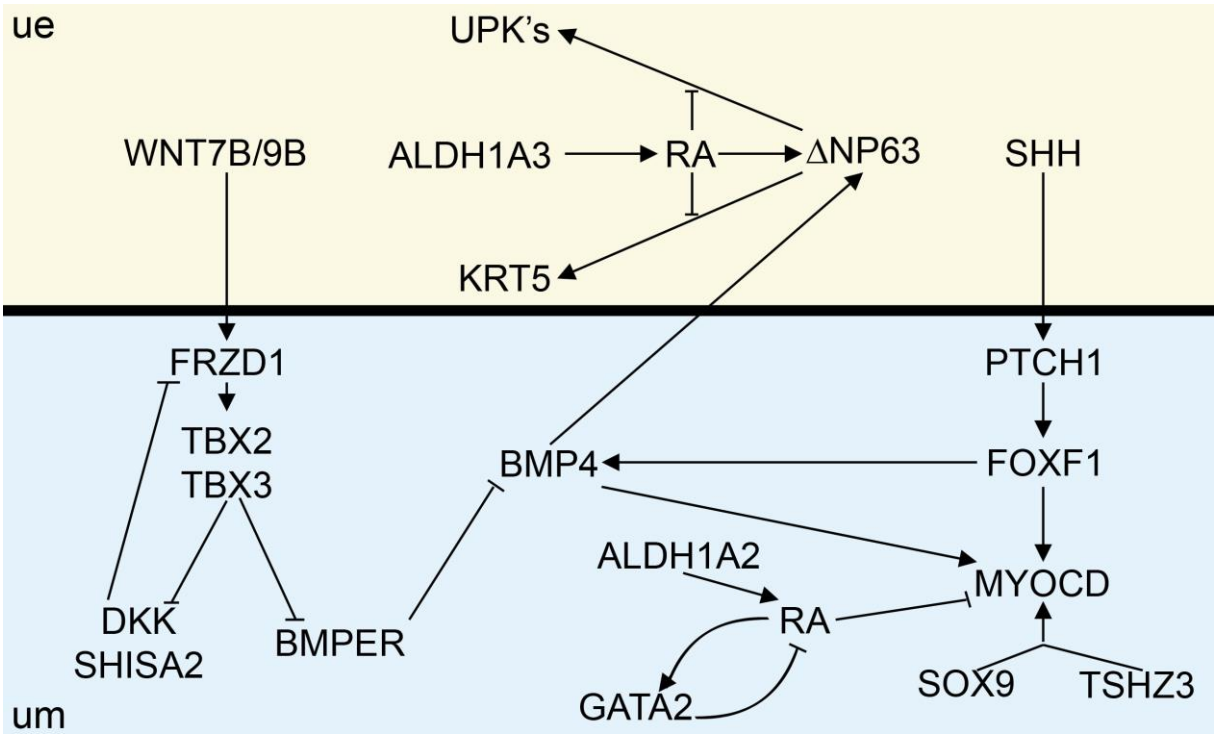

Figure 4: Molecular control of early ureter development in mice.
Early ureter development is controlled by a complex system of signaling pathways and TF genes. ue, ureteric epithelium; um, ureteric mesenchyme.

The BMP4 signaling pathway

BMP4 is a member of the Transforming Growth Factor β (TGFβ) superfamily with very important functions during embryogenesis (Hogan, 1995, Wozney et al., 1988). BMP4 occurs as a dimer that binds to two different receptor types, which are mutually dependent on one another for signal transduction: BMPR1 and BMPR2. Both receptors occur as dimers and form two distinct subgroups according to sequence similarities, protein characteristics and function during signal transduction. Today four different type I receptors (*ACVRL1, ACVR, BMPRIA* and

BMPRIB) and three different type II receptors (*ACTVRIIA, ACTVRIIB* and *BMPRII*) have been identified (Sanchez-Duffhues et al., 2020). Nonetheless, all BMP receptors share a common protein structure with a short extracellular binding domain, followed by a transmembrane domain and an intracellular serine threonine kinase domain (Gomez-Puerto et al., 2019). While BMPR2 harbors a constitutively active, i.e. phosphorylated kinase domain, the kinase domain of BMPR1 becomes transphosphorylated by BMPR2 only after ligand binding (Sanchez-Duffhues et al., 2020, Kawabata et al., 1998, Miyazono et al., 2005). This leads to an activation of different intracellular cascades, one of them being Small Mothers against decapentaplegic homolog (SMAD) signaling. SMAD proteins are classified into different subgroups: receptor regulated (R) SMADs (SMAD1, 5, 9), common partner SMADs (of which SMAD4 is the only one known so far) and inhibitory (I) SMADs (Miyazono et al., 2005). Activated BMPR1 leads to phosphorylation of R-SMADs, which form dimers and bind to SMAD4. This SMAD complex translocates into the nucleus to act as transcriptional co-activator (Sanchez-Duffhues et al., 2020, Kawabata et al., 1998, Miyazono et al., 2005). BMP signals are alternatively and/or additionally mediated by different cytoplasmatic kinases including different MAP-kinases, e.g. P38 and ERK1/2 or the PI3K-AKT signaling pathway (Zhang, 2017).

Due to gastrulation defects *Bmp4* null mice are embryonic lethal between E6.5 and E10.5, i.e. prior to kidney and ureter development (Lawson et al., 1999, Winnier et al., 1995). Therefore, BMP4 function in ureter and kidney development was initially studied in *ex vivo* culture systems and in individuals with heterozygous loss of *Bmp4*. These analyses indicated that BMP4 controls the budding process, supports the survival of the MM, interferes with the branching process during kidney organogenesis and controls ureteric SMC development and *Upk* expression (Raatikainen-Ahokas et al., 2000, Brenner-Anantharam et al., 2007, Miyazaki et al., 2000, Wang et al., 2009, Miyazaki et al., 2003, Michos et al., 2007). Later work showed that BMP4 acts downstream of the SHH-FOXF1 signaling axis to control mesenchymal and epithelial cytodifferentiation (Bohnenpoll et al., 2017c). Finally, conditional inactivation of *Bmp4* in the UM revealed that mutants with complete loss of *Bmp4* display short dilated ureters with associated hydronephrosis at birth as a consequence of physical and functional obstruction. These ureters are hypoplastic due to reduced proliferation in both tissue rudiments and fail to initiate epithelial and mesenchymal differentiation. BMP4 function in this context is mediated by SMAD-dependent and SMAD-independent mechanisms. In the UM phosphorylated (P-) SMAD1/5/9 downstream of BMP4 cooperates with SMAD4 to induce SMC differentiation. AKT has only a minor contribution to SMC formation but controls mesenchymal proliferation. Mesenchymal proliferation is additionally but only slightly influenced by combinatoric action of P-SMAD1/5/9 and P-P38. In the UE phosphorylation of SMAD1/5/9 after ligand binding was detected, but a contribution of SMAD signaling to UE development remains unexplored. Proliferation and differentiation are both mediated by P-AKT, P-ERK and P-P38, with AKT being the most relevant factor

(Mamo et al., 2017). A functional target of BMP4 in the UM is the TF gene *Gata6* which in turn, is required for activation of *Myocd* and SMC development in the UM (Kurz et al., 2022). Whether BMP4 affects other signaling pathways in the early ureter is unknown as is the set of TF genes controlled by BMP4 in the epithelial and mesenchymal differentiation programs.

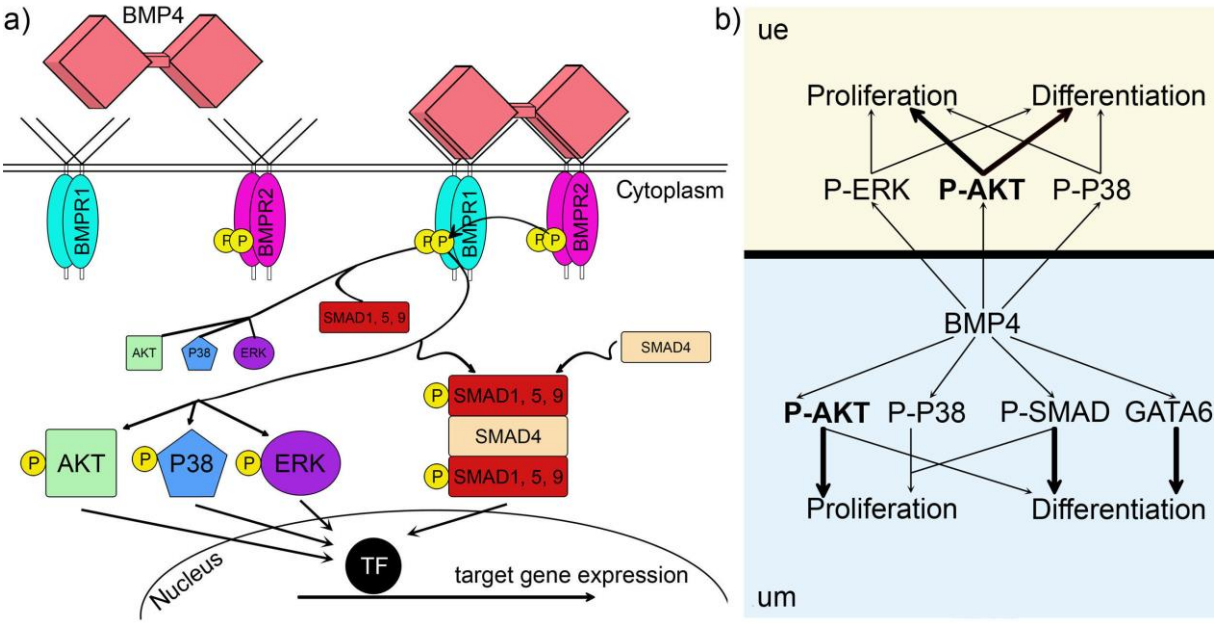

Figure 5: The BMP4 signaling pathway.
(a) Scheme of the BMP4 signaling pathway. BMP4 binds to its receptors BMPR1 and BMPR2 thereby activating i.e., phosphorylating different downstream effectors like R-SMADs, ERK, AKT and P38. (b) Function of BMP4 during murine ureter cytodifferentiation. ue, ureteric epithelium; um, ureteric mesenchyme.

The FGF signaling pathway

Fibroblast Growth Factors (FGFs) are signaling proteins that coordinate numerous cellular programs in development and homeostasis (Ornitz and Itoh, 2015). In mammals, the FGF superfamily consists of 22 secreted ligands that can be subdivided into seven subfamilies. While few FGFs act in an autocrine fashion independent from receptors, most of them have a paracrine or endocrine mode of activity which is mediated by selective binding to one of four receptors, namely FGFR1, FGFR2, FGFR3 and FGFR4 (Ornitz and Itoh, 2015).
FGFRs are receptor tyrosine kinases (RTK) with an intracellular and an extracellular domain. The latter is comprised of three immunoglobulin like domains (DI-DIII) and an acetic box (AB) followed by a transmembrane domain (TM). The former harbors two tyrosine kinase domains (TK) (Lee et al., 1989). Ligand specificity is dependent on DII and DIII whereas DI and AB control ligand binding and harbor autoinhibitory features (Yeh et al., 2003, Werner et al., 1992, Wang et al., 1995). *Fgfr1, Fgfr2* and *Fgfr3* encode different splicing variants that differ in DIII. While the N-terminal part of this domain is encoded in the invariable exon 7 (or IIIa), the C-terminal part consists of the two mutually exclusive exons 8 (or IIIb) and 9 (or IIIc) (Johnson et

al., 1991). The different splicing variants of *Fgfr2* are expressed in a tissue specific manner: *Fgfr2IIIb* is mostly expressed in epithelial tissues, whereas *Fgfr2IIIc* is the predominant isoform in the mesenchyme (Orr-Urtreger et al., 1993).

a)

	Family	FGF	Receptor specificity
secreted FGFs	FGF1 subfamily	FGF1	all FGFRs
		FGF2	**FGFR 1c, 3c** (2c, 1b, 4Δ)
	FGF4 subfamily	FGF4	**FGFR 1c, 2c** (3, 4Δ)
		FGF5	
		FGF6	
	FGF7 subfamily	FGF3	**FGFR 2b** (1b)
		FGF7	
		FGF10	
		FGF22	
	FGF8 subfamily	FGF8	**FGFR 3c** (4Δ, 2c, 1c, 3b)
		FGF17	
		FGF18	
	FGF9 subfamily	FGF9	**FGFR 3c** (2c, 1c, 3b, 4Δ)
		FGF16	
		FGF20	
	FGF15/19 subfamily	FGF15/19	FGFR 1c, 2c, 3c, 4Δ
		FGF21	FGFR 1c, 3c
		FGF23	FGFR 1c, 3c, 4
intracellular FGFs	FGF11 subfamily	FGF11	non-signal proteins serving as cofactors for other molecules
		FGF12	
		FGF13	
		FGF14	

b)

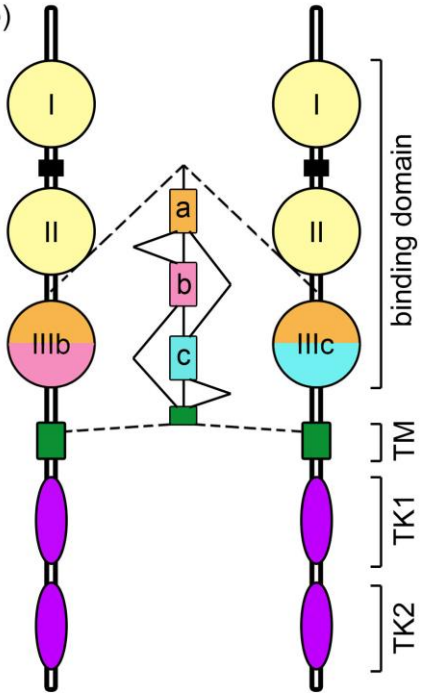

Figure 6: The FGF family.
(a) The FGF family consists of four different receptors and 22 ligands that can be subdivided into seven subfamilies. The ligands show different binding preferences to different receptors. Main receptors are written in bold (Ornitz and Itoh, 2015). (b) Schematic protein structure of FGFR1-4. The protein consists of three extracellular binding domains (I, II, III), followed by a transmembrane domain (TM) and two intracellular tyrosine kinase domains (TK1, TK2). For binding domain III two alternative splicing variants are known that are mutually exclusive. While the first exon (IIIa) is invariant in all isoforms, splicing variant IIIb is mostly expressed in epithelia but IIIc is the dominant isoform in mesenchymal tissues. Idea for graphical design adapted from (Ornitz and Itoh, 2015).

Quiescent FGFRs occur as monomers or inactive dimers within the cell membrane (Schlessinger et al., 1978, Livnah et al., 1999). Binding of a ligand to its receptor results in receptor dimerization and conformational changes, leading to transphosphorylation of the kinase domains (Schlessinger et al., 2000, Chen et al., 2008). Activated kinase domains feature binding sites for Src-homology-2-(SH2) domains (Songyang et al., 1993). Two prominent molecules binding this domain are phospholipase Cγ (PLCγ) and signal transducer and activator of transcription (STAT) controlling the mobility of immune cells and regulating proliferation (Mohammadi et al., 1991, Hartwig et al., 1992, Sahni et al., 1999, Dudka et al., 2010). To allow additional binding of proteins without SH2 domain to FGFRs, FGFR substrate α (FRS2α) is continuously bound to FGFR at the intracellular receptor domain. Activation of FGFR results in phosphorylation of FRS2α which in turn is able to bind growth factor receptor bound 2 (GRB2) (Kouhara et al., 1997, Gotoh, 2008). Activation of GRB2 leads to phosphorylation of

AKT and different MAPK (like ERK1/2 and P38) promoting cell survival, inhibiting apoptosis and increasing proliferation and differentiation (Ong et al., 2001, Lowenstein et al., 1992, Gotoh, 2008).

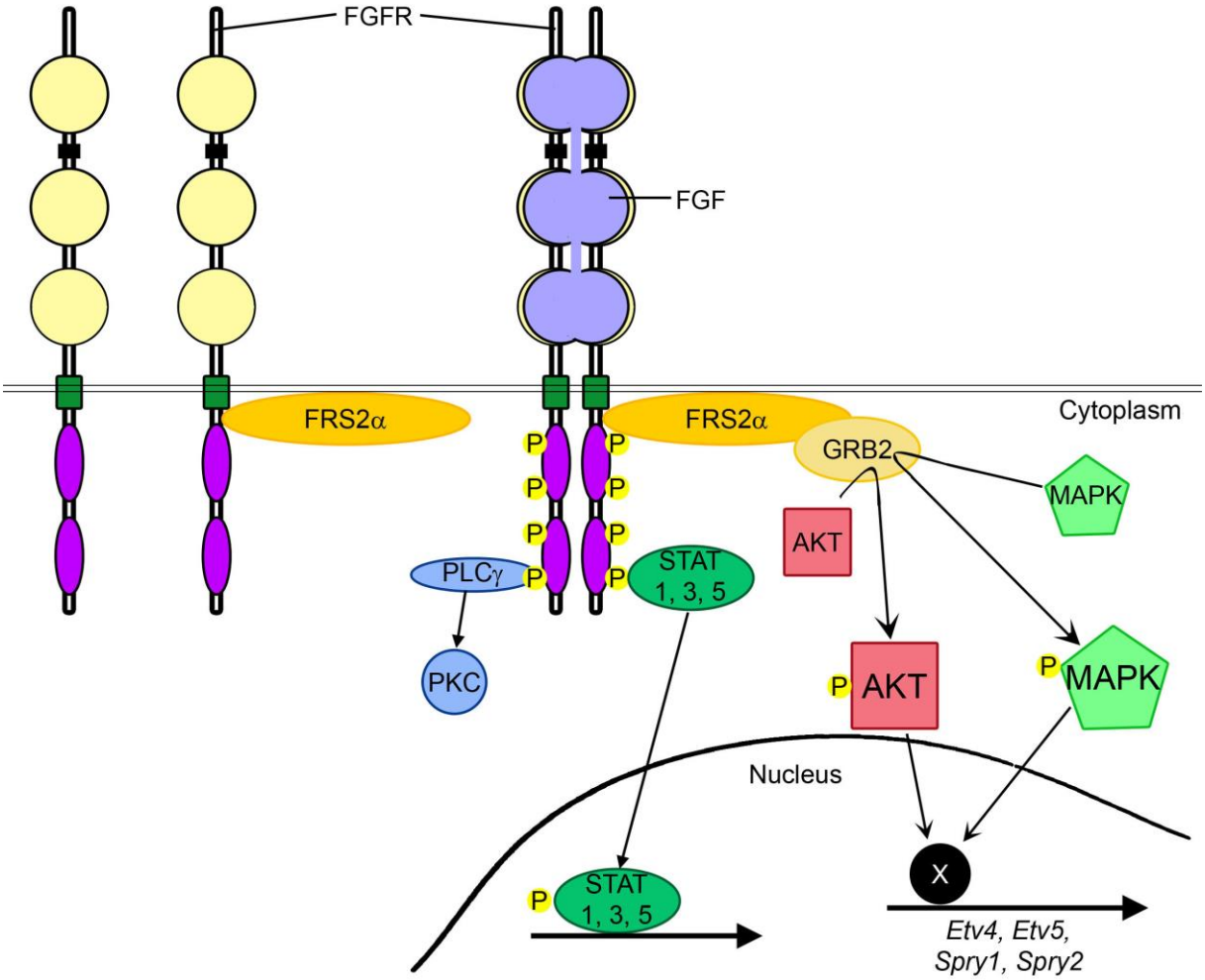

Figure 7: The FGF signaling pathway.
Canonical FGF signaling is activated by transphosphorylation of two receptors after ligand binding. While PLCγ and STAT are able to bind directly to phosphorylated kinase domains activation of MAPK signaling is only possible via the adapter proteins FRS2α und GRB2. Phosphorylation leads to transcription of different target genes such as *Etv* and *Spry.* Idea for graphical design adapted from (Ornitz and Itoh, 2015).

Initial studies reported important functions of FGF signaling in the development of the urinary system. Addition of FGF2 to isolated rat MM cells prevented apoptosis and promoted cell condensation (Barasch et al., 1997, Perantoni et al., 1995). Mice suffering from genetic inactivation of *Fgf8*, *Fgf10* or *Fgfr2IIIb* presented overall normal kidney morphology but the kidneys were significantly smaller (Ohuchi et al., 2000, Qiao et al., 1999, Revest et al., 2001).

The laboratory of Carlton Bates addressed the role of *Fgfr1* and *Fgfr2* in the development of the murine UB, MM and bladder. Conditional inactivation of *Fgfr2* from the UB using a *Hoxb7cre* mouse line resulted in smaller kidneys that displayed considerable smaller number

of nephrons due to reduced branching morphogenesis and tip proliferation and at the same time increased tip apoptosis. *Fgfr1* plays no or only a minor role in this context (Zhao et al., 2004). Unlike in the ND both, *Fgfr1* and *Fgfr2*, have functional relevance in the MM but again with *Fgfr2* being more important. FGFR2 also impacts on the budding process. Inactivation of *Fgfr2* in the whole trunk mesenchyme using *Pax3cre* driver induces multiple UBs, resulting in duplex kidneys and ureters as well as hydroureter and VUR after birth. While *Pax3cre* mediated inactivation of *Fgfr1* alone did not obviously disrupt kidney development, the additional inactivation of *Fgfr2* resulted in complete kidney agenesis due to an inability of the MM to condense (Poladia et al., 2006, Hains et al., 2008, Hains et al., 2010). Mice lacking *Fgfr2* in the peri-ND stroma suffer from an extended CND interfering with distal ureter maturation. On a molecular level *Fgfr2* enhances *Bmp4* expression in the peri-ND mesenchyme (Walker et al., 2013). During murine bladder development FGFR2 controls mesenchymal patterning. Conditional inactivation of *Fgfr2* in the bladder mesenchyme led to increased LP and decreased SMC development as a consequence of increased SHH signaling (Ikeda et al., 2017). However, the function of FGF signaling during ureter development remains unexplored.

Aim of the thesis

Previous work characterized various signaling pathways important for ureter development (Airik and Kispert, 2007, Bohnenpoll and Kispert, 2014). Although FGF signaling was implicated in the development of a large number of organs, its role in the context of ureter development remains completely unexplored (Ornitz and Itoh, 2015). Moreover, the transcriptional targets downstream of the signaling pathways that guide ureter cyto-differentiation from homogeneous, uncommitted precursor cells are widely unknown. Therefore, this thesis aims to address the role of FGF signaling in murine ureter development and identify TF genes that control ureter cyto-differentiation downstream of BMP4 signaling.

Previous work from the lab characterized expression of *Fgfr1* and *Fgfr2* in the early, undifferentiated UE and UM. In the first project the function of FGF signaling in the UE shall be addressed. For this purpose, the spatiotemporal expression of ligands and target genes shall be determined by using the RNA section *in situ* hybridization (SISH) technique. Mice with conditional (*Pax2cre*-mediated) inactivation of *Fgfr1* and *Fgfr2* shall be analyzed for morphological, histological and cellular changes of the ureter at different time points of embryonic development. To identify the underlying molecular mechanisms, unbiased transcriptional profiling by microarray technology shall be performed. Candidate genes shall be validated by SISH for spatial resolution, and by real-time quantitative PCR (RT-qPCR) for quantification. Subsequent rescue experiments by application of chemicals and/or proteins in explant ureter cultures shall verify downstream effectors of FGF signaling. Additional pharmacological loss-of-function experiments in wildtype ureter explant cultures shall provide deeper insight into molecular mechanisms controlling ureter development.

The second project shall address the function of FGF signaling in the ureteric mesenchyme. Morphological, histological, and cellular changes after conditional ($Tbx18^{cre}$-mediated) inactivation of both receptors shall be determined at different time points during ureter development. Functional consequences of phenotypical changes shall be examined in ureter explant cultures by screening for peristaltic activities. Molecular causes underlying the phenotypical changes shall again be addressed by using microarray technology analyzing the transcriptome of mutant ureters. Candidate genes shall be validated by SISH for spatial resolution and by RT-qPCR for quantification. Finally, pharmacological loss- and gain-of-function experiments shall define the functional relevance of signaling pathways for ureter cyto-differentiation.

BMP4 signaling was described to guide ureteric cyto-differentiation in both compartments, the epithelium and the mesenchyme, of the murine ureter, but the transcriptional targets remain widely unexplored (Mamo et al., 2017). The third project therefore aims to identify TF genes that guide ureter cyto-differentiation in the UE and the UM, respectively. For this purpose, unbiased transcriptional profiling of ureters with conditional ($Tbx18^{cre}$-mediated) inactivation of *Bmp4* (*Bmp4cKO*) shall define TF genes, which expression depends on BMP4 signaling.

Moreover, short term inhibition or activation of the BMP4 signaling pathway by applying NOGGIN or BMP4, respectively to ureter explant cultures and subsequent microarray analysis shall determine direct targets of BMP4. Candidate TF genes shall be analyzed by SISH for spatial expression. The molecular mechanisms, by which BMP4 signaling controls the expression of additional indirect targets, shall be investigated by inspection of known signaling pathways that act during ureter development in *Bmp4cKO* ureters. Subsequent pharmacological activation and inhibition experiments in wildtype ureter explant cultures shall provide deeper insight into the regulation of TF genes. Furthermore, the importance of SMAD mediators for cyto-differentiation of the UE shall be addressed by analyzing cellular changes in ureters with conditional (*Pax2cre*-mediated) inactivation of *Smad4*. Moreover, the role of SMAD mediators in the UE and the UM for transduction of BMP4 signals to activate TF gene expression shall be investigated by using microarray technology. Again, candidate genes shall be validated by SISH for spatial resolution.

Together this thesis shall determine the functional relevance of FGF signaling in both compartments of the murine ureter during its development and shall identify TF genes downstream of BMP4 signaling important for ureteric cyto-differentiation.

Part 1 – Molecular function of FGFR2 in the development of the murine ureteric epithelium

FGFR2 signaling enhances the SHH-BMP4 signaling axis in early ureter development

Max Meuser[1,*], Lena Deuper[1,*], Carsten Rudat[1], Nurullah Aydogdu[1], Hauke Thiesler[2], Patricia Zarnovican[2], Herbert Hildebrandt[2], Mark-Oliver Trowe[1] and Andreas Kispert[1,**]

[1]Institut für Molekularbiologie, Medizinische Hochschule Hannover, 30625 Hannover, Germany

[2]Klinik für Gastroenterologie, Hepatologie und Endokrinologie, Medizinische Hochschule Hannover, Hannover, Germany

* These authors contributed equally to this work

**Correspondence to: Andreas Kispert, Institut für Molekularbiologie, OE5250, Medizinische Hochschule Hannover, Carl-Neuberg-Str. 1, D-30625 Hannover, Germany. Phone: +49 511 5324017, Fax: +49 511 5324283, E-Mail: kispert.andreas@mh-hannover.de

KEY WORDS: FGF, FGFR2, Urothelium, Ureter, Epithelial differentiation, SHH, BMP4

Type of authorship: Co-First author
Type of article: Research article
Share of the work: 40%
Contribution to the publication: (co-) planned and performed experiments, analyzed data, prepared figures, assisted in writing the paper

Journal: Development
Impact factor: 6.862
Number of citations: 1
Date of publication: 09.12.2021
DOI: 10.1242/dev.200021

Permission

CCC Marketplace

This is a License Agreement between Lena Deuper ("User") and Copyright Clearance Center, Inc. ("CCC") on behalf of the Rightsholder identified in the order details below. The license consists of the order details, the Marketplace Order General Terms and Conditions below, and any Rightsholder Terms and Conditions which are included below.

All payments must be made in full to CCC in accordance with the Marketplace Order General Terms and Conditions below.

Order Date	26-Oct-2022	Type of Use	Republish in a thesis/dissertation
Order License ID	1283309-1		
ISSN	1477-9129	Publisher	COMPANY OF BIOLOGISTS,
		Portion	Chapter/article

LICENSED CONTENT

Publication Title	Development	Rightsholder	The Company of Biologists Ltd.
Article Title	FGFR2 signaling enhances the SHH-BMP4 signaling axis in early ureter development	Publication Type	e-Journal
		Issue	1
		Volume	149
Author/Editor	Company of Biologists.	URL	http://dev.biologists.org/
Date	01/01/1987		
Language	English		
Country	United Kingdom of Great Britain and Northern Ireland		

REQUEST DETAILS

Portion Type	Chapter/article	Rights Requested	Main product
Page Range(s)	all	Distribution	Worldwide
Total Number of Pages	21	Translation	Original language of publication
Format (select all that apply)	Print, Electronic	Copies for the Disabled?	No
Who Will Republish the Content?	Author of requested content	Minor Editing Privileges?	No
		Incidental Promotional Use?	No
Duration of Use	Life of current edition		
Lifetime Unit Quantity	Up to 499	Currency	EUR

NEW WORK DETAILS

Title	Molecular control of murine ureter development - The function of FGF and BMP4 signaling	Institution Name	Gottfried Wilhelm Leibniz Universität Hannover
		Expected Presentation Date	2022-11-01
Instructor Name	Prof. Dr. rer. nat. Andreas Kispert		

ADDITIONAL DETAILS

Order Reference Number	N/A

The Requesting Person/Organization to Appear on the License	Lena Deuper

REUSE CONTENT DETAILS

Title, Description or Numeric Reference of the Portion(s)	FGFR2 signaling enhances the SHH-BMP4 signaling axis in early ureter development	**Title of the Article/Chapter the Portion Is From**	FGFR2 signaling enhances the SHH-BMP4 signaling axis in early ureter development
Editor of Portion(s)	Meuser, Max; Deuper, Lena; Rudat, Carsten; Aydoğdu, Nurullah; Thiesler, Hauke; Zarnovican, Patricia; Hildebrandt, Herbert; Trowe, Mark-Oliver; Kispert, Andreas	**Author of Portion(s)**	Meuser, Max; Deuper, Lena; Rudat, Carsten; Aydoğdu, Nurullah; Thiesler, Hauke; Zarnovican, Patricia; Hildebrandt, Herbert; Trowe, Mark-Oliver; Kispert, Andreas
Volume of Serial or Monograph	149	**Issue, if Republishing an Article From a Serial**	1
Page or Page Range of Portion	dev200021	**Publication Date of Portion**	2022-01-12

© 2022. Published by The Company of Biologists Ltd | Development (2022) 149, dev200021. doi:10.1242/dev.200021

RESEARCH ARTICLE

FGFR2 signaling enhances the SHH-BMP4 signaling axis in early ureter development

Max Meuser[1,*], Lena Deuper[1,*], Carsten Rudat[1], Nurullah Aydoğdu[1], Hauke Thiesler[2], Patricia Zarnovican[2], Herbert Hildebrandt[2], Mark-Oliver Trowe[1] and Andreas Kispert[1,‡]

ABSTRACT

The patterned array of basal, intermediate and superficial cells in the urothelium of the mature ureter arises from uncommitted epithelial progenitors of the distal ureteric bud. Urothelial development requires signaling input from surrounding mesenchymal cells, which, in turn, depend on cues from the epithelial primordium to form a layered fibro-muscular wall. Here, we have identified FGFR2 as a crucial component in this reciprocal signaling crosstalk in the murine ureter. Loss of *Fgfr2* in the ureteric epithelium led to reduced proliferation, stratification, intermediate and basal cell differentiation in this tissue, and affected cell survival and smooth muscle cell differentiation in the surrounding mesenchyme. Loss of *Fgfr2* impacted negatively on epithelial expression of *Shh* and its mesenchymal effector gene *Bmp4*. Activation of SHH or BMP4 signaling largely rescued the cellular defects of mutant ureters in explant cultures. Conversely, inhibition of SHH or BMP signaling in wild-type ureters recapitulated the mutant phenotype in a dose-dependent manner. Our study suggests that FGF signals from the mesenchyme enhance, via epithelial FGFR2, the SHH-BMP4 signaling axis to drive urothelial and mesenchymal development in the early ureter.

KEY WORDS: FGF, FGFR2, Urothelium, Ureter, Epithelial differentiation, SHH, BMP4

INTRODUCTION

The urothelium is a stratified epithelium that lines the inner surface of the urinary drainage system. In the ureter and bladder, it consists of three major cell types that are organized in radial layers of variable thickness. Large binucleated superficial (S-) or umbrella cells border the lumen and primarily account for the essential barrier function of the tissue. They are sealed by tight junctions and are covered by crystalline plaques of specialized surface proteins: uroplakins (UPKs). Underneath, much smaller intermediate (I) cells form one to several layers depending on species and organ, and serve as precursors for S and basal (B) cells. These small B cells abundantly express keratin 5 (KRT5) and provide an anchor to the basal lamina and the surrounding fibro-muscular wall (Dalghi et al., 2020; Wang et al., 2017).

This urothelial cytoarchitecture derives from highly coordinated proliferation, patterning and differentiation processes that act on epithelial progenitors (the cloacal epithelium in the bladder, the distal ureteric bud in the ureter) starting around embryonic day (E) 10.5 of mouse development (Wang et al., 2017; Yamany et al., 2014). After an initial phase of proliferative expansion, the mono-layered epithelial primordia stratify concomitant with the expression of the transcription factor ΔNP63, indicating I-cell differentiation. After 2 days, the adluminal layer starts to express S-cell markers. B-cell differentiation occurs 2 additional days later (Bohnenpoll et al., 2017a; Gandhi et al., 2013).

Urothelial development in the bladder and ureter does not occur in a cell-autonomous fashion but requires signaling input from adjacent mesenchymal cells, which, in turn, depend on signals from the epithelial primordium to develop into a layered fibro-muscular wall (Balsara and Li, 2017; Bohnenpoll and Kispert, 2014; Cunha et al., 1991; Wang et al., 2017). To date, members of three classes of secreted proteins have been characterized as essential mesenchymal signals for urothelial development: bone morphogenetic protein 4 (BMP4), retinoic acid (RA) and fibroblast growth factors (FGFs). Analysis of conditionally mutant mice showed that *Bmp4* is required in the ureteric mesenchyme (UM) for stratification and cytodifferentiation of the adjacent ureteric epithelium (UE) (Mamo et al., 2017). Expression of *Bmp4* in the UM depends on the transcription factor FOXF1, which, in turn, requires input from an epithelial sonic hedgehog (SHH) signal. SHH acts through this FOXF1-BMP4 axis to control not only epithelial differentiation but also survival, proliferation and smooth muscle cell (SMC) differentiation of surrounding mesenchymal cells, thereby coupling the development of the two tissues (Bohnenpoll et al., 2017c; Yu et al., 2002). *Bmp4* expression receives an additional input from the canonical (CTNNB1-dependent) branch of WNT signaling triggered by WNT ligands from the UE (Trowe et al., 2012). RA has been found to prevent the differentiation of B and S cells in ureter explant cultures (Bohnenpoll et al., 2017b). In the bladder, loss of RA signaling led to a single-layered epithelium with B cells, indicating that, in this context, RA signaling is required for S-cell specification (Gandhi et al., 2013).

Embryos deficient for *Fgf7* exhibit a thinning of the bladder urothelium, particularly of the I-cell layers. *In vitro*, FGF7 stimulated I-cell proliferation and delayed their differentiation into S cells (Tash et al., 2001). Furthermore, FGF10 was shown to act as a mitogen for urothelial cells (Bagai et al., 2002; Zhang et al., 2006). How these mesenchymal FGF signals are transmitted to the epithelium and what targets their signaling pathway has is unknown, as is the interaction of FGF signaling with other signaling systems in this context.

Here, we set out to analyze the role of FGF signaling in urothelial development using the murine ureter as a model. We provide genetic evidence that FGFR2 signaling enhances SHH-BMP4 signaling activity, which is essential for epithelial and mesenchymal proliferation, and differentiation in this organ.

[1]Institute of Molecular Biology, Medizinische Hochschule Hannover, 30625 Hannover, Germany. [2]Institute of Clinical Biochemistry, Medizinische Hochschule Hannover, 30625 Hannover, Germany.
*These authors contributed equally to this work

‡Author for correspondence (kispert.andreas@mh-hannover.de)

A.K., 0000-0002-8154-0257

Handling Editor: Liz Robertson
Received 16 July 2021; Accepted 9 December 2021

RESEARCH ARTICLE

Development (2022) 149, dev200021. doi:10.1242/dev.200021

RESULTS

Fgfr2 is transiently expressed in the epithelium of the developing ureter

Previous work described expression of *Fgf7* and *Fgf10* in the early bladder mesenchyme, while expression of *Fgfr1* and *Fgfr2* was found in the adjacent cloacal epithelium (Cancilla et al., 1999; Dudley et al., 1999; Peters et al., 1992; Tash et al., 2001). To determine whether the expression of these FGF signaling components is conserved in ureter development, we performed *in situ* hybridization analysis on transverse sections of the trunk region of E12.5 to E18.5 wild-type embryos (Fig. 1). At E12.5, both *Fgfr1* and *Fgfr2* were expressed in the UE and UM, *Fgfr2* more strongly and enhanced in the UE. Expression of both genes continued at lower levels at E14.5 and disappeared in both tissues until E18.5. Expression of *Fgf7* and *Fgf10*, the encoded proteins of which predominantly bind to the epithelial (IIIb) isoform of FGFR2 (Igarashi et al., 1998; Jans, 1994; Ornitz and Itoh, 2015), occurred weakly in the UM, particularly at E14.5 (Fig. 1A). We did not detect specific expression of other FGF ligand genes in the UM or the UE from E12.5 to E16.5 (Fig. S1). Importantly, *Spry1* and *Spry2*, target genes of the FGF signaling pathway (Hanafusa et al., 2002), were strongly expressed in the UE at E12.5 and at E14.5 (Fig. 1B). These findings suggest that mesenchymal FGF7 and FGF10 predominantly activate epithelial FGFR2 signaling in early ureter development.

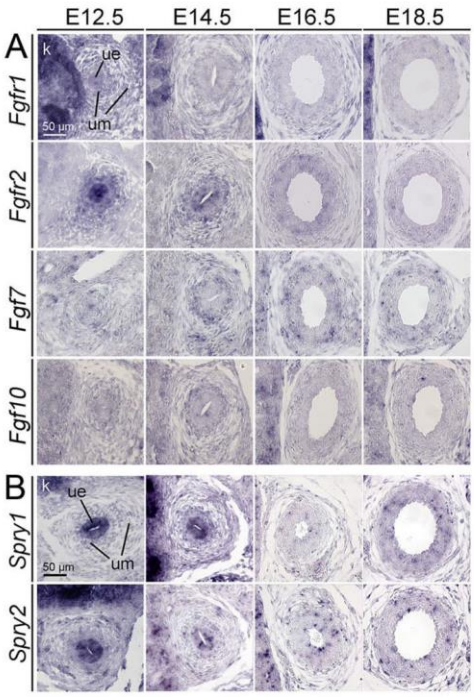

Fig. 1. FGF signaling during embryonic ureter development. (A,B) RNA *in situ* hybridization analysis on transverse sections through the posterior trunk region at the proximal (kidney) level of the ureter of wild-type embryos from E12.5 to E18.5 for expression of two FGFR genes (*Fgfr1* and *Fgfr2*) and two genes encoding FGF ligands (*Fgf7* and *Fgf10*) (A), and of two transcriptional targets of FGF signaling (*Spry1* and *Spry2*) (B). $n \geq 3$ for all probes, stages and genotypes. k, kidney; ue, ureteric epithelium; um, ureteric mesenchyme.

Loss of *Fgfr2* in the UE leads to hydroureter formation and absence of I- and B-cell layers in the urothelium at birth

To explore the specific role of *Fgfr1* and/or *Fgfr2* in the UE, we used a conditional gene inactivation approach with floxed alleles of *Fgfr1* and *Fgfr2* (Hoch and Soriano, 2006; Yu et al., 2003), and a *Pax2-cre* line that mediates recombination in the nephric duct, the precursor of the UE and of the renal collecting duct system (Bohnenpoll et al., 2017a; Trowe et al., 2011). We mated *Pax2-cre/+;Fgfr1*$^{fl/+}$*;Fgfr2*$^{fl/+}$ males with *Fgfr1*$^{fl/fl}$*;Fgfr2*$^{fl/fl}$ females and analyzed the genotype distribution at different time points of embryogenesis. At all stages, *Pax2-cre/+;Fgfr1*$^{fl/fl}$*;Fgfr2*$^{fl/+}$ embryos were found at approximately one-half of the expected frequency, and *Pax2-cre/+;Fgfr1*$^{fl/fl}$*;Fgfr2*$^{fl/fl}$ embryos at a quarter, indicating that homozygous loss of *Fgfr1* accounts for lethality before E12.5, which is further enhanced by removal of *Fgfr2* function (Table S1). Notably, expression of *Spry1* and *Spry2* was strongly reduced at E12.5 and E14.5 in the UE of embryos with loss of two alleles of *Fgfr2*, indicating that FGFR1 does not contribute in a major fashion to FGF signaling in this tissue (Fig. S2).

Morphological inspection of whole urogenital systems at the end of embryonic development, at E18.5, revealed that conditional loss of two and more alleles of *Fgfr1* and *Fgfr2* led with variable severity and penetrance to sex-independent hydroureter formation (Fig. 2A; Table S2A). Approximately 40% of *Pax2-cre/+;Fgfr1*$^{fl/+}$*;Fgfr2*$^{fl/+}$ (n=32) and 30% of *Pax2-cre/+;Fgfr1*$^{fl/fl}$*;Fgfr2*$^{fl/+}$ urogenital systems (n=11) presented with mild unilateral hydroureter, whereas *Pax2-cre/+;Fgfr1*$^{fl/+}$*;Fgfr2*$^{fl/fl}$ (n=26) and *Pax2-cre/+;Fgfr1*$^{fl/fl}$*;Fgfr2*$^{fl/fl}$ (n=8) urogenital systems had an increased occurrence (~85%) of strong bilateral hydroureter. In the last two genotypes, we detected one case each of ureter/kidney agenesis. Loss of both alleles of *Fgfr2* (*Pax2-cre/+;Fgfr1*$^{fl/+}$*;Fgfr2*$^{fl/fl}$; *Pax2-cre/+;Fgfr1*$^{fl/fl}$*;Fgfr2*$^{fl/fl}$) was additionally affected with uni- or bilateral dilatation of the epididymis, while kidney size and ureter length was strongly reduced in *Pax2-cre/+;Fgfr1*$^{fl/fl}$*;Fgfr2*$^{fl/fl}$ urogenital systems only (Fig. 2A; Table S2A). Histological analysis confirmed hydroureter formation upon loss of two or more alleles of *Fgfr1* and/or *Fgfr2*; however, this did not translate into hydronephrosis in any of the genotypes (Fig. 2B, Fig. S3A).

To test for patency of the ureter and its junctions, we injected ink into the renal pelvis of isolated urogenital systems and observed its flow to the bladder upon mild hydrostatic pressure. In most of the embryos with conditional loss of two or three alleles of *Fgfr1* and/or *Fgfr2* (*Pax2-cre/+;Fgfr1*$^{fl/+}$*;Fgfr2*$^{fl/+}$; *Pax2-cre/+;Fgfr1*$^{fl/fl}$*;Fgfr2*$^{fl/+}$; *Pax2-cre/+;Fgfr1*$^{fl/+}$*;Fgfr2*$^{fl/fl}$), the ureteric lumen was contiguous and the distal ureter inserted normally in the dorsal bladder neck. In 60% of *Pax2-cre/+;Fgfr1*$^{fl/fl}$*;Fgfr2*$^{fl/fl}$ urogenital systems (n=5), the ink did not reach the bladder, either due to insertion of the distal ureter into the urethra (1 out of 5) or due to ureteropelvic junction obstruction (n=2) (Table S2B). Histological analysis of the ureter-bladder connection of these specimens confirmed these findings (Fig. S3B). We conclude that loss of *Fgfr2* is associated with strong hydroureter formation. Additional loss of *Fgfr1* contributes to kidney hypoplasia and to increased physical obstruction along the ureter and its junctions.

We next used immunofluorescence analysis of marker proteins to judge cytodifferentiation of the epithelial and mesenchymal tissues of the ureter (Fig. 2C, columns 1-5). Expression of CDH1, a marker of the lateral-basal membrane of epithelial cells, was found in all mutants but the epithelium appeared mono-layered in mutants with loss of two alleles of *Fgfr2*. Expression of KRT5, ΔNP63 and UPK1B combinatorially marked B cells

RESEARCH ARTICLE

Development (2022) 149, dev200021. doi:10.1242/dev.200021

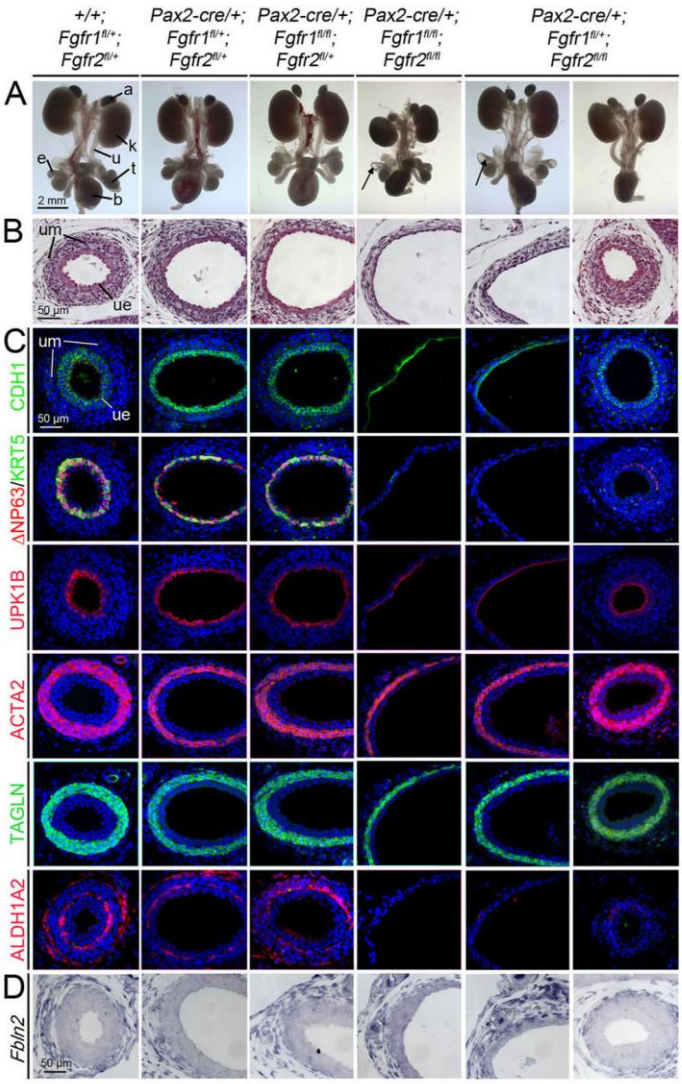

Fig. 2. Ureter anomalies in E18.5 embryos with conditional loss of *Fgfr1* and *Fgfr2* in the UE. (A) Morphology of whole urogenital systems of male embryos. Arrows indicate a dilated epididymis. For quantification data see Table S2A. (B) Hematoxylin and Eosin staining of transverse sections of the proximal ureter. (C,D) Analysis of marker expression for the basolateral membrane of epithelial cells (CDH1), for urothelial cell types [KRT5, ΔNP63 and UPK1B combinatorially mark B cells ($KRT5^+\Delta NP63^+UPK1B^-$), I cells ($KRT5^-\Delta NP63^+UPK1B^{low}$) and S cells ($KRT5^-\Delta NP63^-UPK1B^{high}$)], for SMCs (ACTA2 and TAGLN) and for the *lamina propria* (ALDH1A2) by immunofluorescence (C), and of the *tunica adventitia* marker *Fbln2* by *in situ* hybridization (D). Nuclei are counterstained with DAPI (C,D). $n \geq 3$ for all probes, assays and genotypes (B-D). a, adrenal; b, bladder; e, epididymis; k, kidney; t, testis; u, ureter; ue, ureteric epithelium; um, ureteric mesenchyme.

($KRT5^+\Delta NP63^+UPK1B^-$), I cells ($KRT5^-\Delta NP63^+UPK1B^+$) and S cells ($KRT5^-\Delta NP63^-UPK1B^+$) (Bohnenpoll et al., 2017c) in the control and in mutants with loss of one allele of *Fgfr2*. In mutants with a complete loss of *Fgfr2*, the mono-layered epithelium expressed the S-cell marker UPK1B, whereas KRT5- and ΔNP63-expressing B and I cells were largely absent. Expression of markers for SMCs (ACTA2 and TAGLN) and the *tunica adventitia* (*Fbln2*) occurred in the mesenchymal wall of all mutants; expression of a marker of the *lamina propria* (ALDH1A2) was absent in ureters with complete loss of *Fgfr2* function (Fig. 2C,D, columns 1-5).

Loss and/or reduction of ΔNP63, KRT5 and ALDH1A2 expression was also detected in a rare undilated *Pax2-cre/+;Fgfr1$^{fl/+}$;Fgfr2$^{fl/fl}$* ureter, confirming the dilatation-independent nature of these changes (Fig. 2, column 6). We conclude that loss of *Fgfr2* in the UE compromises differentiation of I and B cells but also affects the development of *lamina propria* fibrocytes in the UM.

Early onset of cellular defects in *Fgfr2*-deficient ureters

To define both the onset as well as the progression of cellular defects in ureters with complete loss of *Fgfr2*, we analyzed earlier embryonic stages (Fig. 3). We used *Pax2-cre/+;Fgfr1$^{fl/+}$;Fgfr2$^{fl/fl}$* (from now on termed *Fgfr2cKO*) embryos for this and all subsequent assays, as they exhibited the same ureteric cytodifferentiation defects as *Pax2-cre/+Fgfr1$^{fl/fl}$;Fgfr2$^{fl/fl}$* embryos but presented in a normal Mendelian ratio. *Fgfr2cKO* ureters exhibited a clear histological division of the UM into an inner layer with rhomboid-shaped condensed cells and an outer layer with loosely organized fibroblast-like cells from E12.5 onwards, as in the control. However, both the UE and the UM were hypoplastic (Fig. 3A). The UE appeared less stratified at E14.5 and subsequent stages, and did not activate expression of ΔNP63 and KRT5. Expression of UPK1B occurred normally from E15.5 onwards. Expression of SMC markers was delayed by 1 day (Fig. 3B, Fig. S4 for higher magnification images of histological and CDH1 staining).

Development (2022) 149, dev200021. doi:10.1242/dev.200021

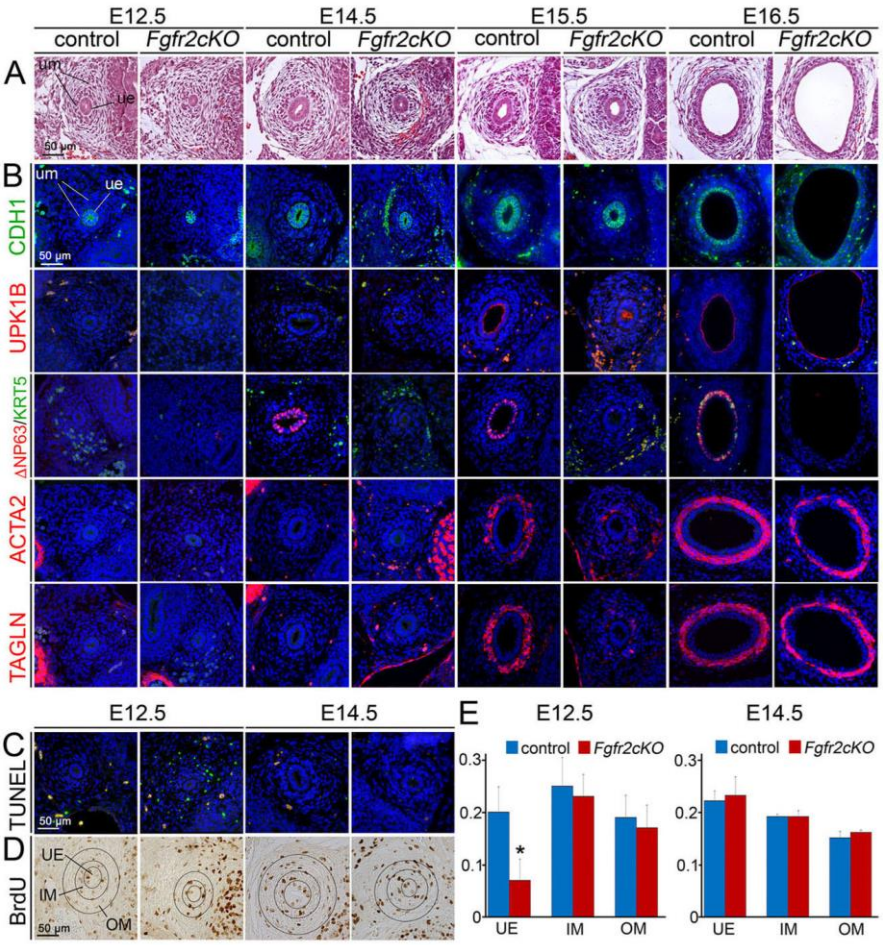

Fig. 3. Early onset of cellular changes in *Fgfr2cKO* ureters. (A) Hematoxylin and Eosin (HE) staining of transverse sections of the proximal region of the developing ureter at the indicated stages. (B) Analysis of marker expression for the epithelium (CDH1), for urothelial cell types (KRT5, ΔNP63 and UPK1B) and for SMCs (ACTA2 and TAGLN) in the developing ureter by immunofluorescence at the indicated stages. Nuclei are counterstained with DAPI (blue). (C) Immunofluorescence analysis (green) of apoptosis by the TUNEL assay on proximal ureter sections at E12.5 and E14.5. Nuclei are counterstained with DAPI (blue). Loss of *Fgfr2* in the UE leads to an increase in apoptosis in outer mesenchymal cells. (D) Determination of cellular proliferation by a BrdU incorporation assay on transverse sections of the proximal ureter at E12.5 and E14.5. Black circles mark the epithelium (UE) and the inner (IM) and outer (OM) mesenchymal compartments of the ureter in which proliferation was quantified. (E) Quantification of BrdU-positive cells (Table S3). E12.5, control versus mutant: UE, 0.2±0.05 versus 0.07±0.04, P=0.02; IM, 0.25±0.05 versus 0.23±0.04, P=0.42; OM, 0.19±0.04 versus 0.17±0.04, P=0.5. E14.5, control versus mutant: UE, 0.22±0.01 versus 0.23±0.03, P=0.56; IM, 0.19±0.01 versus 0.19±0.01, P=0.36; OM, 0.15±0.01 versus 0.16±0.01, P=0.09. Data are mean±s.d. *P<0.05; two-tailed Student's t-test. $n\geq3$, for all probes, assays and genotypes. ue, ureteric epithelium; um, ureteric mesenchyme.

Given the obvious tissue hypoplasia in *Fgfr2cKO* ureters from E12.5 onwards, we analyzed whether changes in apoptosis and/or proliferation may be causative. In fact, the TUNEL assay detected apoptotic cells in the outer region of the UM at E12.5 (Fig. 3C). Moreover, the BrdU incorporation assay revealed strongly reduced proliferation in the UE of mutant embryos at this stage (Fig. 3D,E; Table S3). Hence, epithelial FGFR2 signaling plays a crucial role in epithelial proliferation, stratification and I-/B-cell differentiation, and (indirectly) in mesenchymal apoptosis and differentiation.

Reduced activity of a *Shh-Foxf1-Bmp4* module in *Fgfr2cKO* ureters

We next performed transcriptional profiling by microarray analysis of E13.5 *Fgfr2cKO* and control ureters to identify molecular changes that may underlie the cellular defects in these mutants. Using an intensity threshold of 100 and fold changes of at least 1.5, we identified 97 genes that were consistently upregulated and 49 genes that were downregulated in *Fgfr2cKO* ureters (Fig. 4A; Tables S4 and S5). Functional annotation by DAVID did not find enrichment of meaningful terms in the list of upregulated genes (Table S6). However, in the pool of downregulated genes terms associated with SHH/SMO activity and AP1 signaling were over-represented (Table S7).

In fact, among the most downregulated genes were *Hhip*, *Ptch1* and *Foxf1*, which have previously been found to depend on SHH signaling in the ureter (Bohnenpoll et al., 2017c), *Shh* itself and AP1/immediate early genes (*Fosb*, *Egr1*, *Fos* and *Egr2*). Moreover, *Hoxb8*, a gene linked to proliferation control (Guo et al., 2019; Wang et al., 2019), was strongly reduced as was *Aldh1a3*, a gene encoding an RA-synthesizing enzyme, and *Elf5* (Fig. 4A), an epithelial target of RA signaling in the ureter (Bohnenpoll et al., 2017b). *Spry1* and *Spry2*, direct targets of FGF signaling (Hanafusa et al., 2002), were reduced confirming our previous analysis (Fig. S2).

We used *in situ* hybridization analysis to validate these changes in E12.5 and E14.5 *Fgfr2cKO* ureters. We detected reduced expression of *Hoxb8*, *Aldh1a3* and *Elf5* in the UE at E12.5 (Fig. 4B,C). Expression of *Shh* was strongly reduced in the UE, as was expression of *Ptch1* and *Foxf1* in the UM at E12.5 and E14.5 (Fig. 4D). Expression of *Fosb*, *Egr1* and *Fos* was not detected in the control or was unchanged in the mutant (Fig. S5).

Given the strong downregulation of the *Shh-Foxf1* axis, we also analyzed expression of the effector gene of this pathway: *Bmp4* (−1.2 in the microarray) (Mamo et al., 2017). *Bmp4* expression was clearly reduced in the UM both at E12.5 and E14.5. Moreover, expression of Id genes (*Id2*, *Id3* and *Id4*), direct transcriptional

RESEARCH ARTICLE

Development (2022) 149, dev200021. doi:10.1242/dev.200021

A

Gene	avgFC	Gene	avgFC	Gene	avgFC
Hoxb8	**-3.1**	Hs3st6	-1.9	Gabbr2	-1.6
Nhlrc4	-2.4	Fam150b	-1.8	Dclk3	-1.6
9030625G05Rik	-2.4	Ldoc1	-1.8	Ccdc172	-1.6
Fosb	-2.3	Degs2	-1.8	Afm	-1.6
Gsta2	-2.3	Egr2	-1.8	A_55_P2028852	-1.6
Hhip	-2.2	Sel1l3	-1.8	**Elf5**	**-1.6**
Calcr	-2.2	Kcnj16	-1.8	Atp1b1	-1.6
Gm10639	-2.1	Tfap2b	-1.8	Nr1h5	-1.5
TC1605611	-2.1	Srrm2	-1.8	Iqck	-1.5
Mapk4	-2.0	Arhgef38	-1.8		
A930017K11Rik	-2.0	**Aldh1a3**	**-1.7**	**Ptch1**	**-2.0 (-1.3/-2.7)**
Prr7	-1.9	Gprc5b	-1.7	**Bmp4**	**-1.2 (1.0/-1.4)**
Mia	-1.9	Tmem229a	-1.7	Aldh1a2	-1.3 (-1.2/-1.3)
Fos	-1.9	A4galt	-1.7	Rarb	1 (-1.1/1.1)
Rbm47	-1.9	**Shh**	**-1.7**	**Wnt7b**	**-1.6 (-1.4/-1.7)**
Mllt3	-1.9	E330013P04R	-1.7	Wnt9b	-1.4 (-1.4/-1.4)
Egr1	-1.9	**Foxf1**	**-1.7**	**Axin2**	**-1.2 (1.0/-1.5)**
Sprr2f	-1.9	Clu	-1.7		
Espn	-1.9	Map7	-1.7	**Spry1**	**-1.8 (-1.4/-2.2)**
Frmd5	-1.9	Tfrc	-1.6	**Spry2**	**-1.8 (-1.4/-2.2)**

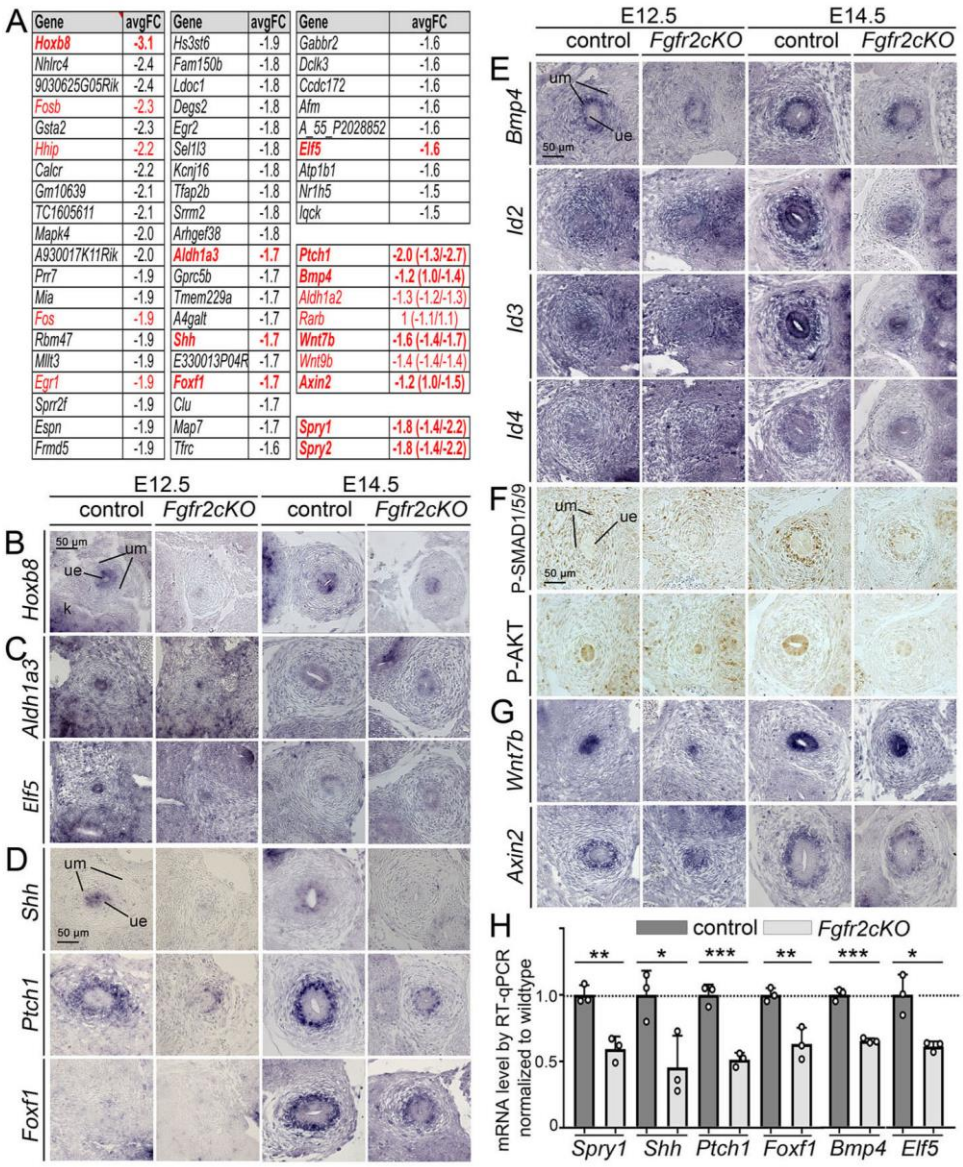

Fig. 4. The *Shh-Foxf1-Bmp4* signaling axis is compromised in *Fgfr2cKO* ureters. (A) Table of transcripts with reduced expression in microarrays of E13.5 *Fgfr2cKO* ureters. Shown are average fold changes (avgFC). Genes in red are validated by *in situ* hybridization, the ones in bold show reduced expression in this assay. All genes in the lower right column did not fulfill the initial filter criteria but were additionally validated. (B-E,G) *In situ* hybridization analysis on transverse sections of the proximal ureter of E12.5 and E14.5 control and *Fgfr2cKO* embryos for expression of *Hoxb8* (B), of an epithelial RA component (*Aldh1a3*) and target (*Elf5*) (C), of components and targets of SHH signaling (*Shh*, *Ptch1* and *Foxf1*) (D), of *Bmp4* and direct transcriptional targets of its activity (*Id2*, *Id3* and *Id4*) (E), and of an epithelial WNT ligand gene (*Wnt7b*) and a target of WNT signaling (*Axin2*) (G). (F) Immunohistochemical detection of activated, i.e. phosphorylated, forms of cytoplasmic effectors of BMP4 signaling (P-SMAD1/5/9 and P-AKT) on transverse sections of the proximal ureter of E12.5 and E14.5 control and *Fgfr2cKO* embryos. $n \geq 3$ for all probes, genotypes and stages. (H) RT-qPCR results of expression of selected signaling components and targets in three independent total RNA pools of E14.5 *Fgfr2cKO* and control ureters. For statistical values, see Table S8. Differences were considered significant (*$P<0.05$), highly significant (**$P \leq 0.01$) or extremely significant (***$P \leq 0.001$); two-tailed Student's *t*-test. Data are mean±s.d. k, kidney; ue, ureteric epithelium; um, ureteric mesenchyme.

targets of BMP signaling (Hollnagel et al., 1999; Liu and Harland, 2003), was reduced both in the UE and UM of *Fgfr2cKO* embryos at E14.5 (Fig. 4E). As BMP4 signaling is mediated by different cytoplasmic effector proteins in the developing ureter (Mamo et al., 2017), we analyzed their activated, i.e. phosphorylated, forms by immunohistochemistry. We found reduced expression of P-SMAD1/5/9 in the UM, and of P-AKT in the UE at E14.5, while P-ERK1/2 and P-P38 expression was unaffected (Fig. 4F; Fig. S6).

In agreement with the microarray data, other signaling systems involved in ureteric proliferation and differentiation were either not

Development (2022) 149, dev200021. doi:10.1242/dev.200021

or only marginally affected. Expression of mesenchymal RA signaling components (*Aldh1a2*) and targets (*Rarb*) (Mendelsohn et al., 1991) was unchanged (Fig. S5). Expression of *Wnt7b* was weakly reduced in the UE at E12.5; *Wnt9b* expression in the UE was normal; expression of *Axin2* was weakly reduced in the UM (Fig. 4G, Fig. S5).

Finally, RT-qPCR analysis confirmed significantly reduced expression of *Spry1*, *Shh*, *Ptch1*, *Foxf1*, *Bmp4* and *Elf5* in E14.5 *Fgfr2cKO* ureters (Fig. 4H; Table S8). We conclude that the *Shh-Foxf1-Bmp4* axis is strongly affected by loss of epithelial *Fgfr2* in the early ureter, whereas RA and WNT signaling are only partly and weakly compromised.

SHH and BMP4 signaling mediates FGFR2 function

To test the individual contribution of reduced SHH, BMP4, RA and WNT signaling activity to the proliferation and cytodifferentiation defects of *Fgfr2cKO* ureters, we performed pharmacological pathway rescue experiments in *ex vivo* cultures (Fig. 5). As we were not able to confirm expression (changes) of AP1 components and targets in the UM of mutants (Fig. S5), we excluded this pathway from further investigation.

Fgfr2cKO ureters explanted at E13.5 and cultured for 4 days in minimal medium (DMEM only) exhibited a short ureter with epithelial tissue hypoplasia. Moreover, the ratio of $\Delta NP63^+$ to $CDH1^+$ cells dropped to around 50% (control: 90%), the thickness of the SMC layer (marked by TAGLN) was reduced and expression of the *lamina propria* marker ALDH1A2 was nearly absent, highly reminiscent of the changes observed *in vivo*. Addition of 2 µM of the SHH signaling/SMO agonist purmorphamine (Li et al., 2008) or of 100 ng/ml BMP4 increased the percentage of $\Delta NP63^+$ cells in *Fgfr2cKO* ureter explants almost to control level and rescued epithelial hypoplasia. In the case of reactivation of the SHH signaling pathway, mesenchymal aspects of the *Fgfr2cKO* phenotype were also rescued: expression of ALDH1A2 was restored as was the thickness of the SMC layer. Addition of BMP4 rescued the mesenchymal phenotype partly. Addition of 1 µM RA enhanced the loss of $\Delta NP63^+$ and $ALDH1A2^+$ cells, and did not rescue the tissue hypoplasia of the mutant ureter. The WNT agonist BIO (Sato et al., 2004) rescued the epithelial hypoplasia but left all other parameters in *Fgfr2cKO* ureters unaffected (Fig. 5; Table S9). Hence, SHH and BMP4 signaling are functional mediators of FGFR2 activity in the UE.

Inhibition of SHH or BMP4 signaling dose-dependently compromises epithelial and mesenchymal differentiation in the ureter

Previous work has shown that the genetic ablation of SHH and BMP4 signaling leads to tissue hypoplasia and a complete lack of cytodifferentiation (Bohnenpoll et al., 2017c; Mamo et al., 2017). To explore the consequences of a partial reduction of these signaling activities for ureter development, we explanted E13.5 wild-type ureters and cultured them for 4 days in DMEM supplemented with increasing concentrations of the SMO antagonist cyclopamine (Chen et al., 2002; Cooper et al., 1998) or noggin (NOG), which sequesters BMP4 from its receptor (Zimmerman et al., 1996). In both cases, we detected a dose-dependent decrease of stratification and of $\Delta NP63^+$ cells, a reciprocal increase of luminal $\Delta NP63^-$ cells that were lined by UPK expression at low and medium doses, and an ablation (cyclopamine) or reduction (NOG) of the SMC layer. At the highest doses of NOG, UPK expression was partially reduced. Expression of ALDH1A2 was strongly affected by mild reduction of SHH signaling, whereas reduction of BMP4 signaling had a weaker but dose-dependent effect (Fig. 6A-E; Fig. S7 for higher magnification images of histological and CDH1 staining; Table S10). We conclude that reduction of SHH or BMP4 signaling largely recapitulates the phenotypic changes in *Fgfr2cKO* ureters.

DISCUSSION

Epithelial FGFR2 signaling controls multiple cellular programs in both the mesenchymal and epithelial compartment of the ureter

Previous work described the role of FGFR signaling in the development of numerous components of the urinary system, but its role(s) in ureter development has remained unexplored (Walker et al., 2016). Based on their expression in the early UE, we used a conditional gene targeting experiment to analyze the specific function of *Fgfr1* and *Fgfr2* in this tissue. Our phenotypic characterization of compound and double mutants revealed that FGFR2 function maintains the structural integrity of the ureter by controlling different cellular programs in both the epithelial and mesenchymal tissue compartment of this organ.

Owing to our breeding strategy, we recovered only *Fgfr1-Fgfr2* compound mutants for phenotypic analysis. Although we cannot formally exclude a (minor) contribution of heterozygous loss of *Fgfr1* to the observed phenotypic changes of the ureter in embryos with homozygous loss of *Fgfr2*, we are convinced that control of early ureter development is exerted almost exclusively by FGFR2. First, *Fgfr2* is much more strongly expressed than *Fgfr1* in the UE from E12.5 to E14.5. Second, complete loss of *Fgfr1* with combined loss of one allele of *Fgfr2* did not result in changes in FGF signaling, i.e. *Spry1* and *Spry2* expression, in the UE, whereas complete loss of *Fgfr2* did. Third, complete loss of *Fgfr2* but not of *Fgfr1* resulted in severe ureteric cytodifferentiation defects. Fourth, FGF7 and FGF10, the two ligands with expression in the UM, predominantly signal through the epithelial isoform of FGFR2 (Igarashi et al., 1998; Jans, 1994; Ornitz and Itoh, 2015), whereas specific expression of FGF ligands that preferentially signal through FGFR1 was not detected in the early ureter. Fifth, previous studies using a *Hoxb7cre* line for recombination in the ureteric bud lineage did not detect defects in the urogenital system of *Hoxb7cre/+;Fgfr1*$^{fl/fl}$ embryos, whereas *Hoxb7cre/+;Fgfr2*$^{fl/fl}$ embryos exhibited renal hypo(dys)plasia due to reduced branching morphogenesis, and thinning of the early ureter and hydroureter, which are highly reminiscent of the phenotypic changes observed in our *Pax2-cre/+;Fgfr1*$^{fl/+}$*;Fgfr2*$^{fl/fl}$ embryos (Sims-Lucas et al., 2011; Zhao et al., 2004).

Although we detected embryonic lethality in our compound mutants, *Hoxb7cre/+;Fgfr1*$^{fl/fl}$, *Hoxb7cre/+;Fgfr2*$^{fl/fl}$ and *Hoxb7cre/+;Fgfr1*$^{fl/fl}$*;Fgfr2*$^{fl/fl}$ mice exhibited a normal Mendelian distribution at embryonic and adult stages (Sims-Lucas et al., 2011; Zhao et al., 2004). The *Pax2-cre* line used in our conditional gene targeting experiments also recombines outside the nephric duct epithelium (and its derivatives), particularly strongly in the midbrain-hindbrain region and the branchial arches at E9.5 (Kuschert et al., 2001). These expression domains are likely to give rise to vessels in the brain but also to the second heart field from which the atria, the right ventricle and the outflow region are derived (Kelly et al., 2001; Mjaatvedt et al., 2001). Given the known role of FGF signaling in the second heart field region and in vessel development (Park et al., 2008; Yang et al., 2015), deletion of *Fgfr1* and/or *Fgfr2* might contribute to embryonic lethality due to cardiac/circulatory insufficiency.

The study by Zhao et al. characterized the function of *Fgfr2* in renal development, but it did not explain the thinning of the early

Development (2022) 149, dev200021. doi:10.1242/dev.200021

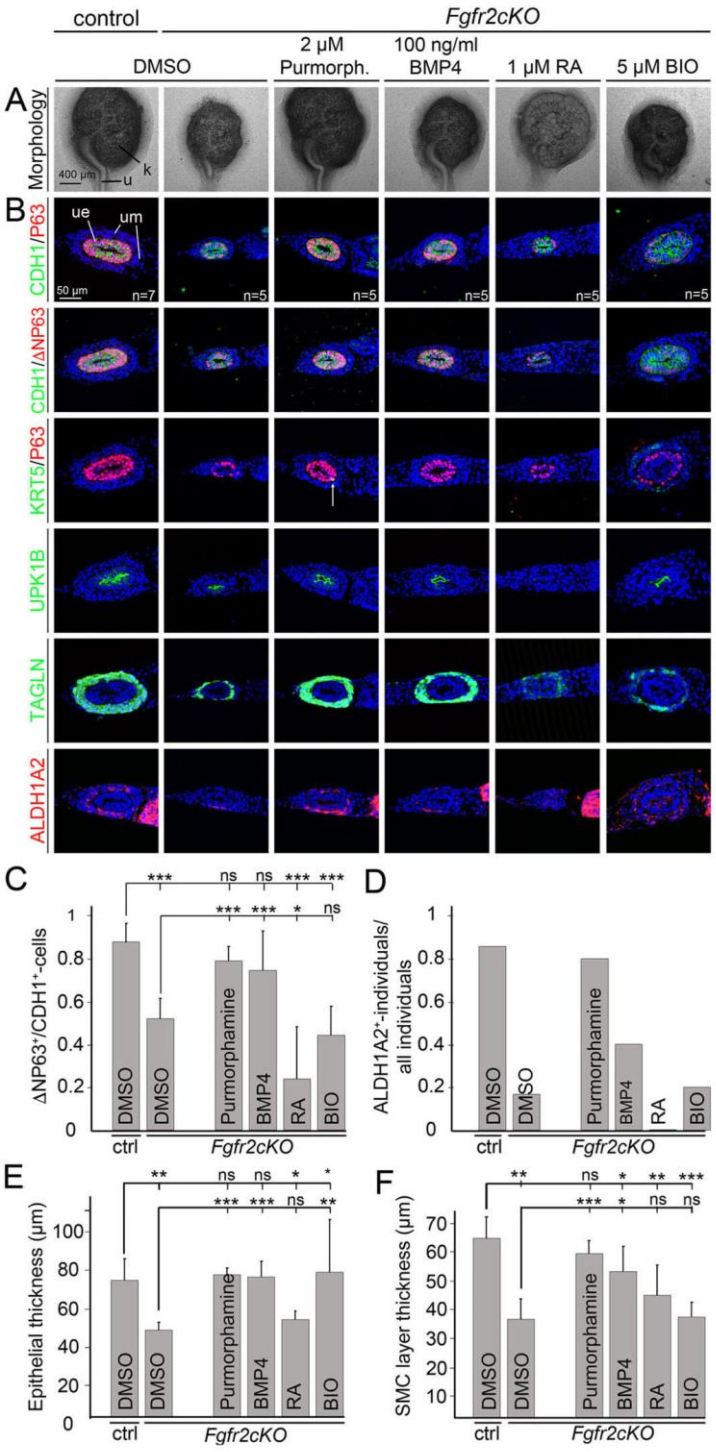

Fig. 5. Restoration of SHH or BMP4 signaling rescues epithelial and mesenchymal proliferation and differentiation defects in *Fgfr2cKO* ureters in explant cultures. E13.5 control and *Fgfr2cKO* ureters were cultured for 4 days in DMEM supplemented with DMSO (as a control), 2 µM of the SHH signaling agonist purmorphamine (Purmorph.), 100 ng/ml BMP4, 1 µM RA or 5 µM WNT signaling activator BIO. (A) Bright-field images of kidney (k) and ureter (u) explants after 4 days of culture. (B) Immunofluorescence analysis on transverse sections of the proximal ureter for expression of markers for the epithelium (CDH1), urothelium (KRT5, ΔNP63 and UPK1B), SMCs (TAGLN) and *lamina propria* (ALDH1A2). The arrow (row 3, column 3) points to a single KRT5$^+$ cell. *n*=7 for the control; *n*=5 for the mutant for all assays (B-F). ue, ureteric epithelium; um, ureteric mesenchyme. (C-F) Quantification on transverse sections of the proximal ureter of the ratio of ΔNP63$^+$ to CDH1$^+$ epithelial cells (C), of the percentage of sections with ALDH1A2$^+$ cells (D), of the epithelial thickness (E) and of the SMC layer thickness (F). For statistical values, see Table S9. Differences were considered non-significant (ns; $P>0.05$), significant (*$P<0.05$), highly significant (**$P\leq0.01$) or extremely significant (***$P\leq0.001$); two-tailed Student's *t*-test. The upper lines refer to the statistical difference compared with the DMSO-treated control (ctrl), the lower lines refer to DMSO-treated *Fgfr2cKO* ureter explants. Data are mean±s.d.

ureter and hydroureter formation in these mice (Zhao et al., 2004). Our study shows that these defects relate to an independent function of FGFR2 signaling in the development of the distal aspect of the ureteric bud. Epithelial *Fgfr2* was required for proliferation, stratification and I-/B-cell differentiation in the UE but its loss also had an impact on apoptosis, and SMC as well as *lamina propria* differentiation in the UM. Although work in the bladder assigned FGF7 and FGF10 a role as mitogens for I cells (Bagai et al., 2002;

RESEARCH ARTICLE

Development (2022) 149, dev200021. doi:10.1242/dev.200021

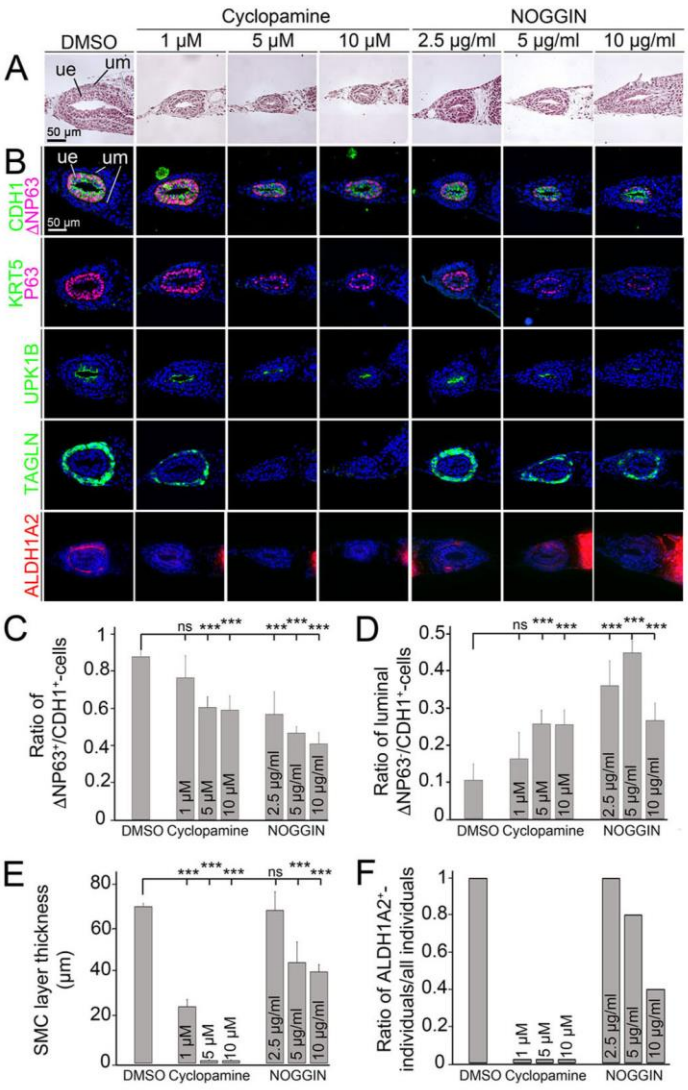

Fig. 6. Inhibition of SHH or BMP4 signaling dose-dependently compromises epithelial and mesenchymal differentiation in the ureter. E13.5 wild-type ureters were cultured for 4 days with increasing concentrations of the SHH signaling inhibitor cyclopamine or the BMP4 antagonist noggin (NOG). (A,B) Transverse sections of the proximal region of E13.5 ureters cultured for 4 days under the indicated conditions were analyzed by Hematoxylin and Eosin staining (A), and by (co-)immunofluorescence analysis for expression of the epithelial marker CDH1 with ΔNP63, the B-cell marker KRT5 with P63, the S-cell marker UPK1B and the SMC marker TAGLN (B). ue, ureteric epithelium; um, ureteric mesenchyme. (C-F) Transverse sections of the proximal ureter cultured in the presence of increasing concentrations of cyclopamine or NOG were quantified for the ratio of $\Delta NP63^+$ cells to $CDH1^+$ cells (C), for the ratio of $\Delta NP63^-$ luminal cells to $CDH1^+$ cells (D), for the thickness of the SMC layer (E), and for the ratio of $ALDH1A2^+$ individuals to all individuals (F) compared with the DMSO control. For statistical values, see Table S10. Differences were considered non-significant (ns) with $P>0.05$ or extremely significant ($^{***}P\leq0.001$); two-tailed Student's *t*-test. $n\geq5$ for all assays. Data are mean±s.d.

Tash et al., 2001; Zhang et al., 2006), our findings indicate a broader function for epithelial FGFR signaling – using a relay system – to coordinate the development of both tissue compartments in the early ureter.

Our ink injection experiments revealed that in *Fgfr2cKO* urogenital systems physical obstruction occurs only in 20% of the specimens, indicating that delayed SMC differentiation contributes or causes hydroureter formation, as observed in other mouse models (Weiss et al., 2019). Luminal occlusion in distal ureter regions due to epithelial hypoplasia and/or distal ureter maturation defects due to delayed ureter budding may contribute to this defect, as reported for *Hoxb7-cre/+;Fgfr2*$^{fl/fl}$ mice (Sims-Lucas et al., 2011; Zhao et al., 2004). Our *Fgfr1/Fgfr2* double mutants exhibited an increased incidence of hydroureter formation due to ureteropelvic junction obstruction, a blind-ending distal ureter and ectopic urethral connectivity. They also showed strong renal and ureter hypoplasia. We assume that these defects reflect the combined function of *Fgfr1* and *Fgfr2* in UB formation, and branching morphogenesis of the collecting duct system from the proximal UB tip region, as previously reported (Sims-Lucas et al., 2011; Zhao et al., 2004).

Shh is a functional target of FGFR2 in the UE

Fgfr2cKO ureters exhibit a spectrum of phenotypic changes in both the epithelial and mesenchymal compartment that are similar in nature but reduced in severity compared with those seen when the SHH-FOXF1-BMP4 signaling axis is lost. Moreover, the temporal window of epithelial FGFR2 signaling activity aligns with the expression profile of *Shh* and *Bmp4* in the ureter; both are strongly downregulated after E14.5 (Bohnenpoll et al., 2017c; Mamo et al., 2017; Yu et al., 2002). Expression of *Shh* as well as of *Ptch1*, *Foxf1* and *Bmp4*, which represent the *Shh* effector level, was reduced in *Fgfr2cKO* ureters. Activation of SHH/SMO signaling by purmorphamine and addition of BMP4 largely rescued the proliferation and differentiation defects in *Fgfr2cKO* ureters. Finally, reduction of SHH and BMP4 signaling in wild-type ureters recapitulated the phenotypic changes observed in *Fgfr2cKO* ureters

Development (2022) 149, dev200021. doi:10.1242/dev.200021

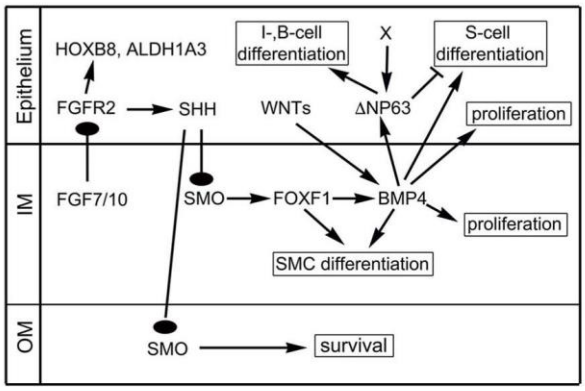

Fig. 7. Model of FGFR2 signaling function in the early ureter. FGFR2 signaling in the UE augments *Shh* expression and, hence, the SHH-FOXF1-BMP4 signaling axis in the UM, which accounts for mesenchymal and epithelial proliferation and differentiation (processes are boxed). FGFR2 may activate expression of additional genes in the UE (*Hoxb8* and *Aldh1a3*) independently of *Shh*. Factor X provides an unknown input for ΔNP63 expression. Arrows indicate activating interactions, dots indicate ligand receptor interaction. IM, inner mesenchyme; OM, outer mesenchyme.

in a dose-dependent manner. Together, this provides compelling evidence that FGFs act via FGFR2 to enhance *Shh* expression and consequently SHH-FOXF1-BMP4 activity in the early ureter (Fig. 7).

It is important to note that the FGF7/10-FGFR2-SHH-BMP4 signaling axis has previously been characterized in the early development of other organs, including the urethra, the limb, the palate and the eyelid (Huang et al., 2009; Petiot et al., 2005; Revest et al., 2001; Rice et al., 2004). The primordia of all of these organs, as well as of the ureter and bladder are characterized by a composite design with epithelial and mesenchymal tissue compartments. The coordinated development of these compartments is assured by reciprocal signaling systems in which the FGF7/10-FGFR2-SHH-BMP4 module seems of outstanding relevance.

Our microarray analysis identified *Hoxb8* as the most downregulated gene in the *Fgfr2cKO* ureter. As *Hoxb8* has been implicated in proliferation control (Guo et al., 2019; Wang et al., 2019), its reduced expression in the UE may contribute to urothelial hypoplasia. Importantly, *Hoxb8* does not depend on SHH signaling in the ureter (Bohnenpoll et al., 2017c), and can be ectopically induced in neural tissues of the chick by FGF treatment (Bel-Vialar et al., 2002). This suggests that FGFR2 signaling regulates a set of genes independently of the SHH-FOXF1-BMP4 signaling axis.

Urothelial cell fates may depend on gradients of BMP4

Fgfr2cKO ureters displayed a mono-layered urothelium consisting of S cells. This phenotype is highly reminiscent of that seen in the bladder and ureters of mice with conditional loss of ΔNP63 in the respective epithelial primordium (Cheng et al., 2006; Pignon et al., 2013; Weiss et al., 2013). Failure to activate ΔNP63 in *Fgfr2cKO* ureters, therefore, likely accounts for the lack of stratification and B-cell differentiation in the mutant urothelium.

Expression and lineage tracing analysis uncovered that S and B cells are terminally differentiated cell types that arise from a common progenitor by an I-cell intermediate. The I cells were recognized as $\Delta NP63^{+}$ cells lacking high expression of UPKs and KRT5 (Bohnenpoll et al., 2017a; Gandhi et al., 2013). Differentiation of S cells in absence of ΔNP63 shows that stratification is not a prerequisite for S-cell differentiation, and suggests that S-cell differentiation is normally inhibited by ΔNP63 in I cells.

Mice with conditional loss of *Smo* or *Bmp4* in the UM do not activate ΔNP63 in the urothelium, and lack stratification and B- and S-cell differentiation (Bohnenpoll et al., 2017c; Mamo et al., 2017). In *Fgfr2cKO* ureters, *Shh* and, consequently, *Bmp4* expression is reduced but not lost, suggesting that ΔNP63 expression and stratification requires higher levels of SHH and BMP4 signaling than S-cell differentiation. This notion is supported by the restoration of ΔNP63 expression in *Fgfr2cKO* ureters by purmorphamine and BMP4 treatment, on the one hand, and a relatively higher decrease in I cells compared with S cells by increasing doses of cyclopamine and NOG in wild-type ureters, on the other hand. Administration of BMP4 to early kidney explants leads to UPK expression in collecting duct cells (Mills et al., 2017; Wang et al., 2009), indicating that BMP4 is required and sufficient to activate S-cell differentiation. It is conceivable that ectopic induction of I-cell differentiation and of ΔNP63 expression, respectively, require higher levels of BMP4 and/or additional positive signals, similar to the situation in other epithelia (Terakawa et al., 2016). Alternatively, concurrent repression of an inhibitor may allow induction of ΔNP63.

Interestingly, the epithelium covering the renal papilla is monolayered and consists of S cells only. It is conceivable that out of the reach of FGF7/FGF10 signals, the SHH-BMP4 axis is not sufficiently augmented to activate ΔNP63 and to drive stratification at this site.

FGFR2 signaling and urothelial regeneration

Our expression analysis showed that *Fgfr2* is strongly downregulated after E14.5, excluding a role for FGFR2 signaling in later (fetal) development and homeostasis. This is consistent with the mature urothelium being quiescent. However, under conditions of injury or infection, proliferation of I cells and differentiation into S and B cells resume to repair the urothelium within days. Interestingly, recent reports revealed that FGF7 and FGFR2 function is reused in this program (Girshovich et al., 2012; Narla et al., 2020). Whether an FGF7-FGFR2 module employs the SHH-BMP4 signaling axis in regeneration similar to the embryonic situation is an interesting question for future research.

MATERIALS AND METHODS

Mice

Mice with *loxP* sites flanking exon 4 of the *Fgfr1* locus (*Fgfr1*$^{tm5.1Sor}$; synonym: *Fgfr1*^{fl}) (Hoch and Soriano, 2006) and mice with *loxP* sites flanking exons 7 to 10 of the *Fgfr2* locus (*Fgfr2*^{tm1Dor}; synonym: *Fgfr2*^{fl}) (Yu et al., 2003) were obtained from the Jackson Laboratory. *Tg(Pax2-cre)1AKis* (synonym: *Pax2-cre*) mice were previously generated in the lab (Bohnenpoll et al., 2017a; Trowe et al., 2011). All mice were maintained on a NMRI outbred background. Embryos for expression analysis of genes encoding FGF signaling components as well as for loss-of-function experiments were obtained from NMRI mice; embryos for phenotype analysis were generated by mating *Pax2-cre/+;Fgfr1*$^{fl/+}$;*Fgfr2*$^{fl/+}$ males with *Fgfr1*$^{fl/fl}$;*Fgfr2*$^{fl/fl}$ females. *Cre*-negative littermates were used as controls. For timed pregnancies, vaginal plugs detected in the morning after mating were designated as embryonic day (E) 0.5 at noon. Urogenital systems and embryos were dissected in PBS, fixed in 4% paraformaldehyde (PFA) in PBS and stored in methanol at −20°C. For genotyping by PCR, genomic DNA prepared from yolk sacs or ear clip biopsies was used.

Mice were housed in rooms with controlled light and temperature. The experiments were carried out in accordance with the German Animal Welfare Legislation and approved by the local Institutional Animal Care and

Development (2022) 149, dev200021. doi:10.1242/dev.200021

Research Advisory Committee and permitted by the Lower Saxony State Office for Consumer Protection and Food Safety (AZ 33.12-42502-04-13/1356, AZ42500/1H).

Organ cultures

Ureters for explant cultures were dissected in L-15 Leibovitz medium (F1315, Biochrom), explanted on 0.4 µm polyester membrane Transwell supports (657610, Greiner Bio-One) and cultured at the air-liquid interface with DMEM/F12 (21331020, Gibco) supplemented with 1×penicillin/streptomycin (15140122, Gibco), 1×NEAA (11140035, Gibco), 1×pyruvate (11360070, Gibco) and 1×glutamax (35050038, Gibco) in a humidified incubator with 5% CO_2 at 37°C. Pathway activating components were dissolved as follows: recombinant human BMP4 (100 ng/µl in 4 mM HCl/0.1% BSA; PHP171, Abd Serotec), purmorphamine (2 µM in DMSO; 540220, Merck), retinoic acid (RA; 1 µM in DMSO; R2625, Sigma-Aldrich), 6-bromoindirubin-3′-oxime (BIO, 5 µM in DMSO; S7198, Selleckchem), cyclopamine (1-10 µM in DMF; S11465, Selleckchem) and NOG (2.5-10 µg/ml in double distilled H_2O; Z0320525, Genescript). Medium containing DMSO or components was refreshed every second day.

Morphological, histological and immunohistochemical analyses

Kidney size and ureter length was measured using the segmented line tool from Image J (Schindelin et al., 2012). Ureter length was measured from the pelvic region to the bladder insertion site. Kidney size was calculated by measuring the cranial to caudal length and the medial to lateral width.

Embryos, urogenital systems and ureter explants were fixed in 4% PFA, embedded in paraffin wax and sectioned at 5 µm. Sections were stained with Hematoxylin and Eosin according to standard procedures.

Immunofluorescence staining as well as immunohistochemistry was performed on 5 µm paraffin wax-embedded sections using the following primary antibodies and dilutions: monoclonal mouse-anti-BrdU (1:250; WH0007348M2, Sigma-Aldrich) polyclonal rabbit-anti-KRT5 (1:200; PRB-160P, BioLegend), polyclonal rabbit-anti-ΔNP63 (1:100; clone Poly6190, 619001, BioLegend), monoclonal mouse-anti-P63 (1:200; clone 4A4, ab735, Abcam), monoclonal mouse-anti-UPK1B (1:200; clone1E1, WH0007348M2, Sigma-Aldrich), polyclonal rabbit-anti-TAGLN (1:200; ab14106, Abcam), polyclonal mouse-anti-ACTA2 (1:200; A5228; clone 1A4; Merck), polyclonal rabbit-anti-ALDH1A2 (1:200; ab75674, Abcam), polyclonal rabbit-anti-CDH1 (1:200, a kind gift from Dr R. Kemler, MPI, Freiburg, Germany), monoclonal rabbit-anti-P-SMAD1/5/9 (1:100; 13280, Cell Signaling), monoclonal rabbit-anti-P-P38 MAPK (1:100; 4631, Cell Signaling), monoclonal rabbit-anti-P-AKT (1:100; 9271, Cell Signaling) and monoclonal rabbit-anti-P-ERK1/2 (1:100; 9102, Cell Signaling). Fluorescent staining was performed using the following secondary antibodies: biotinylated goat-anti-rabbit IgG (1:200; 111065033, Dianova), biotinylated goat-anti-mouse IgG (1:200; 115-065-166, Jackson ImmunoResearch), Alexa488-conjugated goat-anti-rabbit IgG (1:400; A11034, Molecular Probes) and Alexa555-conjugated goat-anti-mouse IgG (1:400; A21422, Molecular Probes). The signals of ΔNP63, P63 and ALDH1A2 were amplified using the Tyramide Signal Amplification system (NEL702001KT, Perkin Elmer). For co-staining with primary antibodies of the same host (ΔNP63 and KRT5 or CDH1), the staining was performed sequentially and the epitope of the first antibody was blocked with goat-anti-rabbit FAB fragment (1:50; 111007003, Dianova). The signals of P-SMAD1/5/9, P-AKT, P-ERK1/2 and P-P38 were amplified using the DAB amplification system (#NEL938001EA, Perkin Elmer). For antigen retrieval, paraffin wax-embedded sections were deparaffinized, pressure-cooked for 15 min in antigen unmasking solution (H3300, Vector Laboratories), treated with 3% H_2O_2/PBS for blocking of endogenous peroxidases, washed in PBST (0.05% Tween-20 in PBS) and incubated in TNB Blocking Buffer (NEL702001KT, Perkin Elmer). Sections were then incubated with primary antibodies at 4°C overnight. Nuclei were stained with 4′,6-diamidino-2-phenylindole (DAPI, 6335.1, Carl Roth).

Cellular assays

In vivo cell proliferation rates of E12.5 and E14.5 ureters were assayed by detection of incorporated 5-bromo-2′-deoxyuridine (BrdU) on 5 µm sections (Bussen et al., 2004). Five to 25 sections of each specimen were analyzed. The BrdU labeling index was defined as the number of BrdU-positive nuclei relative to the total number of nuclei detected by DAPI counterstaining in histologically defined compartments of the ureter. Apoptosis in tissues was assessed by the terminal deoxynucleotidyl transferase dUTP nick end labeling (TUNEL) assay using ApopTag Plus Fluorescein In Situ Apoptosis Detection Kit (S7111; Merck) on 5 µm paraffin wax-embedded sections.

In situ hybridization analysis

Section *in situ* hybridization on 10 µm paraffin wax-embedded sections using digoxigenin-labeled antisense riboprobes was performed as previously described (Moorman et al., 2001).

Reverse transcription-polymerase chain reaction (RT-PCR)

RNA extraction and RT-PCR analysis for gene expression was performed on pools of 20 ureters each of E14.5 control and *Pax2-cre/+;Fgfr1*$^{fl/+}$*;Fgfr2*$^{fl/fl}$ embryos. We isolated total RNA using TRIzol (#15596-018, Thermo Fisher Scientific) and synthesized cDNA from total RNA applying RevertAid H Minus reverse transcriptase (#EP0452, Thermo Fisher Scientific) as described previously (Thiesler et al., 2021). The NCBI tool Primer3 version4.1 was used to design specific primers (Table S11) (Untergasser et al., 2012; Werneburg et al., 2015). RT-quantitative (q)PCR of mouse genes was performed in 10 µl 1:2 diluted BIO SyGreen Lo-ROX mix (PCR Biosystems) with 400 nM primers and 1 ng/µl cDNA applying a QuantStudio3 PCR system fluorometric thermal cycler (Thermo Fisher Scientific). Data were processed by QuantStudio data analysis software (version 1.5.1, Thermo Fisher Scientific) using the comparative threshold cycle ($\Delta\Delta C_T$) method.

Microarray analysis

Two independent pools each of control and mutant ureters were used for microarray analysis. Pool sizes were as follows: 50 ureters each from male and female E13.5 *cre*-negative and *Pax2-cre/+;Fgfr1*$^{fl/(+\ or\ fl)}$*;Fgfr2*$^{fl/fl}$ embryos. Total RNA from each pool was extracted using peqGOLD RNApure (30-1010, VWR international) and subsequently processed by the Research Core Unit Transcriptomics of Hannover Medical School. Agilent whole Mouse Genome Oligo v2 (4×44K) Microarrays (G4846A; Agilent Technologies) were used for transcriptome analysis. Normalized expression data were filtered using Microsoft Excel. Functional enrichment analysis for up- and downregulated genes was performed with DAVID 6.8 web-software (david.ncifcrf.gov), and terms were selected based on *P*-value. Microarray data have been deposited in GEO under accession number GSE178093.

Statistics

Statistical analysis was performed using the unpaired, two-tailed Student's *t*-test (GraphPad Prism version 7.03 and Microsoft Excel). Values are indicated as mean±s.d. $P<0.05$ was considered significant.

Image documentation

Sections were photographed using a DM5000 microscope (Leica Camera) with a Leica DFC300FX digital camera or a Leica DMI6000B microscope with a Leica DFC350FX digital camera. All images were then processed using Adobe Photoshop CS4.

Acknowledgements

We thank Rolf Kemler for the anti-CDH1 antiserum. Microarray data used in this publication were generated by the Research Core Unit Genomics (RCUG) at Hannover Medical School. Nurullah Aydoğdu was supported by the Hannover Biomedical Research School (HBRS) and the MD/PhD program Molecular Medicine.

Competing interests

The authors declare no competing or financial interests.

Author contributions

Conceptualization: M.M., L.D., A.K.; Methodology: M.M., L.D., H.T., M.-O.T.; Software: M.-O.T.; Validation: L.D.; Formal analysis: M.M., L.D., N.A., H.T., P.Z.,

M.-O.T.; Investigation: M.M., L.D., C.R., N.A., H.T., P.Z.; Data curation: M.-O.T.; Writing - original draft: M.M., L.D., H.T., A.K.; Writing - review & editing: M.M., L.D., C.R., N.A., H.T., P.Z., H.H., A.K.; Visualization: L.D.; Supervision: C.R., H.H., A.K.; Project administration: A.K.; Funding acquisition: A.K.

Funding
This work was supported by a grant from by the Deutsche Forschungsgemeinschaft (German Research Foundation) (DFG KI 728/12-1 to A.K.).

Data availability
Microarray data have been deposited in GEO under accession number GSE178093.

Peer review history
The peer review history is available online at https://journals.biologists.com/dev/article-lookup/doi/10.1242/dev.200021.

References

Bagai, S., Rubio, E., Cheng, J. F., Sweet, R., Thomas, R., Fuchs, E., Grady, R., Mitchell, M. and Bassuk, J. A. (2002). Fibroblast growth factor-10 is a mitogen for urothelial cells. *J. Biol. Chem.* **277**, 23828-23837. doi:10.1074/jbc.M201658200

Balsara, Z. R. and Li, X. (2017). Sleeping beauty: awakening urothelium from its slumber. *Am. J. Physiol. Renal Physiol.* **312**, F732-F743. doi:10.1152/ajprenal.00337.2016

Bel-Vialar, S., Itasaki, N. and Krumlauf, R. (2002). Initiating Hox gene expression: in the early chick neural tube differential sensitivity to FGF and RA signaling subdivides the HoxB genes in two distinct groups. *Development* **129**, 5103-5115. doi:10.1242/dev.129.22.5103

Bohnenpoll, T. and Kispert, A. (2014). Ureter growth and differentiation. *Semin. Cell Dev. Biol.* **36**, 21-30. doi:10.1016/j.semcdb.2014.07.014

Bohnenpoll, T., Feraric, S., Nattkemper, M., Weiss, A.-C., Rudat, C., Meuser, M., Trowe, M.-O. and Kispert, A. (2017a). Diversification of cell lineages in ureter development. *J. Am. Soc. Nephrol.* **28**, 1792-1801. doi:10.1681/ASN.2016080849

Bohnenpoll, T., Weiss, A.-C., Labuhn, M., Lüdtke, T. H., Trowe, M.-O. and Kispert, A. (2017b). Retinoic acid signaling maintains epithelial and mesenchymal progenitors in the developing mouse ureter. *Sci. Rep.* **7**, 14803. doi:10.1038/s41598-017-14790-2

Bohnenpoll, T., Wittern, A. B., Mamo, T. M., Weiss, A.-C., Rudat, C., Kleppa, M.-J., Schuster-Gossler, K., Wojahn, I., Lüdtke, T. H.-W., Trowe, M.-O. et al. (2017c). A SHH-FOXF1-BMP4 signaling axis regulating growth and differentiation of epithelial and mesenchymal tissues in ureter development. *PLoS Genet.* **13**, e1006951. doi:10.1371/journal.pgen.1006951

Bussen, M., Petry, M., Schuster-Gossler, K., Leitges, M., Gossler, A. and Kispert, A. (2004). The T-box transcription factor Tbx18 maintains the separation of anterior and posterior somite compartments. *Genes Dev.* **18**, 1209-1221. doi:10.1101/gad.300104

Cancilla, B., Ford-Perriss, M. D. and Bertram, J. F. (1999). Expression and localization of fibroblast growth factors and fibroblast growth factor receptors in the developing rat kidney. *Kidney Int.* **56**, 2025-2039. doi:10.1046/j.1523-1755.1999.00781.x

Chen, J. K., Taipale, J., Cooper, M. K. and Beachy, P. A. (2002). Inhibition of Hedgehog signaling by direct binding of cyclopamine to Smoothened. *Genes Dev.* **16**, 2743-2748. doi:10.1101/gad.1025302

Cheng, W., Jacobs, W. B., Zhang, J. J., Moro, A., Park, J.-H., Kushida, M., Qiu, W., Mills, A. A. and Kim, P. C. W. (2006). DeltaNp63 plays an anti-apoptotic role in ventral bladder development. *Development* **133**, 4783-4792. doi:10.1242/dev.02621

Cooper, M. K., Porter, J. A., Young, K. E. and Beachy, P. A. (1998). Teratogen-mediated inhibition of target tissue response to Shh signaling. *Science* **280**, 1603-1607. doi:10.1126/science.280.5369.1603

Cunha, G. R., Young, P., Higgins, S. J. and Cooke, P. S. (1991). Neonatal seminal vesicle mesenchyme induces a new morphological and functional phenotype in the epithelia of adult ureter and ductus deferens. *Development* **111**, 145-158. doi:10.1242/dev.111.1.145

Dalghi, M. G., Montalbetti, N., Carattino, M. D. and Apodaca, G. (2020). The Urothelium: Life in a Liquid Environment. *Physiol. Rev.* **100**, 1621-1705. doi:10.1152/physrev.00041.2019

Dudley, A. T., Godin, R. E. and Robertson, E. J. (1999). Interaction between FGF and BMP signaling pathways regulates development of metanephric mesenchyme. *Genes Dev.* **13**, 1601-1613. doi:10.1101/gad.13.12.1601

Gandhi, D., Molotkov, A., Batourina, E., Schneider, K., Dan, H., Reiley, M., Laufer, E., Metzger, D., Liang, F., Liao, Y. et al. (2013). Retinoid signaling in progenitors controls specification and regeneration of the urothelium. *Dev. Cell* **26**, 469-482. doi:10.1016/j.devcel.2013.07.017

Girshovich, A., Vinsonneau, C., Perez, J., Vandermeersch, S., Verpont, M.-C., Placier, S., Jouanneau, C., Letavernier, E., Baud, L. and Haymann, J.-P. (2012). Ureteral obstruction promotes proliferation and differentiation of the renal urothelium into a bladder-like phenotype. *Kidney Int.* **82**, 428-435. doi:10.1038/ki.2012.110

Guo, J., Zhang, T. and Dou, D. (2019). Knockdown of HOXB8 inhibits tumor growth and metastasis by the inactivation of Wnt/beta-catenin signaling pathway in osteosarcoma. *Eur. J. Pharmacol.* **854**, 22-27. doi:10.1016/j.ejphar.2019.04.004

Hanafusa, H., Torii, S., Yasunaga, T. and Nishida, E. (2002). Sprouty1 and Sprouty2 provide a control mechanism for the Ras/MAPK signalling pathway. *Nat. Cell Biol.* **4**, 850-858. doi:10.1038/ncb867

Hoch, R. V. and Soriano, P. (2006). Context-specific requirements for Fgfr1 signaling through Frs2 and Frs3 during mouse development. *Development* **133**, 663-673. doi:10.1242/dev.02242

Hollnagel, A., Oehlmann, V., Heymer, J., Rüther, U. and Nordheim, A. (1999). Id genes are direct targets of bone morphogenetic protein induction in embryonic stem cells. *J. Biol. Chem.* **274**, 19838-19845. doi:10.1074/jbc.274.28.19838

Huang, J., Dattilo, L. K., Rajagopal, R., Liu, Y., Kaartinen, V., Mishina, Y., Deng, C.-X., Umans, L., Zwijsen, A., Roberts, A. B. et al. (2009). FGF-regulated BMP signaling is required for eyelid closure and to specify conjunctival epithelial cell fate. *Development* **136**, 1741-1750. doi:10.1242/dev.034082

Igarashi, M., Finch, P. W. and Aaronson, S. A. (1998). Characterization of recombinant human fibroblast growth factor (FGF)-10 reveals functional similarities with keratinocyte growth factor (FGF-7). *J. Biol. Chem.* **273**, 13230-13235. doi:10.1074/jbc.273.21.13230

Jans, D. A. (1994). Nuclear signaling pathways for polypeptide ligands and their membrane receptors? *FASEB J.* **8**, 841-847. doi:10.1096/fasebj.8.11.8070633

Kelly, R. G., Brown, N. A. and Buckingham, M. E. (2001). The arterial pole of the mouse heart forms from Fgf10-expressing cells in pharyngeal mesoderm. *Dev. Cell.* **1**, 435-440. doi:10.1016/S1534-5807(01)00040-5

Kuschert, S., Rowitch, D. H., Haenig, B., McMahon, A. P. and Kispert, A. (2001). Characterization of Pax-2 regulatory sequences that direct transgene expression in the Wolffian duct and its derivatives. *Dev. Biol.* **229**, 128-140. doi:10.1006/dbio.2000.9971

Li, X. J., Hu, B. Y., Jones, S. A., Zhang, Y. S., Lavaute, T., Du, Z. W. and Zhang, S. C. (2008). Directed differentiation of ventral spinal progenitors and motor neurons from human embryonic stem cells by small molecules. *Stem Cells* **26**, 886-893. doi:10.1634/stemcells.2007-0620

Liu, K. J. and Harland, R. M. (2003). Cloning and characterization of Xenopus Id4 reveals differing roles for Id genes. *Dev. Biol.* **264**, 339-351. doi:10.1016/j.ydbio.2003.08.017

Mamo, T. M., Wittern, A. B., Kleppa, M.-J., Bohnenpoll, T., Weiss, A.-C. and Kispert, A. (2017). BMP4 uses several different effector pathways to regulate proliferation and differentiation in the epithelial and mesenchymal tissue compartments of the developing mouse ureter. *Hum. Mol. Genet.* **26**, 3553-3563. doi:10.1093/hmg/ddx242

Mendelsohn, C., Ruberte, E., LeMeur, M., Morriss-Kay, G. and Chambon, P. (1991). Developmental analysis of the retinoic acid-inducible RAR-beta 2 promoter in transgenic animals. *Development* **113**, 723-734. doi:10.1242/dev.113.3.723

Mills, C. G., Lawrence, M. L., Munro, D. A. D., Elhendawi, M., Mullins, J. J. and Davies, J. A. (2017). Asymmetric BMP4 signalling improves the realism of kidney organoids. *Sci. Rep.* **7**, 14824. doi:10.1038/s41598-017-14809-8

Mjaatvedt, C. H., Nakaoka, T., Moreno-Rodriguez, R., Norris, R. A., Kern, M. J., Eisenberg, C. A., Turner, D. and Markwald, R. R. (2001). The outflow tract of the heart is recruited from a novel heart-forming field. *Dev. Biol.* **238**, 97-109. doi:10.1006/dbio.2001.0409

Moorman, A. F., Houweling, A. C., de Boer, P. A. J. and Christoffels, V. M. (2001). Sensitive nonradioactive detection of mRNA in tissue sections: novel application of the whole-mount in situ hybridization protocol. *J. Histochem. Cytochem.* **49**, 1-8. doi:10.1177/002215540104900101

Narla, S. T., Bushnell, D. S., Schaefer, C. M., Nouraie, M., Tometich, J. T., Hand, T. W. and Bates, C. M. (2020). Loss of fibroblast growth factor receptor 2 (FGFR2) leads to defective bladder urothelial regeneration after Cyclophosphamide injury. *Am J. Pathol.* **191**, 631-651. doi:10.1016/j.ajpath.2020.12.011

Ornitz, D. M. and Itoh, N. (2015). The fibroblast growth factor signaling pathway. *Wiley Interdiscip. Rev. Dev. Biol.* **4**, 215-266. doi:10.1002/wdev.176

Park, E. J., Watanabe, Y., Smyth, G., Miyagawa-Tomita, S., Meyers, E., Klingensmith, J., Camenisch, T., Buckingham, M. and Moon, A. M. (2008). An FGF autocrine loop initiated in second heart field mesoderm regulates morphogenesis at the arterial pole of the heart. *Development* **135**, 3559-3610. doi:10.1242/dev.025437

Peters, K. G., Werner, S., Chen, G. and Williams, L. T. (1992). Two FGF receptor genes are differentially expressed in epithelial and mesenchymal tissues during limb formation and organogenesis in the mouse. *Development* **114**, 233-243. doi:10.1242/dev.114.1.233

Petiot, A., Perriton, C. L., Dickson, C. and Cohn, M. J. (2005). Development of the mammalian urethra is controlled by Fgfr2-IIIb. *Development* **132**, 2441-2450. doi:10.1242/dev.01778

Pignon, J. C., Grisanzio, C., Geng, Y., Song, J., Shivdasani, R. A. and Signoretti, S. (2013). p63-expressing cells are the stem cells of developing prostate, bladder, and colorectal epithelia. *Proc. Natl. Acad. Sci. USA* **110**, 8105-8110. doi:10.1073/pnas.1221216110

Revest, J.-M., Spencer-Dene, B., Kerr, K., De Moerlooze, L., Rosewell, I. and Dickson, C. (2001). Fibroblast growth factor receptor 2-IIIb acts upstream of Shh and Fgf4 and is required for limb bud maintenance but not for the induction of Fgf8, Fgf10, Msx1, or Bmp4. *Dev. Biol.* **231**, 47-62. doi:10.1006/dbio.2000.0144

Rice, R., Spencer-Dene, B., Connor, E. C., Gritli-Linde, A., McMahon, A. P., Dickson, C., Thesleff, I. and Rice, D. P. C. (2004). Disruption of Fgf10/Fgfr2b-coordinated epithelial-mesenchymal interactions causes cleft palate. *J. Clin. Invest.* **113**, 1692-1700. doi:10.1172/JCI20384

Sato, N., Meijer, L., Skaltsounis, L., Greengard, P. and Brivanlou, A. H. (2004). Maintenance of pluripotency in human and mouse embryonic stem cells through activation of Wnt signaling by a pharmacological GSK-3-specific inhibitor. *Nat. Med.* **10**, 55-63. doi:10.1038/nm979

Schindelin, J., Arganda-Carreras, I., Frise, E., Kaynig, V., Longair, M., Pietzsch, T., Preibisch, S., Rueden, C., Saalfeld, S., Schmid, B. et al. (2012). Fiji: an open-source platform for biological-image analysis. *Nat. Methods* **9**, 676-682. doi:10.1038/nmeth.2019

Sims-Lucas, S., Cusack, B., Eswarakumar, V. P., Zhang, J., Wang, F. and Bates, C. M. (2011). Independent roles of Fgfr2 and Frs2alpha in ureteric epithelium. *Development* **138**, 1275-1280. doi:10.1242/dev.062158

Tash, J. A., David, S. G., Vaughan, E. E. and Herzlinger, D. A. (2001). Fibroblast growth factor-7 regulates stratification of the bladder urothelium. *J. Urol.* **166**, 2536-2541. doi:10.1016/S0022-5347(05)65630-3

Terakawa, J., Rocchi, A., Serna, V. A., Bottinger, E. P., Graff, J. M. and Kurita, T. (2016). FGFR2IIIb-MAPK activity is required for epithelial cell fate decision in the lower mullerian duct. *Mol. Endocrinol.* **30**, 783-795. doi:10.1210/me.2016-1027

Thiesler, H., Beimdiek, J. and Hildebrandt, H. (2021). Polysialic acid and Siglec-E orchestrate negative feedback regulation of microglia activation. *Cell. Mol. Life Sci.* **78**, 1637-1653. doi:10.1007/s00018-020-03601-z

Trowe, M.-O., Airik, R., Weiss, A.-C., Farin, H. F., Foik, A. B., Bettenhausen, E., Schuster-Gossler, K., Taketo, M. M. and Kispert, A. (2012). Canonical Wnt signaling regulates smooth muscle precursor development in the mouse ureter. *Development* **139**, 3099-3108. doi:10.1242/dev.077388

Trowe, M.-O., Maier, H., Petry, M., Schweizer, M., Schuster-Gossler, K. and Kispert, A. (2011). Impaired stria vascularis integrity upon loss of E-cadherin in basal cells. *Dev. Biol.* **359**, 95-107. doi:10.1016/j.ydbio.2011.08.030

Untergasser, A., Cutcutache, I., Koressaar, T., Ye, J., Faircloth, B. C., Remm, M. and Rozen, S. G. (2012). Primer3-new capabilities and interfaces. *Nucleic Acids Res.* **40**, e115. doi:10.1093/nar/gks596

Walker, K. A., Sims-Lucas, S. and Bates, C. M. (2016). Fibroblast growth factor receptor signaling in kidney and lower urinary tract development. *Pediatr. Nephrol.* **31**, 885-895. doi:10.1007/s00467-015-3151-1

Wang, G. J., Brenner-Anantharam, A., Vaughan, E. D. and Herzlinger, D. (2009). Antagonism of BMP4 signaling disrupts smooth muscle investment of the ureter and ureteropelvic junction. *J. Urol.* **181**, 401-407. doi:10.1016/j.juro.2008.08.117

Wang, C., Ross, W. T. and Mysorekar, I. U. (2017). Urothelial generation and regeneration in development, injury, and cancer. *Dev. Dyn.* **246**, 336-343. doi:10.1002/dvdy.24487

Wang, T., Lin, F., Sun, X., Jiang, L., Mao, R., Zhou, S., Shang, W., Bi, R., Lu, F. and Li, S. (2019). HOXB8 enhances the proliferation and metastasis of colorectal cancer cells by promoting EMT via STAT3 activation. *Cancer Cell Int.* **19**, 3. doi:10.1186/s12935-018-0717-6

Weiss, R. M., Guo, S., Shan, A., Shi, H., Romano, R.-A., Sinha, S., Cantley, L. G. and Guo, J.-K. (2013). Brg1 determines urothelial cell fate during ureter development. *J. Am. Soc. Nephrol.* **24**, 618-626. doi:10.1681/ASN.2012090902

Weiss, A. C., Bohnenpoll, T., Kurz, J., Blank, P., Airik, R., Ludtke, T. H., Kleppa, M. J., Deuper, L., Kaiser, M., Mamo, T. M. et al. (2019). Delayed onset of smooth muscle cell differentiation leads to hydroureter formation in mice with conditional loss of the zinc finger transcription factor gene Gata2 in the ureteric mesenchyme. *J. Pathol.* **248**, 452-463. doi:10.1002/path.5270

Werneburg, S., Buettner, F. F., Mühlenhoff, M. and Hildebrandt, H. (2015). Polysialic acid modification of the synaptic cell adhesion molecule SynCAM 1 in human embryonic stem cell-derived oligodendrocyte precursor cells. *Stem Cell Res.* **14**, 339-346. doi:10.1016/j.scr.2015.03.001

Yamany, T., Van Batavia, J. and Mendelsohn, C. (2014). Formation and regeneration of the urothelium. *Curr. Opin. Organ Transplant.* **19**, 323-330. doi:10.1097/MOT.0000000000000084

Yang, X., Liaw, L., Prudovsky, I., Brooks, P. C., Vary, C., Oxburgh, L. and Friesel, R. (2015). Fibroblast growth factor signaling in the vasculature. *Curr. Atheroscler. Rep.* **17**, 509. doi:10.1007/s11883-015-0509-6

Yu, J., Carroll, T. J. and McMahon, A. P. (2002). Sonic hedgehog regulates proliferation and differentiation of mesenchymal cells in the mouse metanephric kidney. *Development* **129**, 5301-5312. doi:10.1242/dev.129.22.5301

Yu, K., Xu, J., Liu, Z., Sosic, D., Shao, J., Olson, E. N., Towler, D. A. and Ornitz, D. M. (2003). Conditional inactivation of FGF receptor 2 reveals an essential role for FGF signaling in the regulation of osteoblast function and bone growth. *Development* **130**, 3063-3074. doi:10.1242/dev.00491

Zhang, D., Kosman, J., Carmean, N., Grady, R. and Bassuk, J. A. (2006). FGF-10 and its receptor exhibit bidirectional paracrine targeting to urothelial and smooth muscle cells in the lower urinary tract. *Am. J. Physiol. Renal Physiol.* **291**, F481-F494. doi:10.1152/ajprenal.00025.2006

Zhao, H., Kegg, H., Grady, S., Truong, H.-T., Robinson, M. L., Baum, M. and Bates, C. M. (2004). Role of fibroblast growth factor receptors 1 and 2 in the ureteric bud. *Dev. Biol.* **276**, 403-415. doi:10.1016/j.ydbio.2004.09.002

Zimmerman, L. B., De Jesus-Escobar, J. M. and Harland, R. M. (1996). The Spemann organizer signal noggin binds and inactivates bone morphogenetic protein 4. *Cell* **86**, 599-606. doi:10.1016/S0092-8674(00)80133-6

Supplementary Figures

Development: doi:10.1242/dev.200021: Supplementary information

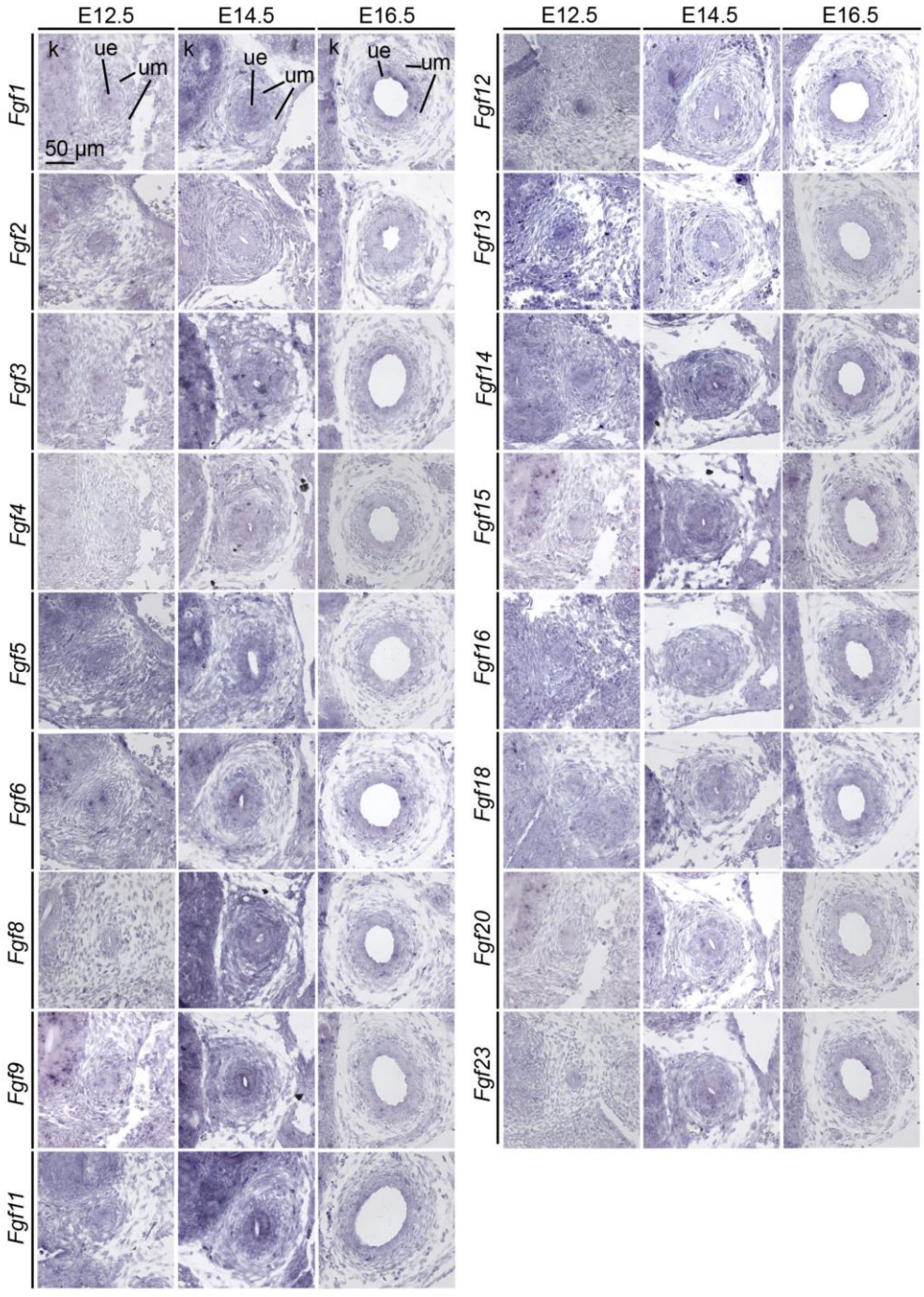

Fig. S1. FGF ligand genes do not show specific expression in the mesenchymal or the epithelial compartment of the early ureter. RNA *in situ* hybridization analysis on transverse sections through the posterior trunk region at the proximal (kidney) level of the ureter for expression of genes encoding FGF ligand genes in wildtype embryos from E12.5 to E16.5. Due to expanded colorimetric detection a homogenous bluish background developed in most cases, but no specific signal was detected in the UE or the UM for any of the probes. n>=3 for all probes and stages. k, kidney; ue, ureteric epithelium; um, ureteric mesenchyme.

Development: doi:10.1242/dev.200021: Supplementary information

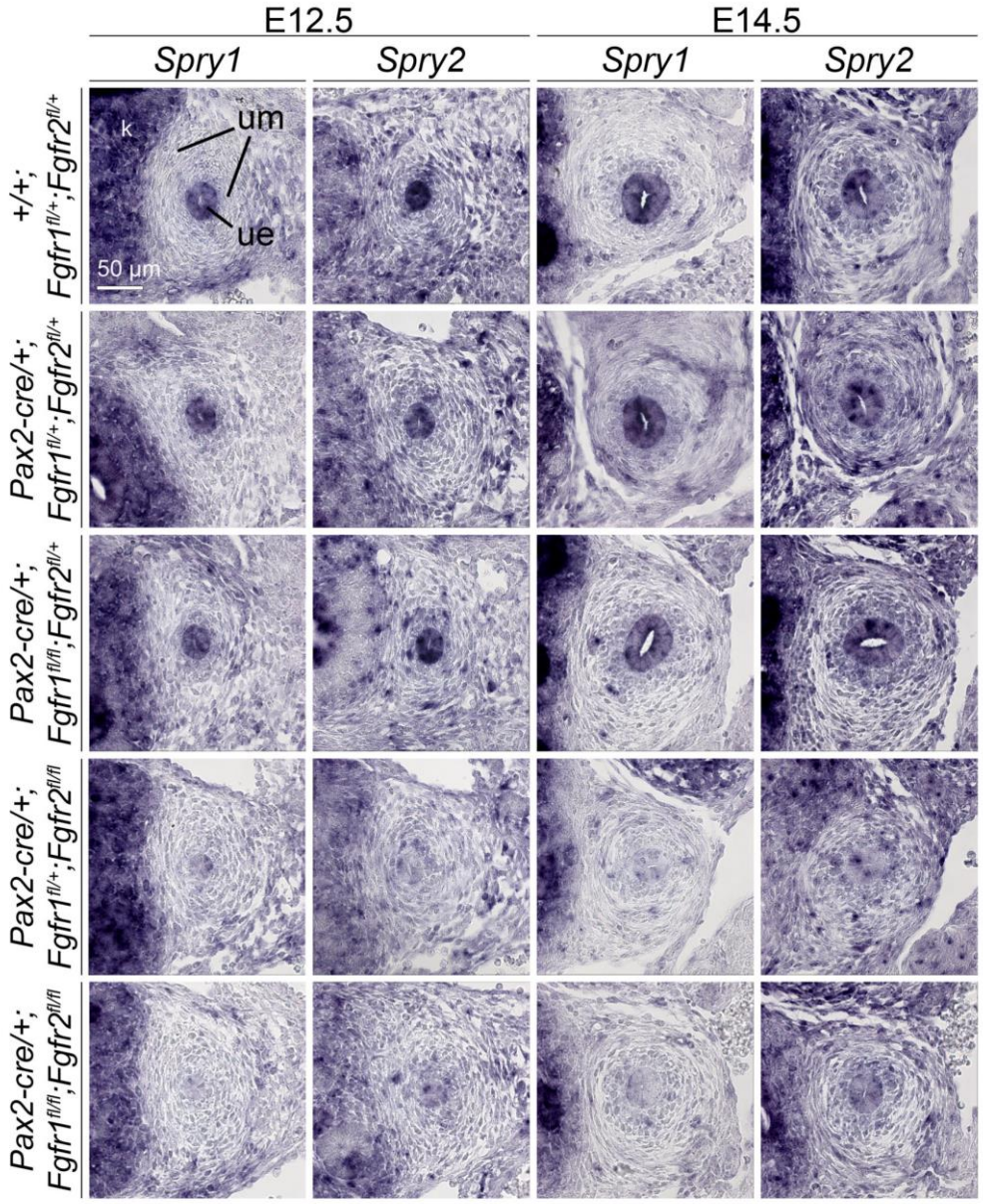

Fig. S2. FGF signaling is specifically diminished in the UE of embryos with conditional loss of *Fgfr2* in this tissue. RNA *in situ* hybridization analysis of expression of transcriptional targets of FGF signaling (*Spry1*, *Spry2*) on transverse sections through the posterior trunk region at the proximal level of the ureter of E12.5 and E14.5 embryos with conditional loss of *Fgfr1* and/or *Fgfr2*. n>=3 for all probes, stages and genotypes. k, kidney; ue, ureteric epithelium; um, ureteric mesenchyme.

Development: doi:10.1242/dev.200021: Supplementary information

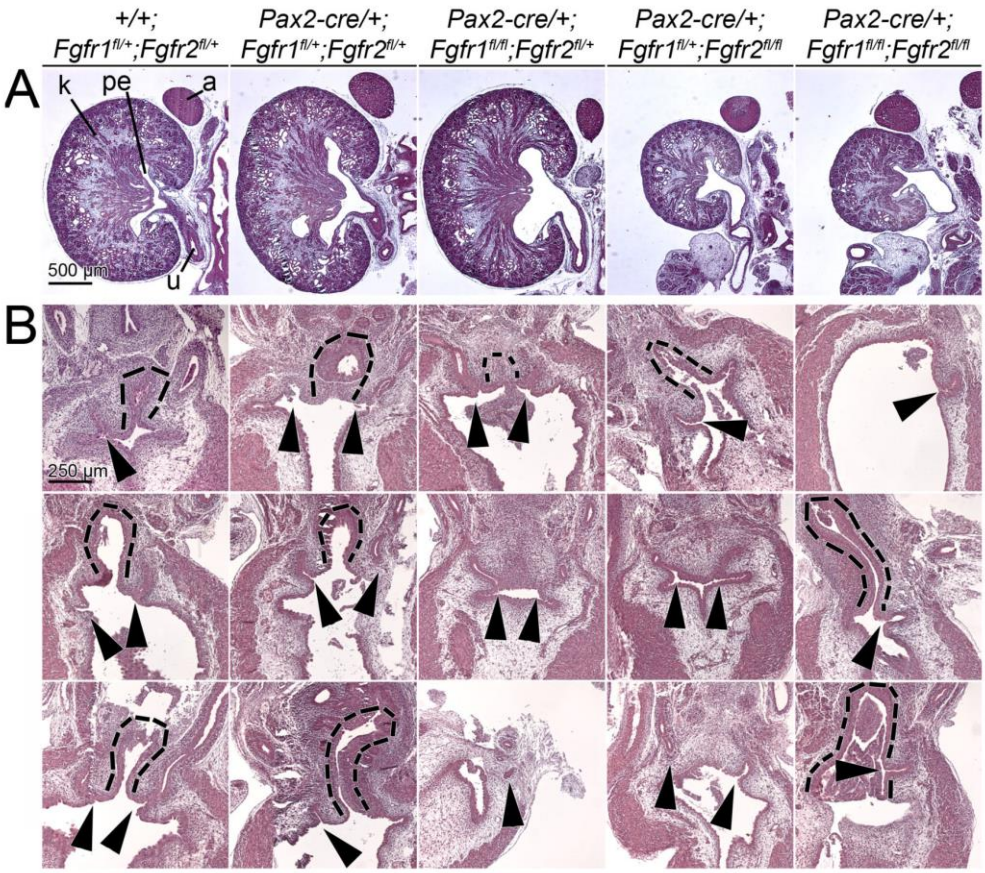

Fig. S3. Histological analysis of the urogenital system of mice with conditional loss of *Fgfr1* and/or *Fgfr2* in the UE. HE staining of sagittal sections of the kidney (A) and the ureter insertion into the bladder (B) at E18.5. (B) Dotted lines mark the urethra; arrowheads mark the ureter insertion. Note the blind ending ureter in the third *Pax2-cre/+;Fgfr1*$^{fl/fl}$*;Fgfr2*$^{fl/+}$ specimen, and the urethral insertion in the third *Pax2-cre/+;Fgfr1*$^{fl/+}$*;Fgfr2*$^{fl/fl}$ specimen. n>=3 for all genotypes. a, adrenal; k, kidney; pe, pelvis; u, ureter.

Development: doi:10.1242/dev.200021: Supplementary information

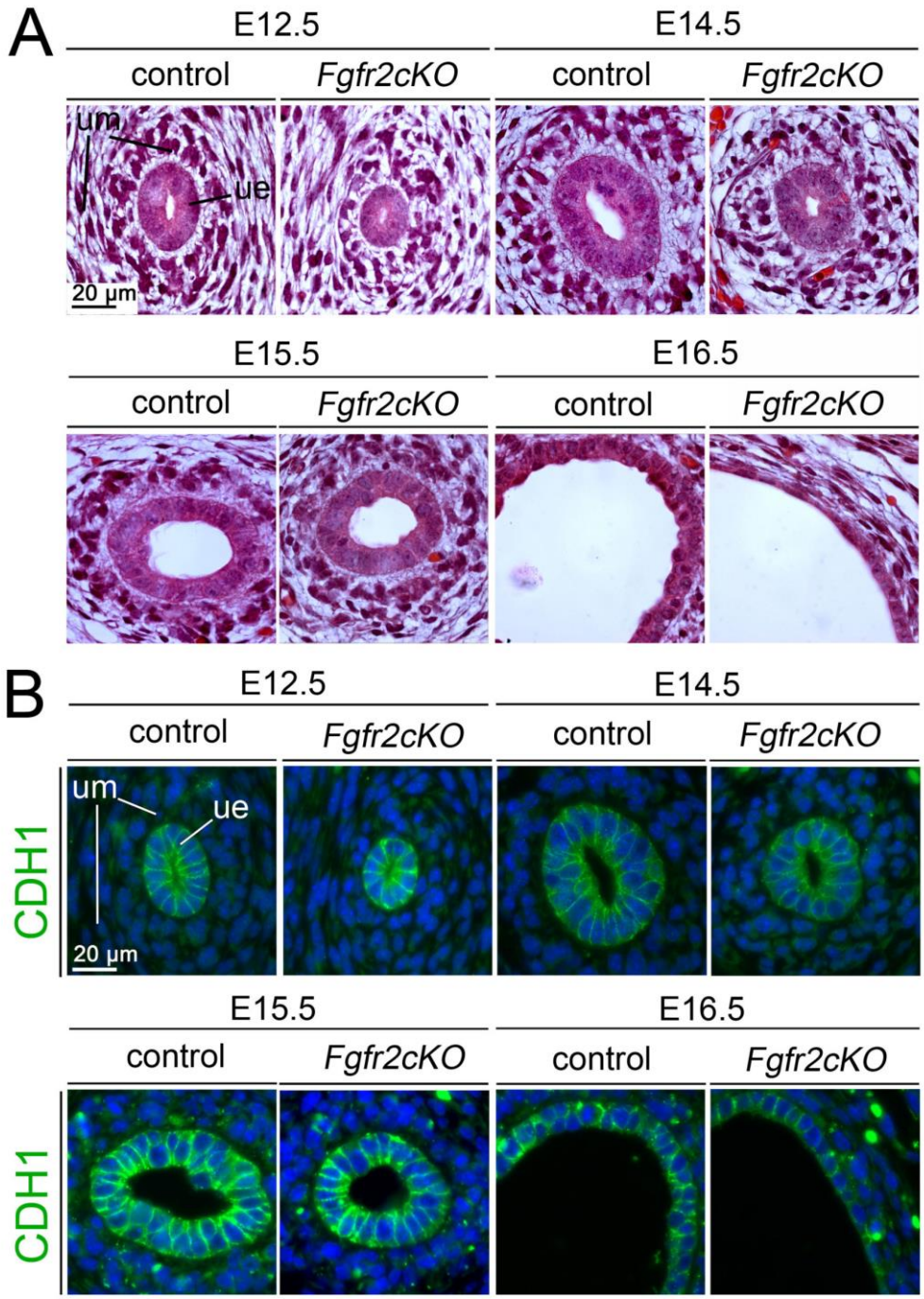

Fig. S4. *Fgfr2cKO* ureters are hypoplastic and exhibit reduced stratification in development. (Higher magnification of images shown in Fig. 3A,B). (A) Hematoxylin and Eosin (HE) staining of transverse sections of the proximal region of the developing ureter at the indicated stages. (B) Analysis of CDH1 expression by immunofluorescence on adjacent sections. Nuclei are counter-stained with DAPI (blue). n>=3, for all probes, assays and genotypes. ue, ureteric epithelium; um, ureteric mesenchyme.

Development: doi:10.1242/dev.200021: Supplementary information

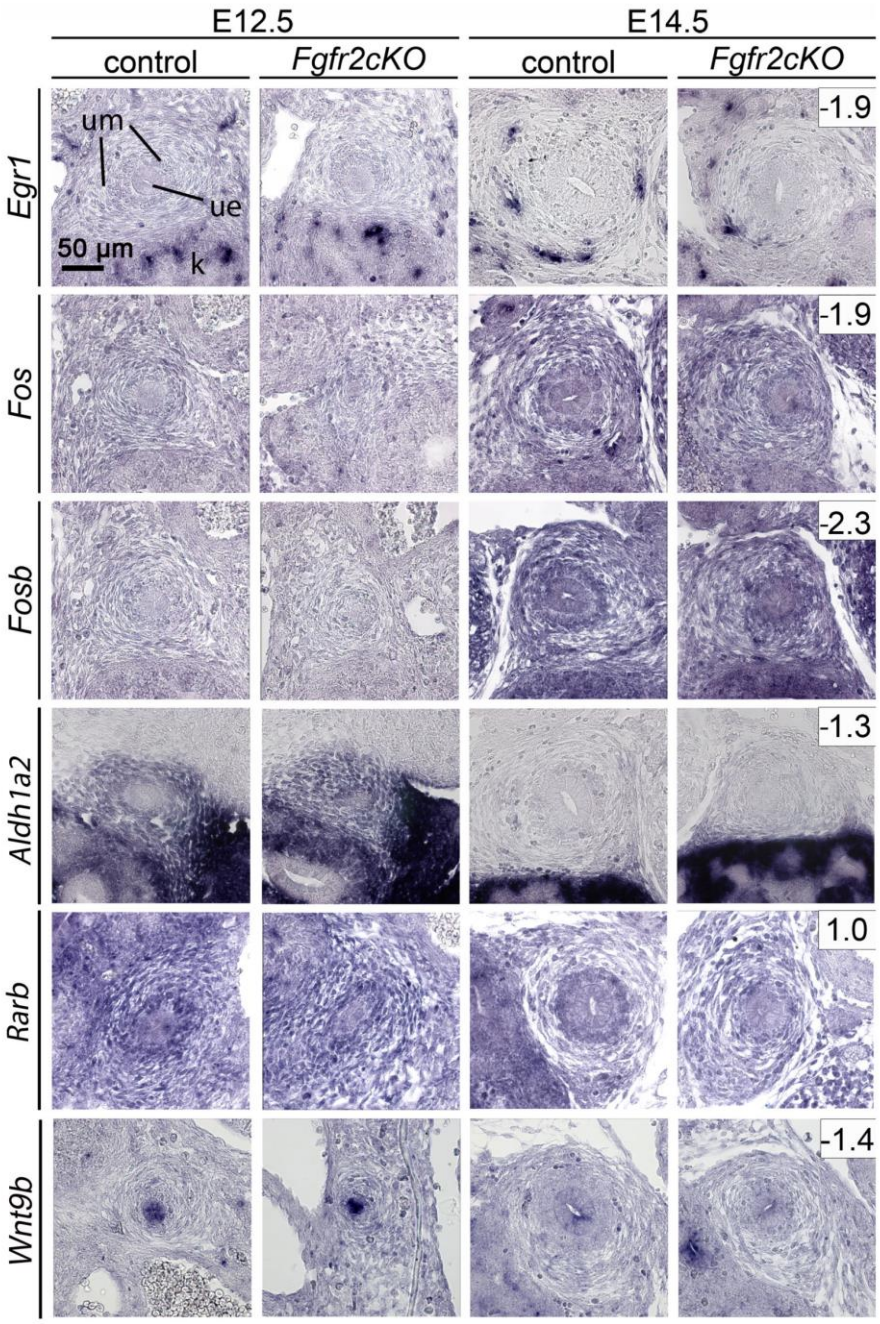

Fig. S5. Expression of immediate early genes, of mesenchymal RA signaling components and of *Wnt9b* is unchanged in *Fgfr2cKO* ureters at E12.5 and E14.5. *In situ* hybridization analysis on transverse sections of the proximal ureter of E12.5 and E14.5 control and *Fgfr2cKO* embryos for expression of immediate early genes (*Egr1, Fos, Fosb)*, of RA signaling components in the UM (*Aldh1a2*, *Rarb*), and of *Wnt9b*. Numbers indicate fold change in the E13.5 microarray analysis. n>=3 for all probes and genotypes k, kidney; ue, ureteric epithelium; um, ureteric mesenchyme.

Development: doi:10.1242/dev.200021: Supplementary information

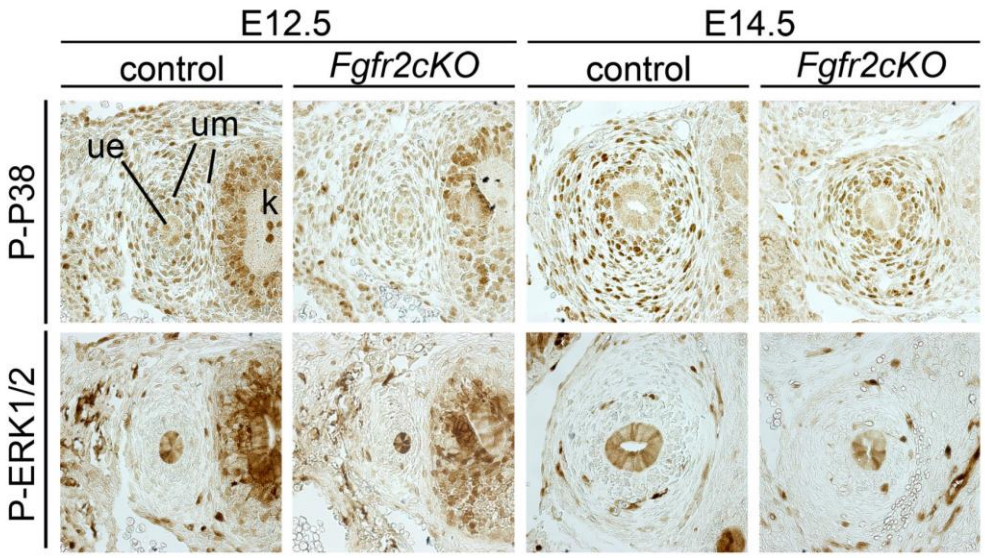

Fig. S6. Phosphorylation of P38 and of ERK1/2 is not changed in *Fgfr2cKO* ureters. Immunohistochemical detection of activated, i.e. phosphorylated forms of cytoplasmic effectors of BMP4 signaling (P-P38, P-ERK1/2) on transverse sections of the proximal ureter of E12.5 and E14.5 control and *Fgfr2cKO* embryos. n>=3 for all probes, genotypes and stages. k, kidney; ue, ureteric epithelium; um, ureteric mesenchyme.

Development: doi:10.1242/dev.200021: Supplementary information

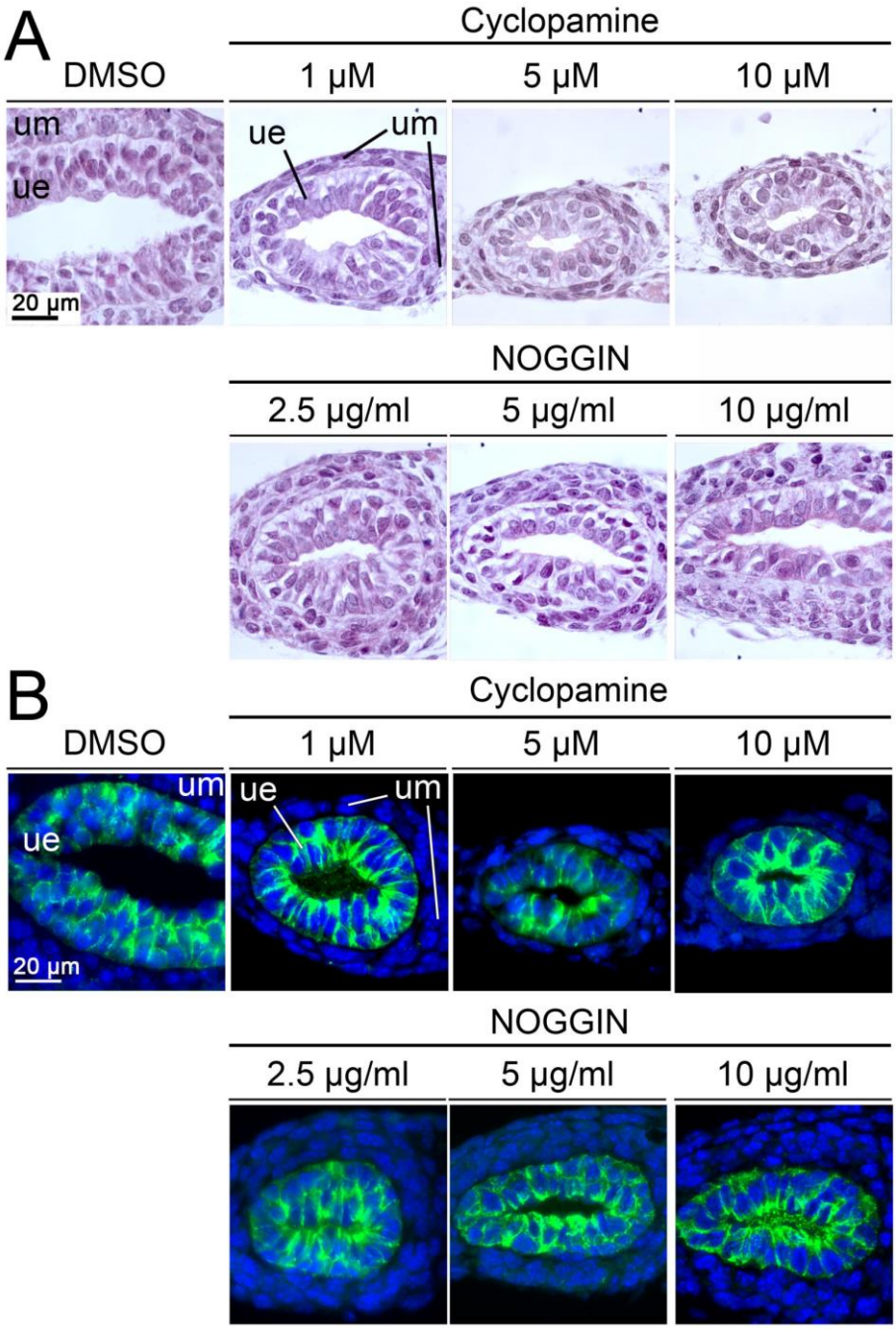

Fig. S7. Inhibition of SHH or BMP4 signaling leads dose-dependently to hypoplastic ureters with reduced stratification. (Higher magnification of images shown in Fig. 6A,B). (A,B) E13.5 wildtype ureters were cultured for 4 days with increasing concentrations of the SHH signaling inhibitor cyclopamine or the BMP4 antagonist NOGGIN, and transverse sections of the proximal region were analyzed by Hematoxylin and Eosin staining (A) and by immunofluorescence for expression of the epithelial marker CDH1. Nuclei are counter-stained with DAPI (blue). n>=3, for all probes, assays and genotypes. ue, ureteric epithelium; um, ureteric mesenchyme.

Development: doi:10.1242/dev.200021: Supplementary information

Table S1. Genotype distribution of embryos obtained from matings of *Pax2-cre/+;Fgfr1fl/;Fgfr2fl/+* males with *Fgfr1fl/fl;Fgfr2fl/fl* females at E12.5, E14.5, E16.5 and E18.5.

Click here to download Table S1

Table S2. A. Distribution of phenotypic changes in urogenital systems of E18.5 embryos obtained from matings of *Pax2-cre/+; Fgfr1fl/;Fgfr2fl/+* males with *Fgfr1fl/fl;Fgfr2fl/fl* females.

Click here to download Table S2

Table S3. Quantification of the BrdU incorporation assay of proximal sections of control and *Fgfr2cKO* ureters at E12.5 and E14.5.

Click here to download Table S3

Table S4. List of genes with increased expression in the microarray of E13.5 ureters of *Fgfr2cKO* and control embryos. Shown are the gene names, the intensity of the two control and mutant ureter samples, the individual and the average fold change (FC).

Click here to download Table S4

Table S5. List of genes with decreased expression in the microarray of E13.5 ureters of *Fgfr2cKO* and control embryos. Shown are the gene names, the intensity of the two control and mutant ureter samples, the individual and the average fold change (FC).

Click here to download Table S5

Development: doi:10.1242/dev.200021: Supplementary information

Table S6. Functional annotation by DAVID for genes with increased expression in the microarray of E13.5 *Fgfr2cKO* ureters.

Click here to download Table S6

Table S7. Functional annotation by DAVID for genes with decreased expression in the microarray of E13.5 *Fgfr2cKO* ureters.

Click here to download Table S7

Table S8. RT-qPCR analysis of gene expression in E13.5 *Fgfr2cKO* ureters (relates to Figure 4H).

Click here to download Table S8

Table S9. Pharmacological rescue experiments in explants of E13.5 *Fgfr2cKO* ureters cultured for 4 days.

Click here to download Table S9

Table S10. Pharmacological inhibition of SHH and BMP4 signaling in explant cultures of E13.5 ureters. E13.5 wildtype ureters were cultured for 4 days with increasing concentrations of the SHH signaling inhibitor cyclopamine or the BMP4 antagonist NOGGIN.

Click here to download Table S10

Table S11. List of primers for RT-qPCR analysis of gene expression in E13.5 *Fgfr2cKO* ureters.

Click here to download Table S11

Supplementary Tables

Genotype	***+/+; Fgfr1$^{fl/+}$; Fgfr2$^{fl/+}$***	***Pax2-cre/+; Fgfr1$^{fl/+}$; Fgfr2$^{fl/+}$***	***Pax2-cre/+; Fgfr1$^{fl/fl}$; Fgfr2$^{fl/+}$***	***Pax2-cre/+; Fgfr1$^{fl/+}$; Fgfr2$^{fl/fl}$***	***Pax2-cre/+; Fgfr1$^{fl/fl}$; Fgfr2$^{fl/fl}$***
expected genotype frequency	50%	12.5%	12.5%	12.5%	12.5%
stages, numbers obtained	obtained numbers (obtained frequency)				
E12.5, n=454	273 (60%)	71 (16%)	24 (5%)	72 (16%)	14 (3%)
E13.5, n=434	270 (62%)	73 (17%)	21 (5%)	59 (14%)	11 (2%)
E14.5, n=354	214 (60%)	56 (16%)	14 (4%)	57 (16%)	13 (4%)
E16.5, n=84	48 (58%)	12 (14%)	6 (7%)	17 (20%)	1 (1%)
E18.5, n=449	271 (60%)	80 (18%)	30 (7%)	54 (12%)	14 (3%)

Table S1: Genotype distribution of embryos obtained from matings of *Pax2-cre/+;Fgfr1$^{fl/+}$;Fgfr2$^{fl/+}$* males with *Fgfr1$^{fl/fl}$;Fgfr2$^{fl/fl}$* females at E12.5, E14.5, E16.5 and E18.5.

Observation	Genotype			control	*Pax2-cre/+; Fgfr1*$^{fl/+}$*; Fgfr2*$^{fl/+}$	*Pax2-cre/+; Fgfr1*$^{fl/fl}$*; Fgfr2*$^{fl/+}$	*Pax2-cre/+; Fgfr1*$^{fl/+}$*; Fgfr2*$^{fl/fl}$	*Pax2-cre/+; Fgfr1*$^{fl/fl}$*; Fgfr2*$^{fl/fl}$
number of specimen analysed				55	32	11	26	8
Sex	female			23 out of 55 (40%)	12 out of 32 (37%)	6 out of 11 (55%)	8 out of 26 (31%)	5 out of 8 (63%)
	male			32 out of 55 (60%)	20 out of 32 (63%)	5 out of 11 (45%)	18 out of 26 (69%)	3 out of 8 (37%)
Ureter anomalies	female	normal ureter		21 out of 23 (90%)	7 out of 12 (58%)	5 out of 7 (84%)	2 out of 8 (25%)	1 out of 5 (20%)
		weak hydroureter	unilateral	2 out of 23 (10%)	3 out of 12 (25%)	1 out of 6 (16%)	2 out of 8 (25%)	2 out of 5 (40%)
			bilateral	0 out of 23 (0%)	0 out of 12 (0%)	0 out of 6 (0%)	0 out of 8 (0%)	1 out of 5 (20%)
		strong hydroureter	unilateral	0 out of 23 (0%)	2 out of 12 (17%)	0 out of 6 (0%)	2 out of 8 (25%)	1 out of 5 (20%)
			bilateral	0 out of 23 (0%)	0 out of 12 (0%)	0 out of 6 (0%)	2 out of 8 (25%)	1 out of 5 (20%)
	male	normal ureter		30 out of 32 (94%)	12 out of 20 (60%)	3 out of 5 (60%)	2 out of 18 (12%)	0 out of 3 (0%)
		weak hydroureter	unilateral	1 out of 32 (3%)	5 out of 20 (25%)	1 out of 5 (20%)	4 out of 18 (22%)	1 out of 3 (33%)
			bilateral	0 out of 32 (0%)	1 out of 20 (5%)	1 out of 5 (20%)	4 out of 18 (22%)	1 out of 3 (33%)
		strong hydroureter	unilateral	1 out of 32 (3%)	1 out of 20 (5%)	0 out of 5 (0%)	0 out of 18 (0%)	1 out of 3 (33%)
			bilateral	0 out of 32 (0%)	1 out of 20 (5%)	0 out of 5 (0%)	8 out of 18 (44%)	0 out of 3 (0%)
kidney/ureter agenesis		unilateral		1 out of 55 (2%)	0 out of 32 (0%)	0 out of 11 (0%)	1 out of 26 (4%)	1 out of 8 (13%)
		bilateral		0 out of 55 (0%)	0 out of 32 (0%)	0 out of 11 (0%)	0 out of 24 (0%)	0 out of 8 (0%)
Epididymal dilatation		unilateral		2 out of 32 (6%)	1 out of 20 (5%)	0 out of 5 (0%)	4 out of 18 (22%)	0 out of 3 (0%)
		bilateral		0 out of 32 (0%)	0 out of 20 (0%)	0 out of 5 (0%)	10 out of 18 (56%)	3 out of 3 (100%)
number of kidneys analysed				74	32	6	18	9
Kidney size		height	mean	2.87 mm (± 0.4)	2.84 mm (± 0.21)	2.65 mm (± 0.24)	2.58 mm (± 0.49)	1.08 mm (± 0.53)
			p-value		0.3931	0.1270	0.0038	2.9 E-17
		width	mean	1.69 mm (± 0.12)	1.68 mm (± 0,11)	1.69 mm (± 0.19)	1.64 mm (± 0.26)	0.93 mm (± 0.31)
			p-value		0.2711	0.7139	0.0914	1.7 E-16
number of ureters analysed				74	32	6	18	8
Ureter length			mean	2.97 mm (± 0.27)	3 mm (± 0.24)	2.81 mm (± 0.38)	3.09 mm (± 0.35)	2.00 mm (± 0.51)
			p-value		0.5503	0.2013	0.1171	8.1 E-5

Table S2A. Distribution of phenotypic changes in urogenital systems of E18.5 embryos obtained from matings of *Pax2cre/+; Fgfr1*$^{fl/+}$*;Fgfr2*$^{fl/+}$ males with *Fgfr1*$^{fl/fl}$*;Fgfr2*$^{fl/fl}$ females.

ink injektion	control	*Pax2-cre/+; Fgfr1fl/+;Fgfr2fl/+*	*Pax2-cre/+; Fgfr1fl/fl;Fgfr2fl/+*	*Pax2-cre/+; Fgfr1fl/+;Fgfr2fl/fl*	*Pax2-cre/+; Fgfr1fl/fl;Fgfr2fl/fl*
number of specimen	36 (100%)	16 (100%)	3 (100%)	9 (100%)	5 (100%)
normal	34 (94%)	16 (100%)	2 (67%)	7 (78%)	2 (40%)
ink did not reach the bladder	2 (6%)	0 (0%)	1 (33%)	2 (22%)	3 (60%)
stenosis	0 (0%)	0 (0%)	0 (0%)	1 (11%)	0 (0%)
distal ending on the urethra	1 (3%)	0 (0%)	0 (0%)	0 (0%)	1 (20%)
blind ending	1 (3%)	0 (0%)	1 (33%)	1 (11%)	0 (0%)
UPJO	0 (0%)	0 (0%)	0 (0%)	0 (0%)	2 (40%)

Table S2B. Analysis of the patency of the ureter and its junctions by ink injections in E18.5 embryos obtained from matings of *Pax2cre/+; Fgfr1*$^{fl/+}$*;Fgfr2*$^{fl/+}$ males with *Fgfr1*$^{fl/fl}$*;Fgfr2*$^{fl/fl}$ females.

E12.5	U		IM		OM	
	Mean	SD	Mean	SD	Mean	SD
Control (n=3)	0.2	0.049	0.247	0.012	0.207	0.017
***Fgfr2cKO* (n=3)**	0.07	0.040	0.233	0.025	0.230	0.028
p-Value	0.0288		0.5438		0.3853	

E14.5	U		IM		OM	
	Mean	SD	Mean	SD	Mean	SD
Control (n=3)	0.217	0.017	0.1867	0.005	0.147	0.012
***Fgfr2cKO* (n=3)**	0.207	0.017	0,197	0.010	0.163	0.005
p-Value	0.5879		0.2739		0.1907	

Table S3. Quantification of the BrdU incorporation assay of proximal sections of control and *Fgfr2cKO* ureters at E12.5 and E14.5. U, urothelium; IM, inner mesenchyme; OM, outer mesenchyme; SD, standard derivation. The statistical significance was calculated by a two-tailed Student's t-test.

	Intensities				Fold change (FC)		
GeneName_RCUT	**control 1**	**mutant 1**	**control 2**	**mutant 2**	**FC 1**	**FC 2**	**avgFC**
Prm1	311	2553	106	2340	8.2	22.1	15.2
S100a8	92	539	117	622	5.9	5.3	5.6
Gm5483	33	158	31	186	4.8	6.1	5.4
S100a9	452	1963	430	2620	4.3	6.1	5.2
Stfa2l1	36	182	31	164	5.0	5.3	5.2
ENSMUST00000085379	132	792	134	503	6.0	3.8	4.9
BC100530	173	845	185	816	4.9	4.4	4.6
Stfa1	133	614	121	517	4.6	4.3	4.4
Stfa3	58	247	66	274	4.3	4.1	4.2
Serpina1a	93	533	114	272	5.7	2.4	4.1
Gm8893	82	482	100	214	5.9	2.1	4.0
Serpina1c	100	537	120	256	5.4	2.1	3.7
Serpina1e	80	413	92	184	5.2	2.0	3.6
Upk3a	87	341	108	322	3.9	3.0	3.4
Afp	650	3215	908	1591	4.9	1.8	3.3
Camp	91	286	83	282	3.1	3.4	3.3
Nefm	68	252	187	511	3.7	2.7	3.2
Serpina6	132	544	119	210	4.1	1.8	3.0
Dhh	139	233	99	416	1.7	4.2	2.9
Alb	86	366	90	139	4.2	1.5	2.9
Serpinf2	42	126	64	118	3.0	1.9	2.5
Apela	723	1769	807	1903	2.4	2.4	2.4
Prmt1	2330	6394	4234	8370	2.7	2.0	2.4
Ms4a7	956	2039	616	1581	2.1	2.6	2.4
Myh8	109	195	99	263	1.8	2.6	2.2
Stfa2	194	449	255	531	2.3	2.1	2.2
C1qa	161	292	137	352	1.8	2.6	2.2
Myog	131	297	138	288	2.3	2.1	2.2
Rab13	210	570	353	530	2.7	1.5	2.1
Fgf11	630	1578	847	1423	2.5	1.7	2.1
Myom2	64	113	67	157	1.8	2.4	2.1
Vgll2	213	375	189	443	1.8	2.3	2.1
Fcgr3	61	116	59	129	1.9	2.2	2.0
ENSMUST00000153890	1260	2811	1800	3344	2.2	1.9	2.0
Aldh2	343	778	448	809	2.3	1.8	2.0
Atp6v1c2	106	200	95	202	1.9	2.1	2.0
Insm2	85	156	95	207	1.8	2.2	2.0
Hba-a2	57755	142513	82351	124425	2.5	1.5	2.0
Hbb-b2	23870	53114	40418	68104	2.2	1.7	2.0
Acta1	108	247	151	241	2.3	1.6	1.9
Ms4a6d	105	194	103	209	1.8	2.0	1.9
Gdf5	1001	1955	855	1645	2.0	1.9	1.9
ENSMUST00000128900	291	644	564	935	2.2	1.7	1.9
Trem2	577	1140	541	1022	2.0	1.9	1.9
Hba-a1	70100	157796	107116	168856	2.3	1.6	1.9
Hbb-bt	44449	96888	66383	103996	2.2	1.6	1.9
Myl1	617	1137	692	1316	1.8	1.9	1.9
Pfdn2	1106	2314	1654	2721	2.1	1.6	1.9
Ccdc50	258	574	402	609	2.2	1.5	1.9

AF251705	130	263	93	158	2.0	1.7	1.9
Tnnc2	693	1346	708	1239	1.9	1.8	1.8
Alas2	1430	2895	2355	3906	2.0	1.7	1.8
Asic4	868	1712	888	1514	2.0	1.7	1.8
Rab7b	56	114	75	121	2.0	1.6	1.8
Fkbp2	2123	4369	3086	4725	2.1	1.5	1.8
A_55_P2145656	82	138	107	202	1.7	1.9	1.8
Grap	54	104	81	135	1.9	1.7	1.8
Tceal7	151	293	163	266	1.9	1.6	1.8
Myl4	1176	2046	1285	2314	1.7	1.8	1.8
Hp	79	136	98	179	1.7	1.8	1.8
Mpeg1	813	1306	788	1511	1.6	1.9	1.8
Gda	83	131	82	157	1.6	1.9	1.8
Tyrobp	912	1475	890	1669	1.6	1.9	1.7
St6galnac6	1286	2363	1886	3110	1.8	1.6	1.7
C1qb	286	480	262	467	1.7	1.8	1.7
Csf1r	2758	4832	2574	4342	1.8	1.7	1.7
Adgre1	330	600	277	447	1.8	1.6	1.7
Meg3	1582	2834	2185	3553	1.8	1.6	1.7
Zfp791	3534	5939	3922	6785	1.7	1.7	1.7
Myom3	121	206	114	194	1.7	1.7	1.7
Apobec1	249	443	280	448	1.8	1.6	1.7
Cpxm1	3072	5601	3828	5943	1.8	1.6	1.7
Pfdn6	2567	4394	3324	5531	1.7	1.7	1.7
C2	125	229	139	213	1.8	1.5	1.7
Otop1	55	101	82	125	1.8	1.5	1.7
Ccl24	99	155	81	146	1.6	1.8	1.7
Dmrt2	155	274	105	166	1.8	1.6	1.7
Foxi1	443	706	395	688	1.6	1.7	1.7
C1qc	962	1552	754	1279	1.6	1.7	1.7
Hbb-bh1	14184	25528	15259	23040	1.8	1.5	1.7
Vav1	307	520	276	445	1.7	1.6	1.7
Dcaf12l2	599	994	608	997	1.7	1.6	1.6
Aif1	893	1494	976	1554	1.7	1.6	1.6
2310047M10Rik	270	453	321	503	1.7	1.6	1.6
Tnnc1	78	135	87	133	1.7	1.5	1.6
Tmem160	967	1609	1278	2012	1.7	1.6	1.6
Ms4a6c	72	119	75	118	1.7	1.6	1.6
Elavl3	111	170	268	442	1.5	1.7	1.6
Gpr182	99	157	105	167	1.6	1.6	1.6
Cx3cr1	205	311	206	340	1.5	1.6	1.6
Mef2a	941	1473	1018	1599	1.6	1.6	1.6
Igf1	808	1263	811	1241	1.6	1.5	1.5
Cldn5	1038	1567	1447	2275	1.5	1.6	1.5
Hspb2	164	254	203	310	1.6	1.5	1.5
Isg20	183	282	318	490	1.5	1.5	1.5
A_55_P2061421	17858	27329	20108	30938	1.5	1.5	1.5

Table S4. List of genes with increased expression in the microarray of E13.5 ureters of *Fgfr2cKO* and control embryos. Shown are the gene names, the intensity of the two control and mutant ureter samples, the individual and the average (avg) fold change (FC).

	Intensities				Fold change (FC)		
GeneName_RCUT	**control 1**	**mutant 1**	**control 2**	**mutant 2**	**FC 1**	**FC 2**	**avgFC**
Hoxb8	4049	1540	2394	683	-2.6	-3.5	-3.1
Nhlrc4	207	102	229	81	-2.0	-2.8	-2.4
9030625G05Rik	125	62	136	50	-2.0	-2.7	-2.4
Fosb	6737	3258	6583	2644	-2.1	-2.5	-2.3
Gsta2	140	62	115	51	-2.3	-2.3	-2.3
Hhip	1675	949	1790	677	-1.8	-2.6	-2.2
Calcr	163	63	143	80	-2.6	-1.8	-2.2
Gm10639	422	175	313	170	-2.4	-1.8	-2.1
TC1605611	1490	597	1201	701	-2.5	-1.7	-2.1
Mapk4	129	77	141	59	-1.7	-2.4	-2.0
A930017K11Rik	247	137	265	126	-1.8	-2.1	-2.0
Prr7	1088	598	786	383	-1.8	-2.1	-1.9
Mia	1078	568	1291	658	-1.9	-2.0	-1.9
Fos	11268	5792	10197	5458	-1.9	-1.9	-1.9
Rbm47	258	165	244	110	-1.6	-2.2	-1.9
Mllt3	211	140	196	86	-1.5	-2.3	-1.9
Egr1	17217	10467	16512	7781	-1.6	-2.1	-1.9
Sprr2f	164	100	185	87	-1.6	-2.1	-1.9
Espn	153	77	140	79	-2.0	-1.8	-1.9
Frmd5	242	125	196	108	-1.9	-1.8	-1.9
Hs3st6	2505	1174	2230	1413	-2.1	-1.6	-1.9
Fam150b	153	82	144	80	-1.9	-1.8	-1.8
Ldoc1	555	366	661	309	-1.5	-2.1	-1.8
Degs2	533	259	547	343	-2.1	-1.6	-1.8
Egr2	270	132	230	143	-2.0	-1.6	-1.8
Sel1l3	614	316	548	323	-1.9	-1.7	-1.8
Kcnj16	3144	1801	2521	1333	-1.7	-1.9	-1.8
Tfap2b	1115	596	943	561	-1.9	-1.7	-1.8
Srrm2	312	205	294	147	-1.5	-2.0	-1.8
Arhgef38	191	107	154	88	-1.8	-1.7	-1.8
Aldh1a3	1683	1115	1428	727	-1.5	-2.0	-1.7
Gprc5b	3997	2574	2849	1485	-1.6	-1.9	-1.7
Tmem229a	419	265	360	193	-1.6	-1.9	-1.7
A4galt	244	153	196	109	-1.6	-1.8	-1.7
Shh	176	95	159	102	-1.8	-1.6	-1.7
E330013P04Rik	134	81	142	83	-1.7	-1.7	-1.7
Foxf1	2882	1880	3316	1846	-1.5	-1.8	-1.7
Clu	7715	4395	8067	5189	-1.8	-1.6	-1.7
Map7	224	140	166	97	-1.6	-1.7	-1.7
Tfrc	582	352	383	237	-1.7	-1.6	-1.6
Gabbr2	319	199	326	200	-1.6	-1.6	-1.6
Dclk3	181	109	195	125	-1.7	-1.6	-1.6
Ccdc172	134	86	169	101	-1.6	-1.7	-1.6

Afm	835	525	705	439	-1.6	-1.6	-1.6
A_55_P2028852	177	113	185	114	-1.6	-1.6	-1.6
Elf5	867	533	818	524	-1.6	-1.6	-1.6
Atp1b1	4276	2738	3311	2066	-1.6	-1.6	-1.6
Nr1h5	510	335	410	266	-1.5	-1.5	-1.5
Iqck	251	166	249	165	-1.5	-1.5	-1.5

Table S5. List of genes with decreased expression in the microarray of E13.5 ureters of *Fgfr2cKO* and control embryos. Shown are the gene names, the intensity of the two control and mutant ureter samples, the individual and the average (avg) fold change (FC).

Category	Term	Count	%	PValue	Genes	List Total	Pop Hits	Pop Total	Fold Enrichment	Bonferroni	Benjamini	FDR
INTERPRO	IPR001713:Proteinase inhibitor I25A, stefin A	6	6,666666667	1,95E-09	GM5483, STFA2L1, BC100530, STFA1, STFA3, STFA2	85	14	20594	103,8352941	3,72E-07	3,72E-07	2,42E-06
GOTERM_CC_DIRECT	GO:0072562~blood microparticle	10	11,11111111	5,41E-09	HBA-A1, HBA-A2, C1QB, HBB-BH1, ACTA1, SERPINF2, ALB, HP, HBB-BT, C1QC	85	133	19662	17,39230429	5,79E-07	5,79E-07	6,08E-06
GOTERM_MF_DIRECT	GO:0019825~oxygen binding	6	6,666666667	7,35E-08	HBA-A1, HBA-A2, HBB-BH1, ALB, HBB-B2, HBB-BT	75	26	17446	53,68	1,33E-05	1,33E-05	9,06E-05
KEGG_PATHWAY	mmu04610:Complement and coagulation cascades	8	8,888888889	1,42E-07	C1QA, C1QB, SERPINF2, SERPINA1A, SERPINA1C, SERPINA1E, C2, C1QC	43	76	7691	18,82741738	1,21E-05	1,21E-05	1,53E-04
SMART	SM00043:CY	6	6,666666667	1,52E-07	GM5483, STFA2L1, BC100530, STFA1, STFA3, STFA2	49	28	10425	45,59037901	6,98E-06	6,98E-06	1,43E-04
INTERPRO	IPR000010:Proteinase inhibitor I25, cystatin	6	6,666666667	1,56E-07	GM5483, STFA2L1, BC100530, STFA1, STFA3, STFA2	85	31	20594	46,89335863	2,99E-05	1,49E-05	1,95E-04
GOTERM_CC_DIRECT	GO:0005833~hemoglobin complex	5	5,555555556	2,15E-07	HBA-A1, HBA-A2, HBB-BH1, HBB-B2, HBB-BT	85	13	19662	88,96832579	2,30E-05	1,15E-05	2,42E-04
INTERPRO	IPR018073:Proteinase inhibitor I25, cystatin, conserved site	5	5,555555556	2,50E-07	GM5483, STFA2L1, STFA1, STFA3, STFA2	85	14	20594	86,52941176	4,77E-05	1,59E-05	3,11E-04
UP_KEYWORDS	Secreted	23	25,55555556	2,61E-07	DHH, S100A8, CAMP, GDF5, S100A9, IGF1, SERPINA1E, HP, C1QC, CCL24, C1QA, AFP, C1QB, SERPINA6, SERPINA1A, ALB, SERPINF2, APELA, SERPINA1C, CPXM1, C2, TREM2, OTOP1	88	1685	22680	3,517939034	3,80E-05	3,80E-05	3,10E-04
UP_KEYWORDS	Oxygen transport	5	5,555555556	3,55E-07	HBA-A1, HBA-A2, HBB-BH1, HBB-B2, HBB-BT	88	16	22680	80,53977273	5,18E-05	2,59E-05	4,22E-04
INTERPRO	IPR009050:Globin-like	5	5,555555556	4,52E-07	HBA-A1, HBA-A2, HBB-BH1, HBB-B2, HBB-BT	85	16	20594	75,71323529	8,62E-05	2,16E-05	5,62E-04
INTERPRO	IPR000971:Globin	5	5,555555556	4,52E-07	HBA-A1, HBA-A2, HBB-BH1, HBB-B2, HBB-BT	85	16	20594	75,71323529	8,62E-05	2,16E-05	5,62E-04
GOTERM_MF_DIRECT	GO:0005344~oxygen transporter activity	5	5,555555556	5,22E-07	HBA-A1, HBA-A2, HBB-BH1, HBB-B2, HBB-BT	75	16	17446	72,69166667	9,45E-05	4,73E-05	6,44E-04
INTERPRO	IPR012292:Globin, structural domain	5	5,555555556	5,89E-07	HBA-A1, HBA-A2, HBB-BH1, HBB-B2, HBB-BT	85	17	20594	71,25951557	1,12E-04	2,25E-05	7,32E-04
GOTERM_CC_DIRECT	GO:0005576~extracellular region	24	26,66666667	7,45E-07	DHH, S100A8, CAMP, GDF5, S100A9, FGF11, IGF1, HP, SERPINA1E, C1QC, CCL24, C1QA, AFP, C1QB, SERPINA6, SERPINA1A, ALB, SERPINF2, APELA, SERPINA1C, CPXM1, C2, TREM2, OTOP1	85	1753	19662	3,166927284	7,97E-05	2,66E-05	8,37E-04
GOTERM_CC_DIRECT	GO:0031838~haptoglobin-hemoglobin complex	4	4,444444444	7,48E-07	HBA-A1, HBA-A2, HP, HBB-BT	85	5	19662	185,0541176	8,00E-05	2,00E-05	8,40E-04
GOTERM_MF_DIRECT	GO:0004869~cysteine-type endopeptidase inhibitor activity	6	6,666666667	1,28E-06	GM5483, STFA2L1, BC100530, STFA1, STFA3, STFA2	75	45	17446	31,01511111	2,32E-04	7,73E-05	0,001579809
UP_KEYWORDS	Muscle protein	6	6,666666667	1,67E-06	MYL4, ACTA1, TNNC2, TNNC1, MYL1, MYH8	88	52	22680	29,73776224	2,43E-04	8,11E-05	0,001981796
GOTERM_BP_DIRECT	GO:0045087~innate immune response	11	12,22222222	5,10E-06	C1QA, C1QB, S100A8, CAMP, S100A9, C2, TREM2, C1QC, CSF1R, ISG20, TYROBP	75	400	18082	6,630066667	0,002853777	0,002853777	0,007465744
UP_SEQ_FEATURE	site:Reactive site	4	4,444444444	6,69E-06	BC100530, STFA1, STFA3, STFA2	80	9	18012	100,0666667	0,001578308	0,001578308	0,008615641
UP_KEYWORDS	Protease inhibitor	7	7,777777778	7,22E-06	SERPINF2, SERPINA1A, SERPINA1C, SERPINA1E, STFA1, STFA3, STFA2	88	121	22680	14,90984222	0,001054248	2,64E-04	0,008586747
GOTERM_MF_DIRECT	GO:0004866~endopeptidase inhibitor activity	5	5,555555556	8,60E-06	SERPINA1A, SERPINA1C, SERPINA1E, STFA1, STFA2	75	31	17446	37,51827957	0,001556023	3,89E-04	0,010606596
UP_SEQ_FEATURE	short sequence motif:Secondary area of contact	4	4,444444444	9,53E-06	BC100530, STFA1, STFA3, STFA2	80	10	18012	90,06	0,002246847	0,001124055	0,012268935
UP_SEQ_FEATURE	metal ion-binding site:Iron (heme distal ligand)	4	4,444444444	1,31E-05	HBA-A1, HBA-A2, HBB-BH1, HBB-B2	80	11	18012	81,87272727	0,00307837	0,001027178	0,016816101
GOTERM_CC_DIRECT	GO:0005615~extracellular space	20	22,22222222	1,48E-05	DHH, S100A8, ACTA1, CAMP, GDF5, S100A9, IGF1, SERPINA1E, HP, C1QC, CCL24, AFP, ALB, SERPINF2, SERPINA1A, SERPINA6, APELA, SERPINA1C, CPXM1, OTOP1	85	1504	19662	3,076032541	0,001583242	3,17E-04	0,01664413
UP_KEYWORDS	Immunity	10	11,11111111	2,35E-05	C1QA, C1QB, ADGRE1, S100A8, S100A9, HP, C2, C1QC, CSF1R, ISG20	88	401	22680	6,427114033	0,003419695	6,85E-04	0,027883428
GOTERM_BP_DIRECT	GO:0002376~immune system process	10	11,11111111	2,56E-05	C1QA, C1QB, ADGRE1, S100A8, S100A9, HP, C2, C1QC, CSF1R, ISG20	75	383	18082	6,2948651	0,014249022	0,007150073	0,03748566
UP_SEQ_FEATURE	metal ion-binding site:Iron (heme proximal ligand)	4	4,444444444	2,85E-05	HBA-A1, HBA-A2, HBB-BH1, HBB-B2	80	14	18012	64,32857143	0,006714671	0,001682911	0,036743355
UP_SEQ_FEATURE	region of interest:RCL	4	4,444444444	2,85E-05	SERPINA1A, SERPINA1C, SERPINA1E, GM8893	80	14	18012	64,32857143	0,006714671	0,001682911	0,036743355
GOTERM_CC_DIRECT	GO:0070062~extracellular exosome	27	30	3,07E-05	GDA, S100A8, CLDN5, S100A9, HP, C1QC, ALB, SERPINA6, SERPINA1A, SERPINA1C, C2, ACTA1, CAMP, SERPINA1E, UPK3A, FCGR3, C1QA, HBA-A1, PFDN2, C1QB, HBA-A2, ATP6V1C2, SERPINF2, ALDH2, RAB13, HBB-BT, FKBP2	85	2674	19662	2,335668089	0,00328377	5,48E-04	0,034547584
UP_KEYWORDS	Innate immunity	8	8,888888889	3,98E-05	C1QA, C1QB, S100A8, S100A9, C2, C1QC, CSF1R, ISG20	88	241	22680	8,555262165	0,005791894	9,68E-04	0,047277488
UP_SEQ_FEATURE	chain:Stefin-1	3	3,333333333	5,68E-05	BC100530, STFA1, STFA3	80	3	18012	225,15	0,01332046	0,002678401	0,073120773
UP_SEQ_FEATURE	chain:Stefin-3	3	3,333333333	5,68E-05	BC100530, STFA1, STFA3	80	3	18012	225,15	0,01332046	0,002678401	0,073120773
INTERPRO	IPR023795:Protease inhibitor I4, serpin, conserved site	5	5,555555556	6,01E-05	SERPINF2, SERPINA6, SERPINA1A, SERPINA1C, SERPINA1E	85	52	20594	23,29638009	0,01140639	0,001910164	0,074686385
GOTERM_MF_DIRECT	GO:0031720~haptoglobin binding	3	3,333333333	1,06E-04	HBA-A1, HBA-A2, HBB-BT	75	4	17446	174,46	0,018988526	0,003826883	0,130499558
UP_SEQ_FEATURE	domain:EF-hand 1	7	7,777777778	1,16E-04	MYL4, S100A8, TNNC2, AIF1, TNNC1, S100A9, MYL1	80	174	18012	9,057758621	0,026918951	0,004537657	0,148736881
KEGG_PATHWAY	mmu05150:Staphylococcus aureus infection	5	5,555555556	1,48E-04	C1QA, C1QB, C2, C1QC, FCGR3	43	50	7691	17,88604651	0,012460498	0,006249779	0,158581598
UP_KEYWORDS	Complement pathway	4	4,444444444	1,49E-04	C1QA, C1QB, C2, C1QC	88	27	22680	38,18181818	0,021548046	0,003107105	0,177182256
INTERPRO	IPR000215:Serpin family	5	5,555555556	1,62E-04	SERPINF2, SERPINA6, SERPINA1A, SERPINA1C, SERPINA1E	85	67	20594	18,08077261	0,030530859	0,004419723	0,201735776

INTERPRO	IPR023796:Serpin domain	5	5,555555556	1,62E-04	SERPINF2, SERPINA6, SERPINA1A, SERPINA1C, SERPINA1E	85	67	20594	18,08077261	0,030530859	0,004419723	0,201735776
GOTERM_BP_DIRECT	GO:0098869~cellular oxidant detoxification	3	3,333333333	1,64E-04	HBA-A1, HBA-A2, HBB-BT	75	5	18082	144,656	0,08771319	0,030136835	0,239538264
GOTERM_BP_DIRECT	GO:0048821~erythrocyte development	4	4,444444444	1,79E-04	HBA-A1, HBA-A2, HBB-B2, HBB-BT	75	27	18082	35,71753086	0,095555378	0,024795952	0,262035935
GOTERM_BP_DIRECT	GO:0030593~neutrophil chemotaxis	5	5,555555556	1,83E-04	CCL24, S100A8, S100A9, VAV1, FCGR3	75	69	18082	17,4705314	0,097258603	0,020255867	0,266947252
SMART	SM00093:SERPIN	5	5,555555556	2,45E-04	SERPINF2, SERPINA6, SERPINA1A, SERPINA1C, SERPINA1E	49	67	10425	15,87724642	0,011213234	0,005622423	0,231436221
INTERPRO	IPR002048:EF-hand domain	7	7,777777778	3,03E-04	MYL4, S100A8, TNNC2, AIF1, TNNC1, S100A9, MYL1	85	223	20594	7,605275653	0,056273586	0,007213727	0,376503233
INTERPRO	IPR002337:Haemoglobin, beta	3	3,333333333	4,53E-04	HBB-BH1, HBB-B2, HBB-BT	85	8	20594	90,85588235	0,08290995	0,009570532	0,562093306
UP_SEQ_FEATURE	signal peptide	27	30	5,71E-04	DHH, MPEG1, GDF5, HP, C1QC, CCL24, SERPINA6, ALB, SERPINA1A, SERPINA1C, C2, CSF1R, TYROBP, ADGRE1, CAMP, IGF1, SERPINA1E, GM8893, UPK3A, FCGR3, C1QA, C1QB, AFP, SERPINF2, CPXM1, TREM2, FKBP2	80	3124	18012	1,945918694	0,126117081	0,019074152	0,732646319
GOTERM_BP_DIRECT	GO:0015671~oxygen transport	3	3,333333333	7,28E-04	HBB-BH1, HBB-B2, HBB-BT	75	10	18082	72,328	0,334869578	0,065704045	1,059632345
KEGG_PATHWAY	mmu05143:African trypanosomiasis	4	4,444444444	8,78E-04	HBA-A1, HBA-A2, HBB-B2, HBB-BT	43	35	7691	20,44119601	0,071924538	0,02457377	0,940322322
INTERPRO	IPR011992:EF-hand-like domain	7	7,777777778	8,79E-04	MYL4, S100A8, TNNC2, AIF1, TNNC1, S100A9, MYL1	85	273	20594	6,212368024	0,154690042	0,016664771	1,088518188
UP_SEQ_FEATURE	domain:EF-hand 2	6	6,666666667	9,80E-04	MYL4, S100A8, TNNC2, TNNC1, S100A9, MYL1	80	173	18012	7,80867052	0,206526113	0,028502741	1,253935395
UP_KEYWORDS	Antioxidant	3	3,333333333	0,001478559	S100A8, S100A9, HP	88	15	22680	51,54545455	0,194288375	0,026642334	1,743312249
GOTERM_BP_DIRECT	GO:0006958~complement activation, classical pathway	4	4,444444444	0,001481666	C1QA, C1QB, C2, C1QC	75	55	18082	17,53406061	0,564102491	0,1118558	2,145888329
UP_SEQ_FEATURE	site:Reactive bond	4	4,444444444	0,001624602	SERPINA1A, SERPINA1C, SERPINA1E, GM8893	80	53	18012	16,99245283	0,318676355	0,04173921	2,071316994
GOTERM_MF_DIRECT	GO:0004867~serine-type endopeptidase inhibitor activity	5	5,555555556	0,001850256	SERPINF2, SERPINA6, SERPINA1A, SERPINA1C, SERPINA1E	75	123	17446	9,455826558	0,284809666	0,054335819	2,257401974
UP_SEQ_FEATURE	disulfide bond	22	24,44444444	0,002179029	GPR182, ADGRE1, ASIC4, CAMP, GDF5, IGF1, HP, C1QC, FCGR3, CCL24, C1QA, ST6GALNAC6, AFP, C1QB, ALB, SERPINF2, CX3CR1, CPXM1, PRM1, C2, TREM2, CSF1R	80	2510	18012	1,973426295	0,402387023	0,050178487	2,769087945
KEGG_PATHWAY	mmu05144:Malaria	4	4,444444444	0,002208098	HBA-A1, HBA-A2, HBB-B2, HBB-BT	43	48	7691	14,90503876	0,171298969	0,045887754	2,350201485
BIOCARTA	m_classicPathway:Classical Complement Pathway	3	3,333333333	0,002760086	C1QA, C1QB, C2	10	12	1289	32,225	0,10218584	0,10218584	2,48215256
UP_KEYWORDS	Disulfide bond	23	25,55555556	0,002963593	GPR182, ADGRE1, ASIC4, CAMP, GDF5, IGF1, HP, C1QC, FCGR3, CCL24, C1QA, ST6GALNAC6, AFP, C1QB, ALB, SERPINF2, CX3CR1, CPXM1, PRM1, C2, TREM2, CSF1R, TYROBP	88	3124	22680	1,897479921	0,351651528	0,047006733	3,466200077
GOTERM_BP_DIRECT	GO:0060395~SMAD protein signal transduction	4	4,444444444	0,003874172	AFP, APELA, GDF5, MEG3	75	77	18082	12,524329	0,886249723	0,237931417	5,520588113
UP_KEYWORDS	Acute phase	3	3,333333333	0,004120584	SERPINF2, SERPINA1A, HP	88	25	22680	30,92727273	0,452749269	0,058503662	4,789279448
UP_KEYWORDS	Thiol protease inhibitor	3	3,333333333	0,004120584	STFA1, STFA3, STFA2	88	25	22680	30,92727273	0,452749269	0,058503662	4,789279448
UP_KEYWORDS	Serine protease inhibitor	4	4,444444444	0,004152644	SERPINF2, SERPINA1A, SERPINA1C, SERPINA1E	88	84	22680	12,27272727	0,45531536	0,053734092	4,825703184
UP_KEYWORDS	Heme	5	5,555555556	0,004271823	HBA-A1, HBA-A2, HBB-BH1, HBB-B2, HBB-BT	88	171	22680	7,535885167	0,46475042	0,050751992	4,960996051
GOTERM_MF_DIRECT	GO:0016209~antioxidant activity	3	3,333333333	0,004611625	S100A8, S100A9, HP	75	24	17446	29,07666667	0,566834174	0,112653062	5,539427802
GOTERM_MF_DIRECT	GO:0042802~identical protein binding	9	10	0,004887557	PRMT1, ALB, SERPINA1A, GDF5, CLDN5, SERPINA1C, ALDH2, SERPINA1E, TYROBP	75	625	17446	3,349632	0,588034933	0,104928871	5,861758809
GOTERM_BP_DIRECT	GO:0003009~skeletal muscle contraction	3	3,333333333	0,00503911	TNNC2, TNNC1, MYH8	75	26	18082	27,81846154	0,940930217	0,26972734	7,124220656
INTERPRO	IPR007237:CD20-like	3	3,333333333	0,005400645	MS4A7, MS4A6C, MS4A6D	85	27	20594	26,92026144	0,644531514	0,089743609	6,514416625
BIOCARTA	m_compPathway:Complement Pathway	3	3,333333333	0,006260225	C1QA, C1QB, C2	10	18	1289	21,48333333	0,21722987	0,115257026	5,55089711
GOTERM_MF_DIRECT	GO:0020037~heme binding	5	5,555555556	0,006524431	HBA-A1, HBA-A2, HBB-BH1, HBB-B2, HBB-BT	75	175	17446	6,646095238	0,694190001	0,123346513	7,75318927
UP_SEQ_FEATURE	domain:C1q	3	3,333333333	0,007141948	C1QA, C1QB, C1QC	80	29	18012	23,29137931	0,815765782	0,142536818	8,814018469
UP_SEQ_FEATURE	domain:EF-hand 3	4	4,444444444	0,007479615	MYL4, TNNC2, TNNC1, MYL1	80	91	18012	9,896703297	0,829977349	0,137268679	9,212433842
KEGG_PATHWAY	mmu05133:Pertussis	4	4,444444444	0,007501759	C1QA, C1QB, C2, C1QC	43	74	7691	9,66813325	0,472735661	0,120155994	7,78188912
INTERPRO	IPR001073:Complement C1q protein	3	3,333333333	0,007531726	C1QA, C1QB, C1QC	85	32	20594	22,71397059	0,764019105	0,113375482	8,975810988
GOTERM_MF_DIRECT	GO:0004601~peroxidase activity	3	3,333333333	0,007622282	HBA-A1, HBA-A2, HBB-BT	75	31	17446	22,51096774	0,749655663	0,129329606	9,002138011
SMART	SM00110:C1Q	3	3,333333333	0,007786431	C1QA, C1QB, C1QC	49	29	10425	22,00914849	0,302028883	0,112954663	7,122045848
INTERPRO	IPR002339:Haemoglobin, pi	2	2,222222222	0,008141276	HBA-A1, HBA-A2	85	2	20594	242,2823529	0,790147014	0,11317153	9,668797225
GOTERM_BP_DIRECT	GO:0070488~neutrophil aggregation	2	2,222222222	0,008168412	S100A8, S100A9	75	2	18082	241,0933333	0,989878524	0,36828035	11,30729715
PIR_SUPERFAMILY	PIRSF002520:serum albumin	2	2,222222222	0,008282676	AFP, ALB	6	3	1807	200,7777778	0,04867831	0,04867831	3,902310543
UP_SEQ_FEATURE	chain:Hemoglobin subunit alpha	2	2,222222222	0,008752936	HBA-A1, HBA-A2	80	2	18012	225,15	0,874416743	0,147514389	10,70043647
UP_SEQ_FEATURE	chain:Alpha-1-antitrypsin 1-5	2	2,222222222	0,008752936	SERPINA1E, GM8893	80	2	18012	225,15	0,874416743	0,147514389	10,70043647
GOTERM_BP_DIRECT	GO:0006953~acute-phase response	3	3,333333333	0,009009124	SERPINF2, SERPINA1A, HP	75	35	18082	20,66514286	0,99370483	0,369173736	12,40081702
UP_SEQ_FEATURE	domain:Collagen-like	3	3,333333333	0,009183565	C1QA, C1QB, C1QC	80	33	18012	20,46818182	0,88665675	0,144033372	11,19855719
GOTERM_MF_DIRECT	GO:0005509~calcium ion binding	9	10	0,009371515	DHH, MYL4, ADGRE1, S100A8, TNNC2, AIF1, TNNC1, S100A9, MYL1	75	699	17446	2,995021459	0,818089845	0,143525835	10,96005253
UP_KEYWORDS	Antimicrobial	4	4,444444444	0,01084264	S100A8, CAMP, S100A9, HP	88	119	22680	8,663101604	0,796414689	0,115237618	12,15332774
UP_KEYWORDS	Methylation	10	11,11111111	0,011275714	MYL4, ACTA1, ALB, S100A9, MYL1, HBB-B2, RAB13, HBB-BT, MYH8, NEFM	88	960	22680	2,684659091	0,809023696	0,111532816	12,60938062
GOTERM_BP_DIRECT	GO:0010466~negative regulation of peptidase activity	4	4,444444444	0,012265459	SERPINF2, SERPINA1C, SERPINA1E, STFA2	75	117	18082	8,242507123	0,999003367	0,43781671	16,51891648
GOTERM_BP_DIRECT	GO:0006935~chemotaxis	4	4,444444444	0,012549044	CCL24, S100A8, S100A9, CX3CR1	75	118	18082	8,172655367	0,999151407	0,419575009	16,8688771
GOTERM_MF_DIRECT	GO:0005506~iron ion binding	5	5,555555556	0,01257918	HBA-A1, HBA-A2, HBB-BH1, HBB-B2, HBB-BT	75	212	17446	5,486163522	0,898862389	0,173817375	14,45014505

GOTERM_MF_DIRECT	GO:0043177~organic acid binding	2	2,222222222	0,012671805	HBA-A1, HBA-A2	75	3	17446	155,0755556	0,900565144	0,162687474	14,54903093
GOTERM_MF_DIRECT	GO:0002020~protease binding	4	4,444444444	0,013492897	SERPINF2, SERPINA1A, SERPINA1C, SERPINA1E	75	117	17446	7,952592593	0,914465925	0,161072896	15,42105119
KEGG_PATHWAY	mmu05020:Prion diseases	3	3,333333333	0,013810999	C1QA, C1QB, C1QC	43	33	7691	16,26004228	0,693371066	0,178825372	13,89687027
GOTERM_BP_DIRECT	GO:0006911~phagocytosis, engulfment	3	3,333333333	0,014601036	AIF1, TREM2, FCGR3	75	45	18082	16,07288889	0,999735286	0,444755779	19,36071964
UP_KEYWORDS	Myosin	3	3,333333333	0,014635151	MYL4, MYL1, MYH8	88	48	22680	16,10795455	0,88380924	0,133680468	16,0741052
GOTERM_MF_DIRECT	GO:0030414~peptidase inhibitor activity	4	4,444444444	0,01541714	SERPINF2, SERPINA1C, SERPINA1E, STFA2	75	123	17446	7,564661247	0,939929524	0,170956335	17,43270264
UP_KEYWORDS	Metal-binding	22	24,44444444	0,016158697	DHH, INSM2, HBB-BH1, GDA, APOBEC1, S100A8, TNNC2, AIF1, TNNC1, S100A9, DMRT2, VAV1, ISG20, HBA-A1, HBA-A2, AFP, ALB, ZFP791, CPXM1, HBB-B2, HBB-BT, C2	88	3395	22680	1,670103093	0,907304758	0,138131337	17,60354157
INTERPRO	IPR021177:Serum albumin/Alpha-fetoprotein	2	2,222222222	0,016217054	AFP, ALB	85	4	20594	121,1411765	0,955968416	0,199933618	18,4035456
GOTERM_BP_DIRECT	GO:0002793~positive regulation of peptide secretion	2	2,222222222	0,016270996	S100A8, S100A9	75	4	18082	120,5466667	0,999897608	0,457976927	21,33709093
GOTERM_BP_DIRECT	GO:0060048~cardiac muscle contraction	3	3,333333333	0,016505901	MYL4, TNNC1, MYL1	75	48	18082	15,06833333	0,999910425	0,441514959	21,61144839
GOTERM_MF_DIRECT	GO:0031721~hemoglobin alpha binding	2	2,222222222	0,016860435	HBB-BH1, HBB-BT	75	4	17446	116,3066667	0,95393761	0,174990111	18,91260018
UP_SEQ_FEATURE	domain:Albumin 1	2	2,222222222	0,017430219	AFP, ALB	80	4	18012	112,575	0,984232487	0,241682847	20,25688398
UP_SEQ_FEATURE	domain:Albumin 2	2	2,222222222	0,017430219	AFP, ALB	80	4	18012	112,575	0,984232487	0,241682847	20,25688398
UP_SEQ_FEATURE	domain:Albumin 3	2	2,222222222	0,017430219	AFP, ALB	80	4	18012	112,575	0,984232487	0,241682847	20,25688398
UP_KEYWORDS	S-nitrosylation	3	3,333333333	0,017659521	S100A8, HBB-B2, HBB-BT	88	53	22680	14,58833619	0,92582495	0,141886807	19,08516974
UP_KEYWORDS	Signal	27	30	0,018407285	DHH, MPEG1, GDF5, HP, C1QC, CCL24, SERPINA6, ALB, SERPINA1A, APELA, SERPINA1C, C2, CSF1R, TYROBP, ADGRE1, CAMP, IGF1, SERPINA1E, UPK3A, FCGR3, C1QA, C1QB, AFP, SERPINF2, CPXM1, TREM2, FKBP2	88	4543	22680	1,531727133	0,933629719	0,139889812	19,81422512
INTERPRO	IPR008983:Tumour necrosis factor-like domain	3	3,333333333	0,018418134	C1QA, C1QB, C1QC	85	51	20594	14,25190311	0,971294402	0,210780562	20,64566025
GOTERM_MF_DIRECT	GO:0051015~actin filament binding	4	4,444444444	0,018579895	MYL4, TNNC2, AIF1, TNNC1	75	132	17446	7,048888889	0,966445863	0,181008902	20,64383436
INTERPRO	IPR014760:Serum albumin, N-terminal	2	2,222222222	0,020230545	AFP, ALB	85	5	20594	96,91294118	0,979831939	0,216495476	22,44917484
INTERPRO	IPR000264:ALB/AFP/VDB	2	2,222222222	0,020230545	AFP, ALB	85	5	20594	96,91294118	0,979831939	0,216495476	22,44917484
INTERPRO	IPR020857:Serum albumin, conserved site	2	2,222222222	0,020230545	AFP, ALB	85	5	20594	96,91294118	0,979831939	0,216495476	22,44917484
INTERPRO	IPR002338:Haemoglobin, alpha	2	2,222222222	0,020230545	HBA-A1, HBA-A2	85	5	20594	96,91294118	0,979831939	0,216495476	22,44917484
INTERPRO	IPR002777:Prefoldin beta-like	2	2,222222222	0,020230545	PFDN2, PFDN6	85	5	20594	96,91294118	0,979831939	0,216495476	22,44917484
GOTERM_BP_DIRECT	GO:0071224~cellular response to peptidoglycan	2	2,222222222	0,020297766	CAMP, TREM2	75	5	18082	96,43733333	0,999989703	0,491103903	25,9186491
GOTERM_BP_DIRECT	GO:0018119~peptidyl-cysteine S-nitrosylation	2	2,222222222	0,020297766	S100A8, S100A9	75	5	18082	96,43733333	0,999989703	0,491103903	25,9186491
GOTERM_CC_DIRECT	GO:0016459~myosin complex	3	3,333333333	0,020829075	MYL4, MYL1, MYH8	85	52	19662	13,34524887	0,894837599	0,275120555	21,069635
GOTERM_MF_DIRECT	GO:0035662~Toll-like receptor 4 binding	2	2,222222222	0,021031535	S100A8, S100A9	75	5	17446	93,04533333	0,978662915	0,192441167	23,05357469
SMART	SM00103:ALBUMIN	2	2,222222222	0,022814896	AFP, ALB	49	5	10425	85,10204082	0,654112758	0,233109009	19,59871509
GOTERM_BP_DIRECT	GO:0007519~skeletal muscle tissue development	3	3,333333333	0,023563035	MEG3, VGLL2, MYOG	75	58	18082	12,47034483	0,999998412	0,523766505	29,44993396
UP_KEYWORDS	Inflammatory response	4	4,444444444	0,024111907	CCL24, S100A8, S100A9, CSF1R	88	161	22680	6,403162055	0,971659808	0,171013391	25,18120516
INTERPRO	IPR020858:Serum albumin-like	2	2,222222222	0,024227856	AFP, ALB	85	6	20594	80,76078431	0,990762649	0,240852229	26,29440038
GOTERM_MF_DIRECT	GO:0030492~hemoglobin binding	2	2,222222222	0,025185177	HP, HBB-BT	75	6	17446	77,53777778	0,990116642	0,215724482	26,98329767
GOTERM_BP_DIRECT	GO:0050729~positive regulation of inflammatory response	3	3,333333333	0,027478176	CCL24, S100A8, S100A9	75	63	18082	11,48063492	0,999999833	0,560104583	33,47718571
UP_KEYWORDS	Glycoprotein	23	25,55555556	0,028803179	GPR182, ADGRE1, MPEG1, ASIC4, GDF5, SERPINA1E, HP, UPK3A, FCGR3, CCL24, C1QA, ST6GALNAC6, C1QB, AFP, SERPINA6, SERPINA1A, SERPINF2, SERPINA1C, CPXM1, C2, TREM2, NEFM, CSF1R	88	3815	22680	1,553794829	0,985976423	0,192127285	29,3460428
SMART	SM00054:EFh	4	4,444444444	0,028907181	S100A8, TNNC2, TNNC1, S100A9	49	145	10425	5,869106263	0,740585548	0,236517945	24,21365233
GOTERM_CC_DIRECT	GO:0016272~prefoldin complex	2	2,222222222	0,029529281	PFDN2, PFDN6	85	7	19662	66,0907563	0,959531167	0,33028491	28,60386467
UP_SEQ_FEATURE	glycosylation site:O-linked (Gal...)	2	2,222222222	0,030305706	C1QA, C1QB	80	7	18012	64,32857143	0,999298832	0,364868148	32,71027688
KEGG_PATHWAY	mmu04380:Osteoclast differentiation	4	4,444444444	0,030994396	TREM2, CSF1R, FCGR3, TYROBP	43	126	7691	5,678110004	0,931176851	0,317720886	28,73303857
GOTERM_BP_DIRECT	GO:0048743~positive regulation of skeletal muscle fiber develo	2	2,222222222	0,032280767	MEG3, MYOG	75	8	18082	60,27333333	0,99999999	0,600991243	38,12476023
GOTERM_MF_DIRECT	GO:0050786~RAGE receptor binding	2	2,222222222	0,033440374	S100A8, S100A9	75	8	17446	58,15333333	0,997879757	0,26494593	34,25150401
GOTERM_CC_DIRECT	GO:0005861~troponin complex	2	2,222222222	0,033676803	TNNC2, TNNC1	85	8	19662	57,82941176	0,974408406	0,334540045	31,95960482
GOTERM_BP_DIRECT	GO:0043434~response to peptide hormone	3	3,333333333	0,036024015	SERPINA1A, SERPINA1C, SERPINA1E	75	73	18082	9,907945205	0,999999999	0,624076858	41,53543507
GOTERM_MF_DIRECT	GO:0050544~arachidonic acid binding	2	2,222222222	0,037542072	S100A8, S100A9	75	9	17446	51,69185185	0,999018032	0,280937652	37,60990255
INTERPRO	IPR008160:Collagen triple helix repeat	3	3,333333333	0,038570305	C1QA, C1QB, C1QC	85	76	20594	9,56377709	0,99945393	0,341226638	38,6938536
GOTERM_BP_DIRECT	GO:0070374~positive regulation of ERK1 and ERK2 cascade	4	4,444444444	0,041893574	CCL24, SERPINF2, TREM2, CSF1R	75	188	18082	5,12964539	1	0,663569366	46,53274681
UP_KEYWORDS	Collagen	3	3,333333333	0,042295313	C1QA, C1QB, C1QC	88	85	22680	9,096256684	0,998181072	0,259517121	40,16949983
GOTERM_BP_DIRECT	GO:0048661~positive regulation of smooth muscle cell prolifera	3	3,333333333	0,04253552	SERPINF2, AIF1, IGF1	75	80	18082	9,041	1	0,652961156	47,05445517
GOTERM_BP_DIRECT	GO:0034097~response to cytokine	3	3,333333333	0,043499296	SERPINA1A, SERPINA1C, SERPINA1E	75	81	18082	8,929382716	1	0,645738855	47,82881563
GOTERM_MF_DIRECT	GO:0001948~glycoprotein binding	3	3,333333333	0,044342096	SERPINA1A, SERPINA1C, SERPINA1E	75	79	17446	8,833417722	0,99972789	0,311438183	42,83221406
UP_KEYWORDS	Hydroxylation	3	3,333333333	0,045021025	C1QA, C1QB, C1QC	88	88	22680	8,786157025	0,998800235	0,263400108	42,16238726
KEGG_PATHWAY	mmu05322:Systemic lupus erythematosus	4	4,444444444	0,045672525	C1QA, C1QB, C2, C1QC	43	147	7691	4,866951432	0,981194654	0,391465555	39,52580191
UP_KEYWORDS	Polymorphism	4	4,444444444	0,046537313	HBA-A1, GDF5, HBB-B2, HBB-BT	88	209	22680	4,932579382	0,99904865	0,261035628	43,24451142
GOTERM_CC_DIRECT	GO:0005581~collagen trimer	3	3,333333333	0,049122234	C1QA, C1QB, C1QC	85	83	19662	8,360878809	0,995436037	0,416643271	43,23138419
GOTERM_CC_DIRECT	GO:0043209~myelin sheath	4	4,444444444	0,049146671	HBA-A1, ALB, HBB-BT, NEFM	85	192	19662	4,819117647	0,99544857	0,387502455	43,24778103
GOTERM_BP_DIRECT	GO:0030335~positive regulation of cell migration	4	4,444444444	0,050592664	CCL24, AIF1, IGF1, CSF1R	75	203	18082	4,750607553	1	0,687436786	53,21173389
UP_KEYWORDS	Chemotaxis	3	3,333333333	0,050660772	CCL24, S100A8, S100A9	88	94	22680	8,225338491	0,999494724	0,271135139	46,09419781

GOTERM_BP_DIRECT	GO:0002523~leukocyte migration involved in inflammatory resp	2	2,222222222	0,05193193	S100A8, S100A9	75	13	18082	37,09128205	1	0,682927267	54,16808612
GOTERM_BP_DIRECT	GO:0006954~inflammatory response	5	5,555555556	0,052497292	CCL24, S100A8, AIF1, S100A9, CSF1R	75	344	18082	3,504263566	1	0,673215543	54,5663103
UP_KEYWORDS	Iron	5	5,555555556	0,056273946	HBA-A1, HBA-A2, HBB-BH1, HBB-B2, HBB-BT	88	375	22680	3,436363636	0,999787427	0,286982286	49,76298312
GOTERM_MF_DIRECT	GO:0015643~toxic substance binding	2	2,222222222	0,0577944	ALB, NEFM	75	14	17446	33,23047619	0,999979089	0,374052728	51,99955787
UP_SEQ_FEATURE	calcium-binding region:2; high affinity	2	2,222222222	0,063831565	S100A8, S100A9	80	15	18012	30,02	0,999999826	0,59975489	57,22040903
UP_SEQ_FEATURE	calcium-binding region:1; low affinity	2	2,222222222	0,063831565	S100A8, S100A9	80	15	18012	30,02	0,999999826	0,59975489	57,22040903
GOTERM_BP_DIRECT	GO:0014002~astrocyte development	2	2,222222222	0,067368973	S100A8, S100A9	75	17	18082	28,36392157	1	0,752145283	63,95352126
GOTERM_BP_DIRECT	GO:0045445~myoblast differentiation	2	2,222222222	0,067368973	IGF1, MYOG	75	17	18082	28,36392157	1	0,752145283	63,95352126
INTERPRO	IPR001751:S100/Calbindin-D9k, conserved site	2	2,222222222	0,07095679	S100A8, S100A9	85	18	20594	26,92026144	0,999999215	0,522825954	59,97002366
GOTERM_BP_DIRECT	GO:0010613~positive regulation of cardiac muscle hypertrophy	2	2,222222222	0,071189327	MEF2A, IGF1	75	18	18082	26,78814815	1	0,759750155	66,05444266
GOTERM_BP_DIRECT	GO:0001774~microglial cell activation	2	2,222222222	0,071189327	AIF1, CX3CR1	75	18	18082	26,78814815	1	0,759750155	66,05444266
GOTERM_MF_DIRECT	GO:0017091~AU-rich element binding	2	2,222222222	0,073693075	APOBEC1, ELAVL3	75	18	17446	25,84592593	0,999999039	0,438594556	61,08425683
GOTERM_BP_DIRECT	GO:0010951~negative regulation of endopeptidase activity	2	2,222222222	0,074994243	STFA1, STFA2	75	19	18082	25,37824561	1	0,766638359	68,03302112
GOTERM_CC_DIRECT	GO:0043292~contractile fiber	2	2,222222222	0,078159467	TNNC1, MYL1	85	19	19662	24,34922601	0,999834739	0,515997562	59,94010577
UP_KEYWORDS	Growth factor	3	3,333333333	0,085606491	GDF5, FGF11, IGF1	88	127	22680	6,088045812	0,999997884	0,395010827	65,48275933
KEGG_PATHWAY	mmu04530:Tight junction	3	3,333333333	0,086294618	CLDN5, RAB13, MYH8	43	90	7691	5,962015504	0,999953385	0,573581367	62,12746839
UP_KEYWORDS	Motor protein	3	3,333333333	0,086755962	MYL4, MYL1, MYH8	88	128	22680	6,040482955	0,999998239	0,387822987	65,99498362
UP_SEQ_FEATURE	glycosylation site:N-linked (GlcNAc...)	22	24,44444444	0,087148293	GPR182, ADGRE1, MPEG1, ASIC4, GDF5, GM8893, SERPINA1E, HP, UPK3A, FCGR3, CCL24, C1QA, ST6GALNAC6, AFP, SERPINA6, SERPINF2, SERPINA1A, SERPINA1C, CPXM1, C2, TREM2, CSF1R	80	3563	18012	1,390204884	1	0,697445899	69,08084794
GOTERM_BP_DIRECT	GO:0045766~positive regulation of angiogenesis	3	3,333333333	0,087916904	CCL24, CAMP, CX3CR1	75	121	18082	5,977520661	1	0,810311547	73,97963403
UP_SEQ_FEATURE	calcium-binding region:2	3	3,333333333	0,089381769	TNNC2, AIF1, TNNC1	80	114	18012	5,925	1	0,687453565	70,0406782
GOTERM_CC_DIRECT	GO:0031430~M band	2	2,222222222	0,089935853	MYOM2, MYOM3	85	22	19662	21,02887701	0,999958245	0,539604447	65,33074051
GOTERM_BP_DIRECT	GO:0006937~regulation of muscle contraction	2	2,222222222	0,090060743	TNNC2, TNNC1	75	23	18082	20,96463768	1	0,808258098	74,86020534
BIOCARTA	m_hsp27PathwayStress Induction of HSP Regulation	2	2,222222222	0,093888523	ACTA1, HSPB2	10	14	1289	18,41428571	0,978616262	0,722437235	59,20451505
GOTERM_BP_DIRECT	GO:0006457~protein folding	3	3,333333333	0,096680593	PFDN2, PFDN6, FKBP2	75	128	18082	5,650625	1	0,821909425	77,40720825
INTERPRO	IPR009053:Prefoldin	2	2,222222222	0,097186867	PFDN2, PFDN6	85	25	20594	19,38258824	0,999999997	0,623331211	71,96740694
UP_KEYWORDS	Calcium	7	7,777777778	0,098051136	DHH, ADGRE1, S100A8, TNNC2, AIF1, TNNC1, S100A9	88	827	22680	2,181488403	0,999999714	0,416144814	70,67083009

Table S6. Functional annotation by DAVID for genes with increased expression in the microarray of E13.5 *Fgfr2cKO* ureters.

Category	Term	Count	%	PValue	Genes	List Total	Pop Hits	Pop Total	Fold Enric	Bonferro	Benjamini	FDR
GOTERM_BP_DIRECT	GO:0006366~transcription from RNA polymerase II promoter	5	10,63829787	1,58E-04	EGR1, FOS, EGR2, TFAP2B, FOSB	37	138	18082	17,7066	0,07784	0,077843	0,228428996
GOTERM_MF_DIRECT	GO:0043565~sequence-specific DNA binding	8	17,0212766	2,67E-04	EGR1, FOS, HOXB8, ELF5, FOXF1, TFAP2B, FOSB, NR1H5	37	633	17446	5,9591	0,03153	0,031533	0,306036567
GOTERM_MF_DIRECT	GO:0003700~transcription factor activity, sequence-specific DNA binding	9	19,14893617	3,56E-04	EGR1, FOS, EGR2, HOXB8, ELF5, FOXF1, TFAP2B, FOSB, NR1H5	37	883	17446	4,80591	0,04183	0,021136	0,407878891
GOTERM_BP_DIRECT	GO:0060441~epithelial tube branching involved in lung morphogenesis	3	6,382978723	0,00103476	FOXF1, HHIP, SHH	37	24	18082	61,0878	0,41144	0,232821	1,484707092
GOTERM_MF_DIRECT	GO:0001077~transcriptional activator activity, RNA polymerase II core promoter proximal region sequence-specific binding	5	10,63829787	0,002238541	EGR1, FOS, EGR2, TFAP2B, FOSB	37	270	17446	8,73173	0,2358	0,085742	2,539764652
GOTERM_BP_DIRECT	GO:0045944~positive regulation of transcription from RNA polymerase II promoter	8	17,0212766	0,003068176	EGR1, FOS, EGR2, ELF5, FOXF1, TFAP2B, FOSB, SHH	37	995	18082	3,92927	0,79264	0,408113	4,342729038
GOTERM_BP_DIRECT	GO:0035914~skeletal muscle cell differentiation	3	6,382978723	0,005356001	EGR1, FOS, EGR2	37	55	18082	26,6565	0,93605	0,497124	7,465976908
GOTERM_BP_DIRECT	GO:0045893~positive regulation of transcription, DNA-templated	6	12,76595745	0,005369769	EGR1, FOS, EGR2, FOXF1, TFAP2B, SHH	37	576	18082	5,09065	0,9365	0,423826	7,484481445
INTERPRO	IPR021849:Protein of unknown function DUF3446	2	4,255319149	0,005525653	EGR1, EGR2	39	3	20594	352,034	0,5107	0,510703	6,240634848
GOTERM_CC_DIRECT	GO:0005634~nucleus	21	44,68085106	0,005544361	EGR1, EGR2, ELF5, CLU, SEL1L3, SPRR2F, FOSB, GPRC5B, FOS, TFRC, HOXB8, SRRM2, FOXF1, MAPK4, DCLK3, TFAP2B, RBM47, HHIP, LDOC1, NR1H5, MLLT3	40	6019	19662	1,71499	0,35904	0,359037	5,739410745
GOTERM_BP_DIRECT	GO:0072659~protein localization to plasma membrane	3	6,382978723	0,006761097	CALCR, ATP1B1, MAP7	37	62	18082	23,6469	0,96899	0,439489	9,336828809
UP_KEYWORDS	Activator	6	12,76595745	0,006950261	EGR1, EGR2, ELF5, FOXF1, TFAP2B, MLLT3	45	624	22680	4,84615	0,45108	0,451084	7,244988919
KEGG_PATHWAY	mmu04024:cAMP signaling pathway	4	8,510638298	0,007245671	FOS, ATP1B1, GABBR2, HHIP	17	197	7691	9,18603	0,39012	0,390124	7,208285586
GOTERM_CC_DIRECT	GO:0016323~basolateral plasma membrane	4	8,510638298	0,007540334	KCNJ16, ATP1B1, TFRC, MAP7	40	203	19662	9,68571	0,45421	0,261221	7,731398368
GOTERM_MF_DIRECT	GO:0000979~RNA polymerase II core promoter sequence-specific DNA binding	3	6,382978723	0,008414536	EGR1, FOS, TFAP2B	37	67	17446	21,1125	0,63724	0,223923	9,244568196
GOTERM_BP_DIRECT	GO:0007224~smoothened signaling pathway	3	6,382978723	0,008785887	FOXF1, HHIP, SHH	37	71	18082	20,6494	0,98909	0,475581	11,97094114
GOTERM_BP_DIRECT	GO:0060438~trachea development	2	4,255319149	0,009916184	FOXF1, SHH	37	5	18082	195,481	0,99392	0,471548	13,41021949
UP_KEYWORDS	Signal-anchor	5	10,63829787	0,010207455	PRR7, ATP1B1, HS3ST6, A4GALT, TFRC	45	439	22680	5,74032	0,58619	0,356721	10,47352044
INTERPRO	IPR003080:Glutathione S-transferase, alpha class	2	4,255319149	0,011021572	GSTA2, GM10639	39	6	20594	176,017	0,76061	0,510729	12,09264058
UP_KEYWORDS	DNA-binding	9	19,14893617	0,011073023	EGR1, FOS, EGR2, HOXB8, ELF5, FOXF1, TFAP2B, FOSB, NR1H5	45	1604	22680	2,82793	0,61618	0,273268	11,31414755
GOTERM_BP_DIRECT	GO:0097070~ductus arteriosus closure	2	4,255319149	0,011887917	FOXF1, TFAP2B	37	6	18082	162,901	0,99781	0,493556	15,86864396
GOTERM_BP_DIRECT	GO:0030323~respiratory tube development	2	4,255319149	0,011887917	FOXF1, SHH	37	6	18082	162,901	0,99781	0,493556	15,86864396
GOTERM_MF_DIRECT	GO:0044212~transcription regulatory region DNA binding	4	8,510638298	0,012138443	EGR1, FOS, EGR2, FOXF1	37	233	17446	8,09465	0,76904	0,254056	13,08101443
GOTERM_BP_DIRECT	GO:0060463~lung lobe morphogenesis	2	4,255319149	0,015819937	FOXF1, SHH	37	8	18082	122,176	0,99972	0,558005	20,57845866
INTERPRO	IPR000837:Fos transforming protein	2	4,255319149	0,016487913	FOS, FOSB	39	9	20594	117,345	0,88289	0,510754	17,5801672
GOTERM_BP_DIRECT	GO:0090090~negative regulation of canonical Wnt signaling pathway	3	6,382978723	0,017523849	EGR1, SHH, MLLT3	37	102	18082	14,3736	0,99988	0,560838	22,54219238
GOTERM_BP_DIRECT	GO:0007398~ectoderm development	2	4,255319149	0,017780238	ELF5, SHH	37	9	18082	108,601	0,9999	0,534875	22,83373446
GOTERM_BP_DIRECT	GO:0007626~locomotory behavior	3	6,382978723	0,019511312	ALDH1A3, GPRC5B, ESPN	37	108	18082	13,5751	0,99996	0,539776	24,77558339
UP_KEYWORDS	Nucleus	16	34,04255319	0,020150076	EGR1, EGR2, ELF5, CLU, FOSB, FOS, HOXB8, SRRM2, MAPK4, FOXF1, DCLK3, TFAP2B, RBM47, LDOC1, NR1H5, MLLT3	45	4534	22680	1,77856	0,82633	0,354449	19,70826317
GOTERM_BP_DIRECT	GO:0009952~anterior/posterior pattern specification	3	6,382978723	0,020886641	HOXB8, SHH, MLLT3	37	112	18082	13,0903	0,99998	0,537886	26,28584304
GOTERM_BP_DIRECT	GO:0048617~embryonic foregut morphogenesis	2	4,255319149	0,021689459	FOXF1, SHH	37	11	18082	88,855	0,99999	0,526915	27,15432901
KEGG_PATHWAY	mmu04380:Osteoclast differentiation	3	6,382978723	0,027502829	CALCR, FOS, FOSB	17	126	7691	10,7717	0,84989	0,612561	24,94171488
GOTERM_CC_DIRECT	GO:0072562~blood microparticle	3	6,382978723	0,028585778	AFM, TFRC, CLU	40	133	19662	11,0876	0,90174	0,538556	26,53259057
GOTERM_BP_DIRECT	GO:0006355~regulation of transcription, DNA-templated	10	21,27659574	0,031197243	EGR1, FOS, EGR2, HOXB8, ELF5, FOXF1, TFAP2B, FOSB, SHH, MLLT3	37	2279	18082	2,14437	1	0,637313	36,7409518
GOTERM_MF_DIRECT	GO:0003690~double-stranded DNA binding	3	6,382978723	0,03197398	EGR1, FOS, FOSB	37	136	17446	10,401	0,97975	0,477916	31,13593091

					TFRC, CLU, HHIP, GPRC5B,						
GOTERM_CC_DIRECT	GO:0009986~cell surface	5	10,63829787	0,035246641	SHH	40	629	19662	3,90739	0,94334	0,512105	31,71471481
GOTERM_BP_DIRECT	GO:0007405~neuroblast proliferation	2	4,255319149	0,037175627	HHIP, SHH	37	19	18082	51,4424	1	0,680496	42,15296842
GOTERM_BP_DIRECT	GO:0048557~embryonic digestive tract morphogenesis	2	4,255319149	0,041009773	FOXF1, SHH	37	21	18082	46,5431	1	0,696111	45,39360892
GOTERM_BP_DIRECT	GO:0051412~response to corticosterone	2	4,255319149	0,041009773	FOS, FOSB	37	21	18082	46,5431	1	0,696111	45,39360892
GOTERM_BP_DIRECT	GO:0031668~cellular response to extracellular stimulus	2	4,255319149	0,042921276	FOS, TFRC	37	22	18082	44,4275	1	0,693388	46,94532813
GOTERM_BP_DIRECT	GO:0060425~lung morphogenesis	2	4,255319149	0,046733175	FOXF1, SHH	37	24	18082	40,7252	1	0,706309	49,91797662
KEGG_PATHWAY	mmu04340:Hedgehog signaling pathway	2	4,255319149	0,048823328	HHIP, SHH	17	24	7691	37,701	0,96675	0,678446	40,24735994
GOTERM_CC_DIRECT	GO:0043005~neuron projection	4	8,510638298	0,050209429	CALCR, FOS, CLU, GABBR2	40	420	19662	4,68143	0,98377	0,561423	42,16935302
GOTERM_BP_DIRECT	GO:0010107~potassium ion import	2	4,255319149	0,050530311	KCNJ16, ATP1B1	37	26	18082	37,5925	1	0,717533	52,72437011
INTERPRO	IPR004046:Glutathione S-transferase, C-terminal	2	4,255319149	0,05568525	GSTA2, GM10639	39	31	20594	34,0678	0,99938	0,842415	48,64045529
GOTERM_BP_DIRECT	GO:0030316~osteoclast differentiation	2	4,255319149	0,056198459	CALCR, TFRC	37	29	18082	33,7036	1	0,739741	56,64239313
UP_KEYWORDS	Transcription regulation	8	17,0212766	0,056439909	EGR1, EGR2, HOXB8, ELF5, FOXF1, TFAP2B, NR1H5, MLLT3	45	1799	22680	2,24125	0,99324	0,63184	46,55187817
GOTERM_BP_DIRECT	GO:0032570~response to progesterone	2	4,255319149	0,05808052	FOS, FOSB	37	30	18082	32,5802	1	0,736049	57,87500063
INTERPRO	IPR004045:Glutathione S-transferase, N-terminal	2	4,255319149	0,059172258	GSTA2, GM10639	39	33	20594	32,0031	0,99962	0,792718	50,80323212
GOTERM_BP_DIRECT	GO:0071310~cellular response to organic substance	2	4,255319149	0,063704838	EGR1, EGR2	37	33	18082	29,6183	1	0,75445	61,36690051
GOTERM_BP_DIRECT	GO:0031016~pancreas development	2	4,255319149	0,063704838	FOXF1, SHH	37	33	18082	29,6183	1	0,75445	61,36690051
UP_KEYWORDS	Transcription	8	17,0212766	0,065128952	EGR1, EGR2, HOXB8, ELF5, FOXF1, TFAP2B, NR1H5, MLLT3	45	1859	22680	2,16891	0,99695	0,619132	51,62658965
GOTERM_MF_DIRECT	GO:0004364~glutathione transferase activity	2	4,255319149	0,06595331	GSTA2, GM10639	37	33	17446	28,5766	0,99972	0,689521	54,30681383
GOTERM_BP_DIRECT	GO:0002053~positive regulation of mesenchymal cell proliferation	2	4,255319149	0,071153162	FOXF1, SHH	37	37	18082	26,4164	1	0,779456	65,57747806
INTERPRO	IPR011042:Six-bladed beta-propeller, TolB-like	2	4,255319149	0,072995343	NHLRC4, HHIP	39	41	20594	25,7586	0,99994	0,803998	58,58287
GOTERM_BP_DIRECT	GO:0006351~transcription, DNA-templated	8	17,0212766	0,075011264	EGR1, EGR2, HOXB8, ELF5, FOXF1, TFAP2B, NR1H5, MLLT3	37	1885	18082	2,07407	1	0,784648	67,58658445
GOTERM_MF_DIRECT	GO:0000977~RNA polymerase II regulatory region sequence-specific DNA binding	3	6,382978723	0,07599868	EGR1, ELF5, FOXF1	37	221	17446	6,40064	0,99992	0,694445	59,64060867
GOTERM_BP_DIRECT	GO:0031623~receptor internalization	2	4,255319149	0,076701569	CALCR, TFRC	37	40	18082	24,4351	1	0,779817	68,43195137
GOTERM_MF_DIRECT	GO:0003677~DNA binding	8	17,0212766	0,080098749	EGR1, FOS, EGR2, HOXB8, ELF5, FOXF1, TFAP2B, FOSB	37	1847	17446	2,04229	0,99996	0,671489	61,64926853
INTERPRO	IPR010987:Glutathione S-transferase, C-terminal-like	2	4,255319149	0,081534136	GSTA2, GM10639	39	46	20594	22,9588	0,99998	0,791405	62,80861483
BIOCARTA	m_arenrf2Pathway:Oxidative Stress Induced Gene Expression Via Nrf2	2	4,255319149	0,085404637	GSTA2, FOS	7	19	1289	19,3835	0,95194	0,95194	54,39158299
GOTERM_BP_DIRECT	GO:0045597~positive regulation of cell differentiation	2	4,255319149	0,087701881	CLU, SHH	37	46	18082	21,2479	1	0,813331	73,45155647
GOTERM_BP_DIRECT	GO:0032870~cellular response to hormone stimulus	2	4,255319149	0,089522835	FOS, FOSB	37	47	18082	20,7959	1	0,809064	74,20700042
GOTERM_CC_DIRECT	GO:1903561~extracellular vesicle	2	4,255319149	0,092814329	ATP1B1, TFRC	40	49	19662	20,0633	0,99959	0,727134	64,49731645
GOTERM_BP_DIRECT	GO:0009953~dorsal/ventral pattern formation	2	4,255319149	0,093154149	HHIP, SHH	37	49	18082	19,947	1	0,811532	75,65412788
INTERPRO	IPR004827:Basic-leucine zipper domain	2	4,255319149	0,09503153	FOS, FOSB	39	54	20594	19,5575	1	0,800165	68,69321753
GOTERM_BP_DIRECT	GO:0007611~learning or memory	2	4,255319149	0,09677138	EGR1, EGR2	37	51	18082	19,1648	1	0,813813	77,02021095
GOTERM_BP_DIRECT	GO:0051591~response to cAMP	2	4,255319149	0,09677138	FOS, FOSB	37	51	18082	19,1648	1	0,813813	77,02021095

Table S7. Functional annotation by DAVID for genes with decreased expression in the microarray of E13.5 *Fgfr2cK*O ureters.

gene	genotype	biological replicates			mean	SD	normalized biological replicates			mean	SD	Student's t-test, unpaired
		#1	#2	#3			#1	#2	#3			
Bmp4	control	1	1.087	1.067	1.0513	0.0372	0.9512	1.0339	1.0149	1.0000	0.0354	p = 0.0002
	Fgfr2cKO	0.68	0.708	0.671	0.6863	0.0158	0.6468	0.6734	0.6382	0.6528	0.0150	
Elf5	control	1	0.737	0.873	0.8700	0.1074	1.1494	0.8471	1.0034	1.0000	0.1234	p = 0.0124
	Fgfr2cKO	0.553	0.494	0.547	0.5313	0.0265	0.6356	0.5678	0.6287	0.6107	0.0305	
Foxf1	control	1	1.107	1.046	1.0510	0.0438	0.9515	1.0533	0.9952	1.0000	0.0417	p = 0.0084
	Fgfr2cKO	0.542	0.797	0.65	0.6630	0.1045	0.5157	0.7583	0.6185	0.6308	0.0994	
Ptch1	control	1	1.143	1.153	1.0987	0.0699	0.9102	1.0404	1.0495	1.0000	0.0636	p = 0.0008
	Fgfr2cKO	0.574	0.502	0.615	0.5637	0.0467	0.5225	0.4569	0.5598	0.5130	0.0425	
Shh	control	1	0.758	1.092	0.9500	0.1409	1.0526	0.7979	1.1495	1.0000	0.1483	p = 0.0343
	Fgfr2cKO	0.342	0.264	0.689	0.4317	0.1847	0.3600	0.2779	0.7253	0.4544	0.1944	
Spry1	control	1	1.134	1.007	1.0470	0.0616	0.9551	1.0831	0.9618	1.0000	0.0588	p = 0.0039
	Fgfr2cKO	0.513	0.702	0.648	0.6210	0.0795	0.4900	0.6705	0.6189	0.5931	0.0759	

Table S8. RT-qPCR analysis of gene expression in E14.5 *Fgfr2cKO* ureters. The statistical significance was calculated by a two-tailed Student's t-test. SD, standard derivation.

Ratio ΔNP63⁺ cells to CDH1⁺ cells				
	Mean	SD	p-Value	
			Control (DMSO)	*Fgfr2cKO* (DMSO)
Control (DMSO) n=7	0.8825	0.0871		4.87E-05
Fgfr2cKO (DMSO) n=5	0.5224	0.0960	4.87E-05	
Fgfr2cKO (Pur-morphamine) n=5	0.7935	0.0665	0.0848	0.0008
Fgfr2cKO (BMP4) n=5	0.7490	0.1844	0.1214	0.0407
Fgfr2cKO (RA) n=5	0.2391	0.2458	1.12E-05	0.0217
Fgfr2cKO (BIO) n=5	0.4445	0.1354	4.38E-05	0.3246

Ratio of ALDH1A2⁺ individuals to all individuals			
	individuals analyzed	ALDH1A2⁺ individuals	ALDH1A2⁺ / ALDH1A2⁻
Ctrl (DMSO)	7	6	0.8571
Fgfr2cKO (DMSO)	6	1	0.1667
Fgfr2cKO (Pur-morphamine)	5	4	0.8
Fgfr2cKO (BMP4)	5	2	0.4
Fgfr2cKO (RA)	4	0	0
Fgfr2cKO (BIO)	5	1	0.2

Epithelial thickness (µm)				
	Mean	SD	p-Value	
			Control (DMSO)	*Fgfr2cKO* (DMSO)
Control (DMSO) n=7	75.13	11.13		0.0102
Fgfr2cKO (DMSO) n=5	49.24	4.27	0.0102	
Fgfr2cKO (Pur-morphamine) n=5	77.94	3.52	0.2292	6.48E-06
Fgfr2cKO (BMP4) n=5	76.84	8.10	0.3396	0.0003
Fgfr2cKO (RA) n=5	54.79	4.47	0.0448	0.1103
Fgfr2cKO (BIO) n=5	79.23	27.21	0.0330	0.0038

Mesenchymal thickness (µm)				
	Mean	SD	p-Value	
			Control (DMSO)	*Fgfr2cKO* (DMSO)
Control (DMSO) n=7	61.55	7.42		0.0001
Fgfr2cKO (DMSO) n=5	33.69	7.09	0.0001	
Fgfr2cKO (Pur-morphamine) n=5	56.25	4.51	0.2240	0.0007
Fgfr2cKO (BMP4) n=5	50.13	8.70	0.0496	0.0190
Fgfr2cKO (RA) n=5	37.25	13.28	0.0042	0.6487
Fgfr2cKO (BIO) n=5	38.00	8.00	0.0007	0.4430

Table S9. Pharmacological rescue experiments in explants of E13.5 *Fgfr2cKO* ureters cultured for 4 days. Quantification of the ratio of ΔNP63⁺ cells to CDH1⁺ cells, of individuals with ALDH1A2⁺ cells and of the thickness of the epithelial layer and the SMC layer. The statistical significance was calculated by a two-tailed Student's t-test. SD, standard derivation.

Ratio ΔNP63⁺ cells to CDH1⁺ cells									
	Mean	SD		p-Value					
				1 µM Cyclopamine	5 µM Cyclopamine	10 µM Cyclopamine	2.5 µg/ml NOGGIN	5 µg/ml NOGGIN	10 µg/ml NOGGIN
Control (DMSO) n=5	0.8253	0.0409	Ctrl DMSO	0.0735	2.83E-05	7.74E-05	0.0007	1.91E-07	7.26E-07
1 µM Cyclo-pamine (n=5)	0.7138	0.1141	1 µM Cyclopamine		0.0329	0.0294			
5 µM Cyclo-pamine (n=5)	0.5686	0.0538	5 µM Cyclopamine			0.7362			
10 µM Cyclo-pamine (n=5)	0.5547	0.0710	10 µM Cyclopamine						
2.5 µg/ml NOGGIN (n=5)	0.5335	0.1140	2.5 µg/ml NOGGIN					0.1085	0.0301
5 µg/ml NOGGIN (n=5)	0.4375	0.0335	5 µg/ml NOGGIN						0.1066
10 µg/ml NOGGIN (n=5)	0.3825	0.0589	10 µg/ml NOGGIN						

Ratio ΔNP63⁺ luminal cells to CDH1⁺ cells									
	Mean	SD		p-Value					
				1 µM Cyclopamine	5 µM Cyclopamine	10 µM Cyclopamine	2.5 µg/ml NOGGIN	5 µg/ml NOGGIN	10 µg/ml NOGGIN
Control (DMSO) n=5	0.1016	0.0419	Ctrl DMSO	0.1638	0.0003	0.0005	9.93E-05	5.42E-07	4.96E-04
1 µM Cyclo-pamine (n=5)	0.1575	0.0699	1 µM Cyclopamine		0.0309	0.0362			
5 µM Cyclo-pamine (n=5)	0.2495	0.0361	5 µM Cyclopamine			0.9368			
10 µM Cyclo-pamine (n=5)	0.2475	0.0392	10 µM Cyclopamine						
2.5 µg/ml NOGGIN (n=5)	0.3507	0.0659	2.5 µg/ml NOGGIN					0.0290	0.0342
5 µg/ml NOGGIN (n=5)	0.4373	0.0312	5 µg/ml NOGGIN						9.76E-05
10 µg/ml NOGGIN (n=5)	0.2588	0.0463	10 µg/ml NOGGIN						

Mesenchymal thickness (µm)									
	Mean	SD		p-Value					
				1 µM Cyclopamine	5 µM Cyclopamine	10 µM Cyclopamine	2.5 µg/ml NOGGIN	5 µg/ml NOGGIN	10 µg/ml NOGGIN
Control (DMSO) n=5	70.38	1.42	Ctrl DMSO	6.76E-09	1.21E-13	1.21E-13	0.7721	0.0003	0.0003
1 µM Cyclo-pamine (n=5)	25.31	3.29	1 µM Cyclopamine		3.20E-07	3.20E-07			
5 µM Cyclo-pamine (n=5)	0.00	0.00	5 µM Cyclopamine			nd			
10 µM Cyclo-pamine (n=5)	0.00	0.00	10 µM Cyclopamine						
2.5 µg/ml NOGGIN (n=5)	68.72	10.97	2.5 µg/ml NOGGIN					0.0090	0.0049
5 µg/ml NOGGIN (n=5)	45.13	8.31	5 µg/ml NOGGIN						1
10 µg/ml NOGGIN (n=5)	40.94	9.36	10 µg/ml NOGGIN						

Component	number of Individuals	number of ALDH1A2+ individuals	ratio ALDH1A2+ individuals / all individuals
Ctrl DMSO	5	5	100.00%
1 µM Cyclopamine	5	0	0.00%
5 µM Cyclopamine	5	0	0.00%
10 µM Cyclopamine	5	0	0.00%
2.5 µg/ml NOGGIN	5	5	100.00%
5 µg/ml NOGGIN	5	4	80.00%
10 µg/ml NOGGIN	5	2	40.00%

Table S10. Pharmacological inhibition of SHH and BMP4 signaling in explant cultures of E13.5 ureters. E13.5 wildtype ureters were cultured for 4 days with increasing concentrations of the SHH signaling inhibitor cyclopamine or the BMP4 antagonist NOGGIN. Quantification of the ratio of ΔNP63⁺ cells to CDH1⁺ cells, of the ratio of ΔNP63⁻ luminal cells to CDH1⁺ cells, of the thickness of the SMC layer and of individuals with ALDH1A2⁺ cells. The statistical significance was calculated by a two-tailed Student's t-test. SD, standard derivation. nd, not defined.

Gene	Forward primer	Reverse primer
Bmp4	5′-CACGAAGAACATCTGGAGAACA-3′	5′-GGTTGAAGAGGAAACGAAAAGC-3′
Elf5	5′-ACTGCATCTCCTTCTGTCACT-3′	5′-AGTAACCTTGCGAGCGAATG-3′
Foxf1	5′-CAAGGCATCCCTCGGTATCA-3′	5′-AGATCCTCCGCCTGTTGTATG-3′
Gapdh	5′-ATGACATCAAGAAGGTGGTG-3′	5′-CATACCAGGAAATGAGCTTG-3′
Ppia	5′-GATTCATGTGCCAGGGTGGT-3′	5′-GCCATTCAGTCTTGGCAGTG-3′
Ptch1	5′-CATCAAAGTGTCGCCCCAAA-3′	5′-AACAGGCATAGGCAAGCATC-3′
Shh	5′-AGCGGCAGATATGAAGGGAA-3′	5′-GTCTTTGCACCTCTGAGTCATC-3′
Spry1	5′-ACACTCAGCCTGCTACGATT-3′	5′-CCTTTCCTGCTTTTCGGGTC-3′

Table S11. List of primers for RT-qPCR analysis of gene expression in E13.5 *Fgfr2cKO* ureters.

Part 2 – Molecular function of FGFR2 in the development of the murine ureteric mesenchyme

Mesenchymal FGFR1 and FGFR2 control patterning of the ureteric mesenchyme by balancing SHH and BMP4 signaling

Lena Deuper[1], Max Meuser[1], Hauke Thiesler[2], Ullrich W. H. Jany[1], Carsten Rudat[1], Herbert Hildebrandt[2], Mark-Oliver Trowe[1] and Andreas Kispert[1,*].

[1]Institut für Molekularbiologie, Medizinische Hochschule Hannover, 30625 Hannover, Germany

[2]Klinik für Gastroenterologie, Hepatologie und Endokrinologie, Medizinische Hochschule Hannover, Hannover, Germany

*Correspondence to: Andreas Kispert, Institut für Molekularbiologie, OE5250, Medizinische Hochschule Hannover, Carl-Neuberg-Str. 1, D-30625 Hannover, Germany. Phone: +49 511 5324017, Fax: +49 511 5324283, E-Mail: kispert.andreas@mh-hannover.de

KEY WORDS: FGF, Patterning, Smooth muscle cells, Ureter, Lamina propria, SHH, BMP4

Type of authorship: First author
Type of article: Research article
Share of the work: 75%
Contribution to the publication: (co-) planned and performed experiments, analyzed data, prepared figures, assisted in writing the paper

Journal: Development
Impact factor: 6.862
Number of citations: 0
Date of publication: 19.08.2022
DOI: 10.1242/dev.200767

Permission

CCC Marketplace

This is a License Agreement between Lena Deuper ("User") and Copyright Clearance Center, Inc. ("CCC") on behalf of the Rightsholder identified in the order details below. The license consists of the order details, the Marketplace Order General Terms and Conditions below, and any Rightsholder Terms and Conditions which are included below.

All payments must be made in full to CCC in accordance with the Marketplace Order General Terms and Conditions below.

Order Date	26-Oct-2022	Type of Use	Republish in a thesis/dissertation
Order License ID	1283309-2	Publisher	COMPANY OF BIOLOGISTS,
ISSN	1477-9129	Portion	Chapter/article

LICENSED CONTENT

Publication Title	Development	Rightsholder	The Company of Biologists Ltd.
Article Title	Mesenchymal FGFR1 and FGFR2 control patterning of the ureteric mesenchyme by balancing SHH and BMP4 signaling	Publication Type	e-Journal
		Issue	17
		Volume	149
Author/Editor	Company of Biologists.	URL	http://dev.biologists.org/
Date	01/01/1987		
Language	English		
Country	United Kingdom of Great Britain and Northern Ireland		

REQUEST DETAILS

Portion Type	Chapter/article	Rights Requested	Main product
Page Range(s)	all	Distribution	Worldwide
Total Number of Pages	25	Translation	Original language of publication
Format (select all that apply)	Print, Electronic	Copies for the Disabled?	No
Who Will Republish the Content?	Author of requested content	Minor Editing Privileges?	No
		Incidental Promotional Use?	No
Duration of Use	Life of current edition		
Lifetime Unit Quantity	Up to 499	Currency	EUR

NEW WORK DETAILS

Title	Molecular control of murine ureter development - The function of FGF and BMP4 signaling	Institution Name	Gottfried Wilhelm Leibniz Universität Hannover
		Expected Presentation Date	2022-11-01
Instructor Name	Prof. Dr. rer. nat. Andreas Kispert		

ADDITIONAL DETAILS

Order Reference Number	N/A

The Requesting Person/Organization to Appear on the License	Lena Deuper

REUSE CONTENT DETAILS

Title, Description or Numeric Reference of the Portion(s)	Mesenchymal FGFR1 and FGFR2 control patterning of the ureteric mesenchyme by balancing SHH and BMP4 signaling	Title of the Article/Chapter the Portion Is From	Mesenchymal FGFR1 and FGFR2 control patterning of the ureteric mesenchyme by balancing SHH and BMP4 signaling
Editor of Portion(s)	Deuper, Lena; Meuser, Max; Thiesler, Hauke; Jany, Ulrich W. H.; Rudat, Carsten; Hildebrandt, Herbert; Trowe, Mark-Oliver; Kispert, Andreas	Author of Portion(s)	Deuper, Lena; Meuser, Max; Thiesler, Hauke; Jany, Ulrich W. H.; Rudat, Carsten; Hildebrandt, Herbert; Trowe, Mark-Oliver; Kispert, Andreas
Volume of Serial or Monograph	149	Issue, if Republishing an Article From a Serial	17
Page or Page Range of Portion	dev200767	Publication Date of Portion	2022-09-12

© 2022. Published by The Company of Biologists Ltd | Development (2022) 149, dev200767. doi:10.1242/dev.200767

RESEARCH ARTICLE

Mesenchymal FGFR1 and FGFR2 control patterning of the ureteric mesenchyme by balancing SHH and BMP4 signaling

Lena Deuper[1], Max Meuser[1], Hauke Thiesler[2], Ulrich W. H. Jany[1], Carsten Rudat[1], Herbert Hildebrandt[2], Mark-Oliver Trowe[1] and Andreas Kispert[1,*]

ABSTRACT

The coordinated development of the mesenchymal and epithelial progenitors of the murine ureter depends on a complex interplay of diverse signaling activities. We have recently shown that epithelial FGFR2 signaling regulates stratification and differentiation of the epithelial compartment by enhancing epithelial *Shh* expression, and mesenchymal SHH and BMP4 activity. Here, we show that FGFR1 and FGFR2 expression in the mesenchymal primordium impinges on the SHH/BMP4 signaling axis to regulate mesenchymal patterning and differentiation. Mouse embryos with conditional loss of *Fgfr1* and *Fgfr2* in the ureteric mesenchyme exhibited reduced mesenchymal proliferation and prematurely activated lamina propria formation at the expense of the smooth muscle cell program. They also manifested hydroureter at birth. Molecular profiling detected increased SHH, WNT and retinoic acid signaling, whereas BMP4 signaling in the mesenchyme was reduced. Pharmacological activation of SHH signaling in combination with inhibition of BMP4 signaling recapitulated the cellular changes in explant cultures of wild-type ureters. Additional experiments suggest that mesenchymal FGFR1 and FGFR2 act as a sink for FGF ligands to dampen activation of *Shh* and BMP receptor gene expression by epithelial FGFR2 signaling.

KEY WORDS: FGF, Patterning, Smooth muscle cells, Ureter, Lamina propria, SHH, BMP4

INTRODUCTION

The ureters are a pair of straight tubes that account by means of peristaltic contractions for the active transport of urine from the renal pelvises to the bladder. The structural basis for this activity is an outer mesenchymal tissue compartment with a three-layered organization of fibroelastic material on the inside (the lamina propria) and outside (the tunica adventitia), and contractile smooth muscle cells (SMCs) in the middle (the tunica muscularis) (Velardo, 1981). This ordered arrangement of fibrocytes and SMCs is the result of a complex interplay of proliferation, patterning and differentiation processes that occurs in the common progenitor pool of these cell types. In the mouse, ureteric mesenchyme (UM) progenitors are first recognized around embryonic day (E) 11.0 as a homogenous population of *Tbx18*$^{+}$ mesenchymal cells. These cells surround the distal aspect of the epithelial ureteric bud, the primordium of the specialized three-layered inner epithelial lining of the ureter, the urothelium (Bohnenpoll et al., 2013). The mesenchymal cells directly adjacent to the ureteric epithelium (UE) acquire at E12.5 a rhomboid shape, express at E14.5 *Myocd*, the master regulator of SMC differentiation (Wang et al., 2001; Wang and Olson, 2004), and activate until birth a cascade of SMC structural genes. Notably, from E14.5 to E16.5 some of these cells switch off *Myocd* expression, populate the region between the committed SMCs and the UE, multiply and start to produce abundant extracellular matrix to form the lamina propria. The cells in the outer layer of the UM retain their loose organization and differentiate from E13.5 onwards into adventitial fibrocytes (Bohnenpoll et al., 2017a).

Proliferation, patterning and SMC differentiation of the UM depends on signals from the adjacent UE (Baskin et al., 1996; Bohnenpoll and Kispert, 2014; Cunha, 1976), of which SHH and WNTs have been characterized as essential. *Shh* is expressed from E11.5 to E14.5 in the UE and activates SMO-dependent signaling in the adjacent UM to assure survival in the outer region, and proliferation and SMC differentiation in the inner region. The latter functions are mediated by the transcription factor FOXF1 and the signaling molecule BMP4 (Bohnenpoll et al., 2017c; Yu et al., 2002). BMP4 also acts *in trans* to activate proliferation, stratification and differentiation of the UE (Mamo et al., 2017). Epithelial WNTs suppress the outer adventitial fate and foster SMC differentiation, at least partly through induction of the transcriptional repressors TBX2 and TBX3 (Aydoğdu et al., 2018; Trowe et al., 2012). SMC differentiation is negatively impacted by retinoic acid (RA), which is produced by ALDH1A2 in the UM and by ALDH1A1 and ALDH1A3 in the UE (Bohnenpoll et al., 2017b). How these signaling pathways are temporally and spatially regulated and integrated to activate *Myocd* and the SMC program in the inner layer of the UM precisely at E14.5 is not known but feed-forward and feed-back mechanisms are central (Meuser et al., 2022; Weiss et al., 2019). Insight into this regulatory network is important because defects in SMC differentiation present a relevant subgroup of human congenital anomalies of the kidney and the urinary tract (Capone et al., 2017).

Fibroblast growth factors (FGFs) are a family of more than 20 secreted proteins that bind with high affinity to at least four members of a family of receptor tyrosine kinases, termed FGFR1-FGFR4. Ligand-receptor interaction activates downstream modules to trigger changes of cell behavior in a variety of biological contexts in both a transcriptionally dependent and independent manner (Laestander and Engström, 2014; Ornitz and Itoh, 2015). Signaling through FGFR1 and FGFR2 has been implicated in the development of numerous tissues and organs, including those of the excretory system (Walker et al., 2016). We have recently shown that *Fgf7* and *Fgf10* are expressed in the UM from E11.5 to E14.5.

[1]Institute of Molecular Biology, Medizinische Hochschule Hannover, 30625 Hannover, Germany. [2]Institute of Clinical Biochemistry, Medizinische Hochschule Hannover, 30625 Hannover, Germany.

*Author for correspondence (kispert.andreas@mh-hannover.de)

M.M., 0000-0001-9621-1889; U.W.H.J., 0000-0003-4506-3817; C.R., 0000-0002-8877-7767; H.H., 0000-0002-1044-0881; M.-O.T., 0000-0002-0011-461X; A.K., 0000-0002-8154-0257

Handling Editor: Liz Robertson
Received 18 March 2022; Accepted 19 August 2022

Development (2022) 149, dev200767. doi:10.1242/dev.200767

Fgfr1 and *Fgfr2* which encode the cognate receptors for these ligands (Igarashi et al., 1998; Jans, 1994), are expressed in the UE at these stages (Meuser et al., 2022). Conditional deletion of *Fgfr2* in the UE resulted in a defect in urothelial stratification and lack of intermediate and basal cell differentiation as well as in delayed SMC and lamina propria differentiation due to a reduction of *Shh* expression and SHH/BMP4 signaling (Meuser et al., 2022). *Fgfr1* and *Fgfr2* are also expressed in the UM at E12.5 and E14.5 (Meuser et al., 2022), indicating a functional relevance for the development of this tissue. Defects in mesenchymal patterning and SMC differentiation in bladders that specifically lack *Fgfr2* in the mesenchymal compartment support this notion (Ikeda et al., 2017).

Here, we used a conditional gene targeting strategy to analyze *Fgfr1* and *Fgfr2* function in the mouse UM. We show that *Fgfr1* and *Fgfr2* maintain the structural and functional integrity of the ureter by patterning the mesenchymal tissue. We provide evidence that mesenchymal FGFR1 and FGFR2 balance SHH and BMP4 signaling by limiting the activation of epithelial FGFR2 signaling.

RESULTS

Loss of *Fgfr1* and *Fgfr2* in the UM leads to hydroureter formation at birth

Fgfr1 and *Fgfr2* are expressed in the epithelial and mesenchymal compartment of the developing ureter at E12.5 and (very weakly) at E14.5 (Fig. S1A). To investigate the mesenchymal function of *Fgfr1* and *Fgfr2* in this organ rudiment, we used a conditional gene inactivation approach with floxed alleles of *Fgfr1* and *Fgfr2* (Hoch and Soriano, 2006; Yu et al., 2003), and a $Tbx18^{cre}$ line that mediates recombination in the UM starting from E10.5 (Airik et al., 2010; Bohnenpoll et al., 2013).

Matings of $Tbx18^{cre/+}$;$Fgfr1^{fl/+}$;$Fgfr2^{fl/+}$ males with $Fgfr1^{fl/fl}$;$Fgfr2^{fl/fl}$ females gave rise to offspring with a normal distribution of all mutant genotypes and with a normal external appearance at all embryonic stages analyzed (Table S1). Morphological inspection of preparations of whole urogenital systems at E18.5, however, revealed hydroureter in 50% of $Tbx18^{cre/+}$;$Fgfr1^{fl/+}$;$Fgfr2^{fl/+}$, in 64% of $Tbx18^{cre/+}$;$Fgfr1^{fl/fl}$;$Fgfr2^{fl/+}$ and in 100% of the mutants with complete loss of *Fgfr2* function ($Tbx18^{cre/+}$;$Fgfr1^{fl/+}$;$Fgfr2^{fl/fl}$, $Tbx18^{cre/+}$;$Fgfr1^{fl/fl}$;$Fgfr2^{fl/fl}$). In the latter two combinations, a shift from mild to strong hydroureter was observed in approximately 20% of the cases (Table S2, Fig. S2, Fig. 1A). This argues for an additive contribution of mutant *Fgfr1* and *Fgfr2* alleles to the observed phenotype with *Fgfr2* being more important. In mutants with complete loss of *Fgfr2* function, the adrenals were drastically reduced in size (Fig. 1A, Fig. S2). We have recently shown that this phenotype relates to a function of *Fgfr2* in expansion of adrenogonadal progenitors in which $Tbx18^{cre}$ also mediates recombination (Hafner et al., 2015).

Given the more robust and severe phenotype of mutants with complete loss of *Fgfr1* and *Fgfr2* function, we concentrated on $Tbx18^{cre/+}$;$Fgfr1^{fl/fl}$;$Fgfr2^{fl/fl}$ (*Fgfr1/2cDKO-UM*) embryos for further analysis. Littermates without the $Tbx18^{cre}$ allele were used as controls. Histological inspection of the urogenital system of *Fgfr1/2cDKO-UM* embryos confirmed the presence of a dilated ureter, which at this stage, however, did not translate into hydronephrotic lesions, i.e. dilatation of the renal pelvis and the renal collecting duct system (Fig. 1B). Ureter dilatation can be caused by physical obstruction along the ureter and/or its junction with the bladder or by functional insufficiency of the peristaltic activity of the mesenchymal wall. To interrogate the first option, we injected ink into the renal pelvis. We observed in all mutants, as in the control, a smooth flow of the ink into the bladder (Fig. 1C). Moreover, histological analysis showed a normal insertion of the distal ureter into the dorsal bladder wall (Fig. 1D, arrows). To test for functional insufficiency, we analyzed proximal ureter sections of E18.5 *Fgfr1/2cDKO-UM* embryos for the presence of SMCs. Considering the dilatation of the ureter, markers of this differentiated cell type appeared either unchanged (ACTA2, TAGLN, *Myocd*, *Myh11*), or weakly (*Tnnt2*, *Tagln*, *Actg2*) or strongly (*Ckm*) reduced in their expression (Fig. 1E,F). Expression of *Aldh1a2*, a marker for fibrocytes of the inner lamina propria,

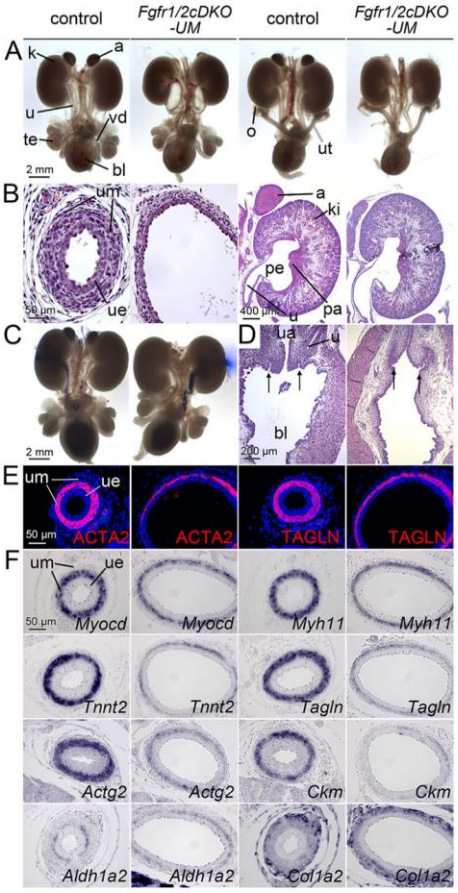

Fig. 1. Ureter anomalies in E18.5 embryos with conditional loss of *Fgfr1* and *Fgfr2* in the UM (*Fgfr1/2cDKO-UM*). (A) Morphology of whole urogenital systems of male (column 1, control: *n*=18; column 2, mutant: *n*=5) and female (column 3, control: *n*=13; column 4, mutant: *n*=4) embryos. (B) Hematoxylin and Eosin staining of transverse sections of the proximal ureter (columns 1 and 2) and of sagittal kidney sections (columns 3 and 4). *n*=3 for all genotypes. (C,D) Analysis of the vesico-ureteric junction by ink injection (control: *n*=8; mutant: *n*=6) (C) and by Hematoxylin and Eosin staining of sagittal bladder sections (control: *n*=3; mutant: *n*=3) (D). Arrows in D indicate the openings of the ureters into the bladder. (E) Immunofluorescence analysis of expression of the SMC proteins ACTA2 and TAGLN on transverse sections of the proximal ureter. Nuclei are counterstained (in blue) with DAPI. (F) Analysis of the expression of markers of SMCs (*Myocd*, *Myh11*, *Tnnt2*, *Tagln*, *Actg2*, *Ckm*), the lamina propria (*Aldh1a2*) and the tunica adventitia (*Col1a2*) by RNA *in situ* hybridization on transverse sections of the proximal ureter. *n*≥3 for all probes and genotypes in D,E. a, adrenal; bl, bladder; k/ki, kidney; o, ovary; pa, papilla; pe, pelvis; te, testis; u, ureter; ua, urethra; ue, ureteric epithelium; um, ureteric mesenchyme; ut, uterus; vd, vas deferens.

Development (2022) 149, dev200767. doi:10.1242/dev.200767

appeared increased in the mutant, whereas *Col1a2*, a marker for outer adventitial fibrocytes, was unchanged (Fig. 1F), again taking the ureter dilatation into account.

Urothelial differentiation was unaffected as revealed by normal expression of KRT5, ΔNP63 and UPK1B, which combinatorially mark basal cells ($KRT5^{+}\Delta NP63^{+}UPK1B^{-}$), intermediate cells ($KRT5^{-}\Delta NP63^{+}UPK1B^{+}$) and superficial cells ($KRT5^{-}\Delta NP63^{-}UPK1B^{+}$) (Bohnenpoll et al., 2017a) (Fig. S3). Together, this argues for defects in SMC differentiation as cause of hydroureter in *Fgfr1/2cDKO-UM* embryos.

Fgfr1/2cDKO-UM ureters exhibit a delay in SMC differentiation and premature lamina propria formation

To define the onset as well as the progression of the mesenchymal differentiation defects, we performed marker analysis at earlier stages of ureter development (Fig. 2). In the control, *Myocd* was strongly activated in the inner layer of the UM at E14.5. *Myh11*, *Tagln*, *Actg2*, ACTA2 and TAGLN followed at E15.5; *Tnnt2* and *Ckm* at E16.5. In *Fgfr1/2cDKO-UM* ureters, all of these markers were very weakly activated at the respective time points and/or were strongly reduced when dilatation occurred at E16.5. *Aldh1a2* was weakly expressed in the entire UM in the control at E14.5 but vanished subsequently. In the mutant, strong expression of *Aldh1a2* was found in the inner layer of the UM from E14.5 to E16.5 (Fig. 2A, arrows). Expression of *Col1a2* was unchanged. Epithelial differentiation was unaffected as indicated by normal activation of ΔNP63 at E14.5, of UPK1B at E15.5 and of KRT5 in few cells of the basal layer of the UE at E16.5 (Fig. S4).

Histological staining detected a normal subdivision of the mutant UM into an inner condensed and an outer loosely organized layer at E12.5 and E14.5 (Fig. S5A). The terminal deoxynucleotidyl transferase dUTP nick end labeling (TUNEL) assay did not expose changes in apoptosis in the UM at either stage (Fig. S5B). In contrast, a 5-bromo-2′-deoxyuridine (BrdU) incorporation assay

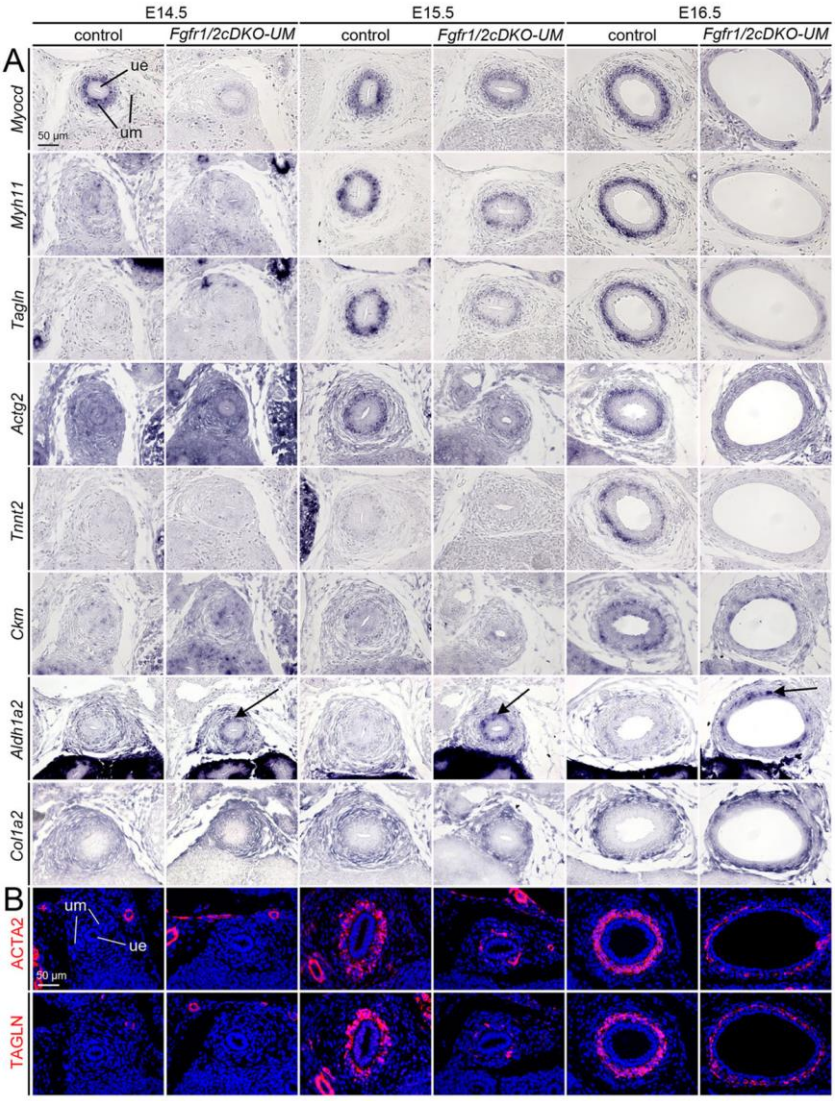

Fig. 2. Early onset of mesenchymal differentiation defects in *Fgfr1/2cDKO-UM* ureters. (A,B) Expression analysis on transverse sections of the proximal ureter region of E14.5, E15.5 and E16.5 embryos for markers of SMCs (*Myocd*, *Myh11*, *Tagln*, *Actg2*, *Tnnt2*, *Ckm*), the lamina propria (*Aldh1a2*) and the tunica adventitia (*Col1a2*) by RNA *in situ* hybridization analysis (A) and for the SMC proteins ACTA2 and TAGLN by immunofluorescence (B). Nuclei are counterstained (in blue) with DAPI in B. Note that *Aldh1a2* is ectopically activated in the inner layer of the UM (arrows). $n \geq 3$ for all probes, genotypes and assays. ue, ureteric epithelium; um, ureteric mesenchyme.

RESEARCH ARTICLE

Development (2022) 149, dev200767. doi:10.1242/dev.200767

revealed reduced proliferation in the inner layer of the UM of mutant embryos at E12.5 (Fig. S5C,D, Table S3). Hence, mesenchymal *Fgfr1* and *Fgfr2* function is required to maintain proliferation in the inner layer of the undifferentiated UM, to suppress lamina propria development and to activate the SMC program in a timely manner.

Delayed onset and compromised progression of peristalsis in *Fgfr1/2cDKO-UM* ureters

As SMC differentiation underlies the peristaltic activity of the ureter, a delayed onset and/or compromised progression of this program may translate into delayed or altered ureter contractions. We tested this hypothesis, by explanting ureters at E13.5 and scoring for peristaltic activity during 8 days of culture (Fig. 3). Wild-type ureters initiated contractions at day 3 of the culture and increased in frequency to 3.5 contractions per minute until day 8 (Fig. 3A,B). Mutant ureters started contractions at day 4 or 5 in culture (Fig. 3A, Table S4A); the contraction frequency was reduced by 50% at day 5 and by 20% at day 8 (Fig. 3B, Table S4B). The contraction intensity was markedly diminished throughout the culture period (Fig. 3C, Table S4C).

Fgfr1/2cDKO-UM ureters explanted at E15.5 behaved similarly. Onset of peristaltic activity was delayed by 2 days, and contraction frequency and intensity were reduced but approached the level of the control at the end of the culture period after 6 days (Fig. S6, Table S5). To investigate whether the SMC phenotype is still compromised at this endpoint, we performed global analysis of transcriptional changes using microarray technology. Using a fold change of at least 1.5 and an intensity threshold of 100 as additional filter, we identified 189 genes that were consistently upregulated and 201 genes that were downregulated in *Fgfr1/2cDKO-UM* ureters (Tables S6 and S7; GEO submission GSE197368). Functional annotation using the DAVID webtool did not uncover any terms related to 'muscle' or 'contraction' in the list of upregulated genes (Tables S8 and S9), and 'regulation of cardiac muscle contraction' at position 97 only in the list of downregulated genes. Manual inspection identified downregulation of the SMC structural genes *Myh6* (−5.0) and *Ckm* (−4.1; it was not detected owing to an intensity <100 in one of the two pools), whereas other SMC-specific genes (*Actg2*, *Acta2*, *Cnn1*, *Myh11*, *Myocd*, *Pcp4l1*, *Tagln*, *Tnnt2*) were unchanged. Expression analysis confirmed downregulation of *Ckm*; *Myh6* provided only unspecific staining. All other SMC markers were unchanged in 6-day explant cultures of E15.5 *Fgfr1/2cDKO-UM* ureters (Fig. S7). Hence, loss of *Fgfr1 and Fgfr2* in the UM does not abrogate SMC differentiation, but delays and partially compromises it. Contraction frequency and intensity can be largely recovered in *ex vivo* culture conditions in the absence of hydrostatic pressure. Interestingly, we found increased and widened expression of *Aldh1a2*/ALDH1A2 (Fig. S7), indicating an expansion of the lamina propria in *ex vivo* conditions.

Altered signaling activities in the UM of *Fgfr1/2cDKO-UM* embryos

We next performed transcriptional profiling by microarray analysis of E14.5 *Fgfr1/2cDKO-UM* and control ureters to identify molecular changes that may underlie the observed cellular defects. Using an intensity threshold of 100 and fold changes of

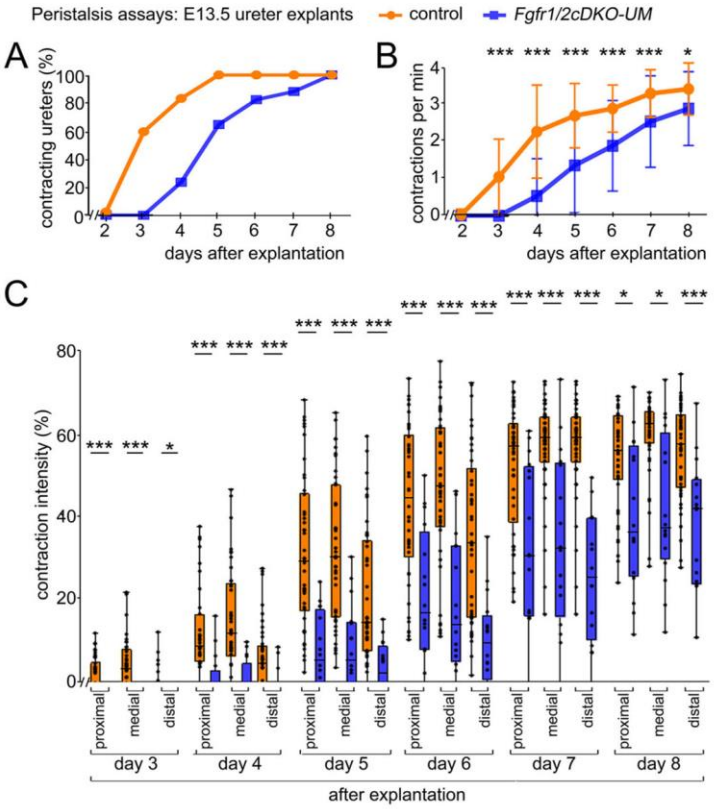

Fig. 3. SMC differentiation and peristaltic activity are delayed but not abrogated in *Fgfr1/2cDKO-UM* ureters. (A-C) E13.5 ureters (control: *n*=42; *Fgfr1/2cDKO-UM*: *n*=17) were explanted and peristaltic activity observed for 8 days in culture. (A) Graph showing the percentage of contracting ureters at any time point of the culture. (B) Graph of the contraction frequency (per min). Values are shown as mean±s.d. (C) Box blot visualizing the contraction intensity. The horizontal line indicates the median. A box contains 50% of all values. Whiskers contain 25% of all values each. Upper and lower whisker borders mark the maximum or minimum value, respectively. **P*<0.05, ****P*<0.001 (two-tailed Student's *t*-test). For detailed values, see Table S4.

RESEARCH ARTICLE

Development (2022) 149, dev200767. doi:10.1242/dev.200767

at least 1.25 in the four individual arrays performed, we identified 148 genes that were consistently downregulated and 170 genes that were upregulated in *Fgfr1/2cDKO-UM* ureters (Fig. 4A, Tables S10, S11; GEO submission GSE197369).

Clustering of functional annotation by DAVID did not reveal enriched terms related to relevant molecular pathways in the list of downregulated genes (Table S12). However, manual inspection of the list (Table S10) found strongly decreased expression of the superficial cell marker *Upk1b* (−3.4), as well as of *Grhl3* (−1.6), which encodes a transcription factor essential for superficial cell differentiation (Yu et al., 2009). *In situ* hybridization analysis confirmed reduced expression of these genes as well as of other UPK genes in the UE of E14.5 *Fgfr1/2cDKO-UM* embryos (Fig. S8).

For the list of upregulated genes, functional annotation clustering found terms related to SHH/SMO signaling as the top-enriched, and related to WNT signaling at position 7 (Fig. 4B, Table S13). Manual inspection of this list identified *Shh* and known targets of its activity in the UM (*Foxl1*, *Foxf1*, *Foxf2*, *Hhip*, *Ptch1*, *Ptch2*) as well as *Wnt9b* and direct targets of WNT signaling activity in the UM (*Sp5*,

A

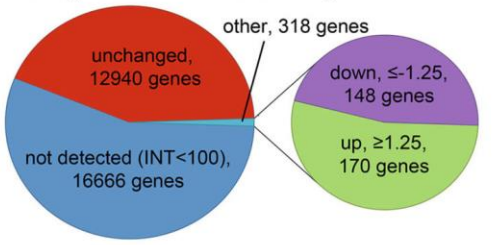

B

Functional annotation clustering for upregulated genes in E14.5 *Fgfr1/2cDKO* ureters

Cluster	Enrichment	Category	Term	P-Value
1	3.22	KEGG_PATHWAY	Hedgehog signaling pathway	3.2E-05
2	2.95	UP_KEYWORDS	Glycoprotein	1.4E-07
3	2.6	INTERPRO	Thrombospondin, type 1 repeat	9.6E-05
4	2.41	GOTERM_CC_DIRECT	proteinaceous extracellular matrix	5.5E-04
5	2.12	GOTERM_BP_DIRECT	cell-cell signaling	1.3E-04
6	2.08	INTERPRO	EGF-like, conserved site	7.2E-05
7	1.94	GOTERM_BP_DIRECT	Wnt signaling pathway	5.5E-03
8	1.89	SMART	EGF	1.7E-03
9	1.84	UP_KEYWORDS	Cell junction	1.7E-03
10	1.75	UP_KEYWORDS	Lipoprotein	6.4E-03

C

Microarray analysis of transcriptional changes in signaling systems in E14.5 *Fgfr1/2cDKO-UM* ureters

relates to	Gene Symbol	FC 1	FC 2	FC 3	FC 4	averageFC
SHH signaling	*Foxl1*	2.1	2.1	1.6	1.9	1.9
	Foxf1	1.5	2.1	1	1.6	1.6
	Ptch1	1.6	1.4	1.5	1.4	1.5
	Ptch2	1.5	1.5	1.4	1.4	1.4
	Hhip	1.6	1.3	1.4	1.8	1.5
	Shh	3.2	1.3	1.5	1.3	1.8
WNT signaling	*Axin2*	2.1	1.7	1.5	1.7	1.8
	Sp5	4.5	5.2	2.3	2.9	3.8
	Wnt7b	1	1.5	1	1.2	1.2
	Wnt9b	2.4	2.6	1.6	1.4	2
RA signaling	*Aldh1a1*	2	2	1.6	1.2	1.7
	Aldh1a2	1.4	1.4	1.4	1.1	1.3
	Aldh1a3	4.7	5.7	3.3	4.1	4.5
	Cyp26a1	1.8	1.9	1.9	2.3	2
	Ecm1	1.3	1.7	1.3	1.8	1.5
	Elf5	1.6	1.6	1.5	1.6	1.6
BMP4 signaling	*Bmp4*	1.2	1.1	1.1	1.3	1.2
	Id2	1	-1.2	1.1	1	1
	Id4	1.2	-1.3	-1.2	1.1	1

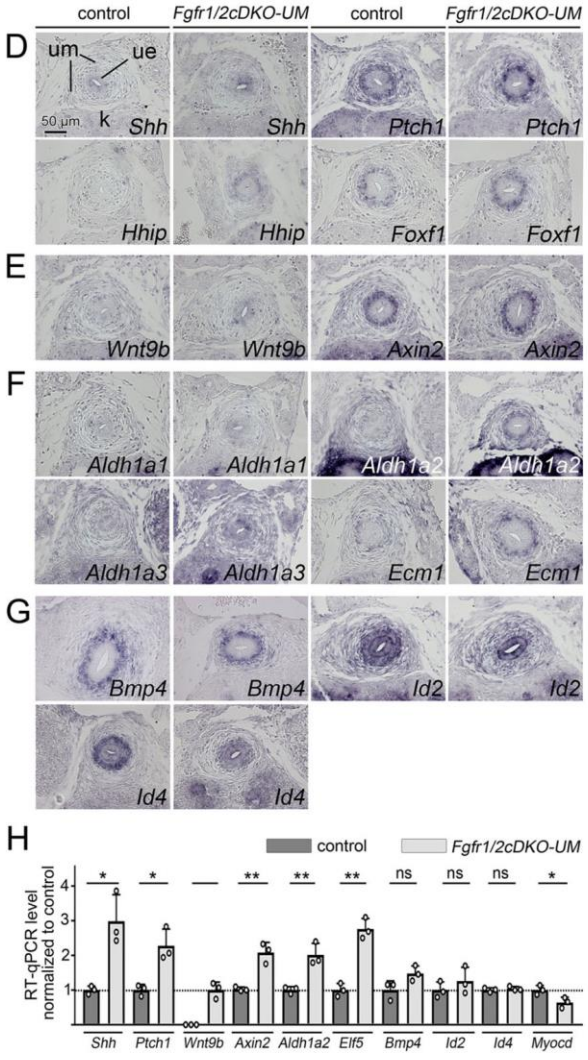

Fig. 4. Altered signaling activities in *Fgfr1/2cDKO-UM* ureters. (A) Pie chart summarizing the results from the microarray analysis of E14.5 control and *Fgfr1/2cDKO-UM* ureters. (B) Functional annotation clustering by DAVID for upregulated genes in the microarrays of E14.5 *Fgfr1/2cDKO-UM* ureters. (C) Changes of signaling components and activities in microarrays of E14.5 *Fgfr1/2cDKO-UM* and control ureters. Shown are the fold changes (FC) of four individual microarrays and the average FC. (D-G) RNA *in situ* hybridization analysis on transverse sections of E14.5 *Fgfr1/2cDKO-UM* and control ureters for expression of components and/or targets of SHH (D), WNT (E), RA (F) and BMP4 (G) signaling. $n \geq 3$ for each probe and genotype. k, kidney; ue, ureteric epithelium; um, ureteric mesenchyme. (H) RT-qPCR results for expression of genes encoding components and targets of SHH signaling (*Shh*, *Ptch1*), WNT signaling (*Wnt9b*, *Axin2*), RA signaling (*Aldh1a2*, *Elf5*), BMP4 signaling (*Bmp4*, *Id2*, *Id4*) and of *Myocd* in three independent RNA pools of E14.5 control and *Fgfr1/2cDKO-UM* ureters. Note that *Wnt9b* expression was normalized to the mutant because expression was not detectable in the control. *$P \leq 0.05$; **$P \leq 0.01$ (two-tailed Student's *t*-test). ns, not significant ($P > 0.05$). Values are shown as mean±s.d. For values and statistics, see Table S14A.

Development (2022) 149, dev200767. doi:10.1242/dev.200767

Axin2) (Bohnenpoll et al., 2017c; Trowe et al., 2012). Furthermore, genes encoding RA-synthesizing enzymes (*Aldh1a1*, *Aldh1a2*, *Aldh1a3*) were upregulated, as were direct targets of RA signaling activity in the UM (*Cyp26a1*, *Ecm1*) and in the UE (*Elf5*) (Bohnenpoll et al., 2017b). The effector gene of both SHH and WNT signaling, *Bmp4* (Bohnenpoll et al., 2017c; Mamo et al., 2017), was weakly upregulated (+1.2), whereas the direct target genes *Id2* and *Id4* (Hollnagel et al., 1999; Liu and Harland, 2003) were unchanged (Fig. 4C).

RNA *in situ* hybridization analysis confirmed increased expression of components and targets of SHH, WNT and RA signaling activity in E14.5 *Fgfr1/2cDKO-UM* ureters (Fig. 4D-F). Expression of *Bmp4* appeared unchanged whereas *Id2* and *Id4* expression was reduced in the UM (Fig. 4G).

Given that RNA *in situ* hybridization detected only weak expression changes, we performed reverse transcription-quantitative polymerase chain reaction (RT-qPCR) analysis for additional validation and quantification. We found an almost threefold increased expression of *Shh*, and a twofold increase of *Ptch1*. *Wnt9b*, *Axin2*, *Aldh1a2* and *Elf5* exhibited increased mRNA expression as well. *Bmp4* expression was unchanged, as was expression of *Id2* and *Id4*. The latter may reflect opposing changes of BMP4 signaling in the UE and UM. *Myocd* expression was significantly reduced (Fig. 4H, Table S14A). We conclude from these three independent assays that SHH, WNT and RA signaling are increased whereas BMP4 signaling is reduced in the mesenchymal compartment of *Fgfr1/2cDKO-UM* ureters at E14.5.

Mesenchymal FGFR1 and FGFR2 may act as a sink for FGF ligands

We recently reported that loss of epithelial *Fgfr2* expression leads to a decrease of *Shh* expression and of SHH, WNT and RA signaling activity in E14.5 ureters (Meuser et al., 2022), i.e. to molecular changes opposite to those found here for the mesenchymal knockout of *Fgfr1* and *Fgfr2*. In fact, the comparison of the list of genes with decreased expression in the epithelial *Fgfr2* knockout (*Pax2cre/+;Fgfr1*$^{fl/+}$*;Fgfr2*$^{fl/fl}$; *Fgfr1/2cDKO-UE*; note that *Fgfr1* was also deleted because of the chosen breeding strategy, but did not contribute to the described cellular and molecular changes) (Table S15) with that of genes with increased expression in the mesenchymal deletion of these receptor genes (*Tbx18*$^{cre/+}$*;Fgfr1*$^{fl/fl}$*;Fgfr2*$^{fl/fl}$; *Fgfr1/2cDKO-UM*) (Table S11) presented here, delivered an overlap of 47 genes (Fig. 5A). This overlap contained *Shh* and targets of its activity (*Hhip*, *Ptch1*, *Ptch2*), but also *Aldh1a3* and *Wnt9b*, suggesting that the increase of *Shh* expression, and of SHH, RA and WNT signaling is due to increased epithelial FGFR2 signaling in *Fgfr1/2cDKO-UM* ureters (Fig. 5B).

To substantiate this hypothesis, we analyzed expression of known direct targets of FGFR signaling, namely *Spry1* (Hanafusa et al., 2002) (microarray: +1.3) as well as *Etv4* and *Etv5* (Firnberg and Neubüser, 2002; Liu et al., 2003) (microarray: +1.2) in E14.5 *Fgfr1/2cDKO-UM* ureters by RNA *in situ* hybridization on sections. In fact, we found increased expression of *Spry1* in the UE. Mesenchymal expression of *Spry1* was not detected by this method (Fig. S9A). Section *in situ* hybridization was not sensitive enough to detect specific expression of *Etv4* and *Etv5* in the ureter at this stage, whereas in whole-mounts of E13.5 ureters cultured for 36 h an epithelial expression was apparent (Fig. S9B,C). Notably, expression of *Fgfr1* and *Fgfr2* appeared unchanged in the UE of E14.5 *Fgfr1/2cDKO-UM* embryos (Fig. S9D). RT-qPCR analysis confirmed increased expression of *Spry1*, *Etv4* and *Etv5*, with the latter reaching significance (Fig. 5C, Table S14B).

It is conceivable that in *Fgfr1/2cDKO-UM* ureters FGF ligands normally bound by the mesenchymal receptors excessively bind to epithelial FGFR2, thereby overactivating FGF signaling and, hence, *Shh* expression in the UE. We tested this hypothesis by treating explant cultures of E12.5 wild-type ureters for 18 h with 100 ng/µl of FGF10, the major ligand of FGFR2 (Igarashi et al., 1998; Jans, 1994). RT-qPCR detected an almost twofold increase in expression of *Shh*. Importantly, upon loss of *Fgfr1 and Fgfr2* in the epithelial compartment (in *Fgfr1/2cDKO-UE* ureters), *Shh* expression was reduced to 50% and could not be increased by FGF10, validating that FGF10 controls *Shh* expression via epithelial FGFR2 signaling (Fig. 5D, Table S14C).

Our *in situ* hybridization analysis revealed a decrease of mesenchymal expression of *Id2* and *Id4*, target genes of BMP4 signaling. We wondered whether altered expression of BMPR genes underlies this change. RNA section *in situ* hybridization analysis (with extended color development) provided the impression that *Bmpr1a*, *Bmpr1b* and *Bmpr2* exhibit increased expression in the epithelial compartment in *Fgfr1/2cDKO-UM* ureters at E14.5, but the level of expression of all of these genes was extremely low, making detection of changes by this method challenging (Fig. S9E). However, RT-qPCR analysis detected a 1.5-fold increase of expression of *Bmpr1a*, *Bmpr1b* and *Bmpr2* in E14.5 *Fgfr1/2cDKO-UM* ureters (Fig. 5E, Table S14D) and a 50% decrease in expression in *Fgfr1/2cDKO-UE* ureters at E14.5 (Fig. 5F, Table S14E). Moreover, E12.5 wild-type ureters cultured for 18 h with 100 ng/µl of FGF10 showed a slight but significant increase of *Bmpr1b* and *Bmpr2* expression (Fig. 5G, Table S14F). Together, this suggests that expression of BMPR genes in the UE is enhanced by epithelial FGFR2 signaling, which, in turn, is controlled by the amount of free FGF ligand, i.e. ligand not bound to mesenchymal FGFR1 and FGFR2.

A combination of increased SHH signaling and decreased BMP4 signaling recapitulates the phenotypic changes of *Fgfr1/2cDKO-UM* ureters

Our molecular analysis revealed increased SHH and decreased BMP4 signaling in the UM of *Fgfr1/2cDKO-UM*. To analyze the relative contribution of these changes to the delayed onset of SMC differentiation in mutant ureters, we treated explants of E13.5 wild-type ureters with 2 µM of the SHH signaling agonist purmorphamine (Li et al., 2008) and/or with the BMP4 antagonist noggin (NOG; 10 µg/ml) (Zimmerman et al., 1996) and scored peristaltic activity over an 8-day culture period. Addition of purmorphamine accelerated the onset of peristalsis by 1 day (starting at day 2-3 rather than at day 3-4 as in the control) whereas NOG-treated ureters acquired marginal peristaltic activity only after 7 days. Remarkably, a combination of the two treatments resulted in a delay of 1-2 days in the onset of peristaltic activity, similar to that observed in *Fgfr1/2cDKO-UM* ureters (Fig. 6A, Table S16A). Moreover, the contraction frequency of ureters treated with purmorphamine and NOG remained lower compared with that of control and of purmorphamine-treated ureters throughout the whole culture period (Fig. 6B, Table S16B).

Marker analysis revealed a premature onset at day 2 and an expansion of SMC differentiation upon purmorphamine treatment, whereas NOG abolished SMC markers in the ureter explants throughout the entire culture period. In the purmorphamine/NOG double-treated ureters, SMC differentiation was reduced at day 4 but was prominent and expanded at the endpoint at day 8.

Development (2022) 149, dev200767. doi:10.1242/dev.200767

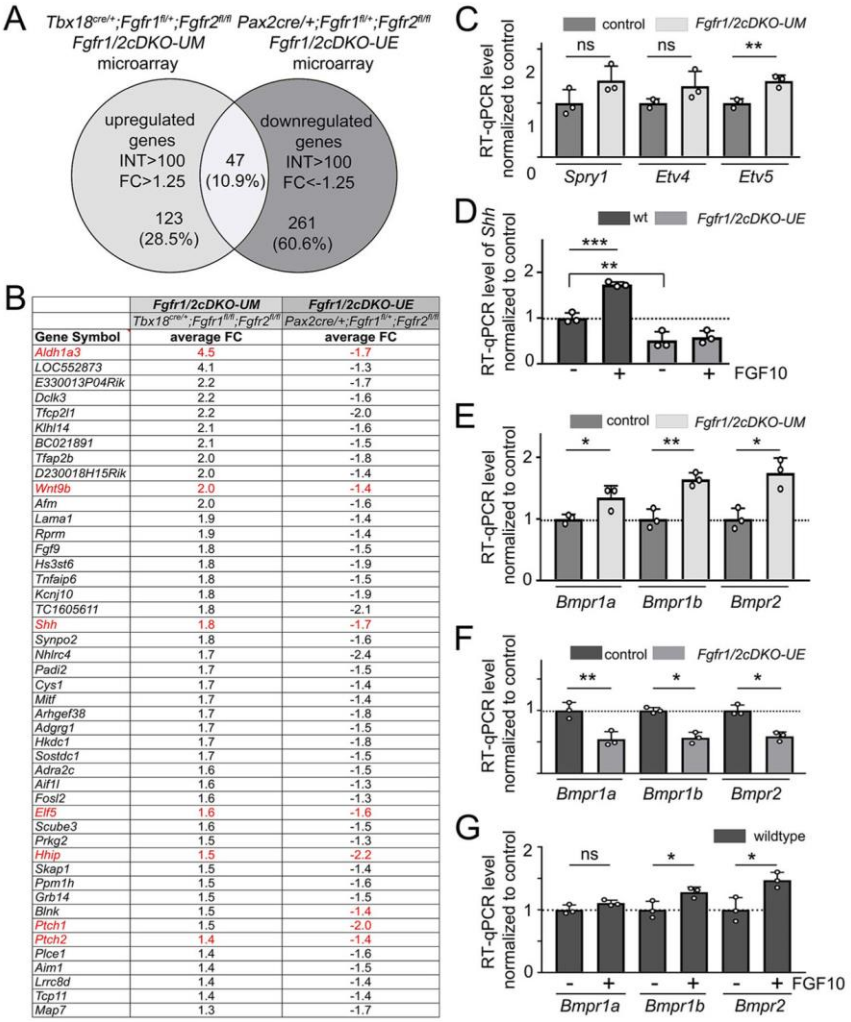

Gene Symbol	Fgfr1/2cDKO-UM Tbx18cre/+;Fgfr1fl/fl;Fgfr2fl/fl average FC	Fgfr1/2cDKO-UE Pax2cre/+;Fgfr1fl/+;Fgfr2fl/fl average FC
Aldh1a3	4.5	-1.7
LOC552873	4.1	-1.3
E330013P04Rik	2.2	-1.7
Dclk3	2.2	-1.6
Tfcp2l1	2.2	-2.0
Klhl14	2.1	-1.6
BC021891	2.1	-1.5
Tfap2b	2.0	-1.8
D230018H15Rik	2.0	-1.4
Wnt9b	2.0	-1.4
Afm	2.0	-1.6
Lama1	1.9	-1.4
Rprm	1.9	-1.4
Fgf9	1.8	-1.5
Hs3st6	1.8	-1.9
Tnfaip6	1.8	-1.5
Kcnj10	1.8	-1.9
TC1605611	1.8	-2.1
Shh	1.8	-1.7
Synpo2	1.8	-1.6
Nhlrc4	1.7	-2.4
Padi2	1.7	-1.5
Cys1	1.7	-1.4
Mitf	1.7	-1.4
Arhgef38	1.7	-1.8
Adgrg1	1.7	-1.5
Hkdc1	1.7	-1.8
Sostdc1	1.7	-1.5
Adra2c	1.6	-1.5
Aif1l	1.6	-1.3
Fosl2	1.6	-1.3
Elf5	1.6	-1.6
Scube3	1.6	-1.5
Prkg2	1.5	-1.3
Hhip	1.5	-2.2
Skap1	1.5	-1.4
Ppm1h	1.5	-1.6
Grb14	1.5	-1.5
Blnk	1.5	-1.4
Ptch1	1.5	-2.0
Ptch2	1.4	-1.4
Plce1	1.4	-1.6
Aim1	1.4	-1.5
Lrrc8d	1.4	-1.4
Tcp11	1.4	-1.4
Map7	1.3	-1.7

Fig. 5. Loss of mesenchymal *Fgfr1* and *Fgfr2* expression leads to increased epithelial FGFR2 signaling. (A) Diagram showing the large overlap of genes upregulated in the microarray of the mesenchymal *Fgfr1/2* knockout (*Fgfr1/2cDKO-UM*; *Tbx18*$^{cre/+}$;*Fgfr1*$^{fl/fl}$;*Fgfr2*$^{fl/fl}$) and downregulated in the epithelial knockout of *Fgfr1/2* in the ureter at E14.5 (*Fgfr1/2cDKO-UE*; *Pax2cre/+;Fgfr1*$^{fl/+}$;*Fgfr2*$^{fl/fl}$). For complete gene lists, see Tables S11 and S15. (B) List of 47 genes from the overlap of the gene lists shown in A. Genes marked in red are components and/or targets of SHH signaling (*Shh*, *Hhip*, *Ptch1*, *Ptch2*), RA signaling (*Aldh1a3*, *Elf5*) and WNT signaling (*Wnt9b*). (C) RT-qPCR results for expression of *Spry1*, *Etv4* and *Etv5* in three independent RNA pools of E14.5 control and *Fgfr1/2cDKO-UM* ureters. **$P \leq 0.01$ (two-tailed Student's *t*-test). For values and statistics, see Table S14B. (D) RT-qPCR results for expression of *Shh* in three independent RNA pools each of explants of E12.5 wild-type and *Fgfr1/2cDKO-UE* ureters treated with 100 ng/µl FGF10 for 18 h; **$P \leq 0.01$; ***$P \leq 0.001$ (two-way ANOVA followed by Tukey's multiple comparisons test; selected comparisons with significant difference shown). For values and complete statistics, see Table S14C. (E) RT-qPCR results for expression of BMPR genes in three independent RNA pools of E14.5 control and *Fgfr1/2cDKO-UM* ureters. *$P \leq 0.05$; **$P \leq 0.01$ (two-tailed Student's *t*-test). For values and statistics, see Table S14D. (F) RT-qPCR results for expression of BMPR genes in three independent RNA pools of E14.5 control and *Fgfr1/2cDKO-UE* ureters. *$P \leq 0.05$; **$P \leq 0.01$ (two-tailed Student's *t*-test). For values and statistics, see Table S14E. (G) RT-qPCR results for expression of BMPR genes in three independent RNA pools each of explants of E12.5 wild-type ureters treated with 100 ng/µl FGF10 for 18 h. *$P \leq 0.05$ (two-tailed Student's *t*-test). For values and statistics, see Table S14F. Values in C-G are shown as mean ±s.d. FC, fold change; INT, intensity; ns, not significant; wt, wild type.

Purmorphamine treatment enhanced ALDH1A2 expression as did the loss of BMP4 signaling at day 2, whereas purmorphamine/NOG treatment led to an expanded peri-epithelial ALDH1A2 domain at the endpoint, again recapitulating the observation in *Fgfr1/2cDKO-UM* ureters (Fig. 6C). Together, we conclude that a combination of increased SHH signaling and decreased BMP4 signaling recapitulates the phenotypic changes of *Fgfr1/2cDKO-UM* ureters (Fig. 7).

DISCUSSION

FGFR1 and FGFR2 maintain the structural and functional integrity of the ureter by patterning the UM

We addressed FGFR1 and FGFR2 function in the UM by a specific conditional gene-targeting approach based on the exclusive expression of *Tbx18* in this tissue (Bohnenpoll et al., 2013). Combined mesenchymal loss of *Fgfr1* and *Fgfr2* by our *Tbx18*^{cre} knock-in line (Airik et al., 2010) resulted in hydroureter formation

RESEARCH ARTICLE

Development (2022) 149, dev200767. doi:10.1242/dev.200767

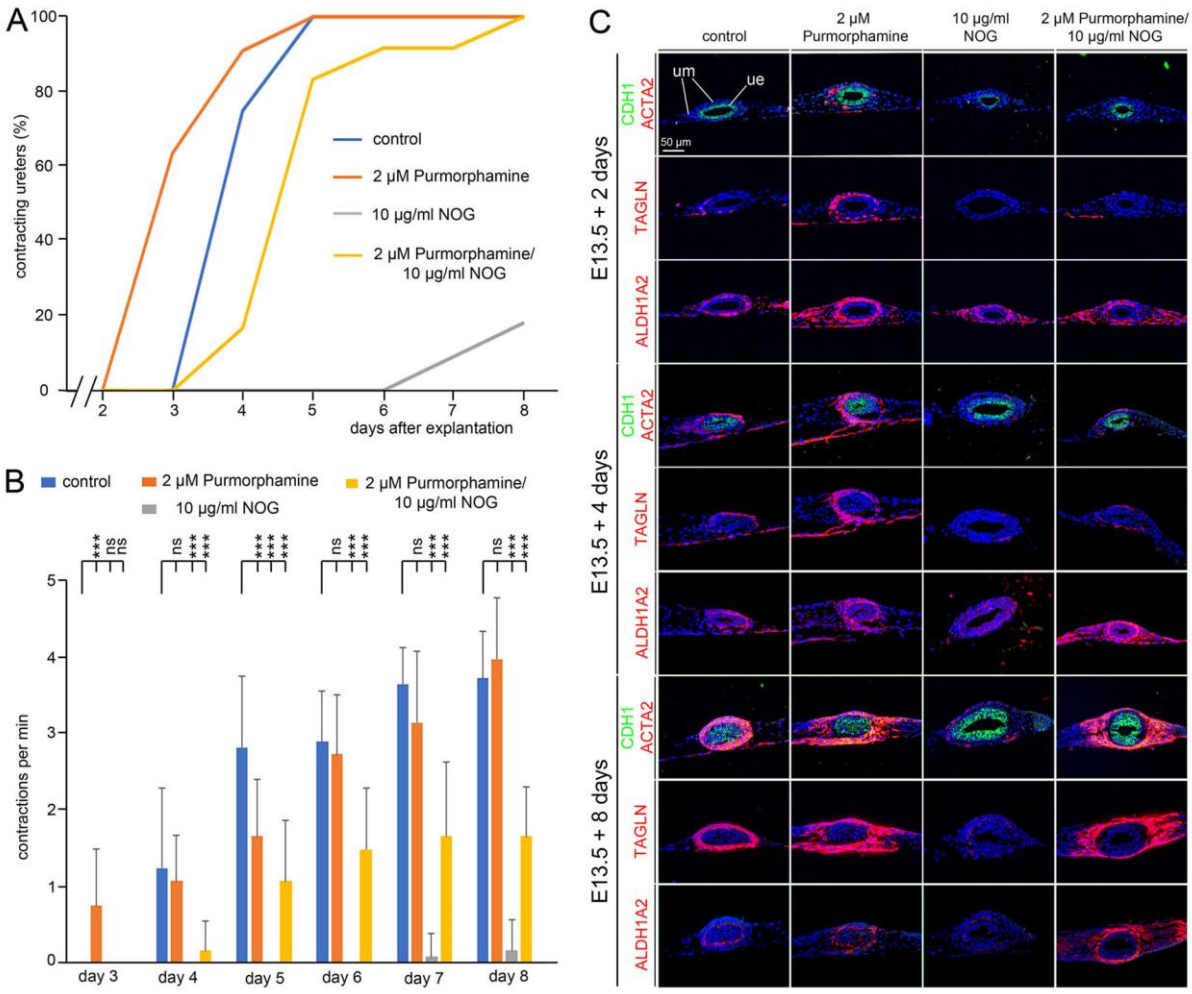

Fig. 6. The combination of increased SHH and reduced BMP4 signaling recapitulates the phenotypic changes of *Fgfr1*|*2cDKO-UM* ureters. (A-C) Wild-type ureters were explanted at E13.5 and cultured for 8 days in minimal medium supplemented with DMSO (control, *n*=12), 2 µM purmorphamine (*n*=11), 10 µg/ml NOG (*n*=11) or 2 µM purmorphamine with 10 µg/ml NOG (*n*=12) and analyzed for peristaltic activity and SMC differentiation. (A) Graph showing the percentage of contracting ureters at different time points of the culture. (B) Graph of the contraction frequency (per min) at day 3-8 of the culture. Values are shown as mean±s.d. ***P<0.001 (two-tailed Student's t-test). For detailed values, see Table S16. (C) (Co-)immunofluorescence analysis of expression of the epithelial marker CDH1 together with the SMC marker ACTA2, of the SMC marker TAGLN, and of the lamina propria marker ALDH1A2 on transverse section of E13.5 ureter explants cultured for 2, 4 and 8 days. Nuclei are counterstained (in blue) with DAPI. *n*=5 for each marker, genotype and stage. ue, ureteric epithelium; um, ureteric mesenchyme.

but did not affect the overall composition of the excretory system and the integrity and size of its other major organs, the kidney and the bladder. The luminal path from the pelvis to the bladder was unaffected. Moreover, we did not find gross urothelial defects in *Fgfr1/2cDKO-UM* ureters. Absence of these phenotypic traits not only proves that hydroureter in *Fgfr1/2cDKO-UM* embryos arises from functional insufficiency of the outer mesenchymal coat, it also confirms that mesenchymal and epithelial lineages outside the UM were not affected to any substantial degree by our conditional targeting approach.

Our breeding strategy only allowed for recovery of *Fgfr1* and *Fgfr2* compound mutants for phenotypic analysis. However, the genotype-phenotype correlation clearly argues that loss of *Fgfr2* is the dominant factor for hydroureter formation, but that loss of *Fgfr1* contributed at least partly to this morphological defect.

Owing to postnatal lethality of *Fgfr1/2cDKO-UM* mice we could not analyze adolescent or adult mice for uro- and nephropathy. However, we assume that the hydroureter worsens leading to dilatation of the pelvis and the renal collecting system (hydronephrosis), a condition that would ultimately destroy the renal parenchyma. *Fgfr1/2cDKO-UM* ureters regained considerable peristaltic performance when relieved from urinary pressure in an *ex vivo* culture setting. Although this confirms that increased hydrostatic pressure exacerbates the SMC defects *in vivo*, it suggests that *in vivo* a temporary artificial bypass may provide a means for (re-)differentiation of contractile SMCs and a regain of peristaltic activity. Irrespective of such a therapeutic option for a subgroup of congenital forms of hydroureter in human patients, *Fgfr1 and Fgfr2* present relevant candidates to include in mutational screens for genetic causes of this disease entity.

Development (2022) 149, dev200767. doi:10.1242/dev.200767

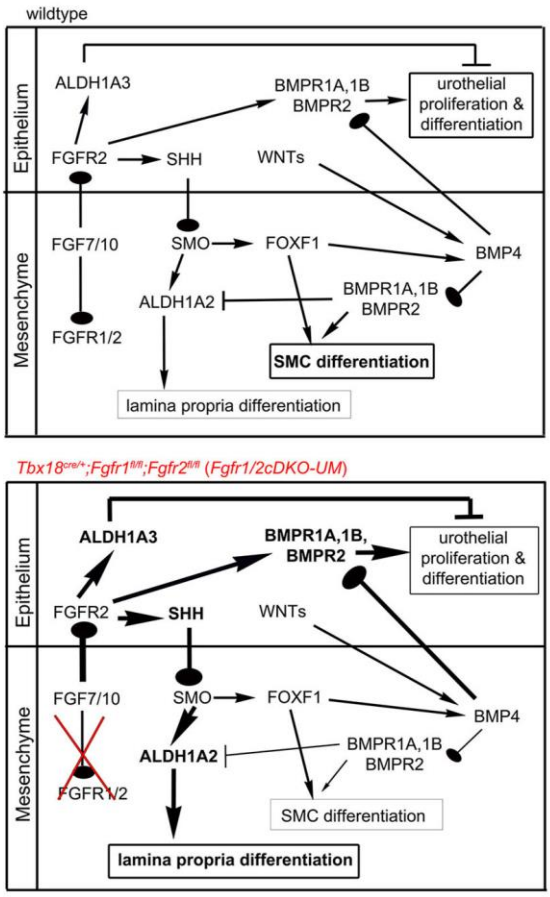

Fig. 7. Model of how mesenchymal FGFR1 and FGFR2 expression regulates various signaling pathways to assure normal patterning and SMC differentiation of the UM around E14.5. Top: In the wild type, mesenchymal FGFR1 and FGFR2 compete with epithelial FGFR2 for binding to FGF7 and FGF10. This dampens the expression of *Aldh1a3*, *Shh* and BMPR genes by epithelial FGFR2 signaling. BMP4 in the mesenchyme represses *Aldh1a2* expression and, together with FOXF1, activates SMC differentiation leading in sum to SMC differentiation around E14.5, whereas lamina propria fibrocyte differentiation is suppressed. Bottom: Loss of mesenchymal FGFR1 and FGFR2 (*Tbx18*$^{cre/+}$;*Fgfr1*$^{fl/fl}$;*Fgfr2*$^{fl/fl}$; *Fgfr1/2cDKO-UM*, marked in red) leads to overactivation of epithelial FGFR2 signaling and enhanced epithelial expression of *Shh*, BMPR genes and *Aldh1a3*. Increased SHH signaling leads to increased expression of *Aldh1a2* in the mesenchyme. BMP4 binding shifts to epithelial BMPR. Less BMP4 is available in the mesenchyme to repress *Aldh1a2* and to activate the SMC program leading to premature lamina propria formation at E14.5. The effects on epithelial development are minor because the inhibitory effect of RA on differentiation is counteracted by increased epithelial BMPR signaling. Arrows indicate activating interactions, ovals ligand receptor interaction, bars inhibitory interactions. The width of arrows, bars and boxes indicates the relative level of activation.

Our cellular and molecular profiling detected decreased proliferation, delayed SMC differentiation and precocious lamina propria formation in *Fgfr1/2cDKO-UM* ureters. Analyses of other mouse models revealed that a 1-day delay in activation of *Myocd* and SMC structural genes does not compromise ureter integrity whereas a delay of two or more days leads to hydroureter formation (Kurz et al., 2022; Weiss et al., 2019). This relates to the onset of urine production in the kidney around E16.5, which generates a hydrostatic pressure that widens the ureter when SMCs are absent at this time point. Given our finding that SMC differentiation is delayed by 1 day in *Fgfr1/2cDKO-UM* ureters, we assume that precocious lamina propria formation contributed to hydroureter formation. This may occur by deposition of extracellular matrix that compromises SMC coupling or by the emergence of a 'myofibroblastic' cell type that lacks the contractile strength of SMCs.

Although the ureter and bladder arise from different primordia in different germ layers, the role of *Fgfr1* and *Fgfr2* seems to be conserved in the early development of these organs. Loss of *Fgf7* led to urothelial stratification defects in the bladder (Tash et al., 2001), and conditional deletion of *Fgfr2* in the bladder mesenchyme resulted in expansion of the lamina propria at the expense of the SMC layer (Ikeda et al., 2017). We posit that integration of FGF signaling in the epithelial and mesenchymal primordia of these organs contributed during evolution to the structural and functional divergence from components of the renal drainage system, the collecting ducts and the pelvis, that preserved a mono-layered epithelial lining and (myo)fibroblastic character of the surrounding mesenchyme.

The combination of increased SHH and decreased BMP4 signaling accounts for defects in mesenchymal patterning in *Fgfr1/2cDKO-UM* ureters

Our molecular profiling experiments identified altered activities of a number of signaling pathways that had previously been implicated in the development of the UM (Bohnenpoll et al., 2017b,c; Mamo et al., 2017; Trowe et al., 2012). SHH, WNT and RA signaling were increased whereas BMP4 signaling was decreased in the UM at E14.5, i.e. prior to onset of differentiation of SMCs and lamina propria fibrocytes. Increased SHH signaling was also detected in E16.5 bladders lacking mesenchymal *Fgfr2* expression but the activity of the other pathways was not analyzed in that context (Ikeda et al., 2017).

The work of several labs has identified SHH signaling as a crucial pathway for mesenchymal proliferation and SMC differentiation in both the bladder and the ureter (Bohnenpoll et al., 2017c; Cao et al., 2010; Shiroyanagi et al., 2007; Yu et al., 2002). Yu et al. reported that ureters with conditional deletion of *Shh* from the UE not only lacked the SMC layer but were also deficient for the lamina propria. Based on the finding that SHH administration to isolated UM led to SMC induction at low doses only, they concluded that the patterning of the UM into an inner layer of lamina propria fibrocytes and outer SMCs depends on a SHH signaling gradient (Yu et al., 2002). A similar finding was reported for the bladder mesenchyme (Cao et al., 2010).

Although this interpretation seems plausible at first sight, it is clearly not supported by the profile of *Shh* expression in the ureter. *Shh* expression in the UE is relatively high from E11.5 to E14.5 when *Myocd* induction occurs and SMC differentiation starts, but drops sharply thereafter and only rises to low levels from E18.5 onwards when lamina propria fibrocytes emerge in the innermost region of the UM (Bohnenpoll et al., 2017c). Our ureter explant culture experiments showed that increased SHH signaling (triggered by administration of purmorphamine to E12.5 ureters) leads to premature expression of SMC markers after 2 days and a widening of the SMC layer after 8 days, incompatible with the previous notion that high doses of SHH inhibit SMC differentiation. Remarkably, increased SHH signaling resulted in a strongly increased and overlapping expression of ALDH1A2, an RA biosynthetic enzyme

Development (2022) 149, dev200767. doi:10.1242/dev.200767

and lamina marker, after 2 days, suggesting that SHH signaling induces SMC and lamina fates simultaneously. ALDH1A2 expression largely extended into the outer region of the UM, in which expression of SMC markers was absent, suggesting that additional signals are required to induce SMCs close to the UE or to prevent this differentiation in the outer region.

Inhibition of BMP4 signaling with NOG resulted in a complete loss of SMC differentiation, and increased ALDH1A2 expression after 2 days, but not thereafter. This supports our previous findings that BMP4 signaling is essential for SMC differentiation and cooperates with SHH signaling (Bohnenpoll et al., 2017c). It also points out that BMP4 signaling represses ALDH1A2 expression induced by endogenous SHH signaling. Finally, combinatorial activation of SHH and inhibition of BMP4 resulted in ectopic and increased ALDH1A2 expression starting after 2 days and a delayed onset of SMC differentiation.

We previously showed that RA is sufficient to increase expression of *Wnt9b* in the UE and enhance WNT signaling activity in the UM in explant cultures of ureters (Bohnenpoll et al., 2017b). Together with our current finding that forced ectopic activation of SHH signaling induces expression of ALDH1A2, we deduce that increased RA and WNT signaling in *Fgfr1/2cDKO-UM* ureters results from the increase of *Shh* expression in the UE. However, increased RA signaling may contribute to delayed SMC differentiation and account for reduced expression of components and regulators of S-cell differentiation at E14.5, as previously reported (Bohnenpoll et al., 2017b).

We conclude that the major phenotypic traits of *Fgfr1/2cDKO-UM* ureters – delayed SMC differentiation and premature and expanded lamina propria formation – are due to a combination of increased SHH and decreased BMP signaling in the UM. Our findings confirm our previous results that SMC differentiation is promoted by combined SHH and BMP4 signaling activities and, surprisingly, suggest that lamina development is induced by SHH signaling but requires absence of BMP4 signaling.

The molecular function of FGFR1 and FGFR2 in the UM: limitation of FGF ligands for activation of epithelial FGFR2 signaling

Molecular analysis of fetal bladders with loss of *Fgfr2* in the mesenchymal compartment revealed that increased mesenchymal SHH signaling was not associated with increased epithelial *Shh* expression but correlated with increased mesenchymal expression of the genes *Boc* and *Cdon*, which encode PTCH1 co-receptors. It was concluded that FGFR2 signaling normally dampens *Cdon* and *Boc* expression and SHH signaling activity in bladder mesenchyme for proper patterning of the muscle and lamina propria (Ikeda et al., 2017).

Although our transcriptional profiling experiment found increased SHH signaling activity in the UM, we did not find alterations in *Boc* and *Cdon* expression in our microarray. However, and in clear contrast to the situation in the developing bladder, our microarrays detected increased expression of *Shh*, which we confirmed in two independent assays. This suggests that increased SHH signaling in the UM results from increased *Shh* expression in the UE.

This '*trans*' effect of mesenchymal *Fgfr1* and *Fgfr2* loss might be due to a complicated feedback mechanism employing a mesenchymally expressed secondary signal. However, our findings rather point towards a role of mesenchymal FGFR1 and FGFR2 to limit the concentration of FGF ligands for activation of FGFR2-mediated *Shh* transcription in the UE. First, loss of mesenchymal *Fgfr1* and *Fgfr2* led to increased FGF signaling activity in the adjacent UE (read-out: *Spry1*, *Etv4*, *Etv5*). Second, loss of epithelial *Fgfr2* resulted in decreased *Shh* expression, and decreased SHH, RA and WNT signaling activity in the UM (Meuser et al., 2022), i.e. to molecular changes opposite to those observed in the mesenchymal *Fgfr1* and *Fgfr2* deletion. Third, administration of FGF10, the primary ligand of FGFR2, to ureter explants led to increased *Shh* expression but only when FGFR2 was present in the epithelium. Fourth, and finally, our recent study showed that expression of *Spry1*, a transcriptional target of FGF signaling activity, in the UE is dependent on epithelial FGFR2 signaling but cannot be detected by *in situ* hybridization analysis in the UM (Meuser et al., 2022), indicating that mesenchymal FGFR1 and FGFR2 signaling elicits no or only a minor transcriptional response in this tissue.

Our *in situ* hybridization results revealed reduced expression of the BMP target genes *Id2* and *Id4* in the UM of *Fgfr1/2cDKO-UM* embryos. Although the sensitivity of this method was not sufficient to detect changes of *Id2/Id4* expression in the UE, it is conceivable that epithelial BMP4 signaling, and hence target gene expression, is enhanced considering the overall unchanged *Id2/Id4* levels both in our microarrays and in RT-qPCR analysis of whole *Fgfr1/2cDKO-UM* ureters.

There are (at least) two possible explanations for the regulation of BMP signaling in the ureter by mesenchymal FGFR1 and FGFR2. First, it is conceivable that mesenchymal FGFR1 and FGFR2 exert a (weak) signaling activity to enhance BMP signaling in the UM. This may be achieved in a transcription-independent manner, e.g. by downstream kinases that activate components and effectors of the BMP signaling machinery, or in a transcription-dependent manner, e.g. by enhancing expression of genes encoding BMP signaling components in the UM. In this scenario, loss of FGFR1 and FGFR2 signaling function in the UM would lead to reduced mesenchymal BMP4 signaling and more BMP4 would be available to bind to and activate BMP4 receptors in the UE.

Alternatively, mesenchymal FGFR1 and FGFR2 may again, as explained before for *Shh* expression, act as a sink for FGFs to control activation of FGFR2 signaling in the UE. Here, epithelial FGFR2 should control expression of genes encoding components of epithelial BMP signaling, such as BMP4 receptor genes in the UE. Loss of mesenchymal FGFR1 and FGFR2 would lead to increased expression of epithelial BMP4 receptors, which could outcompete mesenchymal BMP4 receptors for binding the limited amount of BMP4 ligand.

Although we cannot rule out that mesenchymal FGFR1 and FGFR2 exert a weak signaling activity that controls mesenchymal BMP4 signaling, our findings favor a 'sink' role for mesenchymal FGFR1 and FGFR2. Expression of all three BMPR genes (*Bmpr1a*, *Bmpr1b*, *Bmpr2*) was decreased in *Fgfr1/2cDKO-UE* ureters and increased in *Fgfr1/2cDKO-UM* ureters at E14.5, and exogenous FGF10 caused increased expression of the receptor genes, compatible with the notion that epithelial FGFR2 signaling activity enhances expression of these receptor genes, whereas mesenchymal FGFR1 and FGFR2 limit epithelial activation of these genes by limiting FGF ligand availability.

Together, our findings suggest that FGFR1 and FGFR2 exert a largely signaling-independent function in the UM by binding of FGF ligands and preventing them from activating FGFR2 in the UE. This balances SHH and BMP4 signaling and favors the differentiation of the inner region of the UM into SMCs, which is crucial to maintain the integrity of the ureter (Fig. 7).

Development (2022) 149, dev200767. doi:10.1242/dev.200767

MATERIALS AND METHODS

Mice

Mice with *loxP* sites flanking exon 4 of the *Fgfr1* locus (*Fgfr1*$^{tm5.1Sor}$; synonym: *Fgfr1*^{fl}) (Hoch and Soriano, 2006), and mice with *loxP* sites flanking exons 8-10 of the *Fgfr2* locus (*Fgfr2*^{tm1Dor}; synonym: *Fgfr2*^{fl}) (Yu et al., 2003) were obtained from The Jackson Laboratory. *Tbx18*$^{tm4(cre)Akis}$ (synonym: *Tbx18*^{cre}) mice used for recombination in the mesenchymal progenitors of the ureter (Bohnenpoll et al., 2013) were previously generated in the lab (Airik et al., 2010), as were *Tg(Pax2-cre)1AKis* (synonym: *Pax2-cre*) mice for recombination in the UE (Bohnenpoll et al., 2017a; Trowe et al., 2011). All mice were maintained on an NMRI outbred background. Mutant embryos were generated by mating *Tbx18*$^{cre/+}$;*Fgfr1*$^{fl/+}$;*Fgfr2*$^{fl/+}$ or *Pax2-cre*/+$^{+/+}$;*Fgfr1*$^{fl/+}$;*Fgfr2*$^{fl/+}$ males with *Fgfr1*$^{fl/fl}$;*Fgfr2*$^{fl/fl}$ females. *Cre*-negative littermates were used as controls. For timed pregnancies, vaginal plugs detected in the morning after mating were designated as E0.5 at noon. Urogenital systems and embryos were dissected in PBS, fixed in 4% paraformaldehyde in PBS and stored in methanol at −20°C. Genotyping was performed by PCR on genomic DNA prepared from yolk sacs, embryo tissues or ear clips.

Mice were housed in rooms with controlled light and temperature at the central animal laboratory of the Medizinische Hochschule Hannover. The experiments were in accordance with the German Animal Welfare Legislation and approved by the local Institutional Animal Care and Research Advisory Committee and permitted by the Lower Saxony State Office for Consumer Protection and Food Safety (AZ 33.12-42502-04-13/1356, AZ42500/1H).

Organ cultures and peristalsis assays

Ureters from murine embryos of different stages were dissected in L-15 Leibovitz medium (F1315, Biochrom), explanted on 0.4 µm polyester membrane Transwell supports (3450, Corning) and cultured at the air-liquid interface. Explants were cultured in DMEM/F12 (21331020, Gibco) with 1× penicillin/streptomycin (15140122, Gibco), 1× pyruvate (11360070, Gibco) and 1× GlutaMAX (35050038, Gibco) in a humidified incubator with 5% CO_2 at 37°C. For cultures of *Fgfr1/2cDKO-UM* ureters, we added 10% fetal calf serum (Biochrom) to the medium.

For pharmacological perturbation experiments, we dissolved the following compounds in DMSO or ddH_2O and used them at the indicated final concentrations: eukaryotic FGF10 (100 ng/µl, in ddH_2O; USC-EPB882HU61-10, BIOZOL), purmorphamine (2 µM, in DMSO; 540220, Merck), noggin (10 µg/ml, in ddH_2O; ZO3205, BIOZOL/GenScript). Medium was refreshed every second day.

For evaluating contraction frequency and intensity of cultured ureters, 1 min videos of each ureter were taken using a frame rate of 5 per sec with a Leica DM6000 microscope with Leica DFC350FX digital camera and analyzed using Fiji (Schindelin et al., 2012). The contraction intensity was analyzed at 25%, 50% and 75% of the total ureter length by calculating the relative width of the ureter during contraction and relaxation. Graphs were plotted in Microsoft Excel v.14 (Microsoft Corporation).

Histological and immunohistochemical analyses

Embryos, urogenital systems and ureter explants were fixed in 4% paraformaldehyde, paraffin wax embedded and sectioned at 5 µm. Sections were stained with Hematoxylin and Eosin according to standard procedures.

Immunofluorescence staining was performed on 5-µm paraffin wax sections using the following primary antibodies and dilutions: polyclonal rabbit anti-KRT5 (1:250; PRB-160P, BioLegend), polyclonal rabbit anti-ΔNP63 (1:250; clone Poly6190, 619001, BioLegend), monoclonal mouse anti-UPK1B (1:250; clone1E1, WH0007348M2, Sigma-Aldrich), polyclonal rabbit anti-TAGLN (1:200; ab14106, Abcam), polyclonal rabbit anti-ACTA2 (1:200, A5228; clone 1A4; Merck), polyclonal rabbit anti-ALDH1A2 (1:200; ab75674, Abcam), polyclonal rabbit anti-CDH1 (a kind gift from Dr R. Kemler, MPI, Freiburg, Germany) and monoclonal mouse anti-BrdU (1:250; 1170376, clone BMC9318, Roche). Fluorescent staining was performed using the following secondary antibodies: biotinylated goat anti-rabbit IgG (1:200; 111065033, Dianova), biotinylated donkey anti-goat IgG (1:200; 705-065-003; Dianova), biotinylated goat anti-mouse IgG (1:200; 115-065-166, Jackson ImmunoResearch), Alexa 488-conjugated goat anti-rabbit IgG (1:500; A11034, Molecular Probes) and Alexa 555-conjugated goat anti-mouse IgG (1:500; A21422, Molecular Probes). The signals of ΔNP63 and ALDH1A2 were amplified using the Tyramide Signal Amplification system (NEL702001KT, Perkin Elmer). For antigen retrieval, paraffin sections were deparaffinized, pressure-cooked for 20 min in antigen unmasking solution (H3300, Vector Laboratories), treated with 3% H_2O_2/PBS for blocking of endogenous peroxidases, washed in PBST (0.05% Tween-20 in PBS) and incubated in TNB Blocking Buffer (NEL702001KT, Perkin Elmer). Sections were then incubated with primary antibodies at 4°C overnight. Nuclei were stained with 4′,6-diamidino-2-phenylindole (DAPI; 6335.1, Carl Roth). At least three specimens of each genotype were used for each analysis.

Cellular assays

In vivo cell proliferation rates were assayed by detection of incorporated BrdU on 5-µm paraffin wax sections (Bussen et al., 2004). Twelve sections of each specimen (n=3) were analyzed. The BrdU labeling index was defined as the number of BrdU-positive nuclei relative to the total number of nuclei detected by DAPI counterstaining in histologically defined compartments of the ureter.

Apoptosis in tissues was evaluated by the TUNEL assay using ApopTag Plus Fluorescein In Situ Apoptosis Detection Kit (S7111; Merck) on 5-µm paraffin sections.

RNA *in situ* hybridization analysis

Non-radioactive *in situ* hybridization analysis of gene expression was performed on 10-µm transversal paraffin wax sections of the proximal ureter using digoxigenin-labeled antisense riboprobes as previously described (Moorman et al., 2001).

RT-qPCR

RNA extraction and RT-qPCR analysis for gene expression was performed on three independent pools of 20 ureters each of E14.5 control, *Fgfr1/2cDKO-UM* and *Fgfr1/2cDKO-UE* embryos or of ten ureters each of E12.5 control and *Fgfr1/2cDKO-UE* embryos after 18 h of culture as previously described (Meuser et al., 2022). Primers are listed in Table S17.

Microarray analysis

For microarray analysis, ureters were either isolated at E15.5, explanted on Transwell membranes, cultivated for 6 days and then stored at −80°C or were isolated at E14.5 and directly frozen and stored at −80°C. Two independent pools of control and mutant ureters (five ureters each from male and female embryos) were collected for the E15.5+6 day microarray. Four independent pools of control and mutant ureters (20 ureters each for male and female embryos) were used for microarray analysis at E14.5. Total RNA from each pool was extracted using peqGOLD RNApure (30-1010, VWR International) and subsequently processed by the Research Core Unit Transcriptomics of Hannover Medical School. Whole Mouse Genome Oligo v2 (4×44K) Microarrays (G4846A; Agilent Technologies) were used for transcriptome analysis. Normalized expression data were filtered using Microsoft Excel (Microsoft Corporation). Functional enrichment analysis for up- and downregulated genes was performed with DAVID 6.8 web-software (https://david.ncifcrf.gov/) using default settings, and terms were selected based on P-value.

Statistics

Statistical analysis was performed using unpaired, two-tailed Student's t-test or a two-way analysis of variance (ANOVA) followed by Tukey's multiple comparisons test as indicated (GraphPad Prism version 7.03 and Microsoft Excel). Values are presented as mean±s.d. with P<0.05 considered significant.

Image documentation

Sections were photographed using a DM5000 microscope (Leica Camera, Wetzlar, Germany) with Leica DFC300FX digital camera or a Leica

DMI6000B microscope with Leica DFC350FX digital camera. All images were then processed in Adobe Photoshop CS3 or CS4.

Acknowledgements
We thank Rolf Kemler (MPI for Immunobiology, Freiburg) for the CDH1 antibody, and Patricia Zarnovican for excellent technical support. Microarray data used in this publication were generated by the Research Core Unit Genomics (RCUG) at Hannover Medical School.

Competing interests
The authors declare no competing or financial interests.

Author contributions
Conceptualization: L.D., H.T., A.K.; Methodology: M.M., H.T., M.-O.T.; Software: M.-O.T.; Validation: L.D., H.T.; Formal analysis: L.D., M.M., H.T., U.W.H.J., M.-O.T.; Investigation: L.D., M.M., H.T., U.W.H.J., C.R., M.-O.T.; Resources: C.R.; Data curation: L.D., H.T., M.-O.T.; Writing - original draft: L.D., A.K.; Writing - review & editing: L.D., M.M., H.T., U.W.H.J., C.R., H.H., M.-O.T., A.K.; Visualization: L.D., H.T.; Supervision: C.R., H.H., A.K.; Project administration: A.K.; Funding acquisition: H.H., A.K.

Funding
This work was supported by a grant from the German Research Council (Deutsche Forschungsgemeinschaft; DFG KI728/9-2) to A.K.

Data availability
Microarray data have been deposited in Gene Expression Omnibus under accession numbers GSE197368 and GSE197369.

Peer review history
The peer review history is available online at https://journals.biologists.com/dev/lookup/doi/10.1242/dev.200767.reviewer-comments.pdf.

References

Airik, R., Trowe, M.-O., Foik, A., Farin, H. F., Petry, M., Schuster-Gossler, K., Schweizer, M., Scherer, G., Kist, R. and Kispert, A. (2010). Hydroureternephrosis due to loss of Sox9-regulated smooth muscle cell differentiation of the ureteric mesenchyme. *Hum. Mol. Genet.* **19**, 4918-4929. doi:10.1093/hmg/ddq426

Aydoğdu, N., Rudat, C., Trowe, M.-O., Kaiser, M., Lüdtke, T. H., Taketo, M. M., Christoffels, V. M., Moon, A. and Kispert, A. (2018). TBX2 and TBX3 act downstream of canonical WNT signaling in patterning and differentiation of the mouse ureteric mesenchyme. *Development* **145**, dev171827. doi:10.1242/dev.171827

Baskin, L. S., Hayward, S. W., Young, P. and Cunha, G. R. (1996). Role of mesenchymal-epithelial interactions in normal bladder development. *J. Urol.* **156**, 1820-1827. doi:10.1016/S0022-5347(01)65545-9

Bohnenpoll, T. and Kispert, A. (2014). Ureter growth and differentiation. *Semin. Cell Dev. Biol.* **36**, 21-30. doi:10.1016/j.semcdb.2014.07.014

Bohnenpoll, T., Bettenhausen, E., Weiss, A.-C., Foik, A. B., Trowe, M.-O., Blank, P., Airik, R. and Kispert, A. (2013). Tbx18 expression demarcates multipotent precursor populations in the developing urogenital system but is exclusively required within the ureteric mesenchymal lineage to suppress a renal stromal fate. *Dev. Biol.* **380**, 25-36. doi:10.1016/j.ydbio.2013.04.036

Bohnenpoll, T., Feraric, S., Nattkemper, M., Weiss, A.-C., Rudat, C., Meuser, M., Trowe, M.-O. and Kispert, A. (2017a). Diversification of cell lineages in ureter development. *J. Am. Soc. Nephrol.* **28**, 1792-1801. doi:10.1681/ASN.2016080849

Bohnenpoll, T., Weiss, A.-C., Labuhn, M., Lüdtke, T. H., Trowe, M.-O. and Kispert, A. (2017b). Retinoic acid signaling maintains epithelial and mesenchymal progenitors in the developing mouse ureter. *Sci. Rep.* **7**, 14803. doi:10.1038/s41598-017-14790-2

Bohnenpoll, T., Wittern, A. B., Mamo, T. M., Weiss, A.-C., Rudat, C., Kleppa, M.-J., Schuster-Gossler, K., Wojahn, I., Ludtke, T. H.-W., Trowe, M.-O. et al. (2017c). A SHH-FOXF1-BMP4 signaling axis regulating growth and differentiation of epithelial and mesenchymal tissues in ureter development. *PLoS Genet.* **13**, e1006951. doi:10.1371/journal.pgen.1006951

Bussen, M., Petry, M., Schuster-Gossler, K., Leitges, M., Gossler, A. and Kispert, A. (2004). The T-box transcription factor Tbx18 maintains the separation of anterior and posterior somite compartments. *Genes Dev.* **18**, 1209-1221. doi:10.1101/gad.300104

Cao, M., Tasian, G., Wang, M.-H., Liu, B., Cunha, G. and Baskin, L. (2010). Urothelium-derived Sonic hedgehog promotes mesenchymal proliferation and induces bladder smooth muscle differentiation. *Differentiation* **79**, 244-250. doi:10.1016/j.diff.2010.02.002

Capone, V. P., Morello, W., Taroni, F. and Montini, G. (2017). Genetics of congenital anomalies of the kidney and urinary tract: the current state of play. *Int. J. Mol. Sci.* **18**, 796. doi:10.3390/ijms18040796

Cunha, G. R. (1976). Epithelial-stromal interactions in development of the urogenital system. *Int. Rev. Cytol.* **47**, 137-194. doi:10.1016/S0074-7696(08)60088-1

Firnberg, N. and Neubüser, A. (2002). FGF signaling regulates expression of Tbx2, Erm, Pea3, and Pax3 in the early nasal region. *Dev. Biol.* **247**, 237-250. doi:10.1006/dbio.2002.0696

Hafner, R., Bohnenpoll, T., Rudat, C., Schultheiss, T. M. and Kispert, A. (2015). Fgfr2 is required for the expansion of the early adrenocortical primordium. *Mol. Cell. Endocrinol.* **413**, 168-177. doi:10.1016/j.mce.2015.06.022

Hanafusa, H., Torii, S., Yasunaga, T. and Nishida, E. (2002). Sprouty1 and Sprouty2 provide a control mechanism for the Ras/MAPK signalling pathway. *Nat. Cell Biol.* **4**, 850-858. doi:10.1038/ncb867

Hoch, R. V. and Soriano, P. (2006). Context-specific requirements for Fgfr1 signaling through Frs2 and Frs3 during mouse development. *Development* **133**, 663-673. doi:10.1242/dev.02242

Hollnagel, A., Oehlmann, V., Heymer, J., Rüther, U. and Nordheim, A. (1999). Id genes are direct targets of bone morphogenetic protein induction in embryonic stem cells. *J. Biol. Chem.* **274**, 19838-19845. doi:10.1074/jbc.274.28.19838

Igarashi, M., Finch, P. W. and Aaronson, S. A. (1998). Characterization of recombinant human fibroblast growth factor (FGF)-10 reveals functional similarities with keratinocyte growth factor (FGF-7). *J. Biol. Chem.* **273**, 13230-13235. doi:10.1074/jbc.273.21.13230

Ikeda, Y., Zabbarova, I., Schaefer, C. M., Bushnell, D., De Groat, W. C., Kanai, A. and Bates, C. M. (2017). Fgfr2 is integral for bladder mesenchyme patterning and function. *Am. J. Physiol. Renal Physiol.* **312**, F607-F618. doi:10.1152/ajprenal.00463.2016

Jans, D. A. (1994). Nuclear signaling pathways for polypeptide ligands and their membrane receptors? *FASEB J.* **8**, 841-847. doi:10.1096/fasebj.8.11.8070633

Kurz, J., Weiss, A.-C., Thiesler, H., Qasrawi, F., Deuper, L., Kaur, J., Rudat, C., Lüdtke, T. H., Wojahn, I., Hildebrandt, H. et al. (2022). Notch signaling is a novel regulator of visceral smooth muscle cell differentiation in the murine ureter. *Development* **149**, dev199735. doi:10.1242/dev.199735

Laestander, C. and Engström, W. (2014). Role of fibroblast growth factors in elicitation of cell responses. *Cell Prolif.* **47**, 3-11. doi:10.1111/cpr.12084

Li, X.-J., Hu, B.-Y., Jones, S. A., Zhang, Y.-S., LaVaute, T., Du, Z.-W. and Zhang, S.-C. (2008). Directed differentiation of ventral spinal progenitors and motor neurons from human embryonic stem cells by small molecules. *Stem Cells* **26**, 886-893. doi:10.1634/stemcells.2007-0620

Liu, K. J. and Harland, R. M. (2003). Cloning and characterization of Xenopus Id4 reveals differing roles for Id genes. *Dev. Biol.* **264**, 339-351. doi:10.1016/j.ydbio.2003.08.017

Liu, Y., Jiang, H., Crawford, H. C. and Hogan, B. L. M. (2003). Role for ETS domain transcription factors Pea3/Erm in mouse lung development. *Dev. Biol.* **261**, 10-24. doi:10.1016/S0012-1606(03)00359-2

Mamo, T. M., Wittern, A. B., Kleppa, M.-J., Bohnenpoll, T., Weiss, A.-C. and Kispert, A. (2017). BMP4 uses several different effector pathways to regulate proliferation and differentiation in the epithelial and mesenchymal tissue compartments of the developing mouse ureter. *Hum. Mol. Genet.* **26**, 3553-3563. doi:10.1093/hmg/ddx242

Meuser, M., Deuper, L., Rudat, C., Aydoğdu, N., Thiesler, H., Zarnovican, P., Hildebrandt, H., Trowe, M.-O. and Kispert, A. (2022). FGFR2 signaling enhances the SHH-BMP4 signaling axis in early ureter development. *Development* **149**, dev200021. doi:10.1242/dev.200021

Moorman, A. F. M., Houweling, A. C., de Boer, P. A. J. and Christoffels, V. M. (2001). Sensitive nonradioactive detection of mRNA in tissue sections: novel application of the whole-mount in situ hybridization protocol. *J. Histochem. Cytochem.* **49**, 1-8. doi:10.1177/002215540104900101

Ornitz, D. M. and Itoh, N. (2015). The Fibroblast Growth Factor signaling pathway. *Wiley Interdiscip. Rev. Dev. Biol.* **4**, 215-266. doi:10.1002/wdev.176

Schindelin, J., Arganda-Carreras, I., Frise, E., Kaynig, V., Longair, M., Pietzsch, T., Preibisch, S., Rueden, C., Saalfeld, S., Schmid, B. et al. (2012). Fiji: an open-source platform for biological-image analysis. *Nat. Methods* **9**, 676-682. doi:10.1038/nmeth.2019

Shiroyanagi, Y., Liu, B., Cao, M., Agras, K., Li, J., Hsieh, M. H., Willingham, E. J. and Baskin, L. S. (2007). Urothelial sonic hedgehog signaling plays an important role in bladder smooth muscle formation. *Differentiation* **75**, 968-977. doi:10.1111/j.1432-0436.2007.00187.x

Tash, J. A., David, S. G., Vaughan, E. E. and Herzlinger, D. A. (2001). Fibroblast growth factor-7 regulates stratification of the bladder urothelium. *J. Urol.* **166**, 2536-2541. doi:10.1016/S0022-5347(05)65630-3

Trowe, M.-O., Maier, H., Petry, M., Schweizer, M., Schuster-Gossler, K. and Kispert, A. (2011). Impaired stria vascularis integrity upon loss of E-cadherin in basal cells. *Dev. Biol.* **359**, 95-107. doi:10.1016/j.ydbio.2011.08.030

Trowe, M.-O., Airik, R., Weiss, A.-C., Farin, H. F., Foik, A. B., Bettenhausen, E., Schuster-Gossler, K., Taketo, M. M. and Kispert, A. (2012). Canonical Wnt signaling regulates smooth muscle precursor development in the mouse ureter. *Development* **139**, 3099-3108. doi:10.1242/dev.077388

Development (2022) 149, dev200767. doi:10.1242/dev.200767

Velardo, J. T. (1981). Histology of the ureter. In *The Ureter* (ed. H. Bergman), pp. 13-54. New York: Springer-Verlag.
Walker, K. A., Sims-Lucas, S. and Bates, C. M. (2016). Fibroblast growth factor receptor signaling in kidney and lower urinary tract development. *Pediatr. Nephrol.* **31**, 885-895. doi:10.1007/s00467-015-3151-1
Wang, D.-Z. and Olson, E. N. (2004). Control of smooth muscle development by the myocardin family of transcriptional coactivators. *Curr. Opin. Genet. Dev.* **14**, 558-566. doi:10.1016/j.gde.2004.08.003
Wang, D.-Z., Chang, P. S., Wang, Z., Sutherland, L., Richardson, J. A., Small, E., Krieg, P. A. and Olson, E. N. (2001). Activation of cardiac gene expression by myocardin, a transcriptional cofactor for serum response factor. *Cell* **105**, 851-862. doi:10.1016/S0092-8674(01)00404-4
Weiss, A. C., Bohnenpoll, T., Kurz, J., Blank, P., Airik, R., Lüdtke, T. H., Kleppa, M. J., Deuper, L., Kaiser, M., Mamo, T. M. et al. (2019). Delayed onset of smooth muscle cell differentiation leads to hydroureter formation in mice with conditional loss of the zinc finger transcription factor gene Gata2 in the ureteric mesenchyme. *J. Pathol.* **248**, 452-463. doi:10.1002/path.5270
Yu, J., Carroll, T. J. and McMahon, A. P. (2002). Sonic hedgehog regulates proliferation and differentiation of mesenchymal cells in the mouse metanephric kidney. *Development* **129**, 5301-5312. doi:10.1242/dev.129.22.5301
Yu, K., Xu, J., Liu, Z., Sosic, D., Shao, J., Olson, E. N., Towler, D. A. and Ornitz, D. M. (2003). Conditional inactivation of FGF receptor 2 reveals an essential role for FGF signaling in the regulation of osteoblast function and bone growth. *Development* **130**, 3063-3074. doi:10.1242/dev.00491
Yu, Z., Mannik, J., Soto, A., Lin, K. K. and Andersen, B. (2009). The epidermal differentiation-associated Grainyhead gene Get1/Grhl3 also regulates urothelial differentiation. *EMBO J.* **28**, 1890-1903. doi:10.1038/emboj.2009.142
Zimmerman, L. B., De Jesús-Escobar, J. M. and Harland, R. M. (1996). The Spemann organizer signal noggin binds and inactivates bone morphogenetic protein 4. *Cell* **86**, 599-606. doi:10.1016/S0092-8674(00)80133-6

Supplementary Figures

Development: doi:10.1242/dev.200767: Supplementary information

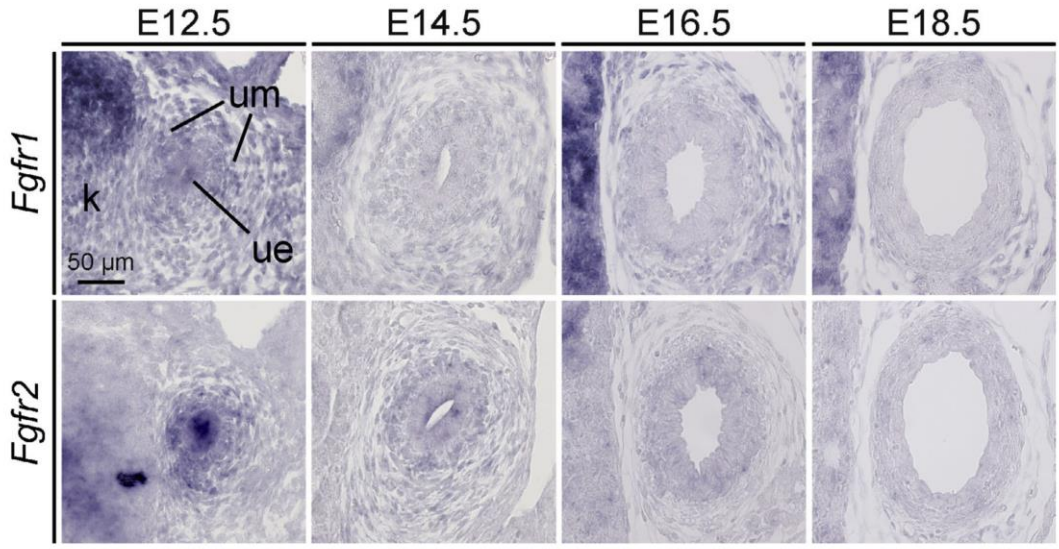

Fig. S1. *Fgfr1* and *Fgfr2* are expressed in the mesenchymal compartment of the developing ureter. RNA *in situ* hybridization analysis of *Fgfr1* and *Fgfr2* expression on transverse sections of the proximal ureter of E12.5 and E14.5 embryos. *n*=3 for each marker and stage. k, kidney; ue, ureteric epithelium; um, ureteric mesenchyme.

Development: doi:10.1242/dev.200767: Supplementary information

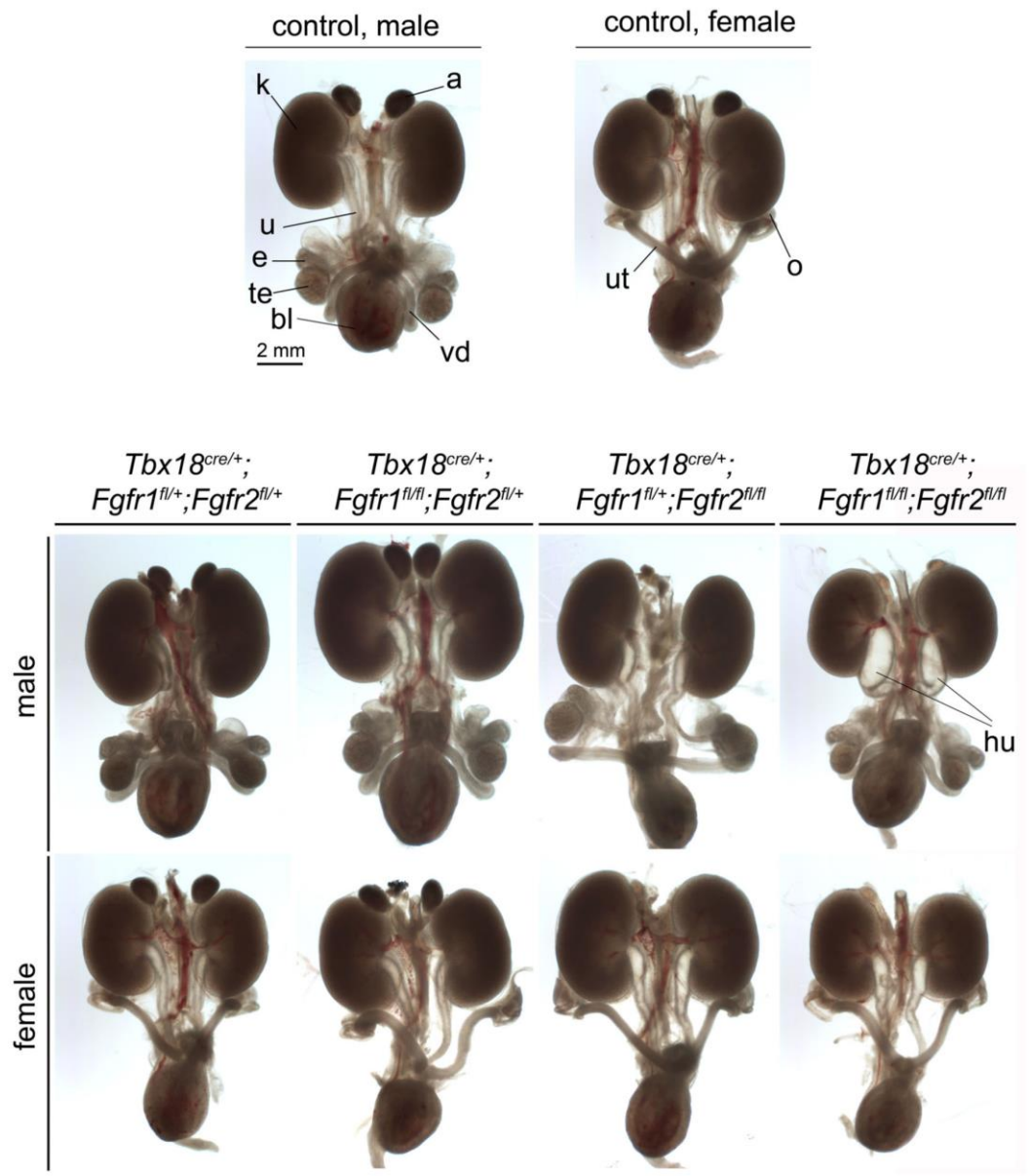

Fig. S2. Phenotypic variation of hydroureter formation upon loss of one or two alleles of *Fgfr1* and/or *Fgfr2* in the UM. Morphology of whole urogenital systems of male and female embryos at E18.5. Genotypes and sex are as indicated. For numbers see Table S2. a, adrenal; bl, bladder; e, epididymis; hu, hydroureter; k, kidney; o, ovary; te, testis; u, ureter; ut, uterus; vd, vas deferens.

Development: doi:10.1242/dev.200767: Supplementary information

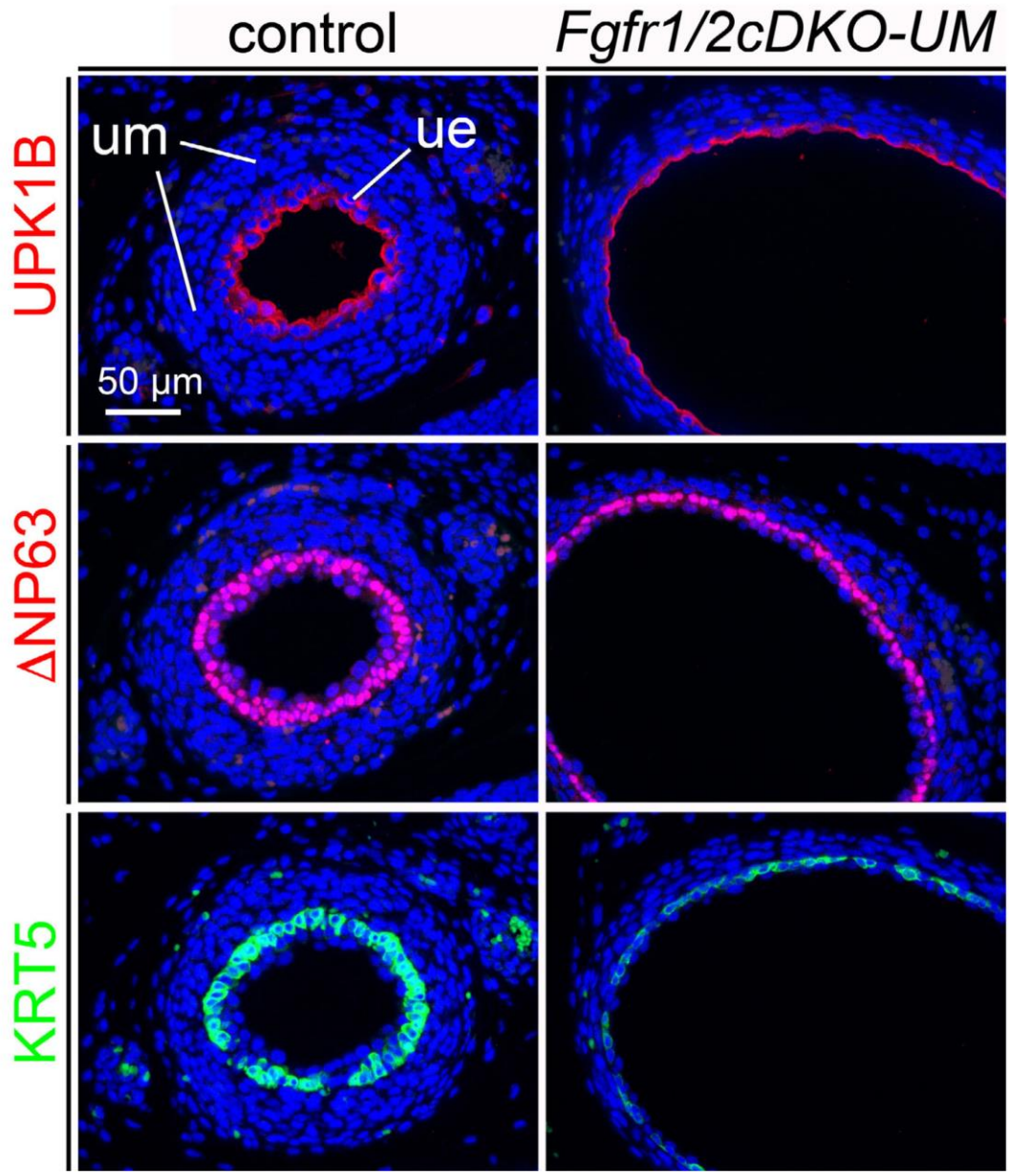

Fig. S3. Urothelial differentiation is not affected in *Fgfr1/2cDKO-UM* ureters at E18.5. Immunofluorescence analysis of expression of the urothelial marker proteins UPK1B (cytoplasmatic and extracellular, for superficial cells), ΔNP63 (nuclear, for intermediate and basal cells) and KRT5 (cytoplasmatic, for basal cells) on transverse sections of the proximal ureter of control and *Fgfr1/2cDKO-UM* embryos at E18.5. Nuclei are counterstained (in blue) with DAPI. Genotypes and antibodies are as indicated. $n \geq 3$ for each marker and genotype. ue, ureteric epithelium; um, ureteric mesenchyme.

Development: doi:10.1242/dev.200767: Supplementary information

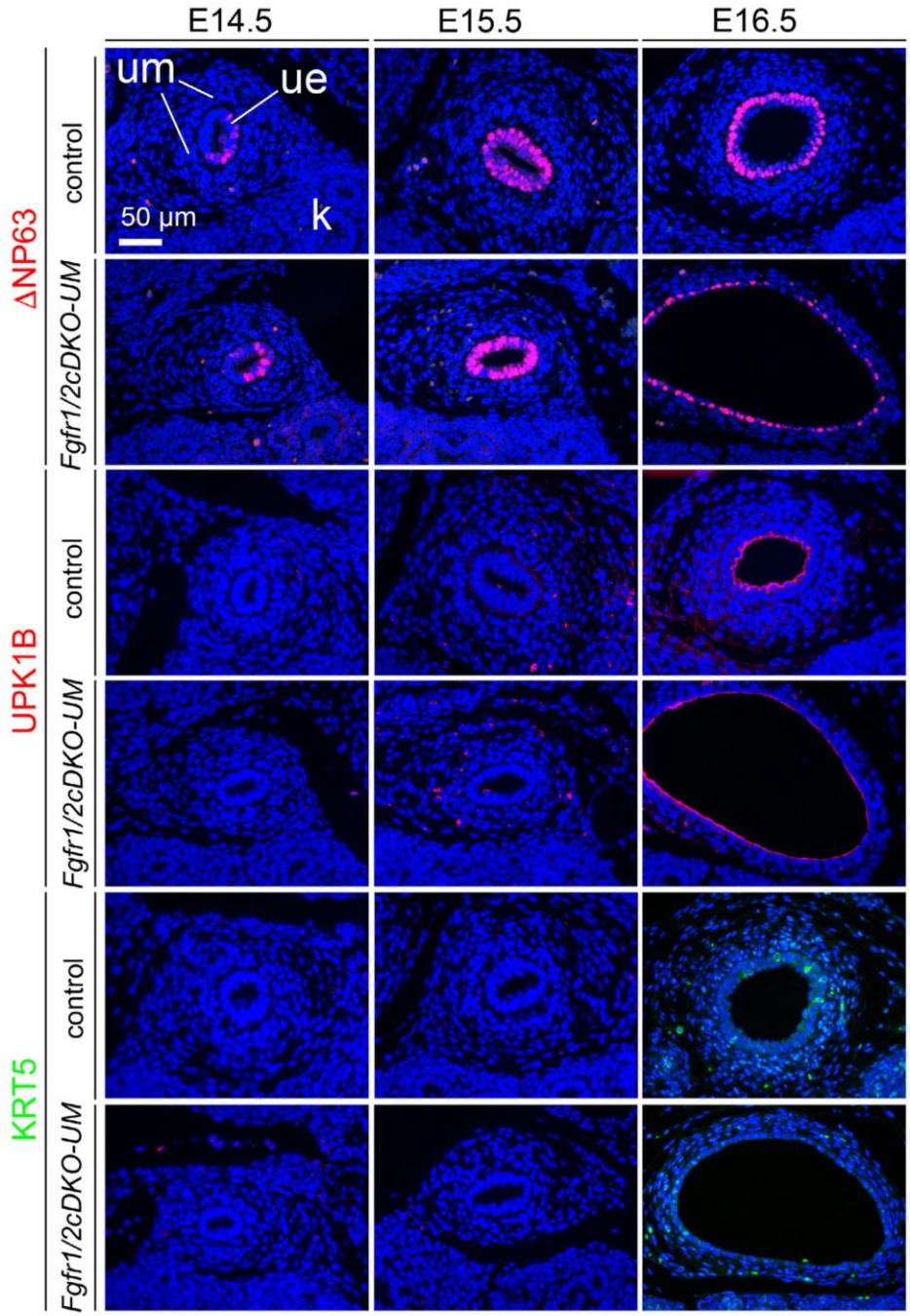

Fig. S4. Onset and progression of urothelial differentiation is not affected in *Fgfr1/2cDKO-UM* ureters at E14.5 to E16.5. Immunofluorescence analysis of expression of the urothelial marker proteins UPK1B (cytoplasmatic and extracellular, for superficial cells), ΔNP63 (nuclear, for intermediate and basal cells) and KRT5 (cytoplasmatic, for basal cells) on transverse sections of the proximal ureter of control and *Fgfr1/2cDKO-UM* embryos at E14.5, E15.5 and E16.5. Nuclei are counterstained (in blue) with DAPI. Genotypes and antibodies are as indicated. $n \geq 3$ for each marker, stage and genotype. k, kidney; ue, ureteric epithelium; um, ureteric mesenchyme.

Development: doi:10.1242/dev.200767: Supplementary information

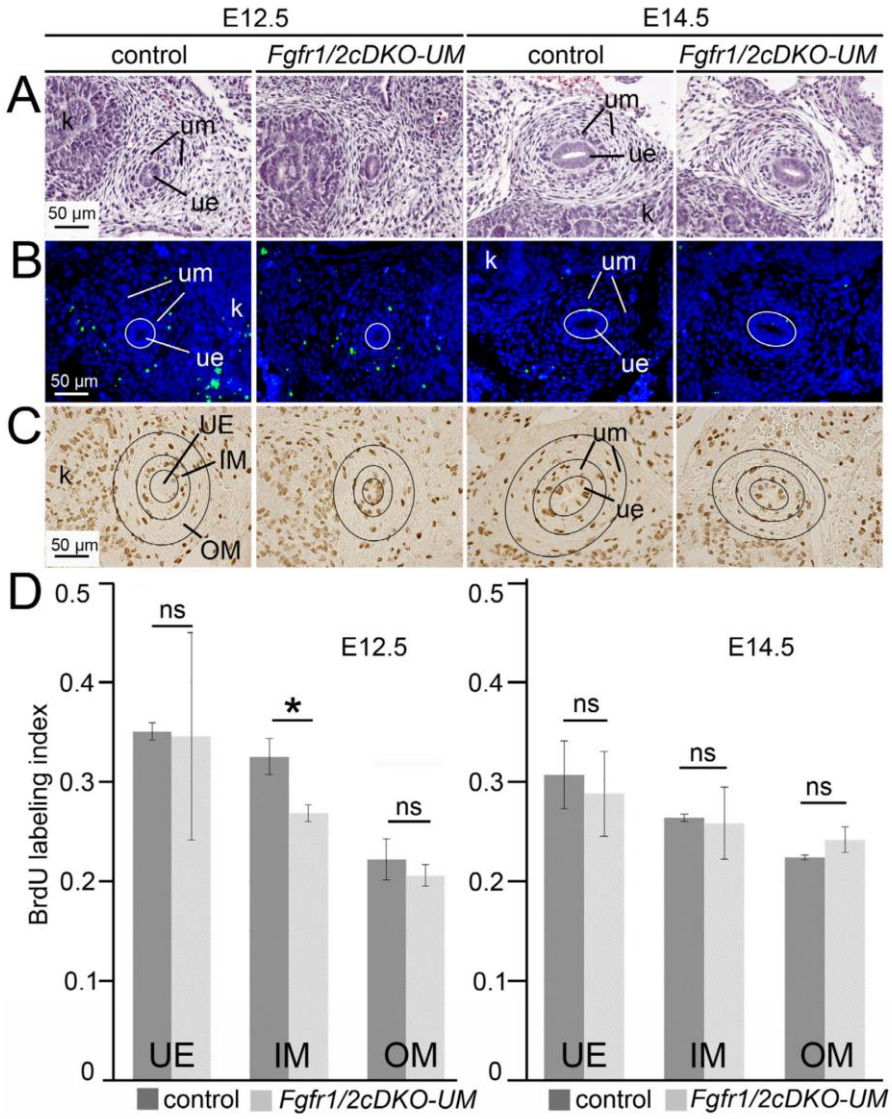

Fig. S5. *Fgfr1/2cDKO-UM* ureters exhibit reduced proliferation in the inner layer of the UM at E12.5. (A) Haematoxylin and eosin staining of transverse sections of the proximal ureter of control and *Fgfr1/2cDKO-UM* embryos at E12.5 and E14.5. (B) Immunofluorescence analysis (green) of apoptosis by the TUNEL assay on proximal ureter sections of control and *Fgfr1/2cDKO-UM* embryos at E12.5 and E14.5. Nuclei are counter-stained with DAPI (blue). *n*≥3 for each assay, stage and genotype. The white line indicates the ureteric epithelium. (C) Determination of cellular proliferation by the BrdU incorporation assay on transverse sections of the proximal ureter of control and *Fgfr1/2cDKO-UM* embryos at E12.5 and E14.5. Black circles mark the epithelium (UE) and the inner (IM) and outer (OM) mesenchymal compartments of the ureter in which proliferation was quantified (D). Quantification of BrdU-positive cells. Values are displayed as mean±sd. *, P<0.05; two-tailed Student's t-test. For detailed values see Table S3. k, kidney; ue, ureteric epithelium; um, ureteric mesenchyme.

Development: doi:10.1242/dev.200767: Supplementary information

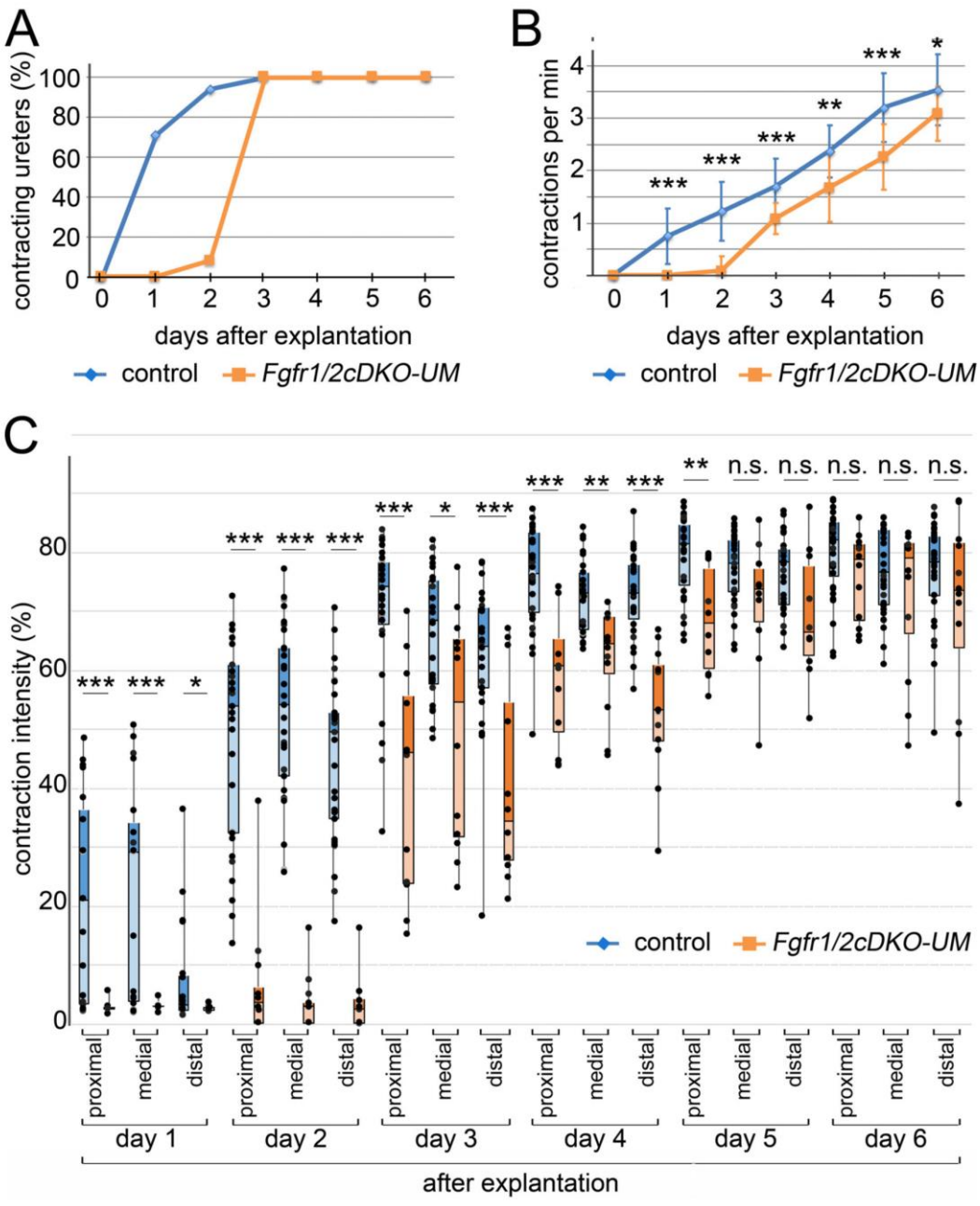

Fig. S6. Peristaltic activity in *Fgfr1/2cDKO-UM* ureters is delayed and reduced but not abrogated. (A-C) E15.5 ureters (control, *n*=32; *Fgfr1/2cDKO-UM, n*=12) were explanted and peristaltic activity observed for 6 days in culture. (A) Diagram showing the percentage of contracting ureters at any time-point of the culture. (B) Diagram of the contraction frequency (per min). (C) Box blot visualizing the contraction intensity. Statistical values are shown as mean±sd. *, P<0.05; **, P<0.01; ***, P<0.001; two-tailed Student's t-test. For detailed values see Table S5.

Development: doi:10.1242/dev.200767: Supplementary information

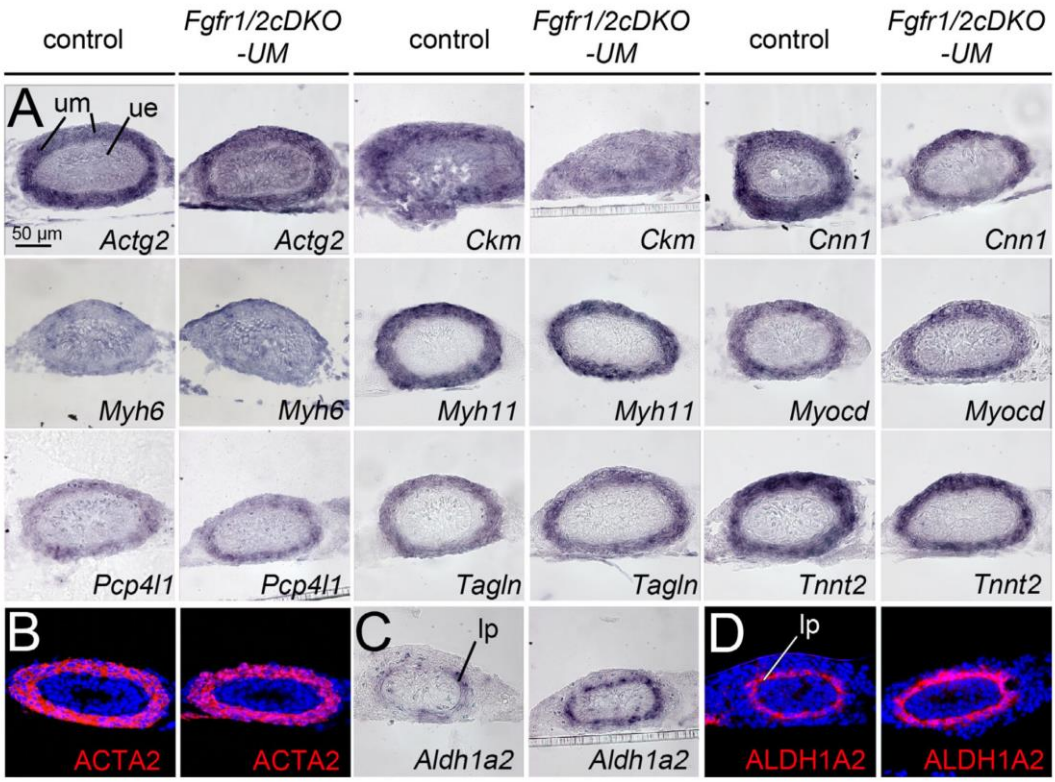

Fig. S7. SMC markers are largely unchanged in 6-day cultures of E15.5 *Fgfr1/2cDKO-UM* ureters. (A-D) Expression analysis on transverse sections of E15.5 ureter explants cultured for 6 days by RNA *in situ* hybridization (A,C) and by immunofluorescence (B,D) for SMC markers (A,B) and the *lamina propria* marker *Aldh1a2*/ALDH1A2 (C,D). $n \geq 3$ for each marker, assay and genotype. lp, lamina propria; ue, ureteric epithelium; um, ureteric mesenchyme.

Development: doi:10.1242/dev.200767: Supplementary information

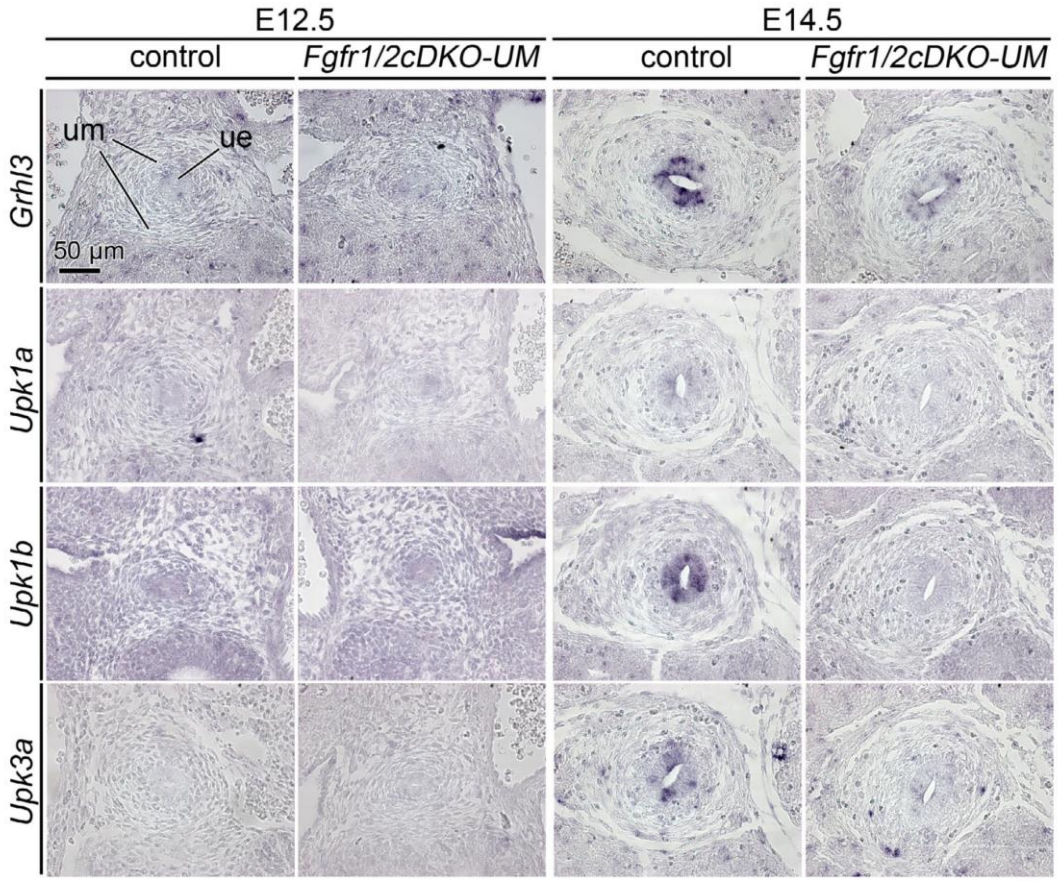

Fig. S8. Markers of superficial cells exhibit reduced expression in *Fgfr1/2cDKO-UM* ureters at E14.5. RNA *in situ* hybridization analysis on transverse sections of E12.5 and E14.5 ureters for expression of *Grhl3*, *Upk1a, Upk1b* and *Upk3a*. $n \geq 3$ for each probe, stage and genotype. ue, ureteric epithelium; um, ureteric mesenchyme.

Development: doi:10.1242/dev.200767: Supplementary information

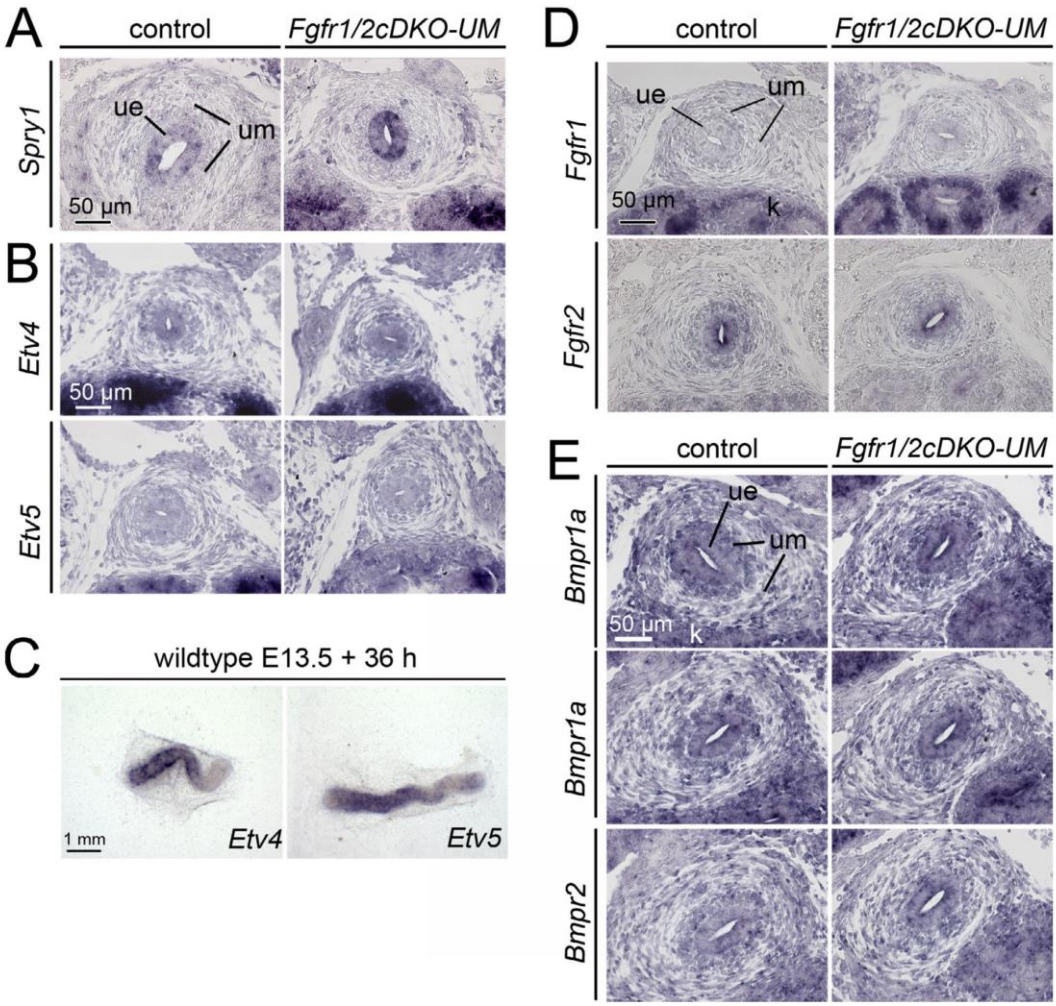

Fig. S9. Loss of mesenchymal *Fgfr1* and *Fgfr2* expression leads to increased epithelial FGFR2 signaling. (A-E) RNA *in situ* hybridization analysis of expression of *Spry1* (A), *Etv4* and *Etv5* (B,C), *Fgfr1* and *Fgfr2* (D) as well as *Bmpr1a*, *Bmpr1b* and *Bmpr2* (E) on transverse sections of the proximal ureter of *Fgfr1/2cKO-UM* and control embryos at E14.5 (A,B,D,E), and on whole E13.5 wild-type ureters cultured for 36 h (C). $n \geq 3$ for each probe and genotype. k, kidney; ue, ureteric epithelium; um, ureteric mesenchyme.

Development: doi:10.1242/dev.200767: Supplementary information

Table S1. Genotype distribution of embryos obtained from matings of *Tbx18*$^{cre/+;}$*Fgfr1*$^{fl/+;}$ *Fgfr2*$^{fl/+}$ males with *Fgfr1*$^{fl/fl}$;*Fgfr2*$^{fl/fl}$ females at E12.5, E14.5, E16.5 and E18.5.

Click here to download Table S1

Table S2. Distribution of hydroureter formation in urogenital systems of embryos obtained from matings of *Tbx18*$^{cre/+;}$*Fgfr1*$^{fl/+}$;*Fgfr2*$^{fl/+}$ males with *Fgfr1*$^{fl/fl}$;*Fgfr2*$^{fl/fl}$ females at E18.5.

Click here to download Table S2

Table S3. Quantification of the BrdU incorporation assay of proximal sections of control and *Fgfr1/2cDKO-UM* embryos at E12.5 and E14.5.

Click here to download Table S3

Table S4. Statistics on the peristaltic activity of explants of E13.5 *Fgfr1/2cDKO-UM* ureters cultured for 6 days.

Click here to download Table S4

Table S5. Statistics on the peristaltic activity of explants of E15.5 *Fgfr1/2cDKO-UM* ureters cultured for 6 days.

Click here to download Table S5

Table S6. List of genes with increased expression in the microarray of E15.5 ureters of *Fgfr1/2cDKO-UM* and control embryos cultured for 6 days.

Click here to download Table S6

Table S7. List of genes with decreased expression in the microarray of E15.5 ureters of *Fgfr1/2cDKO-UM* and control embryos cultured for 6 days.

Click here to download Table S7

Development: doi:10.1242/dev.200767: Supplementary information

Table S8. Functional annotation by DAVID for genes with increased expression in the microarray of E15.5 *Fgfr1/2cDKO-UM* ureter explants cultured for 6 days.

Click here to download Table S8

Table S9. Functional annotation by DAVID for genes with decreased expression in the microarray of E15.5 *Fgfr1/2cDKO-UM* ureter explants cultured for 6 days.

Click here to download Table S9

Table S10. List of genes with decreased expression in the microarray of E14.5 ureters of *Fgfr1/2cDKO-UM* and control embryos.

Click here to download Table S10

Table S11. List of genes with increased expression in the microarray of E14.5 ureters of *Fgfr1/2cDKO-UM* and control embryos.

Click here to download Table S11

Table S12. Functional annotation clustering by DAVID for genes with decreased expression in the microarray of E14.5 *Fgfr1/2cDKO-UM* ureters.

Click here to download Table S12

Table S13. Functional annotation clustering by DAVID for genes with increased expression in the microarray of E14.5 *Fgfr1/2cDKO-UM* ureters.

Click here to download Table S13

Development: doi:10.1242/dev.200767: Supplementary information

Table S14. Expression analyses by RT-qPCR analysis.

Click here to download Table S14

Table S15. Genes with decreased expression in microarrays of E13.5 *Pax2cre/; Fgfr1*$^{fl/+}$*;Fgfr2*$^{fl/fl}$ *(Fgfr1/2cDKO-UE)* ureters.

Click here to download Table S15

Table S16. Statistical analysis of contraction frequencies of explants of E13.5 ureters cultured for 8 days in the presence of purmorphamine and/or NOGGIN.

Click here to download Table S16

Table S17. Primers for qRT-PCR analysis of gene expression.

Click here to download Table S17

Supplementary Tables

Genotype	*Tbx18*$^{+/+}$	*Tbx18*$^{cre/+}$ *Fgfr1*$^{fl/+}$ *Fgfr2*$^{fl/+}$	*Tbx18*$^{cre/+}$ *Fgfr1*$^{fl/fl}$ *Fgfr2*$^{fl/+}$	*Tbx18*$^{cre/+}$ *Fgfr1*$^{fl/+}$ *Fgfr2*$^{fl/fl}$	*Tbx18*$^{cre/+}$ *Fgfr1*$^{fl/fl}$ *Fgfr2*$^{fl/fl}$
(expected frequency)	50%	(12.5%)	(12.5%)	(12.5%)	(12.5%)
Stage/Numbers	Numbers (obtained frequency)				
E12.5, n=448	279 (63%)	27 (6%)	50 (11%)	46 (10%)	46 (10%)
E14.5, n=386	205 (53%)	29 (8%)	39 (10%)	59 (15%)	54 (14%)
E15.5, n=183	88 (48%)	17 (9%)	24 (13%)	29 (16%)	25 (14%)
E16.5, n=37	18 (49%)	6 (16%)	6 (16%)	4 (11%)	3 (8%)
E18.5, n=185	106 (57%)	9 (5%)	22 (12%)	23 (12%)	25 (14%)

Table S1. Genotype distribution of embryos obtained from matings of *Tbx18*$^{cre/+}$*;Fgfr1*$^{fl/+}$*;Fgfr2*$^{fl/+}$ males with *Fgfr1*$^{fl/fl}$*;Fgfr2*$^{fl/fl}$ females at E12.5, E14.5, E16.5 and E18.5.

Genotype / **Phenotype**	*Tbx18*$^{+/+}$	*Tbx18*$^{cre/+}$*; Fgfr1*$^{fl/+}$*; Fgfr2*$^{fl/+}$	*Tbx18*$^{cre/+}$*; Fgfr1*$^{fl/fl}$*; Fgfr2*$^{fl/+}$	*Tbx18*$^{cre/+}$*; Fgfr1*$^{fl/+}$*; Fgfr2*$^{fl/fl}$	*Tbx18*$^{cre/+}$*; Fgfr1*$^{fl/fl}$*; Fgfr2*$^{fl/fl}$
normal	26 (84%)	3 (50%)	3 (38%)	0 (0%)	0 (0%)
mild hydroureter	5 (16%)	3 (50%)	5 (64%)	10 (84%)	7 (78%)
strong hydroureter	0 (0%)	0 (0%)	0 (0%)	2 (16%)	2 (22%)

Table S2. Distribution of hydroureter formation in urogenital systems of embryos obtained from matings of *Tbx18*$^{cre/+}$*;Fgfr1*$^{fl/+}$*;Fgfr2*$^{fl/+}$ males with *Fgfr1*$^{fl/fl}$*;Fgfr2*$^{fl/fl}$ females at E18.5.

E12.5	U		IM		OM	
	Mean	SD	Mean	SD	Mean	SD
control (n=3)	0.3508	0.0087	0.3255	0.0183	0.222	0.0206
***Fgfr1/2cDKO-UM* (n=3)**	0.3459	0.1043	0.2685	0.0084	0.2059	0.0108
p-Value	0.9796		0.0204		0.3384	
E14.5	**U**		**IM**		**OM**	
	Mean	SD	Mean	SD	Mean	SD
control (n=3)	0.3053	0.034	0.2626	0.0036	0.2229	0.0024
***Fgfr1/2cDKO-UM* (n=3)**	0.2866	0.0425	0.2572	0.0359	0.2406	0.0126
p-Value	0.5854		0.7735		0.1328	

Table S3. Quantification of the BrdU incorporation assay of proximal sections of control and *Fgfr1/2cDKO-UM* embryos at E12.5 and E14.5. The statistical significance was calculated by a two-tailed Student's t-test. SD, standard derivation; U, urothelium; IM, inner mesenchyme; OM, outer mesenchyme.

	day 2	**day 3**	**day 4**	**day 5**	**day 6**	**day 7**	**day 8**
control (n=42)	0.0238	0.5952	0.8333	1	1	1	1
***Fgfr1/2cDKO-UM* (n=17)**	0	0	0.2352	0.6471	0.8235	0.8824	1

Table S4A. Statistics on the peristaltic activity of explants of E13.5 control and *Fgfr1/2cDKO-UM* ureters cultured for 8 days. The onset of peristaltic activity is shown as the number of contracting ureters to all ureters at day 2 to 8 days of culture.

	day 2	**day 3**	**day 4**	**day 5**	**day 6**	**day 7**	**day 8**
control average (n=42)	0.0238	1.0476	2.2619	2.6905	2.881	3.2857	3.4048
***Fgfr1/2cDKO-UM* average (n=17)**	0	0	0.5294	1.3529	1.8824	2.5294	2.8824
SD control	0.1543	1.0110	1.2506	0.8692	0.6325	0.6357	0.7005
SD *Fgfr1/2cDKO-UM*	0	0	0.5294	1.3529	1.8824	2.5294	2.8824
p-Value	0.5293	8E-05	4.4E-06	1.9E-05	0.0001	0.0029	0.0257

Table S4B. Statistical analysis of the peristaltic frequency of E13.5 control and *Fgfr1/2cDKO-UM* ureters over 8 days of culture. Shown are the average and corresponding standard deviations of peristaltic contractions per minute after 2 to 8 days after ureter explantation at E13.5. One minute was video-monitored. The statistical significance was calculated by a two-tailed Student's t-test. SD, standard derivation.

	Day 2			Day 3			Day 4			Day 5			Day 6			Day 7			Day 8		
	proximal	medial	distal	proximal	medial	distal	proximal	medial	distal	proximal	medial	distal	proximal	medial	distal	proximal	medial	distal	proximal	medial	distal
control median	0.0000	0.0000	0.0000	0.0000	0.0387	0.0000	0.0931	0.1265	0.0519	0.3081	0.3168	0.1523	0.4654	0.4972	0.3526	0.5955	0.6172	0.5273	0.5840	0.6515	0.6003
Fgfr1/2cDKO-UM median	0.0000	0.0000	0.0000	0.0000	0.0000	0.0000	0.0000	0.0000	0.0000	0.0598	0.0599	0.0617	0.1777	0.1479	0.1009	0.3219	0.3391	0.2677	0.3806	0.3913	0.4395
SD control	0.0115	0.0069	0.0000	0.0364	0.0648	0.0254	0.1051	0.1308	0.0795	0.1909	0.1806	0.1699	0.1928	0.1884	0.2079	0.1559	0.1224	0.1525	0.1230	0.0984	0.1190
SD *Fgfr1/2cDKO-UM*	0.0000	0.0000	0.0000	0.0000	0.0000	0.0000	0.0486	0.0376	0.0290	0.0867	0.1002	0.0529	0.1635	0.1611	0.1044	0.1938	0.2121	0.1548	0.1706	0.1801	0.1552
p-Value	0.3232	0.3232	nd	1.2E-05	5.3E-06	0.0383	7.1E-06	1.7E-07	0.0003	2.3E-08	1.6E-07	6.5E-06	8.7E-05	2.4E-06	2.1E-07	0.0027	0.0007	1.5E-05	0.0260	0.0016	0.0005

Table S4C. Statistical analysis of contraction intensities of E13.5 ureters from control (n=42) and *Fgfr1/2cDKO-UM* (n=17) embryos after 2 to 8 days of culture. Shown is the maximal intensity of one peristaltic contraction from day 2 to 8 of culture after ureter explantation at E13.5. The proximal level equals to 25%, medial to 50% and distal to 75% of the entire ureter length. One minute was video-monitored. Contraction intensity was calculated measuring the diameter of the ureter in a relaxed and a contracted state. The statistical significance was calculated by a two-tailed Student's t-test. SD, standard derivation. nd, not defined.

	day 1	day 2	day 3	day 4	day 5	day 6
control (n=24)	0.7200	0.9375	1	1	1	1
***Fgfr1/2cDKO* (n=12)**	0	0.0833	1	1	1	1

Table S5A. Onset of peristaltic activity of explants of E15.5 *Fgfr1/2cDKO* ureters in culture. Shown are the number of control and mutant ureters that exhibit peristaltic contraction waves at each day of the 6-day culture period.

	day 1	day 2	day 3	day 4	day 5	day 6
control average (n=24)	0.75	1.22	1.70	2.37	3.19	3.53
***Fgfr1/2cDKO-UM* average (n=12)**	0.00	0.17	1.08	1.67	2.10	3.08
SD control	0.53	0.55	0.53	0.49	0.65	0.67
SD *Fgfr1/2cDKO-UM*	0.00	0.39	0.29	0.65	0.57	0.51
p-Value	4.79E-07	1.05E-07	2.72E-05	0.0039	8.33E-05	0.0264

Table S5B. Statistical analysis of the peristaltic frequency of E15.5 control and *Fgfr1/2cDKO-UM* ureters over 6 days of culture. Shown are the average and corresponding standard deviations of peristaltic contractions per minute at day 1 to 6 after ureter explantation at E15.5. One minute was video-monitored. The statistical significance was calculated by a two-tailed Student's t-test. SD, standard derivation.

	Day 1			Day 2			Day 3			Day 4			Day 5			Day 6		
	proximal	medial	distal	proximal	medial	distal	proximal	medial	distal	proximal	medial	distal	proximal	medial	distal	proximal	medial	distal
control median	0.2102	0.2197	0.0766	0.4836	0.5310	0.4521	0.7009	0.6676	0.6264	0.7581	0.7267	0.7280	0.7936	0.7725	0.7650	0.8021	0.7695	0.7671
Fgfr1/2cDKO-UM median	0.0304	0.0310	0.0272	0.0660	0.0366	0.0443	0.4141	0.5022	0.4050	0.5897	0.6207	0.5312	0.6837	0.7157	0.6926	0.7601	0.7257	0.7016
SD control	0.1728	0.1827	0.0929	0.1733	0.1455	0.1385	0.1271	0.1037	0.1244	0.0869	0.0605	0.0696	0.0692	0.0606	0.0636	0.0724	0.0708	0.0848
SD *Fgfr1/2cDKO-UM*	0.0132	0.0091	0.0057	0.1057	0.0454	0.0580	0.1896	0.1956	0.1715	0.1123	0.0888	0.1113	0.0906	0.1085	0.1083	0.0744	0.1303	0.1645
p-Value	0.0003	0.0003	0.0333	7.1E-11	9.9E-19	4.7E-16	0.0002	0.0154	0.0009	0.0002	0.0017	4.8E-05	0.0040	0.1429	0.0699	0.1095	0.2882	0.2106

Table S5C. Statistical analysis of contraction intensities of E15.5 ureters from control (n=24) and *Fgfr1/2cDKO-UM* (n=12) embryos after 1 to 6 days of culture. Shown is the maximal intensity of one peristaltic contraction at day 1 to 6 of culture after ureter explantation at E15.5. The proximal level equals to 25%, medial to 50% and distal to 75% of the entire ureter length. One minute was video-monitored. Contraction intensity equals to Multi-Kymograph grey value ratios. The statistical significance was calculated by a two-tailed Student's t-test. SD, standard derivation.

	Intensities				Fold change (FC)		
GeneName_RCUT	**control 1**	**mutant 1**	**control 2**	**mutant 2**	**FC 1**	**FC 2**	**avgFC**
Ackr4	59	1054	89	854	17.8	9.6	13.7
Cdh16	93	1433	84	313	15.3	3.7	9.5
Egr4	85	535	100	536	6.3	5.4	5.8
D030062O11Rik	36	104	37	150	2.9	4.1	3.5
Epha8	102	288	113	436	2.8	3.8	3.3
Akap12	173	547	246	456	3.2	1.9	2.5
Tfcp2l1	173	493	166	349	2.9	2.1	2.5
Gm13178	196	417	169	435	2.1	2.6	2.4
Itln1	126	390	262	420	3.1	1.6	2.4
Pnmal2	64	156	83	179	2.4	2.2	2.3
Msln	458	970	531	1297	2.1	2.4	2.3
Crym	873	2262	966	1848	2.6	1.9	2.3
Scnn1b	180	447	171	344	2.5	2.0	2.2
Mei1	127	221	102	276	1.7	2.7	2.2
Kcnj10	167	456	233	393	2.7	1.7	2.2
Fam78b	712	1490	704	1607	2.1	2.3	2.2
Fut9	113	263	118	241	2.3	2.0	2.2
Ipcef1	423	1034	534	1009	2.4	1.9	2.2
Sowaha	61	126	54	118	2.1	2.2	2.1
Smtnl2	173	325	182	430	1.9	2.4	2.1
Hoxb8	673	1175	794	1951	1.7	2.5	2.1
Vipr1	354	660	505	1160	1.9	2.3	2.1
Gm5083	68	116	51	123	1.7	2.4	2.1
Rimkla	200	384	247	534	1.9	2.2	2.0
Arc	130	297	108	190	2.3	1.8	2.0
Grik3	223	500	328	588	2.2	1.8	2.0
Notumos	144	298	177	349	2.1	2.0	2.0
Adra2a	360	665	450	973	1.8	2.2	2.0
Sp5	120	246	185	358	2.1	1.9	2.0
Upk1a	32216	57526	30520	67356	1.8	2.2	2.0
Gata3	5074	8706	5885	13359	1.7	2.3	2.0
Bcl11a	82	185	115	200	2.2	1.7	2.0
Klhl14	68	126	68	145	1.9	2.1	2.0
Pnliprp1	206	364	253	561	1.8	2.2	2.0
Upb1	213	381	209	455	1.8	2.2	2.0
Unc13c	472	1032	519	915	2.2	1.8	2.0
Myh14	852	1397	791	1808	1.6	2.3	2.0
Ptch1	272	584	336	585	2.2	1.7	1.9
Fzd10	395	674	510	1114	1.7	2.2	1.9
Tgm5	396	686	425	913	1.7	2.1	1.9
Cntnap2	248	476	217	422	1.9	1.9	1.9
Ksr2	137	307	148	237	2.2	1.6	1.9
Fgfr2	196	385	185	347	2.0	1.9	1.9

Col23a1	61	117	70	133	1.9	1.9	1.9
Lef1	190	391	235	407	2.1	1.7	1.9
A_55_P1953783	120	272	198	302	2.3	1.5	1.9
Cntn3	99	206	128	216	2.1	1.7	1.9
Slco2a1	575	1019	632	1260	1.8	2.0	1.9
Lppr5	301	611	394	681	2.0	1.7	1.9
Slc9a4	116	215	92	175	1.9	1.9	1.9
Clstn2	459	852	604	1128	1.9	1.9	1.9
Kcnb2	67	112	73	147	1.7	2.0	1.9
AA986860	2145	3617	1812	3644	1.7	2.0	1.8
Kif26b	59	116	90	156	2.0	1.7	1.8
Adora1	335	677	441	737	2.0	1.7	1.8
Akr1b7	104	193	94	171	1.9	1.8	1.8
Apol8	235	497	325	503	2.1	1.5	1.8
Scube2	163	318	164	281	2.0	1.7	1.8
Sox9	212	455	304	461	2.1	1.5	1.8
Negr1	68	130	79	137	1.9	1.8	1.8
Tdrp	2002	3875	2258	3893	1.9	1.7	1.8
Rhbg	76	123	59	119	1.6	2.0	1.8
Kcnmb4	256	480	357	632	1.9	1.8	1.8
Gstm1	36216	69303	35998	61606	1.9	1.7	1.8
Erc2	106	223	171	258	2.1	1.5	1.8
AI661453	1202	1810	1508	3168	1.5	2.1	1.8
Ap1s3	1790	2865	1828	3665	1.6	2.0	1.8
Adamts17	410	771	584	1005	1.9	1.7	1.8
Tmco4	2236	3768	2320	4442	1.7	1.9	1.8
Flrt1	1475	2749	1747	3033	1.9	1.7	1.8
Rspo1	385	627	382	751	1.6	2.0	1.8
Nrip3	331	584	363	664	1.8	1.8	1.8
Tmem132c	274	476	300	556	1.7	1.9	1.8
1700047E10Rik	288	594	267	407	2.1	1.5	1.8
Tmem145	108	172	140	278	1.6	2.0	1.8
Plce1	129	222	117	216	1.7	1.8	1.8
Extl1	104	192	130	224	1.9	1.7	1.8
Cck	165	314	176	294	1.9	1.7	1.8
Cldn8	2474	4897	2654	4212	2.0	1.6	1.8
Nedd4l	183	326	226	400	1.8	1.8	1.8
Acer2	86	152	66	117	1.8	1.8	1.8
Casz1	451	873	651	1049	1.9	1.6	1.8
Hoxd3	192	360	213	357	1.9	1.7	1.8
Dner	168	304	203	352	1.8	1.7	1.8
Cdh1	3249	5399	3677	6895	1.7	1.9	1.8
Pllp	475	787	541	1016	1.7	1.9	1.8
Sh3gl2	382	656	355	640	1.7	1.8	1.8
1110035H17Rik	61	106	70	125	1.7	1.8	1.8

Grhl3	2835	4935	2728	4812	1.7	1.8	1.8
Mycl	483	797	512	944	1.7	1.8	1.7
Plagl2	78	142	86	144	1.8	1.7	1.7
Cspg5	336	505	366	727	1.5	2.0	1.7
5031439G07Rik	85	157	74	121	1.9	1.6	1.7
Thsd4	499	910	460	763	1.8	1.7	1.7
Ajap1	158	282	166	282	1.8	1.7	1.7
Pou3f3	74	133	69	116	1.8	1.7	1.7
Fgfr4	173	317	226	364	1.8	1.6	1.7
Ntng1	180	304	221	387	1.7	1.8	1.7
Foxa1	7147	11579	8244	15049	1.6	1.8	1.7
Wnt4	5555	8403	6893	13296	1.5	1.9	1.7
Pvrl4	207	365	279	470	1.8	1.7	1.7
Tox3	91	140	90	169	1.5	1.9	1.7
Rnf186	81	122	57	110	1.5	1.9	1.7
Palm3	78	135	83	139	1.7	1.7	1.7
Kcng1	159	245	208	391	1.5	1.9	1.7
Fam183b	240	450	270	418	1.9	1.5	1.7
Jag2	312	529	376	650	1.7	1.7	1.7
Usp27x	83	142	96	165	1.7	1.7	1.7
Wnt10a	295	447	407	773	1.5	1.9	1.7
Scube3	713	1171	874	1542	1.6	1.8	1.7
Tmem229a	351	641	425	670	1.8	1.6	1.7
Crebl2	139	260	140	213	1.9	1.5	1.7
Nkd1	3144	5014	4259	7651	1.6	1.8	1.7
Ppcdc	76	142	79	119	1.9	1.5	1.7
Prss12	92	169	156	240	1.8	1.5	1.7
Foxl1	607	933	843	1541	1.5	1.8	1.7
Col26a1	397	685	516	843	1.7	1.6	1.7
Mgat3	717	1138	765	1351	1.6	1.8	1.7
Adssl1	1312	2227	1489	2463	1.7	1.7	1.7
Sfrp2	7770	11849	8925	16285	1.5	1.8	1.7
Ppp1r26	164	264	214	371	1.6	1.7	1.7
Tyro3	4370	7576	5890	9500	1.7	1.6	1.7
Gm6403	133	230	170	273	1.7	1.6	1.7
Lrrc8b	564	945	639	1064	1.7	1.7	1.7
Llgl2	1326	2143	1406	2405	1.6	1.7	1.7
Cpm	422	659	397	699	1.6	1.8	1.7
Gldc	971	1607	1080	1797	1.7	1.7	1.7
Faah	106	188	117	181	1.8	1.5	1.7
Evpl	4158	6482	4770	8275	1.6	1.7	1.6
Fgfr3	2429	3894	2611	4391	1.6	1.7	1.6
Rgl3	2235	3756	2760	4420	1.7	1.6	1.6
Grhl2	88	147	77	123	1.7	1.6	1.6
Cux2	215	336	263	452	1.6	1.7	1.6

Diap1	161	282	168	256	1.7	1.5	1.6
Wnt6	388	590	563	986	1.5	1.8	1.6
Shisa2	122	191	159	270	1.6	1.7	1.6
Engase	440	714	562	925	1.6	1.6	1.6
Fam160a1	508	762	623	1100	1.5	1.8	1.6
Mzf1	265	436	342	554	1.6	1.6	1.6
Cyp4f15	397	670	333	525	1.7	1.6	1.6
Cutal	96	148	102	176	1.5	1.7	1.6
Itpr3	3995	6323	4691	7822	1.6	1.7	1.6
Nckap5	178	280	188	315	1.6	1.7	1.6
Kctd1	320	488	373	641	1.5	1.7	1.6
D430019H16Rik	1488	2448	2000	3184	1.6	1.6	1.6
Tmem191c	809	1221	1065	1838	1.5	1.7	1.6
4930426D05Rik	93	151	96	154	1.6	1.6	1.6
Plekhh1	2677	4478	3219	5014	1.7	1.6	1.6
Smcp	90	148	74	118	1.6	1.6	1.6
ENSMUST00000071101	61	105	83	126	1.7	1.5	1.6
Ror2	1683	2589	2180	3647	1.5	1.7	1.6
Prkar1b	81	136	91	138	1.7	1.5	1.6
Gm13547	90	144	78	125	1.6	1.6	1.6
Aldh5a1	987	1604	1503	2360	1.6	1.6	1.6
Hoxd11	1580	2675	1929	2896	1.7	1.5	1.6
Nr2f1	8866	13767	10888	17850	1.6	1.6	1.6
Abcc3	3732	5899	3722	5991	1.6	1.6	1.6
Sapcd2	426	716	449	675	1.7	1.5	1.6
Trim41	13038	21382	16884	26082	1.6	1.5	1.6
Epb4.1l4b	4141	6682	4706	7389	1.6	1.6	1.6
Sprn	523	834	520	824	1.6	1.6	1.6
Ppp1r10	119	192	124	192	1.6	1.6	1.6
Slc7a8	326	491	311	516	1.5	1.7	1.6
Arhgef10l	3653	5733	4780	7598	1.6	1.6	1.6
Sncaip	2312	3581	2580	4153	1.5	1.6	1.6
Lrrc8e	1224	1841	1144	1887	1.5	1.6	1.6
Mal	31908	49382	32262	51742	1.5	1.6	1.6
C77080	4510	7046	5949	9439	1.6	1.6	1.6
Ism1	423	639	459	751	1.5	1.6	1.6
9530068E07Rik	18816	29520	23794	37540	1.6	1.6	1.6
Aifm3	72	112	67	107	1.6	1.6	1.6
Sesn3	1901	3082	2129	3232	1.6	1.5	1.6
Col16a1	2251	3503	2746	4330	1.6	1.6	1.6
Map3k4	4440	7036	5451	8380	1.6	1.5	1.6
Tmem132a	6321	9554	8549	13740	1.5	1.6	1.6
Zbtb32	244	371	256	407	1.5	1.6	1.6
Fbf1	114	178	134	208	1.6	1.6	1.6
Gm15800	2606	4124	3355	5124	1.6	1.5	1.6

Rap1gap	299	475	319	483	1.6	1.5	1.6
Mvb12b	4063	6229	5713	8868	1.5	1.6	1.5
A_55_P2020072	932	1440	1056	1620	1.5	1.5	1.5
Tmem25	242	373	247	379	1.5	1.5	1.5
Nudt11	546	855	717	1080	1.6	1.5	1.5
Igdcc4	2409	3686	2985	4573	1.5	1.5	1.5
Inadl	1168	1785	1314	2014	1.5	1.5	1.5
Gm10748	187	285	202	310	1.5	1.5	1.5
Hpn	255	384	306	474	1.5	1.5	1.5
Tigar	273	413	292	449	1.5	1.5	1.5
Slc35g1	7613	11462	8926	13524	1.5	1.5	1.5

Table S6. List of genes with increased expression in the microarray of E15.5 ureters of *Fgfr1/2cDKO-UM* and control embryos cultured for 6 days. Shown are the gene names, the intensity of the two control and mutant ureter samples, the individual and the average (avg) fold change (FC).

	Intensities				**Fold change (FC)**		
Gene name	**control 1**	**mutant 1**	**control 2**	**mutant 2**	**FC 1**	**FC 2**	**avgFC**
Cfd	18721	7988	13456	768	-2.3	-17.5	-9.9
Mup20	1054	609	640	37	-1.7	-17.3	-9.5
Ces1d	384	172	284	17	-2.2	-16.6	-9.4
Mrap	2060	678	1518	106	-3.0	-14.3	-8.7
Mup1	4768	2235	2522	205	-2.1	-12.3	-7.2
Wfdc21	286	177	288	24	-1.6	-12.1	-6.9
Cidec	1509	849	1215	114	-1.8	-10.7	-6.2
Thrsp	3715	1047	3003	346	-3.5	-8.7	-6.1
Retn	1668	615	1588	171	-2.7	-9.3	-6.0
Adipoq	5356	2371	4374	451	-2.3	-9.7	-6.0
Ces1f	183	66	127	15	-2.8	-8.5	-5.6
Mup3	219	126	133	15	-1.7	-8.9	-5.3
ENSMUST00000120662	969	519	498	58	-1.9	-8.6	-5.2
Myh6	1938	333	1880	451	-5.8	-4.2	-5.0
Fabp4	15497	7075	15194	2103	-2.2	-7.2	-4.7
LOC100048884	5444	2731	2635	361	-2.0	-7.3	-4.6
Mup19	7333	3908	3931	532	-1.9	-7.4	-4.6
Mup2	2741	1678	1663	221	-1.6	-7.5	-4.6
ENSMUST00000178663	203	102	107	15	-2.0	-7.1	-4.6
Mup17	2500	1319	1199	177	-1.9	-6.8	-4.3
Gpd1	4581	1984	3579	563	-2.3	-6.4	-4.3
Pck1	244	117	210	38	-2.1	-5.5	-3.8
Scd1	18931	8858	13712	2512	-2.1	-5.5	-3.8
Slc36a2	1835	1034	1653	298	-1.8	-5.5	-3.7
Hp	11614	5132	7812	1752	-2.3	-4.5	-3.4
Plin1	1386	894	1297	263	-1.5	-4.9	-3.2
Ifi205	605	238	605	168	-2.5	-3.6	-3.1

Itih4	904	548	698	157	-1.6	-4.4	-3.0
C6	230	107	159	41	-2.1	-3.9	-3.0
Mup5	395	245	209	47	-1.6	-4.4	-3.0
F13a1	481	198	465	139	-2.4	-3.3	-2.9
TC1687046	327	154	137	38	-2.1	-3.6	-2.8
Acp5	2981	1509	3841	1041	-2.0	-3.7	-2.8
LOC102636514	110	46	164	53	-2.4	-3.1	-2.7
Rxrg	140	64	116	36	-2.2	-3.2	-2.7
AW112010	883	573	960	260	-1.5	-3.7	-2.6
Gm1987	434	131	364	196	-3.3	-1.9	-2.6
Vstm2l	140	60	120	43	-2.3	-2.8	-2.6
Cartpt	1209	754	1499	442	-1.6	-3.4	-2.5
A530016L24Rik	151	79	104	34	-1.9	-3.0	-2.5
Mup4	1877	1173	1023	304	-1.6	-3.4	-2.5
Gja5	438	182	336	132	-2.4	-2.5	-2.5
Cxcl1	308	191	413	124	-1.6	-3.3	-2.5
Cav3	1347	600	1187	456	-2.2	-2.6	-2.4
Phox2b	149	65	199	82	-2.3	-2.4	-2.4
Nefl	709	292	715	312	-2.4	-2.3	-2.4
Serpina3f	255	116	139	56	-2.2	-2.5	-2.3
Aspn	1002	471	985	393	-2.1	-2.5	-2.3
A_55_P2145656	831	371	665	281	-2.2	-2.4	-2.3
Tppp3	1461	600	1285	601	-2.4	-2.1	-2.3
Cox8b	5553	2808	4652	1793	-2.0	-2.6	-2.3
Krtap1-4	209	135	123	42	-1.6	-2.9	-2.2
Gimap6	470	206	383	176	-2.3	-2.2	-2.2
C3	8182	4395	6510	2501	-1.9	-2.6	-2.2
Sprr2d	201	104	273	107	-1.9	-2.5	-2.2
Ly6c1	416	234	350	132	-1.8	-2.6	-2.2
Ly6d	9879	5036	6886	2803	-2.0	-2.5	-2.2
Stmn3	221	105	309	138	-2.1	-2.2	-2.2
Gimap4	122	55	131	61	-2.2	-2.1	-2.2
Cpa2	149	56	116	70	-2.7	-1.7	-2.2
Dusp26	230	111	286	127	-2.1	-2.3	-2.2
Rgcc	1900	1231	1764	633	-1.5	-2.8	-2.2
Ifi44	196	121	212	79	-1.6	-2.7	-2.2
Camp	412	255	437	165	-1.6	-2.7	-2.1
Lrg1	444	287	255	94	-1.5	-2.7	-2.1
Stmn2	661	371	839	343	-1.8	-2.4	-2.1
Svopl	401	158	385	229	-2.5	-1.7	-2.1
P2ry12	108	62	115	47	-1.7	-2.4	-2.1
Esm1	1563	964	1615	630	-1.6	-2.6	-2.1
Sgcd	577	242	546	304	-2.4	-1.8	-2.1
Poln	162	96	159	64	-1.7	-2.5	-2.1
Mc2r	137	71	140	63	-1.9	-2.2	-2.1

Nr1h3	712	451	614	238	-1.6	-2.6	-2.1
Saa2	107	54	114	53	-2.0	-2.2	-2.1
Apoc1	7891	5145	6746	2595	-1.5	-2.6	-2.1
4631405J19Rik	150	64	129	73	-2.3	-1.8	-2.1
Agtr2	2498	1657	3125	1202	-1.5	-2.6	-2.1
Gem	2689	1199	2626	1409	-2.2	-1.9	-2.1
Gja4	744	294	464	296	-2.5	-1.6	-2.0
Dbh	743	361	854	419	-2.1	-2.0	-2.0
Slc6a12	152	84	138	61	-1.8	-2.3	-2.0
Prlr	3545	1976	2968	1303	-1.8	-2.3	-2.0
Maob	567	237	459	277	-2.4	-1.7	-2.0
Icam2	2943	1489	2946	1428	-2.0	-2.1	-2.0
Cnr1	425	271	506	205	-1.6	-2.5	-2.0
Lama4	6516	3138	6377	3318	-2.1	-1.9	-2.0
Apln	864	500	873	385	-1.7	-2.3	-2.0
Sntg2	826	415	775	388	-2.0	-2.0	-2.0
Dpt	2255	1012	1968	1122	-2.2	-1.8	-2.0
Ifitm6	271	148	265	124	-1.8	-2.1	-2.0
Rims1	193	96	147	75	-2.0	-2.0	-2.0
Gng3	215	120	222	104	-1.8	-2.1	-2.0
Mamdc2	352	155	287	173	-2.3	-1.7	-2.0
Mustn1	542	322	453	205	-1.7	-2.2	-1.9
Gpihbp1	1478	746	1105	582	-2.0	-1.9	-1.9
Prph	268	136	251	133	-2.0	-1.9	-1.9
Fcgr2b	729	451	834	370	-1.6	-2.3	-1.9
Dclk3	245	115	245	142	-2.1	-1.7	-1.9
Chil1	230	119	142	76	-1.9	-1.9	-1.9
Phf11d	1566	927	1408	665	-1.7	-2.1	-1.9
Mrap2	390	239	438	202	-1.6	-2.2	-1.9
Capn3	513	269	582	308	-1.9	-1.9	-1.9
Sox7	222	126	241	119	-1.8	-2.0	-1.9
Isg15	297	180	308	146	-1.7	-2.1	-1.9
Batf	282	163	273	135	-1.7	-2.0	-1.9
Tescl	173	85	152	92	-2.0	-1.7	-1.9
Ednrb	2451	1248	2156	1238	-2.0	-1.7	-1.9
Ppbp	106	69	195	90	-1.5	-2.2	-1.8
Acsl1	750	494	616	284	-1.5	-2.2	-1.8
Tnnc2	800	414	735	421	-1.9	-1.7	-1.8
Olfr523	327	212	220	105	-1.5	-2.1	-1.8
Mme	193	112	185	97	-1.7	-1.9	-1.8
Sult1a1	214	119	175	96	-1.8	-1.8	-1.8
Agpat9	1305	852	1220	588	-1.5	-2.1	-1.8
Abca17	259	155	145	75	-1.7	-1.9	-1.8
Sgcg	161	106	154	74	-1.5	-2.1	-1.8
Cd52	2033	1312	2004	979	-1.6	-2.0	-1.8

Afap1l1	641	312	542	352	-2.1	-1.5	-1.8
Sgca	253	130	185	114	-1.9	-1.6	-1.8
Tpmt	666	363	599	346	-1.8	-1.7	-1.8
Scg2	147	92	212	108	-1.6	-2.0	-1.8
Sncg	388	249	294	148	-1.6	-2.0	-1.8
Phf11a	520	337	482	241	-1.5	-2.0	-1.8
Ltc4s	1183	698	895	485	-1.7	-1.8	-1.8
Mmp9	139	75	208	125	-1.9	-1.7	-1.8
Ly6k	185	103	159	93	-1.8	-1.7	-1.8
A_55_P2112097	1591	1036	140	71	-1.5	-2.0	-1.8
Bche	3900	2011	3485	2225	-1.9	-1.6	-1.8
Fcna	279	165	214	119	-1.7	-1.8	-1.7
Adamdec1	921	515	951	561	-1.8	-1.7	-1.7
Cd33	155	91	130	73	-1.7	-1.8	-1.7
Emcn	247	147	205	115	-1.7	-1.8	-1.7
Cdh13	519	277	394	249	-1.9	-1.6	-1.7
Lgals9	1724	1136	1403	727	-1.5	-1.9	-1.7
B230114P17Rik	234	147	227	124	-1.6	-1.8	-1.7
Grap	170	90	167	110	-1.9	-1.5	-1.7
Akr1c14	561	315	514	315	-1.8	-1.6	-1.7
Vat1l	210	122	299	177	-1.7	-1.7	-1.7
Upp1	272	167	247	139	-1.6	-1.8	-1.7
Pde4b	864	481	799	498	-1.8	-1.6	-1.7
Ostn	187	123	250	133	-1.5	-1.9	-1.7
Igfbp3	3208	2025	2916	1607	-1.6	-1.8	-1.7
Tie1	132	74	111	68	-1.8	-1.6	-1.7
Cox7a1	1255	796	1133	623	-1.6	-1.8	-1.7
Sulf1	2609	1449	2174	1367	-1.8	-1.6	-1.7
Ccm2l	130	74	126	78	-1.8	-1.6	-1.7
Nhlh1	2346	1286	1152	749	-1.8	-1.5	-1.7
Cd209d	310	168	247	164	-1.8	-1.5	-1.7
4833415N18Rik	1109	611	728	481	-1.8	-1.5	-1.7
Phox2a	202	116	293	185	-1.7	-1.6	-1.7
Ifitm1	5233	3209	5036	2985	-1.6	-1.7	-1.7
Tmprss3	3792	2228	2183	1354	-1.7	-1.6	-1.7
Agpat2	1557	989	1187	683	-1.6	-1.7	-1.7
Esam	659	371	608	398	-1.8	-1.5	-1.7
Phf11b	684	447	577	328	-1.5	-1.8	-1.6
Adra1b	10286	5850	5873	3854	-1.8	-1.5	-1.6
Dpysl5	6035	3528	3615	2311	-1.7	-1.6	-1.6
Itih3	466	278	505	316	-1.7	-1.6	-1.6
1500015O10Rik	3047	1858	2985	1840	-1.6	-1.6	-1.6
Astn1	153	94	177	109	-1.6	-1.6	-1.6
Arhgap26	1356	792	985	643	-1.7	-1.5	-1.6
Cldn15	1091	672	680	420	-1.6	-1.6	-1.6

Cd300a	1517	883	884	585	-1.7	-1.5	-1.6
Pcdh12	235	141	247	158	-1.7	-1.6	-1.6
Ccdc169	644	382	306	198	-1.7	-1.5	-1.6
Nrn1	131	79	114	74	-1.7	-1.6	-1.6
Acot3	4161	2509	2441	1571	-1.7	-1.6	-1.6
Gpr84	171	111	167	101	-1.5	-1.6	-1.6
Catsperd	1371	851	836	532	-1.6	-1.6	-1.6
Ecscr	951	624	1011	612	-1.5	-1.7	-1.6
Abca9	141	94	107	64	-1.5	-1.7	-1.6
Tnmd	129	83	143	89	-1.6	-1.6	-1.6
Rbakdn	235	147	146	93	-1.6	-1.6	-1.6
Ushbp1	479	297	430	280	-1.6	-1.5	-1.6
Naip7	534	355	322	196	-1.5	-1.6	-1.6
Adrb1	287	187	160	99	-1.5	-1.6	-1.6
Prkar2b	857	537	634	411	-1.6	-1.5	-1.6
Th	1296	843	1000	626	-1.5	-1.6	-1.6
Nat8l	113	73	102	64	-1.5	-1.6	-1.6
Nos3	884	565	911	582	-1.6	-1.6	-1.6
Gfra3	273	169	291	193	-1.6	-1.5	-1.6
Myo18b	313	196	361	236	-1.6	-1.5	-1.6
Tmem100	312	203	290	183	-1.5	-1.6	-1.6
Proz	726	470	444	282	-1.5	-1.6	-1.6
Cav2	796	496	600	399	-1.6	-1.5	-1.6
Mfng	560	356	459	300	-1.6	-1.5	-1.6
Sfrp1	4343	2789	3276	2117	-1.6	-1.5	-1.6
Fcrls	610	403	402	253	-1.5	-1.6	-1.6
Rac2	2992	1956	2216	1412	-1.5	-1.6	-1.5
Irak3	614	393	496	325	-1.6	-1.5	-1.5
AA416453	292	195	192	121	-1.5	-1.6	-1.5
Rgs2	494	314	423	280	-1.6	-1.5	-1.5
Rarres2	9925	6557	9292	5983	-1.5	-1.6	-1.5
8430419L09Rik	5751	3704	3698	2447	-1.6	-1.5	-1.5
Mef2a	3083	2014	2029	1329	-1.5	-1.5	-1.5
Sp6	273	181	178	115	-1.5	-1.5	-1.5
Coq10b	1376	891	1358	902	-1.5	-1.5	-1.5
Ralgps1	3485	2258	2295	1527	-1.5	-1.5	-1.5
4930589L23Rik	583	387	386	252	-1.5	-1.5	-1.5
Snrnp27	478	314	318	210	-1.5	-1.5	-1.5
Hpca	1981	1307	1207	795	-1.5	-1.5	-1.5

Table S7. List of genes with decreased expression in the microarray of E15.5 ureters of *Fgfr1/2cDKO-UM* and control embryos cultured for 6 days. Shown are the gene names, the intensity of the two control and mutant ureter samples, the individual and the average (avg) fold change (FC).

#	Category	Term	Count	%	PValue	Genes	List Total	Pop Hits	Pop Total	Fold Enrichment	Bonferroni	Benjamini	FDR
1	UP_KEYWORDS	Glycoprotein	58	0.230772291	1.24E-07	LRRC8E, IGDCC4, CLSTN2, LRRC8B, SLC9A4, GRIK3, JAG2, CSPG5, VIPR1, ADORA1, WNT4, TMEM145, RSPO1, CNTNAP2, WNT6, NEGR1, WNT10A, TYRO3, SCUBE3, SCUBE2, TMEM132A, ACKR4, TMEM25, TMEM132C, MGAT3, ROR2, CNTN3, FGFR2, KCNMB4, FGFR4, CPM, FUT9, FGFR3, 9530068E07RIK, ITLN1, RHBG, CDH1, EXTL1, SLCO2A1, COL26A1, UPK1A, DNER, MSLN, ADRA2A, SCNN1B, PRSS12, SPRN, FLRT1, HPN, KCNB2, ACER2, NTNG1, COL16A1, FZD10, CDH16, EPHA8, ABCC3, PTCH1	173	3815	22680	1.993106008	2.09E-05	2.09E-05	1.51E-04
2	GOTERM_CC_DIRECT	GO:0016020~membrane	86	0.342179605	2.88E-06	CLDN8, LRRC8E, IGDCC4, CLSTN2, SMCP, LRRC8B, SLC9A4, GRIK3, SLC7A8, JAG2, RNF186, KCNJ10, CSPG5, VIPR1, ADORA1, AP1S3, TMEM145, CNTNAP2, NEGR1, KCNG1, MVB12B, TYRO3, ARC, COL23A1, TMEM132A, AJAP1, ACKR4, GRHL2, TMEM25, TMEM132C, PLCE1, MGAT3, KSR2, KLHL14, ROR2, PLLP, ERC2, CNTN3, UNC13C, TMCO4, SH3GL2, FGFR2, KCNMB4, FGFR4, CPM, NKD1, FUT9, FGFR3, 9530068E07RIK, RAP1GAP, TFCP2L1, ITLN1, AKAP12, RHBG, CDH1, EXTL1, TMEM229A, SLCO2A1, SHISA2, DNER, UPK1A, MSLN, IPCEF1, PALM3, SCNN1B, PRSS12, SPRN, HPN, FLRT1, ADSSL1, KCNB2, ACER2, NTNG1, MAL, ITPR3, TMEM191C, FZD10, CDH16, SLC35G1, EPHA8, FAAH, PRKAR1B, ABCC3, APOL8, PTCH1, MYH14	160	6998	19662	1.510192198	4.80E-04	4.80E-04	0.003499615
3	UP_SEQ_FEATURE	glycosylation site:N-linked (GlcNAc...)	56	0.222814626	3.37E-06	LRRC8E, IGDCC4, CLSTN2, LRRC8B, SLC9A4, JAG2, CSPG5, VIPR1, ADORA1, WNT4, TMEM145, RSPO1, CNTNAP2, WNT6, NEGR1, WNT10A, TYRO3, SCUBE3, SCUBE2, TMEM132A, ACKR4, TMEM25, TMEM132C, MGAT3, ROR2, CNTN3, FGFR2, KCNMB4, CPM, FGFR4, FUT9, FGFR3, 9530068E07RIK, ITLN1, RHBG, CDH1, EXTL1, SLCO2A1, COL26A1, UPK1A, DNER, MSLN, ADRA2A, SCNN1B, PRSS12, SPRN, HPN, KCNB2, ACER2, NTNG1, COL16A1, FZD10, CDH16, EPHA8, ABCC3, PTCH1	156	3563	18012	1.814719661	0.001854378	0.001854378	0.004924719
4	GOTERM_MF_DIRECT	GO:0043565~sequence-specific DNA binding	18	0.071618987	8.77E-06	FOXL1, TFCP2L1, FOXA1, LEF1, GRHL3, SOX9, GRHL2, HOXD11, HOXB8, HOXD3, GATA3, BCL11A, SP5, POU3F3, CUX2, CREBL2, NR2F1, PLAGL2	137	633	17446	3.62112983	0.002750855	0.002750855	0.011803867
5	UP_KEYWORDS	Developmental protein	22	0.087534317	1.68E-05	WNT10A, ARC, FLRT1, NKD1, FOXA1, JAG2, NTNG1, CSPG5, HOXD11, WNT4, FZD10, SHISA2, EPHA8, HOXB8, SFRP2, DNER, HOXD3, CASZ1, ROR2, POU3F3, WNT6, KIF26B	173	976	22680	2.955083862	0.002817245	0.001409616	0.020444131
6	GOTERM_BP_DIRECT	GO:0050680~negative regulation of epithelial cell proliferation	7	0.027851828	2.52E-05	FGFR2, HPN, FGFR3, SFRP2, CDH1, PTCH1, SOX9	147	72	18082	11.95899471	0.028580497	0.028580497	0.040508813
7	UP_SEQ_FEATURE	topological domain:Extracellular	39	0.155174472	3.00E-05	FGFR2, CLDN8, KCNMB4, IGDCC4, FGFR4, FGFR3, 9530068E07RIK, CLSTN2, SLC9A4, RHBG, JAG2, CDH1, KCNJ10, CSPG5, VIPR1, ADORA1, SHISA2, UPK1A, DNER, ADRA2A, CNTNAP2, SCNN1B, TYRO3, HPN, COL23A1, TMEM132A, MAL, AJAP1, ACKR4, ITPR3, TMEM25, TMEM132C, FZD10, CDH16, EPHA8, ABCC3, ROR2, PLLP, PTCH1	156	2256	18012	1.996010638	0.016375127	0.008221359	0.043798657
8	GOTERM_CC_DIRECT	GO:0016323~basolateral plasma membrane	10	0.039788326	4.18E-05	CLDN8, CDH16, SLC9A4, RHBG, ABCC3, SLC7A8, KCNJ10, CDH1, AJAP1, ADORA1	160	203	19662	6.053571429	0.006948428	0.00348027	0.050771413
9	UP_KEYWORDS	Cell membrane	50	0.198941631	6.10E-05	LRRC8E, CLDN8, IGDCC4, CLSTN2, LRRC8B, SLC9A4, GRIK3, SLC7A8, KCNJ10, CSPG5, VIPR1, ADORA1, NEGR1, KCNG1, TYRO3, ARC, COL23A1, ACKR4, AJAP1, TMEM25, PLCE1, ROR2, CNTN3, UNC13C, FGFR2, NKD1, CPM, FGFR4, FGFR3, ITLN1, RHBG, CDH1, SLCO2A1, DNER, MSLN, ADRA2A, PALM3, IPCEF1, SCNN1B, SPRN, FLRT1, HPN, KCNB2, NTNG1, MAL, FZD10, CDH16, SLC35G1, EPHA8, PRKAR1B	173	3759	22680	1.743791778	0.010192839	0.003409223	0.074222002
10	UP_KEYWORDS	Wnt signaling pathway	9	0.035809493	6.13E-05	WNT10A, FZD10, WNT4, NKD1, RSPO1, SFRP2, LEF1, ROR2, WNT6	173	176	22680	6.703888597	0.01024811	0.002571933	0.074626404
11	GOTERM_MF_DIRECT	GO:0004714~transmembrane receptor protein tyrosine kinase activity	6	0.023872996	6.22E-05	FGFR2, TYRO3, FGFR4, FGFR3, EPHA8, ROR2	137	54	17446	14.14922952	0.019352135	0.009723339	0.083708152
12	KEGG_PATHWAY	mmu05217:Basal cell carcinoma	6	0.023872996	6.24E-05	WNT10A, FZD10, WNT4, LEF1, PTCH1, WNT6	62	54	7691	13.78315412	0.006712812	0.006712812	0.070198613
13	UP_SEQ_FEATURE	topological domain:Cytoplasmic	45	0.179047467	6.48E-05	FGFR2, CLDN8, KCNMB4, IGDCC4, FGFR4, FUT9, FGFR3, 9530068E07RIK, CLSTN2, SLC9A4, RHBG, JAG2, CDH1, KCNJ10, CSPG5, VIPR1, EXTL1, ADORA1, SHISA2, UPK1A, DNER, ADRA2A, CNTNAP2, SCNN1B, KCNG1, TYRO3, HPN, COL23A1, KCNB2, TMEM132A, MAL, AJAP1, ACKR4, ITPR3, TMEM25, TMEM132C, FZD10, MGAT3, CDH16, EPHA8, FAAH, ABCC3, ROR2, PLLP, PTCH1	156	2880	18012	1.804086538	0.035035818	0.011817714	0.09458431
14	GOTERM_BP_DIRECT	GO:0007275~multicellular organism development	22	0.087534317	8.07E-05	WNT10A, ARC, FLRT1, NKD1, FOXA1, JAG2, NTNG1, CSPG5, HOXD11, WNT4, FZD10, SHISA2, EPHA8, HOXB8, SFRP2, DNER, HOXD3, CASZ1, ROR2, POU3F3, WNT6, KIF26B	147	1029	18082	2.629883051	0.088660622	0.045359032	0.129640118
15	GOTERM_BP_DIRECT	GO:0010628~positive regulation of gene expression	13	0.051724824	9.74E-05	FGFR2, WNT10A, FGFR4, HPN, HOXD3, GATA3, BCL11A, LEF1, POU3F3, GRHL3, CUX2, WNT6, SOX9	147	399	18082	4.00774044	0.106060879	0.0366828	0.156538079
16	GOTERM_CC_DIRECT	GO:0005886~plasma membrane	62	0.246687622	9.88E-05	CLDN8, LRRC8E, IGDCC4, CLSTN2, LRRC8B, SLC9A4, GRIK3, SLC7A8, JAG2, KCNJ10, CSPG5, VIPR1, ADORA1, GLDC, NEGR1, KCNG1, MVB12B, TYRO3, ARC, COL23A1, AJAP1, ACKR4, GRHL2, TMEM25, PLCE1, KSR2, ROR2, CNTN3, UNC13C, FGFR2, FGFR4, CPM, NKD1, FGFR3, ITLN1, AKAP12, RHBG, CDH1, LLGL2, SLCO2A1, UPK1A, DNER, MSLN, ADRA2A, PALM3, IPCEF1, NEDD4L, SCNN1B, PRSS12, SPRN, HPN, FLRT1, KCNB2, NTNG1, MAL, ITPR3, FZD10, CDH16, SLC35G1, EPHA8, PRKAR1B, PTCH1	160	4874	19662	1.563197579	0.016364842	0.005484977	0.120104333
17	INTERPRO	IPR013098:Immunoglobulin I-set	8	0.031830661	1.42E-04	FGFR2, TYRO3, IGDCC4, FGFR4, FGFR3, ROR2, CNTN3, NEGR1	159	147	20594	7.048817011	0.055525065	0.055525065	0.198155884
18	GOTERM_BP_DIRECT	GO:0090090~negative regulation of canonical Wnt signaling pathway	7	0.027851828	1.78E-04	WNT4, NKD1, SFRP2, LEF1, ROR2, CDH1, SOX9	147	102	18082	8.441643324	0.185344153	0.049956382	0.286019857
19	GOTERM_CC_DIRECT	GO:0009986~cell surface	16	0.063661322	1.84E-04	FGFR2, CPM, HPN, COL23A1, FGFR3, SCUBE3, CLSTN2, CDH1, CSPG5, WNT4, FZD10, MSLN, CNTNAP2, ROR2, SCNN1B, WNT6	160	629	19662	3.125914149	0.030342967	0.007673617	0.224168353
20	GOTERM_BP_DIRECT	GO:0061144~alveolar secondary septum development	3	0.011936498	1.93E-04	FGFR4, FGFR3, FOXA1	147	3	18082	123.0068027	0.199422802	0.043509539	0.310305874
21	GOTERM_BP_DIRECT	GO:0090263~positive regulation of canonical Wnt signaling pathway	6	0.023872996	2.07E-04	FGFR2, WNT4, FGFR3, RSPO1, SFRP2, ROR2	147	67	18082	11.01553457	0.21193572	0.038918375	0.332247079
22	UP_KEYWORDS	Disulfide bond	42	0.16711097	2.58E-04	FGFR2, IGDCC4, ADAMTS17, FGFR4, CPM, FGFR3, GRIK3, SLC7A8, JAG2, CDH1, CSPG5, EXTL1, VIPR1, ADORA1, ISM1, SLCO2A1, COL26A1, WNT4, RSPO1, UPK1A, DNER, MSLN, ADRA2A, CNTNAP2, WNT6, NEGR1, PRSS12, WNT10A, TYRO3, PNLIPRP1, FLRT1, HPN, SCUBE3, SCUBE2, ALDH5A1, NTNG1, TMEM25, FZD10, SFRP2, PRKAR1B, ROR2, CNTN3	173	3124	22680	1.762524702	0.042362482	0.008619824	0.313214466

23	GOTERM_BP_DIRECT	GO:0045165~cell fate commitment	6	0.023872996	2.90E-04	FGFR2, WNT10A, WNT4, ROR2, WNT6, SOX9	147	72	18082	10.25056689	0.284022195	0.046608302	0.465754879
24	GOTERM_CC_DIRECT	GO:0005887~integral component of plasma membrane	22	0.087534317	2.99E-04	FGFR2, LRRC8E, IGDCC4, KCNMB4, HPN, FLRT1, FGFR4, FGFR3, GRIK3, RHBG, SLC7A8, JAG2, KCNJ10, ITPR3, SLCO2A1, EPHA8, UPK1A, ABCC3, ADRA2A, ROR2, PTCH1, SCNN1B	160	1126	19662	2.400999112	0.048706352	0.009936798	0.363014076
25	UP_KEYWORDS	Lipoprotein	17	0.067640154	3.06E-04	WNT10A, SPRN, CPM, NKD1, ITLN1, AKAP12, NTNG1, MAL, ADORA1, WNT4, MSLN, ADRA2A, PALM3, APOL8, CNTN3, WNT6, NEGR1	173	780	22680	2.857269898	0.050123835	0.008533986	0.371988784
26	GOTERM_MF_DIRECT	GO:0005515~protein binding	51	0.202920463	3.19E-04	CLDN8, GRIK3, JAG2, RGL3, KCNJ10, ADORA1, GSTM1, USP27X, WNT4, MAP3K4, RSPO1, GATA3, CNTNAP2, WNT6, SCUBE2, TRIM41, LEF1, GRHL3, MYCL, KSR2, KLHL14, ROR2, ERC2, SH3GL2, KIF26B, FGFR2, KCNMB4, NKD1, FGFR4, CCK, FGFR3, RAP1GAP, CDH1, SOX9, FBF1, SESN3, COL26A1, UPK1A, MSLN, BCL11A, POU3F3, NEDD4L, SCNN1B, ADSSL1, NTNG1, PPP1R10, ITPR3, SFRP2, EPHA8, THSD4, PTCH1	137	4092	17446	1.58712032	0.095457901	0.032889137	0.429008869
27	GOTERM_BP_DIRECT	GO:0016055~Wnt signaling pathway	9	0.035809493	3.41E-04	WNT10A, FZD10, WNT4, NKD1, RSPO1, SFRP2, LEF1, ROR2, WNT6	147	213	18082	5.197470538	0.324779491	0.047904082	0.547234998
28	INTERPRO	IPR016248:Tyrosine-protein kinase, fibroblast growth factor receptor	3	0.011936498	3.47E-04	FGFR2, FGFR4, FGFR3	159	4	20594	97.14150943	0.130368653	0.067459734	0.483840925
29	UP_KEYWORDS	Membrane	89	0.354116102	3.85E-04	CLDN8, LRRC8E, IGDCC4, CLSTN2, SMCP, SLC9A4, LRRC8B, GRIK3, JAG2, SLC7A8, RNF186, KCNJ10, CSPG5, VIPR1, ADORA1, AP1S3, TMEM145, CUTAL, CNTNAP2, NEGR1, KCNG1, MVB12B, TYRO3, ARC, COL23A1, TMEM132A, D430019H16RIK, AJAP1, ACKR4, GRHL2, TMEM25, TMEM132C, PLCE1, MGAT3, KSR2, KLHL14, ROR2, PLLP, CNTN3, UNC13C, TMCO4, SH3GL2, FGFR2, ADAMTS17, KCNMB4, FGFR4, CPM, NKD1, FUT9, FGFR3, 9530068E07RIK, RAP1GAP, ITLN1, AKAP12, RHBG, CDH1, EXTL1, TMEM229A, SLCO2A1, SHISA2, DNER, UPK1A, MSLN, ADRA2A, IPCEF1, PALM3, NEDD4L, SCNN1B, SPRN, HPN, FLRT1, ADSSL1, KCNB2, ACER2, NTNG1, MAL, ITPR3, TMEM191C, FZD10, NCKAP5, CDH16, SLC35G1, EPHA8, FAAH, PRKAR1B, ABCC3, GM13178, APOL8, PTCH1	173	8683	22680	1.343745902	0.062586091	0.009190416	0.46729997
30	PIR_SUPERFAMILY	PIRSF000628:fibroblast growth factor receptor	3	0.011936498	4.37E-04	FGFR2, FGFR4, FGFR3	17	4	1807	79.72058824	0.006530528	0.006530528	0.303226111
31	GOTERM_BP_DIRECT	GO:0007155~cell adhesion	13	0.051724824	5.78E-04	TYRO3, FLRT1, CDH16, CLSTN2, EPHA8, MSLN, CNTNAP2, CDH1, AJAP1, CNTN3, COL16A1, NEGR1, GRHL2	147	485	18082	3.297089557	0.486254488	0.071331118	0.92631577
32	GOTERM_MF_DIRECT	GO:0005007~fibroblast growth factor-activated receptor activity	3	0.011936498	5.94E-04	FGFR2, FGFR4, FGFR3	137	5	17446	76.40583942	0.170212832	0.045575281	0.796394366
33	GOTERM_BP_DIRECT	GO:0001658~branching involved in ureteric bud morphogenesis	5	0.019894163	6.02E-04	WNT4, PTCH1, WNT6, SOX9, HOXD11	147	48	18082	12.81320862	0.500143199	0.066993734	0.964248405
34	UP_KEYWORDS	GPI-anchor	7	0.027851828	7.07E-04	SPRN, CPM, ITLN1, MSLN, NTNG1, CNTN3, NEGR1	173	140	22680	6.554913295	0.112104008	0.014752681	0.858006117
35	INTERPRO	IPR001245:Serine-threonine/tyrosine-protein kinase catalytic domain	7	0.027851828	7.20E-04	FGFR2, TYRO3, FGFR4, KSR2, FGFR3, EPHA8, ROR2	159	139	20594	6.522691281	0.251362248	0.091990119	1.000162421
36	KEGG_PATHWAY	mmu04550:Signaling pathways regulating pluripotency of stem cells	7	0.027851828	7.39E-04	FGFR2, WNT10A, FZD10, WNT4, FGFR4, FGFR3, WNT6	62	138	7691	6.29230949	0.076742896	0.039137312	0.829029113
37	UP_KEYWORDS	Cell adhesion	12	0.047745991	7.89E-04	TYRO3, FLRT1, CDH16, CLSTN2, EPHA8, MSLN, CNTNAP2, CDH1, CNTN3, AJAP1, COL16A1, NEGR1	173	459	22680	3.427405644	0.124235112	0.014631637	0.95680208
38	KEGG_PATHWAY	mmu04310:Wnt signaling pathway	7	0.027851828	8.27E-04	WNT10A, FZD10, WNT4, NKD1, SFRP2, LEF1, WNT6	62	141	7691	6.158430565	0.085525744	0.029362287	0.927809247
39	INTERPRO	IPR007604:CP2 transcription factor	3	0.011936498	8.60E-04	TFCP2L1, GRHL3, GRHL2	159	6	20594	64.76100629	0.292338992	0.082816324	1.193468079
40	INTERPRO	IPR008266:Tyrosine-protein kinase, active site	6	0.023872996	9.99E-04	FGFR2, TYRO3, FGFR4, FGFR3, EPHA8, ROR2	159	99	20594	7.849818944	0.330909564	0.077222568	1.38556047
41	GOTERM_CC_DIRECT	GO:0031225~anchored component of membrane	7	0.027851828	0.001015952	SPRN, CPM, ITLN1, MSLN, NTNG1, CNTN3, NEGR1	160	141	19662	6.100797872	0.15612446	0.027895247	1.228735111
42	UP_KEYWORDS	Ion channel	10	0.039788326	0.001096375	LRRC8E, KCNMB4, LRRC8B, KCNB2, GRIK3, KCNJ10, PLLP, ITPR3, SCNN1B, KCNG1	173	336	22680	3.901734104	0.168307087	0.018260421	1.326738628
43	KEGG_PATHWAY	mmu04390:Hippo signaling pathway	7	0.027851828	0.001182597	WNT10A, FZD10, WNT4, LEF1, CDH1, WNT6, LLGL2	62	151	7691	5.750587481	0.119967195	0.031444046	1.323555922
44	UP_SEQ_FEATURE	transmembrane region	55	0.218835794	0.001408184	CLDN8, LRRC8E, IGDCC4, CLSTN2, LRRC8B, SLC9A4, SLC7A8, JAG2, RNF186, KCNJ10, CSPG5, VIPR1, ADORA1, TMEM145, CNTNAP2, KCNG1, TYRO3, COL23A1, TMEM132A, AJAP1, ACKR4, TMEM25, TMEM132C, MGAT3, ROR2, PLLP, TMCO4, FGFR2, KCNMB4, FGFR4, FUT9, 9530068E07RIK, FGFR3, RHBG, CDH1, EXTL1, SLCO2A1, SHISA2, UPK1A, DNER, ADRA2A, SCNN1B, HPN, KCNB2, ACER2, MAL, ITPR3, TMEM191C, FZD10, CDH16, SLC35G1, EPHA8, FAAH, ABCC3, PTCH1	156	4312	18012	1.472723705	0.539317989	0.176145889	2.035453662
45	GOTERM_BP_DIRECT	GO:0007267~cell-cell signaling	6	0.023872996	0.001487282	FGFR2, WNT10A, WNT4, FGFR3, ADRA2A, WNT6	147	103	18082	7.165444819	0.819700584	0.144218054	2.36532427
46	UP_SEQ_FEATURE	signal peptide	43	0.171089802	0.001555549	FGFR2, IGDCC4, FGFR4, CPM, FGFR3, 9530068E07RIK, CCK, CLSTN2, ITLN1, JAG2, CDH1, CSPG5, VIPR1, ISM1, SOWAHA, COL26A1, WNT4, RSPO1, SHISA2, DNER, MSLN, CNTNAP2, WNT6, NEGR1, PRSS12, SPRN, WNT10A, TYRO3, PNLIPRP1, SCUBE3, SCUBE2, NTNG1, TMEM132A, COL16A1, TMEM25, TMEM132C, FZD10, CDH16, SFRP2, EPHA8, THSD4, ROR2, CNTN3	156	3124	18012	1.589259332	0.575234407	0.15738368	2.246214908
47	UP_SEQ_FEATURE	lipid moiety-binding region:GPI-anchor amidated serine	5	0.019894163	0.001880867	CPM, ITLN1, MSLN, NTNG1, CNTN3	156	61	18012	9.46406053	0.644933856	0.158504992	2.70999396
48	GOTERM_BP_DIRECT	GO:0001837~epithelial to mesenchymal transition	4	0.01591533	0.001964013	FGFR2, WNT4, LEF1, SOX9	147	31	18082	15.87184551	0.895941483	0.171854837	3.112326981
49	GOTERM_BP_DIRECT	GO:0060349~bone morphogenesis	4	0.01591533	0.002154461	FGFR2, FGFR3, SFRP2, SP5	147	32	18082	15.37585034	0.916462485	0.173833061	3.409243776
50	GOTERM_CC_DIRECT	GO:0043195~terminal bouton	6	0.023872996	0.002259844	CCK, GRIK3, ERC2, UNC13C, ADORA1, PRSS12	160	113	19662	6.525	0.314646851	0.05254367	2.714276779
51	UP_KEYWORDS	Phosphoprotein	77	0.306370111	0.002376311	IGDCC4, PPP1R26, SMCP, LRRC8B, SLC9A4, GRIK3, TDRP, RGL3, SLC7A8, JAG2, KCNJ10, CSPG5, GSTM1, MAP3K4, GATA3, CNTNAP2, NEGR1, MVB12B, TYRO3, ALDH5A1, TRIM41, C77080, AA986860, LEF1, PLEKHH1, ACKR4, PLCE1, KSR2, EVPL, ROR2, PLLP, ERC2, CUX2, UNC13C, SH3GL2, KIF26B, FGFR2, KCNMB4, AI661453, FGFR4, FGFR3, 9530068E07RIK, RAP1GAP, SMTNL2, AKAP12, CDH1, FBF1, LLGL2, SOWAHA, DNER, MSLN, SAPCD2, BCL11A, CASZ1, ADRA2A, IPCEF1, PALM3, NEDD4L, SCNN1B, ARHGEF10L, CREBL2, FLRT1, KCNB2, UPB1, S031439G07RIK, FOXA1, KCTD1, PPP1R10, ITPR3, RIMKLA, CDH16, EPHA8, FAAH, PRKAR1B, ABCC3, PTCH1, MYH14	173	7617	22680	1.325268015	0.329475713	0.035683715	2.855157541
52	GOTERM_BP_DIRECT	GO:0045893~positive regulation of transcription, DNA-templated	13	0.051724824	0.002494375	WNT4, GATA3, POU3F3, LEF1, ROR2, CDH1, PTCH1, GRHL3, WNT6, SOX9, TOX3, GRHL2, CREBL2	147	576	18082	2.7761952	0.943561985	0.185621026	3.937066369
53	INTERPRO	IPR003598:Immunoglobulin subtype 2	8	0.031830661	0.002698826	FGFR2, TYRO3, IGDCC4, FGFR4, FGFR3, ROR2, CNTN3, NEGR1	159	242	20594	4.281719424	0.662569211	0.165619554	3.701903683

54	UP_KEYWORDS	Signal	51	0.202920463	0.002844878	FGFR2, KCNMB4, ADAMTS17, IGDCC4, FGFR4, CPM, FGFR3, 9530068E07RIK, CCK, CLSTN2, GRIK3, ITLN1, JAG2, CDH1, CSPG5, EXTL1, VIPR1, ISM1, SOWAHA, COL26A1, WNT4, TMEM145, SHISA2, RSPO1, DNER, MSLN, CNTNAP2, WNT6, NEGR1, PRSS12, PLAGL2, SPRN, WNT10A, TYRO3, PNLIPRP1, FLRT1, SCUBE3, SCUBE2, NTNG1, TMEM132A, COL16A1, TMEM25, TMEM132C, FZD10, CDH16, SFRP2, EPHA8, THSD4, IROR2, PTCH1, CNTN3	173	4543	22680	1.471717271	0.380362461	0.039100111	3.409234455
55	GOTERM_MF_DIRECT	GO:0005109~frizzled binding	4	0.01591533	0.003202123	WNT10A, WNT4, ROR2, WNT6	137	38	17446	13.40453323	0.634715861	0.182427711	4.223868372
56	INTERPRO	IPR020635:Tyrosine-protein kinase, catalytic domain	5	0.019894163	0.003509547	FGFR2, TYRO3, FGFR4, FGFR3, EPHA8	159	81	20594	7.995185962	0.75666579	0.182825627	4.788843456
57	GOTERM_BP_DIRECT	GO:0060487~lung epithelial cell differentiation	3	0.011936498	0.004052659	FOXA1, SOX9, GRHL2	147	12	18082	30.75170068	0.99066597	0.267729937	6.322348613
58	GOTERM_BP_DIRECT	GO:0048568~embryonic organ development	4	0.01591533	0.004094364	FGFR2, GATA3, PTCH1, GRHL2	147	40	18082	12.30068027	0.991105184	0.255574809	6.385416312
59	SMART	SM00408:IGc2	8	0.031830661	0.004851689	FGFR2, TYRO3, IGDCC4, FGFR4, FGFR3, ROR2, CNTN3, NEGR1	91	242	10425	3.787121969	0.363839999	0.363839999	5.185046374
60	UP_KEYWORDS	Golgi apparatus	14	0.055703657	0.004991024	FGFR2, FUT9, RAP1GAP, CLSTN2, ACER2, TMEM132A, MAL, CDH1, CSPG5, AP1S3, PLCE1, MGAT3, FAAH, MSLN	173	753	22680	2.437417958	0.568544774	0.062614711	5.910162823
61	GOTERM_BP_DIRECT	GO:0008543~fibroblast growth factor receptor signaling pathway	4	0.01591533	0.005024994	FGFR2, FGFR4, FLRT1, FGFR3	147	43	18082	11.44249328	0.996967442	0.288997509	7.782448376
62	GOTERM_CC_DIRECT	GO:0005789~endoplasmic reticulum membrane	14	0.055703657	0.005138138	LRRC8E, TYRO3, HPN, FLRT1, CLSTN2, LRRC8B, TMEM132A, CSPG5, ITPR3, EXTL1, SLC35G1, SHISA2, FAAH, KLHL14	160	710	19662	2.423133803	0.576956838	0.101955029	6.073448329
63	SMART	SM00219:TyrKc	5	0.019894163	0.005211079	FGFR2, TYRO3, FGFR4, FGFR3, EPHA8	91	81	10425	7.071632072	0.384855153	0.215688298	5.559234599
64	KEGG_PATHWAY	mmu05205:Proteoglycans in cancer	7	0.027851828	0.005212916	WNT10A, FZD10, PLCE1, WNT4, PTCH1, ITPR3, WNT6	62	203	7691	4.27753059	0.431337085	0.106754203	5.7152732
65	GOTERM_CC_DIRECT	GO:0000139~Golgi membrane	10	0.039788326	0.005604445	MGAT3, PLCE1, FUT9, CLSTN2, RAP1GAP, FAAH, TMEM132A, MAL, CSPG5, CUX2	160	403	19662	3.049317618	0.60881506	0.0990325	6.607529986
66	UP_SEQ_FEATURE	domain:Ig-like C2-type 1	6	0.023872996	0.005702062	FGFR2, TYRO3, FGFR4, FGFR3, CNTN3, NEGR1	156	132	18012	5.248251748	0.956937784	0.361926203	8.006297507
67	GOTERM_BP_DIRECT	GO:0007417~central nervous system development	5	0.019894163	0.00585871	ALDH5A1, DNER, CASZ1, GRHL3, SOX9	147	89	18082	6.910494535	0.998844482	0.313214815	9.017369188
68	GOTERM_BP_DIRECT	GO:0060070~canonical Wnt signaling pathway	5	0.019894163	0.00585871	FZD10, MGAT3, WNT4, RSPO1, LEF1	147	89	18082	6.910494535	0.998844482	0.313214815	9.017369188
69	UP_SEQ_FEATURE	domain:Ig-like C2-type 2	6	0.023872996	0.005884578	FGFR2, TYRO3, FGFR4, FGFR3, CNTN3, NEGR1	156	133	18012	5.208791209	0.961073429	0.33352975	8.252422049
70	GOTERM_BP_DIRECT	GO:0071805~potassium ion transmembrane transport	5	0.019894163	0.006093452	HPN, SLC9A4, KCNB2, KCNJ10, KCNG1	147	90	18082	6.833711262	0.999119498	0.309448088	9.362265181
71	GOTERM_BP_DIRECT	GO:0000122~negative regulation of transcription from RNA polymerase II promoter	14	0.055703657	0.006200666	FGFR2, FGFR3, TFCP2L1, FOXA1, LEF1, SOX9, GATA3, BCL11A, MZF1, POU3F3, PTCH1, CUX2, CRYM, NR2F1	147	729	18082	2.36227056	0.999222312	0.300898451	9.519382716
72	UP_SEQ_FEATURE	domain:Ig-like C2-type 3	5	0.019894163	0.007030545	FGFR2, FGFR4, FGFR3, CNTN3, NEGR1	156	88	18012	6.560314685	0.979358607	0.350246275	9.783806207
73	KEGG_PATHWAY	mmu04916:Melanogenesis	5	0.019894163	0.007694338	WNT10A, FZD10, WNT4, LEF1, WNT6	62	99	7691	6.265070055	0.565779124	0.129801261	8.329842987
74	GOTERM_CC_DIRECT	GO:0005794~Golgi apparatus	19	0.07559782	0.007740531	FGFR2, FGFR4, FUT9, FGFR3, RAP1GAP, CLSTN2, ACER2, TMEM132A, CDH1, MAL, CSPG5, AP1S3, PLCE1, WNT4, COL26A1, FAAH, MSLN, CNTNAP2, PTCH1	160	1190	19662	1.962069328	0.726840011	0.121702375	9.018641079
75	UP_KEYWORDS	Ion transport	12	0.047745991	0.007773969	LRRC8E, KCNMB4, LRRC8B, SLC9A4, KCNB2, GRIK3, KCNJ10, PLP, ITPR3, SCNN1B, KCNG1, SLCO2A1	173	619	22680	2.541484961	0.730484624	0.089400524	9.064656459
76	GOTERM_BP_DIRECT	GO:0006811~ion transport	12	0.047745991	0.007846122	LRRC8E, KCNMB4, LRRC8B, SLC9A4, KCNB2, GRIK3, KCNJ10, PLP, ITPR3, SCNN1B, KCNG1, SLCO2A1	147	584	18082	2.527537042	0.99988453	0.350620623	11.89890809
77	GOTERM_MF_DIRECT	GO:0001228~transcriptional activator activity, RNA polymerase II transcription regulatory region sequence-specific binding	5	0.019894163	0.008910631	FOXA1, LEF1, GRHL3, SOX9, GRHL2	137	104	17446	6.122262774	0.939823804	0.37400511	11.34681652
78	GOTERM_BP_DIRECT	GO:0001709~cell fate determination	3	0.011936498	0.009101741	GATA3, JAG2, PTCH1	147	18	18082	20.50113379	0.999973118	0.380205203	13.67506604
79	GOTERM_BP_DIRECT	GO:0030111~regulation of Wnt signaling pathway	3	0.011936498	0.009101741	FOXL1, SFRP2, LEF1	147	18	18082	20.50113379	0.999973118	0.380205203	13.67506604
80	INTERPRO	IPR005817:Wnt	3	0.011936498	0.009181013	WNT10A, WNT4, WNT6	159	19	20594	20.45084409	0.975468911	0.370907363	12.07993623
81	INTERPRO	IPR018161:Wnt protein, conserved site	3	0.011936498	0.009181013	WNT10A, WNT4, WNT6	159	19	20594	20.45084409	0.975468911	0.370907363	12.07993623
82	GOTERM_MF_DIRECT	GO:0017016~Ras GTPase binding	3	0.011936498	0.01045514	PLCE1, RAP1GAP, RGL3	137	20	17446	19.10145985	0.963124066	0.375907441	13.18790736
83	GOTERM_CC_DIRECT	GO:0005783~endoplasmic reticulum	20	0.079576652	0.010587511	CLDN8, LRRC8E, FLRT1, FGFR4, AIFM3, FGFR3, CLSTN2, LRRC8B, TMEM132A, MAL, CSPG5, ITPR3, EXTL1, ADORA1, COL26A1, SHISA2, SLC35G1, FAAH, UPK1A, KLHL14	160	1323	19662	1.857709751	0.830946655	0.149213985	12.1433874
84	UP_KEYWORDS	Tyrosine-protein kinase	5	0.019894163	0.0108449	FGFR2, TYRO3, FGFR4, FGFR3, EPHA8	173	113	22680	5.800808225	0.839890058	0.114963422	12.432722
85	UP_SEQ_FEATURE	compositionally biased region:Poly-Gly	7	0.027851828	0.010858257	Ai661453, IGDCC4, POU3F3, LEF1, ERC2, HOXD11, NR2F1	156	215	18012	3.75921288	0.997532873	0.451446301	14.72803129
86	GOTERM_BP_DIRECT	GO:0022409~positive regulation of cell-cell adhesion	3	0.011936498	0.01118435	RAP1GAP, CDH1, KIF26B	147	20	18082	18.45102041	0.999997614	0.430420699	16.5472113
87	SMART	SM00097:WNT1	3	0.011936498	0.011456691	WNT10A, WNT4, WNT6	91	19	10425	18.08849046	0.657547638	0.300372741	11.85138093
88	GOTERM_CC_DIRECT	GO:0043025~neuronal cell body	11	0.043767159	0.011708276	HPN, CCK, RAP1GAP, KCNB2, DNER, KLHL14, ROR2, ERC2, ITPR3, NEGR1, ADORA1	160	534	19662	2.531390449	0.860098784	0.151174423	13.34624343
89	GOTERM_BP_DIRECT	GO:0009887~organ morphogenesis	5	0.019894163	0.011801334	FGFR2, WNT10A, PRKAR1B, PTCH1, WNT6	147	109	18082	5.642513886	0.999998837	0.434100303	17.38073666
90	UP_SEQ_FEATURE	domain:EGF-like 4	4	0.01591533	0.01182602	SCUBE3, SCUBE2, DNER, JAG2	156	55	18012	8.397202797	0.998559949	0.448341	15.93747207
91	KEGG_PATHWAY	mmu05200:Pathways in cancer	9	0.035809493	0.012185807	FGFR2, WNT10A, FZD10, WNT4, FGFR3, LEF1, CDH1, PTCH1, WNT6	62	395	7691	2.826418947	0.733971422	0.172349658	12.89493022
92	UP_SEQ_FEATURE	domain:EGF-like 8; calcium-binding	3	0.011936498	0.012628815	SCUBE3, SCUBE2, DNER	156	20	18012	17.31923077	0.999079027	0.44150335	16.92860256
93	GOTERM_BP_DIRECT	GO:0009952~anterior/posterior pattern specification	5	0.019894163	0.01293445	ARC, HOXB8, SFRP2, HOXD3, HOXD11	147	112	18082	5.491375121	0.999996689	0.450851767	18.89123999
94	GOTERM_BP_DIRECT	GO:0010719~negative regulation of epithelial to mesenchymal transition	3	0.011936498	0.013455479	HPN, SFRP2, FOXA1	147	22	18082	16.77365492	0.999999831	0.451027807	19.57071
95	GOTERM_BP_DIRECT	GO:0009791~post-embryonic development	5	0.019894163	0.013727141	FGFR2, ALDH5A1, GATA3, PLAGL2, LLGL2	147	114	18082	5.395035207	0.999999877	0.445249341	19.9324997
96	GOTERM_BP_DIRECT	GO:0008544~epidermis development	4	0.01591533	0.013781592	EVPL, PTCH1, GRHL3, GRHL2	147	62	18082	7.935922756	0.999999884	0.43473572	20.00356297
97	GOTERM_CC_DIRECT	GO:0005576~extracellular region	24	0.095491983	0.014059355	FGFR2, WNT10A, PNLIPRP1, HPN, FLRT1, CCK, COL23A1, SCUBE3, SCUBE2, ITLN1, COL16A1, TMEM25, ISM1, GSTM1, COL26A1, WNT4, RSPO1, SFRP2, MSLN, THSD4, PTCH1, APOL8, WNT6, PRSS12	160	1753	19662	1.68243012	0.906010638	0.166307194	15.82057119
98	INTERPRO	IPR000884:Thrombospondin, type 1 repeat	4	0.01591533	0.014249248	ADAMTS17, RSPO1, THSD4, ISM1	159	66	20594	7.849818944	0.996878372	0.473258057	18.15346741
99	INTERPRO	IPR020067:Frizzled domain	3	0.011936498	0.014452249	FZD10, SFRP2, ROR2	159	24	20594	16.19025157	0.997126416	0.443016424	18.38842029
100	GOTERM_BP_DIRECT	GO:0090103~cochlea morphogenesis	3	0.011936498	0.014659696	HPN, GRHL3, SOX9	147	23	18082	16.04436557	0.999999959	0.443531769	21.14142916

Table S8. Functional annotation by DAVID for genes with increased expression in the microarray of E15.5 *Fgfr1/2cDKO-UM* ureter explants cultured for 6 days.

#	Category	Term	Count	%	PValue	Genes	List Total	Pop Hits	Pop Total	Fold Enrichment	Bonferroni	Benjamini	FDR
1	UP_KEYWORDS	Disulfide bond	65	33.50515464	7.40E-13	ASPN, RARRES2, MUP19, MMP9, HP, CD209D, EDNRB, AGTR2, ISG15, PROZ, CPA2, CES1F, ITIH4, MUP17, ESAM, CES1D, TIE1, CFD, GPIHBP1, CAMP, ICAM2, TNMD, FCRLS, RETN, MUP20, ADRB1, SGCG, CD33, CARTPT, SGCD, GM1987, CXCL1, MFNG, C3, FCNA, C6, ASTN1, MME, ACP5, CLDN15, LY6D, CHIL1, WFDC21, BCHE, DPT, MUP5, LY6C1, MUP4, MUP1, MUP3, SLC6A12, MUP2, DBH, ADIPOQ, TMPRSS3, P2RY12, LAMA4, SFRP1, PRLR, FCGR2B, CD300A, VSTM2L, ADRA1B, IGFBP3, ADAMDEC1	187	3124	22680	2.523502708	1.56E-10	1.56E-10	9.35E-10
2	UP_KEYWORDS	Secreted	46	23.71134021	9.57E-13	CXCL1, ASPN, RARRES2, MAMDC2, C3, FCNA, F13A1, MUP19, MMP9, 1500015O10RIK, APOC1, HP, ESM1, OSTN, ISG15, SAA2, CHIL1, BCHE, WFDC21, PROZ, ITIH4, CPA2, MUP17, ITIH3, CFD, SCG2, DPT, MUP5, MUP4, MUP1, MUP3, CAMP, MUP2, LY6K, ADIPOQ, LGALS9, RETN, LAMA4, MUP20, SFRP1, FCGR2B, PPBP, CARTPT, GM1987, IGFBP3, ADAMDEC1	187	1685	22680	3.311001444	2.02E-10	1.01E-10	1.21E-09
3	GOTERM_BP_DIRECT	GO:0031649~heat generation	8	4.12371134	3.32E-11	MUP5, MUP4, ADRB1, MUP20, MUP1, MUP3, MUP19, MUP2	170	15	18082	56.72784314	4.39E-08	4.39E-08	5.44E-08
4	UP_SEQ_FEATURE	signal peptide	64	32.98969072	2.58E-10	ASPN, RARRES2, MUP19, MMP9, CD52, HP, EDNRB, SAA2, PROZ, CPA2, MUP17, ESAM, CES1D, TIE1, ITIH3, CFD, GPIHBP1, APLN, CAMP, ICAM2, FCRLS, RETN, CD33, CARTPT, SGCA, CXCL1, EMCN, MAMDC2, C3, FCNA, APOC1, 1500015O10RIK, ASTN1, ACP5, ESM1, NRN1, OSTN, LY6D, CHIL1, LRG1, BCHE, SCG2, DPT, LY6C1, MUP5, MUP4, MUP1, MUP3, MUP2, LY6K, PCDH12, ADIPOQ, CDH13, LAMA4, SFRP1, PRLR, FCGR2B, CD300A, ECSCR, SULF1, VSTM2L, IGFBP3, ADAMDEC1, GFRA3	168	3124	18012	2.196451436	1.28E-07	1.28E-07	3.71E-07
5	GOTERM_CC_DIRECT	GO:0005576~extracellular region	45	23.19587629	3.04E-10	CXCL1, ASPN, RARRES2, MAMDC2, C3, FCNA, F13A1, MUP19, MMP9, 1500015O10RIK, APOC1, HP, ESM1, OSTN, ISG15, SAA2, CHIL1, BCHE, WFDC21, PROZ, ITIH4, CPA2, MUP17, ITIH3, CFD, SCG2, DPT, MUP5, MUP4, MUP1, MUP3, CAMP, MUP2, LY6K, ADIPOQ, LGALS9, RETN, LAMA4, MUP20, SFRP1, FCGR2B, VSTM2L, CARTPT, IGFBP3, ADAMDEC1	179	1753	19662	2.819715285	5.63E-08	5.63E-08	3.77E-07
6	UP_KEYWORDS	Glycoprotein	67	34.53608247	5.51E-10	ASPN, GPR84, F13A1, MMP9, SERPINA3F, CD52, HP, CD209D, EDNRB, AGTR2, PROZ, ITIH4, ESAM, CES1D, TIE1, ITIH3, CFD, GPIHBP1, ICAM2, TNMD, ADRB1, SGCG, CD33, MC2R, SGCD, SGCA, MFNG, EMCN, ABCA9, MAMDC2, C3, CATSPERD, FCNA, ASTN1, MME, ACP5, MRAP2, ESM1, NRN1, ACSL1, LY6D, CHIL1, BCHE, CNR1, ABCA17, NEFL, LY6C1, MUP3, SLC6A12, PCDH12, LY6K, DBH, ADIPOQ, TMPRSS3, P2RY12, CDH13, LAMA4, SFRP1, PRLR, FCGR2B, CD300A, ECSCR, SULF1, ADRA1B, IGFBP3, ADAMDEC1, GFRA3	187	3815	22680	2.130010303	1.16E-07	3.87E-08	6.96E-07
7	GOTERM_BP_DIRECT	GO:0050873~brown fat cell differentiation	9	4.639175258	7.28E-10	SCD1, RARRES2, LAMA4, ADRB1, RGS2, MRAP, LRG1, FABP4, ADIPOQ	170	34	18082	28.15536332	9.62E-07	4.81E-07	1.19E-06
8	UP_KEYWORDS	Pheromone-binding	7	3.608247423	7.98E-10	MUP5, MUP4, MUP20, MUP3, MUP19, MUP2, MUP17	187	14	22680	60.64171123	1.68E-07	4.21E-08	1.01E-06
9	GOTERM_BP_DIRECT	GO:0006112~energy reserve metabolic process	8	4.12371134	8.33E-10	MUP5, MUP4, MUP20, MUP1, MUP3, MUP19, MUP2, MRAP2	170	22	18082	38.67807487	1.10E-06	3.67E-07	1.36E-06
10	GOTERM_MF_DIRECT	GO:0005009~insulin-activated receptor activity	7	3.608247423	9.15E-10	MUP5, MUP4, MUP20, MUP1, MUP3, MUP19, MUP2	162	13	17446	57.98765432	3.12E-07	3.12E-07	1.25E-06
11	UP_KEYWORDS	Signal	74	38.1443299	1.17E-09	ASPN, RARRES2, MUP19, MMP9, CD52, HP, EDNRB, SAA2, PROZ, CES1F, CPA2, ITIH4, MUP17, ESAM, CES1D, TIE1, ITIH3, CFD, APLN, GPIHBP1, AGPAT2, CAMP, ICAM2, FCRLS, RETN, MUP20, PPBP, CD33, CARTPT, GM1987, SGCA, CXCL1, EMCN, MAMDC2, C3, CATSPERD, C6, FCNA, APOC1, 1500015O10RIK, ASTN1, ACP5, ESM1, NRN1, OSTN, IRAK3, LY6D, CHIL1, LRG1, WFDC21, BCHE, SCG2, DPT, MUP5, LY6C1, MUP4, MUP1, MUP3, MUP2, PCDH12, LY6K, ADIPOQ, CDH13, LAMA4, SFRP1, PRLR, FCGR2B, CD300A, ECSCR, SULF1, VSTM2L, IGFBP3, ADAMDEC1, GFRA3	187	4543	22680	1.975560921	2.48E-07	4.95E-08	1.48E-06
12	INTERPRO	IPR002971:Major urinary protein	8	4.12371134	1.56E-09	MUP5, MUP4, MUP20, MUP1, MUP3, MUP19, MUP2, MUP17	175	26	20594	36.20923077	6.38E-07	6.38E-07	2.19E-06
13	GOTERM_CC_DIRECT	GO:0005615~extracellular space	40	20.6185567	1.60E-09	CXCL1, C3, MUP19, MMP9, C6, 1500015O10RIK, SERPINA3F, HP, OSTN, NRN1, SAA2, CHIL1, BCHE, LRG1, WFDC21, PROZ, CPA2, CES1F, CES1D, CFD, APLN, SCG2, DPT, MUP5, MUP4, MUP1, MUP3, CAMP, MUP2, DBH, ADIPOQ, CDH13, RETN, MUP20, SFRP1, PPBP, SULF1, CARTPT, GM1987, IGFBP3	179	1504	19662	2.921371687	2.97E-07	1.48E-07	1.98E-06
14	GOTERM_BP_DIRECT	GO:0045721~negative regulation of gluconeogenesis	8	4.12371134	1.67E-09	MUP5, MUP4, MUP20, MUP1, MUP3, MUP19, MUP2, ADIPOQ	170	24	18082	35.45490196	2.20E-06	5.50E-07	2.72E-06
15	GOTERM_BP_DIRECT	GO:0071396~cellular response to lipid	7	3.608247423	2.85E-09	MUP5, MUP4, MUP20, MUP1, MUP3, MUP19, MUP2	170	15	18082	49.63686275	3.76E-06	7.52E-07	4.66E-06
16	GOTERM_BP_DIRECT	GO:0045834~positive regulation of lipid metabolic process	7	3.608247423	2.85E-09	MUP5, MUP4, MUP20, MUP1, MUP3, MUP19, MUP2	170	15	18082	49.63686275	3.76E-06	7.52E-07	4.66E-06
17	GOTERM_BP_DIRECT	GO:0042593~glucose homeostasis	13	6.701030928	4.33E-09	CAV3, MUP5, MUP4, MUP20, MUP1, MUP3, CNR1, MUP19, MUP2, ADRA1B, DBH, ADIPOQ, PCK1	170	133	18082	10.3965502	5.72E-06	9.53E-07	7.08E-06
18	GOTERM_BP_DIRECT	GO:0051055~negative regulation of lipid biosynthetic process	7	3.608247423	4.52E-09	MUP5, MUP4, MUP20, MUP1, MUP3, MUP19, MUP2	170	16	18082	46.53455882	5.97E-06	8.53E-07	7.39E-06
19	INTERPRO	IPR002345:Lipocalin	8	4.12371134	6.04E-09	MUP5, MUP4, MUP20, MUP1, MUP3, MUP19, MUP2, MUP17	175	31	20594	30.36903226	2.46E-06	1.23E-06	8.44E-06
20	GOTERM_MF_DIRECT	GO:0036094~small molecule binding	8	4.12371134	1.39E-08	MUP5, MUP4, MUP20, MUP1, MUP3, MUP19, MUP2, MUP17	162	32	17446	26.92283951	4.73E-06	2.36E-06	1.89E-05
21	GOTERM_BP_DIRECT	GO:0010888~negative regulation of lipid storage	7	3.608247423	1.50E-08	MUP5, MUP4, MUP20, MUP1, MUP3, MUP19, MUP2	170	19	18082	39.1869969	1.98E-05	2.47E-06	2.45E-05
22	INTERPRO	IPR022272:Lipocalin conserved site	8	4.12371134	1.50E-08	MUP5, MUP4, MUP20, MUP1, MUP3, MUP19, MUP2, MUP17	175	35	20594	26.89828571	6.12E-06	2.04E-06	2.10E-05
23	GOTERM_BP_DIRECT	GO:0010907~positive regulation of glucose metabolic process	7	3.608247423	2.95E-08	MUP5, MUP4, MUP20, MUP1, MUP3, MUP19, MUP2	170	21	18082	35.45490196	3.89E-05	4.32E-06	4.82E-05
24	GOTERM_BP_DIRECT	GO:0061179~negative regulation of insulin secretion involved in cellular response to glucose stimulus	7	3.608247423	4.02E-08	MUP5, MUP4, MUP20, MUP1, MUP3, MUP19, MUP2	170	22	18082	33.84331551	5.31E-05	5.31E-06	6.58E-05
25	UP_SEQ_FEATURE	disulfide bond	51	26.28865979	6.33E-08	ASPN, MMP9, MUP19, HP, CD209D, EDNRB, AGTR2, PROZ, CPA2, MUP17, CES1D, ESAM, TIE1, CFD, GPIHBP1, CAMP, ICAM2, RETN, ADRB1, SGCG, CD33, SGCD, CARTPT, CXCL1, C3, ASTN1, MME, ACP5, LY6D, CHIL1, BCHE, DPT, LY6C1, MUP5, MUP4, MUP1, MUP3, MUP2, DBH, ADIPOQ, TMPRSS3, P2RY12, LAMA4, SFRP1, PRLR, FCGR2B, CD300A, VSTM2L, ADRA1B, IGFBP3, ADAMDEC1	168	2510	18012	2.178457598	3.15E-05	1.58E-05	9.11E-05

26	INTERPRO	IPR000566:Lipocalin/cytosolic fatty-acid binding protein domain	9	4.639175258	7.40E-08	MUP5, MUP4, MUP20, MUP1, MUP3, MUP19, MUP2, FABP4, MUP17	175	65	20594	16.29415385	3.02E-05	7.55E-06	1.04E-04
27	GOTERM_BP_DIRECT	GO:0045475~locomotor rhythm	7	3.608247423	1.20E-07	MUP5, MUP4, MUP20, MUP1, MUP3, MUP19, MUP2	170	26	18082	28.63665158	1.59E-04	1.44E-05	1.97E-04
28	INTERPRO	IPR012674:Calycin	9	4.639175258	1.67E-07	MUP5, MUP4, MUP20, MUP1, MUP3, MUP19, MUP2, FABP4, MUP17	175	72	20594	14.71	6.81E-05	1.36E-05	2.34E-04
29	INTERPRO	IPR011038:Calycin-like	9	4.639175258	1.86E-07	MUP5, MUP4, MUP20, MUP1, MUP3, MUP19, MUP2, FABP4, MUP17	175	73	20594	14.50849315	7.59E-05	1.27E-05	2.60E-04
30	GOTERM_BP_DIRECT	GO:0070584~mitochondrion morphogenesis	7	3.608247423	4.52E-07	MUP5, MUP4, MUP20, MUP1, MUP3, MUP19, MUP2	170	32	18082	23.26727941	5.97E-04	4.97E-05	7.39E-04
31	GOTERM_BP_DIRECT	GO:0009060~aerobic respiration	7	3.608247423	1.54E-06	MUP5, MUP4, MUP20, MUP1, MUP3, MUP19, MUP2	170	39	18082	19.09110106	0.002033586	1.57E-04	0.002521024
32	UP_KEYWORDS	Lipoprotein	22	11.34020619	1.87E-06	LY6C1, STMN3, IFITM1, STMN2, MME, LY6K, CD52, NRN1, CLDN15, CDH13, EDNRB, LY6D, ADRB1, RAC2, CNR1, MC2R, HPCA, ADRA1B, NOS3, GNG3, GPIHBP1, GFRA3	187	780	22680	3.42081448	3.95E-04	6.58E-05	0.002367378
33	GOTERM_BP_DIRECT	GO:0051897~positive regulation of protein kinase B signaling	9	4.639175258	3.52E-06	MUP5, MUP4, MUP20, CHIL1, MUP1, MUP3, MUP19, MUP2, GM1987	170	97	18082	9.868890237	0.004634964	3.32E-04	0.005753343
34	KEGG_PATHWAY	mmu03320:PPAR signaling pathway	8	4.12371134	1.47E-05	SCD1, ACSL1, PLIN1, RXRG, FABP4, ADIPOQ, PCK1, NR1H3	79	80	7691	9.735443038	0.002223041	0.002223041	0.017618906
35	GOTERM_BP_DIRECT	GO:0032496~response to lipopolysaccharide	11	5.670103093	1.66E-05	CXCL1, EDNRB, IRAK3, PPBP, WFDC21, CNR1, MAOB, TH, ACP5, LGALS9, PCK1	170	197	18082	5.939146014	0.02174237	0.001464408	0.027220138
36	GOTERM_MF_DIRECT	GO:0005215~transporter activity	11	5.670103093	3.42E-05	MUP5, MUP4, MUP20, ABCA9, MUP1, MUP3, MUP19, MUP2, FABP4, MUP17, ABCA17	162	217	17446	5.459008932	0.011595387	0.003880165	0.046586331
37	GOTERM_MF_DIRECT	GO:0005550~pheromone binding	8	4.12371134	7.18E-05	MUP5, MUP4, MUP20, MUP1, MUP3, MUP19, MUP2, MUP17	162	110	17446	7.832098765	0.024189233	0.00610295	0.097782311
38	UP_KEYWORDS	GPI-anchor	8	4.12371134	1.60E-04	LY6C1, CDH13, LY6D, LY6K, CD52, NRN1, GPIHBP1, GFRA3	187	140	22680	6.930481283	0.033213695	0.004813776	0.202202617
39	UP_SEQ_FEATURE	glycosylation site:N-linked (GlcNAc...)	54	27.83505155	1.61E-04	ASPN, GPR84, MMP9, F13A1, SERPINA3F, CD52, HP, CD209D, EDNRB, AGTR2, PROZ, CES1D, ESAM, TIE1, ITIH3, CFD, GPIHBP1, ICAM2, TNMD, ADRB1, SGCG, CD33, MC2R, SGCD, SGCA, MFNG, EMCN, ABCA9, MAMDC2, C3, FCNA, ASTN1, ACP5, MME, CHIL1, BCHE, CNR1, SLC6A12, MUP3, PCDH12, DBH, TMPRSS3, P2RY12, CDH13, LAMA4, SFRP1, PRLR, FCGR2B, CD300A, SULF1, ADRA1B, IGFBP3, ADAMDEC1, GFRA3	168	3563	18012	1.624914799	0.076960915	0.026341416	0.231175875
40	GOTERM_CC_DIRECT	GO:0031225~anchored component of membrane	8	4.12371134	3.02E-04	LY6C1, CDH13, LY6D, LY6K, CD52, NRN1, GPIHBP1, GFRA3	179	141	19662	6.232259598	0.054386418	0.018467765	0.373333833
41	GOTERM_BP_DIRECT	GO:0045776~negative regulation of blood pressure	5	2.577319588	3.08E-04	CNR1, NOS3, ADIPOQ, GJA5, APLN	170	35	18082	15.19495798	0.333909512	0.025075853	0.501954429
42	UP_SEQ_FEATURE	propeptide:Removed in mature form	10	5.154639175	3.87E-04	LY6C1, CDH13, LY6D, ISG15, RAC2, LY6K, CD52, GNG3, NRN1, GFRA3	168	238	18012	4.504801921	0.175362825	0.047059626	0.55568026
43	UP_SEQ_FEATURE	chain:Major urinary protein 1	4	2.06185567	4.01E-04	MUP1, MUP19, MUP2, MUP17	168	16	18012	26.80357143	0.181108632	0.039172867	0.575773154
44	UP_SEQ_FEATURE	chain:Major urinary protein 6	4	2.06185567	4.01E-04	MUP1, MUP19, MUP2, MUP17	168	16	18012	26.80357143	0.181108632	0.039172867	0.575773154
45	UP_SEQ_FEATURE	chain:Major urinary protein 2	4	2.06185567	4.01E-04	MUP1, MUP19, MUP2, MUP17	168	16	18012	26.80357143	0.181108632	0.039172867	0.575773154
46	UP_KEYWORDS	Cell membrane	50	25.77319588	4.73E-04	GPR84, SLC36A2, CD52, GJA4, GJA5, PRKAR2B, EDNRB, AGTR2, NOS3, ESAM, TMEM100, GNG3, TIE1, GPIHBP1, GEM, ADRB1, SGCG, CD33, MC2R, SGCD, OLFR523, SGCA, SNTG2, CAV3, CAV2, RALGPS1, IFITM1, CATSPERD, MRAP, FCNA, ASTN1, MME, MRAP2, NRN1, RIMS1, CLDN15, LY6D, CNR1, LY6C1, LY6K, PCDH12, P2RY12, A530016L24RIK, CDH13, FCGR2B, RGS2, CD300A, ECSCR, ADRA1B, GFRA3	187	3759	22680	1.613240522	0.094984351	0.012397885	0.596266903
47	GOTERM_BP_DIRECT	GO:0071356~cellular response to tumor necrosis factor	7	3.608247423	5.86E-04	GPD1, SFRP1, CHIL1, CAMP, FABP4, GM1987, PCK1	170	110	18082	6.768663102	0.538905515	0.044517061	0.95416639
48	GOTERM_BP_DIRECT	GO:0043407~negative regulation of MAP kinase activity	5	2.577319588	6.84E-04	CAV3, IRAK3, RGS2, CD300A, ADIPOQ	170	43	18082	12.36798906	0.594984951	0.04897301	1.113106783
49	GOTERM_CC_DIRECT	GO:0016011~dystroglycan complex	3	1.546391753	8.01E-04	SGCG, SGCD, SGCA	179	5	19662	65.90614525	0.137701311	0.03636086	0.98603963
50	UP_SEQ_FEATURE	chain:PHD finger protein 11-like	3	1.546391753	8.39E-04	PHF11B, PHF11D, PHF11A	168	5	18012	64.32857143	0.341627554	0.067292918	1.200716708
51	UP_SEQ_FEATURE	chain:PHD finger protein 11	3	1.546391753	8.39E-04	PHF11B, PHF11D, PHF11A	168	5	18012	64.32857143	0.341627554	0.067292918	1.200716708
52	UP_KEYWORDS	Palmitate	10	5.154639175	9.52E-04	EDNRB, ADRB1, STMN3, IFITM1, STMN2, CNR1, MC2R, ADRA1B, NOS3, CLDN15	187	304	22680	3.989586265	0.182034676	0.022078764	1.196848718
53	GOTERM_BP_DIRECT	GO:0045766~positive regulation of angiogenesis	7	3.608247423	9.66E-04	CHIL1, C3, LRG1, MMP9, CAMP, C6, NOS3	170	121	18082	6.153330092	0.721203453	0.065015095	1.569391427
54	UP_KEYWORDS	Cleavage on pair of basic residues	9	4.639175258	0.001051017	CDH13, C3, PROZ, 1500015O10RIK, CARTPT, ITIH3, OSTN, APLN, SCG2	187	248	22680	4.401414525	0.198989474	0.021943773	1.320782967
55	GOTERM_CC_DIRECT	GO:0016012~sarcoglycan complex	3	1.546391753	0.001193613	SGCG, SGCD, SGCA	179	6	19662	54.92178771	0.198243508	0.043227912	1.46697201
56	UP_SEQ_FEATURE	zinc finger region:PHD-type; degenerate	3	1.546391753	0.001250792	PHF11B, PHF11D, PHF11A	168	6	18012	53.60714286	0.46381934	0.085191558	1.785177125
57	GOTERM_BP_DIRECT	GO:0035634~response to stilbenoid	4	2.06185567	0.001585782	LY6D, SAA2, MUP1, MUP3	170	25	18082	17.01835294	0.877111932	0.099517067	2.562967873
58	UP_SEQ_FEATURE	lipid moiety-binding region:GPI-anchor amidated glycine	4	2.06185567	0.001739919	LY6C1, CDH13, LY6K, NRN1	168	26	18012	16.49450549	0.579888112	0.102735219	2.475176709
59	UP_SEQ_FEATURE	domain:UPAR/Ly6	4	2.06185567	0.00194417	LY6C1, LY6D, LY6K, GPIHBP1	168	27	18012	15.88359788	0.620590387	0.102087001	2.761971205
60	GOTERM_CC_DIRECT	GO:0005783~endoplasmic reticulum	24	12.37113402	0.001967801	SCD1, CAV3, CAV2, MAMDC2, MRAP, APOC1, HP, MRAP2, LTC4S, ADIPOQ, TMPRSS3, CIDEC, ACSL1, CHIL1, PLIN1, BCHE, AGPAT9, SULF1, CES1F, ABCA17, CES1D, TMEM100, AGPAT2, NAT8L	179	1323	19662	1.992627218	0.305387972	0.058926126	2.407858673
61	UP_KEYWORDS	Lipid droplet	4	2.06185567	0.002060223	PLIN1, CES1F, CES1D, CIDEC	187	31	22680	15.64947387	0.352835991	0.038787329	2.573886665
62	GOTERM_BP_DIRECT	GO:0001937~negative regulation of endothelial cell proliferation	4	2.06185567	0.002705147	CAV2, TNMD, RGCC, SULF1	170	30	18082	14.18196078	0.97207802	0.156670216	4.3348306
63	GOTERM_CC_DIRECT	GO:0045121~membrane raft	9	4.639175258	0.00272412	CAV3, EDNRB, PRKAR2B, CAV2, FCGR2B, CNR1, SULF1, NOS3, SGCA	179	262	19662	3.773252591	0.396283132	0.0695555	3.319048439
64	GOTERM_CC_DIRECT	GO:0005829~cytosol	29	14.94845361	0.002853145	CAV2, MUP19, TH, ACOT3, RAC2, PLIN1, SULT1A1, PDE4B, CES1F, CES1D, NOS3, THRSP, MUP5, GPD1, MUP4, GIMAP4, GIMAP6, MUP1, MUP3, MUP2, CAPN3, CIDEC, PCK1, MUP20, SFRP1, RGS2, ECSCR, FABP4, SP6	179	1784	19662	1.785573816	0.410562299	0.063937733	3.473710034
65	GOTERM_CC_DIRECT	GO:0070062~extracellular exosome	39	20.10309278	0.002869875	SNCG, PRPH, TPPP3, RARRES2, SLC36A2, C3, C6, MMP9, APOC1, ACP5, MME, HP, PRKAR2B, RAC2, SAA2, CHIL1, LRG1, PROZ, ITIH4, ESAM, ITIH3, CFD, DPT, GPD1, ICAM2, CAMP, MAOB, PCDH12, TPMT, ADIPOQ, PCK1, CDH13, RETN, LAMA4, SFRP1, DUSP26, CD300A, FABP4, IGFBP3	179	2674	19662	1.602056635	0.412389024	0.057365519	3.493747461
66	GOTERM_CC_DIRECT	GO:0005811~lipid particle	5	2.577319588	0.003023713	CAV2, PLIN1, CES1F, CES1D, CIDEC	179	66	19662	8.321482986	0.428924783	0.054483023	3.677820857
67	GOTERM_BP_DIRECT	GO:0048147~negative regulation of fibroblast proliferation	4	2.06185567	0.003259983	AGTR2, SFRP1, CD300A, MMP9	170	32	18082	13.29558824	0.986613015	0.178042774	5.201834767
68	GOTERM_BP_DIRECT	GO:0008285~negative regulation of cell proliferation	11	5.670103093	0.003347025	PHOX2B, CDH13, CAV2, SFRP1, IFITM1, BCHE, RGCC, NOS3, SOX7, IGFBP3, DPT	170	384	18082	3.046905637	0.988071629	0.175153582	5.337177661

69	INTERPRO	IPR016054:Ly-6 antigen / uPA receptor -like	4	2.06185567	0.004024915	LY6C1, LY6D, LY6K, GPIHBP1	175	38	20594	12.38736842	0.807079897	0.209483263	5.485330365
70	GOTERM_BP_DIRECT	GO:0071773~cellular response to BMP stimulus	4	2.06185567	0.004214602	PHOX2B, SFRP1, TNMD, TMEM100	170	35	18082	12.15596639	0.996224621	0.207425631	6.676309325
71	BIOCARTA	m_alternativePathway:Alternative Complement Pathway	3	1.546391753	0.004377769	C3, C6, CFD	18	8	1289	26.85416667	0.193443698	0.193443698	4.119354978
72	GOTERM_BP_DIRECT	GO:0010628~positive regulation of gene expression	11	5.670103093	0.004379803	MUP5, MUP4, MUP20, MUP1, MUP3, MUP19, RGCC, MUP2, MUSTN1, RIMS1, LGALS9	170	399	18082	2.932360313	0.99696768	0.207003997	6.929278458
73	GOTERM_CC_DIRECT	GO:0042383~sarcolemma	6	3.092783505	0.004415227	CAV3, SGCG, SGCD, NOS3, SGCA, SNTG2	179	118	19662	5.585266547	0.558962571	0.071718733	5.328219277
74	UP_SEQ_FEATURE	zinc finger region:PHD-type; atypical	3	1.546391753	0.004448478	PHF11B, PHF11D, PHF11A	168	11	18012	29.24025974	0.891421725	0.199107376	6.215130727
75	GOTERM_BP_DIRECT	GO:0016525~negative regulation of angiogenesis	5	2.577319588	0.00462451	ECSCR, TNMD, RGCC, SULF1, TIE1	170	72	18082	7.386437908	0.997808451	0.209828798	7.302809096
76	GOTERM_BP_DIRECT	GO:0045909~positive regulation of vasodilation	4	2.06185567	0.005322415	AGTR2, NOS3, GJA5, APLN	170	38	18082	11.19628483	0.99913232	0.229795749	8.360404864
77	GOTERM_BP_DIRECT	GO:0006641~triglyceride metabolic process	4	2.06185567	0.005726843	CAV3, SCD1, ACSL1, APOC1	170	39	18082	10.9092006	0.999492952	0.237353674	8.968073962
78	GOTERM_CC_DIRECT	GO:0030424~axon	10	5.154639175	0.006703573	PRPH, SNCG, STMN3, STMN2, CNR1, HPCA, TH, MME, DBH, NEFL	179	370	19662	2.968745282	0.711867934	0.098499512	7.985877596
79	GOTERM_BP_DIRECT	GO:0071347~cellular response to interleukin-1	5	2.577319588	0.006712445	SFRP1, CHIL1, CAMP, GM1987, PCK1	170	80	18082	6.647794118	0.999863206	0.264198025	10.43317327
80	GOTERM_BP_DIRECT	GO:0001525~angiogenesis	8	4.123711340	0.007364041	EMCN, ECSCR, NOS3, TIE1, ESM1, TMEM100, GJA5, SCG2	170	239	18082	3.560324883	0.999944251	0.277807163	11.38958442
81	UP_KEYWORDS	Chemotaxis	5	2.577319588	0.007528381	CXCL1, RARRES2, ECSCR, GM1987, LGALS9	187	94	22680	6.451245876	0.796989595	0.124425325	9.112472852
82	GOTERM_CC_DIRECT	GO:0005901~caveola	5	2.577319588	0.00775041	P2RY12, CAV3, CDH13, CAV2, NOS3	179	86	19662	6.386254385	0.762932692	0.104814157	9.178650674
83	UP_KEYWORDS	Lipid metabolism	10	5.154639175	0.007768232	SCD1, ACSL1, C3, PLIN1, SULT1A1, AGPAT9, CES1D, ABCA17, THRSP, AGPAT2	187	417	22680	2.908475359	0.807083271	0.118893403	9.389980101
84	INTERPRO	IPR018363:CD59 antigen, conserved site	3	1.546391753	0.007879744	LY6C1, LY6D, GPIHBP1	175	16	20594	22.065	0.960350182	0.331994329	10.47572668
85	UP_KEYWORDS	Endoplasmic reticulum	17	8.762886598	0.008159675	SCD1, MRAP, LTC4S, MRAP2, TMPRSS3, CIDEC, ACSL1, CHIL1, PLIN1, AGPAT9, SULF1, CES1F, ABCA17, CES1D, TMEM100, AGPAT2, NAT8L	187	997	22680	2.068022249	0.822494571	0.116162834	9.84073419
86	KEGG_PATHWAY	mmu05416:Viral myocarditis	5	2.577319588	0.008280157	SGCG, RAC2, SGCD, MYH6, SGCA	79	79	7691	6.161672809	0.715069184	0.466210888	9.462366533
87	GOTERM_BP_DIRECT	GO:0045892~negative regulation of transcription, DNA-templated	13	6.701030928	0.008327025	MUP5, MUP4, MUP1, MUP19, MUP3, MUP2, SOX7, CAPN3, ADIPOQ, MUP20, SFRP1, FABP4, NR1H3	170	579	18082	2.388154018	0.99998405	0.299754521	12.78550874
88	GOTERM_BP_DIRECT	GO:0050872~white fat cell differentiation	3	1.546391753	0.009561651	SCD1, WFDC21, FABP4	170	16	18082	19.94338235	0.999996923	0.327407808	14.54500702
89	GOTERM_BP_DIRECT	GO:0048485~sympathetic nervous system development	3	1.546391753	0.0107705	PHOX2A, PHOX2B, GFRA3	170	17	18082	18.77024221	0.999999387	0.351753989	16.23543478
90	GOTERM_BP_DIRECT	GO:0014823~response to activity	4	2.06185567	0.010787461	SULT1A1, TH, ADIPOQ, PCK1	170	49	18082	8.682833133	0.999999401	0.343873459	16.2589276
91	GOTERM_BP_DIRECT	GO:0030819~positive regulation of cAMP biosynthetic process	4	2.06185567	0.010787461	ADRB1, MRAP, MC2R, MRAP2	170	49	18082	8.682833133	0.999999401	0.343873459	16.2589276
92	GOTERM_BP_DIRECT	GO:0006629~lipid metabolic process	11	5.670103093	0.011236034	SCD1, ACSL1, C3, PLIN1, SULT1A1, AGPAT9, CES1D, ABCA17, THRSP, AGPAT2, PCK1	170	459	18082	2.549045239	0.999999671	0.347197423	16.87801456
93	GOTERM_CC_DIRECT	GO:0005886~plasma membrane	59	30.41237113	0.011363956	SNCG, GPR84, SLC36A2, CD52, GJA4, GJA5, EDNRB, PRKAR2B, AGTR2, ITIH4, ESAM, NOS3, TMEM100, GNG3, TIE1, GPIHBP1, ICAM2, GEM, ADRB1, SGCG, CD33, MC2R, SGCD, OLFR523, SGCA, SNTG2, CAV3, CAV2, EMCN, RALGPS1, IFITM1, MRAP, CATSPERD, FCNA, ASTN1, MME, AFAP1L1, MRAP2, NRN1, RIMS1, CLDN15, ACSL1, LY6D, CNR1, LY6C1, LY6K, PCDH12, CAPN3, P2RY12, A530016L24RIK, CDH13, SFRP1, FCGR2B, RGS2, CD300A, ECSCR, SULF1, ADRA1B, GFRA3	179	4874	19662	1.329661664	0.879290051	0.140174935	13.18759803
94	**GOTERM_BP_DIRECT**	**GO:0055117~regulation of cardiac muscle contraction**	**3**	**1.546391753**	**0.013377955**	**CAV3, ADRA1B, GJA5**	**170**	**19**	**18082**	**16.79442724**	**0.999999981**	**0.38994722**	**19.77533798**
95	GOTERM_CC_DIRECT	GO:0016020~membrane	79	40.72164948	0.013886224	PRPH, GPR84, SLC36A2, CD52, LTC4S, GJA4, GJA5, CD209D, EDNRB, PRKAR2B, AGTR2, AGPAT9, PDE4B, ESAM, NOS3, GNG3, TMEM100, TIE1, GPIHBP1, AGPAT2, STMN2, ICAM2, TNMD, GEM, FCRLS, ADRB1, SGCG, CD33, MC2R, SGCD, SGCA, SNTG2, CAV3, CAV2, EMCN, MFNG, RALGPS1, ABCA9, MAMDC2, IFITM1, MRAP, CATSPERD, FCNA, ASTN1, MME, MRAP2, NRN1, RIMS1, CLDN15, LY6D, ACSL1, RAC2, BCHE, CNR1, ABCA17, SCD1, LY6C1, COX7A1, COX8B, SLC6A12, MAOB, PCDH12, LY6K, DBH, TMPRSS3, A530016L24RIK, P2RY12, CDH13, SVOPL, RGS2, PRLR, FCGR2B, CD300A, ECSCR, ADRA1B, COQ10B, NAT8L, IFI205, GFRA3	179	6998	19662	1.240017499	0.924751157	0.15841112	15.88875196
96	COG_ONTOLOGY	Lipid metabolism	4	2.06185567	0.014502129	ACSL1, BCHE, CES1F, CES1D	14	88	2126	6.902597403	0.083918444	0.083918444	6.752555924
97	INTERPRO	IPR019826:Carboxylesterase type B, active site	3	1.546391753	0.014674169	BCHE, CES1F, CES1D	175	22	20594	16.04727273	0.997597927	0.488372326	18.6807067
98	GOTERM_CC_DIRECT	GO:0034364~high-density lipoprotein particle	3	1.546391753	0.015286407	SAA2, APOC1, GPIHBP1	179	21	19662	15.69193935	0.94214544	0.163152931	17.35467848
99	GOTERM_BP_DIRECT	GO:0006631~fatty acid metabolic process	6	3.092783505	0.015633046	SCD1, PRKAR2B, ACSL1, C3, TH, FABP4	170	156	18082	4.090950226	0.999999999	0.430246071	22.7231165
100	GOTERM_BP_DIRECT	GO:0048265~response to pain	3	1.546391753	0.016229968	EDNRB, DBH, GJA4	170	21	18082	15.19495798	1	0.433814546	23.48619584

Table S9. Functional annotation by DAVID for genes with decreased expression in the microarray of E15.5 *Fgfr1/2cDKO-UM* ureter explants cultured for 6 days.

	intensities								fold change (FC)				
Gene Symbol	control 1	mutant 1	control 2	mutant 2	control 3	mutant 3	control 4	mutant 4	FC 1	FC 2	FC 3	FC 4	avgFC
Upk1b	685	185	667	122	734	257	547	314	-3.7	-5.5	-2.9	-1.7	-3.4
Prap1	697	96	254	165	150	73	109	84	-7.2	-1.5	-2.1	-1.3	-3.0
Trnt1	1101	213	1034	290	214	159	401	308	-5.2	-3.6	-1.3	-1.3	-2.8
Aldh3b2	130	53	139	47	158	65	146	73	-2.5	-2.9	-2.4	-2.0	-2.5
Uap1l1	671	184	631	209	344	256	404	225	-3.6	-3.0	-1.3	-1.8	-2.4
Gm9992	578	157	571	199	213	160	245	140	-3.7	-2.9	-1.3	-1.8	-2.4
Anxa8	3349	1150	2942	1219	3629	1425	2912	1679	-2.9	-2.4	-2.5	-1.7	-2.4
Zdhhc22	3489	1206	4238	1388	2121	1572	2935	1372	-2.9	-3.1	-1.3	-2.1	-2.4
Itih2	254	92	253	71	179	135	163	114	-2.7	-3.5	-1.3	-1.4	-2.3
Perp	5704	2105	5129	1887	4294	2292	4384	2831	-2.7	-2.7	-1.9	-1.5	-2.2
Mgat4c	211	89	214	86	105	65	110	52	-2.4	-2.5	-1.6	-2.1	-2.1
Sprr1a	909	435	1015	391	1344	658	1301	811	-2.1	-2.6	-2.0	-1.6	-2.1
Apela	5613	2319	5182	1846	2907	1919	3327	2246	-2.4	-2.8	-1.5	-1.5	-2.1
Fam183b	1109	490	1115	407	633	370	618	425	-2.3	-2.7	-1.7	-1.5	-2.0
Fmo1	453	207	433	194	325	203	440	205	-2.2	-2.2	-1.6	-2.1	-2.0
Batf	672	288	579	292	583	287	537	323	-2.3	-2.0	-2.0	-1.7	-2.0
Ccl11	353	176	329	167	218	132	297	128	-2.0	-2.0	-1.6	-2.3	-2.0
Aspn	609	321	597	283	398	232	523	241	-1.9	-2.1	-1.7	-2.2	-2.0
Rab27b	682	312	750	276	443	334	541	352	-2.2	-2.7	-1.3	-1.5	-1.9
D930019F10Rik	255	123	354	163	195	102	148	96	-2.1	-2.2	-1.9	-1.5	-1.9
Igf1	167	92	164	82	198	102	239	126	-1.8	-2.0	-1.9	-1.9	-1.9
Sdpr	11155	5596	10984	4192	6217	4476	7706	4768	-2.0	-2.6	-1.4	-1.6	-1.9
Ndufa4l2	614	228	573	305	503	393	488	294	-2.7	-1.9	-1.3	-1.7	-1.9
Ptn	12472	7565	11356	6102	10914	5807	11340	5379	-1.6	-1.9	-1.9	-2.1	-1.9
Msln	1301	595	1198	644	1457	792	1374	954	-2.2	-1.9	-1.8	-1.4	-1.8
Ptprd	200	77	172	81	167	126	152	120	-2.6	-2.1	-1.3	-1.3	-1.8
Fxyd3	3648	1535	3476	1683	3338	2076	3032	2397	-2.4	-2.1	-1.6	-1.3	-1.8
Cck	426	199	415	201	374	269	384	234	-2.1	-2.1	-1.4	-1.6	-1.8
Lmcd1	965	480	1116	505	1261	890	1418	899	-2.0	-2.2	-1.4	-1.6	-1.8
Fibin	4757	2762	4808	2104	3855	2579	4342	2607	-1.7	-2.3	-1.5	-1.7	-1.8
Vcam1	8095	4701	6689	4890	5995	2906	6397	3202	-1.7	-1.4	-2.1	-2.0	-1.8
Atp8a2	314	185	297	175	287	147	323	190	-1.7	-1.7	-1.9	-1.7	-1.8
Snap91	215	151	268	94	173	130	173	123	-1.4	-2.9	-1.3	-1.4	-1.8
Hpgd	577	325	574	273	494	282	482	362	-1.8	-2.1	-1.8	-1.3	-1.7
Clec1b	261	174	251	168	184	97	226	109	-1.5	-1.5	-1.9	-2.1	-1.7
Zfp949	953	543	1235	570	1004	664	864	585	-1.8	-2.2	-1.5	-1.5	-1.7
Fam167b	574	359	542	336	590	296	675	396	-1.6	-1.6	-2.0	-1.7	-1.7
Trim29	135	62	133	89	205	124	166	111	-2.2	-1.5	-1.7	-1.5	-1.7
Krt20	219	126	214	139	293	140	239	160	-1.7	-1.5	-2.1	-1.5	-1.7
Tmprss13	108	74	127	65	155	81	134	89	-1.5	-2.0	-1.9	-1.5	-1.7
Ly6g6e	128	75	121	64	106	64	110	75	-1.7	-1.9	-1.7	-1.5	-1.7
Ebf2	116	77	113	77	114	54	129	81	-1.5	-1.5	-2.1	-1.6	-1.7
Lypd2	1151	611	1025	590	780	518	779	513	-1.9	-1.7	-1.5	-1.5	-1.7

Colec11	419	289	438	263	457	333	513	240	-1.5	-1.7	-1.4	-2.1	-1.7
Serpina3f	465	237	420	236	330	217	317	234	-2.0	-1.8	-1.5	-1.4	-1.7
Cebpa	241	112	165	117	236	156	212	137	-2.1	-1.4	-1.5	-1.5	-1.7
Hba-x	7796	4898	6840	4089	7847	6167	10349	5045	-1.6	-1.7	-1.3	-2.1	-1.6
Casp4	854	524	767	482	716	354	533	403	-1.6	-1.6	-2.0	-1.3	-1.6
Cmbl	692	371	632	381	548	348	565	404	-1.9	-1.7	-1.6	-1.4	-1.6
Gimap6	4437	2251	3573	2618	2967	2145	3545	1996	-2.0	-1.4	-1.4	-1.8	-1.6
S100a5	263	133	244	145	236	150	227	178	-2.0	-1.7	-1.6	-1.3	-1.6
Ifi203	185	101	167	124	197	99	165	125	-1.8	-1.3	-2.0	-1.3	-1.6
Tmem37	10066	5790	9580	5531	7796	5014	7745	5423	-1.7	-1.7	-1.6	-1.4	-1.6
Pf4	2851	1824	2656	1803	2001	1252	2395	1331	-1.6	-1.5	-1.6	-1.8	-1.6
2200002D01Rik	2671	1512	2703	1431	2001	1356	1913	1486	-1.8	-1.9	-1.5	-1.3	-1.6
Fam212a	308	209	318	220	345	213	462	245	-1.5	-1.4	-1.6	-1.9	-1.6
Crabp1	6118	4027	5653	3758	3983	2518	4624	2563	-1.5	-1.5	-1.6	-1.8	-1.6
Grap	602	342	552	398	388	234	440	280	-1.8	-1.4	-1.7	-1.6	-1.6
Entpd2	409	225	409	255	351	237	396	271	-1.8	-1.6	-1.5	-1.5	-1.6
ENS-MUST00000199575	270	142	242	141	378	275	348	253	-1.9	-1.7	-1.4	-1.4	-1.6
Cthrc1	3009	1649	2934	1583	2223	1618	2265	1745	-1.8	-1.9	-1.4	-1.3	-1.6
Car3	21565	15481	20800	11701	18594	14301	25949	13859	-1.4	-1.8	-1.3	-1.9	-1.6
Pon3	1974	1158	1811	988	1239	928	1358	950	-1.7	-1.8	-1.3	-1.4	-1.6
8430408G22Rik	417	293	436	299	678	424	822	456	-1.4	-1.5	-1.6	-1.8	-1.6
Cbr2	131	88	120	70	142	95	127	80	-1.5	-1.7	-1.5	-1.6	-1.6
Tmem204	626	323	509	342	494	336	478	354	-1.9	-1.5	-1.5	-1.4	-1.6
Grhl3	802	580	1057	549	1483	1003	1547	1059	-1.4	-1.9	-1.5	-1.5	-1.6
Ifi27l2a	1333	893	1252	943	873	463	871	579	-1.5	-1.3	-1.9	-1.5	-1.6
Ccl24	248	138	230	175	174	121	193	117	-1.8	-1.3	-1.4	-1.6	-1.5
Serpina3g	297	186	277	191	286	214	344	190	-1.6	-1.4	-1.3	-1.8	-1.5
C1qb	502	299	463	250	381	289	371	279	-1.7	-1.9	-1.3	-1.3	-1.5
Gem	607	370	526	400	687	423	685	428	-1.6	-1.3	-1.6	-1.6	-1.5
Rab3b	500	383	540	295	619	440	627	387	-1.3	-1.8	-1.4	-1.6	-1.5
Clec1a	229	143	218	134	159	104	184	131	-1.6	-1.6	-1.5	-1.4	-1.5
Gimap4	3783	2428	3386	2370	2392	1753	3228	1786	-1.6	-1.4	-1.4	-1.8	-1.5
Krt19	13801	7732	13406	7522	14290	11286	14605	11071	-1.8	-1.8	-1.3	-1.3	-1.5
Hsd17b14	266	155	291	183	357	240	315	236	-1.7	-1.6	-1.5	-1.3	-1.5
Guca1a	214	128	164	131	128	90	139	78	-1.7	-1.3	-1.4	-1.8	-1.5
Emcn	1400	903	1311	808	1222	817	1313	905	-1.5	-1.6	-1.5	-1.5	-1.5
Fgfr1	594	349	546	366	821	547	645	454	-1.7	-1.5	-1.5	-1.4	-1.5
BC028528	1856	1194	1771	1078	1577	979	1378	1062	-1.6	-1.6	-1.6	-1.3	-1.5
Grrp1	5351	3105	4589	3506	3523	2234	3891	2608	-1.7	-1.3	-1.6	-1.5	-1.5
Ctnna2	1834	1243	1906	1128	1662	1146	1594	1094	-1.5	-1.7	-1.5	-1.5	-1.5
Xaf1	179	114	174	114	200	120	163	125	-1.6	-1.5	-1.7	-1.3	-1.5
Asb4	3496	2538	3273	2091	2202	1638	2893	1642	-1.4	-1.6	-1.3	-1.8	-1.5
ENS-MUST00000128900	870	635	937	538	733	531	969	622	-1.4	-1.7	-1.4	-1.6	-1.5
Klhl6	242	150	227	138	186	132	186	136	-1.6	-1.6	-1.4	-1.4	-1.5
Procr	1766	1405	1922	1406	2923	1673	2936	1779	-1.3	-1.4	-1.7	-1.6	-1.5

Hbb-bh1	9192	6356	7472	4579	4939	3793	6121	3765	-1.4	-1.6	-1.3	-1.6	-1.5
Vsig2	769	519	807	556	902	532	848	619	-1.5	-1.5	-1.7	-1.4	-1.5
Sh3bgrl2	148	91	147	83	105	84	112	84	-1.6	-1.8	-1.3	-1.3	-1.5
Sdcbp2	379	238	368	242	373	257	339	243	-1.6	-1.5	-1.5	-1.4	-1.5
9230102K24Rik	335	218	289	221	206	129	213	141	-1.5	-1.3	-1.6	-1.5	-1.5
Tyrobp	1686	1012	1552	1142	1322	983	1339	847	-1.7	-1.4	-1.3	-1.6	-1.5
Adora2b	269	176	238	178	213	160	268	154	-1.5	-1.3	-1.3	-1.7	-1.5
Il2rg	184	123	189	109	171	125	184	137	-1.5	-1.7	-1.4	-1.3	-1.5
Fcer1g	1580	1022	1653	1106	1226	915	1163	754	-1.5	-1.5	-1.3	-1.5	-1.5
Hapln1	2226	1523	2146	1342	1559	1064	1819	1304	-1.5	-1.6	-1.5	-1.4	-1.5
BC049762	254	168	202	161	158	102	167	106	-1.5	-1.3	-1.6	-1.6	-1.5
Col14a1	1069	768	950	676	1255	801	1367	890	-1.4	-1.4	-1.6	-1.5	-1.5
Ifitm1	1451	927	1233	960	976	672	1161	730	-1.6	-1.3	-1.5	-1.6	-1.5
AI314604	106	68	130	77	120	89	113	88	-1.6	-1.7	-1.4	-1.3	-1.5
Ms4a6c	121	85	128	83	121	79	106	76	-1.4	-1.5	-1.5	-1.4	-1.5
Lgals9	335	256	343	206	336	259	390	250	-1.3	-1.7	-1.3	-1.6	-1.5
S100a13	3480	2331	3009	2245	2418	1686	2760	1764	-1.5	-1.3	-1.4	-1.6	-1.5
Ugt1a6b	553	414	555	349	441	320	462	305	-1.3	-1.6	-1.4	-1.5	-1.5
Sntg1	167	124	159	103	111	85	119	74	-1.3	-1.5	-1.3	-1.6	-1.5
Gas2	5368	3874	5065	3193	3317	2615	3619	2308	-1.4	-1.6	-1.3	-1.6	-1.5
Pon2	317	216	334	193	354	272	358	276	-1.5	-1.7	-1.3	-1.3	-1.4
BC025446	142	107	131	90	256	162	212	149	-1.3	-1.5	-1.6	-1.4	-1.4
Ppp2r2b	688	454	689	405	609	486	673	514	-1.5	-1.7	-1.3	-1.3	-1.4
Sfn	278	161	238	174	405	309	358	261	-1.7	-1.4	-1.3	-1.4	-1.4
Adgrl4	143	110	133	92	142	113	215	123	-1.3	-1.4	-1.3	-1.7	-1.4
S100a16	9134	6566	9247	6001	7467	5663	8467	5612	-1.4	-1.5	-1.3	-1.5	-1.4
H2-T10	481	336	481	299	460	328	473	359	-1.4	-1.6	-1.4	-1.3	-1.4
Tmem140	192	149	231	138	211	140	173	136	-1.3	-1.7	-1.5	-1.3	-1.4
Dapk2	230	157	192	151	212	123	187	146	-1.5	-1.3	-1.7	-1.3	-1.4
Gm11744	188	119	192	147	149	104	147	105	-1.6	-1.3	-1.4	-1.4	-1.4
Ipo11	128	85	123	90	133	93	125	89	-1.5	-1.4	-1.4	-1.4	-1.4
Sult1a1	705	487	642	504	569	413	703	438	-1.4	-1.3	-1.4	-1.6	-1.4
Ushbp1	2029	1404	2069	1538	2417	1602	2201	1575	-1.4	-1.3	-1.5	-1.4	-1.4
Rnd2	571	372	532	348	532	408	542	409	-1.5	-1.5	-1.3	-1.3	-1.4
Nrros	3129	2175	3220	2071	2868	2207	2787	2003	-1.4	-1.6	-1.3	-1.4	-1.4
Pecam1	414	299	460	265	491	385	449	349	-1.4	-1.7	-1.3	-1.3	-1.4
Fap	12110	8809	10885	7111	7843	5769	7944	5694	-1.4	-1.5	-1.4	-1.4	-1.4
A_55_P1953377	14433	9616	14227	9643	15944	12122	15921	11686	-1.5	-1.5	-1.3	-1.4	-1.4
Trem2	938	584	917	649	656	520	571	418	-1.6	-1.4	-1.3	-1.4	-1.4
Plod2	2476	1798	2152	1448	1747	1374	2083	1422	-1.4	-1.5	-1.3	-1.5	-1.4
Aspa	100	80	118	75	103	80	104	73	-1.3	-1.6	-1.3	-1.4	-1.4
Kcnk6	1290	909	1388	1059	1509	1020	1403	1053	-1.4	-1.3	-1.5	-1.3	-1.4
Postn	23180	18502	22838	16403	20220	14201	20427	13936	-1.3	-1.4	-1.4	-1.5	-1.4
Tmem255a	120	91	105	84	146	90	133	103	-1.3	-1.3	-1.6	-1.3	-1.4
Aldh3b1	108	80	102	80	107	75	141	99	-1.3	-1.3	-1.4	-1.4	-1.4

Tnfaip8l1	7475	4799	6308	5005	5225	3906	5792	4493	-1.6	-1.3	-1.3	-1.3	-1.4
Lamb3	566	411	657	501	1028	713	932	721	-1.4	-1.3	-1.4	-1.3	-1.4
Lmo2	4072	3118	3853	3046	3488	2443	3818	2727	-1.3	-1.3	-1.4	-1.4	-1.3
Cep162	295	235	274	199	253	199	243	163	-1.3	-1.4	-1.3	-1.5	-1.3
Ifitm3	6043	4525	5711	4155	5792	4585	6247	4399	-1.3	-1.4	-1.3	-1.4	-1.3
Twist1	1739	1379	1632	1254	1370	1028	1474	987	-1.3	-1.3	-1.3	-1.5	-1.3
HQ258995	716	554	666	470	812	588	675	521	-1.3	-1.4	-1.4	-1.3	-1.3
Lama4	4114	3278	4404	3315	5449	4237	6127	4118	-1.3	-1.3	-1.3	-1.5	-1.3
Has2	4259	3325	4416	3238	4023	2939	4257	3233	-1.3	-1.4	-1.4	-1.3	-1.3
Gm266	315	235	268	201	311	248	363	262	-1.3	-1.3	-1.3	-1.4	-1.3
Tnfaip2	155	116	151	118	246	180	235	177	-1.3	-1.3	-1.4	-1.3	-1.3
H2-Q2	958	696	851	635	916	728	848	640	-1.4	-1.3	-1.3	-1.3	-1.3
H2-Q8	366	280	333	263	418	312	341	260	-1.3	-1.3	-1.3	-1.3	-1.3
ENS-MUST00000174699	496	384	447	345	541	404	465	362	-1.3	-1.3	-1.3	-1.3	-1.3
Gm11127	466	352	419	333	486	360	399	317	-1.3	-1.3	-1.3	-1.3	-1.3

Table S10. List of genes with decreased expression in the microarray of E14.5 ureters of *Fgfr1/2cDKO-UM* and control embryos. Shown are the gene names, the intensity of the four control and mutant ureter samples, the individual and the average fold change (FC, avgFC).

	intensities								**fold change (FC)**				
Gene Symbol	**control 1**	**mutant 1**	**control 2**	**mutant 2**	**control 3**	**mutant 3**	**control 4**	**mutant 4**	**FC 1**	**FC 2**	**FC 3**	**FC 4**	**avgFC**
D030062O11Rik	41	195	37	207	34	165	35	209	4.8	5.5	4.9	6.1	5.3
Aldh1a3	619	2912	496	2824	856	2849	820	3388	4.7	5.7	3.3	4.1	4.5
LOC552873	44	280	56	272	219	494	144	421	6.3	4.9	2.3	2.9	4.1
Sp5	54	245	49	256	145	335	121	357	4.5	5.2	2.3	2.9	3.8
Dlc1	28	132	29	190	259	363	188	370	4.7	6.5	1.4	2.0	3.6
Gria1	79	258	73	304	134	227	111	312	3.3	4.2	1.7	2.8	3.0
Cntn1	1289	3443	1222	3396	1458	3008	1221	3174	2.7	2.8	2.1	2.6	2.5
B4galnt2	116	382	115	323	164	329	213	267	3.3	2.8	2.0	1.3	2.3
Kcnma1	172	380	225	376	162	436	177	427	2.2	1.7	2.7	2.4	2.2
E330013P04Rik	72	178	74	170	61	151	79	118	2.5	2.3	2.5	1.5	2.2
Dclk3	47	151	56	129	70	121	79	112	3.2	2.3	1.7	1.4	2.2
Tfcp2l1	2807	6681	3016	8046	3421	7183	4156	6090	2.4	2.7	2.1	1.5	2.2
Slc7a8	412	857	329	1099	373	522	320	555	2.1	3.3	1.4	1.7	2.1
Klhl14	218	561	222	561	281	489	291	454	2.6	2.5	1.7	1.6	2.1
1700011H14Rik	1478	3655	1401	3222	977	1825	1080	1877	2.5	2.3	1.9	1.7	2.1
D430041D05Rik	615	1198	527	1393	815	1183	617	1379	1.9	2.6	1.5	2.2	2.1
BC021891	253	666	272	619	348	616	381	585	2.6	2.3	1.8	1.5	2.1
Tfap2b	293	839	323	658	345	596	410	607	2.9	2.0	1.7	1.5	2.0
D230018H15Rik	192	416	264	450	232	434	272	631	2.2	1.7	1.9	2.3	2.0
Epha8	588	1026	597	1299	1165	1727	679	1785	1.7	2.2	1.5	2.6	2.0
Wnt9b	204	491	205	529	316	512	344	492	2.4	2.6	1.6	1.4	2.0
AI593442	350	670	335	643	409	731	304	721	1.9	1.9	1.8	2.4	2.0

Itga4	1397	3010	1757	2774	2052	4212	1823	3876	2.2	1.6	2.1	2.1	2.0
Spink8	1756	3948	1707	3326	1328	2583	1523	2680	2.2	1.9	1.9	1.8	2.0
Cyp26a1	77	139	68	128	105	202	94	216	1.8	1.9	1.9	2.3	2.0
Afm	231	500	213	469	215	370	195	344	2.2	2.2	1.7	1.8	2.0
Nlgn1	141	342	138	293	103	192	145	202	2.4	2.1	1.9	1.4	1.9
Lama1	1981	4755	2100	5105	3182	4018	2971	5000	2.4	2.4	1.3	1.7	1.9
Foxl1	1668	3557	1847	3960	2543	4079	2117	3925	2.1	2.1	1.6	1.9	1.9
Rprm	3107	4756	2696	4811	1873	4382	1978	3930	1.5	1.8	2.3	2.0	1.9
Fbxo32	149	284	138	331	186	247	156	303	1.9	2.4	1.3	2.0	1.9
Fhod3	284	642	303	538	346	613	321	541	2.3	1.8	1.8	1.7	1.9
4122401K19Rik	142	381	198	361	297	417	261	414	2.7	1.8	1.4	1.6	1.9
Celsr1	1501	3448	1583	3456	1775	2744	1717	2473	2.3	2.2	1.5	1.4	1.9
Hoxd13	359	826	329	638	468	836	506	725	2.3	1.9	1.8	1.4	1.9
Habp2	1669	3251	1397	3105	1600	2758	1964	3066	1.9	2.2	1.7	1.6	1.9
Kcnd3	1225	2525	1551	2589	1208	2270	1171	2119	2.1	1.7	1.9	1.8	1.9
Fgf9	630	1222	662	1133	561	1213	589	935	1.9	1.7	2.2	1.6	1.8
Usp2	380	848	389	939	586	835	568	744	2.2	2.4	1.4	1.3	1.8
AW011956	160	328	161	372	216	336	217	313	2.1	2.3	1.6	1.4	1.8
Tinag	140	239	120	185	124	245	131	275	1.7	1.5	2.0	2.1	1.8
Hs3st6	1381	2093	1094	2724	1099	1969	1299	1958	1.5	2.5	1.8	1.5	1.8
Nell1	1339	2528	1427	2487	1140	2237	1287	2182	1.9	1.7	2.0	1.7	1.8
G6pc2	150	313	142	323	100	166	140	176	2.1	2.3	1.7	1.3	1.8
Tnfaip6	101	175	76	185	86	146	100	138	1.7	2.4	1.7	1.4	1.8
Kcnj10	126	233	132	297	159	288	176	235	1.8	2.2	1.8	1.3	1.8
TC1605611	1962	3255	1334	3164	1397	1949	1244	2233	1.7	2.4	1.4	1.8	1.8
Shh	64	206	86	108	98	146	120	150	3.2	1.3	1.5	1.3	1.8
Emx2	298	662	361	594	420	783	486	693	2.2	1.6	1.9	1.4	1.8
Gdf5	281	487	255	592	233	357	203	313	1.7	2.3	1.5	1.5	1.8
Dcdc2a	405	827	420	733	527	868	488	814	2.0	1.7	1.6	1.7	1.8
Spsb4	1133	1884	1076	2004	1142	2213	1329	2166	1.7	1.9	1.9	1.6	1.8
Fbxw25	60	135	73	113	108	205	116	164	2.2	1.5	1.9	1.4	1.8
Synpo2	212	480	231	430	263	361	275	432	2.3	1.9	1.4	1.6	1.8
Lrp2	418	903	500	789	500	991	614	817	2.2	1.6	2.0	1.3	1.8
Axin2	197	412	219	379	312	460	250	431	2.1	1.7	1.5	1.7	1.8
Nhlrc4	145	296	176	354	224	348	218	303	2.0	2.0	1.6	1.4	1.7
Fut9	273	450	270	453	225	369	207	410	1.6	1.7	1.6	2.0	1.7
LOC102637947	52151	94663	61495	128135	58873	93829	68005	96115	1.8	2.1	1.6	1.4	1.7
Pappa2	169	294	171	301	373	560	280	533	1.7	1.8	1.5	1.9	1.7
AK136433	104	130	87	184	91	129	68	143	1.3	2.1	1.4	2.1	1.7
Padi2	1003	1504	875	2356	1241	1556	1046	1456	1.5	2.7	1.3	1.4	1.7
1810041L15Rik	1977	3532	1901	4057	2777	3648	2586	4150	1.8	2.1	1.3	1.6	1.7
AK132033	9566	14760	10675	23555	16892	29494	16144	21634	1.5	2.2	1.7	1.3	1.7
Kcnc2	52	106	55	102	81	121	93	133	2.0	1.9	1.5	1.4	1.7
Cntn3	539	1071	611	1015	676	1018	558	932	2.0	1.7	1.5	1.7	1.7
Btc	125	218	141	184	78	149	104	187	1.7	1.3	1.9	1.8	1.7

Ism1	376	727	401	660	485	734	468	773	1.9	1.6	1.5	1.7	1.7
Cys1	1005	1847	1004	1877	1387	2147	1317	1960	1.8	1.9	1.5	1.5	1.7
Gm13178	85	169	91	188	119	162	106	140	2.0	2.1	1.4	1.3	1.7
Mitf	946	2279	1117	1654	1174	1789	1131	1421	2.4	1.5	1.5	1.3	1.7
Kif26b	71	126	75	127	105	148	77	136	1.8	1.7	1.4	1.8	1.7
Arhgef38	166	284	177	230	132	282	163	241	1.7	1.3	2.1	1.5	1.7
Adamts18	106	191	142	228	100	193	126	163	1.8	1.6	1.9	1.3	1.7
Adgrg1	1008	1640	972	1865	1407	2312	1398	2029	1.6	1.9	1.6	1.5	1.7
TC1616199	9217	13587	10068	21802	15605	25741	14626	19702	1.5	2.2	1.6	1.3	1.7
Hkdc1	1561	3003	1800	3372	2405	3529	2461	3369	1.9	1.9	1.5	1.4	1.7
Plch1	669	1198	638	1119	597	827	638	1087	1.8	1.8	1.4	1.7	1.7
Dpp4	272	526	270	398	204	376	295	406	1.9	1.5	1.8	1.4	1.7
Nudt10	1564	2828	1494	2776	1737	2309	1665	2716	1.8	1.9	1.3	1.6	1.7
Sostdc1	184	302	213	334	265	441	251	437	1.6	1.6	1.7	1.7	1.7
Cbln1	214	311	208	371	195	324	193	320	1.5	1.8	1.7	1.7	1.6
Adra2c	783	1333	713	1423	918	1315	972	1375	1.7	2.0	1.4	1.4	1.6
Slc16a10	163	251	150	287	208	311	206	331	1.5	1.9	1.5	1.6	1.6
Hr	89	129	75	177	133	171	101	147	1.5	2.3	1.3	1.4	1.6
Tox3	894	1668	1000	1679	974	1486	1088	1573	1.9	1.7	1.5	1.4	1.6
4930426D05Rik	295	451	307	547	383	566	349	594	1.5	1.8	1.5	1.7	1.6
Megf10	506	839	514	782	622	881	508	953	1.7	1.5	1.4	1.9	1.6
Aif1l	5434	9001	4983	9891	6723	8672	5952	9171	1.7	2.0	1.3	1.5	1.6
Fosl2	4522	6348	3992	7912	5394	7259	4557	7666	1.4	2.0	1.3	1.7	1.6
3930401B19Rik	3573	5548	4049	6945	7075	11882	6160	8823	1.6	1.7	1.7	1.4	1.6
Col2a1	1827	3562	2098	3311	2560	3316	2313	3543	1.9	1.6	1.3	1.5	1.6
Veph1	396	667	430	741	465	722	494	682	1.7	1.7	1.6	1.4	1.6
Elf5	532	862	525	822	494	747	494	806	1.6	1.6	1.5	1.6	1.6
Nr2f1	14907	28711	17500	28058	18288	23353	15762	23741	1.9	1.6	1.3	1.5	1.6
Fam149a	1897	3233	1987	3126	2098	3158	2229	3409	1.7	1.6	1.5	1.5	1.6
Lrriq1	114	172	95	183	130	182	120	177	1.5	1.9	1.4	1.5	1.6
Hoxd12	799	1186	717	1543	749	1043	834	1067	1.5	2.2	1.4	1.3	1.6
Adamts8	92	145	82	154	132	185	126	177	1.6	1.9	1.4	1.4	1.6
Tnfrsf19	258	481	287	400	299	503	352	461	1.9	1.4	1.7	1.3	1.6
Scube3	3797	6625	3919	6471	4669	6713	4644	6428	1.7	1.7	1.4	1.4	1.6
Prkg2	176	221	152	287	186	250	176	296	1.3	1.9	1.3	1.7	1.5
Hhip	1065	1704	1337	1732	1613	2339	1180	2150	1.6	1.3	1.4	1.8	1.5
Sema5b	160	284	160	278	253	322	260	358	1.8	1.7	1.3	1.4	1.5
Skap1	197	291	169	306	169	242	204	291	1.5	1.8	1.4	1.4	1.5
Ecm1	140	186	131	227	278	353	180	327	1.3	1.7	1.3	1.8	1.5
Plac8	11458	15036	8508	16497	7974	10334	7974	12612	1.3	1.9	1.3	1.6	1.5
Ppm1h	520	915	584	891	686	1003	664	901	1.8	1.5	1.5	1.4	1.5
Fam78b	777	1057	846	1242	1083	1566	837	1531	1.4	1.5	1.4	1.8	1.5
Smoc2	13897	25298	17040	25359	17435	23878	19050	27039	1.8	1.5	1.4	1.4	1.5
Cobll1	961	1747	1044	1710	1291	1677	1317	1737	1.8	1.6	1.3	1.3	1.5
Nt5dc3	2048	3359	2342	3160	2334	3715	2143	3171	1.6	1.3	1.6	1.5	1.5

Gcnt3	95	140	80	136	95	132	101	151	1.5	1.7	1.4	1.5	1.5
Pnliprp1	426	613	383	511	445	768	468	717	1.4	1.3	1.7	1.5	1.5
Htr2b	225	340	214	285	172	229	149	275	1.5	1.3	1.3	1.8	1.5
Fgfr2	674	1087	753	1046	871	1299	799	1217	1.6	1.4	1.5	1.5	1.5
Nedd4l	374	617	373	621	408	533	368	512	1.6	1.7	1.3	1.4	1.5
Grb14	939	1514	960	1484	1176	1698	1162	1615	1.6	1.5	1.4	1.4	1.5
Blnk	1062	1698	1034	1568	1202	1613	1145	1752	1.6	1.5	1.3	1.5	1.5
Khdrbs2	123	181	138	181	135	223	144	223	1.5	1.3	1.7	1.5	1.5
Gnal	160	258	180	247	143	222	125	180	1.6	1.4	1.6	1.4	1.5
Aff1	731	1217	780	1289	1048	1320	923	1271	1.7	1.7	1.3	1.4	1.5
Avpr1a	400	668	462	683	642	825	602	909	1.7	1.5	1.3	1.5	1.5
Cry1	145	216	145	224	136	214	143	188	1.5	1.5	1.6	1.3	1.5
Ptch1	465	763	532	749	536	800	535	726	1.6	1.4	1.5	1.4	1.5
LOC102634401	194	310	213	319	183	259	179	247	1.6	1.5	1.4	1.4	1.5
Fmn2	187	335	192	282	266	351	236	307	1.8	1.5	1.3	1.3	1.5
Lrrc4	335	461	317	475	293	443	289	434	1.4	1.5	1.5	1.5	1.5
Cxadr	2959	4552	2733	3918	2590	3667	2674	3989	1.5	1.4	1.4	1.5	1.5
Actg1	48018	94006	65424	88350	58935	75072	54610	69935	2.0	1.4	1.3	1.3	1.5
Bcl11a	844	1128	833	1430	693	880	598	919	1.3	1.7	1.3	1.5	1.5
Ust	94	147	86	147	91	114	95	125	1.6	1.7	1.3	1.3	1.5
Rad54l2	826	1456	971	1404	1173	1523	1047	1348	1.8	1.4	1.3	1.3	1.4
Ptch2	92	141	102	150	135	195	122	165	1.5	1.5	1.4	1.4	1.4
Tmtc1	88	125	80	130	123	171	118	158	1.4	1.6	1.4	1.3	1.4
Plce1	101	150	103	160	100	129	91	130	1.5	1.5	1.3	1.4	1.4
Aim1	2911	5134	3737	5345	4379	5591	4143	5228	1.8	1.4	1.3	1.3	1.4
6330403L08Rik	520	899	615	898	740	930	651	819	1.7	1.5	1.3	1.3	1.4
Lrrc8d	1635	2320	1600	2553	1965	2592	1917	2632	1.4	1.6	1.3	1.4	1.4
Wisp1	2654	3913	2660	4170	3094	4266	2962	3795	1.5	1.6	1.4	1.3	1.4
Dpp6	285	405	285	455	480	606	431	611	1.4	1.6	1.3	1.4	1.4
D430019H16Rik	6303	11172	7413	10128	8040	10080	7640	9950	1.8	1.4	1.3	1.3	1.4
Plcb1	702	1067	773	1064	754	955	674	1029	1.5	1.4	1.3	1.5	1.4
Ylpm1	198	339	218	310	249	319	234	299	1.7	1.4	1.3	1.3	1.4
Camta1	416	587	429	602	380	607	471	593	1.4	1.4	1.6	1.3	1.4
Nav2	183	281	198	300	277	366	246	313	1.5	1.5	1.3	1.3	1.4
Nudt11	1573	2562	1438	1968	1465	2009	1568	1987	1.6	1.4	1.4	1.3	1.4
Traf3	4607	6932	4946	7104	4576	5815	4133	5777	1.5	1.4	1.3	1.4	1.4
Tanc1	383	542	428	555	537	713	445	689	1.4	1.3	1.3	1.5	1.4
Thsd7b	121	176	134	168	139	220	166	211	1.5	1.3	1.6	1.3	1.4
Trp53bp2	840	1256	839	1266	855	1091	832	1073	1.5	1.5	1.3	1.3	1.4
Ccdc85c	1736	2566	1781	2642	2504	3211	2255	2898	1.5	1.5	1.3	1.3	1.4
Tcp11	441	565	429	642	368	500	363	494	1.3	1.5	1.4	1.4	1.4
Rnf43	2202	3113	2622	3449	3451	4359	2949	4423	1.4	1.3	1.3	1.5	1.4
Pcdh7	126	181	132	172	108	137	108	156	1.4	1.3	1.3	1.4	1.4
Kdf1	1105	1553	1220	1801	1595	2092	1502	1881	1.4	1.5	1.3	1.3	1.4
A430105I19Rik	281	395	274	386	350	440	286	392	1.4	1.4	1.3	1.4	1.4

Dusp8	158	197	136	187	225	350	223	280	1.3	1.4	1.6	1.3	1.4
Penk	31439	39353	31498	42367	30259	39984	29054	43762	1.3	1.3	1.3	1.5	1.4
Pde4dip	182	252	171	235	232	295	197	273	1.4	1.4	1.3	1.4	1.4
Ap1s3	4724	5965	4875	6336	4287	6295	4152	5740	1.3	1.3	1.5	1.4	1.4
Casz1	90	116	85	115	89	129	95	125	1.3	1.4	1.4	1.3	1.4
2310079F09Rik	458	581	552	806	705	891	560	787	1.3	1.5	1.3	1.4	1.3
Map7	222	298	216	304	293	378	282	378	1.3	1.4	1.3	1.3	1.3
Trpv4	239	319	235	328	354	466	303	393	1.3	1.4	1.3	1.3	1.3
Nphp3	215	270	224	291	188	271	173	229	1.3	1.3	1.4	1.3	1.3
BB187676	143	201	127	165	101	127	103	136	1.4	1.3	1.3	1.3	1.3
Prdm6	331	415	325	419	325	452	277	367	1.3	1.3	1.4	1.3	1.3
Pcgf5	213	279	202	263	256	328	236	311	1.3	1.3	1.3	1.3	1.3
Hoxd11	3224	4114	3770	4784	3103	3892	3205	4388	1.3	1.3	1.3	1.4	1.3

Table S11. List of genes with increased expression in the microarray of E14.5 ureters of *Fgfr1/2cDKO-UM* and control embryos. Shown are the gene names, the intensity of the four control and mutant ureter samples, the individual and the average fold change (FC, avgFC).

Annotation Cluster1	**Enrichment Score: 5.021541264321461**											
Category	Term	Count	%	PValue	Genes	List Total	Pop Hits	Pop Total	Fold Enrichment	Bonferroni	Benjamini	FDR
UP_KEYWORDS	Secreted	28	19.58041958	3.45E-06	ASPN, CTHRC1, CCK, POSTN, PF4, SFN, CCL24, LAMB3, CASP4, APELA, FAP, MSLN, BC028528, PTN, PRAP1, ITIH2, FIBIN, HAPLN1, IGF1, COLEC11, S100A13, LGALS9, CCL11, C1QB, LAMA4, COL14A1, TREM2, PON3	140	1685	22680	2.691988131	6.00E-04	6.00E-04	0.004224877
GOTERM_CC_DIRECT	GO:0005576~extracellular region	30	20.97902098	3.53E-06	LYPD2, ASPN, CTHRC1, CCK, POSTN, PF4, SFN, CCL24, LAMB3, CASP4, APELA, FAP, MSLN, BC028528, PTN, PRAP1, ITIH2, FIBIN, HAPLN1, IGF1, COLEC11, S100A13, LGALS9, CCL11, C1QB, LAMA4, COL14A1, PON2, TREM2, PON3	132	1753	19662	2.549136545	5.36E-04	5.36E-04	0.004224799
UP_SEQ_FEATURE	signal peptide	40	27.97202797	7.08E-05	LYPD2, ASPN, FGFR1, CTHRC1, EMCN, FXYD3, CCK, POSTN, PF4, CCL24, VCAM1, LAMB3, PROCR, PLOD2, UGT1A6B, MSLN, NRROS, FCER1G, BC028528, PTN, PRAP1, IL2RG, ITIH2, FIBIN, TYROBP, H2-Q2, PTPRD, IGF1, COLEC11, H2-Q8, CCL11, C1QB, VSIG2, LAMA4, COL14A1, PECAM1, PON2, TREM2, PON3, ADGRL4	124	3124	18012	1.859898393	0.029836734	0.029836734	0.099636687
Annotation Cluster 2	**Enrichment Score: 3.8186171268655165**											
Category	Term	Count	%	PValue	Genes	List Total	Pop Hits	Pop Total	Fold Enrichment	Bonferroni	Benjamini	FDR
UP_KEYWORDS	Disulfide bond	39	27.27272727	1.87E-05	ASPN, FGFR1, ADORA2B, POSTN, PF4, CCL24, VCAM1, LAMB3, PROCR, FAP, MSLN, FCER1G, PTN, IL2RG, H2-T10, FIBIN, RAB27B, ENTPD2, TMPRSS13, TYROBP, H2-Q2, HAPLN1, PTPRD, GM11127, IGF1, COLEC11, H2-Q8, CLEC1A, CCL11, C1QB, VSIG2, LAMA4, COL14A1, PECAM1, PON2, TREM2, PON3, ADGRL4, CLEC1B	140	3124	22680	2.02240717	0.003240055	0.001621342	0.022840904
UP_SEQ_FEATURE	signal peptide	40	27.97202797	7.08E-05	LYPD2, ASPN, FGFR1, CTHRC1, EMCN, FXYD3, CCK, POSTN, PF4, CCL24, VCAM1, LAMB3, PROCR, PLOD2, UGT1A6B, MSLN, NRROS, FCER1G, BC028528, PTN, PRAP1, IL2RG, ITIH2, FIBIN, TYROBP, H2-Q2, PTPRD, IGF1, COLEC11, H2-Q8, CCL11, C1QB, VSIG2, LAMA4, COL14A1, PECAM1, PON2, TREM2, PON3, ADGRL4	124	3124	18012	1.859898393	0.029836734	0.029836734	0.099636687
UP_KEYWORDS	Signal	48	33.56643357	9.47E-05	LYPD2, ASPN, FGFR1, CTHRC1, LY6G6E, FXYD3, EMCN, CCK, POSTN, PF4, CCL24, VCAM1, LAMB3, PROCR, PLOD2, UGT1A6B, APELA, MSLN, NRROS, FCER1G, BC028528, PTN, PRAP1, IL2RG, ITIH2, H2-T10, FIBIN, ENTPD2, TYROBP, H2-Q2, PTPRD, TMEM204, GM11127, IGF1, COLEC11, H2-Q8, CCL11, C1QB, VSIG2, BC025446, LAMA4, COL14A1, IFI27L2A, PECAM1, PON2, TREM2, ADGRL4, PON3	140	4543	22680	1.711644288	0.016338578	0.005476126	0.115888624
UP_KEYWORDS	Glycoprotein	42	29.37062937	1.42E-04	LYPD2, ASPN, FGFR1, CTHRC1, EMCN, SNAP91, ADORA2B, SERPINA3F, POSTN, PF4, CCL24, VCAM1, LAMB3, PROCR, PLOD2, FAP, UPK1B, MSLN, NRROS, BC028528, IL2RG, ITIH2, FIBIN, ENTPD2, TMPRSS13, HAPLN1, PTPRD, TMEM204, MGAT4C, H2-Q8, CLEC1A, CCL11, C1QB, VSIG2, LAMA4, COL14A1, PECAM1, PON2, TREM2, PON3, ADGRL4, CLEC1B	140	3815	22680	1.783486239	0.024354503	0.006145036	0.173400958
UP_SEQ_FEATURE	disulfide bond	32	22.37762238	6.13E-04	ASPN, FGFR1, ADORA2B, POSTN, PF4, CCL24, VCAM1, LAMB3, PROCR, FAP, FCER1G, PTN, IL2RG, RAB27B, TMPRSS13, H2-Q2, HAPLN1, PTPRD, IGF1, COLEC11, H2-Q8, CCL11, CLEC1A, C1QB, VSIG2, LAMA4, PECAM1, PON2, TREM2, PON3, ADGRL4, CLEC1B	124	2510	18012	1.851895643	0.230810545	0.122965534	0.859890382
UP_SEQ_FEATURE	glycosylation site:N-linked (GlcNAc...)	40	27.97202797	0.001129185	LYPD2, ASPN, FGFR1, CTHRC1, EMCN, ADORA2B, SERPINA3F, POSTN, GM9992, CCL24, VCAM1, LAMB3, PROCR, PLOD2, UGT1A6B, FAP, MSLN, NRROS, BC028528, IL2RG, ITIH2, FIBIN, ENTPD2, TMPRSS13, H2-Q2, HAPLN1, PTPRD, TMEM204, MGAT4C, H2-Q8, CLEC1A, VSIG2, LAMA4, COL14A1, PECAM1, PON2, TREM2, PON3, ADGRL4, CLEC1B	124	3563	18012	1.630738866	0.38341807	0.148867977	1.578797411

Annotation Cluster 3	**Enrichment Score: 1.7469255219510995**											
Category	Term	Count	%	PValue	Genes	List Total	Pop Hits	Pop Total	Fold Enrichment	Bonferroni	Benjamini	FDR
UP_KEYWORDS	Immunity	9	6.293706294	0.003361713	H2-Q2, C1QB, CASP4, IFITM1, SERPINA3G, IFITM3, NRROS, H2-Q8, LGALS9	140	401	22680	3.635910224	0.443408339	0.070622644	4.040377525
GOTERM_BP_DIRECT	GO:0045087~innate immune response	8	5.594405594	0.014015826	C1QB, CASP4, IFITM1, IFITM3, NRROS, FCER1G, TREM2, TYROBP	116	400	18082	3.117586207	0.999983459	0.66745101	19.42200919
GOTERM_BP_DIRECT	GO:0002376~immune system process	7	4.895104895	0.035663777	C1QB, CASP4, IFITM1, SERPINA3G, IFITM3, NRROS, LGALS9	116	383	18082	2.848969119	1	0.84868535	42.62642204
UP_KEYWORDS	Innate immunity	5	3.496503497	0.061219711	C1QB, CASP4, IFITM1, IFITM3, NRROS	140	241	22680	3.360995851	0.999983168	0.476177579	53.87131726
Annotation Cluster 4	**Enrichment Score: 1.6850967321815948**											
Category	Term	Count	%	PValue	Genes	List Total	Pop Hits	Pop Total	Fold Enrichment	Bonferroni	Benjamini	FDR
GOTERM_BP_DIRECT	GO:0071356~cellular response to tumor necrosis factor	6	4.195804196	6.86E-04	CCL24, CEBPA, CCL11, VCAM1, HAS2, POSTN	116	110	18082	8.502507837	0.414553984	0.234855559	1.044606269
GOTERM_BP_DIRECT	GO:0071347~cellular response to interleukin-1	3	2.097902098	0.092062059	CCL24, CCL11, HAS2	116	80	18082	5.845474138	1	0.944832292	77.18069765
GOTERM_BP_DIRECT	GO:0030335~positive regulation of cell migration	4	2.797202797	0.13938292	CCL24, CCL11, IGF1, HAS2	116	203	18082	3.071513504	1	0.968050519	89.93857948
Annotation Cluster 5	**Enrichment Score: 1.6034429593994273**											
Category	Term	Count	%	PValue	Genes	List Total	Pop Hits	Pop Total	Fold Enrichment	Bonferroni	Benjamini	FDR
UP_KEYWORDS	Extracellular matrix	7	4.895104895	0.003320676	ASPN, HAPLN1, CTHRC1, LAMA4, LAMB3, COL14A1, POSTN	140	235	22680	4.825531915	0.439406412	0.079354172	3.991973673
GOTERM_CC_DIRECT	GO:0005578~proteinaceous extracellular matrix	8	5.594405594	0.005307227	ASPN, HAPLN1, CTHRC1, LAMA4, LAMB3, COL14A1, PTN, POSTN	132	316	19662	3.771001151	0.554628647	0.183078042	6.170554439
GOTERM_CC_DIRECT	GO:0031012~extracellular matrix	5	3.496503497	0.133501786	ASPN, HAPLN1, COL14A1, LMCD1, POSTN	132	294	19662	2.533240569	1	0.861941746	82.00548369
GOTERM_BP_DIRECT	GO:0030198~extracellular matrix organization	3	2.097902098	0.163925643	LAMA4, LAMB3, POSTN	116	114	18082	4.102087114	1	0.97704705	93.53710915
Annotation Cluster 6	**Enrichment Score: 1.5839224688073503**											
Category	Term	Count	%	PValue	Genes	List Total	Pop Hits	Pop Total	Fold Enrichment	Bonferroni	Benjamini	FDR
UP_KEYWORDS	Collagen	4	2.797202797	0.01543902	C1QB, CTHRC1, COL14A1, COLEC11	140	85	22680	7.623529412	0.933286177	0.218173243	17.35102183
GOTERM_CC_DIRECT	GO:0005581~collagen trimer	4	2.797202797	0.018035957	C1QB, CTHRC1, COL14A1, COLEC11	132	83	19662	7.178532311	0.937117615	0.326463267	19.57484159
UP_SEQ_FEATURE	domain:Collagen-like	3	2.097902098	0.021273597	C1QB, CTHRC1, COLEC11	124	33	18012	13.20527859	0.999899298	0.841288777	26.13115222
INTERPRO	IPR008160:Collagen triple helix repeat	3	2.097902098	0.077931003	C1QB, COL14A1, COLEC11	126	76	20594	6.451754386	1	0.738446788	65.81519367
Annotation Cluster 7	**Enrichment Score: 1.459463997603681**											
Category	Term	Count	%	PValue	Genes	List Total	Pop Hits	Pop Total	Fold Enrichment	Bonferroni	Benjamini	FDR
INTERPRO	IPR011161:MHC class I-like antigen recognition	5	3.496503497	4.26E-04	H2-Q2, PROCR, GM11127, H2-T10, H2-Q8	126	58	20594	14.09003831	0.112829076	0.112829076	0.562051424
INTERPRO	IPR011162:MHC classes I/II-like antigen recognition protein	5	3.496503497	8.24E-04	H2-Q2, PROCR, GM11127, H2-T10, H2-Q8	126	69	20594	11.84380032	0.206878192	0.109426136	1.085293024
INTERPRO	IPR001039:MHC class I, alpha chain, alpha1/alpha2	4	2.797202797	0.002571964	H2-Q2, GM11127, H2-T10, H2-Q8	126	45	20594	14.52839506	0.515022554	0.214329378	3.349611569
INTERPRO	IPR003006:Immunoglobulin/major histocompatibility complex, conserved site	4	2.797202797	0.015025441	H2-Q2, GM11127, H2-T10, H2-Q8	126	85	20594	7.691503268	0.985795409	0.507879499	18.15062511
KEGG_PATHWAY	mmu04514:Cell adhesion molecules (CAMs)	5	3.496503497	0.015575516	H2-Q2, VCAM1, PECAM1, H2-T10, H2-Q8	47	162	7691	5.050564749	0.843135742	0.370666283	16.44415177
GOTERM_BP_DIRECT	GO:0002474~antigen processing and presentation of peptide antigen via MHC class I	3	2.097902098	0.021944085	H2-Q2, H2-T10, H2-Q8	116	36	18082	12.98994253	0.99999997	0.792653079	28.78454495
INTERPRO	IPR003597:Immunoglobulin C1-set	4	2.797202797	0.023649526	H2-Q2, GM11127, H2-T10, H2-Q8	126	101	20594	6.473047305	0.998799911	0.489587457	27.14022607
SMART	SM00407:IGc1	4	2.797202797	0.024059941	H2-Q2, GM11127, H2-T10, H2-Q8	67	98	10425	6.350898568	0.799586234	0.552324039	22.04247198
GOTERM_MF_DIRECT	GO:0042605~peptide antigen binding	3	2.097902098	0.034913401	H2-Q2, H2-T10, H2-Q8	115	45	17446	10.11362319	0.999861461	0.948256347	36.9766829
KEGG_PATHWAY	mmu05332:Graft-versus-host disease	3	2.097902098	0.03840613	H2-Q2, H2-T10, H2-Q8	47	52	7691	9.440671031	0.990159459	0.483240554	36.12214221
KEGG_PATHWAY	mmu05330:Allograft rejection	3	2.097902098	0.043941342	H2-Q2, H2-T10, H2-Q8	47	56	7691	8.766337386	0.995020616	0.484596991	40.2060023
KEGG_PATHWAY	mmu04940:Type I diabetes mellitus	3	2.097902098	0.052760391	H2-Q2, H2-T10, H2-Q8	47	62	7691	7.917982155	0.998331746	0.508682225	46.22288401
GOTERM_MF_DIRECT	GO:0005102~receptor binding	7	4.895104895	0.053311261	H2-Q2, LAMA4, PTPRD, H2-T10, H2-Q8, LGALS9, TYROBP	115	412	17446	2.577501055	0.999998873	0.897992101	50.91951108
KEGG_PATHWAY	mmu05320:Autoimmune thyroid disease	3	2.097902098	0.067047915	H2-Q2, H2-T10, H2-Q8	47	71	7691	6.914294276	0.999722411	0.494621408	54.80829343
KEGG_PATHWAY	mmu05416:Viral myocarditis	3	2.097902098	0.080697094	H2-Q2, H2-T10, H2-Q8	47	79	7691	6.214112577	0.999951234	0.507950861	61.82257784
KEGG_PATHWAY	mmu05166:HTLV-I infection	5	3.496503497	0.081794764	H2-Q2, VCAM1, H2-T10, IL2RG, H2-Q8	47	276	7691	2.964461918	0.999957646	0.488954597	62.34102626
KEGG_PATHWAY	mmu04145:Phagosome	4	2.797202797	0.081888523	H2-Q2, H2-T10, COLEC11, H2-Q8	47	171	7691	3.827796441	0.999958154	0.467458209	62.38501143
KEGG_PATHWAY	mmu04612:Antigen processing and presentation	3	2.097902098	0.086022472	H2-Q2, H2-T10, H2-Q8	47	82	7691	5.986766995	0.999975431	0.464392641	64.27838334

KEGG_PATHWAY	mmu05169:Epstein-Barr virus infection	3	2.097902098	0.195200338	H2-Q2, H2-T10, H2-Q8	47	136	7691	3.609668335	1	0.722311475	91.66981016
KEGG_PATHWAY	mmu04144:Endocytosis	4	2.797202797	0.204270491	H2-Q2, H2-T10, IL2RG, H2-Q8	47	261	7691	2.507866634	1	0.72305316	92.68318688
KEGG_PATHWAY	mmu05168:Herpes simplex infection	3	2.097902098	0.354658051	H2-Q2, H2-T10, H2-Q8	47	208	7691	2.360167758	1	0.873465687	99.33447751
KEGG_PATHWAY	mmu05203:Viral carcinogenesis	3	2.097902098	0.404188095	H2-Q2, H2-T10, H2-Q8	47	231	7691	2.1251727	1	0.895973543	99.7331524
Annotation Cluster 8	**Enrichment Score: 1.3749292868524985**											
Category	Term	Count	%	PValue	Genes	List Total	Pop Hits	Pop Total	Fold Enrichment	Bonferroni	Benjamini	FDR
KEGG_PATHWAY	mmu00980:Metabolism of xenobiotics by cytochrome P450	4	2.797202797	0.006466353	CBR2, UGT1A6B, ALDH3B2, ALDH3B1	47	64	7691	10.22739362	0.534902113	0.534902113	7.155462003
KEGG_PATHWAY	mmu00982:Drug metabolism - cytochrome P450	4	2.797202797	0.007043292	FMO1, UGT1A6B, ALDH3B2, ALDH3B1	47	66	7691	9.917472598	0.565712771	0.340995274	7.770609531
KEGG_PATHWAY	mmu05204:Chemical carcinogenesis	4	2.797202797	0.017355304	UGT1A6B, SULT1A1, ALDH3B2, ALDH3B1	47	92	7691	7.114708603	0.87329647	0.338457511	18.15676254
GOTERM_BP_DIRECT	GO:0008152~metabolic process	5	3.496503497	0.340133496	ASPA, UGT1A6B, ALDH3B2, UAP1L1, ALDH3B1	116	463	18082	1.683361883	1	0.998267233	99.82707278
KEGG_PATHWAY	mmu01100:Metabolic pathways	9	6.293706294	0.496405774	ASPA, CBR2, NDUFA4L2, UGT1A6B, MGAT4C, ALDH3B2, UAP1L1, ALDH3B1, CMBL	47	1269	7691	1.160555304	1	0.944475696	99.96105086
Annotation Cluster 9	**Enrichment Score: 1.2137865060813848**											
Category	Term	Count	%	PValue	Genes	List Total	Pop Hits	Pop Total	Fold Enrichment	Bonferroni	Benjamini	FDR
KEGG_PATHWAY	mmu05200:Pathways in cancer	7	4.895104895	0.02907692	CEBPA, FGFR1, LAMA4, LAMB3, IGF1, DAPK2, CTNNA2	47	395	7691	2.899919203	0.969252535	0.440283358	28.65915868
GOTERM_BP_DIRECT	GO:0030324~lung development	4	2.797202797	0.044666088	CEBPA, FGFR1, PTN, IGF1	116	124	18082	5.02836485	1	0.861943	50.29559919
GOTERM_BP_DIRECT	GO:0042127~regulation of cell proliferation	4	2.797202797	0.175838577	CEBPA, FGFR1, IGF1, PF4	116	227	18082	2.746771988	1	0.979095218	94.81111425
Annotation Cluster 10	**Enrichment Score: 1.1874846600287634**											
Category	Term	Count	%	PValue	Genes	List Total	Pop Hits	Pop Total	Fold Enrichment	Bonferroni	Benjamini	FDR
KEGG_PATHWAY	mmu00980:Metabolism of xenobiotics by cytochrome P450	4	2.797202797	0.006466353	CBR2, UGT1A6B, ALDH3B2, ALDH3B1	47	64	7691	10.22739362	0.534902113	0.534902113	7.155462003
KEGG_PATHWAY	mmu00982:Drug metabolism - cytochrome P450	4	2.797202797	0.007043292	FMO1, UGT1A6B, ALDH3B2, ALDH3B1	47	66	7691	9.917472598	0.565712771	0.340995274	7.770609531
INTERPRO	IPR020904:Short-chain dehydrogenase/reductase, conserved site	3	2.097902098	0.021192361	CBR2, HSD17B14, HPGD	126	37	20594	13.25225225	0.997568046	0.487669051	24.67669069
INTERPRO	IPR002347:Glucose/ribitol dehydrogenase	3	2.097902098	0.051486534	CBR2, HSD17B14, HPGD	126	60	20594	8.172222222	0.999999646	0.681003114	50.30713472
UP_KEYWORDS	NAD	4	2.797202797	0.102719129	CBR2, ALDH3B2, HPGD, ALDH3B1	140	183	22680	3.540983607	0.999999994	0.559553481	73.48569373
INTERPRO	IPR016040:NAD(P)-binding domain	4	2.797202797	0.120849555	CBR2, HSD17B14, FMO1, HPGD	126	199	20594	3.285315466	1	0.851158454	81.80395912
GOTERM_BP_DIRECT	GO:0055114~oxidation-reduction process	7	4.895104895	0.260561709	CBR2, PLOD2, HSD17B14, FMO1, ALDH3B2, HPGD, ALDH3B1	116	676	18082	1.61413487	1	0.993326864	99.01296135
UP_KEYWORDS	Oxidoreductase	6	4.195804196	0.354492208	CBR2, PLOD2, FMO1, ALDH3B2, HPGD, ALDH3B1	140	639	22680	1.521126761	1	0.921036091	99.53040182
GOTERM_MF_DIRECT	GO:0016491~oxidoreductase activity	6	4.195804196	0.360509119	CBR2, PLOD2, FMO1, ALDH3B2, HPGD, ALDH3B1	115	604	17446	1.506996833	1	0.992246391	99.69966754
Annotation Cluster 11	**Enrichment Score: 1.14726099345195**											
Category	Term	Count	%	PValue	Genes	List Total	Pop Hits	Pop Total	Fold Enrichment	Bonferroni	Benjamini	FDR
GOTERM_MF_DIRECT	GO:0050839~cell adhesion molecule binding	4	2.797202797	0.011253834	VCAM1, FGFR1, PTPRD, POSTN	115	71	17446	8.546723821	0.94095228	0.94095228	13.672929
INTERPRO	IPR013783:Immunoglobulin-like fold	14	9.79020979	0.016114991	H2-Q2, FGFR1, HAPLN1, PTPRD, GM11127, H2-Q8, VCAM1, VSIG2, COL14A1, EBF2, PECAM1, H2-T10, IL2RG, TREM2	126	1099	20594	2.082094834	0.989592162	0.479086289	19.34035928
UP_SEQ_FEATURE	domain:Ig-like C2-type 3	4	2.797202797	0.022397456	VCAM1, FGFR1, PTPRD, PECAM1	124	88	18012	6.602639296	0.999938415	0.801278108	27.31697262
INTERPRO	IPR007110:Immunoglobulin-like domain	11	7.692307692	0.053470587	H2-Q2, VCAM1, FGFR1, HAPLN1, VSIG2, PTPRD, PECAM1, GM11127, H2-T10, TREM2, H2-Q8	126	920	20594	1.954227053	0.999999803	0.668122683	51.66483732
INTERPRO	IPR003598:Immunoglobulin subtype 2	5	3.496503497	0.060128631	VCAM1, FGFR1, VSIG2, PTPRD, PECAM1	126	242	20594	3.376951331	0.999999973	0.663477486	55.97440926
UP_SEQ_FEATURE	domain:Ig-like C2-type 1	4	2.797202797	0.061796575	VCAM1, FGFR1, PTPRD, PECAM1	124	132	18012	4.401759531	1	0.967047357	59.28128007
UP_SEQ_FEATURE	domain:Ig-like C2-type 2	4	2.797202797	0.062919704	VCAM1, FGFR1, PTPRD, PECAM1	124	133	18012	4.368663594	1	0.954518965	59.96251292
SMART	SM00408:IGc2	5	3.496503497	0.066887283	VCAM1, FGFR1, VSIG2, PTPRD, PECAM1	67	242	10425	3.214814358	0.989633047	0.6809103	50.72864975
UP_KEYWORDS	Immunoglobulin domain	7	4.895104895	0.076002727	VCAM1, FGFR1, HAPLN1, VSIG2, PTPRD, PECAM1, TREM2	140	481	22680	2.357588358	0.999998937	0.534253071	62.0209435
INTERPRO	IPR003599:Immunoglobulin subtype	7	4.895104895	0.09589287	VCAM1, FGFR1, HAPLN1, VSIG2, PTPRD, PECAM1, TREM2	126	518	20594	2.208708709	1	0.792726443	73.64849349
SMART	SM00409:IG	7	4.895104895	0.108725933	VCAM1, FGFR1, HAPLN1, VSIG2, PTPRD, PECAM1, TREM2	67	518	10425	2.102662364	0.999497954	0.781148883	69.17553761
UP_SEQ_FEATURE	domain:Ig-like V-type	3	2.097902098	0.168334709	HAPLN1, VSIG2, TREM2	124	108	18012	4.034946237	1	0.994801644	92.54498113
INTERPRO	IPR013098:Immunoglobulin I-set	3	2.097902098	0.224410333	VCAM1, FGFR1, PTPRD	126	147	20594	3.335600907	1	0.966644209	96.53364913
INTERPRO	IPR013106:Immunoglobulin V-set	3	2.097902098	0.853415988	HAPLN1, VSIG2, TREM2	126	554	20594	0.885078219	1	0.999999996	100

Annotation Cluster 12	**Enrichment Score: 1.0775854852255906**											
Category	Term	Count	%	PValue	Genes	List Total	Pop Hits	Pop Total	Fold Enrichment	Bonferroni	Benjamini	FDR
KEGG_PATHWAY	mmu05200:Pathways in cancer	7	4.895104895	0.02907692	CEBPA, FGFR1, LAMA4, LAMB3, IGF1, DAPK2, CTNNA2	47	395	7691	2.899919203	0.969252535	0.440283358	28.65915868
KEGG_PATHWAY	mmu04151:PI3K-Akt signaling pathway	6	4.195804196	0.057091339	FGFR1, LAMA4, LAMB3, IGF1, IL2RG, PPP2R2B	47	351	7691	2.797235861	0.999028561	0.500262919	48.97058234
KEGG_PATHWAY	mmu04510:Focal adhesion	3	2.097902098	0.352472233	LAMA4, LAMB3, IGF1	47	207	7691	2.371569534	1	0.881962379	99.30821872
Annotation Cluster 13	**Enrichment Score: 1.0356844379019052**											
Category	Term	Count	%	PValue	Genes	List Total	Pop Hits	Pop Total	Fold Enrichment	Bonferroni	Benjamini	FDR
INTERPRO	IPR001806:Small GTPase superfamily	5	3.496503497	0.009060767	RND2, RAB3B, GM266, GEM, RAB27B	126	134	20594	6.0986733	0.922515739	0.472401717	11.34492877
UP_KEYWORDS	Prenylation	5	3.496503497	0.015957703	RND2, RAB3B, ALDH3B2, RAB27B, ALDH3B1	140	157	22680	5.159235669	0.939131124	0.208046638	17.88272068
UP_KEYWORDS	GTP-binding	7	4.895104895	0.016692401	RND2, RAB3B, GIMAP4, GM266, GIMAP6, GEM, RAB27B	140	332	22680	3.415662651	0.94654913	0.201728972	18.63048075
INTERPRO	IPR005225:Small GTP-binding protein domain	5	3.496503497	0.018220314	RND2, RAB3B, GM266, GEM, RAB27B	126	165	20594	4.952861953	0.994299069	0.475804577	21.59410085
GOTERM_MF_DIRECT	GO:0005525~GTP binding	7	4.895104895	0.039814483	RND2, RAB3B, GIMAP4, GM266, GIMAP6, GEM, RAB27B	115	383	17446	2.772664321	0.999961204	0.868853247	41.01025678
GOTERM_MF_DIRECT	GO:0019003~GDP binding	3	2.097902098	0.058627016	RAB3B, GEM, RAB27B	115	60	17446	7.585217391	0.999999724	0.884410349	54.38163194
GOTERM_BP_DIRECT	GO:0007264~small GTPase mediated signal transduction	5	3.496503497	0.063919982	RND2, RAB3B, GM266, GEM, RAB27B	116	236	18082	3.302527762	1	0.90385769	63.5986115
UP_SEQ_FEATURE	nucleotide phosphate-binding region:GTP	6	4.195804196	0.067785181	RND2, RAB3B, GIMAP4, GIMAP6, GEM, RAB27B	124	319	18012	2.732126605	1	0.950422469	62.79317363
UP_SEQ_FEATURE	short sequence motif:Effector region	3	2.097902098	0.149184989	RND2, RAB3B, RAB27B	124	100	18012	4.357741935	1	0.995102696	89.72683253
UP_SEQ_FEATURE	lipid moiety-binding region:S-geranylgeranyl cysteine	3	2.097902098	0.173187158	RND2, RAB3B, RAB27B	124	110	18012	3.961583578	1	0.993824915	93.13480639
INTERPRO	IPR027417:P-loop containing nucleoside triphosphate hydrolase	8	5.594405594	0.314676735	RND2, RAB3B, GIMAP4, GM266, GIMAP6, SULT1A1, GEM, RAB27B	126	909	20594	1.438454957	1	0.988015787	99.32553712
GOTERM_MF_DIRECT	GO:0003924~GTPase activity	3	2.097902098	0.397442128	RAB3B, GEM, RAB27B	115	209	17446	2.177574371	1	0.994891182	99.86133298
UP_KEYWORDS	Nucleotide-binding	12	8.391608392	0.513876192	RND2, TRNT1, FGFR1, RAB3B, GIMAP4, GM266, GIMAP6, ATP8A2, GEM, RAB27B, DAPK2, ENTPD2	140	1754	22680	1.108323831	1	0.969384363	99.98543323
UP_KEYWORDS	Methylation	7	4.895104895	0.539012018	RND2, KRT19, RAB3B, SNAP91, ALDH3B2, RAB27B, ALDH3B1	140	960	22680	1.18125	1	0.973792102	99.99239737
GOTERM_MF_DIRECT	GO:0000166~nucleotide binding	12	8.391608392	0.732448056	RND2, TRNT1, FGFR1, RAB3B, GIMAP4, GIMAP6, SULT1A1, ATP8A2, GEM, RAB27B, DAPK2, ENTPD2	115	1936	17446	0.940316206	1	0.999938374	99.99999636
Annotation Cluster 14	**Enrichment Score: 1.0192536164743922**											
Category	Term	Count	%	PValue	Genes	List Total	Pop Hits	Pop Total	Fold Enrichment	Bonferroni	Benjamini	FDR
UP_KEYWORDS	Cell adhesion	10	6.993006993	0.00212792	VCAM1, LAMA4, LAMB3, COL14A1, FAP, PECAM1, MSLN, POSTN, PERP, CTNNA2	140	459	22680	3.529411765	0.309716306	0.059906026	2.575254043
UP_KEYWORDS	Cell junction	5	3.496503497	0.580065566	TMEM204, FAP, PECAM1, PERP, CTNNA2	140	661	22680	1.225416036	1	0.977046999	99.99757433
GOTERM_CC_DIRECT	GO:0030054~cell junction	5	3.496503497	0.709262056	TMEM204, FAP, PECAM1, PERP, CTNNA2	132	718	19662	1.037287921	1	0.998776565	99.9999621
Annotation Cluster 15	**Enrichment Score: 1.0123430169803975**											
Category	Term	Count	%	PValue	Genes	List Total	Pop Hits	Pop Total	Fold Enrichment	Bonferroni	Benjamini	FDR
INTERPRO	IPR016186:C-type lectin-like	4	2.797202797	0.050942323	CLEC1A, HAPLN1, COLEC11, CLEC1B	126	137	20594	4.772100568	0.999999584	0.706053336	49.92861399
INTERPRO	IPR016187:C-type lectin fold	4	2.797202797	0.058436181	CLEC1A, HAPLN1, COLEC11, CLEC1B	126	145	20594	4.508812261	0.999999955	0.676317763	54.91396416
GOTERM_MF_DIRECT	GO:0030246~carbohydrate binding	5	3.496503497	0.06332882	CLEC1A, EMCN, COLEC11, LGALS9, CLEC1B	115	229	17446	3.312322005	0.999999921	0.870551005	57.25454335
UP_KEYWORDS	Lectin	4	2.797202797	0.090466582	CLEC1A, COLEC11, LGALS9, CLEC1B	140	173	22680	3.74566474	0.999999932	0.561749575	68.69437154
UP_SEQ_FEATURE	domain:C-type lectin	3	2.097902098	0.149184989	CLEC1A, COLEC11, CLEC1B	124	100	18012	4.357741935	1	0.995102696	89.72683253
INTERPRO	IPR001304:C-type lectin	3	2.097902098	0.174016922	CLEC1A, COLEC11, CLEC1B	126	124	20594	3.954301075	1	0.931853327	92.02814969
SMART	SM00034:CLECT	3	2.097902098	0.185110954	CLEC1A, COLEC11, CLEC1B	67	124	10425	3.764443909	0.999998643	0.894783638	87.66793527
Annotation Cluster 16	**Enrichment Score: 0.9765332144820323**											
Category	Term	Count	%	PValue	Genes	List Total	Pop Hits	Pop Total	Fold Enrichment	Bonferroni	Benjamini	FDR
UP_KEYWORDS	Chemotaxis	4	2.797202797	0.020139487	CCL24, CCL11, PF4, LGALS9	140	94	22680	6.893617021	0.970987801	0.223423342	22.05607405
SMART	SM00199:SCY	3	2.097902098	0.036943847	CCL24, CCL11, PF4	67	48	10425	9.724813433	0.916630674	0.563146892	31.94694638
INTERPRO	IPR001811:Chemokine interleukin-8-like domain	3	2.097902098	0.037046879	CCL24, CCL11, PF4	126	50	20594	9.806666667	0.99997528	0.618770959	39.31209384
GOTERM_MF_DIRECT	GO:0008009~chemokine activity	3	2.097902098	0.039282767	CCL24, CCL11, PF4	115	48	17446	9.481521739	0.999955445	0.918299671	40.58447729
GOTERM_BP_DIRECT	GO:0006935~chemotaxis	4	2.797202797	0.039494651	CCL24, CCL11, PF4, LGALS9	116	118	18082	5.284044418	1	0.85976234	46.01604322

GOTERM_BP_DIRECT	GO:0070098~chemokine-mediated signaling pathway	3	2.097902098	0.04786098	CCL24, CCL11, PF4	116	55	18082	8.502507837	1	0.852322553	52.77875648
UP_KEYWORDS	Inflammatory response	4	2.797202797	0.076576912	CCL24, CCL11, CASP4, NRROS	140	161	22680	4.02484472	0.999999046	0.517892913	62.30899093
GOTERM_BP_DIRECT	GO:0006955~immune response	5	3.496503497	0.095608208	CCL24, CCL11, H2-Q2, NRROS, PF4	116	272	18082	2.865428499	1	0.939155698	78.50680609
KEGG_PATHWAY	mmu04060:Cytokine-cytokine receptor interaction	4	2.797202797	0.175414443	CCL24, CCL11, IL2RG, PF4	47	242	7691	2.704765254	1	0.69815794	89.00058619
GOTERM_BP_DIRECT	GO:0006954~inflammatory response	5	3.496503497	0.176192644	CCL24, CCL11, CASP4, NRROS, PF4	116	344	18082	2.26568765	1	0.977165028	94.84511398
KEGG_PATHWAY	mmu04062:Chemokine signaling pathway	3	2.097902098	0.328287655	CCL24, CCL11, PF4	47	196	7691	2.504667825	1	0.881675623	98.94750547
UP_KEYWORDS	Cytokine	3	2.097902098	0.347257906	CCL24, CCL11, PF4	140	200	22680	2.43	1	0.922651887	99.46172157
GOTERM_MF_DIRECT	GO:0005125~cytokine activity	3	2.097902098	0.408893241	CCL24, CCL11, PF4	115	214	17446	2.126696465	1	0.993625002	99.8919259
GOTERM_BP_DIRECT	GO:0007186~G-protein coupled receptor signaling pathway	6	4.195804196	0.986979516	CCL24, CCL11, ADORA2B, PF4, ENTPD2, ADGRL4	116	1706	18082	0.548227352	1	1	100
Annotation Cluster 17	**Enrichment Score: 0.9204906477908756**											
Category	Term	Count	%	PValue	Genes	List Total	Pop Hits	Pop Total	Fold Enrichment	Bonferroni	Benjamini	FDR
INTERPRO	IPR013787:S100/CaBP-9k-type, calcium binding, subdomain	3	2.097902098	0.011617162	S100A16, S100A5, S100A13	126	27	20594	18.16049383	0.962504427	0.481443599	14.32340011
SMART	SM01394:SM01394	3	2.097902098	0.011633102	S100A16, S100A5, S100A13	67	26	10425	17.95350172	0.538043958	0.538043958	11.27590309
INTERPRO	IPR011992:EF-hand-like domain	4	2.797202797	0.2305881	GUCA1A, S100A16, S100A5, S100A13	126	273	20594	2.394790395	1	0.96484892	96.88165262
INTERPRO	IPR018247:EF-Hand 1, calcium-binding site	3	2.097902098	0.287264765	GUCA1A, S100A16, S100A5	126	175	20594	2.801904762	1	0.984035084	98.86683001
GOTERM_MF_DIRECT	GO:0005509~calcium ion binding	7	4.895104895	0.306820507	ASPN, GUCA1A, ANXA8, S100A16, S100A5, ADGRL4, S100A13	115	699	17446	1.519213784	1	0.9897536	99.14407985
UP_SEQ_FEATURE	domain:EF-hand 1	3	2.097902098	0.333657596	GUCA1A, S100A5, S100A13	124	174	18012	2.504449388	1	0.999935743	99.6713609
INTERPRO	IPR002048:EF-hand domain	3	2.097902098	0.393065764	GUCA1A, S100A16, S100A5	126	223	20594	2.198804185	1	0.995468296	99.86477894
Annotation Cluster 18	**Enrichment Score: 0.8862305099775343**											
Category	Term	Count	%	PValue	Genes	List Total	Pop Hits	Pop Total	Fold Enrichment	Bonferroni	Benjamini	FDR
UP_SEQ_FEATURE	topological domain:Extracellular	28	19.58041958	0.002374553	FGFR1, EMCN, FXYD3, ADORA2B, TMEM140, VCAM1, PROCR, FAP, UPK1B, FCER1G, NRROS, IL2RG, ENTPD2, TMPRSS13, TYROBP, H2-Q2, PTPRD, TMEM204, MS4A6C, H2-Q8, CLEC1A, VSIG2, PECAM1, ATP8A2, HAS2, TREM2, ADGRL4, CLEC1B	124	2256	18012	1.802848318	0.638508702	0.224602383	3.293169886
GOTERM_CC_DIRECT	GO:0016020~membrane	56	39.16083916	0.075806338	LYPD2, GM11744, TMEM140, CASP4, PLOD2, SDPR, FAP, RAB27B, TMPRSS13, TMEM204, MS4A6C, TMEM255A, GEM, ALDH3B1, CTNNA2, CLEC1A, RND2, VSIG2, GM266, HAS2, TREM2, CLEC1B, FGFR1, FXYD3, EMCN, RAB3B, SNAP91, IFITM1, ADORA2B, IFITM3, VCAM1, TMEM37, ZDHHC22, PROCR, FMO1, MSLN, UPK1B, PTN, FCER1G, NRROS, IL2RG, PPP2R2B, ENTPD2, TYROBP, H2-Q2, GUCA1A, PTPRD, MGAT4C, GAS2, IFI27L2A, PECAM1, ATP8A2, PON2, IFI203, PERP, ADGRL4	132	6998	19662	1.191976928	0.999993749	0.698284662	61.07607911
UP_SEQ_FEATURE	topological domain:Cytoplasmic	27	18.88111888	0.07849579	FGFR1, EMCN, FXYD3, ADORA2B, TMEM140, VCAM1, PROCR, FAP, UPK1B, FCER1G, NRROS, IL2RG, ENTPD2, TMPRSS13, TYROBP, PTPRD, TMEM204, MS4A6C, MGAT4C, CLEC1A, VSIG2, PECAM1, ATP8A2, HAS2, TREM2, ADGRL4, CLEC1B	124	2880	18012	1.361794355	1	0.958445013	68.3821123
UP_SEQ_FEATURE	transmembrane region	36	25.17482517	0.142374053	FGFR1, EMCN, FXYD3, ADORA2B, GM11744, GM9992, TMEM140, VCAM1, TMEM37, ZDHHC22, PROCR, UGT1A6B, FAP, UPK1B, NRROS, FCER1G, IL2RG, ENTPD2, TMPRSS13, TYROBP, H2-Q2, PTPRD, TMEM204, MS4A6C, TMEM255A, MGAT4C, H2-Q8, CLEC1A, VSIG2, PECAM1, ATP8A2, HAS2, PERP, TREM2, ADGRL4, CLEC1B	124	4312	18012	1.212729667	1	0.995822092	88.50580321

UP_KEYWORDS	Membrane	59	41.25874126	0.225831922	LYPD2, GM11744, GM9992, TMEM140, CASP4, PLOD2, UGT1A6B, KCNK6, SDPR, FAP, RAB27B, TMPRSS13, TMEM204, MS4A6C, TMEM255A, GM11127, GEM, ALDH3B1, CTNNA2, CLEC1A, RND2, VSIG2, HAS2, TREM2, CLEC1B, FGFR1, EMCN, FXYD3, RAB3B, SNAP91, IFITM1, ADORA2B, IFITM3, VCAM1, TMEM37, ZDHHC22, PROCR, FMO1, MSLN, UPK1B, FCER1G, NRROS, H2-T10, IL2RG, PPP2R2B, ENTPD2, TYROBP, H2-Q2, GUCA1A, PTPRD, MGAT4C, GAS2, H2-Q8, IFI27L2A, PECAM1, ATP8A2, PON2, PERP, ADGRL4	140	8683	22680	1.100771623	1	0.807865654	95.65004034
UP_KEYWORDS	Transmembrane	45	31.46853147	0.431429177	ASPN, FGFR1, FXYD3, EMCN, ADORA2B, IFITM1, IFITM3, GM11744, GM9992, TMEM140, VCAM1, TMEM37, ZDHHC22, PROCR, UGT1A6B, FMO1, KCNK6, FAP, UPK1B, NRROS, FCER1G, IL2RG, H2-T10, ENTPD2, TMPRSS13, TYROBP, H2-Q2, PTPRD, TMEM204, MS4A6C, TMEM255A, MGAT4C, GM11127, H2-Q8, CLEC1A, VSIG2, IFI27L2A, PECAM1, ATP8A2, PON2, HAS2, TREM2, PERP, ADGRL4, CLEC1B	140	6955	22680	1.048166786	1	0.949061528	99.90076389
UP_KEYWORDS	Transmembrane helix	43	30.06993007	0.570246922	FGFR1, FXYD3, EMCN, ADORA2B, IFITM1, IFITM3, GM11744, GM9992, TMEM140, VCAM1, TMEM37, ZDHHC22, PROCR, UGT1A6B, KCNK6, FAP, UPK1B, NRROS, FCER1G, IL2RG, H2-T10, ENTPD2, TMPRSS13, TYROBP, H2-Q2, PTPRD, TMEM204, MS4A6C, TMEM255A, MGAT4C, GM11127, H2-Q8, CLEC1A, VSIG2, IFI27L2A, PECAM1, ATP8A2, PON2, HAS2, TREM2, PERP, ADGRL4, CLEC1B	140	6938	22680	1.004035745	1	0.976901039	99.99678065
GOTERM_CC_DIRECT	GO:0016021~integral component of membrane	44	30.76923077	0.727500846	FGFR1, FXYD3, EMCN, ADORA2B, IFITM1, IFITM3, GM11744, GM9992, TMEM140, VCAM1, TMEM37, ZDHHC22, PROCR, UGT1A6B, FMO1, KCNK6, FAP, UPK1B, NRROS, FCER1G, IL2RG, H2-T10, ENTPD2, TMPRSS13, TYROBP, H2-Q2, PTPRD, TMEM204, MS4A6C, TMEM255A, MGAT4C, GM11127, H2-Q8, CLEC1A, VSIG2, IFI27L2A, PECAM1, ATP8A2, PON2, HAS2, TREM2, PERP, ADGRL4, CLEC1B	132	6878	19662	0.952893283	1	0.998902171	99.99998255
Annotation Cluster 19	**Enrichment Score: 0.7995669361042614**														
Category	Term	Count	%	PValue	Genes	List Total	Pop Hits	Pop Total	Fold Enrichment	Bonferroni	Benjamini	FDR			
UP_KEYWORDS	Serine protease inhibitor	3	2.097902098	0.093987321	SERPINA3G, SERPINA3F, ITIH2	140	84	22680	5.785714286	0.999999965	0.558605566	70.1466862			
UP_KEYWORDS	Protease inhibitor	3	2.097902098	0.169844841	SERPINA3G, SERPINA3F, ITIH2	140	121	22680	4.016528926	1	0.72625353	89.76977285			
GOTERM_BP_DIRECT	GO:0010466~negative regulation of peptidase activity	3	2.097902098	0.170679621	SERPINA3G, SERPINA3F, ITIH2	116	117	18082	3.996905393	1	0.978538057	94.29132695			
GOTERM_MF_DIRECT	GO:0030414~peptidase inhibitor activity	3	2.097902098	0.192057384	SERPINA3G, SERPINA3F, ITIH2	115	123	17446	3.700106045	1	0.964287474	93.73697456			
GOTERM_MF_DIRECT	GO:0004867~serine-type endopeptidase inhibitor activity	3	2.097902098	0.192057384	SERPINA3G, SERPINA3F, ITIH2	115	123	17446	3.700106045	1	0.964287474	93.73697456			
Annotation Cluster 20	**Enrichment Score: 0.2352033575364828**														
Category	Term	Count	%	PValue	Genes	List Total	Pop Hits	Pop Total	Fold Enrichment	Bonferroni	Benjamini	FDR			
GOTERM_MF_DIRECT	GO:0042802~identical protein binding	7	4.895104895	0.224926446	FGFR1, HSD17B14, PON2, SDCBP2, DAPK2, ENTPD2, TYROBP	115	625	17446	1.699088696	1	0.976412062	96.34860762			
UP_KEYWORDS	Kinase	3	2.097902098	0.933515355	FGFR1, DAPK2, TYROBP	140	707	22680	0.687411598	1	0.99950338	100			
GOTERM_MF_DIRECT	GO:0016301~kinase activity	3	2.097902098	0.938054218	FGFR1, DAPK2, TYROBP	115	674	17446	0.675241904	1	0.999999982	100			

Table S12. Functional annotation clustering by DAVID for genes with decreased expression in the microarray of E14.5 *Fgfr1/2cDKO-UM* ureters.

Annotation Cluster1	**Enrichment Score: 3.224734025879356**											
Category	Term	Count	%	PValue	Genes	List Total	Pop Hits	Pop Total	Fold Enrichment	Bonferroni	Benjamini	FDR
KEGG_PATHWAY	mmu04340:Hedgehog signaling pathway	5	3.012048193	3.17E-05	PTCH1, PTCH2, HHIP, LRP2, SHH	61	24	7691	26.2670765	0.004389829	0.004389829	0.03729115
KEGG_PATHWAY	mmu05217:Basal cell carcinoma	6	3.614457831	5.76E-05	WNT9B, PTCH1, PTCH2, HHIP, AXIN2, SHH	61	54	7691	14.00910747	0.007968667	0.003992303	0.067804531
GOTERM_BP_DIRECT	GO:0007389~pattern specification process	6	3.614457831	7.44E-05	SOSTDC1, HOXD12, HOXD13, PTCH1, SHH, HOXD11	137	58	18082	13.65366222	0.083156887	0.042480751	0.119782771
GOTERM_BP_DIRECT	GO:0030326~embryonic limb morphogenesis	6	3.614457831	1.11E-04	FGF9, GDF5, HOXD13, PTCH1, SHH, HOXD11	137	63	18082	12.57003823	0.121233466	0.042163969	0.178252853
GOTERM_MF_DIRECT	GO:0097108~hedgehog family protein binding	3	1.807228916	3.17E-04	PTCH1, PTCH2, HHIP	129	4	17446	101.4302326	0.095446872	0.04892002	0.426656394
GOTERM_BP_DIRECT	GO:0001658~branching involved in ureteric bud morphogenesis	4	2.409638554	0.005622423	WNT9B, PTCH1, SHH, HOXD11	137	48	18082	10.99878345	0.998611987	0.268989693	8.683261464
GOTERM_BP_DIRECT	GO:0009953~dorsal/ventral pattern formation	4	2.409638554	0.00595656	PTCH1, HHIP, SHH, HOXD11	137	49	18082	10.77431849	0.99906231	0.271606032	9.176358651
GOTERM_BP_DIRECT	GO:0007224~smoothened signaling pathway	3	1.807228916	0.099841439	PTCH1, HHIP, SHH	137	71	18082	5.576847949	1	0.805372641	81.63237777
Annotation Cluster 2	**Enrichment Score: 2.948213654465655**											
Category	Term	Count	%	PValue	Genes	List Total	Pop Hits	Pop Total	Fold Enrichment	Bonferroni	Benjamini	FDR
UP_KEYWORDS	Glycoprotein	53	31.92771084	1.39E-07	KCNC2, FGF9, NELL1, BTC, GDF5, RPRM, CXADR, MEGF10, SHH, WISP1, SOSTDC1, HHIP, DPP6, DPP4, 1810041L15RIK, LRRC4, SCUBE3, AI593442, TNFAIP6, CBLN1, ADAMTS8, WNT9B, CNTN1, CNTN3, FGFR2, ADAMTS18, GCNT3, HS3ST6, FUT9, COL2A1, G6PC2, SMOC2, SEMA5B, B4GALNT2, TNFRSF19, ADRA2C, UST, NLGN1, CELSR1, ITGA4, ECM1, ADGRG1, THSD7B, RNF43, LAMA1, AFM, GRIA1, EPHA8, AVPR1A, PTCH1, PTCH2, LRP2, HTR2B	153	3815	22680	2.059363195	2.41E-05	2.41E-05	1.70E-04
UP_KEYWORDS	Disulfide bond	45	27.10843373	7.97E-07	FGFR2, ADAMTS18, GCNT3, HS3ST6, NELL1, BTC, GDF5, SLC7A8, COL2A1, CXADR, MEGF10, SPINK8, ISM1, SEMA5B, SMOC2, WISP1, SOSTDC1, TNFRSF19, ADRA2C, HHIP, DPP6, DPP4, LRRC4, PNLIPRP1, SCUBE3, NLGN1, CELSR1, ITGA4, THSD7B, RNF43, LAMA1, TNFAIP6, CBLN1, AFM, ADAMTS8, PENK, GRIA1, WNT9B, AVPR1A, CNTN1, PAPPA2, CNTN3, HTR2B, LRP2, HABP2	153	3124	22680	2.135271522	1.38E-04	6.89E-05	9.75E-04
UP_SEQ_FEATURE	glycosylation site:N-linked (GlcNAc...)	53	31.92771084	1.30E-06	KCNC2, FGF9, NELL1, BTC, GDF5, LRRC8D, RPRM, CXADR, MEGF10, SHH, WISP1, SOSTDC1, HHIP, DPP6, DPP4, 1810041L15RIK, LRRC4, SCUBE3, AI593442, TNFAIP6, CBLN1, ADAMTS8, WNT9B, CNTN1, CNTN3, FGFR2, ADAMTS18, GCNT3, HS3ST6, FUT9, G6PC2, SMOC2, SEMA5B, B4GALNT2, TNFRSF19, ADRA2C, UST, NLGN1, CELSR1, ITGA4, ECM1, ADGRG1, THSD7B, RNF43, LAMA1, AFM, GRIA1, EPHA8, AVPR1A, PTCH1, PTCH2, LRP2, HTR2B	141	3563	18012	1.900215573	8.48E-04	8.48E-04	0.001941236
UP_SEQ_FEATURE	disulfide bond	39	23.4939759	2.84E-05	FGFR2, ADAMTS18, GCNT3, HS3ST6, NELL1, BTC, GDF5, CXADR, MEGF10, SPINK8, ISM1, SMOC2, SEMA5B, WISP1, SOSTDC1, TNFRSF19, ADRA2C, HHIP, DPP6, DPP4, LRRC4, PNLIPRP1, SCUBE3, NLGN1, CELSR1, ITGA4, THSD7B, LAMA1, TNFAIP6, CBLN1, AFM, ADAMTS8, PENK, AVPR1A, CNTN1, CNTN3, HTR2B, LRP2, HABP2	141	2510	18012	1.984877511	0.018394478	0.009239927	0.0424684
UP_KEYWORDS	Secreted	27	16.26506024	5.32E-05	ADAMTS18, PNLIPRP1, SCUBE3, FGF9, NELL1, GDF5, BTC, COL2A1, CXADR, ADGRG1, ECM1, SPINK8, SHH, ISM1, SMOC2, LAMA1, AFM, CBLN1, ADAMTS8, WISP1, PENK, SOSTDC1, WNT9B, TNFRSF19, HHIP, DPP4, HABP2	153	1685	22680	2.375283645	0.009155352	0.003061145	0.065030595
GOTERM_CC_DIRECT	GO:0005576~extracellular region	29	17.46987952	6.42E-05	FGFR2, ADAMTS18, FGF9, NELL1, BTC, GDF5, COL2A1, CXADR, SHH, SPINK8, ISM1, SMOC2, WISP1, SOSTDC1, TNFRSF19, HHIP, DPP4, PNLIPRP1, SCUBE3, ECM1, ADGRG1, LAMA1, CBLN1, AFM, ADAMTS8, PENK, WNT9B, PTCH1, HABP2	145	1753	19662	2.24324016	0.011238312	0.011238312	0.078769448

UP_SEQ_FEATURE	signal peptide	42	25.30120482	3.24E-04	FGFR2, ADAMTS18, NELL1, BTC, GDF5, COL2A1, CXADR, MEGF10, SPINK8, SHH, ISM1, SEMA5B, SMOC2, WISP1, SOSTDC1, TNFRSF19, HHIP, 1810041L15RIK, LRRC4, PNLIPRP1, SCUBE3, NLGN1, AI593442, CELSR1, ITGA4, ECM1, ADGRG1, THSD7B, RNF43, LAMA1, TNFAIP6, CBLN1, AFM, ADAMTS8, PENK, EPHA8, GRIA1, WNT9B, CNTN1, CNTN3, LRP2, HABP2	141	3124	18012	1.717438091	0.190812648	0.068142092	0.483243118
UP_KEYWORDS	Signal	49	29.51807229	4.93E-04	NELL1, GDF5, BTC, MITF, CXADR, MEGF10, SHH, SPINK8, WISP1, SOSTDC1, HHIP, 1810041L15RIK, LRRC4, KCND3, SCUBE3, AI593442, D430041D05RIK, PCDH7, TNFAIP6, CBLN1, ADAMTS8, WNT9B, CNTN1, CNTN3, FGFR2, ADAMTS18, COL2A1, ISM1, SMOC2, SEMA5B, TNFRSF19, PNLIPRP1, NLGN1, ITGA4, CELSR1, ECM1, TINAG, ADGRG1, THSD7B, LAMA1, RNF43, AFM, PENK, EPHA8, GRIA1, PAPPA2, PTCH1, LRP2, HABP2	153	4543	22680	1.598839844	0.081848219	0.012124832	0.60213999
UP_KEYWORDS	Cell membrane	41	24.69879518	0.001518588	FGFR2, KCNC2, SLC16A10, LRRC8D, BTC, GDF5, SLC7A8, KCNJ10, PRKG2, CXADR, SKAP1, MEGF10, SHH, VEPH1, AIF1L, TRPV4, TNFRSF19, ADRA2C, HHIP, CYS1, DPP6, DPP4, BLNK, LRRC4, KCNMA1, KCND3, NLGN1, TANC1, CELSR1, ADGRG1, FMN2, RNF43, CBLN1, PLCE1, GRIA1, EPHA8, AVPR1A, CNTN1, MAP7, CNTN3, HTR2B	153	3759	22680	1.616825501	0.231193107	0.028790258	1.84235233
UP_SEQ_FEATURE	topological domain:Cytoplasmic	37	22.28915663	0.002057214	FGFR2, KCNC2, GCNT3, HS3ST6, FUT9, SLC16A10, BTC, KCNJ10, CXADR, MEGF10, G6PC2, SEMA5B, B4GALNT2, TNFRSF19, TRPV4, ADRA2C, DPP6, 1810041L15RIK, DPP4, LRRC4, KCNMA1, KCND3, UST, NLGN1, AI593442, CELSR1, ITGA4, ADGRG1, THSD7B, RNF43, EPHA8, GRIA1, AVPR1A, PTCH1, PTCH2, HTR2B, LRP2	141	2880	18012	1.641164303	0.7393937	0.235817686	3.029851353
GOTERM_CC_DIRECT	GO:0016020~membrane	67	40.36144578	0.007044885	DLC1, KCNC2, SLC16A10, GDF5, BTC, LRRC8D, SLC7A8, RPRM, KCNJ10, PRKG2, CXADR, SKAP1, MEGF10, SHH, ACTG1, AP1S3, VEPH1, AIF1L, TRPV4, HHIP, PLCB1, DPP6, CYS1, 1810041L15RIK, DPP4, LRRC4, KCNMA1, KCND3, TANC1, AI593442, CYP26A1, FMN2, PLCE1, CBLN1, KLHL14, CNTN1, CNTN3, GRB14, FGFR2, GCNT3, HS3ST6, FUT9, TFCP2L1, G6PC2, SEMA5B, TCP11, PLCH1, B4GALNT2, TNFRSF19, ADRA2C, BLNK, UST, NLGN1, ITGA4, CELSR1, ADGRG1, THSD7B, RNF43, GRIA1, EPHA8, TMTC1, AVPR1A, PTCH1, MAP7, PTCH2, HTR2B, LRP2	145	6998	19662	1.298256645	0.711853943	0.116998852	8.309870912
UP_SEQ_FEATURE	topological domain:Extracellular	29	17.46987952	0.007834179	FGFR2, SLC16A10, BTC, KCNJ10, CXADR, MEGF10, SEMA5B, TNFRSF19, TRPV4, ADRA2C, DPP6, DPP4, 1810041L15RIK, KCNMA1, LRRC4, NLGN1, AI593442, ITGA4, CELSR1, ADGRG1, THSD7B, RNF43, EPHA8, GRIA1, AVPR1A, PTCH1, PTCH2, LRP2, HTR2B	141	2256	18012	1.642108043	0.994118026	0.434842846	11.08645314
GOTERM_CC_DIRECT	GO:0005886~plasma membrane	50	30.12048193	0.007942745	KCNC2, SLC16A10, GDF5, BTC, LRRC8D, SLC7A8, KCNJ10, PRKG2, CXADR, MEGF10, SKAP1, SHH, ACTG1, VEPH1, AIF1L, TRPV4, HHIP, DPP6, CYS1, PLCB1, DPP4, KCNMA1, LRRC4, KCND3, TANC1, PCDH7, FMN2, PLCE1, CBLN1, CNTN1, CNTN3, GRB14, FGFR2, TNFRSF19, ADRA2C, NEDD4L, AXIN2, BLNK, NLGN1, ITGA4, CELSR1, ADGRG1, RNF43, PENK, GRIA1, EPHA8, AVPR1A, PTCH1, MAP7, HTR2B	145	4874	19662	1.391054575	0.754265689	0.119786956	9.322099257

UP_KEYWORDS	Membrane	73	43.97590361	0.013628498	DLC1, KCNC2, SLC16A10, LRRC8D, GDF5, BTC, YLPM1, SLC7A8, RPRM, KCNJ10, PRKG2, CXADR, SKAP1, MEGF10, SHH, AP1S3, VEPH1, AIF1L, TRPV4, HHIP, PLCB1, DPP6, CYS1, 1810041L15RIK, DPP4, LRRC4, KCNMA1, KCND3, TANC1, AI593442, CYP26A1, D430019H16RIK, D430041D05RIK, PCDH7, FMN2, PLCE1, CBLN1, KLHL14, CNTN1, CNTN3, GRB14, FGFR2, HS3ST6, GCNT3, FUT9, G6PC2, SEMA5B, TCP11, PLCH1, B4GALNT2, TNFRSF19, ADRA2C, NEDD4L, BLNK, UST, NLGN1, AFF1, ITGA4, CELSR1, ADGRG1, THSD7B, RNF43, GRIA1, EPHA8, TMTC1, AVPR1A, GM13178, PTCH1, MAP7, PTCH2, HTR2B, LRP2, DUSP8	153	8683	22680	1.246248586	0.906887217	0.146374682	15.4564234
GOTERM_CC_DIRECT	GO:0005615~extracellular space	17	10.24096386	0.084150377	PNLIPRP1, FGF9, NELL1, GDF5, BTC, COL2A1, TINAG, ECM1, SHH, SPINK8, ACTG1, TNFAIP6, LAMA1, AFM, SOSTDC1, WNT9B, LRP2	145	1504	19662	1.532712766	0.999999809	0.461429995	65.99560547
UP_SEQ_FEATURE	transmembrane region	42	25.30120482	0.084553918	FGFR2, KCNC2, GCNT3, HS3ST6, FUT9, SLC16A10, LRRC8D, BTC, RPRM, SLC7A8, KCNJ10, CXADR, MEGF10, G6PC2, SEMA5B, TCP11, B4GALNT2, TNFRSF19, TRPV4, ADRA2C, DPP6, 1810041L15RIK, DPP4, LRRC4, KCNMA1, KCND3, UST, NLGN1, AI593442, CELSR1, ITGA4, ADGRG1, THSD7B, RNF43, EPHA8, GRIA1, TMTC1, AVPR1A, PTCH1, PTCH2, HTR2B, LRP2	141	4312	18012	1.244266372	1	0.8819458	73.28328587
UP_KEYWORDS	Transmembrane helix	52	31.3253012	0.238133973	DLC1, KCNC2, SLC16A10, YLPM1, BTC, LRRC8D, RPRM, SLC7A8, KCNJ10, CXADR, MEGF10, TRPV4, DPP6, DPP4, 1810041L15RIK, KCNMA1, LRRC4, KCND3, AI593442, D430041D05RIK, D430019H16RIK, PCDH7, CNTN1, FGFR2, GCNT3, HS3ST6, FUT9, G6PC2, SEMA5B, TCP11, B4GALNT2, TNFRSF19, ADRA2C, NEDD4L, UST, NLGN1, CELSR1, ITGA4, AFF1, ADGRG1, THSD7B, RNF43, GRIA1, EPHA8, TMTC1, AVPR1A, GM13178, PTCH1, PTCH2, LRP2, HTR2B, DUSP8	153	6938	22680	1.111016906	1	0.6247931	96.41339383
UP_KEYWORDS	Transmembrane	52	31.3253012	0.244465215	DLC1, KCNC2, SLC16A10, YLPM1, BTC, LRRC8D, RPRM, SLC7A8, KCNJ10, CXADR, MEGF10, TRPV4, DPP6, DPP4, 1810041L15RIK, KCNMA1, LRRC4, KCND3, AI593442, D430041D05RIK, D430019H16RIK, PCDH7, CNTN1, FGFR2, GCNT3, HS3ST6, FUT9, G6PC2, SEMA5B, TCP11, B4GALNT2, TNFRSF19, ADRA2C, NEDD4L, UST, NLGN1, CELSR1, ITGA4, AFF1, ADGRG1, THSD7B, RNF43, GRIA1, EPHA8, TMTC1, AVPR1A, GM13178, PTCH1, PTCH2, LRP2, HTR2B, DUSP8	153	6955	22680	1.108301264	1	0.61361519	96.76153515
GOTERM_CC_DIRECT	GO:0016021~integral component of membrane	51	30.72289157	0.557452083	DLC1, KCNC2, SLC16A10, YLPM1, BTC, LRRC8D, RPRM, SLC7A8, KCNJ10, CXADR, MEGF10, TRPV4, DPP6, DPP4, 1810041L15RIK, KCNMA1, LRRC4, KCND3, AI593442, D430041D05RIK, D430019H16RIK, CNTN1, FGFR2, GCNT3, HS3ST6, FUT9, G6PC2, SEMA5B, TCP11, B4GALNT2, TNFRSF19, ADRA2C, NEDD4L, UST, NLGN1, CELSR1, ITGA4, AFF1, ADGRG1, THSD7B, RNF43, GRIA1, EPHA8, TMTC1, AVPR1A, GM13178, PTCH1, PTCH2, LRP2, HTR2B, DUSP8	145	6878	19662	1.005466705	1	0.95580091	99.99547632

Annotation Cluster 3	**Enrichment Score: 2.6012388429194218**											
Category	Term	Count	%	PValue	Genes	List Total	Pop Hits	Pop Total	Fold Enrichment	Bonferroni	Benjamini	FDR
INTERPRO	IPR000884:Thrombospondin, type 1 repeat	6	3.614457831	9.57E-05	ADAMTS18, SEMA5B, ADAMTS8, WISP1, THSD7B, ISM1	144	66	20594	13.00126263	0.037092137	0.018721312	0.133135929
SMART	SM00209:TSP1	6	3.614457831	3.32E-04	ADAMTS18, SEMA5B, ADAMTS8, WISP1, THSD7B, ISM1	101	63	10425	9.830268741	0.039415506	0.039415506	0.381349773
UP_SEQ_FEATURE	domain:TSP type-1 1	4	2.409638554	0.002719919	ADAMTS18, SEMA5B, ADAMTS8, THSD7B	141	36	18012	14.19385343	0.83111321	0.256525724	3.987490491
UP_SEQ_FEATURE	domain:TSP type-1 2	4	2.409638554	0.002719919	ADAMTS18, SEMA5B, ADAMTS8, THSD7B	141	36	18012	14.19385343	0.83111321	0.256525724	3.987490491
UP_SEQ_FEATURE	domain:TSP type-1 5	3	1.807228916	0.010398426	ADAMTS18, SEMA5B, THSD7B	141	20	18012	19.16170213	0.998914509	0.462335354	14.45851462
UP_SEQ_FEATURE	domain:TSP type-1 4	3	1.807228916	0.013637639	ADAMTS18, SEMA5B, THSD7B	141	23	18012	16.66234968	0.999872406	0.472958362	18.54766387
UP_SEQ_FEATURE	domain:TSP type-1 3	3	1.807228916	0.01854177	ADAMTS18, SEMA5B, THSD7B	141	27	18012	14.19385343	0.999995076	0.492860157	24.39286645
Annotation Cluster 4	**Enrichment Score: 2.407985731621579**											
Category	Term	Count	%	PValue	Genes	List Total	Pop Hits	Pop Total	Fold Enrichment	Bonferroni	Benjamini	FDR
GOTERM_CC_DIRECT	GO:0005578~proteinaceous extracellular matrix	10	6.024096386	5.45E-04	ADAMTS18, LAMA1, SMOC2, ADAMTS8, WISP1, NAV2, WNT9B, COL2A1, ECM1, SHH	145	316	19662	4.291139241	0.091488098	0.046841093	0.666740487
UP_KEYWORDS	Extracellular matrix	7	4.21686747	0.005134046	ADAMTS18, LAMA1, SMOC2, ADAMTS8, WNT9B, COL2A1, ECM1	153	235	22680	4.415519399	0.589540409	0.077762528	6.103892931
GOTERM_CC_DIRECT	GO:0031012~extracellular matrix	7	4.21686747	0.021339359	ACTG1, FGFR2, ADAMTS18, LAMA1, ADAMTS8, COL2A1, ECM1	145	294	19662	3.228571429	0.977548077	0.223603499	23.25599161
Annotation Cluster 5	Enrichment Score: 2.1158249866392773											
Category	Term	Count	%	PValue	Genes	List Total	Pop Hits	Pop Total	Fold Enrichment	Bonferroni	Benjamini	FDR
GOTERM_BP_DIRECT	GO:0007267~cell-cell signaling	7	4.21686747	1.27E-04	FGFR2, WISP1, FGF9, WNT9B, ADRA2C, CELSR1, SHH	137	103	18082	8.969881653	0.138239371	0.036511219	0.205178714
GOTERM_BP_DIRECT	GO:0051781~positive regulation of cell division	5	3.012048193	3.59E-04	FGFR2, FGF9, BTC, HTR2B, SHH	137	45	18082	14.66504461	0.342424775	0.080420908	0.577034098
GOTERM_BP_DIRECT	GO:0060484~lung-associated mesenchyme development	3	1.807228916	0.002954276	FGFR2, FGF9, SHH	137	11	18082	35.99601858	0.968341309	0.194100642	4.654736938
GOTERM_BP_DIRECT	GO:0060979~vasculogenesis involved in coronary vascular morphogenesis	3	1.807228916	0.004816304	FGFR2, FGF9, SHH	137	14	18082	28.28258603	0.996426487	0.268758463	7.483289824
GOTERM_BP_DIRECT	GO:0002053~positive regulation of mesenchymal cell proliferation	3	1.807228916	0.031502179	FGFR2, FGF9, SHH	137	37	18082	10.70151904	1	0.580507918	40.29081
GOTERM_BP_DIRECT	GO:0030324~lung development	4	2.409638554	0.067015075	FGFR2, NPHP3, FGF9, SHH	137	124	18082	4.257593595	1	0.746411052	67.29133531
GOTERM_BP_DIRECT	GO:0010628~positive regulation of gene expression	7	4.21686747	0.081001607	FGFR2, FGF9, BCL11A, MITF, TRPV4, CNTN1, SHH	137	399	18082	2.315533359	1	0.785677665	74.35637326
GOTERM_BP_DIRECT	GO:0001525~angiogenesis	5	3.012048193	0.106296899	FGFR2, FGF9, ECM1, ADGRG1, SHH	137	239	18082	2.761200867	1	0.813887237	83.64331537
Annotation Cluster 6	**Enrichment Score: 2.078773834414423**											
Category	Term	Count	%	PValue	Genes	List Total	Pop Hits	Pop Total	Fold Enrichment	Bonferroni	Benjamini	FDR
INTERPRO	IPR013032:EGF-like, conserved site	9	5.421686747	7.18E-05	LAMA1, SCUBE3, NELL1, BTC, CELSR1, HHIP, LRP2, MEGF10, HABP2	144	197	20594	6.533629442	0.02796757	0.02796757	0.099931778
INTERPRO	IPR000742:Epidermal growth factor-like domain	9	5.421686747	2.56E-04	LAMA1, SCUBE3, NELL1, BTC, CELSR1, HHIP, LRP2, MEGF10, HABP2	144	237	20594	5.430907173	0.096216188	0.033159459	0.355940594
UP_KEYWORDS	EGF-like domain	8	4.819277108	8.04E-04	SCUBE3, NELL1, BTC, CELSR1, HHIP, LRP2, MEGF10, HABP2	153	224	22680	5.294117647	0.129932854	0.017247638	0.979590242
SMART	SM00181:EGF	8	4.819277108	0.001744073	LAMA1, SCUBE3, NELL1, CELSR1, HHIP, LRP2, MEGF10, HABP2	101	181	10425	4.56211367	0.190401669	0.100223177	1.986832719
GOTERM_MF_DIRECT	GO:0005509~calcium ion binding	13	7.831325301	0.005327947	SMOC2, PNLIPRP1, SCUBE3, NELL1, PLCH1, AIF1L, PADI2, PCDH7, CELSR1, LRP2, PLCB1, SHH, HABP2	129	699	17446	2.5151989	0.815135549	0.245239956	6.94255851
UP_SEQ_FEATURE	domain:EGF-like 4	4	2.409638554	0.008978853	SCUBE3, NELL1, LRP2, MEGF10	141	55	18012	9.290522244	0.997232115	0.445099897	12.6067726
UP_SEQ_FEATURE	domain:EGF-like 1	5	3.012048193	0.011032954	NELL1, HHIP, LRP2, MEGF10, HABP2	141	111	18012	5.754264903	0.99928595	0.453222393	15.27431851
INTERPRO	IPR001881:EGF-like calcium-binding	5	3.012048193	0.011616098	SCUBE3, NELL1, CELSR1, LRP2, HABP2	144	126	20594	5.675154321	0.990099958	0.536617629	15.01301475
INTERPRO	IPR009030:Insulin-like growth factor binding protein, N-terminal	5	3.012048193	0.012907263	WISP1, SCUBE3, NELL1, CELSR1, LRP2	144	130	20594	5.500534188	0.994092649	0.519572853	16.54574032
UP_SEQ_FEATURE	domain:EGF-like 6; calcium-binding	3	1.807228916	0.013637639	NELL1, CELSR1, LRP2	141	23	18012	16.66234968	0.999872406	0.472958362	18.54766387
UP_SEQ_FEATURE	domain:EGF-like 3	4	2.409638554	0.014724643	NELL1, LRP2, MEGF10, HABP2	141	66	18012	7.74210187	0.999937895	0.454153681	19.87849848
UP_SEQ_FEATURE	domain:EGF-like 2	4	2.409638554	0.027733151	HHIP, LRP2, MEGF10, HABP2	141	84	18012	6.083080041	0.999999989	0.619630081	34.30812102
INTERPRO	IPR000152:EGF-type aspartate/asparagine hydroxylation site	4	2.409638554	0.030904894	SCUBE3, NELL1, CELSR1, LRP2	144	98	20594	5.837301587	0.999995882	0.676085914	35.40693769

INTERPRO	IPR009030:Insulin-like growth factor binding protein, N-terminal	5	3.012048193	0.012907263	WISP1, SCUBE3, NELL1, CELSR1, LRP2	144	130	20594	5.500534188	0.994092649	0.519572853	16.54574032
UP_SEQ_FEATURE	domain:EGF-like 6; calcium-binding	3	1.807228916	0.013637639	NELL1, CELSR1, LRP2	141	23	18012	16.66234968	0.999872406	0.472958362	18.54766387
UP_SEQ_FEATURE	domain:EGF-like 3	4	2.409638554	0.014724643	NELL1, LRP2, MEGF10, HABP2	141	66	18012	7.74210187	0.999937895	0.454153681	19.87849848
UP_SEQ_FEATURE	domain:EGF-like 2	4	2.409638554	0.027733151	HHIP, LRP2, MEGF10, HABP2	141	84	18012	6.083080041	0.999999989	0.619630081	34.30812102
INTERPRO	IPR000152:EGF-type aspartate/asparagine hydroxylation site	4	2.409638554	0.030904894	SCUBE3, NELL1, CELSR1, LRP2	144	98	20594	5.837301587	0.999995882	0.676085914	35.40693769
SMART	SM00179:EGF_CA	5	3.012048193	0.032818087	SCUBE3, NELL1, CELSR1, LRP2, HABP2	101	126	10425	4.095945309	0.982360424	0.554038234	31.86133072
UP_SEQ_FEATURE	domain:EGF-like 5	3	1.807228916	0.044020528	SCUBE3, LRP2, MEGF10	141	43	18012	8.912419594	1	0.770043491	48.96169822
UP_SEQ_FEATURE	domain:EGF-like 2; calcium-binding	3	1.807228916	0.061808849	SCUBE3, NELL1, CELSR1	141	52	18012	7.369885434	1	0.823764525	61.4499549
INTERPRO	IPR018097:EGF-like calcium-binding, conserved site	3	1.807228916	0.145998113	SCUBE3, NELL1, LRP2	144	97	20594	4.423109966	1	0.941200389	88.88949297
Annotation Cluster 7	**Enrichment Score: 1.936870485814026**											
Category	Term	Count	%	PValue	Genes	List Total	Pop Hits	Pop Total	Fold Enrichment	Bonferroni	Benjamini	FDR
GOTERM_BP_DIRECT	GO:0016055~Wnt signaling pathway	7	4.21686747	0.005509928	RNF43, NPHP3, WISP1, SOSTDC1, MITF, WNT9B, AXIN2	137	213	18082	4.337548405	0.998416102	0.28777498	8.516685324
UP_KEYWORDS	Wnt signaling pathway	6	3.614457831	0.00673028	RNF43, NPHP3, WISP1, SOSTDC1, WNT9B, AXIN2	153	176	22680	5.053475936	0.68909699	0.085947484	7.93074376
GOTERM_BP_DIRECT	GO:0090090~negative regulation of canonical Wnt signaling pathway	4	2.409638554	0.04170705	NPHP3, SOSTDC1, AXIN2, SHH	137	102	18082	5.175898096	1	0.65277854	49.6584239
Annotation Cluster 8	**Enrichment Score: 1.8929064150221735**											
Category	Term	Count	%	PValue	Genes	List Total	Pop Hits	Pop Total	Fold Enrichment	Bonferroni	Benjamini	FDR
SMART	SM00181:EGF	8	4.819277108	0.001744073	LAMA1, SCUBE3, NELL1, CELSR1, HHIP, LRP2, MEGF10, HABP2	101	181	10425	4.56211367	0.190401669	0.100223177	1.986832719
INTERPRO	IPR002049:EGF-like, laminin	3	1.807228916	0.02721047	LAMA1, CELSR1, MEGF10	144	37	20594	11.59572072	0.999981488	0.663685137	31.89285621
SMART	SM00180:EGF_Lam	3	1.807228916	0.044155023	LAMA1, CELSR1, MEGF10	101	35	10425	8.847241867	0.995764712	0.597764418	40.49915654
Annotation Cluster 9	**Enrichment Score: 1.842097729530089**											
Category	Term	Count	%	PValue	Genes	List Total	Pop Hits	Pop Total	Fold Enrichment	Bonferroni	Benjamini	FDR
UP_KEYWORDS	Cell junction	13	7.831325301	0.001696185	KCNC2, DLC1, LRRC4, CCDC85C, NLGN1, TANC1, CXADR, CBLN1, KDF1, GRIA1, TRPV4, HTR2B, DPP4	153	661	22680	2.915368871	0.254491801	0.028941839	2.05576463
GOTERM_CC_DIRECT	GO:0060076~excitatory synapse	4	2.409638554	0.002491012	FGFR2, LRRC4, GRIA1, NLGN1	145	37	19662	14.65945946	0.355296658	0.136120224	3.014232928
GOTERM_CC_DIRECT	GO:0045211~postsynaptic membrane	7	4.21686747	0.005938214	KCNMA1, KCNC2, LRRC4, CBLN1, GRIA1, NLGN1, TANC1	145	222	19662	4.275675676	0.649446171	0.122808652	7.047956748
GOTERM_CC_DIRECT	GO:0030054~cell junction	13	7.831325301	0.006599668	KCNC2, DLC1, LRRC4, CCDC85C, NLGN1, TANC1, CXADR, CBLN1, KDF1, GRIA1, TRPV4, HTR2B, DPP4	145	718	19662	2.455153203	0.6881994	0.12145481	7.80410365
UP_KEYWORDS	Postsynaptic cell membrane	6	3.614457831	0.00673028	KCNC2, LRRC4, CBLN1, GRIA1, NLGN1, TANC1	153	176	22680	5.053475936	0.68909699	0.085947484	7.93074376
UP_KEYWORDS	Synapse	7	4.21686747	0.033484606	KCNC2, LRRC4, CBLN1, GRIA1, NLGN1, TANC1, HTR2B	153	357	22680	2.906574394	0.997238671	0.225994102	34.08007347
GOTERM_CC_DIRECT	GO:0045202~synapse	7	4.21686747	0.166559348	KCNC2, LRRC4, CBLN1, GRIA1, NLGN1, TANC1, HTR2B	145	505	19662	1.87960396	1	0.632877723	89.30861893
GOTERM_CC_DIRECT	GO:0043197~dendritic spine	3	1.807228916	0.294946993	LRRC4, GRIA1, NLGN1	145	148	19662	2.748648649	1	0.818877212	98.62756387
Annotation Cluster 10	**Enrichment Score: 1.7534485441460566**											
Category	Term	Count	%	PValue	Genes	List Total	Pop Hits	Pop Total	Fold Enrichment	Bonferroni	Benjamini	FDR
UP_KEYWORDS	Lipoprotein	13	7.831325301	0.00637953	KCNMA1, GNAL, NPHP3, GRIA1, WNT9B, AVPR1A, CNTN1, CNTN3, PRKG2, CXADR, HTR2B, CYS1, SHH	153	780	22680	2.470588235	0.669515035	0.088137599	7.532139875
UP_KEYWORDS	Palmitate	7	4.21686747	0.016826826	KCNMA1, GNAL, GRIA1, AVPR1A, CXADR, HTR2B, SHH	153	304	22680	3.413312693	0.94691235	0.158605599	18.75025789
UP_SEQ_FEATURE	lipid moiety-binding region:S-palmitoyl cysteine	5	3.012048193	0.051152103	GNAL, GRIA1, AVPR1A, CXADR, HTR2B	141	179	18012	3.568287175	1	0.774793089	54.3636472
Annotation Cluster 11	Enrichment Score: 1.6062557545005893											
Category	Term	Count	%	PValue	Genes	List Total	Pop Hits	Pop Total	Fold Enrichment	Bonferroni	Benjamini	FDR
SMART	SM00181:EGF	8	4.819277108	0.001744073	LAMA1, SCUBE3, NELL1, CELSR1, HHIP, LRP2, MEGF10, HABP2	101	181	10425	4.56211367	0.190401669	0.100223177	1.986832719
SMART	SM00282:LamG	3	1.807228916	0.058657385	LAMA1, NELL1, CELSR1	101	41	10425	7.552523545	0.999334	0.648269048	50.08985016
INTERPRO	IPR013320:Concanavalin A-like lectin/glucanase, subgroup	5	3.012048193	0.059737476	LAMA1, NELL1, SPSB4, PAPPA2, CELSR1	144	211	20594	3.388954713	1	0.802503075	57.58101154
INTERPRO	IPR001791:Laminin G domain	3	1.807228916	0.061495428	LAMA1, NELL1, CELSR1	144	58	20594	7.397270115	1	0.79129952	58.67194177

Annotation Cluster 12	**Enrichment Score: 1.4595825345609983**											
Category	Term	Count	%	PValue	Genes	List Total	Pop Hits	Pop Total	Fold Enrichment	Bonferroni	Benjamini	FDR
INTERPRO	IPR001711:Phospholipase C, phosphatidylinositol-specific, Y domain	3	1.807228916	0.004738115	PLCE1, PLCH1, PLCB1	144	15	20594	28.60277778	0.846798804	0.374372919	6.398454746
INTERPRO	IPR001192:Phosphoinositide phospholipase C	3	1.807228916	0.004738115	PLCE1, PLCH1, PLCB1	144	15	20594	28.60277778	0.846798804	0.374372919	6.398454746
UP_SEQ_FEATURE	domain:PI-PLC Y-box	3	1.807228916	0.005134321	PLCE1, PLCH1, PLCB1	141	14	18012	27.37386018	0.965311538	0.381335771	7.402289215
UP_SEQ_FEATURE	domain:PI-PLC X-box	3	1.807228916	0.006702059	PLCE1, PLCH1, PLCB1	141	16	18012	23.95212766	0.987613843	0.422413446	9.558562643
GOTERM_MF_DIRECT	GO:0004435~phosphatidylinositol phospholipase C activity	3	1.807228916	0.006758729	PLCE1, PLCH1, PLCB1	129	17	17446	23.86593707	0.882698612	0.263719485	8.729395387
INTERPRO	IPR000909:Phospholipase C, phosphatidylinositol-specific , X domain	3	1.807228916	0.007577514	PLCE1, PLCH1, PLCB1	144	19	20594	22.58114035	0.950437248	0.451683792	10.04852766
SMART	SM00149:PLCYc	3	1.807228916	0.00881795	PLCE1, PLCH1, PLCB1	101	15	10425	20.64356436	0.6575755	0.300391716	9.681310604
SMART	SM00148:PLCXc	3	1.807228916	0.012611326	PLCE1, PLCH1, PLCB1	101	18	10425	17.2029703	0.784689556	0.318813121	13.57636263
INTERPRO	IPR017946:PLC-like phosphodiesterase, TIM beta/alpha-barrel domain	3	1.807228916	0.01293767	PLCE1, PLCH1, PLCB1	144	25	20594	17.16166667	0.994164094	0.474269057	16.58152462
UP_SEQ_FEATURE	domain:C2	4	2.409638554	0.017224747	PLCE1, PLCH1, NEDD4L, PLCB1	141	70	18012	7.299696049	0.99998818	0.486957942	22.86280281
GOTERM_MF_DIRECT	GO:0008081~phosphoric diester hydrolase activity	3	1.807228916	0.055827414	PLCE1, PLCH1, PLCB1	129	52	17446	7.802325581	0.999999987	0.726552375	53.87136717
GOTERM_BP_DIRECT	GO:0035556~intracellular signal transduction	7	4.21686747	0.081752502	PLCE1, PLCH1, DCLK3, SPSB4, DCDC2A, PLCB1, BLNK	137	400	18082	2.309744526	1	0.783735561	74.69186077
INTERPRO	IPR000008:C2 calcium-dependent membrane targeting	4	2.409638554	0.095298561	PLCE1, PLCH1, NEDD4L, PLCB1	144	156	20594	3.667022792	1	0.888946422	75.20045558
KEGG_PATHWAY	mmu00562:Inositol phosphate metabolism	3	1.807228916	0.103251424	PLCE1, PLCH1, PLCB1	61	70	7691	5.403512881	0.999999736	0.661087475	72.31379404
SMART	SM00239:C2	4	2.409638554	0.118399398	PLCE1, PLCH1, NEDD4L, PLCB1	101	125	10425	3.302970297	0.999999761	0.851325272	76.51371017
INTERPRO	IPR011992:EF-hand-like domain	5	3.012048193	0.122627098	SMOC2, PLCE1, PLCH1, AIF1L, PLCB1	144	273	20594	2.619301994	1	0.934108442	83.81991259
UP_KEYWORDS	Lipid degradation	3	1.807228916	0.144874086	PLCE1, PLCH1, PLCB1	153	100	22680	4.447058824	1	0.518945103	85.26569298
GOTERM_BP_DIRECT	GO:0016042~lipid catabolic process	3	1.807228916	0.197894331	PLCE1, PLCH1, PLCB1	137	109	18082	3.632625728	1	0.939018446	97.13506035
GOTERM_BP_DIRECT	GO:0006629~lipid metabolic process	5	3.012048193	0.454648741	NPHP3, PLCE1, PNLIPRP1, PLCH1, PLCB1	137	459	18082	1.437749471	1	0.998483838	99.99427595
UP_KEYWORDS	Lipid metabolism	3	1.807228916	0.771881884	PLCE1, PLCH1, PLCB1	153	417	22680	1.066440965	1	0.965408534	99.9999986
Annotation Cluster 13	**Enrichment Score: 1.4034431010932522**											
Category	Term	Count	%	PValue	Genes	List Total	Pop Hits	Pop Total	Fold Enrichment	Bonferroni	Benjamini	FDR
GOTERM_CC_DIRECT	GO:0043025~neuronal cell body	10	6.024096386	0.016940114	KCNMA1, KCNC2, KCND3, PENK, GRIA1, KLHL14, TANC1, DPP6, HTR2B, SHH	145	534	19662	2.539325843	0.950560325	0.221653518	18.91377996
GOTERM_CC_DIRECT	GO:0030425~dendrite	9	5.421686747	0.028010734	KCNMA1, KCNC2, KCND3, PENK, GRIA1, NLGN1, TANC1, HTR2B, SHH	145	490	19662	2.490612245	0.993263745	0.242545437	29.43475343
GOTERM_MF_DIRECT	GO:0005216~ion channel activity	5	3.012048193	0.036624325	KCNMA1, KCNC2, KCND3, GRIA1, TRPV4	129	170	17446	3.977656179	0.999992424	0.692430422	39.50127643
GOTERM_BP_DIRECT	GO:0007268~chemical synaptic transmission	4	2.409638554	0.140028734	KCNMA1, PENK, GRIA1, HTR2B	137	172	18082	3.069427941	1	0.883159174	91.19968118
Annotation Cluster 14	**Enrichment Score: 1.3112478840336648**											
Category	Term	Count	%	PValue	Genes	List Total	Pop Hits	Pop Total	Fold Enrichment	Bonferroni	Benjamini	FDR
GOTERM_BP_DIRECT	GO:0007389~pattern specification process	6	3.614457831	7.44E-05	SOSTDC1, HOXD12, HOXD13, PTCH1, SHH, HOXD11	137	58	18082	13.65366222	0.083156887	0.042480751	0.119782771
GOTERM_BP_DIRECT	GO:0009952~anterior/posterior pattern specification	6	3.614457831	0.001576007	EMX2, CYP26A1, HOXD13, CELSR1, SHH, HOXD11	137	112	18082	7.070646507	0.84128587	0.168118322	2.50902804
GOTERM_BP_DIRECT	GO:0042733~embryonic digit morphogenesis	4	2.409638554	0.013489675	HOXD12, HOXD13, SHH, HOXD11	137	66	18082	7.99911524	0.999999869	0.410405255	19.65221094
GOTERM_BP_DIRECT	GO:0001501~skeletal system development	4	2.409638554	0.046944173	HOXD12, HOXD13, COL2A1, HOXD11	137	107	18082	4.934033699	1	0.674446719	53.91236747
INTERPRO	IPR020479:Homeodomain, metazoa	3	1.807228916	0.131793548	EMX2, HOXD12, HOXD11	144	91	20594	4.71474359	1	0.938651432	86.02096053
INTERPRO	IPR017970:Homeobox, conserved site	4	2.409638554	0.136454886	EMX2, HOXD12, HOXD13, HOXD11	144	184	20594	3.108997585	1	0.936678415	87.03039422
UP_SEQ_FEATURE	DNA-binding region:Homeobox	4	2.409638554	0.164964019	EMX2, HOXD12, HOXD13, HOXD11	141	180	18012	2.838770686	1	0.971769942	93.2352148
UP_KEYWORDS	Homeobox	4	2.409638554	0.289615056	EMX2, HOXD12, HOXD13, HOXD11	153	280	22680	2.117647059	1	0.658901086	98.47630186
INTERPRO	IPR001356:Homeodomain	4	2.409638554	0.29101666	EMX2, HOXD12, HOXD13, HOXD11	144	271	20594	2.110906109	1	0.985668604	99.16732323
INTERPRO	IPR009057:Homeodomain-like	4	2.409638554	0.430361207	EMX2, HOXD12, HOXD13, HOXD11	144	345	20594	1.658132045	1	0.997119143	99.96043339
SMART	SM00389:HOX	4	2.409638554	0.471802414	EMX2, HOXD12, HOXD13, HOXD11	101	266	10425	1.552147696	1	0.995980528	99.93497055
Annotation Cluster 15	**Enrichment Score: 1.174344028548501**											
Category	Term	Count	%	PValue	Genes	List Total	Pop Hits	Pop Total	Fold Enrichment	Bonferroni	Benjamini	FDR
GOTERM_MF_DIRECT	GO:0043565~sequence-specific DNA binding	14	8.43373494	7.72E-04	CAMTA1, FOSL2, FOXL1, ELF5, TFCP2L1, MITF, EMX2, HOXD12, HOXD13, HOXD11, BCL11A, TFAP2B, SP5, NR2F1	129	633	17446	2.991096905	0.216617757	0.078154993	1.035178833

UP_KEYWORDS	Transcription regulation	21	12.65060241	0.01735988	CAMTA1, KHDRBS2, FOSL2, FOXL1, ELF5, TFCP2L1, MITF, YLPM1, HR, HOXD12, HOXD13, TOX3, HOXD11, PCGF5, PRDM6, BCL11A, CASZ1, TFAP2B, SP5, CRY1, NR2F1	153	1799	22680	1.730373083	0.951666628	0.154910674	19.28762992
UP_KEYWORDS	Transcription	21	12.65060241	0.023777677	CAMTA1, KHDRBS2, FOSL2, FOXL1, ELF5, TFCP2L1, MITF, YLPM1, HR, HOXD12, HOXD13, TOX3, HOXD11, PCGF5, PRDM6, BCL11A, CASZ1, TFAP2B, SP5, CRY1, NR2F1	153	1859	22680	1.67452457	0.984442814	0.187924232	25.50625276
GOTERM_BP_DIRECT	GO:0006351~transcription, DNA-templated	22	13.25301205	0.043014983	CAMTA1, KHDRBS2, FOSL2, FOXL1, ELF5, TFCP2L1, MITF, YLPM1, HR, HOXD12, HOXD13, AFF1, TOX3, HOXD11, PCGF5, PRDM6, BCL11A, CASZ1, TFAP2B, SP5, CRY1, NR2F1	137	1885	18082	1.540413174	1	0.656634884	50.75402551
GOTERM_BP_DIRECT	GO:0006355~regulation of transcription, DNA-templated	24	14.45783133	0.086040819	CAMTA1, KHDRBS2, FOSL2, FOXL1, ELF5, TFCP2L1, MITF, YLPM1, EMX2, HR, HOXD12, HOXD13, TOX3, SHH, HOXD11, PCGF5, PRDM6, BCL11A, CASZ1, SP5, TFAP2B, AXIN2, CRY1, NR2F1	137	2279	18082	1.389929634	1	0.786481783	76.53026651
UP_KEYWORDS	DNA-binding	16	9.638554217	0.119519533	FOSL2, FOXL1, ELF5, TFCP2L1, MITF, EMX2, HR, HOXD12, HOXD13, TOX3, HOXD11, TFAP2B, SP5, CASZ1, RAD54L2, NR2F1	153	1604	22680	1.4786563	1	0.48690551	78.93320144
UP_KEYWORDS	Nucleus	37	22.28915663	0.149255361	CAMTA1, FOSL2, USP2, ELF5, NELL1, TFCP2L1, MITF, YLPM1, HOXD12, HR, HOXD13, SKAP1, HOXD11, PCGF5, TRP53BP2, BCL11A, DCLK3, CASZ1, CRY1, PLCB1, NR2F1, KHDRBS2, FOXL1, EMX2, SYNPO2, AFF1, TOX3, FMN2, RNF43, PRDM6, PPM1H, TFAP2B, SP5, RAD54L2, FBXO32, PDE4DIP, DUSP8	153	4534	22680	1.209683697	1	0.520926975	86.16327208
UP_KEYWORDS	Activator	7	4.21686747	0.241574596	CAMTA1, ELF5, MITF, SP5, TFAP2B, TOX3, NR2F1	153	624	22680	1.662895928	1	0.615852035	96.6066299
GOTERM_CC_DIRECT	GO:0005634~nucleus	49	29.51807229	0.265244621	DLC1, FOSL2, NELL1, ELF5, MITF, YLPM1, HR, HOXD12, HOXD13, CXADR, SKAP1, HOXD11, ACTG1, PCGF5, HHIP, CRY1, CYS1, PLCB1, NR2F1, KHDRBS2, EMX2, NUDT10, NUDT11, TOX3, FMN2, PPM1H, PRDM6, TFAP2B, PDE4DIP, FGFR2, CAMTA1, USP2, TFCP2L1, DCDC2A, TRP53BP2, BCL11A, CASZ1, DCLK3, NEDD4L, AXIN2, FOXL1, SYNPO2, AFF1, PLAC8, RNF43, SP5, FBXO32, RAD54L2, DUSP8	145	6019	19662	1.103904303	1	0.787729629	97.72277896
GOTERM_MF_DIRECT	GO:0003677~DNA binding	17	10.24096386	0.278495889	CAMTA1, FOSL2, FOXL1, ELF5, TFCP2L1, MITF, EMX2, HR, HOXD12, HOXD13, TOX3, HOXD11, CASZ1, TFAP2B, SP5, RAD54L2, NR2F1	129	1847	17446	1.244767337	1	0.951865682	98.76792208
GOTERM_MF_DIRECT	GO:0003700~transcription factor activity, sequence-specific DNA binding	9	5.421686747	0.321747682	FOSL2, FOXL1, ELF5, TFCP2L1, MITF, TFAP2B, HOXD13, AFF1, NR2F1	129	883	17446	1.378440307	1	0.956963486	99.46416312
Annotation Cluster 16	**Enrichment Score: 1.1480458185525872**											
Category	Term	Count	%	PValue	Genes	List Total	Pop Hits	Pop Total	Fold Enrichment	Bonferroni	Benjamini	FDR
GOTERM_BP_DIRECT	GO:0034765~regulation of ion transmembrane transport	5	3.012048193	0.019009699	KCNMA1, KCNC2, KCND3, KCNJ10, NEDD4L	137	135	18082	4.888348202	1	0.454115761	26.5970162
GOTERM_CC_DIRECT	GO:0008076~voltage-gated potassium channel complex	4	2.409638554	0.020296843	KCNMA1, KCNC2, KCND3, DPP6	145	79	19662	6.865822785	0.972920958	0.227238929	22.24675586
GOTERM_MF_DIRECT	GO:0005267~potassium channel activity	4	2.409638554	0.02104081	KCNMA1, KCNC2, KCND3, KCNJ10	129	80	17446	6.762015504	0.998793271	0.526047938	24.90526083
UP_KEYWORDS	Ion channel	7	4.21686747	0.025965963	KCNMA1, KCNC2, KCND3, GRIA1, LRRC8D, TRPV4, KCNJ10	153	336	22680	3.088235294	0.989448236	0.186886559	27.52391165
GOTERM_BP_DIRECT	GO:0071805~potassium ion transmembrane transport	4	2.409638554	0.030429879	KCNMA1, KCNC2, KCND3, KCNJ10	137	90	18082	5.866017843	1	0.576265196	39.21680418
GOTERM_CC_DIRECT	GO:0016324~apical plasma membrane	7	4.21686747	0.033927151	KCNMA1, KCNC2, TRPV4, KCNJ10, PRKG2, LRP2, DPP4	145	328	19662	2.893902439	0.997699945	0.251195425	34.5284651
UP_KEYWORDS	Potassium transport	4	2.409638554	0.035334836	KCNMA1, KCNC2, KCND3, KCNJ10	153	107	22680	5.541506322	0.998017784	0.228419413	35.60764976
GOTERM_MF_DIRECT	GO:0005216~ion channel activity	5	3.012048193	0.036624325	KCNMA1, KCNC2, KCND3, GRIA1, TRPV4	129	170	17446	3.977656179	0.999992424	0.692430422	39.50127643
INTERPRO	IPR005821:Ion transport domain	4	2.409638554	0.038574449	KCNMA1, KCNC2, KCND3, TRPV4	144	107	20594	5.346313603	0.999999821	0.697379121	42.17137709
UP_KEYWORDS	Potassium	4	2.409638554	0.046991714	KCNMA1, KCNC2, KCND3, KCNJ10	153	120	22680	4.941176471	0.99975805	0.283280858	44.50805409
GOTERM_BP_DIRECT	GO:0051260~protein homooligomerization	5	3.012048193	0.061633752	KCNMA1, KCNC2, KCND3, SCUBE3, NLGN1	137	197	18082	3.349883286	1	0.728130309	64.11581905
UP_KEYWORDS	Voltage-gated channel	4	2.409638554	0.063595063	KCNMA1, KCNC2, KCND3, KCNJ10	153	136	22680	4.359861592	0.999988433	0.333674551	55.24579065

UP_SEQ_FEATURE	short sequence motif:Selectivity filter	3	1.807228916	0.063914761	KCNC2, KCND3, KCNJ10	141	53	18012	7.230830992	1	0.821861344	62.72272569
GOTERM_BP_DIRECT	GO:0006813~potassium ion transport	4	2.409638554	0.070905116	KCNMA1, KCNC2, KCND3, KCNJ10	137	127	18082	4.157020518	1	0.75512048	69.42058005
UP_KEYWORDS	Potassium channel	3	1.807228916	0.074390771	KCNMA1, KCNC2, KCND3	153	67	22680	6.637401229	0.999998444	0.359676268	61.16584244
GOTERM_MF_DIRECT	GO:0005244~voltage-gated ion channel activity	4	2.409638554	0.075835725	KCNMA1, KCNC2, KCND3, KCNJ10	129	134	17446	4.037024181	1	0.789357387	65.43151058
GOTERM_MF_DIRECT	GO:0005249~voltage-gated potassium channel activity	3	1.807228916	0.093491877	KCNMA1, KCNC2, KCND3	129	70	17446	5.796013289	1	0.821500703	73.34090931
UP_KEYWORDS	Ion transport	7	4.21686747	0.236076687	KCNMA1, KCNC2, KCND3, GRIA1, LRRC8D, TRPV4, KCNJ10	153	619	22680	1.676328043	1	0.628872106	96.29307514
GOTERM_BP_DIRECT	GO:0006811~ion transport	7	4.21686747	0.276687099	KCNMA1, KCNC2, KCND3, GRIA1, LRRC8D, TRPV4, KCNJ10	137	584	18082	1.582016798	1	0.978033825	99.45841836
GOTERM_BP_DIRECT	GO:0055085~transmembrane transport	5	3.012048193	0.293406021	KCNMA1, KCNC2, KCND3, SLC16A10, TRPV4	137	364	18082	1.812986284	1	0.98191824	99.6284302
UP_KEYWORDS	Transport	12	7.228915663	0.737140915	KCNMA1, KCNC2, AP1S3, FMN2, KCND3, AFM, SLC16A10, GRIA1, LRRC8D, SLC7A8, TRPV4, KCNJ10	153	1901	22680	0.935730421	1	0.956004683	99.99999206
GOTERM_BP_DIRECT	GO:0006810~transport	12	7.228915663	0.818900135	KCNMA1, KCNC2, AP1S3, FMN2, KCND3, AFM, SLC16A10, GRIA1, LRRC8D, SLC7A8, TRPV4, KCNJ10	137	1822	18082	0.869278165	1	0.999999966	100
Annotation Cluster 17	**Enrichment Score: 0.9385877840360088**											
Category	Term	Count	%	PValue	Genes	List Total	Pop Hits	Pop Total	Fold Enrichment	Bonferroni	Benjamini	FDR
GOTERM_BP_DIRECT	GO:0045944~positive regulation of transcription from RNA polymerase II promoter	14	8.43373494	0.036949873	FGFR2, CAMTA1, FOSL2, ELF5, MITF, HOXD13, SKAP1, SHH, PLAC8, PCGF5, TFAP2B, RAD54L2, CYS1, NR2F1	137	995	18082	1.857081026	1	0.615249205	45.47769428
GOTERM_MF_DIRECT	GO:0003682~chromatin binding	7	4.21686747	0.128368828	FOSL2, MITF, TFAP2B, HOXD13, CYS1, TOX3, PLAC8	129	466	17446	2.031506804	1	0.8610171	84.2837067
GOTERM_MF_DIRECT	GO:0001077~transcriptional activator activity, RNA polymerase II core promoter proximal region sequence-specific binding	5	3.012048193	0.137347325	CAMTA1, MITF, TFAP2B, HOXD13, CYS1	129	270	17446	2.504450187	1	0.85705346	86.32952468
GOTERM_MF_DIRECT	GO:0000978~RNA polymerase II core promoter proximal region sequence-specific DNA binding	5	3.012048193	0.270244048	FOSL2, BCL11A, MITF, HOXD13, CYS1	129	359	17446	1.883569778	1	0.951042154	98.56398603
Annotation Cluster 18	**Enrichment Score: 0.9221107145486607**											
Category	Term	Count	%	PValue	Genes	List Total	Pop Hits	Pop Total	Fold Enrichment	Bonferroni	Benjamini	FDR
KEGG_PATHWAY	mmu04924:Renin secretion	3	1.807228916	0.105730438	KCNMA1, PRKG2, PLCB1	61	71	7691	5.327407065	0.99999982	0.644962444	73.20239566
KEGG_PATHWAY	mmu04970:Salivary secretion	3	1.807228916	0.120932695	KCNMA1, PRKG2, PLCB1	61	77	7691	4.912284437	0.999999983	0.673643524	78.10488371
KEGG_PATHWAY	mmu04022:cGMP-PKG signaling pathway	4	2.409638554	0.133944256	KCNMA1, ADRA2C, PRKG2, PLCB1	61	163	7691	3.094036005	0.999999998	0.670606408	81.63336241
Annotation Cluster 19	**Enrichment Score: 0.7818506682737131**											
Category	Term	Count	%	PValue	Genes	List Total	Pop Hits	Pop Total	Fold Enrichment	Bonferroni	Benjamini	FDR
KEGG_PATHWAY	mmu04151:PI3K-Akt signaling pathway	6	3.614457831	0.137527617	FGFR2, LAMA1, FGF9, COL2A1, ITGA4, G6PC2	61	351	7691	2.155247303	0.999999999	0.661214048	82.50916638
KEGG_PATHWAY	mmu04512:ECM-receptor interaction	3	1.807228916	0.150057192	LAMA1, COL2A1, ITGA4	61	88	7691	4.298248882	1	0.659099934	85.27971269
KEGG_PATHWAY	mmu04510:Focal adhesion	4	2.409638554	0.21867605	ACTG1, LAMA1, COL2A1, ITGA4	61	207	7691	2.436366516	1	0.719276471	94.54111516
Annotation Cluster 20	**Enrichment Score: 0.7814403167188648**											
Category	Term	Count	%	PValue	Genes	List Total	Pop Hits	Pop Total	Fold Enrichment	Bonferroni	Benjamini	FDR
GOTERM_MF_DIRECT	GO:0003779~actin binding	6	3.614457831	0.10343321	KCNMA1, FMN2, AIF1L, FHOD3, TRPV4, SYNPO2	129	338	17446	2.400715564	1	0.821841792	77.02041117
GOTERM_CC_DIRECT	GO:0015629~actin cytoskeleton	4	2.409638554	0.183003434	ACTG1, FMN2, AIF1L, SYNPO2	145	201	19662	2.698507463	1	0.659716232	91.62792807
UP_KEYWORDS	Actin-binding	4	2.409638554	0.239089116	FMN2, AIF1L, FHOD3, SYNPO2	153	252	22680	2.352941176	1	0.618902897	96.46802638

Table S13. Functional annotation clustering by DAVID for genes with increased expression in the microarray of E14.5 *Fgfr1/2cDKO-UM* ureters.

gene	genotype	biological replicates					normalized biological replicates					Student's t-test, unpaired
		#1	#2	#3	mean	SD	#1	#2	#3	mean	SD	
Aldh1a2	control	1.0000	1.0210	0.8470	0.9560	0.0775	1.0460	1.0680	0.8860	1.0000	0.0811	p = 0.0072
	Fgfr1/2-cDKO-UM	1.7120	1.7700	2.2900	1.9240	0.2599	1.7908	1.8515	2.3954	2.0126	0.2718	
Axin2	control	1.0000	1.0940	0.9770	1.0237	0.0506	0.9769	1.0687	0.9544	1.0000	0.0494	p = 0.0037
	Fgfr1/2-cDKO-UM	1.7550	2.3260	2.1580	2.0797	0.2396	1.7144	2.2722	2.1081	2.0316	0.2341	
Bmp4	control	1.0000	1.6560	1.6510	1.4357	0.3081	0.6965	1.1535	1.1500	1.0000	0.2146	p = 0.0736
	Fgfr1/2-cDKO-UM	2.0850	2.4500	1.8230	2.1193	0.2571	1.4523	1.7065	1.2698	1.4762	0.1791	
Elf5	control	1.0000	0.8230	1.2100	1.0110	0.1582	0.9892	0.8140	1.1968	1.0000	0.1565	p = 0.001
	Fgfr1/2-cDKO-UM	2.7160	2.5280	3.1250	2.7897	0.2492	2.6864	2.5005	3.0910	2.7593	0.2465	
Id2	control	1.0000	0.7590	0.6320	0.7970	0.1526	1.2547	0.9523	0.7930	1.0000	0.1915	p = 0.384
	Fgfr1/2-cDKO-UM	0.7310	0.9310	1.3500	1.0040	0.2579	0.9172	1.1681	1.6939	1.2597	0.3236	
Id4	control	1.0000	0.9210	1.0450	0.9887	0.0518	1.0115	0.9316	1.0570	1.0000	0.0518	p = 0.4764
	Fgfr1/2-cDKO-UM	1.1000	0.9990	0.9870	1.0287	0.0513	1.1126	1.0105	0.9983	1.0405	0.0513	
Myocd	control	1.0000	1.3080	1.1460	1.1513	0.1258	0.8685	1.1361	0.9954	1.0000	0.1093	p = 0.0372
	Fgfr1/2-cDKO-UM	0.5520	0.7580	0.9010	0.7370	0.1433	0.4794	0.6584	0.7826	0.6401	0.1245	
Ptch1	control	1.0000	1.3730	1.2900	1.2210	0.1599	0.8190	1.1245	1.0565	1.0000	0.1310	p = 0.012
	Fgfr1/2-cDKO-UM	2.3690	3.4530	2.5210	2.7810	0.4792	1.9402	2.8280	2.0647	2.2776	0.3925	
Shh	control	1.0000	1.1470	1.2630	1.1367	0.1076	0.8798	1.0091	1.1111	1.0000	0.0946	p = 0.0114
	Fgfr1/2-cDKO-UM	2.7540	3.0320	4.3830	3.3897	0.7115	2.4229	2.6674	3.8560	2.9821	0.6260	
Wnt9b	control	0.0000	0.0000	0.0000	0.0000	0.0000	0.0000	0.0000	0.0000	0.0000	0.0000	n. d.
	Fgfr1/2-cDKO-UM	1.0000	0.6963	1.1149	0.9371	0.1766	1.0672	0.7431	1.1897	1.0000	0.1884	

Table S14A. RT-qPCR analysis of gene expression in control and *Fgfr1/2DKO-UM* ureters at E14.5. SD, standard derivation.

		biological replicates					normalized biological replicates					
gene	genotype	#1	#2	#3	mean	SD	#1	#2	#3	mean	SD	Student's t-test, unpaired
Spry1	control	1.0000	1.1410	1.5940	1.2450	0.2534	0.8032	0.9165	1.2803	1.0000	0.2035	p = 0.1177
	Fgfr1/2-cDKO-UM	1.5580	2.1480	1.5920	1.7660	0.2705	1.2514	1.7253	1.2787	1.4185	0.2172	
Etv4	control	1.0000	1.1680	1.1240	1.0973	0.0648	0.9113	1.0644	1.0243	1.0000	0.0648	p = 0.1296
	Fgfr1/2-cDKO-UM	1.3270	1.7830	1.2150	1.4417	0.2239	1.2093	1.6248	1.1072	1.3138	0.2239	
Etv5	control	1.0000	1.1310	1.1710	1.1007	0.0664	0.9085	1.0276	1.0639	1.0000	0.0664	p = 0.0066
	Fgfr1/2-cDKO-UM	1.4130	1.5960	1.6410	1.5500	0.0896	1.2838	1.4500	1.4909	1.4082	0.0896	

Table S14B. RT-qPCR analysis of gene expression in control and *Fgfr1/2cDKO-UM* ureters at E14.5. SD, standard derivation.

gene	genotype / treatment	biological replicates			mean	SD	normalized biological replicates			mean	SD	2-Way-ANOVA	Tukey's multiple comparison test	
		#1	#2	#3			#1	#2	#3					
Shh	control / mock	1.0000	0.8190	0.8366	0.8852	0.0815	1.1297	0.9252	0.9451	1.0000	0.0921	genotype: p <0.0001	control / mock vs. control / FGF10	p = 0.0007
	control / FGF10	1.5191	1.5873	1.4961	1.5342	0.0387	1.7161	1.7932	1.6902	1.7332	0.0437	treatment: p = 0.0008	control / mock vs. Fgfr1/2-cDKO-UE / mock	p = 0.0088
	Fgfr1/2-cDKO-UE / mock	0.6465	0.3612	0.3543	0.4540	0.1361	0.7303	0.4080	0.4002	0.5128	0.1538	interaction: p = 0.0025	control / mock vs. Fgfr1/2-cDKO-UE / FGF10	p = 0.0204
	Fgfr1/2-cDKO-UE / FGF10	0.6519	0.4846	0.4087	0.5151	0.1016	0.7364	0.5475	0.4617	0.5819	0.1147		control / FGF10 vs. Fgfr1/2-cDKO-UE / mock	p <0.0001
													control / FGF10 vs.Fgfr1/2-cDKO-UE / FGF10	p <0.,0001
													Fgfr1/2-cDKO-UE / mock vs.Fgfr1/2-cDKO-UE / FGF10	p = 0.9177

Table S14C. RT-qPCR analysis of gene expression in control and *Fgfr1/2cDKO-UE* ureters at E12.5 cultured for 18 h in presence or absence of FGF10. SD, standard derivation.

gene	genotype	biological replicates			mean	SD	normalized biological replicates			mean	SD	Student's t-test, unpaired
		#1	#2	#3			#1	#2	#3			
Bmpr1a	control	1.0000	1.0400	0.9020	0.9807	0.0580	1.0197	1.0605	0.9198	1.0000	0.0591	p = 0.0417
	Fgfr1/2-cDKO-UM	1.1060	1.4300	1.4290	1.3217	0.1525	1.1278	1.4582	1.4572	1.3477	0.1555	
Bmpr1b	control	1.0000	1.1180	1.3630	1.1603	0.1512	0.8618	0.9635	1.1747	1.0000	0.1303	p = 0.0223
	Fgfr1/2-cDKO-UM	1.7860	1.8920	2.0360	1.9047	0.1025	1.5392	1.6306	1.7547	1.6415	0.0883	
Bmpr2	control	1.0000	1.1460	1.4020	1.1827	0.1662	0.8455	0.9690	1.1855	1.0000	0.1405	p = 0.0118
	Fgfr1/2-cDKO-UM	1.7580	2.3160	2.1250	2.0663	0.2315	1.4865	1.9583	1.7968	1.7472	0.1958	

Table S14D. RT-qPCR analysis of gene expression in control and *Fgfr1/2cDKO-UM* ureters at E14.5. SD, standard derivation.

gene	genotype	biological replicates			normalized biological replicates				mean	SD	Student's t-test, unpaired
		#1	#2	#3	mean	SD	#1	#2	#3			
Bmpr1a	control	1.0000	1.1500	1.2910	1.1470	0.1188	0.8718	1.0027	1.1255	1.0000	0.1036	p = 0.0107
	Fgfr1/2-cDKO-UE	0.5590	0.5250	0.7810	0.6217	0.1135	0.4874	0.4577	0.6809	0.5420	0.0990	
Bmpr1b	control	1.0000	0.9650	1.0570	1.0073	0.0379	0.9927	0.9580	1.0493	1.0000	0.0376	p = 0.0016
	Fgfr1/2-cDKO-UE	0.4800	0.5690	0.6580	0.5690	0.0727	0.4765	0.5649	0.6532	0.5649	0.0721	
Bmpr2	control	1.0000	1.1600	1.0030	1.0543	0.0747	0.9485	1.1002	0.9513	1.0000	0.0709	p = 0.0031
	Fgfr1/2-cDKO-UE	0.5350	0.6410	0.6810	0.6190	0.0616	0.5074	0.6080	0.6459	0.5871	0.0584	

Table S14E. RT-qPCR analysis of gene expression in control and *Fgfr1/2cDKO-UE* ureters at E14.5. SD, standard derivation.

gene	genotype	biological replicates			mean	SD	normalized biological replicates			mean	SD	Student's t-test, unpaired
		#1	#2	#3			#1	#2	#3			
Bmpr1a	control / mock	1.0000	1.1210	0.9750	1.0320	0.0638	0.9690	1.0866	0.9444	1.0000	0.0621	p = 0.1078
	control / FGF10	1.1950	1.1060	1.1220	1.1410	0.0387	1.1585	1.0719	1.0874	1.1059	0.0377	
Bmpr1b	control / mock	1.0000	1.1140	1.3060	1.1400	0.1263	0.8772	0.9772	1.1456	1.0000	0.1108	p = 0.0382
	control / FGF10	1.3510	1.4970	1.5260	1.4580	0.0766	1.1851	1.3132	1.3386	1.2790	0.0672	
Bmpr2	control / mock	1.0000	1.2000	1.4690	1.2230	0.1922	1.2015	0.9809	0.8176	1.0000	0.1573	p = 0.0235
	control / FGF10	1.7880	1.9570	1.6540	1.7997	0.1240	1.4621	1.6002	1.3522	1.4715	0.1015	

Table S14F. RT-qPCR analysis of gene expression in control ureters at E12.5 cultured for 18 h in the presence or absence of FGF10. SD, standard derivation.

	Intensities				Fold change (FC)		
Gene Symbol	**control 1**	**mutant 1**	**control 2**	**mutant 2**	**FC 1**	**FC 2**	**avgFC**
Hoxb8	4049	1540	2394	683	-2.6	-3.5	-3.1
Nhlrc4	207	102	229	81	-2.0	-2.8	-2.4
9030625G05Rik	125	62	136	50	-2.0	-2.7	-2.4
Fosb	6737	3258	6583	2644	-2.1	-2.5	-2.3
Gsta2	140	62	115	51	-2.3	-2.3	-2.3
Hhip	1675	949	1790	677	-1.8	-2.6	-2.2
Calcr	163	63	143	80	-2.6	-1.8	-2.2
Gm10639	422	175	313	170	-2.4	-1.8	-2.1
TC1605611	1490	597	1201	701	-2.5	-1.7	-2.1
Mapk4	129	77	141	59	-1.7	-2.4	-2.0
Kifc1	2229	837	1190	867	-2.7	-1.4	-2.0
Ptch1	334	258	360	135	-1.3	-2.7	-2.0
Tfcp2l1	5121	3507	3639	1463	-1.5	-2.5	-2.0
AI661453	151	116	176	67	-1.3	-2.6	-2.0
A930017K11Rik	247	137	265	126	-1.8	-2.1	-2.0
Prr7	1088	598	786	383	-1.8	-2.1	-1.9
Mia	1078	568	1291	658	-1.9	-2.0	-1.9
Kcnj10	512	208	398	291	-2.5	-1.4	-1.9
Fos	11268	5792	10197	5458	-1.9	-1.9	-1.9
Rbm47	258	165	244	110	-1.6	-2.2	-1.9
Mllt3	211	140	196	86	-1.5	-2.3	-1.9
Egr1	17217	10467	16512	7781	-1.6	-2.1	-1.9
Sprr2f	164	100	185	87	-1.6	-2.1	-1.9
Diap1	285	219	228	93	-1.3	-2.5	-1.9
Espn	153	77	140	79	-2.0	-1.8	-1.9
Frmd5	242	125	196	108	-1.9	-1.8	-1.9
Hs3st6	2505	1174	2230	1413	-2.1	-1.6	-1.9
Mdn1	417	306	320	137	-1.4	-2.3	-1.8
Fam150b	153	82	144	80	-1.9	-1.8	-1.8
Ldoc1	555	366	661	309	-1.5	-2.1	-1.8
Degs2	533	259	547	343	-2.1	-1.6	-1.8
Pkhd1	166	118	159	71	-1.4	-2.2	-1.8
Egr2	270	132	230	143	-2.0	-1.6	-1.8
Sel1l3	614	316	548	323	-1.9	-1.7	-1.8
Kcnj16	3144	1801	2521	1333	-1.7	-1.9	-1.8
Eppk1	125	98	145	62	-1.3	-2.4	-1.8
Gprin3	129	87	104	48	-1.5	-2.2	-1.8

Syt6	519	376	588	261	-1.4	-2.3	-1.8
Slc44a1	141	111	144	61	-1.3	-2.3	-1.8
Spry1	2579	1788	2188	1009	-1.4	-2.2	-1.8
Cmtm4	1535	1192	1302	563	-1.3	-2.3	-1.8
Bbx	155	118	106	47	-1.3	-2.2	-1.8
Tfap2b	1115	596	943	561	-1.9	-1.7	-1.8
Spry2	245	177	231	107	-1.4	-2.2	-1.8
Srrm2	312	205	294	147	-1.5	-2.0	-1.8
Sgk2	118	82	121	58	-1.4	-2.1	-1.8
Hkdc1	3376	2256	3518	1736	-1.5	-2.0	-1.8
Arhgef38	191	107	154	88	-1.8	-1.7	-1.8
Ccdc85a	174	128	156	72	-1.4	-2.2	-1.8
Aldh1a3	1683	1115	1428	727	-1.5	-2.0	-1.7
Gprc5b	3997	2574	2849	1485	-1.6	-1.9	-1.7
Hist1h4c	6989	5447	5279	2425	-1.3	-2.2	-1.7
Ascl1	376	258	338	170	-1.5	-2.0	-1.7
Tmem229a	419	265	360	193	-1.6	-1.9	-1.7
Mknk2	141	102	123	60	-1.4	-2.1	-1.7
A4galt	244	153	196	109	-1.6	-1.8	-1.7
Shh	176	95	159	102	-1.8	-1.6	-1.7
Ikzf2	441	314	384	196	-1.4	-2.0	-1.7
Mid1	165	114	130	68	-1.4	-1.9	-1.7
E330013P04Rik	134	81	142	83	-1.7	-1.7	-1.7
Zswim6	894	647	669	340	-1.4	-2.0	-1.7
Foxf1	2882	1880	3316	1846	-1.5	-1.8	-1.7
Ptpn21	498	372	419	211	-1.3	-2.0	-1.7
Fndc1	246	196	296	144	-1.3	-2.1	-1.7
Clu	7715	4395	8067	5189	-1.8	-1.6	-1.7
AW549542	4733	3470	4772	2453	-1.4	-1.9	-1.7
Tcf7l2	280	198	219	116	-1.4	-1.9	-1.7
Map7	224	140	166	97	-1.6	-1.7	-1.7
Hoxd1	296	213	278	146	-1.4	-1.9	-1.6
A_55_P2174736	1056	781	1244	644	-1.4	-1.9	-1.6
Tmem171	132	72	117	81	-1.8	-1.4	-1.6
Tfrc	582	352	383	237	-1.7	-1.6	-1.6
Hist1h4i	2490	1914	2026	1045	-1.3	-1.9	-1.6
Gabbr2	319	199	326	200	-1.6	-1.6	-1.6
Dclk3	181	109	195	125	-1.7	-1.6	-1.6
Ccdc172	134	86	169	101	-1.6	-1.7	-1.6

Hspg2	135	103	130	68	-1.3	-1.9	-1.6
Aqp3	248	176	219	122	-1.4	-1.8	-1.6
Lama5	7979	6198	7020	3678	-1.3	-1.9	-1.6
Afm	835	525	705	439	-1.6	-1.6	-1.6
A_55_P2028852	177	113	185	114	-1.6	-1.6	-1.6
Elf5	867	533	818	524	-1.6	-1.6	-1.6
Rhpn2	1696	1148	1478	873	-1.5	-1.7	-1.6
Rec8	1456	1067	1852	1027	-1.4	-1.8	-1.6
Atp1b1	4276	2738	3311	2066	-1.6	-1.6	-1.6
Synpo2	404	296	363	203	-1.4	-1.8	-1.6
Wnt7b	210	144	245	145	-1.5	-1.7	-1.6
Klhl14	881	531	715	483	-1.7	-1.5	-1.6
Cck	601	446	697	389	-1.3	-1.8	-1.6
Ppm1h	1168	913	1061	571	-1.3	-1.9	-1.6
Plce1	168	115	116	69	-1.5	-1.7	-1.6
Inpp5j	237	164	261	155	-1.4	-1.7	-1.6
Gdnf	536	301	271	204	-1.8	-1.3	-1.6
Pa2g4	6273	4860	6261	3429	-1.3	-1.8	-1.6
Sstr1	727	414	635	469	-1.8	-1.4	-1.6
Papola	4269	2497	2540	1822	-1.7	-1.4	-1.6
Ncoa7	199	153	158	88	-1.3	-1.8	-1.5
Kiss1	123	84	146	90	-1.5	-1.6	-1.5
Mctp2	140	112	140	76	-1.3	-1.8	-1.5
Ammecr1	1609	1237	1186	665	-1.3	-1.8	-1.5
BC021891	1079	654	1074	754	-1.6	-1.4	-1.5
Frem2	2363	1428	2241	1587	-1.7	-1.4	-1.5
Gna14	381	284	359	209	-1.3	-1.7	-1.5
Adra2c	625	493	875	488	-1.3	-1.8	-1.5
Nr1h5	510	335	410	266	-1.5	-1.5	-1.5
Aim1	4064	3242	4481	2482	-1.3	-1.8	-1.5
DV650784	165	100	128	92	-1.7	-1.4	-1.5
Rffl	136	103	142	82	-1.3	-1.7	-1.5
Krt23	695	446	799	538	-1.6	-1.5	-1.5
Hoxb5os	2826	1686	2047	1495	-1.7	-1.4	-1.5
Cntfr	1854	1406	1720	996	-1.3	-1.7	-1.5
Padi2	2167	1533	2038	1254	-1.4	-1.6	-1.5
Ano6	685	509	493	292	-1.3	-1.7	-1.5
Ercc6l2	342	244	177	109	-1.4	-1.6	-1.5
Adgrg1	1624	1272	1695	966	-1.3	-1.8	-1.5

Hook1	139	101	101	61	-1.4	-1.6	-1.5
Setd8	741	562	610	357	-1.3	-1.7	-1.5
Cftr	492	361	547	329	-1.4	-1.7	-1.5
Iqck	251	166	249	165	-1.5	-1.5	-1.5
Lgr5	126	96	111	65	-1.3	-1.7	-1.5
4933408B17Rik	478	326	356	229	-1.5	-1.6	-1.5
Myo9a	376	292	226	131	-1.3	-1.7	-1.5
Spred2	1276	988	1205	701	-1.3	-1.7	-1.5
Gm7325	1677	1304	1601	934	-1.3	-1.7	-1.5
Rasef	213	128	150	114	-1.7	-1.3	-1.5
Sostdc1	134	86	176	123	-1.6	-1.4	-1.5
Hapln3	837	556	782	532	-1.5	-1.5	-1.5
Arglu1	5572	4188	4245	2581	-1.3	-1.6	-1.5
Itga3	107	82	124	75	-1.3	-1.7	-1.5
Zfp955b	869	653	574	351	-1.3	-1.6	-1.5
Cdk14	176	125	129	83	-1.4	-1.5	-1.5
Grb14	1725	1048	1438	1091	-1.6	-1.3	-1.5
Pcyox1l	167	113	140	94	-1.5	-1.5	-1.5
Gyltl1b	1355	881	1107	780	-1.5	-1.4	-1.5
Ipcef1	234	153	196	138	-1.5	-1.4	-1.5
TC1624218	445	337	371	227	-1.3	-1.6	-1.5
2010315B03Rik	182	134	155	98	-1.4	-1.6	-1.5
Scube3	8585	6829	7702	4558	-1.3	-1.7	-1.5
D9Ertd115e	296	234	315	187	-1.3	-1.7	-1.5
ENSMUST00000101281	119	81	106	72	-1.5	-1.5	-1.5
Raly	26250	16837	20031	14462	-1.6	-1.4	-1.5
Chrdl2	156	124	192	114	-1.3	-1.7	-1.5
Lrrc16a	271	202	205	128	-1.3	-1.6	-1.5
Bmp7	1444	928	1201	871	-1.6	-1.4	-1.5
Tnfaip6	273	179	214	153	-1.5	-1.4	-1.5
Fgf9	854	544	814	605	-1.6	-1.3	-1.5
Cds1	198	150	257	162	-1.3	-1.6	-1.5
Asb16	211	153	209	136	-1.4	-1.5	-1.5
Ccl4	162	121	129	82	-1.3	-1.6	-1.5
Kcnd3	1126	879	1307	807	-1.3	-1.6	-1.4
Robo2	1104	759	874	606	-1.5	-1.4	-1.4
Fam199x	190	127	137	98	-1.5	-1.4	-1.4
Adrb3	318	203	240	182	-1.6	-1.3	-1.4
Cited2	1871	1376	1915	1257	-1.4	-1.5	-1.4

Defb28	104	83	107	66	-1.3	-1.6	-1.4
Grhl2	1643	1091	1405	1026	-1.5	-1.4	-1.4
Vstm4	235	161	225	160	-1.5	-1.4	-1.4
Taf15	1702	1204	1188	814	-1.4	-1.5	-1.4
A_55_P2065434	297	237	188	116	-1.3	-1.6	-1.4
Tmem184a	289	221	338	216	-1.3	-1.6	-1.4
Gm13051	340	235	349	247	-1.4	-1.4	-1.4
Ehf	312	234	301	197	-1.3	-1.5	-1.4
Mitf	917	602	537	403	-1.5	-1.3	-1.4
Bmpr1b	705	524	489	324	-1.3	-1.5	-1.4
Fam133b	3170	2444	2272	1461	-1.3	-1.6	-1.4
Ssb	3961	2907	3114	2092	-1.4	-1.5	-1.4
Ttc39a	416	323	436	279	-1.3	-1.6	-1.4
Smtnl2	3126	2492	2873	1803	-1.3	-1.6	-1.4
Hist2h3b	11453	9074	9799	6186	-1.3	-1.6	-1.4
Cited4	339	255	434	287	-1.3	-1.5	-1.4
Plcl1	524	415	352	222	-1.3	-1.6	-1.4
Gabra2	412	325	429	273	-1.3	-1.6	-1.4
A_55_P2107682	195	138	204	143	-1.4	-1.4	-1.4
Bcl11b	474	378	510	323	-1.3	-1.6	-1.4
Lin28b	837	669	711	450	-1.3	-1.6	-1.4
Hist1h1e	20212	14528	11813	8212	-1.4	-1.4	-1.4
Spint2	2578	1819	2607	1846	-1.4	-1.4	-1.4
Ptch2	137	107	136	88	-1.3	-1.5	-1.4
Ago2	5462	4013	4902	3348	-1.4	-1.5	-1.4
Rcor1	171	133	115	75	-1.3	-1.5	-1.4
Arid4b	1001	759	696	463	-1.3	-1.5	-1.4
Nr4a1	6958	5231	7971	5345	-1.3	-1.5	-1.4
4930412O13Rik	1119	890	1249	802	-1.3	-1.6	-1.4
Emid1	8710	6530	9373	6337	-1.3	-1.5	-1.4
Ctnnal1	307	224	226	157	-1.4	-1.4	-1.4
Ildr1	154	123	181	117	-1.3	-1.6	-1.4
Cys1	2112	1670	1863	1207	-1.3	-1.5	-1.4
Fam120c	143	105	100	69	-1.4	-1.4	-1.4
ENSMUST00000059110	1120	742	1006	776	-1.5	-1.3	-1.4
Klhl15	299	235	260	169	-1.3	-1.5	-1.4
Ino80	192	136	159	114	-1.4	-1.4	-1.4
Camkmt	174	123	141	102	-1.4	-1.4	-1.4
Spty2d1	221	172	184	121	-1.3	-1.5	-1.4

Atp6v0a2	1339	1059	1016	661	-1.3	-1.5	-1.4
Mal2	3509	2784	3524	2286	-1.3	-1.5	-1.4
Trim71	709	522	557	387	-1.4	-1.4	-1.4
Kifc5b	187	145	160	106	-1.3	-1.5	-1.4
Lrrc8d	3022	2317	2463	1653	-1.3	-1.5	-1.4
Gm6402	196	154	151	100	-1.3	-1.5	-1.4
A430105D02Rik	173	136	112	74	-1.3	-1.5	-1.4
Lhfpl3	101	78	104	69	-1.3	-1.5	-1.4
Llgl2	853	629	868	606	-1.4	-1.4	-1.4
Wnt9b	695	484	640	472	-1.4	-1.4	-1.4
Sbf2	351	273	257	171	-1.3	-1.5	-1.4
Krt36	136	94	131	98	-1.4	-1.3	-1.4
Ptar1	493	359	385	274	-1.4	-1.4	-1.4
Blnk	1425	1134	1154	762	-1.3	-1.5	-1.4
Btbd11	1076	777	951	686	-1.4	-1.4	-1.4
Rln1	233	184	269	179	-1.3	-1.5	-1.4
Pantr1	1367	972	1312	961	-1.4	-1.4	-1.4
Rprm	4225	3372	3586	2367	-1.3	-1.5	-1.4
Ptger2	209	145	227	173	-1.4	-1.3	-1.4
Wfdc15b	2741	2142	2512	1708	-1.3	-1.5	-1.4
Il3ra	865	660	904	628	-1.3	-1.4	-1.4
Adcy1	229	173	289	202	-1.3	-1.4	-1.4
Mapk8	127	97	102	71	-1.3	-1.4	-1.4
Synrg	764	603	813	550	-1.3	-1.5	-1.4
Frmpd4	123	87	105	79	-1.4	-1.3	-1.4
Nde1	249	194	179	123	-1.3	-1.5	-1.4
Cldn4	441	336	498	349	-1.3	-1.4	-1.4
Lama1	7655	5681	5890	4225	-1.3	-1.4	-1.4
B930095M22Rik	257	180	295	224	-1.4	-1.3	-1.4
Hoxd3	1999	1531	1980	1383	-1.3	-1.4	-1.4
Asxl2	563	406	363	269	-1.4	-1.4	-1.4
Fgd6	334	237	330	248	-1.4	-1.3	-1.4
A_55_P2115364	1939	1545	2130	1442	-1.3	-1.5	-1.4
Pipox	200	138	198	156	-1.5	-1.3	-1.4
Wdr45b	954	710	887	639	-1.3	-1.4	-1.4
Trim35	285	228	198	135	-1.3	-1.5	-1.4
Skap1	279	198	242	184	-1.4	-1.3	-1.4
Epc2	4337	3122	2737	2051	-1.4	-1.3	-1.4
Ints2	122	97	104	71	-1.3	-1.5	-1.4

Tspan15	232	178	268	190	-1.3	-1.4	-1.4
Gm7008	127	96	115	82	-1.3	-1.4	-1.4
A3galt2	141	112	125	85	-1.3	-1.5	-1.4
Tcp11	585	467	667	455	-1.3	-1.5	-1.4
Nupr1l	125	99	130	89	-1.3	-1.5	-1.4
Hyls1	353	270	294	209	-1.3	-1.4	-1.4
Mef2a	221	159	156	118	-1.4	-1.3	-1.4
D230018H15Rik	677	493	571	427	-1.4	-1.3	-1.4
Cyr61	2749	2008	2610	1945	-1.4	-1.3	-1.4
Mfap3l	144	111	126	89	-1.3	-1.4	-1.4
Zgrf1	253	188	215	158	-1.3	-1.4	-1.4
Gpr160	198	146	188	139	-1.4	-1.4	-1.4
Fam132a	10253	7621	10632	7870	-1.3	-1.4	-1.3
Cers6	243	180	187	139	-1.4	-1.3	-1.3
Usp53	105	79	122	89	-1.3	-1.4	-1.3
Hoxd4	5633	4313	4801	3459	-1.3	-1.4	-1.3
Zdhhc23	123	93	111	82	-1.3	-1.4	-1.3
Bcl2l15	265	204	238	171	-1.3	-1.4	-1.3
Zmym2	197	155	131	93	-1.3	-1.4	-1.3
LOC552873	411	296	349	269	-1.4	-1.3	-1.3
Ahcyl2	152	121	146	102	-1.3	-1.4	-1.3
Tfeb	100	78	116	83	-1.3	-1.4	-1.3
Rasgef1b	1538	1187	1497	1078	-1.3	-1.4	-1.3
Arhgdig	219	174	258	182	-1.3	-1.4	-1.3
Twistnb	4323	3393	3246	2308	-1.3	-1.4	-1.3
Tshz1	4493	3527	4243	3017	-1.3	-1.4	-1.3
Zfp958	187	136	138	107	-1.4	-1.3	-1.3
Morc4	142	107	137	102	-1.3	-1.3	-1.3
Mid2	156	122	136	98	-1.3	-1.4	-1.3
Elp4	163	130	120	85	-1.3	-1.4	-1.3
Slc35d1	907	695	667	492	-1.3	-1.4	-1.3
Sdad1	2206	1722	2164	1571	-1.3	-1.4	-1.3
Sycp1	224	177	192	139	-1.3	-1.4	-1.3
Fosl2	5485	4095	4310	3285	-1.3	-1.3	-1.3
Maff	855	648	902	678	-1.3	-1.3	-1.3
Ccdc150	120	91	107	81	-1.3	-1.3	-1.3
Lrrk1	503	391	477	350	-1.3	-1.4	-1.3
Usp37	135	107	126	91	-1.3	-1.4	-1.3
Aqp11	512	375	435	342	-1.4	-1.3	-1.3

Cdkl1	253	190	229	175	-1.3	-1.3	-1.3
Apobec3	113	82	118	94	-1.4	-1.3	-1.3
2900073C17Rik	1021	781	745	560	-1.3	-1.3	-1.3
Prkg2	122	93	109	82	-1.3	-1.3	-1.3
Ripk4	2325	1777	1980	1493	-1.3	-1.3	-1.3
Cystm1	477	367	460	345	-1.3	-1.3	-1.3
A_55_P1994173	6179	4684	6222	4747	-1.3	-1.3	-1.3
Itpr3	10171	8019	7660	5664	-1.3	-1.4	-1.3
Hsd17b7	681	516	569	439	-1.3	-1.3	-1.3
Dusp1	1938	1528	2200	1631	-1.3	-1.3	-1.3
Efna5	4106	3186	4514	3404	-1.3	-1.3	-1.3
Dennd2d	165	129	172	129	-1.3	-1.3	-1.3
Rrp1b	851	674	734	546	-1.3	-1.3	-1.3
6330531I01Rik	126	100	133	100	-1.3	-1.3	-1.3
Arhgef16	1045	787	1174	925	-1.3	-1.3	-1.3
Stau2	2283	1813	1734	1298	-1.3	-1.3	-1.3
Gca	314	243	277	213	-1.3	-1.3	-1.3
Pde8b	272	203	268	215	-1.3	-1.3	-1.3
Jakmip1	219	167	193	151	-1.3	-1.3	-1.3
Znf660	158	121	137	107	-1.3	-1.3	-1.3
Mcf2	199	154	154	120	-1.3	-1.3	-1.3
Thbd	605	479	512	393	-1.3	-1.3	-1.3
AI448005	11035	8528	8072	6343	-1.3	-1.3	-1.3
Aif1l	11460	9116	10920	8375	-1.3	-1.3	-1.3
Trps1	2028	1572	1824	1435	-1.3	-1.3	-1.3
Slc16a7	1086	863	1088	836	-1.3	-1.3	-1.3
Cfap97	1019	780	747	597	-1.3	-1.3	-1.3
A_55_P2005672	11456	9153	13069	10069	-1.3	-1.3	-1.3
Syn3	179	139	173	137	-1.3	-1.3	-1.3
Tnks	201	157	130	103	-1.3	-1.3	-1.3
Kcnk1	1089	853	1253	997	-1.3	-1.3	-1.3
1110059G10Rik	1143	910	1001	784	-1.3	-1.3	-1.3
Sult2b1	106	83	116	92	-1.3	-1.3	-1.3
Capn5	1169	920	1199	955	-1.3	-1.3	-1.3
Ybx3	19487	15338	18474	14774	-1.3	-1.3	-1.3
D8Ertd82e	5273	4214	5579	4415	-1.3	-1.3	-1.3
Prom2	146	117	136	108	-1.3	-1.3	-1.3

Table S15. Genes with decreased expression in microarrays of E13.5 *Pax2cre/+;Fgfr1$^{fl/+}$;Fgfr2$^{fl/fl}$ (Fgfr1/2cDKO-UE)* ureters. The microarrays were filtered for an intensity of >100 in the control RNAs and in fold change (FC) >-1.25 in the two arrays performed.

	day 2	day 3	day 4	day 5	day 6	day 7	day 8
Ctrl	0 out of 12	0 out of 12	9 out of 12	12 out of 12	12 out of 12	12 out of 12	12 out of 12
	0	0	0.7500	1	1	1	1
2 µM Purmorphamine	0 out of 11	7 out of 11	10 out of 11	11 out of 11	11 out of 11	11 out of 11	11 out of 11
	0	0.6364	0.9091	1	1	1	1
10 µg/ml NOGGIN	0 out of 11	0 out of 11	0 out of 11	0 out of 11	0 out of 11	1 out of 11	2 out of 11
	0	0	0	0	0	0.0909	0.1818
2 µM Purmorphamine + 10 µg/ml NOGGIN	0 out of 12	0 out of 12	2 out of 12	10 out of 12	11 out of 12	11 out of 12	12 out of 12
	0	0	0.1667	0.8333	0.9167	0.9167	1

Table S16A. Onset of peristaltic activity of explants of E13.5 ureters cultured for 8 days in the presence of purmorphamine and/or NOGGIN. Shown are the number of control and mutant ureters that exhibit peristaltic contraction waves from day 2 to 8 of the culture period.

		day 2	day 3	day 4	day 5	day 6	day 7	day 8
Ctrl	Mean	0.0000	0.0000	1.2500	2.8333	2.9167	3.6667	3.7500
	SD	0.0000	0.0000	1.0553	0.9374	0.6686	0.4924	0.6216
2 µM Purmorphamine	Mean	0.0000	0.7500	1.0833	1.6667	2.7500	3.1667	4.0000
	SD	0.0000	0.7508	0.6030	0.7508	0.7746	0.9342	0.8090
	p-Value	n.d.	1.1E-03	8.5E-01	9.6E-03	7.8E-01	5.0E-01	5.3E-02
10 µg/ml NOGGIN	Mean	0.0000	0.0000	0.0000	0.0000	0.0000	0.0833	0.1667
	SD	0.0000	0.0000	0.0000	0.0000	0.0000	0.3015	0.4045
	p-Value	n.d.	n.d.	7.8E-04	1.9E-09	2.2E-12	1.8E-15	2.6E-13
2 µM Purmorphamine + 10 µg/ml NOGGIN	Mean	0.0000	0.0000	0.1667	1.0833	1.5000	1.6667	1.6667
	SD	0.0000	0.0000	0.3892	0.7930	0.7977	0.9847	0.6513
	p-Value	n.d.	n.d.	3.0E-03	6.1E-05	1.1E-04	2.5E-06	5.7E-08

Table S16B. Statistical analysis of the peristaltic frequency of E13.5 ureter explants treated with DMSO (Ctrl, n=12), purmorphamine or NOGGIN (n=11), and purmorphamine and NOGGIN (n=12) over 8 days of culture. Shown are the average and corresponding standard deviations of peristaltic contractions per minute after 2 to 8 days after ureter explantation at E13.5. One minute was video-monitored. The statistical significance was calculated by a two-tailed Student's t-test. SD, standard derivation. n.d., not defined.

Gene	Forward primer	Reverse primer
Aldh1a2	5′-CTGGAAAATTGCTCCCGCAT-3′	5′-GAAAGCCAGCCTCCTTGATG-3′
Axin2	5′-GCAGAAGCCACACAGAGAGT-3′	5′-CACCTCTGCTGCCACAAAAC-3′
Bmp4	5′-CACGAAGAACATCTGGAGAACA-3′	5′-GGTTGAAGAGGAAACGAAAAGC-3′
Bmpr1a	5′-CAGGAGGAATCGTGGAGGAA-3′	5′-CAGCGGTTAGACACGATTGG-3′
Bmpr1b	5′-TGTTCTTCACCACGGAGGAA-3′	5′-GCAGCAATGAACCCCAGAAT-3′
Bmpr2	5′-TTGACAGGAGACCGGAAACA-3′	5′-TATCGACCCCGTCCAATCAG-3′
Elf5	5′-ACTGCATCTCCTTCTGTCACT-3′	5′-AGTAACCTTGCGAGCGAATG-3′
Etv4	5′-GTGATGGAGTGATGGGTTATGG-3′	5′-TCCCTTCCTGCTTGATGTCT-3′
Etv5	5′-AAGAGGTTGCTCGCCGT-3′	5′-TGTAGACGTAGCGTTCCCC-3′
Gapdh	5′-ATGACATCAAGAAGGTGGTG-3′	5′-CATACCAGGAAATGAGCTTG-3′
Id2	5′-CTGGACTCGCATCCCACTATC-3′	5′-ATGCCTGCAAGGACAGGATG-3′
Id4	5′-GTGCGATATGAACGACTGCT-3′	5′-CTTTGCTGACTTTCTTGTTGGG-3′
Myocd	5′-CACACCTCAAAGAACCAAATGAAC-3′	5′-TTTTGACAGGGGATAGAGGGG-3′
Ppia	5′-GATTCATGTGCCAGGGTGGT-3′	5′-GCCATTCAGTCTTGGCAGTG-3′
Ptch1	5′-CATCAAAGTGTCGCCCCAAA-3′	5′-AACAGGCATAGGCAAGCATC-3′
Shh	5′-AGCGGCAGATATGAAGGGAA-3′	5′-GTCTTTGCACCTCTGAGTCATC-3′
Spry1	5′-ACACTCAGCCTGCTACGATT-3′	5′-CCTTTCCTGCTTTTCGGGTC-3′
Wnt9b	5′-CCCAAGAGAGGAAGCAAGGA-3′	5′-TTCACAGCCTTGATGCCCA-3′

Table S17. Primer for RT-qPCR analysis of gene expression.

Part 3 – Transcriptional control of BMP4 signaling during early murine ureter development

BMP4 signaling regulates expression of signals and transcription factor genes for coordinated cyto-differentiation in the murine ureter

Lena Deuper[1], Nicolas Hense[1], Tamrat Mamo[1], Florian Bergmann, Mark-Oliver Trowe[1] and Andreas Kispert[1,*]

[1]Institute of Molecular Biology, Medizinische Hochschule Hannover, 30625 Hannover, Germany

[*]Address correspondence to: Andreas Kispert, Institut für Molekularbiologie, OE5250, Medizinische Hochschule Hannover, Carl-Neuberg-Str. 1, D-30625 Hannover, Germany. Phone: +49 511 5324017, Fax: +49 511 5324283, E-Mail: kispert.andreas@mh-hannover.de

Short title: BMP4 in ureter development
Key words: Ureter, Differentiation, Smooth muscle cells, Superficial cells, Urothelium, BMP4, *Grhl3, Pparg, Trp63, Myocd*

Type of authorship: First author
Type of article: Research article
Share of the work: 60%
Contribution to the publication: (co-) planned and performed experiments, analyzed data, prepared figures, assisted in writing the paper

Journal: -
Impact factor: -
Number of citations: -
Date of publication: manuscript in preparation
DOI: -

Abstract

The differentiated cell types of the epithelial and mesenchymal compartments of the murine ureter arise in a highly coordinated fashion from progenitors in the distal ureteric bud epithelium and its surrounding mesenchyme. Previous genetic efforts identified BMP4, a member of the bone morphogenetic protein family, as a crucial mesenchymal signal for cyto-differentiation in both tissue primordia. Here, we used unbiased transcriptional profiling of ureters with genetic or pharmacological inhibition of BMP4 activity combined with specific expression approaches to define the BMP4 controlled gene regulatory network in the early ureter focusing on transcription factor genes as possible drivers of cyto-differentiation. We show that BMP4 directly controls expression of *Snai1*, *Gata6*, *Sox9*, *Tbx18, Myocd, Id2* and *Id4* in the ureteric mesenchyme, and of *Pparg, Msx2* and weakly *Trp63* in the ureteric epithelium. BMP4 indirectly enhances expression of *Grhl3* in the epithelium by repressing the expression of *Aldh1a3* and *Aldh1a2*, respectively, encoding RA synthesizing enzymes. Conditional gene targeting of *Smad4* reveals that BMP4 function is partly mediated by SMAD effectors in both ureteral tissues. Hence, our work links BMP4 with known transcriptional regulators of ureteric cyto-differentiation and uncovers as yet unknown additional factors relevant for this program.

Introduction

The ureters are critical components of the mammalian excretory system by enabling the efficient transport of urine from the renal pelvis to the bladder. Key to the functionality of these tubular organs is a patterned array of specialized cell types both in the outer mesenchymal wall as well as in the inner epithelial lining, the urothelium. In the mesenchymal wall, fibrocytes ensheath contractile smooth muscle cells (SMCs) while layers of basal (B), intermediate (I) and large binucleated superficial (S) cells populate the urothelium. S cells strongly contribute to sealing of the luminal content by harboring tight junctions and expressing uroplakins (UPKs) that form crystalline plaques on the apical surface (Bohnenpoll et al., 2017a, Velardo, 1981, Sun et al., 1996).

The cyto-architecture of the mature ureter derives from a complex interplay of proliferation, patterning and differentiation programs that occurs in the tissue primordia of this organ: the epithelial ureteric bud stalk (UB) and its surrounding mesenchyme. In the mouse, both progenitor pools strongly proliferate from E11.5, when the UB has been established as an outgrowth of the nephric duct, until E14.5, to elongate the tube. Cells of the inner layer of the ureteric mesenchyme (UM) subsequently differentiate into subepithelial *lamina propria* fibrocytes or into medial SMCs. Cells of the outer mesenchymal layer will become adventitial fibrocytes. Epithelial progenitors start to express ΔNP63 and low levels of UPKs and stratify indicating differentiation of I cells. Around E16.5, luminal epithelial cells increase their expression of UPKs and become S cells. B cells are first recognized at E16.5 by expression of KRT5. At E18.5, they populate the entire basal layer of the fully stratified and differentiated urothelium (Bohnenpoll et al., 2017a, Bohnenpoll and Kispert, 2014).

The precise course of these cellular processes ensures the establishment of a peristaltically active sealing tube shortly after onset of urine production in the fetal kidney around E16.5. Failure of SMC differentiation compromises urine removal to the bladder and leads to dilatation of the ureter and the renal drainage system (hydroureter and hydronephrosis) with progressive destruction of the renal parenchyma by the hydrostatic pressure (Kurz et al., 2022). Lack of urothelial cells, particularly S cells, impedes the urothelial barrier function and results in efflux of urine into the interstitial space and subsequent hydroureter and inflammation (Dalghi et al., 2020, Hu et al., 2005, Hu et al., 2002). Given the severity of these defects and the frequent nature of their occurrence in human newborns (Kagan et al., 2022, Khan et al., 2022), it is important to unravel the molecular players driving cyto-differentiation in the ureter.

The exit of the ureteric progenitors from the proliferative phase is controlled by a complex network of signaling activities in which BMP4 has been recognized as a central hub. *Bmp4* is expressed in the undifferentiated UM from E11.5 to E14.5 under the control of epithelial SHH and WNT signals (Bohnenpoll et al., 2017d, Trowe et al., 2012). SHH triggers via SMO

signaling expression of the forkhead transcription factor (TF) gene *Foxf1* while WNTs activate expression of the T-box TF genes *Tbx2* and *Tbx3* via the canonical (CTNNB1-dependent) pathway in the UM (Aydoğdu et al., 2018, Bohnenpoll et al., 2017d). *Shh* expression is enhanced by epithelial FGFR1/2 signaling which is triggered by mesenchymal FGF7 and FGF10 and modulated by mesenchymal FGFR1/2 (Deuper et al., 2022, Meuser et al., 2022). Retinoic acid (RA) synthesized both in the UE and UM maintains the progenitors possibly by counteracting WNT signaling (Bohnenpoll et al., 2017a).

Human patients with heterozygous loss of *BMP4* as well as mice which carry one loss-of-function allele of the orthologous gene, exhibit at birth congenital anomalies of the kidney and the urinary tract including hypo- or dysplastic kidneys, and/or hydroureter with associated hydronephrosis (Miyazaki et al., 2000, Miyazaki et al., 2003, Weber et al., 2008). Pharmacological inhibition experiments in ureter explant systems revealed a requirement for *Bmp4* in SMC and S cell differentiation (Brenner-Anantharam et al., 2007, Wang et al., 2009). We recently showed that conditional (*Tbx18*^{cre}-mediated) loss of both alleles of *Bmp4* in the UM results in complete bilateral hydroureter and hydronephrosis at birth. Proliferation in the mesenchymal and epithelial primordia was severely reduced; SMC and urothelial differentiation failed (Mamo et al., 2017). Genetic analysis identified *Smad4* as an effector of BMP4 signaling in SMC differentiation (Tripathi et al., 2012, Mamo et al., 2017).

Given the complete loss of all differentiated cell types in *Bmp4cKO* ureters, it seems likely that BMP4 possibly via SMADs positively controls the expression of TF genes that activate cell-type specific differentiation programs in the ureteric tissue compartments. In fact, our previous work described that in *Bmp4cKO* ureters the SMC regulatory gene *Myocd* (Wang et al., 2003) is not activated in the UM, while expression of ΔNP63, a TF gene required for stratification and I/ B cell differentiation (Weiss et al., 2013), was abrogated in the UE (Mamo et al., 2017). Whether BMP4 impinges on some of the other TF genes already known to affect the mesenchymal SMC program such as *Gata2*, *Gata6*, *Foxf1*, *Id2*, *Tbx18*, *Tbx2/Tbx3*, *Tshz3* and *Sox9* (Airik et al., 2006, Airik et al., 2010, Aoki et al., 2004, Aydoğdu et al., 2018, Bohnenpoll et al., 2017d, Caubit et al., 2008, Kurz et al., 2022, Weiss et al., 2019) and/or urothelial differentiation including *Pparg*, *Grhl3*, *Foxa1*, *Elf3*, *Klf5* or *Ovol1* (Bell et al., 2011, Böck et al., 2014, Varley et al., 2009, Weiss et al., 2013, Yu et al., 2009) or uses as yet unknown TF genes to execute these programs has remained enigmatic. Using genetic and pharmacological disruption of BMP4 signaling and its *Smad4* effector and subsequent transcriptional profiling experiments, we here show that BMP4 signaling via SMADs directly controls expression of pro-differentiation TF genes but also impacts on signaling pathways, most notably RA signaling to indirectly control expression of crucial TF genes for ureter differentiation.

Results

Loss of *Bmp4* affects expression of genes encoding transcriptional regulators of epithelial and mesenchymal differentiation in the ureter

We previously reported that conditional (*Tbx18*^{cre}-mediated) deletion of *Bmp4* in the UM leads to a complete absence of differentiated cell types both in the epithelial and mesenchymal tissue compartments of the murine ureter at birth. To decipher the molecular programs and unravel TF genes whose loss may underlie these cyto-differentiation defects, we performed by micro-array technology unbiased transcriptional profiling of mutant ureters at E14.5, i.e. at the end of the undifferentiated phase. Using intensities >100 and fold changes ≥-2 in the two individual microarrays performed as filters, we identified 144 down-regulated genes (Fig. 1A, Table S1). Functional annotation using the DAVID software tool (david.ncifcrf.gov) revealed in this gene set enrichment of gene ontology (GO) terms relating to cyto-differentiation of the UE ("epithelial differentiation", "apical plasma membrane urothelial plaque", "cell differentiation", "keratinocyte differentiation" and "skin epidermis development"). GO terms relating to BMP signaling and the cyto-differentiation of the UM ("cell differentiation", "cardiac muscle differentiation", "regulation of smooth muscle differentiation") were less strongly but still significantly enriched (Fig. 1B, Table S2).

Many of the genes associated with the terms "epithelial differentiation" belonged to the group of the top 50 down-regulated genes including various *Upks* (*Upk1a, Upk1b, Upk2*, *Upk3a*) as well as TF genes previously implicated in stratification (*Trp63*) and S cell differentiation (*Pparg* and *Grhl3*) in the ureter and/or bladder (Liu et al., 2019, Pignon et al., 2013, Weiss et al., 2013, Yu et al., 2009). Genes associated with mesenchymal differentiation included the master regulator of SMC differentiation *Myocd* and its activator *Gata6* (Kurz et al., 2022, Wang et al., 2003) as well as SMC structural genes *Myh11*, *Actg2* and *Cnn1* (Fig. 1C).

Besides *Trp63*, *Pparg*, *Grhl3*, *Myocd* and *Gata6*, we curated *Msx2, Hopx*, *Smad9*, *Foxa1*, *Snai1* and *Irf5* as encoded TF genes in the list of 144 down-regulated genes. *Id* genes, direct targets of BMP/SMAD signaling (Hollnagel et al., 1999, Nakahiro et al., 2010), were at the threshold of the filters used as were *Tbx18* and *Foxf1*, TF genes essential for ureteric SMC differentiation (Airik et al., 2006, Bohnenpoll et al., 2017d). *Ovol1*, *Klf5* and *Elf3,* TF genes previously implicated in urothelial differentiation in the ureter and/or the bladder (Bell et al., 2011), were weakly reduced (Fig. 1D).

To validate these findings and to determine the time line and tissue specificity of expression, we performed RNA *in situ* hybridization analysis on proximal sections of E12.5 and E14.5 control and *Bmp4cKO* ureters starting with *Upk*s and selected top-down-regulated structural genes. *Upk1b*, *Rab27*, *Upk3a* and *Upk1a* were expressed in the UE of control embryos at E14.5; *Car3* and *Bmp4* (as a control) expression was found in the UM both at E12.5 and E14.5.

Expression of all these genes was severely reduced or absent in *Bmp4cKO* ureters (Fig. 1E). We did not detect expression of *Aldh3b2*, *Upk2*, *Ivl*, *Trim29*, *Perp* and *Fbxl22* in control or mutant ureters at either stage by this method (Fig. S1A). For the TF genes, we found expression of *Trp63*, *Pparg*, *Msx2* and *Grhl3* in the UE of control embryos at E14.5 which was lost in the mutant. Expression of *Foxa1*, *Klf5* and *Ovol1* was also confined to the UE at E14.5 but expression appeared only weakly reduced in the mutant ureter. *Hopx*, *Myocd* and *Foxf1* were confined to the UM of E14.5 control embryos. Expression in the mutant was lost (*Hopx, Myocd*) or strongly reduced (*Foxf1*). Expression of *Snai1*, *Gata6* and *Tbx18* was found in the UM of control embryos at both E12.5 and E14.5. *Id2* and *Id4* were strongly expressed in the UM and weakly in the UE. In the *Bmp4cKO* ureter, *Snai1*, *Gata6, Id2 and Id4* expression was strongly reduced at both stages, while expression of *Tbx18* appeared weakly reduced (Fig. 1F). Expression of *Smad9* and *Irf5* was not detected in control or mutant ureters while *Id1* and *Id3* were more broadly expressed, but appeared reduced in both tissue compartments (Fig. S1B). Other TF genes previously shown to be expressed in the UM and to be involved in SMC differentiation including *Gata2, Sox9, Tbx2, Tbx3* and *Tshz3* (Airik et al., 2010, Aydoğdu et al., 2018, Caubit et al., 2008, Weiss et al., 2019) were not or marginally affected in the microarray and appeared unchanged (or in case of *Tshz3* rather up-regulated) in the RNA *in situ* hybridization analysis (Fig. S1C).

We conclude from this analysis that *Bmp4* in the UM is essential for expression of *Hopx, Myocd, Snai1, Gata6, Id2, Id4* and *Foxf1* in the UM and of *Trp63*, *Pparg*, *Msx2* and *Grhl3* in the UE. *Tbx18* in the UM and *Foxa1, Klf5* and *Ovol1* in the UE depend only weakly on *Bmp4* (Fig. 1G).

Pharmacological inhibition experiments of explant cultures identify a set of TF genes that may directly depend on BMP4 signaling activity in the ureter

Reduced expression of TF genes in *Bmp4cKO* ureters at E14.5 may reflect the lack of direct BMP4 signaling inputs but may also relate to secondary changes that accumulated over time. To identify genes that are possibly directly controlled by BMP4 signaling, we switched to a short time pharmacological inhibition experiment with the BMP4 inhibitor NOGGIN (Zimmerman et al., 1996) in ureter explant cultures. We explanted ureters at E12.5, treated them for 18 h with 10 µg/ml NOGGIN and monitored transcriptional changes compared to the control by microarray technology. Using the same filters as above, we identified 90 down-regulated genes (Fig. 2A, Table S3). Functional annotation using DAVID did not recover GO terms relating to epithelial and SMC differentiation in this gene pool. Instead “cartilage development”, “negative regulation of osteoblast differentiation” and particularly “TGFß/BMP4” signaling terms were enriched (Fig. 2B, Table S4). This related to strong downregulation of genes encoding BMP signaling antagonists (*Grem2, Chrdl1, Chrdl2, Nog)* and signaling components

(*Smad9*) as well as (known) direct transcriptional targets (*Id* genes, *Smad9*) (Hollnagel et al., 1999, Tsukamoto et al., 2014) (Fig. 2C). Besides *Smad9* and *Id* genes, TF genes with reduced expression were *Tcf24, Sox9, Pparg, Tlx2, Cux2, Snai1, Atoh8, Ahr, Msx2* and *Tbx18*. From the TF genes with reduced expression in E14.5 *Bmp4cKO* ureters, *Irf5*, *Gata6* and *Hopx* were also affected while expression of *Ovol1, Foxa1*, *Trp63*, *Grhl3*, *Myocd, Klf5* and *Foxf1* was weakly reduced or was normal (Fig. 2D). RNA *in situ* hybridization analysis for *Tcf24*, *Tlx2*, *Cux2*, *Atoh8* and *Ahr* did not detect expression on sections of E12.5 ureters cultured for 18 h. *Tcf24* and *Tlx2* were neither detected in control nor in *Bmp4cKO* ureters at E12.5 or E14.5 while *Atoh8* and *Ahr* exhibited weak expression in the UM, which however, was difficult to distinguish from the background (Fig. S2A). *Cux2*, which showed weak expression in E12.5 and E14.5 wildtype UM as well (Fig. S2A), appeared reduced in the NOG-treated ureters (Fig. 2E). We validated other TF genes which showed specific expression in E12.5 control ureters. Expression of *Id2*, *Sox9*, *Snai1*, *Tbx18* and *Gata6* was clearly reduced in the mesenchyme of NOG treated E12.5 ureter explants. Expression of *Id4* was difficult to distinguish from the background (Fig. 2E). Expression of *Pparg* and *Msx2* was not detectable in E12.5 + 18 h ureter cultures. *Id1* and *Id3* were broadly expressed in the ureter but only Id3 expression appeared reduced upon NOG treatment (Fig. S2E).

To characterize whether the set of BMP4 regulated TF genes changes with time, we additionally profiled the transcriptional changes caused by treating E13.75 ureters for 18 h with 10 µg/ml NOG. In this setting, 66 genes with decreased expression were detected (Fig. 2G, Table S5). Functional annotations strongly enriched the terms “TGFß-signaling”, “osteoblast differentiation” and “cartilage development” similar to the situation at E12.5 (Fig. 2H, Table S6). Again, all *Id* genes and *Smad9* were strongly down-regulated. Additional TF genes with reduced expression above or around the filter threshold were *Pparg, Sp5, Ahr, Myocd, Msx2* and *Sox9*. From the TF genes which were reduced in E14.5 *Bmp4cKO* ureters or in E12.5 NOG-treated ureters *Tcf24*, *Cux2*, S*nai1*, *Atoh8*, *Tlx2*, *Irf5*, *Trp63*, *Gata6* and *Tbx18* were reduced as well, whereas *Hopx*, *Grhl3*, *Ovol1*, *Foxa1*, *Klf5* and *Foxf1* were not or only marginally affected (Fig. 2I, J). We performed RNA *in situ* hybridizations for most of these TF genes. We found that in E13.75 ureters treated with NOG for 18 h, expression of *Id2, Id4, Ahr, Myocd, Sox9, Snai1, Gata6* and *Tbx18* was clearly reduced in the UM, and of *Pparg* and *Msx2* in the UE (Fig. 2K). *Sp5* was weakly expressed in the UM of E13.75 treated explants and in E12.5 and E14.5 wildtype ureters. Expression upon NOG-treatment and in *Bmp4cKO* ureters appeared very weak (Fig. S2C, D). Expression of *Cux2* provided a lot of background, however it appeared clearly reduced in the UM upon NOG treatment (Fig. S2F). All other candidates (*Trp63, Hopx, Grhl3, Ovol1, Foxa1, Klf5, Foxf1*) were - as expected from the weak changes - not affected by the treatment (Fig. S2F). Expression of *Id1* and *Id3* again provided only unspecific or no staining (Fig. S2F). We conclude that BMP4 signaling robustly regulates a similar

set of TF genes in the UM (*Id2*, *Id4*, *Cux2*, *Gata6*, *Snai1*, *Sox9* and weakly *Tbx18*) and in the UE (*Msx2*, *Pparg)* at both time-points analyzed (Fig. 2 F, L).

BMP4 administration leads to upregulation of some of the TF genes whose expression depends on BMP4 signaling

To further investigate which TF genes are directly regulated by BMP4, we performed a complementary BMP4 activation experiment. For this, we explanted E12.5 ureters, treated them for 18 h with 100 ng/ml BMP4 and profiled the transcriptional changes by microarray analysis. Using intensity >100 and fold change ≥2 as filters, we obtained 129 genes with increased expression (Fig. 3A, Table S7). Functional annotation found an enrichment of terms relating to BMP signaling and multicellular and cartilage development indicating again that BMP4 signaling components were up-regulated (Fig. 3B, Table S8). 29 of the genes encoded TF genes including ones that were described as targets of BMP signaling in other developmental contexts such as *Tbx20* and *Gata4* (Schultheiss et al., 1997) (Fig. 3C). When we compared the genes with increased expression from this microarray with the list of genes with reduced expression from the microarrays of NOG treated E12.5 and E13.75 ureters, we found a large overlap comprising *Gata6*, *Irf5*, *Cux2*, *Tcf24, Msx2*, *Smad9*, *Snai1*, *Pparg*, *Tlx2* and *Myocd* presenting most likely direct targets of BMP4 signaling in the ureter. Intriguingly, the *Id* genes, *Sox9, Atoh8* and *Ahr* which were strongly decreased upon NOG-treatment were not up-regulated by BMP4, possibly due to saturation of expression in the wildtype (Fig. 3D). RNA *in situ* hybridizations revealed increased expression of *Cux2*, *Gata6*, *Snai1* and *Id2* upon BMP4 treatment, all other TF genes tested were not detected by this method (Fig. 3E, Fig. S3).

BMP4 represses RA signaling to timely activate the ureteric cytodifferentiation programs

Our transcriptional profiling experiments revealed that expression of some of the TF genes is differentially affected by pharmacological short time inhibition of BMP4 signaling and genetic ablation of *Bmp4*. Some TF genes were similarly reduced in both conditions (*Gata6, Irf5, Msx2, Myocd, Pparg, Smad9, Snai1, Tbx18)*, some were more weakly affected in the genetic condition (*Ahr, Atoh8, Cux2, Id* genes, *Sox9, Sp5, Tcf24, Tlx2*) whereas a third group was only or more strongly affected by genetic loss of *Bmp4* (*Foxa1, Foxf1, Klf5, Ovol1* weakly and *Grhl3, Hopx* and *Trp63* strongly).

We hypothesized that the differences in the two latter groups may be due to (secondary) alterations in *Bmp4cKO* ureters of signals and/or signaling activities important for cyto-differentiation (Bohnenpoll et al., 2017a, Bohnenpoll et al., 2017d, Deuper et al., 2022, Meuser et al., 2022, Trowe et al., 2012). We interrogated this possibility by analyzing expression of

components and targets of SHH, WNT, FGFR1/2 and RA signaling in E14.5 *Bmp4cKO* ureters by RNA *in situ* hybridization (Fig. 4A-D).

In the microarray of E14.5 *Bmp4cKO* ureters, we found increased expression of *Shh* (+1.8), *Wnt9b* (+4.4), and of the genes encoding the RA-synthesizing enzymes *Aldh1a1* (+2.9), *Aldh1a2* (+3.7) and *Aldh1a3* (+4.8). In contrast, expression of *Fgf7* (-3.2) and *Fgf10* (-1.5) was reduced. Expression of the SHH signaling targets *Ptch1* (+1.2) and *Hhip1* (-1.4), of the WNT target *Axin2* (+1), of the FGFR receptor genes *Fgfr1* and *Fgfr2*, of the FGF signaling target *Spry1* (-1.3), and of the RA signaling target *Rarb* (+1.2) were marginally affected. The RA signaling target *Stra6 (*+1.9) was increased.

RNA *in situ* hybridization largely reflected these changes. *Shh* expression was clearly increased in the UE while *Ptch1* and *Hhip* appeared unaltered in the UM (Fig. 4A). *Wnt7b* was decreased while *Wnt9b* was strongly increased in the UE. *Axin2* was unchanged in the UM (Fig. 4B). Expression of *Fgf10* in the UM was decreased. Notably, *Fgfr1/2* showed reduced expression in the UM. Expression of *Spry1* appeared unchanged in the UE (Fig. 4C). Expression of RA-synthesizing enzyme *Aldh1a2* was strongly increased in the UM while *Aldh1a3* was strongly increased in the UE; *Aldh1a1* was not detected. *Rarb* and *Stra6* appeared slightly increased in the UM (Fig. 4E).

Owing to the report that RA signaling inhibits cyto-differentiation in the ureter (Bohnenpoll et al., 2017a), we wished to interrogate the possible significance of increased RA (signaling) levels on the expression of TF genes in *Bmp4cKO* ureters. For this, we first interrogated the data from a previous microarray profiling of transcriptional changes induced by treating E12.5 ureter explants for 18 h with RA and the RA signaling antagonist BMS (Bohnenpoll et al., 2017a). Intriguingly, we found for some of the genes with exclusive strongly decreased expression in *Bmp4cKO* ureters (*Grhl3, Trp63,* and *Hopx*), a reduction of expression upon RA treatment and a corresponding increase by BMS treatment suggesting that these genes are repressed by RA signaling. For *Sp5* and *Tlx2*, we found the opposite. Expression of *Foxa1* was also exclusively decreased in *Bmp4cKO* mutants, however RA treatment did not affect its expression and BMS treatment led to a further repression suggesting *Foxa1* expression depends on additional factors. For genes that strongly and quickly responded to BMP4 signaling changes (*Pparg, Msx2*) we found no expression changes upon RA treatment. However, application of BMS slightly decreased the expression of *Pparg* (Fig. 4E). To interrogate the possibility that the decreased expression of some of these TF genes in *Bmp4cKO* ureters is a consequence of increased RA signaling, we explanted E12.5 kidney and ureter rudiments, grew them for 4 days in the presence or absence of 10 µg/ml NOG and/or 1 µM RA and scored for the expression of *Grhl3*, *Trp63*, *Pparg* and *Foxa1* (Fig. 4F). After 4 days of NOG treatment the expression of *Grhl3, Trp63* and *Pparg* was strongly reduced, while *Foxa1* expression was only mildly affected, recapitulating the changes in *Bmp4cKO* mutant ureters (Fig. 4F). As expected, RA treatment did

not affect the expression of *Pparg* and *Foxa1*, but expression of *Grhl3* was nearly absent. Expression of *Trp63* appeared only weakly affected (Fig. 4F). In E12.5 explants treated with a combination of 10 µg/ml NOG and 1 µM BMS, expression of *Grhl3* was regained in half of the individuals analyzed. In contrast, expression of *Trp63* was not detectable under these conditions. Expression of *Pparg* and *Foxa1* was even more reduced (Fig. 4E, F).
We conclude that loss of *Grhl3* in *Bmp4cKO* mutants is due to increased RA signaling. Increased RA signaling also contributes to the reduction of *Trp63* expression whereas *Pparg* is unaffected by altered RA signaling levels.

Epithelial loss of *Smad4* delays urothelial differentiation

We previously reported that the conditional (*Tbx18*^{cre}-mediated) loss of *Smad4* in the UM resulted in weak hydroureter formation due to a delay in the activation of *Myocd* and the SMC differentiation program. To interrogate the relevance of the SMAD effector pathway in the differentiation of the UE, we combined a floxed allele of *Smad4* (Chu et al., 2004), and a *Pax2-cre* line which mediates recombination in the nephric duct, the precursor of the UE and of the renal collecting duct system (Trowe et al., 2011, Bohnenpoll et al., 2017a). We mated *Pax2-cre/+;Smad4*$^{fl/+}$ males with *Smad4*$^{fl/fl}$ females and analyzed the genotype distribution at different time points of embryogenesis. At all stages analyzed, *Pax2-cre/+;Smad4*$^{fl/fl}$ *(Smad4cKO(UE))* mice presented without external morphological defects and at the expected Mendelian frequency (Table S9). To judge whether loss of *Smad4* affects urothelial development, we analyzed by immunofluorescence expression of cyto-differentiation markers on proximal ureter sections from E14.5 to E18.5, and at postnatal day (P) 14 as an end-point. The epithelial marker CDH1 revealed a delay in urothelial stratification in *Smad4cKO(UE)* embryos. At E16.5, the UE was one-layered rather than two-layered as in the control. This was paralleled by reduced expression of ΔNP63, which occurred in few cells at E14.5 and marked all cells in the basal layer at E18.5 only. Few of these cells co-expressed the B cell marker KRT5 contrasting the situation in the control where KRT5 expression occurred in almost all cells of the basal layer. Expression of S100A1 and UPK1B which mark S cells of the luminal layer at E16.5 in the control was activated in some luminal cells at E18.5 only. Stratification and urothelial differentiation appeared unaltered at P14. SMC differentiation was not affected as shown by normal expression of TAGLN (Fig. 5A). Subsequent quantification confirmed reduced presentation of ΔNP63^{+} (B/I cells) from E14.5 to E18.5, of KRT5^{+} basal and of S100A1^{+} S cells from E16.5 to P14 (Fig. 5B, Table S10). We conclude that *Smad4* is required for correct timing and full execution of the urothelial cyto-differentiation programs.

SMAD effectors mediate part of the epithelial and mesenchymal differentiation program downstream of *Bmp4*

To investigate how the SMAD effector pathway affects global and TF gene expression patterns in the epithelial and mesenchymal compartments of the ureter, we independently performed microarray analysis of *Smad4cKO(UE)* ureters and of ureters with mesenchymal loss of *Smad4* (*Tbx18*$^{cre/+;}$*Smad4*$^{fl/fl}$, short: *Smad4cKO(UM))*. Using less stringent conditions for the fold change (intensity>100, fold change ≥-1.5) we identified 68 genes with reduced expression in *Smad4cKO(UE)* ureters (Fig. 6A, Table S11). Functional annotation revealed in this gene set enrichment of GO terms relating to cyto-differentiation of the UE ("skin barrier", "epithelial differentiation", "apical plasma membrane urothelial plaque", "epidermis development" and "skin epidermis development") mimicking a subset of the terms found in the microarrays of *Bmp4cKO* ureters (Fig. 6B, Table S12). In the list of top down-regulated genes, we found various *Upks* (*Upk3a, Upk1a, Upk1b, Upk3bl*), *Aldh3b2, Rab27b, Perp* and *Trim29*, similar to the situation in *Bmp4cKO* ureters (Fig. 6C). TF genes with reduced expression among the top 50 down-regulated genes were *Trp63, Msx2* and *Grhl3*. Manual inspection of the list revealed additional regulation of *Foxi1*, *Elf5* and *Pparg* (Fig. 6D). All these genes were less strongly down-regulated compared to *Bmp4cKO* mutant ureters. Expression of *Ovol1, Klf5* and *Foxa1* was not affected by epithelial loss of *Smad4* (Fig. 6D). *In situ* hybridization analysis confirmed downregulation of *Grhl3, Trp63* and *Pparg* (Fig. 6E). *Foxi1* and *Elf5* expression was not detected in wildtype ureters (Fig. S4A).

In E14.5 *Smad4cKO(UM)* ureters, we found 90 genes to be down-regulated using the same filter criteria as before (Fig. 6F, Table S13). Associated GO terms related to defects in "TGF-ß" and "BMP4-signaling", "muscle protein", "cartilage development", "heart development" and "cardiac muscle tissue development" again reflecting a subset of the terms found for *Bmp4cKO* ureters (Fig. 6G, Table S14). Among the top down-regulated genes, we found *Car3, Myh11, Actg2* and *Cnn1,* also being negatively regulated in *Bmp4cKO* ureters. TF genes with reduced expression comprised *Smad9, Irf5, Myocd, Id2, Id1, Id3, Smad6* and *Hopx* (Fig. 6H, I). Other TF genes including *Snai1, Tbx18, Cux2, Gata6, Atoh8, Sox9, Id4, Foxf1, Sp5* and *Ahr* were not or only very mildly affected. Inspection by *in situ* hybridization confirmed strong downregulation of *Myocd, Id2, Smad6* and *Hopx* in the UM (Fig. 6J). Again, *Smad9* expression was not detectable in either ureter compartment. Expression of *Id1* and *Id3* was reduced in the UM (Fig. S4B).

We next intersected the lists of genes with reduced expression in *Smad4cKO(UM)*, *Smad4cKO(UE)* and *Bmp4cKO* ureters with each other (Fig. 7). In the overlap of the 26 genes between the *Smad4cKO(UE)* and *Bmp4cKO* gene lists were the TF genes *Grhl3*, *Msx2, Trp63* and *Pparg*, i.e. all TF genes with strong downregulation in *Bmp4cKO* ureter. In the overlap of

the 29 genes between the *Smad4cKO(UE)* and *Bmp4cKO* gene lists were the TF genes *Hopx*, *Myocd*, *Smad9* and *Irf5* as well as the *Id* genes (Fig. 6J). We conclude that SMAD effectors mediate parts of the epithelial and mesenchymal differentiation program downstream of BMP4 signaling.

Discussion

Here, we characterized BMP4 signaling as an important regulator of TF gene activation as well as a coordinator of signaling pathways to guide cyto-differentiation in the UE and the UM. Our work indicates that transcriptional activation of some TF genes directly depends on *Bmp4* while others are controlled indirectly. We showed that *Bmp4* represses the expression of *Aldh1a2* in the UM and of *Aldh1a3* in the UE, respectively. Hence, BMP4 signaling limits the activity of RA signaling and thereby indirectly increases *Grhl3* expression. Furthermore, this study confirms that SMAD effectors partly mediate BMP4 function in the UE and the UM.

BMP4 signaling coordinates signaling activities in early ureter development

SHH, WNT, RA and FGF signaling exert important functions during early murine ureter development acting at least partly together in regulatory networks (Bohnenpoll et al., 2017a, Bohnenpoll et al., 2017d, Deuper et al., 2022, Meuser et al., 2022, Trowe et al., 2012). Here, we showed that BMP4 is not only a downstream effector of these signaling pathways but controls their activities in both the mesenchymal and epithelial compartments of the early ureter.

We found that *Bmp4* is required for expression of mesenchymal *Fgf10* and *Fgfr2* while epithelial FGF signals are independent from BMP4 signaling input. During ureter development epithelial FGFR2 is activated by mesenchymal FGF10 (and FGF7) while mesenchymal FGFR2 acts as a sink for FGF ligands to prevent overactivation of the epithelial receptor (Deuper et al., 2022). Since expression of the FGFR2 signaling target *Spry1* is unaffected in the UE, the combined reduction of both *Fgf10* and mesenchymal *Fgfr2* may leave epithelial FGFR2 activation unaffected.

We detected upregulation of *Shh* in the UE of *Bmp4cKO* embryos while SHH signaling targets in the UM appeared unaltered (*Ptch1*) or down-regulated (*Hhip, Foxf1*). The importance of HH signaling during ureter development was deduced from transgenic mice lacking either *Shh* itself or its mediator Smoothened (*Smo*) (Bohnenpoll et al., 2017d, Yu et al., 2002). The role of another homolog of the hedgehog family, *Indian hedgehog (Ihh),* that signals also via PTCH/SMO and controls the same set of target genes including *Hhip*, has not yet been addressed in the ureter (Sigafoos et al., 2021). Interestingly, *Ihh* is strongly down-regulated (-4.6) in *Bmp4cKO* ureters and may therefore compensate the increase of *Shh* expression, resulting in normal or decreased activation of HH targets genes.

The RA signaling pathway was strongly affected by genetic deletion of *Bmp4*. Expression of the RA synthesizing enzymes (*Aldh1a1, Aldh1a2* and *Aldh1a3*) as well as of RA receptor and target genes (*Rarb, Stra6*) was strongly increased. Owing to the fact that RA signaling was previously shown to inhibit ureteric cyto-differentiation and thereby promote proliferation of progenitors (Bohnenpoll et al., 2017a), it is conceivable that increased RA signaling contributes

to the cyto-differentiation defects in *Bmp4cKO* ureters. BMP4 signaling may therefore regulate cyto-differentiation both by inhibiting pro-proliferative RA signaling and by promoting the expression of pro-differentiation TF genes (see below).
Although expression of the WNT signaling target gene *Axin2* was unchanged in *Bmp4cKO* ureters, we found increased expression of the gene encoding the WNT ligand WNT9B. Since *Wnt9b* has been described as a target of RA signaling (Bohnenpoll et al., 2017a), its upregulation might be a consequence of increased RA signaling. Unaltered activity of canonical signaling might be the consequence of downregulation of a second WNT ligand gene, *Wnt7b*, in the UE of *Bmp4cKO* ureter.

BMP4 signaling directs SMC development by controlling *Myocd* activation

We previously showed that *Bmp4* is required in the mesenchymal compartment of the developing ureter for activation of *Myocd,* the master regulator of visceral SMC differentiation (Mamo et al., 2017). Here, we confirmed this finding and collected evidence that *Myocd* expression and hence SMC differentiation is controlled in multiple ways by BMP4 signaling. Importantly, we uncovered that *Myocd* directly depends on *Bmp4*, since application of BMP4 to ureter explant cultures was sufficient to increase its expression. However, we detected a much stronger deregulation in *Bmp4cKO* ureters than in NOG treated ureters, arguing for additional input(s) on *Myocd*. In fact, we found that *Tbx18, Gata6* and *Sox9*, TF genes that were all described to impact on *Myocd* expression and/or SMC differentiation during ureter development (Airik et al., 2006, Airik et al., 2010, Kurz et al., 2022), are also positively regulated by BMP4 signaling. Moreover, *Atoh8* and *Ahr* present additional TF genes which depend directly on *Bmp4* in the UM. Although the function of both TF genes has not yet been addressed in the context of ureter development, *Atoh8* impacts on the expression of *MyoD* (the master regulator of skeletal muscle differentiation) during zebrafish development (Yao et al., 2010).
Moreover, we found that *Foxf1* and *Hopx* are indirectly regulated by BMP4 signaling in the UM. *Foxf1* is the most critical transcriptional activator of *Myocd* expression during ureter development (Bohnenpoll et al., 2017c). The function of *Hopx* was not addressed during ureter development but it was shown that *Hopx* is required for differentiation of cardiomyocytes (Friedman et al., 2018).
Together, our findings suggest that BMP4 signaling directly impinges on *Myocd* expression but may also indirectly activate expression of this gene by inducing and/or maintaining expression of a number of TF genes including *Tbx18, Sox9, Gata6, Atoh8* and *Ahr* in the UM.

Bmp4 controls the expression of TF genes in the urothelium to guide stratification and cyto-differentiation

A number of TF genes has previously been characterized to regulate urothelial cyto-differentiation in the bladder and/or ureter. Whether these TF genes are sufficient to account for all differentiation events or whether additional TF genes are involved has remained enigmatic as has been the activation and regulation, respectively, of these TF genes by BMP4 signaling.
Our study provides compelling evidence that BMP4 signaling directly controls the activation of two TF genes in the UE, namely *Pparg* and *Msx2*. *Pparg* was previously shown to be indispensable for S cell differentiation and uroplakin production in the murine bladder (Liu et al., 2019, Varley et al., 2006, Varley et al., 2004) while *Msx2* was described to impact on the development of the murine vaginal epithelium. The vaginal epithelium of *Msx2* null mice lacks the superficial cell layer and shows abnormal I/B cell layers (Yin et al., 2006). Hence, it is likely that *Bmp4* controls epithelial development and S cell differentiation in the ureter by activating the expression of these TF genes.
Our work also showed that *Ovol1, Klf5, Foxa1* and *Grhl3* are indirectly activated by BMP4 signaling. All of these TF genes are critical for the differentiation of S cells in the murine bladder urothelium (Bell et al., 2011, Yu et al., 2009, Varley et al., 2009) making them candidate regulators of this cyto-differentiation program in the ureter.
Bmp4cKO ureters do not only suffer from a lack of S cell differentiation, they exhibit a complete lack of urothelial differentiation and stratification (Mamo et al., 2017). Our work defined *Trp63* as a downstream effector of *Bmp4*. *Trp63* encodes for P63 protein, of which the ΔN isoform is expressed in the ureter. $\Delta NP63^+$ cells stratify and serve as a precursor population for S and B cells (Bohnenpoll et al., 2017a). Similar to *Myocd, Trp63* seems to depend on *Bmp4* both in a direct and indirect fashion. *Trp63* is strongly down-regulated in *Bmp4cKO* ureters, while its expression upon NOG treatment is only mildly affected. This points to additional factors downstream of *Bmp4* controlling *Trp63* expression.
Taken together this study unraveled a network of TF genes that are likely to control epithelial stratification and cyto-differentiation downstream of BMP4 signaling.

BMP4 represses RA signaling to induce TF gene expression important for cyto-differentiation

Our transcriptional profiling experiments showed that *Grhl3* is strongly down-regulated in *Bmp4cKO* ureters but is unchanged in ureters treated with NOGGIN, strongly indicating that expression of this gene indirectly depends on BMP4 signaling. Interestingly, we described in a previous study that RA signaling represses *Grhl3* expression in the early ureter (Bohnenpoll et al., 2017b). Moreover, we found here that RA signaling is increased in *Bmp4cKO* ureters and

that inhibition of RA signaling by BMS application in NOG treated ureter explants rescued *Grhl3* expression in half of the individuals analyzed providing strong evidence that loss of *Grhl3* expression in *Bmp4cKO* ureters is a consequence of increased RA signaling.
Since *Trp63* expression was decreased in RA treated ureter cultures and up-regulated in BMS treated cultures, we tested whether combined NOG and BMS treatment might at least partly rescue *Trp63* expression. Surprisingly, we found no rescue of *Trp63* by this treatment. This points to additional (up to now unidentified) factors regulated by *Bmp4* that in turn regulate the expression of *Trp63*.
Hopx was also recognized as an indirect target of *Bmp4*. Again, we found reduced expression upon RA treatment and increased expression following BMS treatment. It is possible that *Hopx* is also lost due to increased RA signaling in the background of *Bmp4cKO* ureters. Whether *Hopx* expression can be reinstalled in NOG treated ureters by application of BMS remains to be analyzed.
Hence, our study provides evidence that timely expression of some TF genes including *Grhl3*, relies on suppression of RA signaling by BMP4.

TF genes in the UE are expressed in a temporal asynchrony to TF genes in the UM

Bmp4 expression occurs in the UM from E11.5 to E14.5. Interestingly, we found that *Bmp4*-dependent mesenchymal TF genes are already expressed at E12.5 (with the exception of *Myocd*) whereas expression of direct TF target genes in the UE occurs only at E14.5. There are at least three explanations for this dichotomy: First, expression of BMP4 receptors might differ in the UM and in the UE. Second, inhibitory factors may selectively prevent premature expression of TF genes in the UE. Third, epithelial TF genes require additional inputs for expression that only occur from E14.5 onwards in the UE. Irrespective of the precise molecular explanation, it is obvious that BMP4 signaling impinges differentially on TF gene activation in the epithelial and mesenchymal compartment of the ureter.

Smad4 affects the precise temporal activation of the epithelial differentiation and stratification programs downstream of *Bmp4*

We previously reported that mesenchymal *Smad4* is an important mediator of BMP4 signaling in the activation of *Myocd* expression and SMC differentiation (Mamo et al., 2017). Here, we showed that inactivation of *Smad4* in the UE resulted in a delayed onset of ΔNP63 expression, and a delay in stratification and B and S cell differentiation indicating a similar requirement in the timely activation of epithelial cyto-differentiation.

We used a *Pax2cre* line to inactivate *Smad4* in the UE. Mutants occurred in the expected frequency. This is in contrast to previous studies, that reported embryonic lethality of *Pax2cre/+;Smad4*$^{fl/fl}$ mutants (Laronda et al., 2013). This discrepancy may be due to different genetic backgrounds of the mice and the use of different Cre lines. While our transgene was constructed by fusing a murine 8.5 kbp *Pax2* upstream fragment (Kuschert et al., 2001) to a Cre gene cassette containing a nuclear localization signal (Lewandoski et al., 1997), our colleagues generated their *Pax2-Cre* transgenic line by modification of a *Pax2* bacterial artificial chromosome (BAC) (Ohyama and Groves, 2004). In the *Smad4* line used in our study the first exon was floxed (Chu et al., 2004) while exon 8 was floxed in the line used in the previous study (Yang et al., 2002).

Our study demonstrated the need for *Smad4* to precisely activate ΔNP63 expression at E14.5 in the murine ureter. The dependence of ΔNP63 on SMAD4 mediated BMP4 signaling was described before in the context of the development of the murine vaginal epithelium where inactivation of *Smad4* completely abolished ΔNP63 expression (Laronda et al., 2013). However, in our study ΔNP63 expression was delayed but not absent. This may be due to additional effectors of BMP4 signaling that act cooperatively to induce epithelial differentiation. In fact, we have previously reported that BMP4 function in the mesenchyme is synergistically mediated by SMADs and AKT and P38 kinases. Furthermore, we have demonstrated that the development of the UE at least partly depends on AKT, P38 and ERK kinase activity. However, inhibition of none of these factors alone or in combination was able to abolish ΔNP63 expression (Mamo et al., 2017). Our data suggests that *Smad4* is an additional effector of BMP4 signaling in the UE. Synergistic action of SMAD4 and P38 downstream of TGFß/BMP has previously been described in the oral epithelium where pharmacological inhibition experiments demonstrated that blockage of only one downstream effector delays development, while blockage of both downstream effectors arrests development (Xu et al., 2008). Whether SMAD4 acts synergistically with effector kinases in the development of the murine UE will be an important question of future research.

SMAD effectors partly mediate *Bmp4* function in the UM and the UE

We have shown in this and in a recent study that *Smad4* is important for epithelial and mesenchymal cyto-differentiation in the ureter (Mamo et al., 2017). Here, we provided evidence that the molecular function of BMP4 is also partly mediated by SMADs in both ureteric tissue compartments. We have identified *Grhl3, Pparg* and *Trp63* in the UE and *Myocd, Id2, Smad6* and *Hopx* in the UM as important TF genes regulated by the BMP4-SMAD-signaling axis. However, for most of the genes (except for *Id2*) the expression changes were attenuated in the *Smad4cKO* compared to the *Bmp4cKO* mutants. This points to the possibility that expression of these TF genes only partly depends on SMAD mediators, and that there are additional

downstream effectors of BMP4 that impinge on the same set of target genes. It has been reported that e.g. *Snai1* expression depends on SMAD or MAPK signaling (Simon-Tillaux and Hertig, 2017). Our comparisons of the transcriptional profiles of *Bmp4cKO*, *Smad4cKO(UE)* and *Smad4cKO(UM)* ureters revealed that expression of a large set of genes depends on *Bmp4* but is not affected by the loss of *Smad4* supporting the idea that these genes are exclusively and predominantly regulated by SMAD independent mediators.

Material and Methods

Mice

All mouse lines used in this study were maintained on an NMRI outbred background. In the *Bmp4* allele used (*Bmp4*^{tm3Blh}, synonym: *Bmp4*^{fl}) Cre recombinase recognition sites (loxP) were placed upstream and downstream of exons 3 and 4, within intron 2 and 3' of the poly-adenylation site, such that Cre recombination excises the entire *Bmp4* protein coding sequence (Kulessa and Hogan, 2002). In the *Smad4* allele used (*Smad4*^{tm1Rob}, synonym: *Smad4*^{fl}) the first codon was flanked with *loxP* sites (Chu et al., 2004). Recombination of the *Bmp4*^{fl} and *Smad4*^{fl} allele in the ureteric mesenchyme was achieved with the *Tbx18*$^{tm4(cre)Akis}$ line (synonym: *Tbx18*^{cre}) line previously generated in the lab (Airik et al., 2010) while recombination of the *Smad4*^{fl} allele in the ureteric epithelium used the *Tg(Pax2-cre)1AKis* (synonym: *Pax2-cre*) line (Bohnenpoll et al., 2017a, Trowe et al., 2011).

Embryos for ureter explant cultures were derived from matings of NMRI wildtype mice. Embryos for cellular and molecular analyses were derived from matings of *Tbx18*$^{cre/+}$*;Bmp4*$^{fl/+}$males with *Bmp4*$^{fl/fl}$ females, and from matings of *Pax2-cre/+;Smad4*$^{fl/+}$ and *Tbx18*$^{cre/+}$*;Smad4*$^{fl/+}$ males, respectively, with *Smad4*$^{fl/fl}$ females.

For timed pregnancies, vaginal plugs detected in the morning after mating were designated as embryonic day (E)0.5 at noon. Urogenital systems and embryos were dissected in PBS, fixed in 4% paraformaldehyde (PFA) in PBS and stored in methanol at -20°C. For genotyping by PCR genomic DNA prepared from yolk sacs or ear clip biopsies was used.

Mice were housed in rooms with controlled light and temperature. The experiments were in accordance with the German Animal Welfare Legislation and approved by the local Institutional Animal Care and Research Advisory Committee and permitted by the Lower Saxony State Office for Consumer Protection and Food Safety (AZ 33.12-42502-04-13/1356, AZ42500/1H).

Organ cultures

Ureters for explant cultures were dissected in L-15 Leibovitz medium (#F1315, Biochrom, Berlin, Germany), explanted on 0.4 µm polyester membrane Transwell supports (#3450, Corning) and cultured at the air-liquid interface with DMEM/F12 (#21331020, Gibco, Waltham, MA, USA) supplemented with 10% FCS (S0115, Biochrom), 1x Penicillin/Streptomycin (#15140122, Gibco), 1x non-essential amino acids (#11140035, Gibco), 1x Pyruvate (#11360070, Gibco) and 1x Glutamax (#35050038, Gibco) in a humidified incubator with 5 % CO_2 at 37^{o}C. Pathway activating components were dissolved as follows: recombinant human BMP4 (100 ng/ml in 4 mM HCl/0.1% BSA; #PHP171, Abd Serotec, Oxford, UK), NOGGIN (10 µg/ml in ddH2O; #Z0320525, Genescript), BMS (#3509, Tocris) and retinoic acid (RA; 1 µM in

DMSO; #0695 Trocis). Medium containing DMSO or components was refreshed every second day.

Immunofluorescence analyses

Embryos, urogenital systems and ureter explants were fixed in 4% PFA, paraffin-embedded and sectioned to 5 µm. Immunofluorescence staining was performed using the following primary antibodies and dilutions: polyclonal rabbit-anti-KRT5 (1:200; #PRB-160P, Biolegend, San Diego, CA, USA), polyclonal rabbit-anti-ΔNP63 (1:100; clone Poly6190, #619001, BioLegend), monoclonal mouse-anti-UPK1B (1:200; clone1E1, #WH0007348M2, Sigma-Aldrich), polyclonal rabbit-anti-TAGLN (1:200; #ab14106, Abcam, Cambridge, UK) and polyclonal rabbit-anti-S100A1 (1:200 #C0318-1, Acris Antibodies, Herford, Germany). Fluorescent staining was performed using the following secondary antibodies: biotinylated goat-anti-rabbit IgG (1:200; #111065033; Dianova, Hamburg, Germany), biotinylated goat-anti-mouse IgG (1:200; #115-065-166, Jackson ImmunoResearch, Cambridgeshire, UK), Alexa488-conjugated goat-anti-rabbit IgG (1:400; #A11034; Molecular Probes, Carlsbad, CA, USA), and Alexa555-conjugated goat-anti-mouse IgG (1:400; #A21422; Molecular Probes). The signal of ΔNP63 was amplified using the Tyramide Signal Amplification system (#NEL702001KT, Perkin Elmer, Waltham, MA, USA). For co-stainings with primary antibodies of the same host (ΔNP63 and KRT5 or CDH1) the staining was performed sequentially and the epitope of the first antibody was blocked with goat-anti-rabbit FAB fragment (1:50; 111007003, Dianova). For antigen retrieval, paraffin sections were deparaffinized, pressure-cooked for 15 min in antigen unmasking solution (#H3300, Vector Laboratories, Burlingame, CA, USA), treated with 3% H_2O_2/PBS for blocking of endogenous peroxidases, washed in PBS-T (0.05% Tween-20 in PBS) and incubated in TNB Blocking Buffer (NEL702001KT, Perkin Elmer). Sections were then incubated with primary antibodies at 4ºC overnight. Nuclei were stained with 4',6-diamidino-2-phenylindole (DAPI, # 6335.1, Carl Roth, Karlsruhe, Germany).

In situ hybridization analysis

Section *in situ* hybridization on 10-µm paraffin sections using digoxigenin-labeled antisense riboprobes was performed as previously described (Moorman et al., 2001).

Whole mount *in situ* hybridization analysis

Whole-mount *in situ* hybridization was performed following a standard procedure with digoxigenin-labeled antisense riboprobes (Wilkinson and Nieto, 1993).

Microarray analysis

Two independent pools each of control and mutant or compound treated ureters were used for microarray analysis. Pool sizes were as follows: >20 ureters each form male and female E12.5 or E13.75 ureters, 20 ureters from E14.5 mutant embryos. Total RNA from each pool was extracted using peqGOLD RNApure (#30-1010, VWR international GmbH, Darmstadt, Germany) and subsequently processed by the Research Core Unit Transcriptomics of Hannover Medical School. Agilent whole Mouse Genome Oligo v2 (4x44K) Microarrays (#G4846A; Agilent Technologies Inc, Santa Clara, CA, USA) were used for transcriptome analysis. Normalized expression data were filtered using Microsoft Excel (MicrosoftCorp, Redmond, WA, USA). Functional enrichment analysis for up- and down-regulated genes was performed with DAVID 6.8 web-software (david.ncifcrf.gov), and terms were selected based on p-value.

Statistics

Statistical analysis was performed using the unpaired, two-tailed Student's *t*-test (GraphPad Prism version 7.03, GraphPad Software, San Diego, CA, USA; Excel, MicrosoftCorp). Values are indicated as mean±SD $P<0.05$ was considered significant.

Image documentation

Sections were photographed using a DM5000 microscope (Leica Camera, Wetzlar, Germany) with Leica DFC300FX digital camera or a Leica DMI6000B microscope with Leica DFC350FX digital camera. All images were then processed in Adobe Photoshop CS4 (Adobe, San Jose, CA, USA).

Acknowledgments

We thank Rolf Kemler for the anti-CDH1 antiserum. Microarray data used in this publication were generated by the Research Core Unit Genomics (RCUG) at Hannover Medical School.

Competing interests

No competing interests declared.

Author Contributions

L.D. and A.K. designed the study; L.D., N.H., T.M., F.B., and M.O.T. collected or provided the data; L.D., N.H., M.O.T. and A.K. analyzed the data; L.D. and A.K. drafted the manuscript; A.K. provided funding, A.K. supervised experiments; all authors edited the manuscript and approved it.

Funding

This work was supported by grants from by the Deutsche Forschungsgemeinschaft (German Research Foundation) [DFG KI 728/9-2 and DFG KI 728/12-1, to A.K.]

Data availability

Microarray data have been deposited in Gene Expression Omnibus under accession number GSE178093.

References

AIRIK, R., BUSSEN, M., SINGH, M. K., PETRY, M. & KISPERT, A. 2006. Tbx18 regulates the development of the ureteral mesenchyme. *J Clin Invest,* 116**,** 663-74.

AIRIK, R., TROWE, M. O., FOIK, A., FARIN, H. F., PETRY, M., SCHUSTER-GOSSLER, K., SCHWEIZER, M., SCHERER, G., KIST, R. & KISPERT, A. 2010. Hydroureternephrosis due to loss of Sox9-regulated smooth muscle cell differentiation of the ureteric mesenchyme. *Hum Mol Genet,* 19**,** 4918-29.

AOKI, Y., MORI, S., KITAJIMA, K., YOKOYAMA, O., KANAMARU, H., OKADA, K. & YOKOTA, Y. 2004. Id2 haploinsufficiency in mice leads to congenital hydronephrosis resembling that in humans. *Genes Cells,* 9**,** 1287-96.

AYDOĞDU, N., RUDAT, C., TROWE, M. O., KAISER, M., LÜDTKE, T. H., TAKETO, M. M., CHRISTOFFELS, V. M., MOON, A. & KISPERT, A. 2018. TBX2 and TBX3 act downstream of canonical WNT signaling in patterning and differentiation of the mouse ureteric mesenchyme. *Development,* 145**,** 171827.

BELL, S. M., ZHANG, L., MENDELL, A., XU, Y., HAITCHI, H. M., LESSARD, J. L. & WHITSETT, J. A. 2011. Kruppel-like factor 5 is required for formation and differentiation of the bladder urothelium. *Dev Biol,* 358**,** 79-90.

BÖCK, M., HINLEY, J., SCHMITT, C., WAHLICHT, T., KRAMER, S. & SOUTHGATE, J. 2014. Identification of ELF3 as an early transcriptional regulator of human urothelium. *Dev Biol,* 386**,** 321-30.

BOHNENPOLL, T., FERARIC, S., NATTKEMPER, M., WEISS, A. C., RUDAT, C., MEUSER, M., TROWE, M. O. & KISPERT, A. 2017a. Diversification of Cell Lineages in Ureter Development. *J Am Soc Nephrol,* 28**,** 1792-1801.

BOHNENPOLL, T. & KISPERT, A. 2014. Ureter growth and differentiation. *Semin Cell Dev Biol,* 36**,** 21-30.

BOHNENPOLL, T., WEISS, A. C., LABUHN, M., LÜDTKE, T. H., TROWE, M. O. & KISPERT, A. 2017b. Retinoic acid signaling maintains epithelial and mesenchymal progenitors in the developing mouse ureter. *Sci Rep,* 7**,** 017-14790.

BOHNENPOLL, T., WITTERN, A. B., MAMO, T. M., WEISS, A. C., RUDAT, C., KLEPPA, M. J., SCHUSTER-GOSSLER, K., WOJAHN, I., LUDTKE, T. H., TROWE, M. O. & KISPERT, A. 2017c. A SHH-FOXF1-BMP4 signaling axis regulating growth and differentiation of epithelial and mesenchymal tissues in ureter development. *PLoS Genet,* 13**,** 1006951.

BOHNENPOLL, T., WITTERN, A. B., MAMO, T. M., WEISS, A. C., RUDAT, C., KLEPPA, M. J., SCHUSTER-GOSSLER, K., WOJAHN, I., LÜDTKE, T. H., TROWE, M. O. & KISPERT, A. 2017d. A SHH-FOXF1-BMP4 signaling axis regulating growth and differentiation of epithelial and mesenchymal tissues in ureter development. *PLoS Genet,* 13.

BRENNER-ANANTHARAM, A., CEBRIAN, C., GUILLAUME, R., HURTADO, R., SUN, T. T. & HERZLINGER, D. 2007. Tailbud-derived mesenchyme promotes urinary tract segmentation via BMP4 signaling. *Development,* 134**,** 1967-75.

CAUBIT, X., LYE, C. M., MARTIN, E., CORE, N., LONG, D. A., VOLA, C., JENKINS, D., GARRATT, A. N., SKAER, H., WOOLF, A. S. & FASANO, L. 2008. Teashirt 3 is necessary for ureteral smooth muscle differentiation downstream of SHH and BMP4. *Development,* 135**,** 3301-10.

CHU, G. C., DUNN, N. R., ANDERSON, D. C., OXBURGH, L. & ROBERTSON, E. J. 2004. Differential requirements for Smad4 in TGFbeta-dependent patterning of the early mouse embryo. *Development,* 131**,** 3501-12.

DALGHI, M. G., MONTALBETTI, N., CARATTINO, M. D. & APODACA, G. 2020. The Urothelium: Life in a Liquid Environment. *Physiol Rev,* 100**,** 1621-1705.

DEUPER, L., MEUSER, M., THIESLER, H., JANY, U. W. H., RUDAT, C., HILDEBRANDT, H., TROWE, M. O. & KISPERT, A. 2022. Mesenchymal FGFR1 and FGFR2 control patterning of the ureteric mesenchyme by balancing SHH and BMP4 signaling. *Development,* 149**,** 12.

FRIEDMAN, C. E., NGUYEN, Q., LUKOWSKI, S. W., HELFER, A., CHIU, H. S., MIKLAS, J., LEVY, S., SUO, S., HAN, J. J., OSTEIL, P., PENG, G., JING, N., BAILLIE, G. J., SENABOUTH, A., CHRIST, A. N., BRUXNER, T. J., MURRY, C. E., WONG, E. S., DING, J., WANG, Y., HUDSON, J., RUOHOLA-BAKER, H., BAR-JOSEPH, Z., TAM, P. P. L., POWELL, J. E. & PALPANT, N. J. 2018. Single-Cell Transcriptomic Analysis of Cardiac Differentiation from Human PSCs Reveals HOPX-Dependent Cardiomyocyte Maturation. *Cell Stem Cell,* 23**,** 586-598.

HOLLNAGEL, A., OEHLMANN, V., HEYMER, J., RUTHER, U. & NORDHEIM, A. 1999. Id genes are direct targets of bone morphogenetic protein induction in embryonic stem cells. *J Biol Chem,* 274**,** 19838-45.

HU, C. C., LIANG, F. X., ZHOU, G., TU, L., TANG, C. H., ZHOU, J., KREIBICH, G. & SUN, T. T. 2005. Assembly of urothelial plaques: tetraspanin function in membrane protein trafficking. *Mol Biol Cell,* 16**,** 3937-50.

HU, P., MEYERS, S., LIANG, F. X., DENG, F. M., KACHAR, B., ZEIDEL, M. L. & SUN, T. T. 2002. Role of membrane proteins in permeability barrier function: uroplakin ablation elevates urothelial permeability. *Am J Physiol Renal Physiol,* 283**,** 30.

KAGAN, M., PLENICEANU, O. & VIVANTE, A. 2022. The genetic basis of congenital anomalies of the kidney and urinary tract. *Pediatr Nephrol,* 37**,** 2231-2243.

KHAN, K., AHRAM, D. F., LIU, Y. P., WESTLAND, R., SAMPOGNA, R. V., KATSANIS, N., DAVIS, E. E. & SANNA-CHERCHI, S. 2022. Multidisciplinary approaches for elucidating genetics and molecular pathogenesis of urinary tract malformations. *Kidney Int,* 101**,** 473-484.

KULESSA, H. & HOGAN, B. L. 2002. Generation of a loxP flanked bmp4loxP-lacZ allele marked by conditional lacZ expression. *Genesis,* 32**,** 66-8.

KURZ, J., WEISS, A. C., LÜDTKE, T. H., DEUPER, L., TROWE, M. O., THIESLER, H., HILDEBRANDT, H., HEINEKE, J., DUNCAN, S. A. & KISPERT, A. 2022. GATA6 is a crucial factor for Myocd expression in the visceral smooth muscle cell differentiation program of the murine ureter. *Development,* 149**,** 29.

KUSCHERT, S., ROWITCH, D. H., HAENIG, B., MCMAHON, A. P. & KISPERT, A. 2001. Characterization of Pax-2 regulatory sequences that direct transgene expression in the Wolffian duct and its derivatives. *Dev Biol,* 229**,** 128-40.

LARONDA, M. M., UNNO, K., ISHI, K., SERNA, V. A., BUTLER, L. M., MILLS, A. A., ORVIS, G. D., BEHRINGER, R. R., DENG, C., SINHA, S. & KURITA, T. 2013. Diethylstilbestrol induces vaginal adenosis by disrupting SMAD/RUNX1-mediated cell fate decision in the Müllerian duct epithelium. *Dev Biol,* 381**,** 5-16.

LEWANDOSKI, M., MEYERS, E. N. & MARTIN, G. R. 1997. Analysis of Fgf8 gene function in vertebrate development. *Cold Spring Harb Symp Quant Biol,* 62**,** 159-68.

LIU, C., TATE, T., BATOURINA, E., TRUSCHEL, S. T., POTTER, S., ADAM, M., XIANG, T., PICARD, M., REILEY, M., SCHNEIDER, K., TAMARGO, M., LU, C., CHEN, X., HE, J., KIM, H. & MENDELSOHN, C. L. 2019. Pparg promotes differentiation and regulates mitochondrial gene expression in bladder epithelial cells. *Nat Commun,* 10**,** 019-12332.

MAMO, T. M., WITTERN, A. B., KLEPPA, M. J., BOHNENPOLL, T., WEISS, A. C. & KISPERT, A. 2017a. BMP4 uses several different effector pathways to regulate proliferation and differentiation in the epithelial and mesenchymal tissue compartments of the developing mouse ureter. *Hum Mol Genet,* 26.

MAMO, T. M., WITTERN, A. B., KLEPPA, M. J., BOHNENPOLL, T., WEISS, A. C. & KISPERT, A. 2017b. BMP4 uses several different effector pathways to regulate proliferation and differentiation in the epithelial and mesenchymal tissue compartments of the developing mouse ureter. *Hum Mol Genet,* 26**,** 3553-3563.

MEUSER, M., DEUPER, L., RUDAT, C., AYDOĞDU, N., THIESLER, H., ZARNOVICAN, P., HILDEBRANDT, H., TROWE, M. O. & KISPERT, A. 2022. FGFR2 signaling enhances the SHH-BMP4 signaling axis in early ureter development. *Development,* 149**,** 12.

MIYAZAKI, Y., OSHIMA, K., FOGO, A., HOGAN, B. L. & ICHIKAWA, I. 2000. Bone morphogenetic protein 4 regulates the budding site and elongation of the mouse ureter. *J Clin Invest,* 105**,** 863-73.

MIYAZAKI, Y., OSHIMA, K., FOGO, A. & ICHIKAWA, I. 2003. Evidence that bone morphogenetic protein 4 has multiple biological functions during kidney and urinary tract development. *Kidney Int,* 63**,** 835-44.

MOORMAN, A. F., HOUWELING, A. C., DE BOER, P. A. & CHRISTOFFELS, V. M. 2001. Sensitive nonradioactive detection of mRNA in tissue sections: novel application of the whole-mount in situ hybridization protocol. *J Histochem Cytochem,* 49**,** 1-8.

NAKAHIRO, T., KUROOKA, H., MORI, K., SANO, K. & YOKOTA, Y. 2010. Identification of BMP-responsive elements in the mouse Id2 gene. *Biochem Biophys Res Commun,* 399**,** 416-21.

OHYAMA, T. & GROVES, A. K. 2004. Generation of Pax2-Cre mice by modification of a Pax2 bacterial artificial chromosome. *Genesis,* 38**,** 195-9.

PIGNON, J. C., GRISANZIO, C., GENG, Y., SONG, J., SHIVDASANI, R. A. & SIGNORETTI, S. 2013. p63-expressing cells are the stem cells of developing prostate, bladder, and colorectal epithelia. *Proc Natl Acad Sci U S A,* 110**,** 8105-10.

SCHULTHEISS, T. M., BURCH, J. B. & LASSAR, A. B. 1997. A role for bone morphogenetic proteins in the induction of cardiac myogenesis. *Genes Dev,* 11**,** 451-62.

SIGAFOOS, A. N., PARADISE, B. D. & FERNANDEZ-ZAPICO, M. E. 2021. Hedgehog/GLI Signaling Pathway: Transduction, Regulation, and Implications for Disease. *Cancers,* 13.

SIMON-TILLAUX, N. & HERTIG, A. 2017. Snail and kidney fibrosis. *Nephrol Dial Transplant,* 32**,** 224-233.

SUN, T. T., ZHAO, H., PROVET, J., AEBI, U. & WU, X. R. 1996. Formation of asymmetric unit membrane during urothelial differentiation. *Mol Biol Rep,* 23**,** 3-11.

TRIPATHI, P., WANG, Y., CASEY, A. M. & CHEN, F. 2012. Absence of canonical Smad signaling in ureteral and bladder mesenchyme causes ureteropelvic junction obstruction. *J Am Soc Nephrol,* 23**,** 618-28.

TROWE, M. O., AIRIK, R., WEISS, A. C., FARIN, H. F., FOIK, A. B., BETTENHAUSEN, E., SCHUSTER-GOSSLER, K., TAKETO, M. M. & KISPERT, A. 2012. Canonical Wnt signaling regulates smooth muscle precursor development in the mouse ureter. *Development,* 139**,** 3099-108.

TROWE, M. O., MAIER, H., PETRY, M., SCHWEIZER, M., SCHUSTER-GOSSLER, K. & KISPERT, A. 2011. Impaired stria vascularis integrity upon loss of E-cadherin in basal cells. *Dev Biol,* 359**,** 95-107.

TSUKAMOTO, S., MIZUTA, T., FUJIMOTO, M., OHTE, S., OSAWA, K., MIYAMOTO, A., YONEYAMA, K., MURATA, E., MACHIYA, A., JIMI, E., KOKABU, S. & KATAGIRI, T. 2014. Smad9 is a new type of transcriptional regulator in bone morphogenetic protein signaling. *Sci Rep,* 4.

VARLEY, C. L., BACON, E. J., HOLDER, J. C. & SOUTHGATE, J. 2009. FOXA1 and IRF-1 intermediary transcriptional regulators of PPARgamma-induced urothelial cytodifferentiation. *Cell Death Differ,* 16**,** 103-14.

VARLEY, C. L., GARTHWAITE, M. A., CROSS, W., HINLEY, J., TREJDOSIEWICZ, L. K. & SOUTHGATE, J. 2006. PPARgamma-regulated tight junction development during human urothelial cytodifferentiation. *J Cell Physiol,* 208**,** 407-17.

VARLEY, C. L., STAHLSCHMIDT, J., LEE, W. C., HOLDER, J., DIGGLE, C., SELBY, P. J., TREJDOSIEWICZ, L. K. & SOUTHGATE, J. 2004. Role of PPARgamma and EGFR signalling in the urothelial terminal differentiation programme. *J Cell Sci,* 117**,** 2029-36.

VELARDO, J. 1981. Histology of the ureter. In: *The ureter,* 2nd Ed., edited by Bergman H. *New York, Springer-Verlag*.

WANG, G. J., BRENNER-ANANTHARAM, A., VAUGHAN, E. D. & HERZLINGER, D. 2009. Antagonism of BMP4 signaling disrupts smooth muscle investment of the ureter and ureteropelvic junction. *J Urol,* 181**,** 401-7.

WANG, Z., WANG, D. Z., PIPES, G. C. & OLSON, E. N. 2003. Myocardin is a master regulator of smooth muscle gene expression. *Proc Natl Acad Sci U S A,* 100**,** 7129-34.

WEBER, S., TAYLOR, J. C., WINYARD, P., BAKER, K. F., SULLIVAN-BROWN, J., SCHILD, R., KNÜPPEL, T., ZUROWSKA, A. M., CALDAS-ALFONSO, A., LITWIN, M., EMRE, S., GHIGGERI, G. M., BAKKALOGLU, A., MEHLS, O., ANTIGNAC, C., NETWORK,

E., SCHAEFER, F. & BURDINE, R. D. 2008. SIX2 and BMP4 mutations associate with anomalous kidney development. *J Am Soc Nephrol,* 19**,** 891-903.

WEISS, A. C., BOHNENPOLL, T., KURZ, J., BLANK, P., AIRIK, R., LÜDTKE, T. H., KLEPPA, M. J., DEUPER, L., KAISER, M., MAMO, T. M., COSTA, R., VON HAHN, T., TROWE, M. O. & KISPERT, A. 2019. Delayed onset of smooth muscle cell differentiation leads to hydroureter formation in mice with conditional loss of the zinc finger transcription factor gene Gata2 in the ureteric mesenchyme. *J Pathol,* 248**,** 452-463.

WEISS, R. M., GUO, S., SHAN, A., SHI, H., ROMANO, R. A., SINHA, S., CANTLEY, L. G. & GUO, J. K. 2013. Brg1 determines urothelial cell fate during ureter development. *J Am Soc Nephrol,* 24**,** 618-26.

WILKINSON, D. G. & NIETO, M. A. 1993. Detection of messenger RNA by in situ hybridization to tissue sections and whole mounts. *Methods Enzymol,* 225**,** 361-73.

XU, X., HAN, J., ITO, Y., BRINGAS, P., JR., DENG, C. & CHAI, Y. 2008. Ectodermal Smad4 and p38 MAPK are functionally redundant in mediating TGF-beta/BMP signaling during tooth and palate development. *Dev Cell,* 15**,** 322-9.

YANG, X., LI, C., HERRERA, P. L. & DENG, C. X. 2002. Generation of Smad4/Dpc4 conditional knockout mice. *Genesis,* 32**,** 80-1.

YAO, J., ZHOU, J., LIU, Q., LU, D., WANG, L., QIAO, X. & JIA, W. 2010. Atoh8, a bHLH transcription factor, is required for the development of retina and skeletal muscle in zebrafish. *PLoS One,* 5**,** 0010945.

YIN, Y., LIN, C. & MA, L. 2006. MSX2 promotes vaginal epithelial differentiation and wolffian duct regression and dampens the vaginal response to diethylstilbestrol. *Mol Endocrinol,* 20**,** 1535-46.

YU, J., CARROLL, T. J. & MCMAHON, A. P. 2002. Sonic hedgehog regulates proliferation and differentiation of mesenchymal cells in the mouse metanephric kidney. *Development,* 129**,** 5301-12.

YU, Z., MANNIK, J., SOTO, A., LIN, K. K. & ANDERSEN, B. 2009. The epidermal differentiation-associated Grainyhead gene Get1/Grhl3 also regulates urothelial differentiation. *Embo J,* 28**,** 1890-903.

ZIMMERMAN, L. B., DE JESÚS-ESCOBAR, J. M. & HARLAND, R. M. 1996. The Spemann organizer signal noggin binds and inactivates bone morphogenetic protein 4. *Cell,* 86**,** 599-606.

Figures/Figure Legend

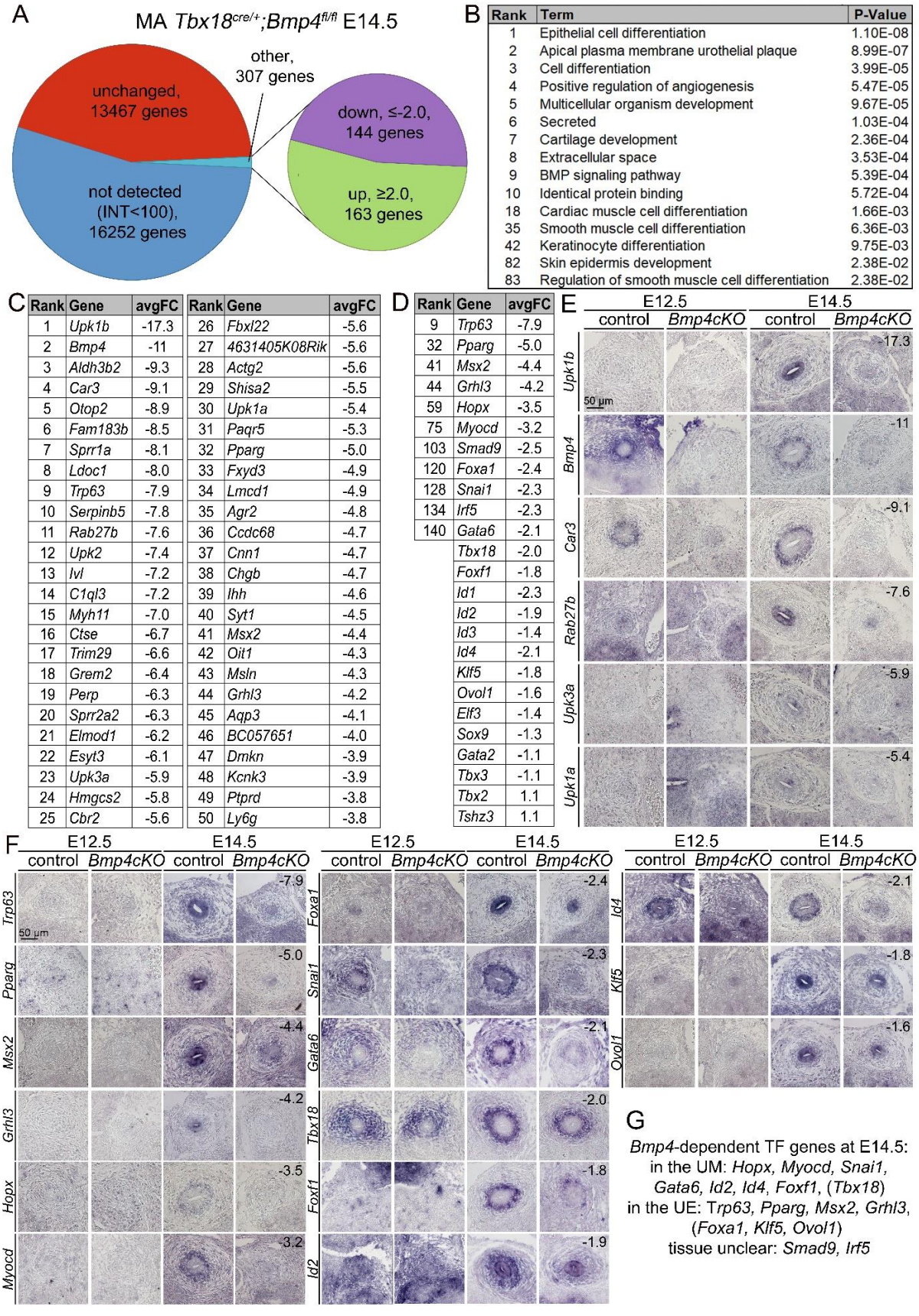

Rank	Term	P-Value
1	Epithelial cell differentiation	1.10E-08
2	Apical plasma membrane urothelial plaque	8.99E-07
3	Cell differentiation	3.99E-05
4	Positive regulation of angiogenesis	5.47E-05
5	Multicellular organism development	9.67E-05
6	Secreted	1.03E-04
7	Cartilage development	2.36E-04
8	Extracellular space	3.53E-04
9	BMP signaling pathway	5.39E-04
10	Identical protein binding	5.72E-04
18	Cardiac muscle cell differentiation	1.66E-03
35	Smooth muscle cell differentiation	6.36E-03
42	Keratinocyte differentiation	9.75E-03
82	Skin epidermis development	2.38E-02
83	Regulation of smooth muscle cell differentiation	2.38E-02

Rank	Gene	avgFC	Rank	Gene	avgFC
1	*Upk1b*	-17.3	26	*Fbxl22*	-5.6
2	*Bmp4*	-11	27	*4631405K08Rik*	-5.6
3	*Aldh3b2*	-9.3	28	*Actg2*	-5.6
4	*Car3*	-9.1	29	*Shisa2*	-5.5
5	*Otop2*	-8.9	30	*Upk1a*	-5.4
6	*Fam183b*	-8.5	31	*Paqr5*	-5.3
7	*Sprr1a*	-8.1	32	*Pparg*	-5.0
8	*Ldoc1*	-8.0	33	*Fxyd3*	-4.9
9	*Trp63*	-7.9	34	*Lmcd1*	-4.9
10	*Serpinb5*	-7.8	35	*Agr2*	-4.8
11	*Rab27b*	-7.6	36	*Ccdc68*	-4.7
12	*Upk2*	-7.4	37	*Cnn1*	-4.7
13	*Ivl*	-7.2	38	*Chgb*	-4.7
14	*C1ql3*	-7.2	39	*Ihh*	-4.6
15	*Myh11*	-7.0	40	*Syt1*	-4.5
16	*Ctse*	-6.7	41	*Msx2*	-4.4
17	*Trim29*	-6.6	42	*Oit1*	-4.3
18	*Grem2*	-6.4	43	*Msln*	-4.3
19	*Perp*	-6.3	44	*Grhl3*	-4.2
20	*Sprr2a2*	-6.3	45	*Aqp3*	-4.1
21	*Elmod1*	-6.2	46	*BC057651*	-4.0
22	*Esyt3*	-6.1	47	*Dmkn*	-3.9
23	*Upk3a*	-5.9	48	*Kcnk3*	-3.9
24	*Hmgcs2*	-5.8	49	*Ptprd*	-3.8
25	*Cbr2*	-5.6	50	*Ly6g*	-3.8

Rank	Gene	avgFC
9	*Trp63*	-7.9
32	*Pparg*	-5.0
41	*Msx2*	-4.4
44	*Grhl3*	-4.2
59	*Hopx*	-3.5
75	*Myocd*	-3.2
103	*Smad9*	-2.5
120	*Foxa1*	-2.4
128	*Snai1*	-2.3
134	*Irf5*	-2.3
140	*Gata6*	-2.1
	Tbx18	-2.0
	Foxf1	-1.8
	Id1	-2.3
	Id2	-1.9
	Id3	-1.4
	Id4	-2.1
	Klf5	-1.8
	Ovol1	-1.6
	Elf3	-1.4
	Sox9	-1.3
	Gata2	-1.1
	Tbx3	-1.1
	Tbx2	1.1
	Tshz3	1.1

Figure 1: *Bmp4* controls the expression of TF genes in the UE and the UM. See figure description on the next page.

Figure 1: *Bmp4* controls the expression of TF genes in the UE and the UM. (A) Pie chart visualizing differentially expressed genes in E14.5 *Bmp4cKO* mutant ureters found by global transcriptome analysis using microarray technology. (B) Functional annotation clustering by DAVID for down-regulated genes in mutant ureters. (C,D) List of top 50 down-regulated genes (C) and TF genes with decreased or unchanged expression (D) in *Bmp4cKO* ureters. Shown is the average fold change (avgFC) from two independent microarrays. Genes in (D) without a rank did not fulfill the initial filter criteria but were additionally inspected due to described expression and/or function in ureter development. (E,F) RNA *in situ* hybridization analysis on transverse ureter sections at the indicated stages of control and *Bmp4cKO* ureters at E12.5 and E14.5. Numbers in the upper right corner reflect the average fold change determined by microarray analysis. $n \geq 3$ for each probe and genotype. (G) Summary of *Bmp4* dependent TF genes in the UE and in the UM.

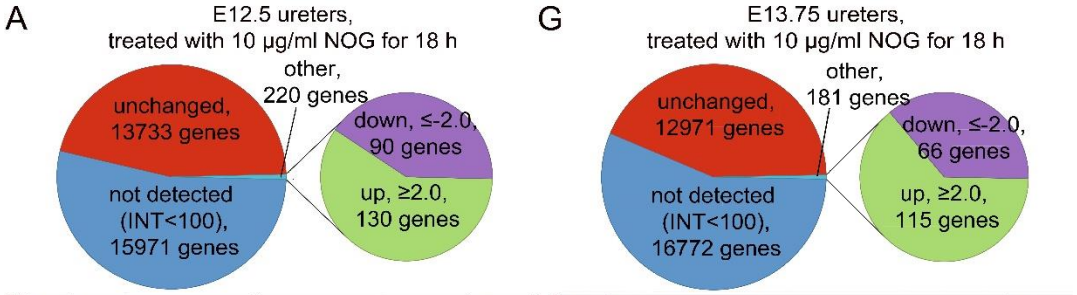

B

Rank	Term	P-Value
1	Cartilage development	3.50E-08
2	Negative regulation of osteoblast differentiation	1.57E-07
3	TGF-beta signaling pathway	1.64E-07
4	DNA-binding protein inhibitor	1.69E-07
5	Multicellular organism development	1.84E-07
6	Cell differentiation	4.06E-07
7	Extracellular region	9.17E-07
8	BMP signaling pathway	2.51E-06
9	Myc-type, basic helix-loop-helix domain	3.15E-06
10	Ossification	3.60E-06

H

Rank	Term	P-Value
1	DNA-binding protein inhibitor	7.67E-08
2	TGF-beta signaling pathway	1.04E-06
3	Negative regulation of osteoblast differentiation	1.25E-06
5	Myc-type, basic helix-loop-helix domain	1.47E-05
6	Cell differentiation	1.62E-05
8	Interaction with IFI204	4.04E-05
9	Circadian regulation of gene expression	4.50E-05
10	Negative regulation of transcription from RNA Pol II promotor	5.57E-05
27	Cartilage development	2.05E-03
33	BMP signaling pathway	3.41E-03

C

Rank	Gene	avgFC	Rank	Gene	avgFC
1	*Grem2*	-8.0	26	*Iigp1*	-3.3
2	*Id2*	-7.3	27	*Hs3st1*	-3.3
3	*Gata5os*	-7.2	28	*Micalcl*	-3.3
4	*Crhbp*	-6.3	29	*Kctd8*	-3.3
5	*Wfdc18*	-6.1	30	*ENSMUST00000131638*	-3.2
6	*Smad9*	-6	31	*Ednrb*	-3.2
7	*Gm4841*	-5.4	32	*Tlx2*	-3
8	*Gpr165*	-5.3	33	*a*	-3
9	*Npy1r*	-5.2	34	*Timp4*	-2.9
10	*Tcf24*	-5.2	35	*Cux2*	-2.9
11	*Sphkap*	-5.1	36	*LOC102633497*	-2.9
12	*Chrdl1*	-5.1	37	*Masp1*	-2.9
13	*Chrdl2*	-4.9	38	*Snai1*	-2.9
14	*Sox9*	-4.8	39	*Gdf5*	-2.8
15	*Brinp3*	-4.6	40	*Cck*	-2.8
16	*Pparg*	-4.2	41	*Id3*	-2.8
17	*Id1*	-4.2	42	*Akr1b7*	-2.8
18	*Id4*	-4	43	*Fgfr3*	-2.8
19	*Ptger2*	-3.9	44	*A_55_P1957123*	-2.8
20	*Gprin3*	-3.8	45	*Gm5105*	-2.8
21	*1010001N08Rik*	-3.7	46	*Kcnip4*	-2.8
22	*Nog*	-3.7	47	*Atoh8*	-2.7
23	*Myl1*	-3.6	48	*BC023105*	-2.7
24	*Sct*	-3.4	49	*Ahr*	-2.7
25	*Cdh18*	-3.4	50	*Col9a3*	-2.7

I

Rank	Gene	avgFC	Rank	Gene	avgFC
1	*Gsdmc3*	-7.0	26	*Tcf24*	-3.1
2	*Id2*	-6.2	27	*Pparg*	-3.1
3	*Ifit3*	-5.7	28	*S100a5*	-3.1
4	*Calcb*	-5.3	29	*Aqp3*	-3.1
5	*Gpr165*	-5.2	30	*Hmgcs2*	-3.0
6	*Grem2*	-4.9	31	*Sst*	-3.0
7	*Smad9*	-4.9	32	*Ugt2b34*	-3.0
8	*Ctse*	-4.8	33	*A_55_P2175050*	-3.0
9	*Id1*	-4.6	34	*Ihh*	-2.9
10	*Ednrb*	-5.2	35	*Calcr*	-2.9
11	*Fa2h*	-4.3	36	*Otor*	-2.9
12	*Iigp1*	-4.3	37	*Sp5*	-2.8
13	*ENSMUST00000131638*	-4.0	38	*Id3*	-2.8
14	*Sct*	-3.9	39	*Ahr*	-2.7
15	*Npy1r*	-3.8	40	*Insc*	-2.6
16	*Ldoc1*	-3.8	41	*Syt1*	-2.6
17	*Gm4951*	-3.7	42	*ENSMUST00000089689*	-2.6
18	*Pdzk1*	-3.7	43	*Ntng1*	-2.6
19	*Phlda2*	-3.5	44	*Myocd*	-2.5
20	*Id4*	-3.4	45	*Msx2*	-2.5
21	*BC023105*	-3.4	46	*Paqr5*	-2.5
22	*Dmkn*	-3.4	47	*Mansc4*	-2.5
23	*Nrn1l*	-3.3	48	*BC025446*	-2.5
24	*Wif1*	-3.3	49	*Maob*	-2.4
25	*Trim9*	-3.2	50	*Hpgd*	-2.4

D

Rank	Gene	avgFC
2	*Id2*	-7.3
6	*Smad9*	-6
10	*Tcf24*	-5.2
14	*Sox9*	-4.8
16	*Pparg*	-4.2
17	*Id1*	-4.2
18	*Id4*	-4
32	*Tlx2*	-3
35	*Cux2*	-2.9
38	*Snai1*	-2.9
41	*Id3*	-2.8
47	*Atoh8*	-2.7
49	*Ahr*	-2.7
56	*Msx2*	-2.6
65	*Tbx18*	-2.4
	Irf5	-2.3
	Gata6	-2.0
	Hopx	-1.8
	Ovol1	-1.7
	Foxa1	-1.5
	Trp63	-1.4
	Grhl3	-1.3
	Myocd	-1.2
	Klf5	-1.1
	Foxf1	1

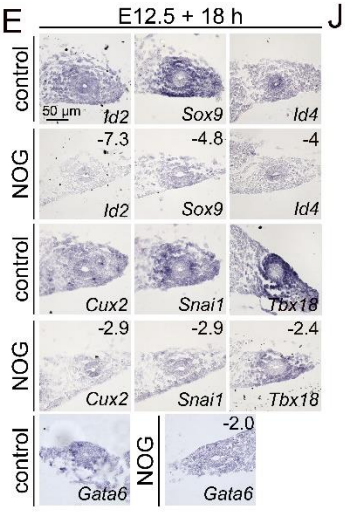

J

Rank	Gene	avgFC
2	*Id2*	-6.2
7	*Smad9*	-4.9
9	*Id1*	-4.6
20	*Id4*	-3.4
27	*Pparg*	-3.1
37	*Sp5*	-2.8
38	*Id3*	-2.8
39	*Ahr*	-2.7
44	*Myocd*	-2.5
45	*Msx2*	-2.5
61	*Sox9*	-2.3
	Tcf24	-3.1
	Cux2	-2.5
	Snai1	-2.4
	Atoh8	-2.4
	Tlx2	-2.1
	Irf5	-1.9
	Tbx18	-1.6
	Gata6	-1.7
	Trp63	-1.7
	Hopx	-1.4
	Grhl3	-1.3
	Ovol1	-1.3
	Foxa1	-1.2
	Klf5	-1.2
	Foxf1	1

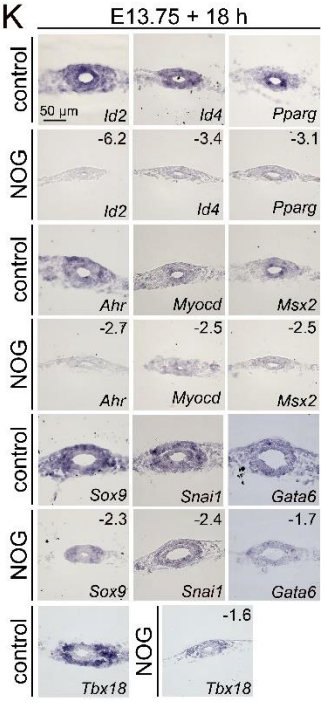

F *BMP4 signaling*-dependent TF genes at E12.5:
in the UM: *Id2, Sox9, Cux2, Snai1, Tbx18, Gata6 (Id4)*
most likely in the UE: *Pparg, Msx2*
tissue unclear: *Tcf24, Id1, Tlx2, Id3, Atoh8, Ahr*

L *BMP4 signaling*-dependent TF genes at E13.75:
in the UM: *Id2, Id4, Ahr, Myocd, Sox9, Cux2, Snai1, Gata6, Tbx18*
in the UE: *Pparg, Msx2*
tissue unclear: *Id1, Id3, Sp5*

Figure 2: Pharmacological inhibition experiments identify TF genes that may directly depend on BMP4 activity in the ureter. See figure description on the next page.

Figure 2: Pharmacological inhibition experiments identify TF genes that may directly depend on BMP4 activity in the ureter. (A,G) Pie chart summarizing microarray results from E12.5 (A) and E13.75 (G) ureters inhibited for 18 h with the BMP4 antagonist NOGGIN (NOG). (B,H) Functional annotation clustering by DAVID for down-regulated genes detected after BMP4 inhibition by NOG. (C,I) List of top 50 genes with strongest decreased expression after NOG treatment. Shown is the average fold change (avgFC) from two independent microarrays. (D,J) List of TF genes with decreased or unaffected expression after NOG treatment. TF genes at the bottom of the lists did not match the initial filter criteria but were manually inspected for being down-regulated in *Bmp4cKO* ureters. (E,K) RNA *in situ* hybridization analysis on transverse ureter sections of control and NOG (10 µg/ml) treated ureters. Numbers in the upper right corner reflect the average fold change from the microarray analysis. $n \geq 3$ for each probe and condition. (F,L) Summary of BMP4 signaling dependent TF genes and their tissue-specificity at the two time-points analyzed. UE, ureteric epithelium; UM ureteric mesenchyme.

A

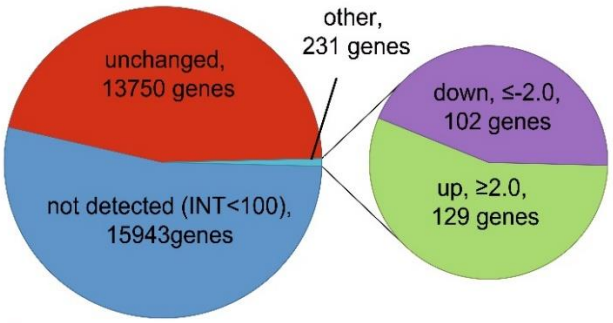

B

Rank	Term	P-Value
1	Regulation of transcription by RNA Pol II	5.34E-10
2	Negative regulation of BMP4 signaling pathway	6.12E-10
3	Sequence-specific double-stranded DNA binding	7.24E-10
4	Protein binding	1.13E-09
5	BMP4-signaling pathway	6.68E-09
6	Sequence specific DNA binding	6.84E-09
7	Multicellular organ development	1.00E-08
8	DNA-binding	1.06E-08
9	N-linked (GlcNAc…) asparagine	1.61E-08
10	Regulation of transcription, DNA templated	2.08E-08
11	Cartilage development	2.96E-08

C

Rank	TF Gene	INT				avgFC
		control 1	treated 1	control 2	treated 2	
3	*Tbx20*	32	194	18	167	7.7
12	*Gata4*	33	186	42	246	5.8
16	*Onecut2*	215	1139	253	1311	5.2
21	*Irx4*	127	487	154	801	4.5
24	*Cux2*	4072	17197	4888	22812	4.4
27	*Smad6*	2280	9212	2614	12233	4.4
33	*Msx1*	528	1946	586	2100	3.6
43	*Myocd*	39	134	52	164	3.3
47	*Zfpm1*	693	2461	1000	2904	3.2
48	*Tcf24*	36	111	38	123	3.2
51	*Msx2*	562	1691	691	2281	3.2
61	*Gata6*	12957	38502	14827	42333	2.9
62	*Irf5*	435	1105	365	1186	2.9
68	*Pitx1*	620	1928	841	2073	2.8
73	*Nkx3-1*	46	147	51	113	2.7
74	*Smad9*	854	2083	923	2742	2.7
75	*Hand1*	428	1046	386	1120	2.7
76	*Snai1*	2972	7930	3358	8976	2.7
77	*Sct*	3036	7497	2681	7517	2.6
78	*Rxrg*	256	603	207	597	2.6
97	*Hoxc9*	1693	3956	1574	4080	2.5
103	*Hoxb13*	91	207	121	304	2.4
104	*Smad7*	989	2072	1054	2821	2.4
107	*Tbx4*	217	544	291	624	2.3
109	*Prrx2*	4050	8512	3657	9066	2.3
114	*Pparg*	4409	10224	4668	10012	2.2
118	*Tlx2*	3509	7815	3334	7101	2.2
127	*Hr*	3450	7016	4566	9401	2.0
128	*Foxo6*	932	1865	1107	2306	2.0

D

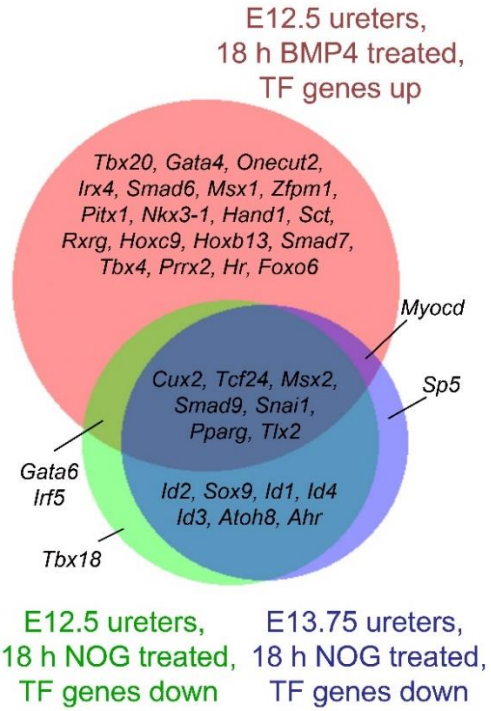

E

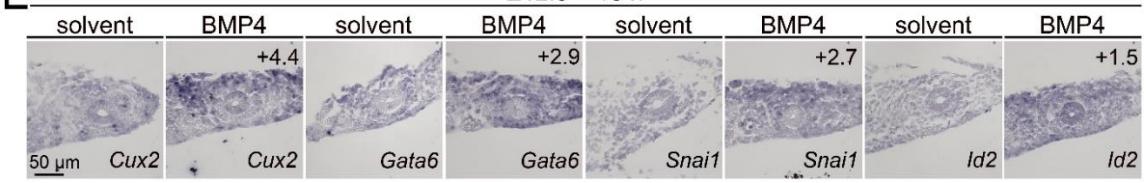

Figure 3: Pharmacological manipulation in ureter explant cultures uncovers TF genes that rapidly and positively respond to BMP4 administration. (A) Pie chart summarizing microarray analysis for control versus BMP4 treated E12.5 + 18 h ureter cultures. (B,C) Functional annotation clustering by DAVID (B) and list of TF genes showing increased expression (C) after BMP4 treatment. (C) Shown are the individual intensities (INT) in control and treated ureters and the average fold change (avgFC) from two independent microarrays. (D) Venn diagram visualizing TF genes with increased expression upon BMP4 and decreased expression upon NOGGIN (NOG) treatment in E12.5 and E13.75 + 18 h ureter cultures. (E) RNA *in situ* hybridization analysis on transverse ureter sections of control individuals and individuals treated with 100 ng/ml BMP4. Numbers in the upper right corner reflect the average fold change from the microarray analysis. *n* ≥3 for each probe and condition.

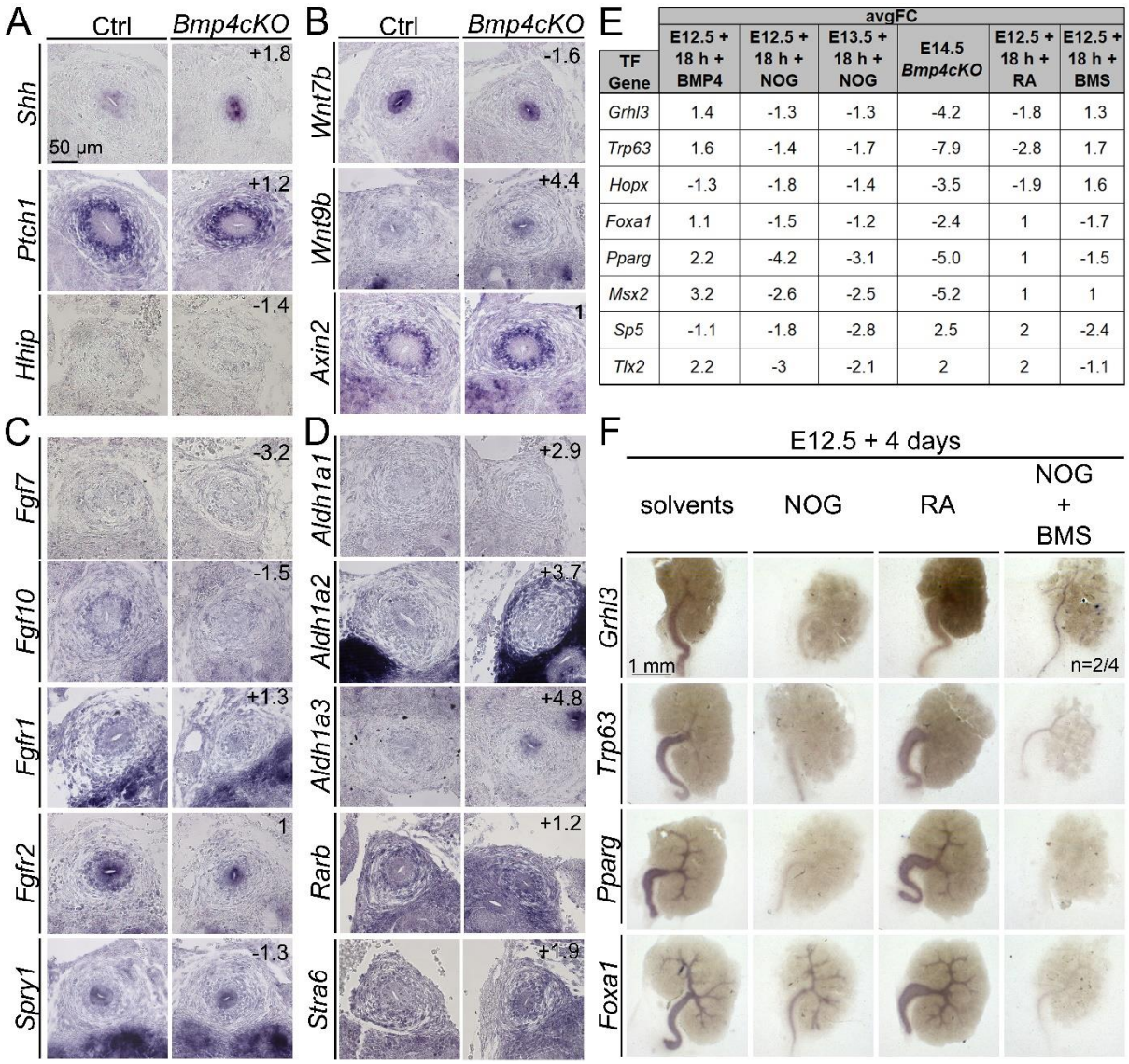

E

TF Gene	avgFC E12.5 + 18 h + BMP4	E12.5 + 18 h + NOG	E13.5 + 18 h + NOG	E14.5 *Bmp4cKO*	E12.5 + 18 h + RA	E12.5 + 18 h + BMS
Grhl3	1.4	-1.3	-1.3	-4.2	-1.8	1.3
Trp63	1.6	-1.4	-1.7	-7.9	-2.8	1.7
Hopx	-1.3	-1.8	-1.4	-3.5	-1.9	1.6
Foxa1	1.1	-1.5	-1.2	-2.4	1	-1.7
Pparg	2.2	-4.2	-3.1	-5.0	1	-1.5
Msx2	3.2	-2.6	-2.5	-5.2	1	1
Sp5	-1.1	-1.8	-2.8	2.5	2	-2.4
Tlx2	2.2	-3	-2.1	2	2	-1.1

Figure 4: Reduced TF gene expression in *Bmp4cKO* ureters is partly caused by increased RA signaling. (A-D) RNA *in situ* hybridization analysis on transverse ureter sections of E14.5 control and *Bmp4cKO* ureters analyzing the expression of components and target genes of SHH (A), WNT (B), FGF (C) and RA signaling (D). Numbers in the upper right corner reflect the average fold change in the *Bmp4cKO* ureter microarray analysis. *n* ≥4 for each probe and genotype. (E) List of selected TF genes with their changes in expression found in microarrays of ureters with manipulation of BMP4 and RA signaling. Shown are the average fold changes (avgFC) after BMP4 (100 ng/ml), NOGGIN (NOG, 10 µg/ml), retinoic acid (RA, 1µM) and BMS189453 (BMS, 1 µM) treatment on E12.5 or E13.5 +18 h ureter cultures and the average fold change in E14.5 *Bmp4cKO* mutant ureters. (F) Whole mount *in situ* hybridization analyzing the expression of different TF genes on E12.5 kidney and ureter rudiments grown for 4 days in presence and/or absence of NOGGIN (NOG, 10 µg/ml), retinoic acid (RA, 1 µM) and/or BMS189453 (BMS, 1 µM). *n* ≥3 for each probe and condition.

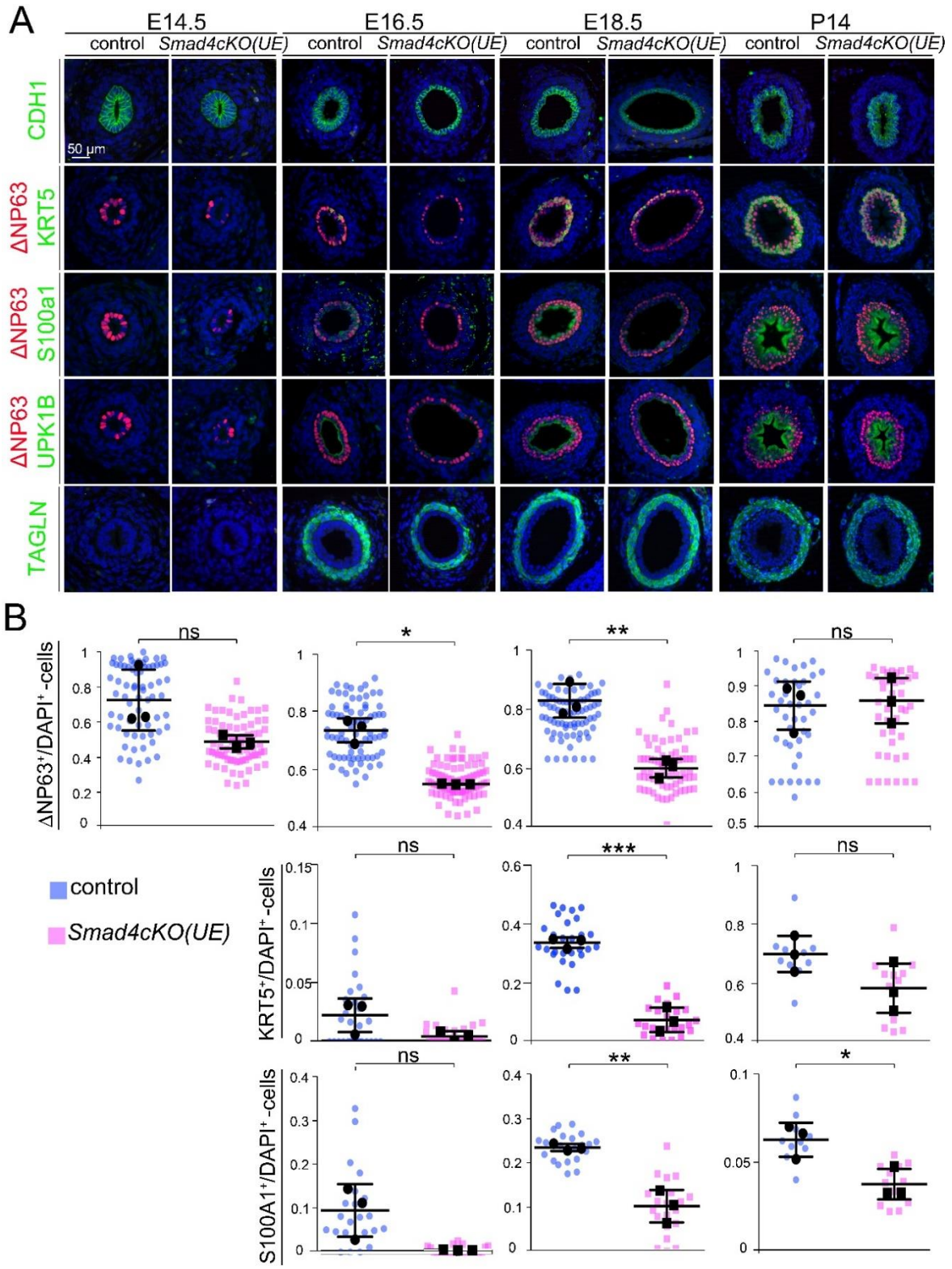

Figure 5: Urothelial differentiation and stratification is delayed in *Smad4cKO(UE)* ureters. (A) Immunofluorescence of different proteins that characterize epithelial cells (CDH1), different urothelial cell types (ΔNP63, KRT5, UPK1B, S100A1) and SMCs (TAGLN) at the indicated stages. Nuclei are counterstained with DAPI (blue). (B) Quantification of the ratio of ΔNP63$^+$/DAPI, KRT5$^+$/DAPI and S100A1$^+$/DAPI cells on transverse ureter sections. For statistics see Table S10. Differences were considered non-significant (ns; P>0.05), significant (*P<0.05), highly significant (*P<0.01) or extremely significant (*P<0.001); two tailed Students *t*-test.

A

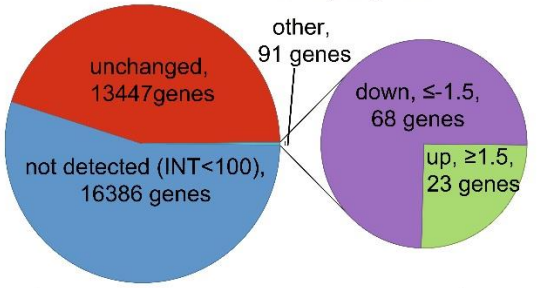

F

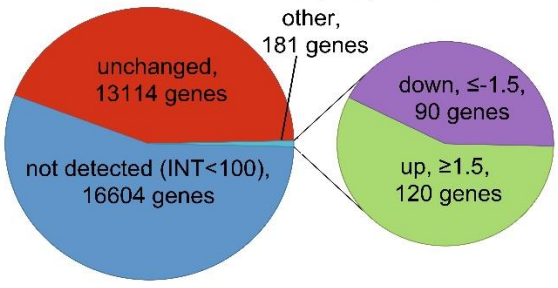

B

Rank	Term	P-Value
1	Establishment of skin barrier	5.57E-08
2	Epithelial cell differentiation	5.34E-07
3	Secreted	5.39E-06
4	Apical plasma membrane urothelial plaque	4.88E-05
5	Extracellular region	5.20E-05
6	Regulation of cellular response to insuline stimulus	3.01E-04
7	Transcriptional activation	3.42E-04
8	Antimicrobial humoral immune response	7.63E-04
9	Epidermis development	8.42E-04
10	Extracellular space	1.12E-03

G

Rank	Term	P-Value
1	N-linked (GlcNAc…) asparagine	4.29E-05
2	TGF-beta signaling pathway	4.81E-05
3	Fibronectin type-III	5.98E-05
4	Multicellular orgnism development	7.28E-05
5	Interaction with IFI204	7.45E-05
6	Muscle protein	1.32E-04
7	Cartilage development	4.53E-04
8	BMP signaling pathway	8.88E-04
9	Heart development	1.07E-03
10	Cardiac muscle tissue development	6.03E-03

C

Rank	Gene Symbol	avgFC
1	*Serpinb5*	-2.3
2	*Prap1*	-2.3
3	*Aldh3b2*	-3.3
4	*Upk3a*	-3.0
5	*Gsdmc3*	-3.0
6	*Ldoc1*	-2.8
7	*Upk1a*	-2.7
8	*Pdzk1*	-2.7
9	*Afp*	-2.7
10	*Anxa8*	-2.7
11	*Upk1b*	-2.7
12	*Perp*	-2.7
13	*S100a14*	-2.5
14	*Fa2h*	-2.5
15	*Cbr2*	-2.4
16	*Wnt10a*	-2.4
17	*Grhl3*	-2.4
18	*Ppbp*	-2.4
19	*A_55_P1953377*	-2.2
20	*Msx2*	-2.2
21	*ENSMUST00000199575*	-2.2
22	*Gp9*	-2.2
23	*Eddm3b*	-2.2
24	*4631405K08Rik*	-2.1
25	*Rab27b*	-2.1

Rank	Gene Symbol	avgFC
26	*Urah*	-2.1
27	*Trim29*	-2.1
28	*Ttr*	-2.1
29	*Tmprss13*	-2.1
30	*Trp63*	-2.1
31	*Aqp3*	-2.0
32	*Fxyd3*	-2.0
33	*Foxi1*	-2.0
34	*Upk3bl*	-2.0
35	*Tmem45b*	-2.0
36	*Paqr5*	-1.9
37	*Slc35g1*	-1.9
38	*Elf5*	-1.9
39	*Sfn*	-1.9
40	*Calml3*	-1.8
41	*Sprr2a2*	-1.8
42	*Dmkn*	-1.8
43	*Prom2*	-1.8
44	*Lgals3*	-1.8
45	*Abcc3*	-1.8
46	*4930434F21Rik*	-1.8
47	*Zbtb32*	-1.8
48	*Grhl1*	-1.7
49	*Crim1*	-1.7
50	*Fam183b*	-1.7

H

Rank	Gene Symbol	avgFC
1	*Myh11*	-6.0
2	*Cnn1*	-4.0
3	*Sct*	-3.9
4	*Actg2*	-4.0
5	*Acta2*	-3.3
6	*Mrap2*	-3.3
7	*Smad9*	-3.3
8	*Car3*	-3.1
9	*Hpgd*	-3.1
10	*Irf5*	-2.3
11	*Syt1*	-2.3
12	*Myocd*	-2.3
13	*Mansc4*	-2.4
14	*Maob*	-2.4
15	*Id2*	-2.4
16	*Epha5*	-2.3
17	*Slitrk5*	-2.3
18	*Id1*	-2.3
19	*Bmp5*	-2.2
20	*A_55_P2041693*	-2.2
21	*Pcdh9*	-2.2
22	*Cfh*	-2.2
23	*Mylk*	-2.2
24	*Cfhr2*	-2.1
25	*Cox8b*	-2.1

Rank	Gene Symbol	avgFC
26	*Srprb*	-2.1
27	*Id3*	-2.1
28	*Lhfpl3*	-2.1
29	*Alpl*	-2.0
30	*Asic1*	-2.0
31	*Sned1*	-2.0
32	*6720482D04*	-2.0
33	*Olfm1*	-2.0
34	*Lactb*	-1.9
35	*A_55_P2175050*	-1.9
36	*Actc1*	-1.9
37	*Sfrp2*	-1.9
38	*Slc38a5*	-1.9
39	*Sdpr*	-1.9
40	*Enpp2*	-1.9
41	*Ecm1*	-1.9
42	*9630023C09Rik*	-1.9
43	*F830014O18Rik*	-1.9
44	*Otop2*	-1.9
45	*Tmeff2*	-1.9
46	*Baiap2l2*	-1.9
47	*Tspan1*	-1.9
48	*Hapln1*	-1.8
49	*Srrm3*	-1.8
50	*Rbp4*	-1.8

D

Rank	Gene symbol	avrgFC
17	*Grhl3*	-2.3
20	*Msx2*	-2.2
30	*Trp63*	-2.1
33	*Foxi1*	-2.0
38	*Elf5*	-1.9
58	*Pparg*	-1.7

Ovol1	-1.2
Klf5	-1.1
Foxa1	1

E

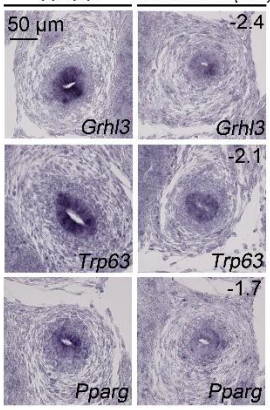

I

Rank	Gene symbol	avrgFC
7	*Smad9*	-3.2
10	*Irf5*	-2.3
12	*Myocd*	-2.3
15	*Id2*	-2.4
18	*Id1*	-1.9
27	*Id3*	-1.9
58	*Smad6*	-1.8
78	*Hopx*	-1.6

Snai1	-1.5
Tbx18	-1.4
Cux2	-1.3
Gata6	-1.2
Atoh8	-1.1
Sox9	-1.1
Id4	1
Foxf1	1
Sp5	1
Ahr	1.2

J

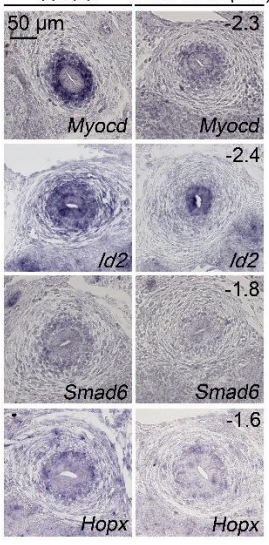

Figure 6: SMAD effectors mediate part of the epithelial and mesenchymal differentiation program downstream of *Bmp4*. See figure description on the next page.

Figure 6: SMAD effectors mediate part of the epithelial and mesenchymal differentiation program downstream of *Bmp4*. (A,F) Pie chart summarizing microarray data from epithelial *(Smad4cKO(UE)*) and mesenchymal (*Smad4cKO(UM)*) *Smad4* mutant ureters. (B,G) Functional annotation clustering by DAVID for genes showing decreased expression upon conditional inactivation of *Smad4*. (C,H) List of the top 50 genes showing decreased expression. Shown is the average fold change (avgFC) from two independent microarray pools. (D,I) TF genes with decreased or unchanged expression. (E,J) RNA *in situ* hybridization analysis on transverse ureter sections of E14.5 control and mutant ureters. Numbers in the upper right corner reflect the average fold change from the microarray analysis. $n \geq 3$ for each probe and genotype.

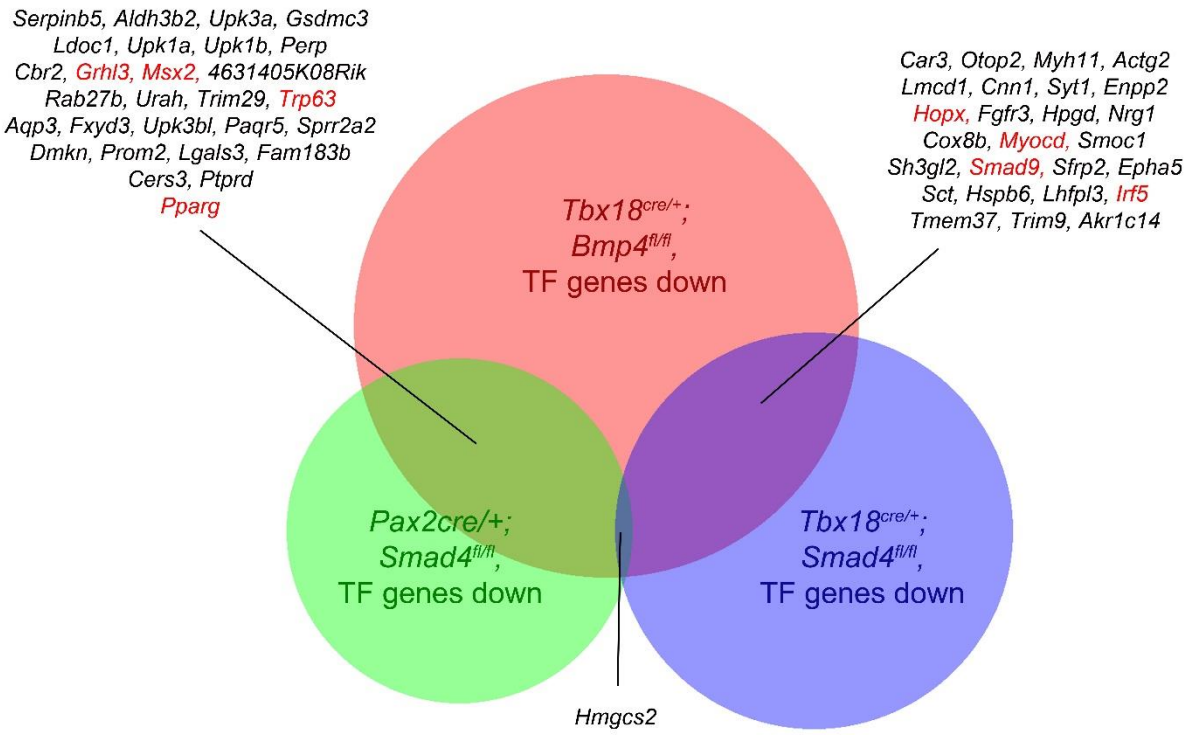

Figure 7: All relevant TF genes for ureteric cytodifferentiation downstream of *Bmp4* are at least partly regulated by *Smad4*. Venn diagram visualizing the intersection of the lists of genes with decreased expression in *Bmp4cKO, Smad4cKO(UE)* and *Smad4cKO(UM)* mutant ureters at E14.5.

Supplementary Figures

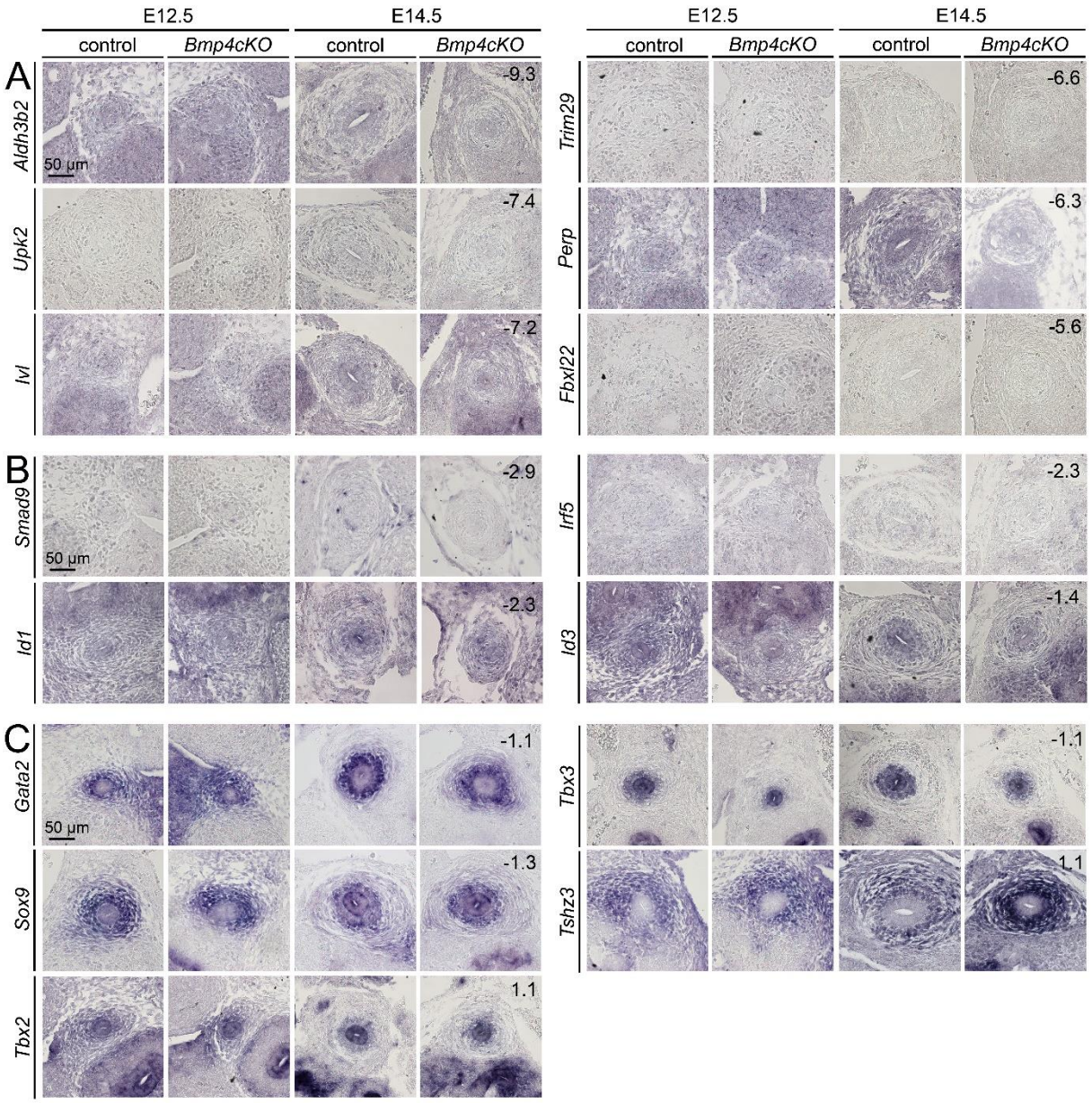

Figure S1: Genes showing no specific or unchanged expression in *Bmp4cKO* mutant ureters. (A-C) RNA *in situ* hybridization on transverse ureter sections for structural genes (A) and TF genes (B,C). Numbers in the upper right corner reflect the average fold change determined by microarray analysis. $n \geq 3$ for each probe and genotype.

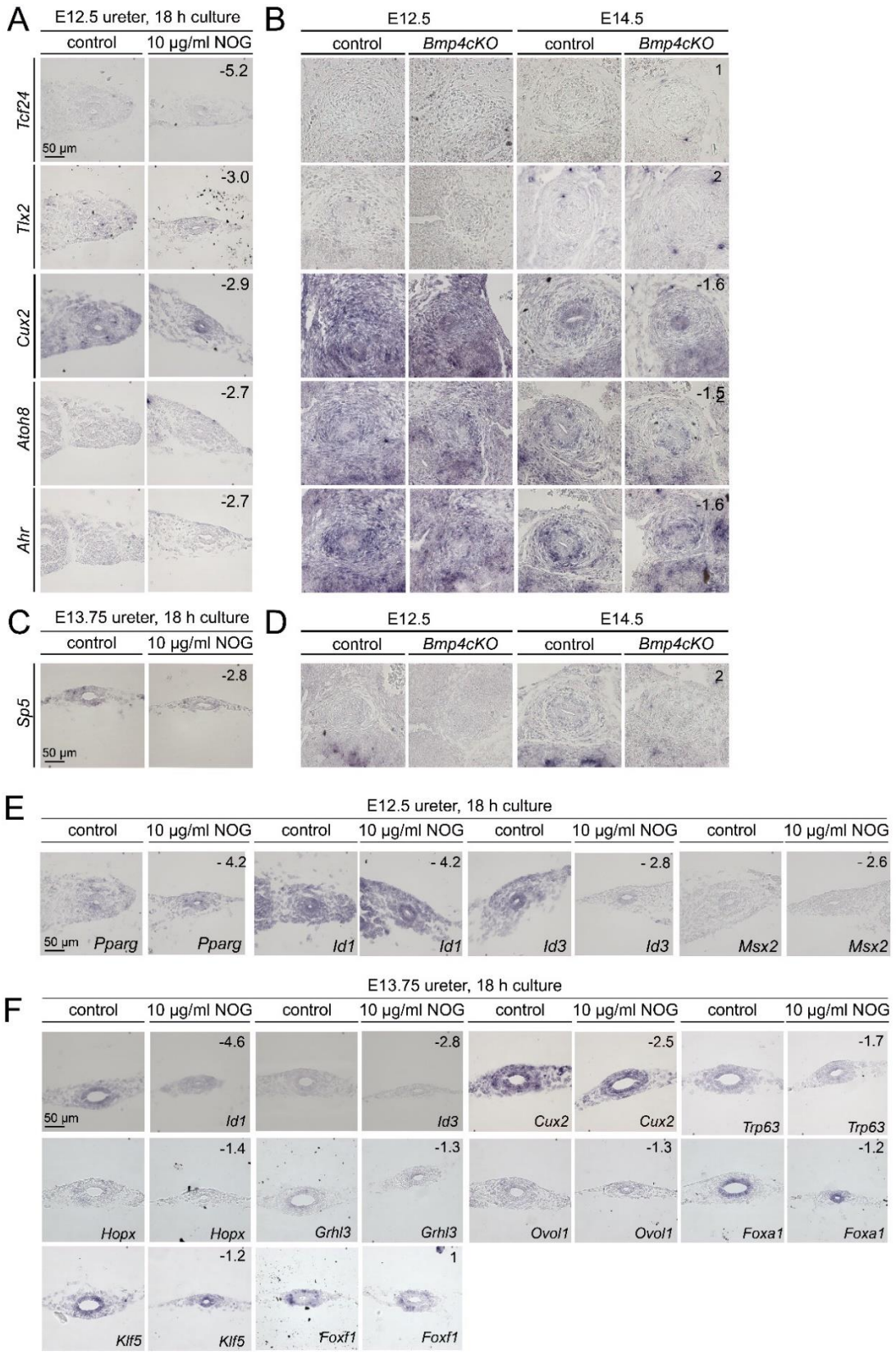

Figure S2: Genes showing no specific or unchanged expression in *Bmp4cKO* mutant ureters or ureter explant cultures. (A-E) RNA *in situ* hybridization on transverse ureter sections on explant cultures (A,C,E) or *Bmp4cKO* ureters (B,D). Shown are genes with no, unspecific or unchanged expression. Numbers in the upper right corner reflect the average fold change determined by microarray analysis. $n \geq 3$ for each probe and genotype or condition.

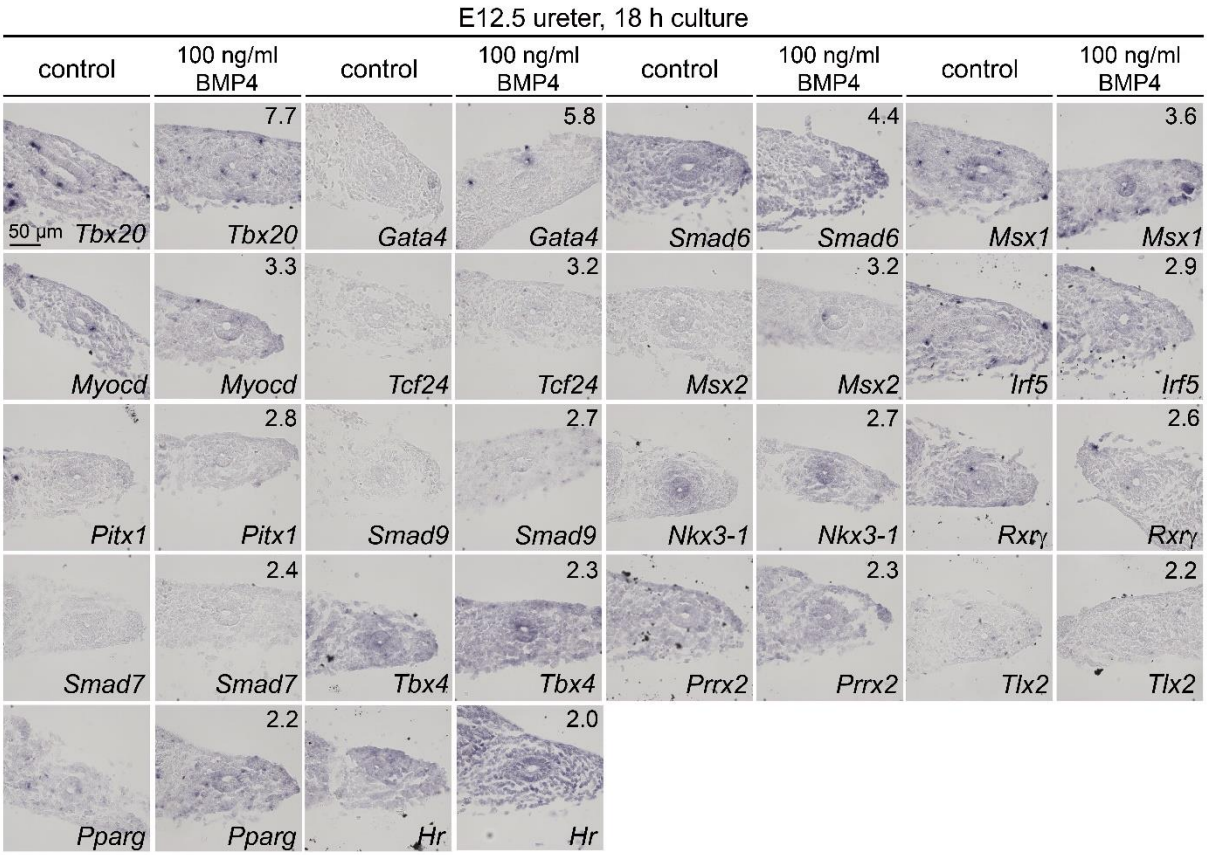

Figure S3: Genes showing no specific expression after BMP4 treatment in ureter explant cultures. RNA *in situ* hybridization on transverse ureter sections on E12.5 + 18 h explant cultures treated with 100 ng/ml BMP4. Shown are genes with no or unspecific expression. Numbers in the upper right corner indicate the average fold change from microarray analysis. $n \geq 3$ for each probe and condition.

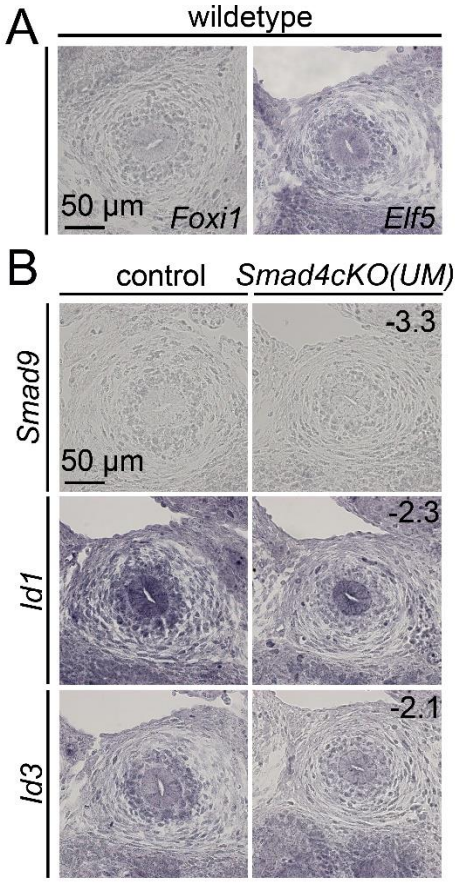

Figure S4: Genes showing no specific or unchanged expression in *Smad4cKO* mutant ureters. (A,B) RNA *in situ* hybridization on E14.5 transverse ureter sections of wildtype (A) and control and *Smad4cKO(UM)* mutant ureters. Numbers in the upper right corner reflect the average fold change determined by microarray analysis. $n \geq 3$ for each probe and genotype.

Supplementary Tables

		Intensities				fold changes (FC)		
Rank	**Gene Symbol**	**control 1**	**mutant 1**	**control 2**	**mutant 2**	**FC1**	**FC2**	**avgFC**
1	*Upk1b*	1844	186	2450	100	-9.9	-24.6	-17.3
2	*Bmp4*	21568	2642	17775	1280	-8.2	-13.9	-11.0
3	*Aldh3b2*	133	23	192	15	-5.7	-12.8	-9.3
4	*Car3*	61822	8735	43802	3946	-7.1	-11.1	-9.1
5	*Otop2*	273	30	284	34	-9.2	-8.5	-8.9
6	*Fam183b*	263	30	308	38	-8.8	-8.1	-8.5
7	*Sprr1a*	1953	484	4018	332	-4.0	-12.1	-8.1
8	*Ldoc1*	704	118	924	93	-6.0	-10.0	-8.0
9	*Trp63*	313	43	571	67	-7.4	-8.5	-7.9
10	*Serpinb5*	101	15	132	15	-6.7	-8.8	-7.8
11	*Rab27b*	1431	213	1614	192	-6.7	-8.4	-7.6
12	*Upk2*	330	73	683	67	-4.5	-10.2	-7.4
13	*Ivl*	113	26	152	15	-4.4	-10.1	-7.2
14	*C1ql3*	354	61	327	38	-5.8	-8.7	-7.2
15	*Myh11*	576	142	1333	134	-4.1	-9.9	-7.0
16	*Ctse*	959	147	1159	168	-6.5	-6.9	-6.7
17	*Trim29*	168	53	325	33	-3.2	-10.0	-6.6
18	*Grem2*	113	15	103	19	-7.5	-5.3	-6.4
19	*Perp*	3436	693	4359	566	-5.0	-7.7	-6.3
20	*Sprr2a2*	215	46	230	29	-4.7	-7.8	-6.3
21	*Elmod1*	160	31	244	34	-5.2	-7.1	-6.2
22	*Esyt3*	290	43	271	49	-6.8	-5.5	-6.1
23	*Upk3a*	4968	987	4215	619	-5.0	-6.8	-5.9
24	*Hmgcs2*	200	43	323	47	-4.7	-6.8	-5.8
25	*Cbr2*	242	59	305	42	-4.1	-7.2	-5.6
26	*Fbxl22*	242	80	524	64	-3.0	-8.2	-5.6
27	*4631405K08Rik*	519	113	660	100	-4.6	-6.6	-5.6
28	*Actg2*	1469	435	3417	440	-3.4	-7.8	-5.6
29	*Shisa2*	2216	390	2874	543	-5.7	-5.3	-5.5
30	*Upk1a*	1372	373	2397	336	-3.7	-7.1	-5.4
31	*Paqr5*	217	54	261	40	-4.0	-6.5	-5.3
32	*Pparg*	2543	553	2362	436	-4.6	-5.4	-5.0
33	*Fxyd3*	12019	2869	12802	2279	-4.2	-5.6	-4.9
34	*Lmcd1*	1845	479	2512	427	-3.8	-5.9	-4.9
35	*Agr2*	112	24	107	21	-4.6	-5.1	-4.8
36	*Ccdc68*	530	149	801	136	-3.6	-5.9	-4.7
37	*Cnn1*	2531	788	4143	669	-3.2	-6.2	-4.7
38	*Chgb*	1325	405	2107	345	-3.3	-6.1	-4.7
39	*Ihh*	233	92	679	102	-2.5	-6.7	-4.6
40	*Syt1*	2418	518	1987	450	-4.7	-4.4	-4.5
41	*Msx2*	389	134	695	118	-2.9	-5.9	-4.4
42	*Oit1*	292	91	482	88	-3.2	-5.5	-4.3

43	*Msln*	694	220	993	182	-3.2	-5.5	-4.3
44	*Grhl3*	1395	558	2761	468	-2.5	-5.9	-4.2
45	*Aqp3*	417	128	528	106	-3.3	-5.0	-4.1
46	*BC057651*	264	75	418	96	-3.5	-4.4	-4.0
47	*Dmkn*	358	93	298	76	-3.8	-3.9	-3.9
48	*Kcnk3*	321	109	387	81	-3.0	-4.8	-3.9
49	*Ptprd*	297	101	358	76	-2.9	-4.7	-3.8
50	*Ly6g*	306	110	393	82	-2.8	-4.8	-3.8
51	*Prom2*	296	112	565	115	-2.6	-4.9	-3.8
52	*Enpp2*	16569	4369	13062	3538	-3.8	-3.7	-3.7
53	*AU015836*	128	34	106	29	-3.7	-3.7	-3.7
54	*Prss22*	123	42	179	41	-2.9	-4.4	-3.7
55	*AI314604*	137	35	135	40	-3.9	-3.4	-3.7
56	*Ugt2b34*	347	102	313	80	-3.4	-3.9	-3.7
57	*ENSMUST00000055719*	976	331	1041	241	-2.9	-4.3	-3.6
58	*Npy1r*	3304	833	2650	871	-4.0	-3.0	-3.5
59	*Hopx*	2333	814	2745	669	-2.9	-4.1	-3.5
60	*Lamc3*	526	159	768	210	-3.3	-3.7	-3.5
61	*Sptlc3*	158	51	161	41	-3.1	-3.9	-3.5
62	*Aqp1*	1589	588	1916	452	-2.7	-4.2	-3.5
63	*1700055N04Rik*	168	69	259	59	-2.5	-4.4	-3.4
64	*Lamb3*	224	109	349	73	-2.1	-4.8	-3.4
65	*Itih2*	329	111	244	64	-3.0	-3.8	-3.4
66	*Fgfr3*	1064	367	1408	366	-2.9	-3.8	-3.4
67	*Hpgd*	2267	748	2429	673	-3.0	-3.6	-3.3
68	*Nrn1l*	654	224	690	190	-2.9	-3.6	-3.3
69	*Upk3bl*	727	309	1251	304	-2.4	-4.1	-3.2
70	*Fgf7*	2184	685	2160	662	-3.2	-3.3	-3.2
71	*Nrg1*	652	251	846	220	-2.6	-3.8	-3.2
72	*Cox8b*	374	129	415	118	-2.9	-3.5	-3.2
73	*Syt8*	173	68	212	55	-2.5	-3.8	-3.2
74	*Pla2g1b*	131	50	117	31	-2.6	-3.7	-3.2
75	*Myocd*	137	65	293	69	-2.1	-4.2	-3.2
76	*Gsdmc3*	275	77	154	57	-3.6	-2.7	-3.1
77	*Urah*	147	53	139	40	-2.8	-3.4	-3.1
78	*Apela*	4216	1676	4354	1224	-2.5	-3.6	-3.0
79	*Smim6*	227	90	211	62	-2.5	-3.4	-3.0
80	*Anxa9*	157	72	247	67	-2.2	-3.7	-2.9
81	*Smoc1*	898	286	931	348	-3.1	-2.7	-2.9
82	*Ednrb*	4863	1636	3468	1251	-3.0	-2.8	-2.9
83	*Ildr1*	111	45	188	57	-2.4	-3.3	-2.9
84	*Sh3gl2*	372	136	436	149	-2.7	-2.9	-2.8
85	*Ppm1e*	439	149	414	154	-2.9	-2.7	-2.8
86	*Ncmap*	355	167	513	146	-2.1	-3.5	-2.8
87	*Fzd9*	268	100	343	118	-2.7	-2.9	-2.8
88	*S100a5*	244	107	218	67	-2.3	-3.3	-2.8
89	*Prkcb*	479	223	625	184	-2.1	-3.4	-2.8

90	*2200002D01Rik*	2145	832	2023	691	-2.6	-2.9	-2.8
91	*Lmo1*	485	229	585	173	-2.1	-3.4	-2.8
92	*Ddc*	374	158	375	121	-2.4	-3.1	-2.7
93	*Nt5e*	237	83	232	89	-2.8	-2.6	-2.7
94	*Ccdc184*	406	179	509	162	-2.3	-3.1	-2.7
95	*Mal*	3410	1300	3465	1249	-2.6	-2.8	-2.7
96	*Pipox*	172	64	175	65	-2.7	-2.7	-2.7
97	*A_55_P2243558*	169	75	197	63	-2.2	-3.1	-2.7
98	*Krt42*	3155	1380	3794	1232	-2.3	-3.1	-2.7
99	*Krt19*	15089	6308	15572	5247	-2.4	-3.0	-2.7
100	*Cers3*	1164	485	1306	456	-2.4	-2.9	-2.6
101	*ENSMUST00000089689*	483	219	520	173	-2.2	-3.0	-2.6
102	*Trim71*	1003	468	1657	553	-2.1	-3.0	-2.6
103	*Smad9*	329	129	410	161	-2.5	-2.5	-2.5
104	*Tmem54*	570	262	653	225	-2.2	-2.9	-2.5
105	*Ptx3*	1510	579	1472	602	-2.6	-2.4	-2.5
106	*Sfrp2*	38888	13460	29715	13794	-2.9	-2.2	-2.5
107	*Sh2d4a*	111	50	150	54	-2.2	-2.8	-2.5
108	*Lrrc75b*	1071	451	1285	484	-2.4	-2.7	-2.5
109	*Iigp1*	2315	941	2025	797	-2.5	-2.5	-2.5
110	*Cmbl*	798	338	722	276	-2.4	-2.6	-2.5
111	*Cytl1*	104	39	116	50	-2.6	-2.3	-2.5
112	*Epha5*	526	211	522	214	-2.5	-2.4	-2.5
113	*Sct*	5952	2618	5696	2149	-2.3	-2.7	-2.5
114	*Lnx1*	376	147	355	152	-2.6	-2.3	-2.4
115	*Rasgrf1*	303	140	368	137	-2.2	-2.7	-2.4
116	*Aspa*	197	76	163	73	-2.6	-2.2	-2.4
117	*Aspn*	461	212	585	220	-2.2	-2.7	-2.4
118	*A930009L07Rik*	114	55	134	49	-2.1	-2.7	-2.4
119	*TC1703733*	432	183	425	173	-2.4	-2.5	-2.4
120	*Foxa1*	5297	2606	7154	2596	-2.0	-2.8	-2.4
121	*Rasef*	214	81	186	88	-2.7	-2.1	-2.4
122	*Crym*	5043	1945	4523	2095	-2.6	-2.2	-2.4
123	*Gm4951*	849	351	689	296	-2.4	-2.3	-2.4
124	*Eif2ak4*	110	44	124	56	-2.5	-2.2	-2.4
125	*Cela1*	284	112	272	125	-2.5	-2.2	-2.4
126	*Insc*	139	64	149	59	-2.2	-2.5	-2.3
127	*Degs2*	428	214	483	179	-2.0	-2.7	-2.3
128	*Snai1*	3016	1448	4461	1714	-2.1	-2.6	-2.3
129	*Fam49a*	262	124	256	99	-2.1	-2.6	-2.3
130	*Hspb6*	3562	1706	4871	1931	-2.1	-2.5	-2.3
131	*Lgals3*	2657	1176	2626	1135	-2.3	-2.3	-2.3
132	*Bnipl*	198	91	220	92	-2.2	-2.4	-2.3
133	*Lhfpl3*	149	65	159	70	-2.3	-2.3	-2.3
134	*Irf5*	354	167	344	144	-2.1	-2.4	-2.3
135	*Zcchc12*	1662	733	1475	671	-2.3	-2.2	-2.2
136	*Tmem140*	119	52	131	60	-2.3	-2.2	-2.2

137	*Tspan8*	6307	2898	5633	2520	-2.2	-2.2	-2.2
138	*Tmem37*	5828	2797	5724	2495	-2.1	-2.3	-2.2
139	*Trim9*	233	104	214	102	-2.2	-2.1	-2.2
140	*Gata6*	13387	6250	12709	6005	-2.1	-2.1	-2.1
141	*Akr1c14*	360	170	377	181	-2.1	-2.1	-2.1
142	*Tmc7*	1031	486	906	438	-2.1	-2.1	-2.1
143	*Dusp10*	340	167	389	192	-2.0	-2.0	-2.0
144	*Krt8*	18611	9219	16856	8290	-2.0	-2.0	-2.0

Table S1. List of genes with decreased expression in microarrays of E14.5 *Bmp4cKO* ureters. Shown are the gene names, the intensity of the two control and mutant ureter samples, the individual and the average (avg) fold change (FC).

Rank	Category	Term	Count	%	PValue	Genes	List Total	Pop Hits	Pop Total	Fold Enrichment	Bonferroni	Benjamini	FDR
1	GOTERM_BP_DIRECT	GO:0030855~epithelial cell differentiation	10	7.462686567	1.10E-08	LGALS3, UPK1B, KRT19, UPK1A, UPK2, GATA6, TRP63, PPARG, KRT42, UPK3A	122	102	20094	16.14754098	1.43E-05	1.43E-05	1.43E-05
2	GOTERM_CC_DIRECT	GO:0120001~apical plasma membrane urothelial plaque	4	2.985074627	9.00E-07	UPK1B, UPK1A, UPK2, UPK3A	131	4	21179	161.6717557	1.62E-04	1.62E-04	1.60E-04
3	GOTERM_BP_DIRECT	GO:0030154~cell differentiation	19	14.17910448	3.99E-05	FOXA1, SYT1, PAQR5, IHH, TRP63, SMAD9, NRG1, EIF2AK4, DMKN, HOPX, BMP4, LGALS3, FGF7, APELA, SFRP2, SMOC1, INSC, PPARG, FGFR3	122	1022	20094	3.062028809	0.050512329	0.023669646	0.023542096
4	GOTERM_BP_DIRECT	GO:0045766~positive regulation of angiogenesis	8	5.970149254	5.47E-05	LGALS3, APELA, SFRP2, HSPB6, PRKCB, GATA6, CELA1, AQP1	122	161	20094	8.184095306	0.068548242	0.023669646	0.023542096
5	GOTERM_BP_DIRECT	GO:0007275~multicellular organism development	19	14.17910448	9.67E-05	TRIM71, FOXA1, EPHA5, MSX2, PAQR5, FZD9, IHH, KRT8, TRP63, SHISA2, HOPX, BMP4, GREM2, APELA, SFRP2, SMOC1, INSC, SNAI1, FGFR3	122	1095	20094	2.857893555	0.118068046	0.031408575	0.031239322
6	UP_KW_CELLULAR_COMPONENT	KW-0964~Secreted	26	19.40298507	1.03E-04	ITIH2, HSPB6, PLA2G1B, LAMC3, SCT, IHH, MSLN, DMKN, LGALS3, FGF7, APELA, SPRR2A2, ENPP2, AGR2, CHGB, URAH, LAMB3, CELA1, C1QL3, ASPN, SERPINB5, BMP4, GREM2, SFRP2, SMOC1, PTX3	119	1709	17960	2.296099247	0.002664544	0.002667963	0.002667963
7	GOTERM_BP_DIRECT	GO:0051216~cartilage development	6	4.47761194	2.36E-04	BMP4, SFRP2, MSX2, IHH, SMAD9, FGFR3	122	92	20094	10.74162509	0.263978882	0.061292062	0.060961774
8	GOTERM_CC_DIRECT	GO:0005615~extracellular space	26	19.40298507	3.53E-04	HPGD, PLA2G1B, SCT, IHH, MSLN, DMKN, PRSS22, LGALS3, FGF7, APELA, ENPP2, AGR2, ANXA9, CHGB, URAH, CELA1, NRG1, C1QL3, ASPN, SERPINB5, BMP4, GREM2, SFRP2, NRN1L, SMOC1, PTX3	131	1969	21179	2.134822574	0.061646149	0.031808458	0.031455031
9	GOTERM_BP_DIRECT	GO:0030509~BMP signaling pathway	6	4.47761194	5.39E-04	BMP4, ZCCHC12, SFRP2, MSX2, SMAD9, PPARG	122	110	20094	8.98390462	0.503452766	0.116648009	0.116019421
10	GOTERM_MF_DIRECT	GO:0042802~identical protein binding	25	18.65671642	5.72E-04	HPGD, RASEF, ILDR1, TRP63, AQP3, AQP1, TRIM29, AGR2, HMGCS2, CTSE, SH3GL2, CBR2, SYT1, C1QL3, IIGP1, BMP4, GREM2, NRN1L, LNX1, PPARG, PTX3, IRF5, ASPA, FGFR3, BNIPL	114	1962	18713	2.091604521	0.168225254	0.184140941	0.184140941
11	UP_KW_PTM	KW-0325~Glycoprotein	43	32.08955224	6.55E-04	ITIH2, LAMC3, UPK2, IHH, MSLN, DMKN, PRSS22, NCMAP, AQP3, AQP1, NT5E, FGF7, UPK1B, UPK1A, EDNRB, TSPAN8, ENPP2, CTSE, PROM2, CHGB, EPHA5, LAMB3, SYT1, FZD9, KRT8, NPY1R, CELA1, TMC7, UPK3A, ASPN, SERPINB5, PTPRD, BMP4, GREM2, NRN1L, SMOC1, SNAI1, PPARG, PTX3, UPK3BL, LY6G, FGFR3, KCNK3	88	4008	12816	1.562465977	0.013664879	0.014409577	0.014409577
12	GOTERM_CC_DIRECT	GO:0001533~cornified envelope	5	3.731343284	6.87E-04	LGALS3, SPRR2A2, SPRR1A, SERPINB5, IVL	131	65	21179	12.4362889	0.116337265	0.040500319	0.040050315
13	GOTERM_BP_DIRECT	GO:0000122~negative regulation of transcription from RNA polymerase II promoter	16	11.94029851	7.68E-04	FOXA1, LMO1, MYOCD, MSX2, GATA6, TRP63, CELA1, HOPX, BMP4, EDNRB, TRIM29, SNAI1, PPARG, CRYM, FGFR3, LMCD1	122	975	20094	2.702849937	0.631585671	0.142594769	0.14182636
14	GOTERM_CC_DIRECT	GO:0005576~extracellular region	24	17.91044776	9.00E-04	ITIH2, HSPB6, LAMB3, LAMC3, PLA2G1B, SCT, IHH, CELA1, MSLN, DMKN, C1QL3, ASPN, SERPINB5, BMP4, GREM2, LGALS3, FGF7, APELA, SFRP2, SMOC1, ENPP2, AGR2, PTX3, CHGB	131	1859	21179	2.087209326	0.149621912	0.040500319	0.040050315
15	UP_KW_MOLECULAR_FUNCTION	KW-9996~Developmental protein	16	11.94029851	0.001345134	TRIM71, FOXA1, MSX2, PAQR5, FZD9, IHH, TRP63, SHISA2, HOPX, BMP4, GREM2, APELA, SFRP2, SMOC1, INSC, SNAI1	75	1044	12158	2.484393359	0.061304229	0.031610643	0.031610643
16	UP_KW_MOLECULAR_FUNCTION	KW-0217~Developmental protein	16	11.94029851	0.001345134	TRIM71, FOXA1, MSX2, PAQR5, FZD9, IHH, TRP63, SHISA2, HOPX, BMP4, GREM2, APELA, SFRP2, SMOC1, INSC, SNAI1	75	1044	12158	2.484393359	0.061304229	0.031610643	0.031610643
17	GOTERM_BP_DIRECT	GO:0010667~negative regulation of cardiac muscle cell apoptotic process	4	2.985074627	0.001540662	MYOCD, SFRP2, HSPB6, NRG1	122	38	20094	17.33735979	0.865051613	0.219305092	0.218123309
18	GOTERM_BP_DIRECT	GO:0055007~cardiac muscle cell differentiation	4	2.985074627	0.001661765	BMP4, MYOCD, GATA6, NRG1	122	39	20094	16.89281211	0.884724311	0.219305092	0.218123309
19	GOTERM_BP_DIRECT	GO:0008284~positive regulation of cell proliferation	12	8.955223881	0.001688261	BMP4, LGALS3, FGF7, MYOCD, EDNRB, SFRP2, PLA2G1B, IHH, ENPP2, TRP63, NRG1, FGFR3	122	640	20094	3.088217213	0.888630772	0.219305092	0.218123309

20	GOTERM_MF_DIRECT	GO:0005515~protein binding	48	35.82089552	0.001924747	TRIM71, ZCCHC12, RASGRF1, GATA6, IHH, ILDR1, TRP63, MSLN, SMIM6, TRIM9, LGALS3, FGF7, UPK1A, EDNRB, TRIM29, LMCD1, SH3GL2, CHGB, EPHA5, LMO1, CBR2, MYOCD, MSX2, SYT1, PRKCB, KRT8, SMAD9, RAB27B, GRHL3, EIF2AK4, C1QL3, ASPN, HOPX, IIGP1, PTPRD, BMP4, KRT19, SFRP2, NRN1L, FXYD3, SNAI1, LNX1, PPARG, PTX3, IRF5, FAM183B, ASPA, FGFR3	114	5338	18713	1.476050561	0.4622523	0.309884286	0.309884286
21	GOTERM_BP_DIRECT	GO:0050680~negative regulation of epithelial cell proliferation	5	3.731343284	0.001975787	BMP4, DUSP10, SFRP2, PPARG, FGFR3	122	88	20094	9.358233979	0.92339444	0.233322437	0.232065118
22	GOTERM_BP_DIRECT	GO:0043065~positive regulation of apoptotic process	9	6.71641791	0.00224611	FOXA1, BMP4, SFRP2, MSX2, HPGD, GATA6, FZD9, IRF5, PPARG	122	383	20094	3.870350554	0.946119091	0.24314145	0.241831219
23	GOTERM_CC_DIRECT	GO:0071944~cell periphery	5	3.731343284	0.002804146	EPHA5, KRT19, KRT8, SPRR1A, ACTG2	131	95	21179	8.509039775	0.3967691	0.100949244	0.099827586
24	GOTERM_BP_DIRECT	GO:0006366~transcription from RNA polymerase II promoter	7	5.223880597	0.003146485	BMP4, MYOCD, MSX2, TRP63, CYTL1, GRHL3, CELA1	122	237	20094	4.86470222	0.983323043	0.297555004	0.295951551
25	GOTERM_BP_DIRECT	GO:0048488~synaptic vesicle endocytosis	4	2.985074627	0.003206905	SYT1, RAB27B, SYT8, SH3GL2	122	49	20094	13.44529943	0.984585767	0.297555004	0.295951551
26	GOTERM_BP_DIRECT	GO:0006833~water transport	3	2.23880597	0.0040837	AQP3, UPK3A, AQP1	122	16	20094	30.88217213	0.995085611	0.347472537	0.345600091
27	UP_SEQ_FEATURE	BINDING:Substrate	10	7.462686567	0.004099321	PTPRD, CBR2, NT5E, DDC, URAH, HPGD, AKR1C14, ENPP2, HMGCS2, ASPA	129	547	22511	3.190198829	0.865283187	1	1
28	GOTERM_BP_DIRECT	GO:0042060~wound healing	5	3.731343284	0.004279877	FGF7, MSX2, NRG1, GRHL3, AQP1	122	109	20094	7.555271469	0.9961952	0.347472537	0.345600091
29	GOTERM_MF_DIRECT	GO:0005544~calcium-dependent phospholipid binding	4	2.985074627	0.004477131	SYT1, ESYT3, ANXA9, SYT8	114	55	18713	11.93811802	0.764223959	0.480545347	0.480545347
30	GOTERM_BP_DIRECT	GO:0050918~positive chemotaxis	3	2.23880597	0.004610037	BMP4, LGALS3, FGF7	122	17	20094	29.06557377	0.997526904	0.352261085	0.350362834
31	GOTERM_CC_DIRECT	GO:0016324~apical plasma membrane	9	6.71641791	0.004637683	UPK1B, UPK1A, UPK2, MAL, NRG1, RAB27B, UPK3A, AQP1, PROM2	131	423	21179	3.43982459	0.566873192	0.1391305	0.137584605
32	UP_SEQ_FEATURE	CARBOHYD:N-linked (GlcNAc...) asparagine	34	25.37313433	0.004718949	ITIH2, LAMC3, UPK2, IHH, MSLN, PRSS22, AQP3, AQP1, NT5E, FGF7, UPK1A, EDNRB, TSPAN8, ENPP2, CTSE, PROM2, EPHA5, LAMB3, SYT1, FZD9, NPY1R, CELA1, TMC7, UPK3A, ASPN, SERPINB5, PTPRD, BMP4, GREM2, SMOC1, PTX3, UPK3BL, FGFR3, KCNK3	129	3706	22511	1.600952991	0.900569633	1	1
33	GOTERM_BP_DIRECT	GO:0003151~outflow tract morphogenesis	4	2.985074627	0.004918571	BMP4, SFRP2, MSX2, NPY1R	122	57	20094	11.55823986	0.99834671	0.354956867	0.353044089
34	GOTERM_BP_DIRECT	GO:0048546~digestive tract morphogenesis	3	2.23880597	0.005751086	SFRP2, AGR2, FGFR3	122	19	20094	26.00603969	0.999442599	0.393192673	0.391073852
35	GOTERM_BP_DIRECT	GO:0051145~smooth muscle cell differentiation	3	2.23880597	0.006365062	BMP4, MYOCD, GATA6	122	20	20094	24.7057377	0.999750148	0.413410809	0.411183037
36	GOTERM_BP_DIRECT	GO:0022010~central nervous system myelination	3	2.23880597	0.007007522	MAL, FGFR3, ASPA	122	21	20094	23.529274	0.999892155	0.418292065	0.416037989
37	GOTERM_BP_DIRECT	GO:0048646~anatomical structure formation involved in morphogenesis	3	2.23880597	0.007678106	FOXA1, BMP4, TRP63	122	22	20094	22.45976155	0.999955157	0.418292065	0.416037989
38	GOTERM_BP_DIRECT	GO:0042733~embryonic digit morphogenesis	4	2.985074627	0.007710292	BMP4, SFRP2, MSX2, IHH	122	67	20094	9.833129435	0.999957007	0.418292065	0.416037989
39	GOTERM_BP_DIRECT	GO:0071456~cellular response to hypoxia	5	3.731343284	0.00772826	GATA6, PPARG, AQP3, KCNK3, AQP1	122	129	20094	6.383911552	0.999958007	0.418292065	0.416037989
40	GOTERM_MF_DIRECT	GO:0001786~phosphatidylserine binding	4	2.985074627	0.008082136	SYT1, ANXA9, GSDMC3, SYT8	114	68	18713	9.655830753	0.92668731	0.65061197	0.65061197
41	GOTERM_BP_DIRECT	GO:1902894~negative regulation of pri-miRNA transcription from RNA polymerase II promoter	3	2.23880597	0.009102223	BMP4, GATA6, PPARG	122	24	20094	20.58811475	0.999993058	0.472951484	0.470402861
42	GOTERM_BP_DIRECT	GO:0030216~keratinocyte differentiation	4	2.985074627	0.009753335	CERS3, TRP63, SPRR1A, IVL	122	73	20094	9.024927015	0.999997044	0.487291634	0.484665736
43	GOTERM_CC_DIRECT	GO:0099523~presynaptic cytosol	3	2.23880597	0.01022688	TRIM9, PRKCB, SH3GL2	131	25	21179	19.40061069	0.842812541	0.230104811	0.227548091
44	GOTERM_CC_DIRECT	GO:0016327~apicolateral plasma membrane	3	2.23880597	0.01022688	KRT19, RASGRF1, KRT8	131	25	21179	19.40061069	0.842812541	0.230104811	0.227548091
45	GOTERM_BP_DIRECT	GO:0003148~outflow tract septum morphogenesis	3	2.23880597	0.011440524	BMP4, MSX2, GATA6	122	27	20094	18.30054645	0.999999677	0.541228881	0.538312328
46	GOTERM_BP_DIRECT	GO:0043627~response to estrogen	4	2.985074627	0.011674467	KRT19, GATA6, PPARG, AQP1	122	78	20094	8.446406053	0.999999763	0.541228881	0.538312328
47	UP_SEQ_FEATURE	METAL:Calcium 1; via carbonyl oxygen	4	2.985074627	0.011855245	SYT1, PRKCB, IHH, ESYT3	129	83	22511	8.409825348	0.997032176	1	1
48	GOTERM_BP_DIRECT	GO:0036342~post-anal tail morphogenesis	3	2.23880597	0.012272481	SFRP2, TRP63, FGFR3	122	28	20094	17.6469555	0.999999892	0.541228881	0.538312328
49	GOTERM_BP_DIRECT	GO:0045669~positive regulation of osteoblast differentiation	4	2.985074627	0.012499512	BMP4, SFRP2, MSX2, TRP63	122	80	20094	8.235245902	0.99999992	0.541228881	0.538312328
50	INTERPRO	IPR018499:Tetraspanin/Peripherin	3	2.23880597	0.01259295	UPK1B, UPK1A, TSPAN8	120	30	20908	17.42333333	0.983103997	1	1
51	INTERPRO	IPR008952:Tetraspanin, EC2 domain	3	2.23880597	0.01259295	UPK1B, UPK1A, TSPAN8	120	30	20908	17.42333333	0.983103997	1	1
52	GOTERM_MF_DIRECT	GO:0005509~calcium ion binding	11	8.208955224	0.012929178	SYT1, PLA2G1B, SMOC1, RASEF, IHH, ENPP2, S100A5, ESYT3, ANXA9, SYT8, ASPN	114	730	18713	2.473479933	0.984858907	0.832639052	0.832639052
53	GOTERM_BP_DIRECT	GO:0014059~regulation of dopamine secretion	3	2.23880597	0.013130134	SYT1, PRKCB, SYT8	122	29	20094	17.0384398	0.999999965	0.550194976	0.547230107
54	UP_KW_PTM	KW-0449~Lipoprotein	13	9.701492537	0.013858206	SYT1, IHH, NPY1R, RAB27B, MSLN, IIGP1, ALDH3B2, NT5E, EDNRB, NRN1L, MAL, DEGS2, LY6G	88	867	12816	2.183705568	0.25402088	0.152440262	0.152440262
55	UP_SEQ_FEATURE	DISULFID:Interchain	5	3.731343284	0.014127807	BMP4, LGALS3, LAMB3, PTX3, CTSE	129	163	22511	5.352879631	0.999035147	1	1
56	UP_SEQ_FEATURE	REPEAT:1	5	3.731343284	0.014127807	LGALS3, DDC, SPRR2A2, SPRR1A, PPM1E	129	163	22511	5.352879631	0.999035147	1	1
57	GOTERM_CC_DIRECT	GO:0070382~exocytic vesicle	3	2.23880597	0.014536106	SYT1, RAB27B, SYT8	131	30	21179	16.16717557	0.928331382	0.290722127	0.287491881
58	UP_SEQ_FEATURE	REPEAT:2	5	3.731343284	0.014713663	LGALS3, DDC, SPRR2A2, SPRR1A, PPM1E	129	165	22511	5.287996241	0.999278094	1	1
59	GOTERM_BP_DIRECT	GO:0009887~animal organ morphogenesis	5	3.731343284	0.015050107	GREM2, FGF7, LAMB3, LAMC3, TRP63	122	157	20094	5.245379555	0.999999997	0.583700029	0.580554609

60	GOTERM_BP_DIRECT	GO:0048714~positive regulation of oligodendrocyte differentiation	3	2.23880597	0.016811073	ENPP2, PPARG, ASPA	122	33	20094	14.97317437	1	0.583700029	0.580554609
61	UP_SEQ_FEATURE	REGION:Necessary for interaction with PNN	2	1.492537313	0.016962265	KRT19, KRT8	129	3	22511	116.3359173	0.999763271	1	1
62	INTERPRO	IPR024831:Uroplakin-3	2	1.492537313	0.016978613	UPK3BL, UPK3A	120	3	20908	116.1555556	0.995970276	1	1
63	UP_SEQ_FEATURE	REPEAT:5	4	2.985074627	0.017005658	LGALS3, SPRR2A2, SPRR1A, PPM1E	129	95	22511	7.34753162	0.999768316	1	1
64	GOTERM_BP_DIRECT	GO:0031424~keratinization	4	2.985074627	0.0171177	SPRR2A2, KRT8, SPRR1A, IVL	122	90	20094	7.320218579	1	0.583700029	0.580554609
65	GOTERM_BP_DIRECT	GO:0050673~epithelial cell proliferation	4	2.985074627	0.0171177	BMP4, FGF7, PPARG, FGFR3	122	90	20094	7.320218579	1	0.583700029	0.580554609
66	GOTERM_MF_DIRECT	GO:0008270~zinc ion binding	11	8.208955224	0.017256379	TRIM71, CAR3, ZCCHC12, TRIM9, TRIM29, PRKCB, GATA6, ENPP2, S100A5, PPARG, LMCD1	114	764	18713	2.363403601	0.996320785	0.926092349	0.926092349
67	GOTERM_BP_DIRECT	GO:1904706~negative regulation of vascular smooth muscle cell proliferation	3	2.23880597	0.017792255	CNN1, MYOCD, PPARG	122	34	20094	14.53278689	1	0.583700029	0.580554609
68	GOTERM_BP_DIRECT	GO:0060197~cloacal septation	2	1.492537313	0.017957418	BMP4, TRP63	122	3	20094	109.8032787	1	0.583700029	0.580554609
69	GOTERM_BP_DIRECT	GO:0061144~alveolar secondary septum development	2	1.492537313	0.017957418	FOXA1, FGFR3	122	3	20094	109.8032787	1	0.583700029	0.580554609
70	GOTERM_BP_DIRECT	GO:0035116~embryonic hindlimb morphogenesis	3	2.23880597	0.018797173	BMP4, MSX2, TRP63	122	35	20094	14.1175644	1	0.583700029	0.580554609
71	GOTERM_BP_DIRECT	GO:0046513~ceramide biosynthetic process	3	2.23880597	0.018797173	CERS3, SPTLC3, DEGS2	122	35	20094	14.1175644	1	0.583700029	0.580554609
72	GOTERM_BP_DIRECT	GO:0031016~pancreas development	3	2.23880597	0.018797173	GATA6, IHH, MSLN	122	35	20094	14.1175644	1	0.583700029	0.580554609
73	GOTERM_BP_DIRECT	GO:0008283~cell proliferation	7	5.223880597	0.018872518	BMP4, RASGRF1, IHH, TRP63, PPARG, NRG1, FGFR3	122	348	20094	3.31302996	1	0.583700029	0.580554609
74	UP_KW_BIOLOGICAL_PROCESS	KW-0221~Differentiation	10	7.462686567	0.01908427	BMP4, LGALS3, APELA, SFRP2, SYT1, PAQR5, SMOC1, INSC, EIF2AK4, DMKN	61	747	11003	2.414686087	0.666568343	1	1
75	GOTERM_BP_DIRECT	GO:0042476~odontogenesis	3	2.23880597	0.019825511	BMP4, MSX2, AQP3	122	36	20094	13.72540984	1	0.585303149	0.58214909
76	GOTERM_BP_DIRECT	GO:0031069~hair follicle morphogenesis	3	2.23880597	0.019825511	FGF7, SNAI1, TRP63	122	36	20094	13.72540984	1	0.585303149	0.58214909
77	GOTERM_BP_DIRECT	GO:0060349~bone morphogenesis	3	2.23880597	0.023047918	SFRP2, MSX2, FGFR3	122	39	20094	12.66960908	1	0.603705916	0.600452689
78	GOTERM_MF_DIRECT	GO:0042056~chemoattractant activity	3	2.23880597	0.023158198	BMP4, LGALS3, FGF7	114	39	18713	12.6268556	0.999471063	0.966233406	0.966233406
79	GOTERM_BP_DIRECT	GO:0001843~neural tube closure	4	2.985074627	0.023758705	TRIM71, BMP4, SFRP2, GRHL3	122	102	20094	6.459016393	1	0.603705916	0.600452689
80	GOTERM_BP_DIRECT	GO:0001649~osteoblast differentiation	4	2.985074627	0.023758705	BMP4, MSX2, IHH, SNAI1	122	102	20094	6.459016393	1	0.603705916	0.600452689
81	GOTERM_BP_DIRECT	GO:0060157~urinary bladder development	2	1.492537313	0.023871865	MYOCD, UPK3A	122	4	20094	82.35245902	1	0.603705916	0.600452689
82	GOTERM_BP_DIRECT	GO:0098773~skin epidermis development	2	1.492537313	0.023871865	GATA6, TRP63	122	4	20094	82.35245902	1	0.603705916	0.600452689
83	GOTERM_BP_DIRECT	GO:0051150~regulation of smooth muscle cell differentiation	2	1.492537313	0.023871865	BMP4, MYOCD	122	4	20094	82.35245902	1	0.603705916	0.600452689
84	GOTERM_MF_DIRECT	GO:0000976~transcription regulatory region sequence-specific DNA binding	6	4.47761194	0.024005799	FOXA1, MSX2, GATA6, TRP63, IRF5, PPARG	114	270	18713	3.647758285	0.999600046	0.966233406	0.966233406
85	GOTERM_BP_DIRECT	GO:0009888~tissue development	3	2.23880597	0.024166826	BMP4, LAMB3, LAMC3	122	40	20094	12.35286885	1	0.603705916	0.600452689
86	GOTERM_BP_DIRECT	GO:0045595~regulation of cell differentiation	3	2.23880597	0.024166826	BMP4, NRG1, CELA1	122	40	20094	12.35286885	1	0.603705916	0.600452689
87	KEGG_PATHWAY	mmu05200:Pathways in cancer	9	6.71641791	0.02454272	BMP4, FGF7, EDNRB, LAMB3, LAMC3, PRKCB, FZD9, PPARG, FGFR3	60	543	8992	2.483977901	0.98641599	1	1
88	GOTERM_BP_DIRECT	GO:0010628~positive regulation of gene expression	9	6.71641791	0.024785198	BMP4, FGF7, MYOCD, AGR2, PPARG, NRG1, GRHL3, EIF2AK4, ACTG2	122	583	20094	2.542614515	1	0.607471183	0.604197666
89	GOTERM_BP_DIRECT	GO:0030513~positive regulation of BMP signaling pathway	3	2.23880597	0.025307615	BMP4, MSX2, GATA6	122	41	20094	12.05157937	1	0.608788733	0.605508116
90	UP_SEQ_FEATURE	TOPO_DOM:Cytoplasmic	28	20.89552239	0.025896166	UPK2, ILDR1, TMEM140, NCMAP, AQP3, AQP1, UPK1B, UPK1A, EDNRB, TSPAN8, PROM2, EPHA5, CERS3, SYT1, PAQR5, FZD9, NPY1R, TMC7, SHISA2, SYT8, UPK3A, PTPRD, FXYD3, MAL, ESYT3, UPK3BL, FGFR3, KCNK3	129	3252	22511	1.502493397	0.99999725	1	1
91	GOTERM_MF_DIRECT	GO:0043565~sequence-specific DNA binding	8	5.970149254	0.02775105	FOXA1, MSX2, GATA6, SNAI1, TRP63, IRF5, PPARG, GRHL3	114	485	18713	2.707614397	0.999884029	0.992870899	0.992870899
92	UP_KW_CELLULAR_COMPONENT	KW-0084~Basement membrane	3	2.23880597	0.028380488	LAMB3, LAMC3, SMOC1	119	40	17960	11.31932773	0.526955583	0.368946343	0.368946343
93	GOTERM_BP_DIRECT	GO:0060513~prostatic bud formation	2	1.492537313	0.029750984	BMP4, TRP63	122	5	20094	65.88196721	1	0.66762031	0.664022664
94	GOTERM_BP_DIRECT	GO:0060512~prostate gland morphogenesis	2	1.492537313	0.029750984	BMP4, SERPINB5	122	5	20094	65.88196721	1	0.66762031	0.664022664
95	GOTERM_BP_DIRECT	GO:0015840~urea transport	2	1.492537313	0.029750984	AQP3, UPK3A	122	5	20094	65.88196721	1	0.66762031	0.664022664
96	UP_KW_PTM	KW-0165~Cleavage on pair of basic residues	6	4.47761194	0.030061005	BMP4, UPK2, SCT, ENPP2, MSLN, CHGB	88	256	12816	3.413352273	0.473215702	0.220447367	0.220447367
97	UP_SEQ_FEATURE	TOPO_DOM:Extracellular	22	16.41791045	0.030808085	EPHA5, PAQR5, FZD9, ILDR1, NPY1R, TMC7, SHISA2, TMEM140, NCMAP, AQP3, SYT8, AQP1, PTPRD, UPK1B, UPK1A, EDNRB, TSPAN8, FXYD3, MAL, UPK3BL, FGFR3, PROM2	129	2408	22511	1.594304515	0.999999767	1	1
98	GOTERM_BP_DIRECT	GO:0030501~positive regulation of bone mineralization	3	2.23880597	0.031329375	BMP4, FZD9, FGFR3	122	46	20094	10.74162509	1	0.66762031	0.664022664
99	GOTERM_BP_DIRECT	GO:0045944~positive regulation of transcription from RNA polymerase II promoter	14	10.44776119	0.031417935	FOXA1, LMO1, ZCCHC12, MYOCD, GATA6, IHH, TRP63, GRHL3, CELA1, BMP4, SFRP2, PPARG, IRF5, CYTL1	122	1216	20094	1.896273727	1	0.66762031	0.664022664
100	GOTERM_BP_DIRECT	GO:0010718~positive regulation of epithelial to mesenchymal transition	3	2.23880597	0.032595252	BMP4, MYOCD, SNAI1	122	47	20094	10.51307987	1	0.66762031	0.664022664

Table S2. Functional annotation by DAVID for genes with decreased expression in E14.5 *Bmp4cKO* ureters.

		Intensities				fold changes (FC)		
Rank	**Gene Symbol**	**control 1**	**NOG 1**	**control 2**	**NOG 2**	**FC1**	**FC2**	**avgFC**
1	*Grem2*	251	40	216	22	-6.2	-9.8	-8.0
2	*Id2*	43029	10261	42291	4028	-4.2	-10.5	-7.3
3	*Gata5os*	119	19	122	15	-6.3	-8.1	-7.2
4	*Crhbp*	166	26	216	36	-6.5	-6.1	-6.3
5	*Wfdc18*	210	51	145	18	-4.1	-8.0	-6.1
6	*Smad9*	1093	208	1013	150	-5.3	-6.7	-6.0
7	*Gm4841*	102	31	132	17	-3.3	-7.6	-5.4
8	*Gpr165*	130	23	108	22	-5.6	-4.9	-5.3
9	*Npy1r*	6327	1354	6163	1078	-4.7	-5.7	-5.2
10	*Tcf24*	216	50	167	28	-4.4	-6.0	-5.2
11	*Sphkap*	191	40	162	30	-4.8	-5.5	-5.1
12	*Chrdl1*	389	75	294	59	-5.2	-5.0	-5.1
13	*Chrdl2*	113	26	134	25	-4.4	-5.4	-4.9
14	*Sox9*	5654	1116	5232	1149	-5.1	-4.6	-4.8
15	*Brinp3*	263	78	346	59	-3.4	-5.9	-4.6
16	*Pparg*	4200	1339	4790	894	-3.1	-5.4	-4.2
17	*Id1*	4434	1570	5138	906	-2.8	-5.7	-4.2
18	*Id4*	14272	4842	13943	2719	-2.9	-5.1	-4.0
19	*Ptger2*	388	114	293	65	-3.4	-4.5	-3.9
20	*Gprin3*	360	109	354	82	-3.3	-4.3	-3.8
21	*1010001N08Rik*	1034	340	1421	320	-3.0	-4.4	-3.7
22	*Nog*	309	96	293	70	-3.2	-4.2	-3.7
23	*Myl1*	208	54	177	53	-3.9	-3.3	-3.6
24	*Sct*	1632	630	1666	393	-2.6	-4.2	-3.4
25	*Cdh18*	171	58	178	47	-3.0	-3.8	-3.4
26	*Iigp1*	3880	1407	3911	993	-2.8	-3.9	-3.3
27	*Hs3st1*	442	172	460	115	-2.6	-4.0	-3.3
28	*Micalcl*	135	46	136	38	-2.9	-3.6	-3.3
29	*Kctd8*	292	119	388	96	-2.4	-4.1	-3.3
30	*ENSMUST00000131638*	1076	470	1190	291	-2.3	-4.1	-3.2
31	*Ednrb*	5395	1854	4628	1337	-2.9	-3.5	-3.2
32	*Tlx2*	4033	1455	2695	836	-2.8	-3.2	-3.0
33	*a*	376	118	238	86	-3.2	-2.8	-3.0
34	*Timp4*	116	40	108	36	-2.9	-3.0	-2.9
35	*Cux2*	6140	2135	5745	1914	-2.9	-3.0	-2.9
36	*LOC102633497*	421	162	541	168	-2.6	-3.2	-2.9
37	*Masp1*	614	220	571	189	-2.8	-3.0	-2.9
38	*Snai1*	4360	1612	3700	1222	-2.7	-3.0	-2.9
39	*Gdf5*	2039	800	1921	612	-2.5	-3.1	-2.8
40	*Cck*	2714	1158	3294	985	-2.3	-3.3	-2.8
41	*Id3*	66190	26689	54551	17080	-2.5	-3.2	-2.8
42	*Akr1b7*	142	56	162	53	-2.5	-3.1	-2.8
43	*Fgfr3*	2035	766	1954	667	-2.7	-2.9	-2.8
44	*A_55_P1957123*	112	46	129	41	-2.4	-3.1	-2.8
45	*Gm5105*	148	54	144	51	-2.7	-2.8	-2.8

46	*Kcnip4*	289	123	320	101	-2.3	-3.2	-2.8
47	*Atoh8*	1387	568	1377	451	-2.4	-3.1	-2.7
48	*BC023105*	258	98	290	103	-2.6	-2.8	-2.7
49	*Ahr*	5475	2180	5141	1799	-2.5	-2.9	-2.7
50	*Col9a3*	287	106	230	88	-2.7	-2.6	-2.7
51	*Sst*	514	210	434	151	-2.4	-2.9	-2.7
52	*Gabra1*	413	169	468	167	-2.5	-2.8	-2.6
53	*Enpp2*	13192	5249	13538	4939	-2.5	-2.7	-2.6
54	*Gabra2*	110	44	105	39	-2.5	-2.7	-2.6
55	*Spag16*	159	78	207	66	-2.0	-3.1	-2.6
56	*Msx2*	533	207	440	172	-2.6	-2.6	-2.6
57	*Akr1c14*	228	101	226	78	-2.2	-2.9	-2.6
58	*Hapln1*	1148	443	1373	543	-2.6	-2.5	-2.6
59	*BC057651*	362	170	415	144	-2.1	-2.9	-2.5
60	*1110032F04Rik*	194	72	204	90	-2.7	-2.3	-2.5
61	*Fzd9*	486	211	436	164	-2.3	-2.7	-2.5
62	*Syt4*	186	69	197	88	-2.7	-2.2	-2.5
63	*Pnlip*	103	47	119	44	-2.2	-2.7	-2.5
64	*Syt1*	3659	1698	3928	1444	-2.2	-2.7	-2.4
65	*Tbx18*	6839	3270	8455	3046	-2.1	-2.8	-2.4
66	*Sstr1*	883	379	888	352	-2.3	-2.5	-2.4
67	*4930431P19Rik*	536	242	675	269	-2.2	-2.5	-2.4
68	*Dleu2*	136	64	167	64	-2.1	-2.6	-2.4
69	*Fam19a2*	1079	510	1145	445	-2.1	-2.6	-2.3
70	*Dkk2*	3385	1611	3608	1394	-2.1	-2.6	-2.3
71	*Elavl2*	1391	595	1596	681	-2.3	-2.3	-2.3
72	*Galnt14*	1006	482	1091	427	-2.1	-2.6	-2.3
73	*A_55_P2015594*	157	76	228	90	-2.1	-2.5	-2.3
74	*Calcr*	130	54	104	47	-2.4	-2.2	-2.3
75	*Gabrb2*	1172	519	1187	524	-2.3	-2.3	-2.3
76	*Phlda2*	219	97	208	92	-2.3	-2.3	-2.3
77	*A_55_P2175050*	283	116	235	114	-2.4	-2.1	-2.3
78	*Traf1*	221	105	219	93	-2.1	-2.3	-2.2
79	*Ihh*	195	94	210	89	-2.1	-2.4	-2.2
80	*Stxbp5l*	376	159	311	150	-2.4	-2.1	-2.2
81	*Sntg1*	457	220	459	195	-2.1	-2.4	-2.2
82	*Edil3*	3210	1388	3151	1514	-2.3	-2.1	-2.2
83	*Cadps*	1570	728	1240	558	-2.2	-2.2	-2.2
84	*Nxpe3*	4798	2364	4831	2108	-2.0	-2.3	-2.2
85	*Pcdh9*	607	278	676	316	-2.2	-2.1	-2.2
86	*CB193388*	2005	935	2461	1134	-2.1	-2.2	-2.2
87	*Pipox*	151	74	176	79	-2.0	-2.2	-2.1
88	*Rab27b*	827	375	750	363	-2.2	-2.1	-2.1
89	*Clstn2*	9357	4464	8565	3985	-2.1	-2.1	-2.1
90	*Gper1*	381	189	337	158	-2.0	-2.1	-2.1

Table S3. List of genes with decreased expression in microarrays of explants of E12.5 ureters treated for 18 h with 10 µg/ml NOGGIN (NOG). Shown are the gene names, the intensity of the two control and treated ureter samples, the individual and the average (avg) fold change (FC).

Rank	Category	Term	Count	%	PValue	Genes	List Total	Pop Hits	Pop Total	Fold Enrichment	Bonferroni	Benjamini	FDR
1	GOTERM_BP_DIRECT	GO:0051216~cartilage development	8	10	3.51E-08	MSX2, NOG, IHH, SMAD9, SOX9, CHRDL2, GDF5, FGFR3	72	92	20094	24.26811594	3.48E-05	3.48E-05	3.39E-05
2	GOTERM_BP_DIRECT	GO:0045668~negative regulation of osteoblast differentiation	7	8.75	1.58E-07	ID2, NOG, ID1, ID3, PPARG, AHR, SOX9	72	69	20094	28.31280193	1.57E-04	6.11E-05	5.95E-05
3	KEGG_PATHWAY	mmu04350:TGF-beta signaling pathway	8	10	1.65E-07	GREM2, ID2, NOG, ID1, ID4, SMAD9, ID3, GDF5	41	95	8992	18.46880616	1.53E-05	1.53E-05	1.52E-05
4	INTERPRO	IPR026052:DNA-binding protein inhibitor	4	5	1.70E-07	ID2, ID1, ID4, ID3	75	4	20908	278.7733333	3.40E-05	3.40E-05	3.36E-05
5	GOTERM_BP_DIRECT	GO:0007275~multicellular organism development	18	22.5	1.84E-07	MSX2, NOG, FZD9, IHH, CHRDL2, CHRDL1, DKK2, TBX18, GREM2, TLX2, ID2, ATOH8, ID1, SNAI1, ID3, FGFR3, EDIL3, CDH18	72	1095	20094	4.587671233	1.83E-04	6.11E-05	5.95E-05
6	GOTERM_BP_DIRECT	GO:0030154~cell differentiation	17	21.25	4.07E-07	SYT4, SYT1, NOG, IHH, SMAD9, CHRDL2, CHRDL1, TBX18, GPER1, ID2, ATOH8, ID1, ID4, ID3, PPARG, SOX9, FGFR3	72	1022	20094	4.642286367	4.04E-04	1.01E-04	9.85E-05
7	GOTERM_CC_DIRECT	GO:0005576~extracellular region	22	27.5	9.18E-07	SPAG16, A, SCT, NOG, IHH, CCK, CHRDL2, GDF5, CHRDL1, DKK2, HAPLN1, AKR1B7, GREM2, CRHBP, SST, ENPP2, WFDC18, MASP1, EDIL3, BRINP3, TIMP4, PNLIP	75	1859	21179	3.341854043	1.33E-04	1.33E-04	1.23E-04
8	GOTERM_BP_DIRECT	GO:0030509~BMP signaling pathway	7	8.75	2.52E-06	MSX2, NOG, ID1, SMAD9, PPARG, GDF5, CHRDL1	72	110	20094	17.75984848	0.002497757	5.00E-04	4.87E-04
9	INTERPRO	IPR011598:Myc-type, basic helix-loop-helix (bHLH) domain	7	8.75	3.15E-06	TCF24, ID2, ATOH8, ID1, ID4, ID3, AHR	75	114	20908	17.11766082	6.30E-04	3.15E-04	3.12E-04
10	GOTERM_BP_DIRECT	GO:0001503~ossification	7	8.75	3.60E-06	CALCR, MSX2, IHH, FZD9, SOX9, CHRDL2, CHRDL1	72	117	20094	16.69729345	0.003575268	5.97E-04	5.81E-04
11	KEGG_PATHWAY	mmu04080:Neuroactive ligand-receptor interaction	11	13.75	5.05E-06	GABRA2, GABRB2, GABRA1, EDNRB, CALCR, SST, SCT, PTGER2, NPY1R, CCK, SSTR1	41	386	8992	6.249968406	4.69E-04	2.35E-04	2.32E-04
12	UP_KW_CELLULAR_COMPONENT	KW-0964~Secreted	20	25	9.79E-06	A, SCT, NOG, IHH, CCK, CHRDL2, GDF5, CHRDL1, DKK2, HAPLN1, GREM2, CRHBP, SST, ENPP2, WFDC18, MASP1, EDIL3, BRINP3, TIMP4, PNLIP	68	1709	17960	3.090902833	2.05E-04	2.06E-04	1.86E-04
13	UP_SEQ_FEATURE	DOMAIN:BHLH	6	7.5	1.03E-05	TCF24, ID2, ID1, ID4, ID3, AHR	78	84	22511	20.61446886	0.003380944	0.003386655	0.003386655
14	SMART	SM00353:HLH	7	8.75	1.11E-05	TCF24, ID2, ATOH8, ID1, ID4, ID3, AHR	50	111	10615	13.38828829	5.87E-04	5.87E-04	5.87E-04
15	UP_KW_MOLECULAR_FUNCTION	KW-9996~Developmental protein	16	20	2.54E-05	MSX2, NOG, FZD9, IHH, CHRDL2, CHRDL1, DKK2, TBX18, GREM2, TLX2, ID2, ATOH8, ID1, SNAI1, ID3, EDIL3	54	1044	12158	3.450546332	8.39E-04	4.20E-04	3.94E-04
16	UP_KW_MOLECULAR_FUNCTION	KW-0217~Developmental protein	16	20	2.54E-05	MSX2, NOG, FZD9, IHH, CHRDL2, CHRDL1, DKK2, TBX18, GREM2, TLX2, ID2, ATOH8, ID1, SNAI1, ID3, EDIL3	54	1044	12158	3.450546332	8.39E-04	4.20E-04	3.94E-04
17	KEGG_PATHWAY	mmu04550:Signaling pathways regulating pluripotency of stem cells	7	8.75	3.18E-05	ID2, ID1, ID4, FZD9, SMAD9, ID3, FGFR3	41	140	8992	10.96585366	0.002949963	9.85E-04	9.74E-04
18	GOTERM_BP_DIRECT	GO:0000122~negative regulation of transcription from RNA polymerase II promoter	14	17.5	3.23E-05	MSX2, NOG, AHR, TBX18, EDNRB, CUX2, ID2, ID1, ID4, SNAI1, ID3, PPARG, SOX9, FGFR3	72	975	20094	4.007350427	0.031607386	0.004588166	0.004468154
19	UP_SEQ_FEATURE	DOMAIN:bHLH	6	7.5	3.32E-05	ID2, ATOH8, ID1, ID4, ID3, AHR	78	107	22511	16.18332135	0.010910236	0.005485003	0.005485003
20	GOTERM_BP_DIRECT	GO:0030514~negative regulation of BMP signaling pathway	5	6.25	4.91E-05	GREM2, NOG, PPARG, CHRDL2, CHRDL1	72	57	20094	24.48099415	0.047605442	0.006096835	0.005937361
21	GOTERM_CC_DIRECT	GO:0031045~dense core granule	4	5	5.21E-05	SYT4, CRHBP, SYT1, CADPS	75	21	21179	53.78793651	0.007519082	0.003773648	0.003487371
22	GOTERM_MF_DIRECT	GO:0046983~protein dimerization activity	7	8.75	5.22E-05	TCF24, ID2, ATOH8, ID1, ID4, ID3, AHR	71	177	18713	10.42341052	0.011427559	0.00574004	0.005609584
23	UP_SEQ_FEATURE	CARBOHYD:N-linked (GlcNAc...) asparagine	28	35	5.62E-05	GABRB2, A, CLSTN2, PTGER2, IHH, CHRDL2, CHRDL1, HAPLN1, CRHBP, CALCR, EDNRB, GPER1, ENPP2, BRINP3, EDIL3, GABRA2, GABRA1, SYT1, NOG, FZD9, NPY1R, SSTR1, GDF5, DKK2, HS3ST1, GREM2, MASP1, FGFR3	78	3706	22511	2.180483485	0.018374675	0.005691253	0.005691253
24	GOTERM_MF_DIRECT	GO:0036122~BMP binding	4	5	6.35E-05	GREM2, CHRDL2, GDF5, CHRDL1	71	21	18713	50.20254863	0.013878848	0.00574004	0.005609584
25	GOTERM_BP_DIRECT	GO:0010629~negative regulation of gene expression	9	11.25	6.50E-05	GPER1, ID2, ATOH8, NOG, ID1, ID3, PPARG, SOX9, FGFR3	72	387	20094	6.490310078	0.062564355	0.007178341	0.006990578
26	UP_SEQ_FEATURE	REGION:Interaction with IFI204	3	3.75	6.90E-05	ID2, ID1, ID3	78	4	22511	216.4519231	0.022508612	0.005691253	0.005691253
27	UP_KW_DOMAIN	KW-0732~Signal	32	40	7.68E-05	GABRB2, A, CLSTN2, SCT, IHH, CHRDL2, CHRDL1, CRHBP, CALCR, EDNRB, ENPP2, WFDC18, BRINP3, EDIL3, TIMP4, GABRA2, GABRA1, 1110032F04RIK, PCDH9, NOG, FZD9, CCK, GDF5, DKK2, HS3ST1, GREM2, SST, COL9A3, MASP1, FGFR3, PNLIP, CDH18	56	4739	15344	1.850179363	0.001074806	0.001075342	0.001075342
28	GOTERM_MF_DIRECT	GO:0005509~calcium ion binding	12	15	7.83E-05	SYT4, PCDH9, SYT1, CLSTN2, MYL1, CADPS, KCNIP4, IHH, ENPP2, MASP1, EDIL3, CDH18	71	730	18713	4.332548717	0.017073363	0.00574004	0.005609584
29	GOTERM_BP_DIRECT	GO:0045892~negative regulation of transcription, DNA-templated	11	13.75	1.06E-04	CUX2, MSX2, ID2, ATOH8, ID1, ID4, SNAI1, ID3, PPARG, AHR, SOX9	72	662	20094	4.637336354	0.100074793	0.010543803	0.010268009
30	GOTERM_BP_DIRECT	GO:0032922~circadian regulation of gene expression	5	6.25	1.23E-04	ID2, ID1, ID4, ID3, AHR	72	72	20094	19.38078704	0.114914335	0.011096668	0.010806413
31	GOTERM_BP_DIRECT	GO:0010628~positive regulation of gene expression	10	12.5	2.06E-04	CALCR, CUX2, GPER1, ID2, NOG, ID1, ID4, ID3, PPARG, SOX9	72	583	20094	4.787021155	0.184823109	0.017027428	0.016582043
32	GOTERM_CC_DIRECT	GO:0045202~synapse	12	15	2.64E-04	KCTD8, GABRA2, GABRB2, SYT4, GABRA1, SYT1, CLSTN2, GPER1, CADPS, CHRDL1, ELAVL2, HAPLN1	75	895	21179	3.786189944	0.037568391	0.012762405	0.011794223
33	GOTERM_BP_DIRECT	GO:0050673~epithelial cell proliferation	5	6.25	2.91E-04	NOG, PPARG, SOX9, FGFR3, TBX18	72	90	20094	15.50462963	0.25102759	0.022231624	0.021650112
34	GOTERM_BP_DIRECT	GO:0050679~positive regulation of epithelial cell proliferation	5	6.25	3.16E-04	NOG, ID1, IHH, SOX9, TBX18	72	92	20094	15.16757246	0.269784907	0.022454744	0.021867397
35	GOTERM_BP_DIRECT	GO:0008284~positive regulation of cell proliferation	10	12.5	4.08E-04	EDNRB, GPER1, ID2, NOG, ID4, IHH, ENPP2, CCK, SOX9, FGFR3	72	640	20094	4.360677083	0.333404378	0.027032597	0.026325507
36	GOTERM_BP_DIRECT	GO:0001649~osteoblast differentiation	5	6.25	4.68E-04	MSX2, NOG, ID4, IHH, SNAI1	72	102	20094	13.68055556	0.3723069	0.027562514	0.026841563
37	GOTERM_BP_DIRECT	GO:0071392~cellular response to estradiol stimulus	4	5	4.71E-04	CRHBP, MSX2, GPER1, SSTR1	72	43	20094	25.96124031	0.374167937	0.027562514	0.026841563
38	GOTERM_BP_DIRECT	GO:0097152~mesenchymal cell apoptotic process	3	3.75	5.44E-04	MSX2, SOX9, GDF5	72	10	20094	83.725	0.417695265	0.030034128	0.029248527
39	GOTERM_MF_DIRECT	GO:0070888~E-box binding	4	5	6.78E-04	ATOH8, SNAI1, PPARG, AHR	71	46	18713	22.91855481	0.138630501	0.032660848	0.031918556
40	GOTERM_MF_DIRECT	GO:0005237~inhibitory extracellular ligand-gated ion channel activity	3	3.75	7.42E-04	GABRA2, GABRB2, GABRA1	71	11	18713	71.8809219	0.150718755	0.032660848	0.031918556
41	GOTERM_BP_DIRECT	GO:0007417~central nervous system development	5	6.25	8.37E-04	NOG, ID3, SOX9, TIMP4, HAPLN1	72	119	20094	11.72619048	0.564834073	0.043772618	0.042627661
42	UP_KW_PTM	KW-1015~Disulfide bond	27	33.75	9.15E-04	GABRB2, A, GALNT14, PTGER2, HAPLN1, CRHBP, CALCR, EDNRB, GPER1, ENPP2, EDIL3, TIMP4, GABRA2, GABRA1, NOG, FZD9, NPY1R, RAB27B, SSTR1, GDF5, DKK2, HS3ST1, GREM2, SST, MASP1, FGFR3, PNLIP	58	3302	12816	1.806804653	0.014540592	0.013280366	0.010936772
43	GOTERM_BP_DIRECT	GO:1904862~inhibitory synapse assembly	3	3.75	9.36E-04	GABRA2, GABRB2, GABRA1	72	13	20094	64.40384615	0.605877598	0.04653289	0.045315732
44	GOTERM_CC_DIRECT	GO:0045211~postsynaptic membrane	6	7.5	0.001040387	KCTD8, GABRA2, GABRB2, GABRA1, CLSTN2, GPER1	75	220	21179	7.701454545	0.140096102	0.037714028	0.034852964
45	GOTERM_MF_DIRECT	GO:0022851~GABA-gated chloride ion channel activity	3	3.75	0.001047623	GABRA2, GABRB2, GABRA1	71	13	18713	60.82231853	0.205941278	0.038412842	0.037539823

46	UP_KW_BIOLOGICAL_PROCESS	KW-0891~Chondrogenesis	3	3.75	0.001528743	NOG, CHRDL2, GDF5	39	17	11003	49.78733032	0.038996986	0.021668709	0.021668709			
47	UP_KW_PTM	KW-0325~Glycoprotein	30	37.5	0.001562396	GABRB2, A, CLSTN2, PTGER2, IHH, CHRDL2, CHRDL1, HAPLN1, CRHBP, CALCR, EDNRB, GPER1, ENPP2, BRINP3, EDIL3, GABRA2, GABRA1, SYT1, NOG, FZD9, NPY1R, SSTR1, GDF5, DKK2, HS3ST1, GREM2, SNAI1, PPARG, MASP1, FGFR3	58	4008	12816	1.653933512	0.024707532	0.013280366	0.010936772			
48	GOTERM_BP_DIRECT	GO:0048712~negative regulation of astrocyte differentiation	3	3.75	0.001617628	NOG, ID4, FGFR3	72	17	20094	49.25	0.799957244	0.076567726	0.074564948			
49	UP_KW_BIOLOGICAL_PROCESS	KW-0090~Biological rhythms	5	6.25	0.001666824	ID2, ID1, ID3, PPARG, AHR	39	149	11003	9.467389434	0.042446396	0.021668709	0.021668709			
50	GOTERM_BP_DIRECT	GO:0002062~chondrocyte differentiation	4	5	0.001722272	IHH, SOX9, CHRDL2, GDF5	72	67	20094	16.66169154	0.819750624	0.077815366	0.075779954			
51	INTERPRO	IPR007743:Interferon-inducible GTPase	3	3.75	0.001822634	BC023105, GM4841, IIGP1	75	18	20908	46.46222222	0.305705803	0.121508963	0.120293874			
52	GOTERM_CC_DIRECT	GO:0030424~axon	8	10	0.00184456	GABRA2, SYT4, CALCR, SYT1, GPER1, NOG, NPY1R, CCK	75	502	21179	4.500185923	0.23486898	0.047891356	0.044258218			
53	UP_SEQ_FEATURE	DOMAIN:IRG-type G	3	3.75	0.001901709	BC023105, GM4841, IIGP1	78	19	22511	45.56882591	0.466428136	0.125512807	0.125512807			
54	GOTERM_CC_DIRECT	GO:1902711~GABA-A receptor complex	3	3.75	0.001981711	GABRA2, GABRB2, GABRA1	75	19	21179	44.58736842	0.249963368	0.047891356	0.044258218			
55	GOTERM_BP_DIRECT	GO:0048511~rhythmic process	5	6.25	0.002113708	ID2, ID1, ID3, PPARG, AHR	72	153	20094	9.12037037	0.877940793	0.091348932	0.088959523			
56	GOTERM_MF_DIRECT	GO:0004890~GABA-A receptor activity	3	3.75	0.002263644	GABRA2, GABRB2, GABRA1	71	19	18713	41.61527057	0.392599103	0.071143107	0.069526218			
57	GOTERM_BP_DIRECT	GO:0043065~positive regulation of apoptotic process	7	8.75	0.00232798	MSX2, GPER1, FZD9, ID3, CCK, PPARG, PHLDA2	72	383	20094	5.100739774	0.901402576	0.096417186	0.093895207			
58	UP_KW_CELLULAR_COMPONENT	KW-0628~Postsynaptic cell membrane	5	6.25	0.002499526	KCTD8, GABRA2, GABRB2, GABRA1, GPER1	68	152	17960	8.688080495	0.051198574	0.01789197	0.016187973			
59	UP_KW_CELLULAR_COMPONENT	KW-0770~Synapse	8	10	0.002555996	KCTD8, GABRA2, GABRB2, GABRA1, SYT1, CLSTN2, GPER1, CADPS	68	500	17960	4.225882353	0.052325911	0.01789197	0.016187973			
60	GOTERM_BP_DIRECT	GO:0007165~signal transduction	13	16.25	0.002856153	GABRA2, GABRB2, GABRA1, PTGER2, FZD9, NPY1R, TRAF1, SSTR1, EDNRB, CALCR, GPER1, PPARG, SOX9	72	1368	20094	2.6521077	0.941753921	0.113560657	0.110590258			
61	INTERPRO	IPR006028:Gamma-aminobutyric acid A receptor	3	3.75	0.002979614	GABRA2, GABRB2, GABRA1	75	23	20908	36.36173913	0.449436193	0.148980711	0.147490904			
62	GOTERM_CC_DIRECT	GO:0005615~extracellular space	16	20	0.002980914	A, SCT, NOG, IHH, CCK, GDF5, DKK2, GREM2, CRHBP, SST, ENPP2, COL9A3, WFDC18, MASP1, TIMP4, PNLIP	75	1969	21179	2.294660572	0.351360397	0.061747503	0.05706321			
63	GOTERM_BP_DIRECT	GO:0051932~synaptic transmission, GABAergic	3	3.75	0.003230816	GABRA2, GABRB2, GABRA1	72	24	20094	34.88541667	0.959910079	0.118941902	0.115830745			
64	GOTERM_BP_DIRECT	GO:0032331~negative regulation of chondrocyte differentiation	3	3.75	0.003230816	IHH, SOX9, GDF5	72	24	20094	34.88541667	0.959910079	0.118941902	0.115830745			
65	GOTERM_BP_DIRECT	GO:0008217~regulation of blood pressure	4	5	0.003393679	EDNRB, NPY1R, PPARG, AHR	72	85	20094	13.13333333	0.96592031	0.120094436	0.116953132			
66	GOTERM_BP_DIRECT	GO:0048708~astrocyte differentiation	3	3.75	0.003503761	ID2, ID4, FGFR3	72	25	20094	33.49	0.969464162	0.120094436	0.116953132			
67	GOTERM_CC_DIRECT	GO:0050680~negative regulation of epithelial cell proliferation	4	5	0.003742144	PPARG, SOX9, GDF5, FGFR3	72	88	20094	12.68560606	0.975927091	0.123989698	0.120746507			
68	GOTERM_CC_DIRECT	GO:0043005~neuron projection	8	10	0.004228623	GABRA2, GABRB2, SYT4, GABRA1, CALCR, SYT1, NPY1R, SSTR1	75	583	21179	3.874945683	0.459061849	0.076229716	0.070446772			
69	UP_KW_LIGAND	KW-0106~Calcium	10	12.5	0.004577984	SYT4, SYT1, CLSTN2, CADPS, KCNIP4, IHH, ENPP2, MASP1, EDIL3, PNLIP	28	836	6582	2.811859193	0.066512235	0.068669756	0.068669756			
70	GOTERM_BP_DIRECT	GO:0030900~forebrain development	4	5	0.004637884	PCDH9, NOG, SSTR1, FGFR3	72	95	20094	11.75087719	0.990154886	0.148711495	0.144821657			
71	GOTERM_BP_DIRECT	GO:0007623~circadian rhythm	4	5	0.00491555	ID2, ID1, ID4, ID3	72	97	20094	11.50859107	0.99253929	0.151296571	0.147339115			
72	GOTERM_CC_DIRECT	GO:0070382~exocytic vesicle	3	3.75	0.004917597	SYT4, SYT1, RAB27B	75	30	21179	28.23866667	0.510715187	0.076229716	0.070446772			
73	GOTERM_BP_DIRECT	GO:0007214~gamma-aminobutyric acid signaling pathway	3	3.75	0.005022924	GABRA2, GABRB2, GABRA1	72	30	20094	27.90833333	0.993298127	0.151296571	0.147339115			
74	GOTERM_CC_DIRECT	GO:0030425~dendrite	8	10	0.005257222	GABRA2, SYT4, CRHBP, CLSTN2, GPER1, KCNIP4, CCK, BRINP3	75	607	21179	3.72173531	0.534343945	0.076229716	0.070446772			
75	GOTERM_BP_DIRECT	GO:0002053~positive regulation of mesenchymal cell proliferation	3	3.75	0.006792737	IHH, SOX9, TBX18	72	35	20094	23.92142857	0.99885805	0.198587676	0.193393229			
76	GOTERM_CC_DIRECT	GO:0043025~neuronal cell body	8	10	0.00714051	GABRA2, SYT4, CALCR, SST, GPER1, KCNIP4, CCK, BRINP3	75	643	21179	3.513364438	0.646222884	0.094124904	0.086984394			
77	UP_KW_BIOLOGICAL_PROCESS	KW-0892~Osteogenesis	3	3.75	0.007167974	MSX2, CHRDL2, CHRDL1	39	37	11003	22.87525988	0.17058818	0.062122444	0.062122444			
78	GOTERM_BP_DIRECT	GO:0008283~cell proliferation	6	7.5	0.007752553	NOG, ID4, IHH, PPARG, SOX9, FGFR3	72	348	20094	4.811781609	0.999563212	0.220172501	0.214413462			
79	GOTERM_CC_DIRECT	GO:0099060~integral component of postsynaptic specialization membrane	3	3.75	0.007805442	GABRA2, GABRB2, GABRA1	75	38	21179	22.29368421	0.678972735	0.094315754	0.087160765			
80	GOTERM_BP_DIRECT	GO:0001708~cell fate specification	3	3.75	0.008382992	IHH, SOX9, TBX18	72	39	20094	21.46794872	0.999767778	0.231203668	0.225156087			
81	GOTERM_MF_DIRECT	GO:0061629~RNA polymerase II sequence-specific DNA binding transcription factor binding	5	6.25	0.008466583	ID2, ID4, PPARG, AHR, TBX18	71	214	18713	6.158022904	0.84596542	0.190935896	0.186596444			
82	GOTERM_BP_DIRECT	GO:0001707~mesoderm formation	3	3.75	0.008804188	TLX2, NOG, SNAI1	72	40	20094	20.93125	0.999847769	0.231203668	0.225156087			
83	GOTERM_BP_DIRECT	GO:0001501~skeletal system development	4	5	0.008838772	NOG, IHH, SOX9, HAPLN1	72	120	20094	9.302777778	0.999852959	0.231203668	0.225156087			
84	INTERPRO	IPR018000:Neurotransmitter-gated ion-channel, conserved site	3	3.75	0.00926871	GABRA2, GABRB2, GABRA1	75	41	20908	20.39804878	0.844698426	0.242750582	0.240323076			
85	GOTERM_MF_DIRECT	GO:0043565~sequence-specific DNA binding	7	8.75	0.009515744	CUX2, MSX2, TLX2, SNAI1, PPARG, AHR, SOX9	71	485	18713	3.80400755	0.877969927	0.190935896	0.186596444			
86	INTERPRO	IPR006201:Neurotransmitter-gated ion-channel	3	3.75	0.009710023	GABRA2, GABRB2, GABRA1	75	42	20908	19.91238095	0.857938412	0.242750582	0.240323076			
87	INTERPRO	IPR006029:Neurotransmitter-gated ion-channel transmembrane domain	3	3.75	0.009710023	GABRA2, GABRB2, GABRA1	75	42	20908	19.91238095	0.857938412	0.242750582	0.240323076			
88	INTERPRO	IPR006202:Neurotransmitter-gated ion-channel ligand-binding	3	3.75	0.009710023	GABRA2, GABRB2, GABRA1	75	42	20908	19.91238095	0.857938412	0.242750582	0.240323076			
89	GOTERM_MF_DIRECT	GO:0004888~transmembrane signaling receptor activity	5	6.25	0.009748132	GABRA2, GABRB2, GABRA1, CALCR, FZD9	71	223	18713	5.909492831	0.884109608	0.190935896	0.186596444			
90	GOTERM_MF_DIRECT	GO:0005230~extracellular ligand-gated ion channel activity	3	3.75	0.009816182	GABRA2, GABRB2, GABRA1	71	40	18713	19.76725352	0.885848547	0.190935896	0.186596444			
91	GOTERM_BP_DIRECT	GO:0009755~hormone-mediated signaling pathway	3	3.75	0.010123382	A, CRHBP, PPARG	72	43	20094	19.47093023	0.999959488	0.258016445	0.251267524			
92	GOTERM_CC_DIRECT	GO:0005794~Golgi apparatus	12	15	0.010374872	SYT4, GALNT14, SYT1, CLSTN2, GPER1, ID1, FZD9, ENPP2, RAB27B, FGFR3, HS3ST1, IIGP1	75	1427	21179	2.374660126	0.779578712	0.115719728	0.10694099			
93	GOTERM_BP_DIRECT	GO:0001837~epithelial to mesenchymal transition	3	3.75	0.010581419	NOG, SNAI1, SOX9	72	44	20094	19.02840909	0.999974427	0.262948252	0.25607033			
94	GOTERM_MF_DIRECT	GO:0048469~cell maturation	3	3.75	0.011048495	ID2, IHH, PPARG	72	45	20094	18.60555556	0.999984006	0.267838625	0.260852263			
95	GOTERM_MF_DIRECT	GO:0030348~syntaxin-3 binding	2	2.5	0.011180814	SYT4, SYT1	71	3	18713	175.7089202	0.915721928	0.190935896	0.186596444			
96	GOTERM_MF_DIRECT	GO:0005231~excitatory extracellular ligand-gated ion channel activity	3	3.75	0.011282576	GABRA2, GABRB2, GABRA1	71	43	18713	18.38814281	0.917608705	0.190935896	0.186596444			
97	UP_KW_BIOLOGICAL_PROCESS	KW-0221~Differentiation	8	10	0.012829779	SYT4, SYT1, GPER1, ATOH8, NOG, SOX9, CHRDL2, CHRDL1	39	747	11003	3.021453335	0.285185754	0.083393561	0.083393561			
98	GOTERM_CC_DIRECT	GO:0034707~chloride channel complex	3	3.75	0.013239641	GABRA2, GABRB2, GABRA1	75	50	21179	16.9432	0.855224294	0.137124851	0.126722276			
99	UP_KW_CELLULAR_COMPONENT	KW-0968~Cytoplasmic vesicle	8	10	0.013259427	GABRA2, GABRB2, SYT4, GABRA1, SYT1, GPER1, CADPS, FGFR3	68	681	17960	3.102703637	0.244450885	0.069611994	0.062982281			
100	KEGG_PATHWAY	mmu05033:Nicotine addiction	3	3.75	0.013527589	GABRA2, GABRB2, GABRA1	41	40	8992	16.44878049	0.718226753	0.248019666	0.245352788			

Table S4. Functional annotation by DAVID for genes with decreased expression in explants of E12.5 ureters treated for 18 h with 10 µg/ml NOGGIN.

		Intensities				fold changes (FC)		
Rank	**Gene Symbol**	**control 1**	**NOG 1**	**control 2**	**NOG 2**	**FC1**	**FC2**	**avgFC**
1	*Gsdmc3*	137	21	208	28	-6.6	-7.5	-7.0
2	*Id2*	37141	7027	36241	5164	-5.3	-7.0	-6.2
3	*Ifit3*	157	69	6340	692	-2.3	-9.2	-5.7
4	*Calcb*	142	20	138	40	-7.1	-3.4	-5.3
5	*Gpr165*	110	32	104	15	-3.4	-7.0	-5.2
6	*Grem2*	214	46	202	39	-4.6	-5.2	-4.9
7	*Smad9*	961	177	798	183	-5.4	-4.4	-4.9
8	*Ctse*	955	202	1093	226	-4.7	-4.8	-4.8
9	*Id1*	8428	1812	8472	1871	-4.7	-4.5	-4.6
10	*Ednrb*	3906	942	3590	773	-4.1	-4.6	-4.4
11	*Fa2h*	261	47	195	63	-5.6	-3.1	-4.3
12	*Iigp1*	3696	1332	6173	1054	-2.8	-5.9	-4.3
13	*ENSMUST00000131638*	1466	612	2750	485	-2.4	-5.7	-4.0
14	*Sct*	1389	343	1731	451	-4.0	-3.8	-3.9
15	*Npy1r*	6478	1546	5605	1602	-4.2	-3.5	-3.8
16	*Ldoc1*	614	221	1159	238	-2.8	-4.9	-3.8
17	*Gm4951*	4352	1839	8713	1751	-2.4	-5.0	-3.7
18	*Pdzk1*	544	172	822	198	-3.2	-4.1	-3.7
19	*Phlda2*	459	150	624	156	-3.1	-4.0	-3.5
20	*Id4*	11456	3031	9216	2959	-3.8	-3.1	-3.4
21	*BC023105*	105	40	104	25	-2.6	-4.2	-3.4
22	*Dmkn*	116	35	140	40	-3.3	-3.5	-3.4
23	*Nrn1l*	442	117	344	123	-3.8	-2.8	-3.3
24	*Wif1*	516	174	508	142	-3.0	-3.6	-3.3
25	*Trim9*	283	86	275	90	-3.3	-3.1	-3.2
26	*Tcf24*	176	47	139	55	-3.7	-2.5	-3.1
27	*Pparg*	5507	1694	5448	1829	-3.3	-3.0	-3.1
28	*S100a5*	133	38	149	55	-3.5	-2.7	-3.1
29	*Aqp3*	533	164	527	179	-3.2	-2.9	-3.1
30	*Hmgcs2*	221	73	295	99	-3.0	-3.0	-3.0
31	*Sst*	346	119	305	101	-2.9	-3.0	-3.0
32	*Ugt2b34*	614	259	914	257	-2.4	-3.6	-3.0
33	*A_55_P2175050*	341	105	322	121	-3.2	-2.7	-3.0
34	*Ihh*	306	90	324	129	-3.4	-2.5	-2.9
35	*Calcr*	152	60	186	56	-2.5	-3.3	-2.9
36	*Otor*	456	217	704	190	-2.1	-3.7	-2.9
37	*Sp5*	343	101	289	127	-3.4	-2.3	-2.8
38	*Id3*	29857	10996	29420	10105	-2.7	-2.9	-2.8
39	*Ahr*	8178	3191	8535	3047	-2.6	-2.8	-2.7
40	*Insc*	363	124	299	128	-2.9	-2.3	-2.6
41	*Syt1*	3553	1358	3219	1225	-2.6	-2.6	-2.6
42	*ENSMUST00000089689*	111	50	170	58	-2.2	-2.9	-2.6
43	*Ntng1*	144	68	146	49	-2.1	-3.0	-2.6
44	*Myocd*	135	52	116	46	-2.6	-2.5	-2.5
45	*Msx2*	365	147	453	177	-2.5	-2.6	-2.5

46	*Paqr5*	179	78	215	79	-2.3	-2.7	-2.5
47	*Mansc4*	780	268	629	300	-2.9	-2.1	-2.5
48	*BC025446*	259	105	351	141	-2.5	-2.5	-2.5
49	*Maob*	2174	769	1625	798	-2.8	-2.0	-2.4
50	*Hpgd*	649	284	604	235	-2.3	-2.6	-2.4
51	*Synpr*	492	230	618	230	-2.1	-2.7	-2.4
52	*Gprin3*	102	47	132	50	-2.2	-2.7	-2.4
53	*Inhbb*	303	133	583	230	-2.3	-2.5	-2.4
54	*Tnfsf13b*	764	336	986	389	-2.3	-2.5	-2.4
55	*Kcne3*	239	116	540	203	-2.0	-2.7	-2.4
56	*3830417A13Rik*	135	60	178	73	-2.3	-2.4	-2.3
57	*Upk3b*	129	54	112	50	-2.4	-2.2	-2.3
58	*Enpp2*	17155	6984	17019	7885	-2.5	-2.2	-2.3
59	*Cck*	818	330	590	281	-2.5	-2.1	-2.3
60	*Rnf186*	851	376	1061	463	-2.3	-2.3	-2.3
61	*Sox9*	4026	1691	3207	1489	-2.4	-2.2	-2.3
62	*Cela1*	688	334	764	329	-2.1	-2.3	-2.2
63	*Ptger2*	276	123	338	164	-2.2	-2.1	-2.2
64	*Rab27b*	1585	739	1625	791	-2.1	-2.1	-2.1
65	*Fxyd3*	4414	2057	4618	2293	-2.1	-2.0	-2.1
66	*Fam132a*	5425	2619	6017	2963	-2.1	-2.0	-2.1

Table S5. List of genes with decreased expression in microarrays of explants of E13.75 ureters treated for 18 h with 10 µg/ml NOGGIN (NOG). Shown are the gene names, the intensity of the two control and treated ureter samples, the individual and the average (avg) fold change (FC).

Rank	Category	Term	Count	%	PValue	Genes	List Total	Pop Hits	Pop Total	Fold Enrichment	Bonferroni	Benjamini	FDR
1	INTERPRO	IPR026052:DNA-binding protein inhibitor	4	6.666666667	7.67E-08	ID2, ID1, ID4, ID3	58	4	20908	360.4827586	1.19E-05	1.19E-05	1.19E-05
2	KEGG_PATHWAY	mmu04350:TGF-beta signaling pathway	7	11.66666667	1.04E-06	GREM2, ID2, ID1, ID4, SMAD9, ID3, INHBB	34	95	8992	19.4873065	7.93E-05	7.93E-05	7.93E-05
3	GOTERM_BP_DIRECT	GO:0045668~negative regulation of osteoblast differentiation	6	10	1.25E-06	ID2, ID1, ID3, PPARG, AHR, SOX9	56	69	20094	31.20186335	0.001068388	0.001068959	0.001051394
4	UP_SEQ_FEATURE	DOMAIN:BHLH	6	10	2.74E-06	TCF24, ID2, ID1, ID4, ID3, AHR	60	84	22511	26.79880952	7.81E-04	7.81E-04	7.76E-04
5	INTERPRO	IPR011598:Myc-type, basic helix-loop-helix (bHLH) domain	6	10	1.47E-05	TCF24, ID2, ID1, ID4, ID3, AHR	58	114	20908	18.97277677	0.0022813	0.001141945	0.001141945
6	GOTERM_BP_DIRECT	GO:0030154~cell differentiation	13	21.66666667	1.62E-05	NTNG1, SYT1, PAQR5, IHH, SMAD9, DMKN, ID2, INSC, ID1, ID4, ID3, PPARG, SOX9	56	1022	20094	4.564264747	0.013707247	0.006900974	0.006787577
7	SMART	SM00353:HLH	6	10	2.15E-05	TCF24, ID2, ID1, ID4, ID3, AHR	34	111	10615	16.87599364	9.22E-04	9.23E-04	9.23E-04
8	UP_SEQ_FEATURE	REGION:Interaction with IFI204	3	5	4.04E-05	ID2, ID1, ID3	60	4	22511	281.3875	0.011443275	0.00575451	0.005714128
9	GOTERM_BP_DIRECT	GO:0032922~circadian regulation of gene expression	5	8.333333333	4.50E-05	ID2, ID1, ID4, ID3, AHR	56	72	20094	24.91815476	0.037620857	0.011861799	0.011666887
10	GOTERM_BP_DIRECT	GO:0000122~negative regulation of transcription from RNA polymerase II promoter	12	20	5.57E-05	MYOCD, EDNRB, MSX2, ID2, ID1, ID4, SP5, ID3, PPARG, CELA1, AHR, SOX9	56	975	20094	4.416263736	0.046340431	0.011861799	0.011666887
11	GOTERM_MF_DIRECT	GO:0046983~protein dimerization activity	6	10	1.42E-04	TCF24, ID2, ID1, ID4, ID3, AHR	54	177	18713	11.7470182	0.024436662	0.024738434	0.024596259
12	KEGG_PATHWAY	mmu04550:Signaling pathways regulating pluripotency of stem cells	6	10	1.42E-04	ID2, ID1, ID4, SMAD9, ID3, INHBB	34	140	8992	11.33445378	0.010758116	0.005407817	0.005407817
13	UP_SEQ_FEATURE	DOMAIN:bHLH	5	8.333333333	1.80E-04	ID2, ID1, ID4, ID3, AHR	60	107	22511	17.53193146	0.049896356	0.017059869	0.01694015
14	UP_KW_PTM	KW-0165~Cleavage on pair of basic residues	7	11.66666667	1.96E-04	CALCB, SST, SCT, ENPP2, INHBB, CCK, TNFSF13B	44	256	12816	7.964488636	0.003530483	0.003732849	0.003536383
15	UP_KW_MOLECULAR_FUNCTION	KW-0372~Hormone	5	8.333333333	4.06E-04	CALCB, SST, SCT, INHBB, CCK	41	107	12158	13.85684978	0.00849355	0.008528093	0.008528093
16	KEGG_PATHWAY	mmu04080:Neuroactive ligand-receptor interaction	8	13.33333333	4.12E-04	EDNRB, CALCB, CALCR, SST, SCT, PTGER2, NPY1R, CCK	34	386	8992	5.481255715	0.030862035	0.010447278	0.010447278
17	UP_KW_PTM	KW-0027~Amidation	4	6.666666667	4.23E-04	CALCB, SST, SCT, CCK	44	44	12816	26.47933884	0.007593042	0.004021879	0.003810201
18	GOTERM_MF_DIRECT	GO:0005179~hormone activity	5	8.333333333	4.31E-04	CALCB, SST, SCT, INHBB, CCK	54	125	18713	13.86148148	0.072325631	0.037529155	0.03731347
19	UP_KW_BIOLOGICAL_PROCESS	KW-0090~Biological rhythms	5	8.333333333	4.45E-04	ID2, ID1, ID3, PPARG, AHR	28	149	11003	13.186721	0.015011327	0.015121774	0.015121774
20	GOTERM_BP_DIRECT	GO:0048511~rhythmic process	5	8.333333333	8.15E-04	ID2, ID1, ID3, PPARG, AHR	56	153	20094	11.72619048	0.500782183	0.138885924	0.136603761
21	GOTERM_BP_DIRECT	GO:0010628~positive regulation of gene expression	8	13.33333333	0.0010129	MYOCD, CALCR, ID2, ID1, ID4, ID3, PPARG, SOX9	56	583	20094	4.923793188	0.578286208	0.143831843	0.141468409
22	INTERPRO	IPR007743:Interferon-inducible GTPase	3	5	0.001086348	BC023105, GM4951, IIGP1	58	18	20908	60.08045977	0.155048037	0.056127991	0.056127991
23	UP_SEQ_FEATURE	DOMAIN:IRG-type G	3	5	0.001122145	BC023105, GM4951, IIGP1	60	19	22511	59.23947368	0.273844389	0.079952844	0.079391771
24	GOTERM_BP_DIRECT	GO:0007507~heart development	6	10	0.001316202	MYOCD, ID2, ID1, ID3, PPARG, SOX9	56	298	20094	7.224592522	0.674418556	0.16020057	0.157568167
25	GOTERM_BP_DIRECT	GO:0008217~regulation of blood pressure	4	6.666666667	0.001635252	EDNRB, NPY1R, PPARG, AHR	56	85	20094	16.88571429	0.752012045	0.162469447	0.159799761
26	GOTERM_BP_DIRECT	GO:0008284~positive regulation of cell proliferation	8	13.33333333	0.001732069	MYOCD, EDNRB, ID2, ID4, IHH, ENPP2, CCK, SOX9	56	640	20094	4.485267857	0.771678891	0.162469447	0.159799761
27	GOTERM_BP_DIRECT	GO:0051216~cartilage development	4	6.666666667	0.002051256	MSX2, IHH, SMAD9, SOX9	56	92	20094	15.60093168	0.826133128	0.162469447	0.159799761
28	GOTERM_BP_DIRECT	GO:0045892~negative regulation of transcription, DNA-templated	8	13.33333333	0.00209761	MSX2, ID2, ID1, ID4, ID3, PPARG, AHR, SOX9	56	662	20094	4.336210617	0.832879626	0.162469447	0.159799761
29	GOTERM_BP_DIRECT	GO:0007623~circadian rhythm	4	6.666666667	0.002385236	ID2, ID1, ID4, ID3	56	97	20094	14.79675994	0.869273625	0.169351779	0.166569004
30	GOTERM_MF_DIRECT	GO:0042802~identical protein binding	14	23.33333333	0.002693279	MAOB, SYT1, HPGD, AHR, AQP3, IFIT3, IIGP1, GREM2, NRN1L, SST, ID1, PPARG, HMGCS2, CTSE	54	1962	18713	2.472741345	0.374536732	0.136685478	0.13589993
31	GOTERM_BP_DIRECT	GO:0007275~multicellular organism development	10	16.66666667	0.002708012	NTNG1, GREM2, MSX2, WIF1, PAQR5, ID2, INSC, ID1, IHH, ID3	56	1095	20094	3.276908023	0.900774076	0.177478948	0.174562627
32	GOTERM_MF_DIRECT	GO:0061629~RNA polymerase II sequence-specific DNA binding transcription factor binding	5	8.333333333	0.003142195	MYOCD, ID2, ID4, PPARG, AHR	54	214	18713	8.096659744	0.42166541	0.136685478	0.13589993
33	GOTERM_BP_DIRECT	GO:0030509~BMP signaling pathway	4	6.666666667	0.003405184	MSX2, ID1, SMAD9, PPARG	56	110	20094	13.04805195	0.945315113	0.193069494	0.18989699
34	GOTERM_BP_DIRECT	GO:0043065~positive regulation of apoptotic process	6	10	0.003903389	MSX2, HPGD, ID3, CCK, PPARG, PHLDA2	56	383	20094	5.621223424	0.964285371	0.193069494	0.18989699
35	GOTERM_CC_DIRECT	GO:0005576~extracellular region	13	21.66666667	0.003996014	CALCB, SCT, IHH, INHBB, CCK, CELA1, DMKN, OTOR, TNFSF13B, GREM2, WIF1, SST, ENPP2	59	1859	21179	2.510252459	0.329949352	0.316248226	0.316248226
36	GOTERM_BP_DIRECT	GO:0006366~transcription from RNA polymerase II promoter	5	8.333333333	0.00401839	MYOCD, MSX2, CELA1, AHR, SOX9	56	237	20094	7.570072333	0.967631384	0.193069494	0.18989699
37	GOTERM_BP_DIRECT	GO:0001503~ossification	4	6.666666667	0.004049428	CALCR, MSX2, IHH, SOX9	56	117	20094	12.26739927	0.968479488	0.193069494	0.18989699
38	GOTERM_BP_DIRECT	GO:0010629~negative regulation of gene expression	6	10	0.004078933	ID2, ID1, ID3, PPARG, SOX9, UPK3B	56	387	20094	5.563122924	0.969265144	0.193069494	0.18989699

39	UP_KW_CELLULAR_COMPONENT	KW-0964~Secreted	13	21.66666667	0.004147355	CALCB, SCT, IHH, INHBB, CCK, CELA1, DMKN, OTOR, TNFSF13B, GREM2, WIF1, SST, ENPP2	55	1709	17960	2.483961913	0.068213572	0.070505035	0.070505035
40	UP_KW_DOMAIN	KW-0732~Signal	23	38.33333333	0.00432168	NTNG1, UGT2B34, CALCB, SCT, IHH, INHBB, CCK, CELA1, UPK3B, DMKN, OTOR, TNFSF13B, SYNPR, GREM2, EDNRB, CALCR, NRN1L, WIF1, FXYD3, SST, MANSC4, ENPP2, CTSE	44	4739	15344	1.692493622	0.058832954	0.060503519	0.060503519
41	GOTERM_BP_DIRECT	GO:0042476~odontogenesis	3	5	0.00436591	MSX2, ID3, AQP3	56	36	20094	29.90178571	0.975956711	0.195776611	0.192559625
42	UP_SEQ_FEATURE	CARBOHYD:N-linked (GlcNAc...) asparagine	19	31.66666667	0.005336243	NTNG1, KCNE3, SYT1, PTGER2, IHH, NPY1R, INHBB, CELA1, UPK3B, AQP3, TNFSF13B, SYNPR, GREM2, EDNRB, CALCR, WIF1, MANSC4, ENPP2, CTSE	60	3706	22511	1.923497931	0.782357499	0.304165843	0.302031346
43	GOTERM_BP_DIRECT	GO:1903547~regulation of growth hormone activity	2	3.333333333	0.005466915	LDOC1, PHLDA2	56	2	20094	358.8214286	0.990633258	0.232890573	0.229063733
44	UP_KW_MOLECULAR_FUNCTION	KW-9996~Developmental protein	10	16.66666667	0.005866795	NTNG1, GREM2, MSX2, WIF1, PAQR5, ID2, INSC, ID1, IHH, ID3	41	1044	12158	2.840388749	0.116236268	0.041067567	0.041067567
45	UP_KW_MOLECULAR_FUNCTION	KW-0217~Developmental protein	10	16.66666667	0.005866795	NTNG1, GREM2, MSX2, WIF1, PAQR5, ID2, INSC, ID1, IHH, ID3	41	1044	12158	2.840388749	0.116236268	0.041067567	0.041067567
46	GOTERM_CC_DIRECT	GO:0005615~extracellular space	13	21.66666667	0.006324965	CALCB, HPGD, SCT, IHH, INHBB, CCK, CELA1, DMKN, TNFSF13B, GREM2, NRN1L, SST, ENPP2	59	1969	21179	2.370014892	0.469802227	0.316248226	0.316248226
47	GOTERM_BP_DIRECT	GO:0048469~cell maturation	3	5	0.006753644	ID2, IHH, PPARG	56	45	20094	23.92142857	0.996891525	0.27400498	0.269502551
48	GOTERM_BP_DIRECT	GO:0010468~regulation of gene expression	6	10	0.008513429	ID2, IHH, PPARG, AHR, SOX9, PHLDA2	56	462	20094	4.660018553	0.999313905	0.329701892	0.324284255
49	GOTERM_BP_DIRECT	GO:0045600~positive regulation of fat cell differentiation	3	5	0.00960999	WIF1, ID2, PPARG	56	54	20094	19.93452381	0.999732745	0.355987446	0.350137887
50	UP_KW_BIOLOGICAL_PROCESS	KW-0805~Transcription regulation	11	18.33333333	0.010236735	MYOCD, MSX2, ID2, ID1, ID4, SP5, SMAD9, ID3, PPARG, AHR, SOX9	28	1873	11003	2.307852185	0.295201052	0.141935199	0.141935199
51	GOTERM_BP_DIRECT	GO:0048709~oligodendrocyte differentiation	3	5	0.010662169	ID2, ID4, SOX9	56	57	20094	18.88533835	0.999891953	0.378506988	0.37228739
52	UP_KW_PTM	KW-0325~Glycoprotein	22	36.66666667	0.011922501	NTNG1, KCNE3, SYT1, PTGER2, IHH, NPY1R, INHBB, CELA1, UPK3B, DMKN, AQP3, TNFSF13B, SYNPR, GREM2, EDNRB, CALCR, NRN1L, WIF1, MANSC4, ENPP2, PPARG, CTSE	44	4008	12816	1.598802395	0.194179768	0.075509175	0.071535008
53	GOTERM_BP_DIRECT	GO:0035458~cellular response to interferon-beta	3	5	0.012140547	GM4951, IFIT3, IIGP1	56	61	20094	17.6469555	0.999969781	0.413749859	0.406951152
54	UP_KW_BIOLOGICAL_PROCESS	KW-0804~Transcription	11	18.33333333	0.012523694	MYOCD, MSX2, ID2, ID1, ID4, SP5, SMAD9, ID3, PPARG, AHR, SOX9	28	1928	11003	2.242016153	0.348510761	0.141935199	0.141935199
55	GOTERM_BP_DIRECT	GO:0003413~chondrocyte differentiation involved in endochondral bone morphogenesis	2	3.333333333	0.013612311	IHH, SOX9	56	5	20094	143.5285714	0.999991516	0.42954402	0.422485785
56	GOTERM_BP_DIRECT	GO:0060512~prostate gland morphogenesis	2	3.333333333	0.013612311	ID4, SOX9	56	5	20094	143.5285714	0.999991516	0.42954402	0.422485785
57	GOTERM_CC_DIRECT	GO:0008021~synaptic vesicle	4	6.666666667	0.013628179	SYNPR, TRIM9, SYT1, NPY1R	59	182	21179	7.889364872	0.746448799	0.454272631	0.454272631
58	GOTERM_MF_DIRECT	GO:0004957~prostaglandin E receptor activity	2	3.333333333	0.014082785	HPGD, PTGER2	54	5	18713	138.6148148	0.915230764	0.490080921	0.487264364
59	GOTERM_BP_DIRECT	GO:0097070~ductus arteriosus closure	2	3.333333333	0.016312859	MYOCD, HPGD	56	6	20094	119.6071429	0.999999179	0.496377002	0.488220572
60	GOTERM_BP_DIRECT	GO:0071407~cellular response to organic cyclic compound	3	5	0.018879167	SP5, SMAD9, PPARG	56	77	20094	13.98005566	0.999999911	0.554656914	0.545542833
61	GOTERM_BP_DIRECT	GO:0042127~regulation of cell proliferation	4	6.666666667	0.020573245	FA2H, PTGER2, CELA1, SOX9	56	213	20094	6.738430584	0.99999998	0.584280149	0.574679302
62	GOTERM_BP_DIRECT	GO:0043433~negative regulation of sequence-specific DNA binding transcription factor activity	3	5	0.02321764	ID2, ID1, ID3	56	86	20094	12.51702658	0.999999998	0.638110633	0.627625247
63	UP_KW_PTM	KW-0449~Lipoprotein	8	13.33333333	0.024080281	NTNG1, EDNRB, SYT1, NRN1L, IHH, NPY1R, RAB27B, IIGP1	44	867	12816	2.687637622	0.355157464	0.114381335	0.108361265
64	GOTERM_BP_DIRECT	GO:0050679~positive regulation of epithelial cell proliferation	3	5	0.026315886	ID1, IHH, SOX9	56	92	20094	11.70069876	1	0.698192053	0.686719413
65	GOTERM_BP_DIRECT	GO:0097152~mesenchymal cell apoptotic process	2	3.333333333	0.02704265	MSX2, SOX9	56	10	20094	71.76428571	1	0.698192053	0.686719413
66	GOTERM_BP_DIRECT	GO:0045444~fat cell differentiation	3	5	0.02846942	ID4, INHBB, PPARG	56	96	20094	11.21316964	1	0.713410165	0.701687463
67	GOTERM_BP_DIRECT	GO:0008285~negative regulation of cell proliferation	5	8.333333333	0.030174712	MYOCD, MSX2, PPARG, SOX9, IFIT3	56	431	20094	4.162661584	1	0.730708827	0.718701875

68	GOTERM_BP_DIRECT	GO:0001649~osteoblast differentiation	3	5	0.031827481	MSX2, ID4, IHH	56	102	20094	10.55357143	1	0.730708827	0.718701875
69	GOTERM_BP_DIRECT	GO:0030850~prostate gland development	2	3.333333333	0.03236437	AHR, SOX9	56	12	20094	59.80357143	1	0.730708827	0.718701875
70	GOTERM_BP_DIRECT	GO:0030183~B cell differentiation	3	5	0.03298006	ID2, AHR, TNFSF13B	56	104	20094	10.35061813	1	0.730708827	0.718701875
71	UP_KW_BIOLOGICAL_PROCESS	KW-0221~Differentiation	6	10	0.032987378	NTNG1, SYT1, PAQR5, INSC, SOX9, DMKN	28	747	11003	3.156339644	0.680336647	0.280392715	0.280392715
72	GOTERM_BP_DIRECT	GO:0043066~negative regulation of apoptotic process	6	10	0.033447939	EDNRB, MSX2, ID1, IHH, SOX9, IFIT3	56	657	20094	3.276908023	1	0.730708827	0.718701875
73	GOTERM_BP_DIRECT	GO:0030903~notochord development	2	3.333333333	0.035014502	ID3, SOX9	56	13	20094	55.2032967	1	0.745808897	0.733553822
74	UP_KW_MOLECULAR_FUNCTION	KW-0678~Repressor	6	10	0.036865434	MSX2, ID2, ID1, ID4, ID3, AHR	41	566	12158	3.143497371	0.545612512	0.193543527	0.193543527
75	GOTERM_BP_DIRECT	GO:0071380~cellular response to prostaglandin E stimulus	2	3.333333333	0.040293406	PTGER2, PPARG	56	15	20094	47.84285714	1	0.837316641	0.823557917
76	GOTERM_MF_DIRECT	GO:0000976~transcription regulatory region sequence-specific DNA binding	4	6.666666667	0.041020913	MSX2, PPARG, AHR, SOX9	54	270	18713	5.13388203	0.999316419	1	1
77	GOTERM_BP_DIRECT	GO:0060487~lung epithelial cell differentiation	2	3.333333333	0.042922216	INSC, SOX9	56	16	20094	44.85287857	1	0.862298879	0.848129649
78	GOTERM_BP_DIRECT	GO:0030334~regulation of cell migration	3	5	0.044061007	SST, ENPP2, PHLDA2	56	122	20094	8.823477752	1	0.862298879	0.848129649
79	GOTERM_BP_DIRECT	GO:0045893~positive regulation of transcription, DNA-templated	6	10	0.044758248	MYOCD, ID2, SMAD9, PPARG, AHR, SOX9	56	712	20094	3.023776083	1	0.862298879	0.848129649
80	GOTERM_BP_DIRECT	GO:0002024~diet induced thermogenesis	2	3.333333333	0.045543955	SCT, PPARG	56	17	20094	42.21428571	1	0.862298879	0.848129649
81	KEGG_PATHWAY	mmu04024:cAMP signaling pathway	4	6.666666667	0.046012124	SST, PTGER2, NPY1R, SOX9	34	220	8992	4.80855615	0.972122297	0.874230365	0.874230365
82	GOTERM_BP_DIRECT	GO:0007189~adenylate cyclase-activating G-protein coupled receptor signaling pathway	3	5	0.046687719	CALCB, CALCR, PTGER2	56	126	20094	8.543367347	1	0.864737754	0.850528448
83	GOTERM_BP_DIRECT	GO:0048715~negative regulation of oligodendrocyte differentiation	2	3.333333333	0.048158642	ID2, ID4	56	18	20094	39.86904762	1	0.873003476	0.858658349
84	GOTERM_MF_DIRECT	GO:0043565~sequence-specific DNA binding	5	8.333333333	0.048208037	MSX2, SP5, PPARG, AHR, SOX9	54	485	18713	3.572546774	0.999815365	1	1
85	GOTERM_CC_DIRECT	GO:0005667~transcription factor complex	4	6.666666667	0.048285846	MSX2, SMAD9, AHR, SOX9	59	298	21179	4.818336936	0.992909893	0.970783689	0.970783689
86	GOTERM_CC_DIRECT	GO:0030424~axon	5	8.333333333	0.048539184	CALCR, SYT1, NRN1L, NPY1R, CCK	59	502	21179	3.575359579	0.99309616	0.970783689	0.970783689
87	GOTERM_BP_DIRECT	GO:0071285~cellular response to lithium ion	2	3.333333333	0.050766297	ID2, PPARG	56	19	20094	37.77067669	1	0.901101774	0.886294937
88	GOTERM_BP_DIRECT	GO:0048745~smooth muscle tissue development	2	3.333333333	0.053366937	IHH, AHR	56	20	20094	35.88214286	1	0.927931238	0.912683542
89	GOTERM_MF_DIRECT	GO:0005515~protein binding	22	36.66666667	0.053674214	NTNG1, MYOCD, MSX2, SYT1, IHH, SMAD9, CCK, RAB27B, AHR, PDZK1, IFIT3, IIGP1, TRIM9, EDNRB, NRN1L, FXYD3, ID2, ID1, ID4, ID3, PPARG, SOX9	54	5338	18713	1.428215589	0.999932224	1	1
90	GOTERM_BP_DIRECT	GO:0048557~embryonic digestive tract morphogenesis	2	3.333333333	0.055960582	ID2, IHH	56	21	20094	34.17346939	1	0.953568314	0.937899351
91	GOTERM_BP_DIRECT	GO:0001502~cartilage condensation	2	3.333333333	0.058547249	SOX9, OTOR	56	22	20094	32.62012987	1	0.978083452	0.962011658
92	GOTERM_BP_DIRECT	GO:0002063~chondrocyte development	2	3.333333333	0.061126957	MSX2, SOX9	56	23	20094	31.20186335	1	0.986766642	0.970552167
93	GOTERM_BP_DIRECT	GO:0032331~negative regulation of chondrocyte differentiation	2	3.333333333	0.063699725	IHH, SOX9	56	24	20094	29.90178571	1	0.986766642	0.970552167
94	GOTERM_BP_DIRECT	GO:1902894~negative regulation of pri-miRNA transcription from RNA polymerase II promoter	2	3.333333333	0.063699725	PPARG, SOX9	56	24	20094	29.90178571	1	0.986766642	0.970552167
95	GOTERM_BP_DIRECT	GO:0050872~white fat cell differentiation	2	3.333333333	0.063699725	ID2, PPARG	56	24	20094	29.90178571	1	0.986766642	0.970552167
96	KEGG_PATHWAY	mmu04972:Pancreatic secretion	3	5	0.065212675	SCT, CCK, RAB27B	34	114	8992	6.959752322	0.994054698	0.991232657	0.991232657
97	GOTERM_MF_DIRECT	GO:0008188~neuropeptide receptor activity	2	3.333333333	0.065844629	GPR165, NPY1R	54	24	18713	28.87808642	0.999992873	1	1
98	GOTERM_BP_DIRECT	GO:0048708~astrocyte differentiation	2	3.333333333	0.06626557	ID2, ID4	56	25	20094	28.70571429	1	1	0.984723854
99	GOTERM_BP_DIRECT	GO:0009887~animal organ morphogenesis	3	5	0.068845925	NTNG1, GREM2, PHLDA2	56	157	20094	6.856460419	1	1	0.984723854
100	GOTERM_BP_DIRECT	GO:0008283~cell proliferation	4	6.666666667	0.069914254	ID4, IHH, PPARG, SOX9	56	348	20094	4.124384236	1	1	0.984723854

Table S6. Functional annotation by DAVID for genes with decreased expression in explants of E13.75 ureters treated for 18 h with 10 µg/ml NOGGIN.

		Intensities				fold changes (FC)		
Rank	**Gene**	**control 1**	**BMP4 1**	**control 2**	**BMP4 2**	**FC1**	**FC2**	**avgFC**
1	*Hsd17b2*	18	178	32	213	9.6	6.7	8.2
2	*Ano2*	42	210	34	369	5.0	10.8	7.9
3	*Tbx20*	32	194	18	167	6.0	9.4	7.7
4	*Nog*	345	2745	403	2664	8.0	6.6	7.3
5	*Phlda2*	370	2278	399	3225	6.1	8.1	7.1
6	*Thbs4*	142	768	160	1395	5.4	8.7	7.1
7	*Bcan*	47	161	33	337	3.5	10.3	6.9
8	*Cpne6*	83	580	147	968	6.9	6.6	6.8
9	*A_55_P2147160*	46	196	37	324	4.3	8.9	6.6
10	*Chrdl2*	116	651	158	1051	5.6	6.6	6.1
11	*Fam25c*	30	195	40	201	6.5	5.1	5.8
12	*Gata4*	33	186	42	246	5.6	5.9	5.8
13	*Grem2*	242	1102	233	1572	4.6	6.7	5.6
14	*Cbln1*	48	214	59	373	4.4	6.3	5.4
15	*Crhbp*	204	991	172	968	4.9	5.6	5.2
16	*Onecut2*	215	1139	253	1311	5.3	5.2	5.2
17	*Rgs6*	27	129	56	304	4.8	5.4	5.1
18	*Asic1*	133	516	179	1088	3.9	6.1	5.0
19	*Wif1*	759	3072	819	4293	4.0	5.2	4.6
20	*Ttr*	30	131	47	229	4.4	4.8	4.6
21	*Irx4*	127	487	154	801	3.8	5.2	4.5
22	*Dkk1*	2582	11394	2739	12484	4.4	4.6	4.5
23	*Ibsp*	52	184	36	194	3.6	5.3	4.5
24	*Cux2*	4072	17197	4888	22812	4.2	4.7	4.4
25	*Sost*	58	253	71	318	4.4	4.5	4.4
26	*Agtr1a*	323	1113	373	1998	3.4	5.4	4.4
27	*Smad6*	2280	9212	2614	12233	4.0	4.7	4.4
28	*Slc25a34*	64	180	57	298	2.8	5.3	4.0
29	*Tacr3*	169	543	125	605	3.2	4.8	4.0
30	*Gbp11*	63	160	47	256	2.5	5.4	4.0
31	*Tmem178*	1107	3468	1409	6192	3.1	4.4	3.8
32	*Chst9*	87	224	58	276	2.6	4.8	3.7
33	*Msx1*	528	1946	586	2100	3.7	3.6	3.6
34	*Kcnh1*	44	145	45	177	3.3	4.0	3.6
35	*Syndig1*	194	692	237	859	3.6	3.6	3.6
36	*Brinp3*	352	866	226	1022	2.5	4.5	3.5
37	*Cidea*	39	113	25	102	2.9	4.1	3.5
38	*Gcgr*	1810	4941	1778	7393	2.7	4.2	3.4
39	*Sprr1a*	2367	11026	4079	8898	4.7	2.2	3.4
40	*3830417A13Rik*	76	189	61	260	2.5	4.2	3.4
41	*Fam189a1*	55	133	79	332	2.4	4.2	3.3
42	*Tmem200a*	840	2209	777	3068	2.6	3.9	3.3
43	*Myocd*	39	134	52	164	3.5	3.1	3.3
44	*Tenm2*	87	307	131	398	3.5	3.0	3.3
45	*Ppapdc1a*	80	225	90	340	2.8	3.8	3.3

46	*a*	355	1253	237	711	3.5	3.0	3.3
47	*Zfpm1*	693	2461	1000	2904	3.6	2.9	3.2
48	*Tcf24*	36	111	38	123	3.1	3.3	3.2
49	*Pcdh17*	293	741	340	1302	2.5	3.8	3.2
50	*Kctd8*	262	719	234	845	2.7	3.6	3.2
51	*Msx2*	562	1691	691	2281	3.0	3.3	3.2
52	*Ttn*	78	179	90	347	2.3	3.8	3.1
53	*Htr3a*	131	417	113	323	3.2	2.9	3.0
54	*Trim9*	190	480	225	787	2.5	3.5	3.0
55	*Fmod*	180	558	250	730	3.1	2.9	3.0
56	*2900001G08Rik*	85	237	95	306	2.8	3.2	3.0
57	*Myl1*	313	715	285	1043	2.3	3.7	3.0
58	*Fgfr3*	1843	4842	2407	7860	2.6	3.3	2.9
59	*Pdlim3*	1166	3540	1388	3924	3.0	2.8	2.9
60	*Pcdh10*	60	167	63	196	2.8	3.1	2.9
61	*Gata6*	12957	38502	14827	42333	3.0	2.9	2.9
62	*Irf5*	435	1105	365	1186	2.5	3.3	2.9
63	*Pi16*	41	110	41	125	2.7	3.1	2.9
64	*4930466F19Rik*	80	178	67	238	2.2	3.5	2.9
65	*4930412O13Rik*	1635	4236	1395	4275	2.6	3.1	2.8
66	*Fam19a2*	931	1990	797	2768	2.1	3.5	2.8
67	*Ldoc1*	1073	2185	1082	3840	2.0	3.5	2.8
68	*Pitx1*	620	1928	841	2073	3.1	2.5	2.8
69	*Asb4*	2923	6737	2102	6860	2.3	3.3	2.8
70	*Ifitm10*	39	116	46	117	3.0	2.5	2.7
71	*Calcr*	97	199	91	310	2.1	3.4	2.7
72	*Rarres1*	254	624	230	689	2.5	3.0	2.7
73	*Nkx3-1*	46	147	51	113	3.2	2.2	2.7
74	*Smad9*	854	2083	923	2742	2.4	3.0	2.7
75	*Hand1*	428	1046	386	1120	2.4	2.9	2.7
76	*Snai1*	2972	7930	3358	8976	2.7	2.7	2.7
77	*Sct*	3036	7497	2681	7517	2.5	2.8	2.6
78	*Rxrg*	256	603	207	597	2.4	2.9	2.6
79	*Gata5os*	79	191	123	341	2.4	2.8	2.6
80	*Gm6403*	163	355	206	619	2.2	3.0	2.6
81	*Esrrg*	197	438	166	493	2.2	3.0	2.6
82	*Syn2*	84	232	96	232	2.8	2.4	2.6
83	*Nefm*	3614	8899	3280	8865	2.5	2.7	2.6
84	*Calcb*	89	201	76	221	2.3	2.9	2.6
85	*Igf1*	1425	2888	1266	3958	2.0	3.1	2.6
86	*Cfh*	207	431	200	614	2.1	3.1	2.6
87	*Trabd2b*	308	847	317	751	2.8	2.4	2.6
88	*Olfm1*	3350	7798	3985	11104	2.3	2.8	2.6
89	*Grin2c*	531	1263	588	1607	2.4	2.7	2.6
90	*Hrct1*	94	212	87	242	2.3	2.8	2.5
91	*Ecel1*	406	838	478	1427	2.1	3.0	2.5
92	*Dmkn*	62	132	77	223	2.1	2.9	2.5

93	*Ppp2r2b*	762	1827	852	2231	2.4	2.6	2.5
94	*Sstr1*	919	2122	864	2332	2.3	2.7	2.5
95	*Syt1*	3657	7778	3788	10643	2.1	2.8	2.5
96	*4930432J09Rik*	82	193	65	168	2.4	2.6	2.5
97	*Hoxc9*	1693	3956	1574	4080	2.3	2.6	2.5
98	*Nrn1l*	525	1134	641	1773	2.2	2.8	2.5
99	*Ceacam10*	87	178	67	190	2.0	2.8	2.4
100	*Baiap2l2*	2383	5298	2465	6508	2.2	2.6	2.4
101	*Thrb*	135	308	167	430	2.3	2.6	2.4
102	*BC100530*	75	170	69	180	2.3	2.6	2.4
103	*Hoxb13*	91	207	121	304	2.3	2.5	2.4
104	*Smad7*	989	2072	1054	2821	2.1	2.7	2.4
105	*Grik3*	87	203	72	173	2.3	2.4	2.4
106	*Ccdc3*	113	272	148	335	2.4	2.3	2.3
107	*Tbx4*	217	544	291	624	2.5	2.1	2.3
108	*Fst*	1834	4334	1975	4514	2.4	2.3	2.3
109	*Prrx2*	4050	8512	3657	9066	2.1	2.5	2.3
110	*Slc18a3*	564	1319	614	1366	2.3	2.2	2.3
111	*Gabra2*	94	204	82	193	2.2	2.4	2.3
112	*Slitrk5*	957	2187	1119	2501	2.3	2.2	2.3
113	*Me1*	1340	2976	1688	3849	2.2	2.3	2.3
114	*Pparg*	4409	10224	4668	10012	2.3	2.1	2.2
115	*Nrg1*	1810	3818	2149	5027	2.1	2.3	2.2
116	*A_55_P2042833*	51	105	50	118	2.1	2.4	2.2
117	*Dlg2*	292	629	281	626	2.2	2.2	2.2
118	*Tlx2*	3509	7815	3334	7101	2.2	2.1	2.2
119	*AA387883*	63	127	69	161	2.0	2.3	2.2
120	*Npy*	563	1173	583	1301	2.1	2.2	2.2
121	*NAP001637-001*	322	723	386	779	2.2	2.0	2.1
122	*Bmper*	19226	39741	19450	41281	2.1	2.1	2.1
123	*Bean1*	621	1270	740	1582	2.0	2.1	2.1
124	*Srrm3*	314	642	406	867	2.0	2.1	2.1
125	*Map1b*	2708	5545	3114	6635	2.0	2.1	2.1
126	*Rorb*	57	118	71	143	2.1	2.0	2.1
127	*Hr*	3450	7016	4566	9401	2.0	2.1	2.0
128	*Foxo6*	932	1865	1107	2306	2.0	2.1	2.0
129	*Unc5b*	6668	13620	7931	15942	2.0	2.0	2.0

Table S7. List of genes with increased expression in microarrays of explants of E12.5 ureters treated for 18 h with 100 ng/ml BMP4 (BMP4). Shown are the gene names, the intensity of the two control and treated ureter samples, the individual and the average (avg) fold change (FC).

Rank	Category	Term	Count	%	PValue	Genes	List Total	Pop Hits	Pop Total	Fold Enrichment	Bonferroni	Benjamini	FDR
1	GOTERM_BP_DIRECT	GO:0006357~regulation of transcription from RNA polymerase II promoter	31	25.40983607	5.34E-10	THRB, ONECUT2, TCF24, GATA6, FOXO6, HR, GATA4, RORB, HOXB13, CUX2, TBX20, MSX1, HOXC9, RXRG, PITX1, NKX3-1, MYOCD, MSX2, IRX4, PRRX2, SMAD9, ESRRG, SMAD6, TBX4, SMAD7, TLX2, HAND1, SNAI1, PPARG, IRF5, ZFPM1	107	1606	20094	3.624922894	6.62E-07	3.80E-07	3.67E-07
2	GOTERM_BP_DIRECT	GO:0030514~negative regulation of BMP signaling pathway	9	7.37704918	6.12E-10	GREM2, BMPER, NOG, PPARG, SOST, CHRDL2, SMAD6, DKK1, SMAD7	107	57	20094	29.65174619	7.59E-07	3.80E-07	3.67E-07
3	GOTERM_MF_DIRECT	GO:1990837~sequence-specific double-stranded DNA binding	19	15.57377049	7.24E-10	THRB, MSX2, ONECUT2, PRRX2, GATA6, ESRRG, GATA4, RORB, HOXB13, CUX2, TLX2, TBX20, SNAI1, IRF5, MSX1, HOXC9, PITX1, RXRG, NKX3-1	102	547	18713	6.37249525	1.82E-07	1.42E-07	1.33E-07
4	GOTERM_MF_DIRECT	GO:0005515~protein binding	59	48.36065574	1.13E-09	TENM2, THRB, CPNE6, GRIK3, HR, RORB, CHRDL2, TRIM9, BMPER, ME1, SOST, PITX1, RGS6, SLC18A3, NKX3-1, MYOCD, MSX2, UNC5B, SSTR1, DKK1, SYN2, ANO2, AGTR1A, TMEM178, OLFM1, NRN1L, MAP1B, HAND1, IRF5, PPARG, ZFPM1, A, BEAN1, CFH, GATA6, GATA4, HOXB13, THBS4, TTN, PDLIM3, TTR, TBX20, MSX1, ASIC1, GABRA2, SYT1, CIDEA, SMAD9, ESRRG, IGF1, GRIN2C, SMAD6, TBX4, SMAD7, DLG2, TLX2, SNAI1, FGFR3, CBLN1	102	5338	18713	2.027760636	2.83E-07	1.42E-07	1.33E-07
5	GOTERM_BP_DIRECT	GO:0030509~BMP signaling pathway	10	8.196721311	6.68E-09	MSX2, BMPER, FST, NOG, SMAD9, PPARG, SOST, MSX1, SMAD6, SMAD7	107	110	20094	17.0722175	8.30E-06	2.77E-06	2.67E-06
6	GOTERM_MF_DIRECT	GO:0043565~sequence-specific DNA binding	17	13.93442623	6.84E-09	THRB, MSX2, GATA6, FOXO6, ESRRG, GATA4, RORB, HOXB13, CUX2, TLX2, HAND1, SNAI1, PPARG, IRF5, MSX1, RXRG, NKX3-1	102	485	18713	6.430584192	1.72E-06	5.72E-07	5.38E-07
7	GOTERM_BP_DIRECT	GO:0007275~multicellular organism development	24	19.67213115	1.00E-08	MSX2, UNC5B, FST, IRX4, NOG, PRRX2, ESRRG, RORB, CHRDL2, HOXB13, DKK1, TBX4, OLFM1, GREM2, WIF1, TLX2, HAND1, TBX20, SNAI1, MSX1, HOXC9, FGFR3, PITX1, NKX3-1	107	1095	20094	4.11604148	1.25E-05	3.12E-06	3.01E-06
8	UP_KW_MOLECULAR_FUNCTION	KW-0238~DNA-binding	29	23.7704918	1.06E-08	THRB, ONECUT2, GATA6, FOXO6, HR, GATA4, RORB, HOXB13, CUX2, TBX20, MSX1, HOXC9, RXRG, PITX1, NKX3-1, MSX2, IRX4, PRRX2, SMAD9, ESRRG, SMAD6, TBX4, SMAD7, TLX2, HAND1, SNAI1, PPARG, IRF5, ZFPM1	70	1588	12158	3.171842389	3.72E-07	3.72E-07	3.62E-07
9	UP_SEQ_FEATURE	CARBOHYD:N-linked (GlcNAc...) asparagine	45	36.8852459	1.61E-08	A, TENM2, CFH, TMEM200A, GRIK3, CHRDL2, THBS4, CRHBP, CALCR, TTR, BMPER, IBSP, WIF1, SLITRK5, SOST, BRINP3, ASIC1, SLC18A3, KCNH1, GABRA2, CHST9, SYT1, UNC5B, FST, GCGR, NOG, ECEL1, TACR3, HTR3A, SSTR1, GRIN2C, DKK1, AGTR1A, ANO2, BCAN, GREM2, OLFM1, TMEM178, CEACAM10, PI16, CCDC3, FMOD, FGFR3, TRABD2B, CBLN1	116	3706	22511	2.356372239	1.62E-05	1.62E-05	1.61E-05
10	GOTERM_BP_DIRECT	GO:0006355~regulation of transcription, DNA-templated	25	20.49180328	2.08E-08	THRB, GATA6, FOXO6, GATA4, RORB, HOXB13, CUX2, TBX20, MSX1, HOXC9, RXRG, PITX1, NKX3-1, MSX2, IRX4, PRRX2, SMAD9, ESRRG, SMAD6, TBX4, SMAD7, TLX2, SNAI1, PPARG, IRF5	107	1237	20094	3.79535959	2.58E-05	5.17E-06	5.00E-06
11	GOTERM_BP_DIRECT	GO:0051216~cartilage development	9	7.37704918	2.96E-08	CFH, MSX2, NOG, PRRX2, SMAD9, MSX1, CHRDL2, PITX1, FGFR3	107	92	20094	18.37119057	3.67E-05	6.12E-06	5.92E-06
12	GOTERM_MF_DIRECT	GO:0000978~RNA polymerase II core promoter proximal region sequence-specific DNA binding	24	19.67213115	4.72E-08	THRB, MSX2, ONECUT2, IRX4, PRRX2, GATA6, FOXO6, SMAD9, ESRRG, GATA4, RORB, HOXB13, TBX4, CUX2, TLX2, HAND1, TBX20, SNAI1, PPARG, IRF5, HOXC9, PITX1, RXRG, NKX3-1	102	1169	18713	3.766517385	1.18E-05	2.96E-06	2.79E-06
13	GOTERM_CC_DIRECT	GO:0030424~axon	16	13.1147541	5.74E-08	GABRA2, SYT1, CFH, NOG, CPNE6, GRIK3, HTR3A, NRG1, BCAN, OLFM1, CALCR, NRN1L, MAP1B, NEFM, SLC18A3, KCNH1	112	502	21179	6.027034718	1.09E-05	1.09E-05	1.00E-05
14	UP_KW_BIOLOGICAL_PROCESS	KW-0805~Transcription regulation	29	23.7704918	2.15E-07	TENM2, THRB, ONECUT2, GATA6, FOXO6, HR, GATA4, RORB, HOXB13, CUX2, TBX20, MSX1, HOXC9, RXRG, PITX1, NKX3-1, MYOCD, MSX2, CIDEA, SMAD9, ESRRG, SMAD6, TBX4, SMAD7, TLX2, HAND1, PPARG, IRF5, ZFPM1	63	1873	11003	2.704150035	7.31E-06	6.80E-06	6.80E-06
15	UP_KW_PTM	KW-0325~Glycoprotein	51	41.80327869	2.23E-07	TENM2, TMEM200A, GRIK3, CHRDL2, DMKN, CRHBP, BMPER, IBSP, NEFM, SOST, SLC18A3, KCNH1, CHST9, UNC5B, FST, NOG, TACR3, HTR3A, SSTR1, DKK1, ANO2, AGTR1A, BCAN, TMEM178, GREM2, OLFM1, NRN1L, PPARG, TRABD2B, A, CFH, THBS4, TTN, CALCR, TTR, WIF1, SLITRK5, BRINP3, ASIC1, GABRA2, SYT1, GCGR, ECEL1, GRIN2C, SNAI1, CEACAM10, PI16, CCDC3, FMOD, FGFR3, CBLN1	87	4008	12816	1.874457981	4.23E-06	4.46E-06	4.46E-06
16	GOTERM_MF_DIRECT	GO:0003677~DNA binding	29	23.7704918	2.51E-07	THRB, ONECUT2, GATA6, FOXO6, HR, GATA4, RORB, HOXB13, CUX2, TBX20, MSX1, HOXC9, RXRG, PITX1, NKX3-1, MSX2, IRX4, PRRX2, SMAD9, ESRRG, SMAD6, TBX4, SMAD7, TLX2, HAND1, SNAI1, PPARG, IRF5, ZFPM1	102	1830	18713	2.907302047	6.30E-05	1.26E-05	1.18E-05
17	UP_KW_BIOLOGICAL_PROCESS	KW-0804~Transcription	29	23.7704918	4.00E-07	TENM2, THRB, ONECUT2, GATA6, FOXO6, HR, GATA4, RORB, HOXB13, CUX2, TBX20, MSX1, HOXC9, RXRG, PITX1, NKX3-1, MYOCD, MSX2, CIDEA, SMAD9, ESRRG, SMAD6, TBX4, SMAD7, TLX2, HAND1, PPARG, IRF5, ZFPM1	63	1928	11003	2.627008826	1.36E-05	6.80E-06	6.80E-06
18	GOTERM_MF_DIRECT	GO:0000981~RNA polymerase II transcription factor activity, sequence-specific DNA binding	22	18.03278689	4.31E-07	MSX2, ONECUT2, TCF24, IRX4, PRRX2, GATA6, FOXO6, SMAD9, GATA4, RORB, HOXB13, TBX4, CUX2, TLX2, HAND1, TBX20, SNAI1, IRF5, MSX1, HOXC9, PITX1, NKX3-1	102	1117	18713	3.613372654	1.08E-04	1.80E-05	1.69E-05
19	GOTERM_BP_DIRECT	GO:0060394~negative regulation of pathway-restricted SMAD protein phosphorylation	5	4.098360656	5.04E-07	NOG, PPARG, SMAD6, DKK1, SMAD7	107	13	20094	72.22861251	6.26E-04	7.85E-05	7.59E-05
20	GOTERM_BP_DIRECT	GO:0007507~heart development	12	9.836065574	5.06E-07	MYOCD, PDLIM3, IRX4, HAND1, PPARG, NRG1, GATA4, MSX1, ZFPM1, AGTR1A, TTN, NKX3-1	107	298	20094	7.562190303	6.28E-04	7.85E-05	7.59E-05
21	INTERPRO	IPR013088:Zinc finger, NHR/GATA-type	7	5.737704918	5.11E-07	THRB, GATA6, PPARG, ESRRG, GATA4, RORB, RXRG	110	57	20908	23.34226475	1.48E-04	7.55E-05	7.32E-05
22	INTERPRO	IPR017970:Homeobox, conserved site	10	8.196721311	5.21E-07	CUX2, MSX2, TLX2, IRX4, PRRX2, MSX1, HOXB13, HOXC9, PITX1, NKX3-1	110	184	20908	10.33003953	1.51E-04	7.55E-05	7.32E-05
23	UP_KW_MOLECULAR_FUNCTION	KW-9996~Developmental protein	21	17.21311475	7.78E-07	MSX2, UNC5B, IRX4, NOG, PRRX2, RORB, CHRDL2, HOXB13, DKK1, TBX4, OLFM1, GREM2, WIF1, TLX2, HAND1, TBX20, SNAI1, MSX1, HOXC9, PITX1, NKX3-1	70	1044	12158	3.493678161	2.72E-05	9.08E-06	8.82E-06
24	UP_KW_MOLECULAR_FUNCTION	KW-0217~Developmental protein	21	17.21311475	7.78E-07	MSX2, UNC5B, IRX4, NOG, PRRX2, RORB, CHRDL2, HOXB13, DKK1, TBX4, OLFM1, GREM2, WIF1, TLX2, HAND1, TBX20, SNAI1, MSX1, HOXC9, PITX1, NKX3-1	70	1044	12158	3.493678161	2.72E-05	9.08E-06	8.82E-06
25	GOTERM_CC_DIRECT	GO:0045202~synapse	19	15.57377049	9.12E-07	GABRA2, TENM2, SYT1, GRIK3, HTR3A, NRG1, GRIN2C, SYN2, KCTD8, BCAN, TRIM9, OLFM1, DLG2, MAP1B, SYNDIG1, SLITRK5, CBLN1, ASIC1, KCNH1	112	895	21179	4.014375499	1.73E-04	8.67E-05	7.98E-05
26	UP_KW_DOMAIN	KW-0371~Homeobox	11	9.016393443	1.22E-06	CUX2, MSX2, ONECUT2, TLX2, IRX4, PRRX2, MSX1, HOXB13, HOXC9, PITX1, NKX3-1	98	219	15344	7.86431833	2.31E-05	2.31E-05	2.31E-05
27	GOTERM_MF_DIRECT	GO:0003700~transcription factor activity, sequence-specific DNA binding	16	13.1147541	1.43E-06	THRB, ONECUT2, GATA6, FOXO6, ESRRG, GATA4, RORB, TBX4, TLX2, TBX20, PPARG, IRF5, HOXC9, PITX1, RXRG, NKX3-1	102	631	18713	4.651937479	3.58E-04	5.11E-05	4.81E-05
28	INTERPRO	IPR001356:Homeodomain	11	9.016393443	1.46E-06	CUX2, MSX2, ONECUT2, TLX2, IRX4, PRRX2, MSX1, HOXB13, HOXC9, PITX1, NKX3-1	110	269	20908	7.772490706	4.25E-04	1.42E-04	1.37E-04
29	UP_KW_CELLULAR_COMPONENT	KW-0770~Synapse	15	12.29508197	1.59E-06	GABRA2, TENM2, SYT1, GRIK3, HTR3A, GRIN2C, SYN2, KCTD8, TRIM9, OLFM1, DLG2, MAP1B, SYNDIG1, CBLN1, KCNH1	108	500	17960	4.988888889	3.98E-05	3.98E-05	3.98E-05
30	GOTERM_CC_DIRECT	GO:0045211~postsynaptic membrane	10	8.196721311	2.41E-06	KCTD8, GABRA2, TENM2, DLG2, GRIK3, SYNDIG1, HTR3A, GRIN2C, CBLN1, KCNH1	112	220	21179	8.595373377	4.59E-04	1.53E-04	1.41E-04

31	GOTERM_BP_DIRECT	GO:0000122~negative regulation of transcription from RNA polymerase II promoter	19	15.57377049	3.22E-06	MYOCD, TENM2, THRB, MSX2, FST, NOG, GATA6, GATA4, HOXB13, DKK1, SMAD7, CUX2, HAND1, TBX20, SNAI1, PPARG, MSX1, FGFR3, ZFPM1	107	975	20094	3.659583034	0.003992188	4.44E-04	4.30E-04
32	UP_KW_CELLULAR_COMPONENT	KW-0628~Postsynaptic cell membrane	9	7.37704918	3.51E-06	KCTD8, GABRA2, TENM2, GRIK3, SYNDIG1, HTR3A, GRIN2C, CBLN1, KCNH1	108	152	17960	9.846491228	8.78E-05	4.39E-05	4.39E-05
33	UP_KW_CELLULAR_COMPONENT	KW-0964~Secreted	27	22.13114754	5.86E-06	A, CALCB, CFH, SCT, CHRDL2, DMKN, THBS4, CRHBP, TTR, BMPER, IBSP, WIF1, NPY, SOST, BRINP3, FST, NOG, IGF1, DKK1, BCAN, GREM2, OLFM1, CEACAM10, PI16, CCDC3, FMOD, CBLN1	108	1709	17960	2.627267408	1.46E-04	4.88E-05	4.88E-05
34	UP_SEQ_FEATURE	DNA_BIND:Homeobox	10	8.196721311	7.03E-06	CUX2, MSX2, ONECUT2, TLX2, PRRX2, MSX1, HOXB13, HOXC9, PITX1, NKX3-1	116	257	22511	7.55098618	0.007052086	0.003538522	0.003513925
35	GOTERM_CC_DIRECT	GO:0005576~extracellular region	26	21.31147541	9.07E-06	A, CALCB, CFH, SCT, CHRDL2, DMKN, THBS4, CRHBP, TTR, BMPER, IBSP, WIF1, NPY, SOST, BRINP3, FST, NOG, IGF1, DKK1, BCAN, GREM2, OLFM1, PI16, CCDC3, FMOD, CBLN1	112	1859	21179	2.64473027	0.001721632	4.31E-04	3.97E-04
36	GOTERM_MF_DIRECT	GO:0004879~RNA polymerase II transcription factor activity, ligand-activated sequence-specific DNA binding	6	4.918032787	9.69E-06	THRB, PPARG, ESRRG, RORB, RXRG, NKX3-1	102	53	18713	20.76914539	0.002428194	3.04E-04	2.86E-04
37	INTERPRO	IPR009057:Homeodomain-like	11	9.016393443	1.02E-05	CUX2, MSX2, ONECUT2, TLX2, IRX4, PRRX2, MSX1, HOXB13, HOXC9, PITX1, NKX3-1	110	335	20908	6.24119403	0.002959614	7.41E-04	7.18E-04
38	GOTERM_BP_DIRECT	GO:0030279~negative regulation of ossification	5	4.098360656	1.80E-05	CALCR, SOST, SMAD6, DKK1, SMAD7	107	30	20094	31.29906542	0.022136116	0.002041644	0.001974193
39	GOTERM_BP_DIRECT	GO:0045944~positive regulation of transcription from RNA polymerase II promoter	20	16.39344262	1.81E-05	MYOCD, THRB, ONECUT2, NOG, PRRX2, GATA6, ESRRG, GATA4, IGF1, RORB, TLX2, HAND1, TBX20, PPARG, IRF5, MSX1, ZFPM1, PITX1, RXRG, NKX3-1	107	1216	20094	3.088723561	0.022207983	0.002041644	0.001974193
40	GOTERM_CC_DIRECT	GO:0043204~perikaryon	9	7.37704918	2.04E-05	OLFM1, CRHBP, DLG2, NPY, MAP1B, CPNE6, GRIK3, NEFM, KCNH1	112	219	21179	7.771159491	0.003864355	7.49E-04	6.90E-04
41	KEGG_PATHWAY	mmu04080:Neuroactive ligand-receptor interaction	12	9.836065574	2.06E-05	GABRA2, CALCB, CALCR, THRB, SCT, NPY, GCGR, GRIK3, TACR3, SSTR1, GRIN2C, AGTR1A	57	386	8992	4.904281429	0.002510028	0.001534788	0.001534788
42	GOTERM_BP_DIRECT	GO:0030154~cell differentiation	18	14.75409836	2.42E-05	THRB, SYT1, FST, IRX4, NOG, CPNE6, SMAD9, NRG1, CHRDL2, SMAD6, DMKN, SMAD7, HAND1, PPARG, FGFR3, ZFPM1, RXRG, NKX3-1	107	1022	20094	3.307533332	0.029536867	0.002498459	0.002415915
43	GOTERM_CC_DIRECT	GO:0005615~extracellular space	26	21.31147541	2.42E-05	A, CALCB, CFH, SCT, DMKN, THBS4, CRHBP, TTR, BMPER, IBSP, NPY, SOST, FST, NOG, RARRES1, NRG1, IGF1, DKK1, BCAN, GREM2, OLFM1, NRN1L, CEACAM10, PI16, FMOD, CBLN1	112	1969	21179	2.496979975	0.004595302	7.49E-04	6.90E-04
44	KEGG_PATHWAY	mmu04350:TGF-beta signaling pathway	7	5.737704918	2.52E-05	GREM2, FST, NOG, SMAD9, FMOD, SMAD6, SMAD7	57	95	8992	11.62400739	0.003064909	0.001534788	0.001534788
45	SMART	SM00389:HOX	11	9.016393443	2.63E-05	CUX2, MSX2, ONECUT2, TLX2, IRX4, PRRX2, MSX1, HOXB13, HOXC9, PITX1, NKX3-1	81	263	10615	5.481152889	0.00223126	0.002233724	0.002207444
46	GOTERM_CC_DIRECT	GO:0005667~transcription factor complex	10	8.196721311	2.76E-05	MSX2, IRX4, GATA6, SMAD9, MSX1, HOXB13, SMAD6, PITX1, ZFPM1, SMAD7	112	298	21179	6.345577661	0.005231978	7.49E-04	6.90E-04
47	GOTERM_BP_DIRECT	GO:0045892~negative regulation of transcription, DNA-templated	14	11.47540984	4.57E-05	THRB, MSX2, GATA6, HR, NRG1, RORB, CUX2, HAND1, TBX20, SNAI1, PPARG, MSX1, PITX1, NKX3-1	107	662	20094	3.971482621	0.055171826	0.004365454	0.004221228
48	GOTERM_BP_DIRECT	GO:0001707~mesoderm formation	5	4.098360656	5.78E-05	TLX2, HAND1, NOG, SNAI1, DKK1	107	40	20094	23.47429907	0.069175555	0.004835798	0.004676033
49	GOTERM_BP_DIRECT	GO:0010628~positive regulation of gene expression	13	10.6557377	5.85E-05	MYOCD, GCGR, NOG, NRG1, GATA4, IGF1, DKK1, TTN, OLFM1, CALCR, CUX2, PPARG, NKX3-1	107	583	20094	4.187525048	0.069970604	0.004835798	0.004676033
50	INTERPRO	IPR017855:SMAD domain-like	4	3.278688525	5.99E-05	SMAD9, IRF5, SMAD6, SMAD7	110	15	20908	50.68606061	0.017225846	0.003475083	0.003367236
51	GOTERM_BP_DIRECT	GO:0030513~positive regulation of BMP signaling pathway	5	4.098360656	6.37E-05	MSX2, TBX20, GATA6, GATA4, MSX1	107	41	20094	22.90175519	0.076064852	0.00494443	0.004781076
52	GOTERM_BP_DIRECT	GO:0009755~hormone-mediated signaling pathway	5	4.098360656	7.71E-05	A, CRHBP, THRB, GCGR, PPARG	107	43	20094	21.83655727	0.091201925	0.005625216	0.00543937
53	UP_SEQ_FEATURE	DNA_BIND:Nuclear receptor	5	4.098360656	8.94E-05	THRB, PPARG, ESRRG, RORB, RXRG	116	46	22511	21.09351574	0.086070099	0.022499346	0.022342945
54	UP_SEQ_FEATURE	ZN_FING:NR C4-type	5	4.098360656	8.94E-05	THRB, PPARG, ESRRG, RORB, RXRG	116	46	22511	21.09351574	0.086070099	0.022499346	0.022342945
55	GOTERM_CC_DIRECT	GO:0098978~glutamatergic synapse	12	9.836065574	9.42E-05	BCAN, OLFM1, TENM2, DLG2, SYT1, GRIK3, NRG1, HTR3A, GRIN2C, SYN2, PCDH17, CBLN1	112	522	21179	4.347085386	0.017745072	0.002237945	0.002061265
56	GOTERM_MF_DIRECT	GO:0000977~RNA polymerase II regulatory region sequence-specific DNA binding	11	9.016393443	9.45E-05	CUX2, MSX2, TCF24, HAND1, PRRX2, TBX20, SNAI1, PPARG, ESRRG, GATA4, MSX1	102	422	18713	4.782153146	0.023429411	0.002634125	0.002476707
57	INTERPRO	IPR001628:Zinc finger, nuclear hormone receptor-type	5	4.098360656	1.05E-04	THRB, PPARG, ESRRG, RORB, RXRG	110	47	20908	20.2205029	0.029961948	0.00448065	0.004341596
58	INTERPRO	IPR001723:Steroid hormone receptor	5	4.098360656	1.14E-04	THRB, PPARG, ESRRG, RORB, RXRG	110	48	20908	19.79924242	0.032512707	0.00448065	0.004341596
59	UP_SEQ_FEATURE	DOMAIN:NR LBD	5	4.098360656	1.15E-04	THRB, PPARG, ESRRG, RORB, RXRG	116	49	22511	19.802076	0.109068275	0.023096172	0.022935623
60	GOTERM_BP_DIRECT	GO:0001657~ureteric bud development	5	4.098360656	1.19E-04	BMPER, NOG, SMAD9, SMAD6, SMAD7	107	48	20094	19.56191589	0.137366283	0.008208684	0.007937486
61	GOTERM_CC_DIRECT	GO:0030054~cell junction	16	13.1147541	1.21E-04	GABRA2, TENM2, SYT1, GRIK3, HTR3A, GRIN2C, SYN2, KCTD8, TRIM9, OLFM1, BAIAP2L2, DLG2, MAP1B, SYNDIG1, CBLN1, KCNH1	112	944	21179	3.205054479	0.022787219	0.002561051	0.002358863
62	INTERPRO	IPR000536:Nuclear hormone receptor, ligand-binding, core	5	4.098360656	1.24E-04	THRB, PPARG, ESRRG, RORB, RXRG	110	49	20908	19.39517625	0.03521251	0.00448065	0.004341596
63	GOTERM_MF_DIRECT	GO:0001228~transcriptional activator activity, RNA polymerase II transcription regulatory region sequence-specific binding	12	9.836065574	1.26E-04	ONECUT2, TLX2, HAND1, PRRX2, TBX20, IRF5, PPARG, ESRRG, GATA4, MSX1, RORB, PITX1	102	526	18713	4.185417133	0.031223101	0.003171893	0.002982337
64	UP_SEQ_FEATURE	REGION:Disordered	87	71.31147541	1.39E-04	TENM2, THRB, ONECUT2, TMEM200A, TCF24, HRCT1, HR, RORB, CHRDL2, DMKN, TRIM9, BAIAP2L2, IBSP, NEFM, SOST, PITX1, RGS6, SLC18A3, NKX3-1, KCNH1, SRRM3, MYOCD, MSX2, FST, NOG, TACR3, LDOC1, NRG1, SSTR1, SYN2, ANO2, AGTR1A, KCTD8, BCAN, TMEM178, GATA5OS, OLFM1, MYL1, MAP1B, HAND1, IRF5, PPARG, ZFPM1, TRABD2B, A, BEAN1, CFH, PCDH10, 4930412O13RIK, GATA6, FOXO6, GATA4, THBS4, PCDH17, TTN, CUX2, WIF1, NPY, TBX20, SYNDIG1, SLITRK5, MSX1, HOXC9, RXRG, GABRA2, IFITM10, SYT1, GCGR, ECEL1, RARRES1, IRX4, PRRX2, SMAD9, FAM189A1, ESRRG, IGF1, GRIN2C, SMAD6, TBX4, SMAD7, DLG2, TLX2, SNAI1, PI16, FMOD, SPRR1A, FGFR3	116	13081	22511	1.290669674	0.130884676	0.023378281	0.02321577
65	GOTERM_MF_DIRECT	GO:0061629~RNA polymerase II sequence-specific DNA binding transcription factor binding	8	6.557377049	1.61E-04	MYOCD, HAND1, TBX20, GATA6, PPARG, GATA4, PITX1, ZFPM1	102	214	18713	6.858347077	0.039517595	0.003665125	0.003446094
66	UP_KW_CELLULAR_COMPONENT	KW-0965~Cell junction	16	13.1147541	1.85E-04	GABRA2, TENM2, SYT1, GRIK3, HTR3A, GRIN2C, SYN2, KCTD8, TRIM9, OLFM1, BAIAP2L2, DLG2, MAP1B, SYNDIG1, CBLN1, KCNH1	108	865	17960	3.076000856	0.004606767	0.001154246	0.001154246
67	GOTERM_BP_DIRECT	GO:0003151~outflow tract morphogenesis	5	4.098360656	2.33E-04	MSX2, NOG, TBX20, GATA4, ZFPM1	107	57	20094	16.47319233	0.251188297	0.015222843	0.014719913
68	GOTERM_CC_DIRECT	GO:0043005~neuron projection	12	9.836065574	2.46E-04	GABRA2, TENM2, DLG2, CALCR, SYT1, NPY, NEFM, HTR3A, SSTR1, ANO2, RGS6, SLC18A3	112	583	21179	3.892244548	0.045742882	0.004681636	0.004312033
69	UP_KW_MOLECULAR_FUNCTION	KW-0010~Activator	13	10.6557377	3.37E-04	MYOCD, ONECUT2, GATA6, CIDEA, FOXO6, ESRRG, GATA4, RORB, TLX2, HAND1, PPARG, ZFPM1, PITX1	70	668	12158	3.380111206	0.011726796	0.002948527	0.002864284

70	GOTERM_BP_DIRECT	GO:0030326~embryonic limb morphogenesis	5	4.098360656	3.43E-04	MSX2, PRRX2, MSX1, DKK1, TBX4	107	63	20094	14.90431687	0.346743724	0.021285637	0.020682404
71	GOTERM_CC_DIRECT	GO:0030425~dendrite	12	9.836065574	3.47E-04	GABRA2, BCAN, CRHBP, TRIM9, TENM2, DLG2, MAP1B, CPNE6, GRIK3, BRINP3, AGTR1A, KCNH1	112	607	21179	3.7383502	0.063855333	0.005997618	0.005524122
72	GOTERM_BP_DIRECT	GO:0042391~regulation of membrane potential	6	4.918032787	3.75E-04	GABRA2, GRIK3, HTR3A, GRIN2C, ASIC1, KCNH1	107	116	20094	9.713503062	0.371829817	0.021469241	0.020759943
73	GOTERM_BP_DIRECT	GO:0003148~outflow tract septum morphogenesis	4	3.278688525	3.81E-04	MSX2, TBX20, GATA6, SMAD6	107	27	20094	27.82139148	0.376504175	0.021469241	0.020759943
74	SMART	SM00399:ZnF_C4	5	4.098360656	4.17E-04	THRB, PPARG, ESRRG, RORB, RXRG	81	47	10615	13.94142369	0.034839757	0.013879016	0.013715734
75	GOTERM_BP_DIRECT	GO:0032526~response to retinoic acid	5	4.098360656	4.34E-04	HSD17B2, GATA6, GATA4, DKK1, RXRG	107	67	20094	14.01145069	0.415746948	0.023435524	0.022661264
76	UP_SEQ_FEATURE	DOMAIN:Homeobox	7	5.737704918	4.64E-04	CUX2, MSX2, ONECUT2, TLX2, PRRX2, PITX1, NKX3-1	116	192	22511	7.075116739	0.379238982	0.066725944	0.066262109
77	GOTERM_BP_DIRECT	GO:0060045~positive regulation of cardiac muscle cell proliferation	4	3.278688525	4.72E-04	TBX20, GATA6, NRG1, GATA4	107	29	20094	25.90267483	0.443269907	0.024397356	0.023591319
78	SMART	SM00430:HOLI	5	4.098360656	4.90E-04	THRB, PPARG, ESRRG, RORB, RXRG	81	49	10615	13.37238599	0.040791919	0.013879016	0.013715734
79	GOTERM_BP_DIRECT	GO:0060536~cartilage morphogenesis	3	2.459016393	5.69E-04	HAND1, SNAI1, MSX1	107	7	20094	80.48331108	0.506540676	0.02727059	0.026369627
80	GOTERM_BP_DIRECT	GO:0009653~anatomical structure morphogenesis	5	4.098360656	5.71E-04	ONECUT2, SMAD9, SMAD6, PITX1, SMAD7	107	72	20094	13.04127726	0.507981008	0.02727059	0.026369627
81	GOTERM_MF_DIRECT	GO:0000976~transcription regulatory region sequence-specific DNA binding	8	6.557377049	6.53E-04	MSX2, HAND1, GATA6, IRF5, PPARG, GATA4, SMAD6, NKX3-1	102	270	18713	5.435875091	0.151271782	0.013663557	0.01284701
82	UP_SEQ_FEATURE	DOMAIN:MH2	3	2.459016393	7.10E-04	SMAD9, SMAD6, SMAD7	116	8	22511	72.77262931	0.510921391	0.079442012	0.078889783
83	UP_SEQ_FEATURE	DOMAIN:MH1	3	2.459016393	7.10E-04	SMAD9, SMAD6, SMAD7	116	8	22511	72.77262931	0.510921391	0.079442012	0.078889783
84	INTERPRO	IPR013790:Dwarfin	3	2.459016393	7.39E-04	SMAD9, SMAD6, SMAD7	110	8	20908	71.27727273	0.192910826	0.01947654	0.018872096
85	INTERPRO	IPR013019:MAD homology, MH1	3	2.459016393	7.39E-04	SMAD9, SMAD6, SMAD7	110	8	20908	71.27727273	0.192910826	0.01947654	0.018872096
86	INTERPRO	IPR001132:SMAD domain, Dwarfin-type	3	2.459016393	7.39E-04	SMAD9, SMAD6, SMAD7	110	8	20908	71.27727273	0.192910826	0.01947654	0.018872096
87	GOTERM_CC_DIRECT	GO:0071144~SMAD2-SMAD3 protein complex	3	2.459016393	7.47E-04	SMAD9, SMAD6, SMAD7	112	8	21179	70.91183036	0.132311477	0.011822457	0.010889105
88	GOTERM_BP_DIRECT	GO:0061312~BMP signaling pathway involved in heart development	3	2.459016393	7.56E-04	MSX2, NOG, MSX1	107	8	20094	70.4228972	0.608823964	0.03427107	0.033138827
89	GOTERM_BP_DIRECT	GO:0043627~response to estrogen	5	4.098360656	7.73E-04	GATA6, PPARG, GATA4, SMAD6, AGTR1A	107	78	20094	12.03810208	0.617092236	0.03427107	0.033138827
90	GOTERM_BP_DIRECT	GO:0035116~embryonic hindlimb morphogenesis	4	3.278688525	8.26E-04	MSX2, MSX1, PITX1, TBX4	107	35	20094	21.46221629	0.641352226	0.035344517	0.034176809
91	GOTERM_BP_DIRECT	GO:0055007~cardiac muscle cell differentiation	4	3.278688525	0.001135782	MYOCD, GATA6, NRG1, GATA4	107	39	20094	19.26096334	0.755931401	0.046983497	0.045431262
92	INTERPRO	IPR020479:Homeodomain, metazoa	5	4.098360656	0.001318559	MSX2, TLX2, MSX1, HOXC9, NKX3-1	110	91	20908	10.44356644	0.317937838	0.03186518	0.030876261
93	GOTERM_BP_DIRECT	GO:0045893~positive regulation of transcription, DNA-templated	12	9.836065574	0.001341563	MYOCD, TBX20, GATA6, SNAI1, SMAD9, PPARG, ESRRG, GATA4, IGF1, SOST, RORB, NKX3-1	107	712	20094	3.165074031	0.810997848	0.053705778	0.051931453
94	UP_SEQ_FEATURE	DOMAIN:Nuclear receptor	4	3.278688525	0.001381109	THRB, PPARG, ESRRG, RXRG	116	43	22511	18.0521251	0.751357262	0.139077691	0.138110914
95	GOTERM_BP_DIRECT	GO:0030512~negative regulation of transforming growth factor beta receptor signaling pathway	5	4.098360656	0.001431662	ONECUT2, CIDEA, PPARG, SMAD6, SMAD7	107	92	20094	10.20621698	0.831018471	0.055521651	0.053687334
96	SMART	SM00524:DWB	3	2.459016393	0.001525088	SMAD9, SMAD6, SMAD7	81	8	10615	49.14351852	0.121668684	0.032408113	0.032026841
97	GOTERM_BP_DIRECT	GO:0070374~positive regulation of ERK1 and ERK2 cascade	7	5.737704918	0.001547541	CALCR, BMPER, NPY, NRG1, GATA4, IGF1, FGFR3	107	235	20094	5.593875522	0.853683877	0.058196916	0.056274213
98	GOTERM_BP_DIRECT	GO:0030900~forebrain development	5	4.098360656	0.001611621	NOG, MSX1, SSTR1, DKK1, FGFR3	107	95	20094	9.883915396	0.864885837	0.058824171	0.056880746
99	GOTERM_MF_DIRECT	GO:0042802~identical protein binding	22	18.03278689	0.001627389	TENM2, THRB, SYT1, CFH, HTR3A, ESRRG, SMAD6, SYN2, THBS4, ANO2, TTN, GREM2, BAAP2L2, TTR, NRN1L, HAND1, ME1, PPARG, IRF5, FGFR3, CBLN1, KCNH1	102	1962	18713	2.057154564	0.335555782	0.031421129	0.029543373
100	INTERPRO	IPR003619:MAD homology 1, Dwarfin-type	3	2.459016393	0.001717799	SMAD9, SMAD6, SMAD7	110	12	20908	47.51818182	0.392613602	0.038320135	0.03713089

Table S8. Functional annotation by DAVID for genes with increased expression in explants of E12.5 ureters treated for 18 h with 100 ng/ml BMP4.

Genotype	***Pax2+/+***	***Pax2-cre/+; Smad4$^{fl/+}$***	***Pax2-cre/+; Smad4$^{fl/fl}$***
expected genotype frequency	50%	25%	25%
stages, numbers obtained	obtained numbers (obtained frequency)		
E14.5, n=270	131 (49%)	67 (25%)	72 (26%)
E16.5, n=42	23 (55%)	12 (28%)	7 (17%)
E18.5, n=54	31 (57%)	10 (19%)	13 (24%)

Table S9. Genotype distribution of embryos obtained from matings of *Pax2-cre/+;Smad4$^{fl/+}$* males with *Smad4$^{fl/fl}$* females at E14.5, E16.5 and E18.5.

stage	Ratio	control		mutant		Unpaired t test (two-tailed)	Welsh Test correction (if F-Test shows significance)	
		Mean	SD	Mean	SD	P value	F- value	Welsh Test
E14.5	ΔNP63$^+$/DAPI$^+$	72.6083	17.4063	48.8190	3.7373	0.0816	0.0881	No
E16.5	ΔNP63$^+$/DAPI$^+$	73.1593	4.1010	54.7509	0.1489	0.0160	0.0026	Yes
	KRT5$^+$/DAPI$^+$	2.2424	1.4076	0.4673	0.4332	0.1051	0.173	No
	S100A1$^+$/DAPI$^+$	9.4898	5.9810	0.4865	0.0993	0.1209	0.0006	Yes
E18.5	ΔNP63$^+$/DAPI$^+$	83.1268	5.7289	59.9053	3.0483	0.0036	0.4543	No
	KRT5$^+$/DAPI$^+$	33.7628	1.8127	7.6482	4.1130	0.0005	0.3253	No
	S100A1$^+$/DAPI$^+$	23.4429	0.7949	10.2203	3.6654	0.0036	0.0898	No
P14	ΔNP63$^+$/DAPI$^+$	84.2938	6.8065	85.6836	6.4299	0.8098	0.9431	No
	KRT5$^+$/DAPI$^+$	70.0992	6.1072	58.4767	8.3664	0.1239	0.6952	No
	S100A1$^+$/DAPI$^+$	6.3112	0.9600	3.8113	0.8595	0.0283	0.8898	No

Table S10. Onset of urothelial differentiation in control and *Smad4cKO(UE)* ureters. Shown are the numbers of differentiated cells in the UE. Statistical significance was calculated using students t-Test. SD, standard derivation.

		Intensities				fold changes (FC)		
Rank	**Gene**	**control 1**	**mutant 1**	**control 2**	**mutant 2**	**FC1**	**FC2**	**avgFC**
1	*Serpinb5*	148	69	165	28	-2.2	-5.8	-4.0
2	*Prap1*	204	132	1295	222	-1.5	-5.8	-3.7
3	*Aldh3b2*	153	63	176	42	-2.4	-4.1	-3.3
4	*Upk3a*	3420	1259	3237	977	-2.7	-3.3	-3.0
5	*Gsdmc3*	446	161	583	182	-2.8	-3.2	-3.0
6	*Ldoc1*	2207	902	2164	704	-2.4	-3.1	-2.8
7	*Upk1a*	3318	1395	3095	1041	-2.4	-3.0	-2.7
8	*Pdzk1*	4722	1736	3914	1523	-2.7	-2.6	-2.6
9	*Afp*	2298	719	4854	2322	-3.2	-2.1	-2.6
10	*Anxa8*	4591	1680	3921	1556	-2.7	-2.5	-2.6
11	*Upk1b*	1197	491	1056	377	-2.4	-2.8	-2.6
12	*Perp*	6882	2771	6384	2408	-2.5	-2.7	-2.6
13	*S100a14*	549	231	524	194	-2.4	-2.7	-2.5
14	*Fa2h*	231	111	213	71	-2.1	-3.0	-2.5
15	*Cbr2*	277	144	327	112	-1.9	-2.9	-2.4
16	*Wnt10a*	211	115	183	65	-1.8	-2.8	-2.3
17	*Grhl3*	2016	1051	1696	625	-1.9	-2.7	-2.3
18	*Ppbp*	174	87	185	73	-2.0	-2.5	-2.3
19	*A_55_P1953377*	21413	11852	20916	7797	-1.8	-2.7	-2.2
20	*Msx2*	490	287	548	198	-1.7	-2.8	-2.2
21	*ENSMUST00000199575*	341	166	308	132	-2.1	-2.3	-2.2
22	*Gp9*	201	73	133	84	-2.8	-1.6	-2.2
23	*Eddm3b*	147	69	159	73	-2.1	-2.2	-2.2
24	*4631405K08Rik*	1160	648	1812	729	-1.8	-2.5	-2.1
25	*Rab27b*	600	319	614	258	-1.9	-2.4	-2.1
26	*Urah*	206	91	177	89	-2.3	-2.0	-2.1
27	*Trim29*	324	181	255	104	-1.8	-2.5	-2.1
28	*Ttr*	115	53	171	83	-2.2	-2.1	-2.1
29	*Tmprss13*	244	143	251	102	-1.7	-2.5	-2.1
30	*Trp63*	584	283	591	289	-2.1	-2.0	-2.1
31	*Aqp3*	1184	612	1080	503	-1.9	-2.1	-2.0
32	*Fxyd3*	4031	1983	3871	1903	-2.0	-2.0	-2.0
33	*Foxi1*	367	181	313	159	-2.0	-2.0	-2.0
34	*Upk3bl*	988	543	961	447	-1.8	-2.2	-2.0
35	*Tmem45b*	993	464	919	516	-2.1	-1.8	-2.0
36	*Paqr5*	374	184	324	184	-2.0	-1.8	-1.9
37	*Slc35g1*	1412	799	1386	688	-1.8	-2.0	-1.9
38	*Elf5*	394	223	389	200	-1.8	-1.9	-1.9
39	*Sfn*	362	204	323	166	-1.8	-1.9	-1.9
40	*Calml3*	167	89	183	101	-1.9	-1.8	-1.8
41	*Sprr2a2*	110	69	111	54	-1.6	-2.0	-1.8
42	*Dmkn*	356	181	292	177	-2.0	-1.7	-1.8
43	*Prom2*	434	263	321	164	-1.7	-2.0	-1.8
44	*Lgals3*	2276	1496	2656	1293	-1.5	-2.1	-1.8
45	*Abcc3*	910	600	935	456	-1.5	-2.0	-1.8

46	*4930434F21Rik*	221	127	220	124	-1.7	-1.8	-1.8
47	*Zbtb32*	135	78	122	69	-1.7	-1.8	-1.8
48	*Grhl1*	223	122	211	129	-1.8	-1.6	-1.7
49	*Crim1*	254	146	210	122	-1.7	-1.7	-1.7
50	*Fam183b*	740	419	719	436	-1.8	-1.6	-1.7
51	*Krt20*	362	200	334	211	-1.8	-1.6	-1.7
52	*Cers3*	2845	1632	2862	1792	-1.7	-1.6	-1.7
53	*Lama3*	323	177	246	163	-1.8	-1.5	-1.7
54	*Ptprd*	173	107	167	99	-1.6	-1.7	-1.7
55	*Slc39a4*	553	340	548	326	-1.6	-1.7	-1.7
56	*Ang*	324	188	326	206	-1.7	-1.6	-1.7
57	*Slco2a1*	1018	629	821	487	-1.6	-1.7	-1.7
58	*Pparg*	3833	2226	3498	2215	-1.7	-1.6	-1.7
59	*Bglap3*	118	68	128	84	-1.7	-1.5	-1.6
60	*Cck*	393	257	388	230	-1.5	-1.7	-1.6
61	*Eaf2*	214	132	223	140	-1.6	-1.6	-1.6
62	*Hmgcs2*	270	169	204	128	-1.6	-1.6	-1.6
63	*Sh3tc2*	765	462	695	462	-1.7	-1.5	-1.6
64	*Ang4*	160	104	176	111	-1.5	-1.6	-1.6
65	*Aldh1a7*	370	242	446	282	-1.5	-1.6	-1.6
66	*Il17re*	1148	720	950	631	-1.6	-1.5	-1.5
67	*Bglap2*	213	141	232	149	-1.5	-1.6	-1.5
68	*Kng1*	130	86	217	143	-1.5	-1.5	-1.5

Table S11. List of genes with decreased expression in microarrays of E14.5 *Smad4cKO(UE)* ureters. Shown are the gene names, the intensity of the two control and mutant ureter samples, the individual and the average (avg) fold change (FC).

Rank	Category	Term	Count	%	PValue	Genes	List Total	Pop Hits	Pop Total	Fold Enrichment	Bonferroni	Benjamini
1	GOTERM_BP_DIRECT	GO:0061436~establishment of skin barrier	6	9.230769231	5.57E-08	FA2H, TRP63, GRHL3, SFN, GRHL1, TMPRSS13	60	35	20094	57.41142857	3.00E-05	3.00E-05
2	GOTERM_BP_DIRECT	GO:0030855~epithelial cell differentiation	7	10.76923077	5.34E-07	LGALS3, UPK1B, UPK1A, TRP63, PPARG, KRT20, UPK3A	60	102	20094	22.98333333	2.88E-04	1.44E-04
3	UP_KW_CELLULAR_COMPONENT	KW-0964~Secreted	19	29.23076923	5.39E-06	WNT10A, URAH, ANG4, LAMA3, CCK, IL17RE, PPBP, AFP, DMKN, PRAP1, KNG1, SERPINB5, LGALS3, TTR, SPRR2A2, BGLAP3, BGLAP2, SFN, ANG	60	1709	17960	3.32787205	1.19E-04	1.19E-04
4	GOTERM_CC_DIRECT	GO:0120001~apical plasma membrane urothelial plaque	3	4.615384615	4.88E-05	UPK1B, UPK1A, UPK3A	62	4	21179	256.1975806	0.004914619	0.002626255
5	GOTERM_CC_DIRECT	GO:0005576~extracellular region	17	26.15384615	5.20E-05	WNT10A, ANG4, LAMA3, CRIM1, CCK, IL17RE, AFP, DMKN, PRAP1, KNG1, SERPINB5, LGALS3, TTR, BGLAP3, BGLAP2, SFN, ANG	62	1859	21179	3.123800517	0.005238876	0.002626255
6	GOTERM_BP_DIRECT	GO:1900076~regulation of cellular response to insulin stimulus	3	4.615384615	3.01E-04	BGLAP3, BGLAP2, PPARG	60	9	20094	111.6333333	0.149831461	0.054098743
7	UP_SEQ_FEATURE	REGION:Transcription activation	3	4.615384615	3.42E-04	TRP63, GRHL3, GRHL1	64	10	22511	105.5203125	0.100888582	0.106330136
8	GOTERM_BP_DIRECT	GO:0061844~antimicrobial humoral immune response mediated by antimicrobial peptide	5	7.692307692	7.63E-04	LGALS3, ANG4, ANG, PPBP, KNG1	60	140	20094	11.96071429	0.337396771	0.090820406
9	GOTERM_BP_DIRECT	GO:0008544~epidermis development	4	6.153846154	8.42E-04	CERS3, TRP63, GRHL3, GRHL1	60	63	20094	21.26349206	0.365103588	0.090820406
10	GOTERM_CC_DIRECT	GO:0005615~extracellular space	15	23.07692308	0.001177058	WNT10A, URAH, ANG4, CCK, PPBP, AFP, DMKN, KNG1, SERPINB5, LGALS3, TTR, BGLAP3, BGLAP2, ANG, S100A14	62	1969	21179	2.602311637	0.112150398	0.033984477
11	GOTERM_CC_DIRECT	GO:0016324~apical plasma membrane	7	10.76923077	0.00134592	UPK1B, UPK1A, RAB27B, PDZK1, UPK3A, SLC39A4, PROM2	62	423	21179	5.652901701	0.127183091	0.033984477
12	UP_KW_PTM	KW-0301~Gamma-carboxyglutamic acid	3	4.615384615	0.001813443	TTR, BGLAP3, BGLAP2	44	19	12816	45.99043062	0.025091097	0.02720164
13	UP_SEQ_FEATURE	DOMAIN:RNAse_Pc	3	4.615384615	0.002044696	ANG4, ANG, EDDM3B	64	24	22511	43.96679688	0.470885986	0.317950172
14	GOTERM_MF_DIRECT	GO:0043565~sequence-specific DNA binding	7	10.76923077	0.002405325	MSX2, ELF5, FOXI1, TRP63, PPARG, GRHL3, GRHL1	54	485	18713	5.001565483	0.327905775	0.349518518
15	INTERPRO	IPR023412:Ribonuclease A-domain	3	4.615384615	0.002729328	ANG4, ANG, EDDM3B	59	28	20908	37.968523	0.361236982	0.227162651
16	GOTERM_BP_DIRECT	GO:0042476~odontogenesis	3	4.615384615	0.00500782	WNT10A, MSX2, AQP3	60	36	20094	27.90833333	0.933196272	0.449869191
17	INTERPRO	IPR000895:Transthyretin/hydroxyisourate hydrolase	2	3.076923077	0.005540552	TTR, URAH	59	2	20908	354.3728814	0.597949331	0.227162651
18	INTERPRO	IPR023416:Transthyretin/hydroxyisourate hydrolase, superfamily	2	3.076923077	0.005540552	TTR, URAH	59	2	20908	354.3728814	0.597949331	0.227162651
19	INTERPRO	IPR023419:Transthyretin, conserved site	2	3.076923077	0.005540552	TTR, URAH	59	2	20908	354.3728814	0.597949331	0.227162651
20	UP_SEQ_FEATURE	DOMAIN:TR_THY	2	3.076923077	0.005589555	TTR, URAH	64	2	22511	351.734375	0.825045293	0.461424382
21	UP_SEQ_FEATURE	TOPO_DOM:Extracellular	15	23.07692308	0.005934719	ABCC3, PAQR5, CRIM1, IL17RE, TMPRSS13, AQP3, PTPRD, GP9, UPK1B, UPK1A, FXYD3, SLCO2A1, UPK3BL, SLC39A4, PROM2	64	2408	22511	2.191036389	0.842950799	0.461424382
22	SMART	SM00095:TR_THY	2	3.076923077	0.006208244	TTR, URAH	34	2	10615	312.2058824	0.258384651	0.297995706
23	GOTERM_MF_DIRECT	GO:0005102~receptor binding	6	9.230769231	0.00705882	PTPRD, WNT10A, ANG4, LAMA3, ANG, KNG1	54	427	18713	4.869372886	0.689271391	0.349518518
24	GOTERM_MF_DIRECT	GO:0000976~transcription regulatory region sequence-specific DNA binding	5	7.692307692	0.007131433	MSX2, FOXI1, TRP63, PPARG, GRHL1	54	270	18713	6.417352538	0.69299835	0.349518518
25	UP_KW_MOLECULAR_FUNCTION	KW-0795~Thyroid hormone	2	3.076923077	0.007384888	TTR, URAH	31	3	12158	261.4623656	0.175286796	0.1920071
26	GOTERM_BP_DIRECT	GO:0048662~negative regulation of smooth muscle cell proliferation	3	4.615384615	0.008074041	ANG4, PPARG, ANG	60	46	20094	21.84130435	0.987343343	0.526015905
27	GOTERM_BP_DIRECT	GO:0007599~hemostasis	3	4.615384615	0.008074041	GP9, ANXA8, KNG1	60	46	20094	21.84130435	0.987343343	0.526015905
28	INTERPRO	IPR024831:Uroplakin-3	2	3.076923077	0.008299504	UPK3BL, UPK3A	59	3	20908	236.2485876	0.745078205	0.272223743
29	GOTERM_MF_DIRECT	GO:0008147~structural constituent of bone	2	3.076923077	0.008473176	BGLAP3, BGLAP2	54	3	18713	231.0246914	0.75439502	0.349518518
30	GOTERM_BP_DIRECT	GO:0010482~regulation of epidermal cell division	2	3.076923077	0.008783197	TRP63, SFN	60	3	20094	223.2666667	0.991391939	0.526015905
31	UP_KW_BIOLOGICAL_PROCESS	KW-0356~Hemostasis	3	4.615384615	0.009946542	GP9, ANXA8, KNG1	38	45	11003	19.30350877	0.336250146	0.203904118
32	UP_KW_BIOLOGICAL_PROCESS	KW-0094~Blood coagulation	3	4.615384615	0.009946542	GP9, ANXA8, KNG1	38	45	11003	19.30350877	0.336250146	0.203904118
33	INTERPRO	IPR002384:Osteocalcin/matrix Gla protein	2	3.076923077	0.011050934	BGLAP3, BGLAP2	59	4	20908	177.1864407	0.838369369	0.302058852
34	UP_SEQ_FEATURE	CARBOHYD:N-linked (GlcNAc...) asparagine	19	29.23076923	0.011103225	ABCC3, WNT10A, LAMA3, CRIM1, IL17RE, AFP, TMPRSS13, AQP3, UPK3A, KNG1, SERPINB5, PTPRD, GP9, UPK1A, TTR, SLCO2A1, UPK3BL, SLC39A4, PROM2	64	3706	22511	1.803279311	0.968958067	0.690620586
35	GOTERM_BP_DIRECT	GO:0032571~response to vitamin K	2	3.076923077	0.011694042	BGLAP3, BGLAP2	60	4	20094	167.45	0.998236109	0.630308872
36	UP_KW_PTM	KW-0325~Glycoprotein	22	33.84615385	0.011922501	ABCC3, WNT10A, LAMA3, CRIM1, IL17RE, AFP, DMKN, TMPRSS13, AQP3, UPK3A, KNG1, SERPINB5, PTPRD, GP9, UPK1B, UPK1A, TTR, SLCO2A1, PPARG, UPK3BL, SLC39A4, PROM2	44	4008	12816	1.598802395	0.154576861	0.08941876
37	UP_KW_DOMAIN	KW-0732~Signal	24	36.92307692	0.01318262	WNT10A, ANG4, LAMA3, CRIM1, CCK, IL17RE, PPBP, EDDM3B, AFP, DMKN, PRAP1, UPK3A, KNG1, PTPRD, GP9, LGALS3, TTR, FXYD3, BGLAP3, BGLAP2, ANG, UPK3BL, SLC39A4, PROM2	50	4739	15344	1.554150665	0.191297777	0.210921918
38	GOTERM_BP_DIRECT	GO:0015840~urea transport	2	3.076923077	0.014596484	AQP3, UPK3A	60	5	20094	133.96	0.999638587	0.655625394
39	GOTERM_BP_DIRECT	GO:0032431~activation of phospholipase A2 activity	2	3.076923077	0.014596484	ANG4, ANG	60	5	20094	133.96	0.999638587	0.655625394
40	GOTERM_CC_DIRECT	GO:0001533~cornified envelope	3	4.615384615	0.015107881	LGALS3, SPRR2A2, SERPINB5	62	65	21179	15.76600496	0.785090858	0.305179196
41	UP_SEQ_FEATURE	TOPO_DOM:Cytoplasmic	17	26.15384615	0.015326656	ABCC3, CERS3, PAQR5, CRIM1, IL17RE, TMPRSS13, AQP3, UPK3A, PTPRD, GP9, UPK1B, UPK1A, FXYD3, SLCO2A1, UPK3BL, SLC39A4, PROM2	64	3252	22511	1.838709832	0.991798969	0.740916726
42	GOTERM_MF_DIRECT	GO:0001228~transcriptional activator activity, RNA polymerase II transcription regulatory region sequence-specific binding	6	9.230769231	0.016311887	ELF5, FOXI1, TRP63, PPARG, GRHL3, GRHL1	54	526	18713	3.952893959	0.933705899	0.512800485

43	INTERPRO	IPR007604:CP2 transcription factor	2	3.076923077	0.016531305	GRHL3, GRHL1	59	6	20908	118.1242938	0.935027642	0.387304857
44	UP_SEQ_FEATURE	DOMAIN:Grh/CP2 DB	2	3.076923077	0.016676582	GRHL3, GRHL1	64	6	22511	117.2447917	0.994647277	0.740916726
45	GOTERM_BP_DIRECT	GO:0002934~desmosome organization	2	3.076923077	0.017490546	PERP, GRHL1	60	6	20094	111.6333333	0.999925954	0.721720341
46	GOTERM_BP_DIRECT	GO:0030216~keratinocyte differentiation	3	4.615384615	0.019491042	CERS3, TRP63, SFN	60	73	20094	13.76301371	0.999975317	0.721720341
47	GOTERM_MF_DIRECT	GO:0046848~hydroxyapatite binding	2	3.076923077	0.019661253	BGLAP3, BGLAP2	54	7	18713	99.01058201	0.962236891	0.512800485
48	UP_KW_MOLECULAR_FUNCTION	KW-0010~Activator	6	9.230769231	0.022425461	ELF5, EAF2, FOXI1, TRP63, PPARG, GRHL1	31	668	12158	3.522696542	0.445505898	0.246464243
49	GOTERM_MF_DIRECT	GO:0070324~thyroid hormone binding	2	3.076923077	0.022438862	TTR, URAH	54	8	18713	86.63425926	0.976354518	0.512800485
50	GOTERM_BP_DIRECT	GO:0007596~blood coagulation	3	4.615384615	0.022596571	GP9, ANXA8, KNG1	60	79	20094	12.71772152	0.999995535	0.721720341
51	GOTERM_CC_DIRECT	GO:0005791~rough endoplasmic reticulum	3	4.615384615	0.02285339	BGLAP3, BGLAP2, TRP63	62	81	21179	12.65173238	0.903187221	0.365094581
52	GOTERM_BP_DIRECT	GO:0001738~morphogenesis of a polarized epithelium	2	3.076923077	0.023253625	LAMA3, TRP63	60	8	20094	83.725	0.999996893	0.721720341
53	GOTERM_CC_DIRECT	GO:0043204~perikaryon	4	6.153846154	0.025303585	BGLAP3, BGLAP2, CCK, KNG1	62	219	21179	6.239210488	0.924871236	0.365094581
54	GOTERM_BP_DIRECT	GO:0032287~peripheral nervous system myelin maintenance	2	3.076923077	0.02612269	FA2H, SH3TC2	60	9	20094	74.42222222	0.999999364	0.721720341
55	GOTERM_MF_DIRECT	GO:0004028~3-chloroallyl aldehyde dehydrogenase activity	2	3.076923077	0.027970936	ALDH3B2, ALDH1A7	54	10	18713	69.30740741	0.990730071	0.512800485
56	GOTERM_MF_DIRECT	GO:0043878~glyceraldehyde-3-phosphate dehydrogenase (NAD+) (non-phosphorylating) activity	2	3.076923077	0.027970936	ALDH3B2, ALDH1A7	54	10	18713	69.30740741	0.990730071	0.512800485
57	UP_KW_MOLECULAR_FUNCTION	KW-0372~Hormone	3	4.615384615	0.028438182	TTR, URAH, CCK	31	107	12158	10.9960808	0.527685355	0.246464243
58	GOTERM_BP_DIRECT	GO:0006144~purine nucleobase metabolic process	2	3.076923077	0.028983469	TTR, URAH	60	10	20094	66.98	0.99999987	0.721720341
59	GOTERM_BP_DIRECT	GO:0007398~ectoderm development	2	3.076923077	0.028983469	ELF5, GRHL3	60	10	20094	66.98	0.99999987	0.721720341
60	GOTERM_BP_DIRECT	GO:0045617~negative regulation of keratinocyte differentiation	2	3.076923077	0.028983469	MSX2, TRP63	60	10	20094	66.98	0.99999987	0.721720341
61	GOTERM_BP_DIRECT	GO:0031640~killing of cells of other organism	3	4.615384615	0.029370118	LGALS3, PPBP, KNG1	60	91	20094	11.04065934	0.999999895	0.721720341
62	GOTERM_BP_DIRECT	GO:0030154~cell differentiation	8	12.30769231	0.029457973	LGALS3, PAQR5, ELF5, FOXI1, TRP63, PPARG, ANG, DMKN	60	1022	20094	2.621526419	0.9999999	0.721720341
63	UP_SEQ_FEATURE	MOTIF:Nucleolar localization signal	2	3.076923077	0.030364418	ANG4, ANG	64	11	22511	63.95170455	0.999931568	1
64	KEGG_PATHWAY	mmu04115:p53 signaling pathway	3	4.615384615	0.031735596	PERP, SFN, SERPINB5	36	72	8992	10.40740741	0.97702296	1
65	GOTERM_MF_DIRECT	GO:0042277~peptide binding	3	4.615384615	0.03325394	ANG4, PPARG, ANG	54	101	18713	10.29317932	0.996228208	0.548690017
66	GOTERM_BP_DIRECT	GO:0001649~osteoblast differentiation	3	4.615384615	0.036197157	MSX2, BGLAP3, BGLAP2	60	102	20094	9.85	0.999999998	0.842554312
67	GOTERM_BP_DIRECT	GO:0006651~diacylglycerol biosynthetic process	2	3.076923077	0.037516333	ANG4, ANG	60	13	20094	51.52307692	0.999999999	0.842554312
68	GOTERM_BP_DIRECT	GO:0019732~antifungal humoral response	2	3.076923077	0.043163913	ANG4, ANG	60	15	20094	44.65333333	1	0.917806674
69	INTERPRO	IPR000294:Gamma-carboxyglutamic acid-rich (GLA) domain	2	3.076923077	0.043488604	BGLAP3, BGLAP2	59	16	20908	44.29661017	0.999318942	0.694809572
70	UP_SEQ_FEATURE	DOMAIN:Gla	2	3.076923077	0.043864703	BGLAP3, BGLAP2	64	16	22511	43.96679688	0.999999126	1
71	GOTERM_MF_DIRECT	GO:0004029~aldehyde dehydrogenase (NAD) activity	2	3.076923077	0.044383512	ALDH3B2, ALDH1A7	54	16	18713	43.31712963	0.999441787	0.665752674
72	GOTERM_CC_DIRECT	GO:0005604~basement membrane	3	4.615384615	0.04482534	ANG4, LAMA3, ANG	62	117	21179	8.758891646	0.990264416	0.565919924
73	GOTERM_BP_DIRECT	GO:0006068~ethanol catabolic process	2	3.076923077	0.045975473	ALDH3B2, ALDH1A7	60	16	20094	41.8625	1	0.917806674
74	GOTERM_BP_DIRECT	GO:0006833~water transport	2	3.076923077	0.045975473	AQP3, UPK3A	60	16	20094	41.8625	1	0.917806674
75	SMART	SM00069:GLA	2	3.076923077	0.04866314	BGLAP3, BGLAP2	34	16	10615	39.02573529	0.908642743	1
76	GOTERM_BP_DIRECT	GO:0009303~rRNA transcription	2	3.076923077	0.048778912	ANG4, ANG	60	17	20094	39.4	1	0.938994064
77	INTERPRO	IPR016160:Aldehyde dehydrogenase, conserved site	2	3.076923077	0.048792258	ALDH3B2, ALDH1A7	59	18	20908	39.3747646	0.999726371	0.694809572
78	GOTERM_MF_DIRECT	GO:0005179~hormone activity	3	4.615384615	0.048899395	TTR, URAH, CCK	54	125	18713	8.316888889	0.999744515	0.672366677
79	UP_SEQ_FEATURE	METAL:Calcium 3	3	4.615384615	0.051428587	BGLAP3, BGLAP2, CALML3	64	130	22511	8.116947115	0.999999926	1
80	GOTERM_BP_DIRECT	GO:0001878~response to yeast	2	3.076923077	0.054361517	ANG4, ANG	60	19	20094	35.25263158	1	1
81	INTERPRO	IPR016161:Aldehyde/histidinol dehydrogenase	2	3.076923077	0.056693595	ALDH3B2, ALDH1A7	59	21	20908	33.74979822	0.999930328	0.694809572
82	INTERPRO	IPR015590:Aldehyde dehydrogenase domain	2	3.076923077	0.056693595	ALDH3B2, ALDH1A7	59	21	20908	33.74979822	0.999930328	0.694809572
83	INTERPRO	IPR016163:Aldehyde dehydrogenase, C-terminal	2	3.076923077	0.056693595	ALDH3B2, ALDH1A7	59	21	20908	33.74979822	0.999930328	0.694809572
84	INTERPRO	IPR016162:Aldehyde dehydrogenase, N-terminal	2	3.076923077	0.056693595	ALDH3B2, ALDH1A7	59	21	20908	33.74979822	0.999930328	0.694809572
85	GOTERM_BP_DIRECT	GO:0001736~establishment of planar polarity	2	3.076923077	0.057140728	TRP63, GRHL3	60	20	20094	33.49	1	1
86	INTERPRO	IPR023411:Ribonuclease A, active site	2	3.076923077	0.059313012	ANG4, ANG	59	22	20908	32.21571649	0.999955843	0.694809572
87	GOTERM_BP_DIRECT	GO:0001836~release of cytochrome c from mitochondria	2	3.076923077	0.065430274	CCK, SFN	60	23	20094	29.12173913	1	1
88	UP_SEQ_FEATURE	BINDING:Substrate	5	7.692307692	0.066959206	PTPRD, CBR2, URAH, ANG4, HMGCS2	64	547	22511	3.215122258	1	1
89	GOTERM_MF_DIRECT	GO:1990837~sequence-specific double-stranded DNA binding	5	7.692307692	0.068853372	MSX2, ELF5, FOXI1, ZBTB32, GRHL1	54	547	18713	3.167614598	0.999992274	0.824161491
90	GOTERM_MF_DIRECT	GO:0003677~DNA binding	10	15.38461538	0.069928864	CERS3, MSX2, ELF5, FOXI1, ZBTB32, TRP63, PPARG, GRHL3, ANG, GRHL1	54	1830	18713	1.893645011	0.999993615	0.824161491
91	GOTERM_BP_DIRECT	GO:0007202~activation of phospholipase C activity	2	3.076923077	0.070916791	ANG4, ANG	60	25	20094	26.792	1	1
92	INTERPRO	IPR001427:Ribonuclease A	2	3.076923077	0.072303252	ANG4, ANG	59	27	20908	26.24984306	0.999955486	0.771886295
93	SMART	SM00092:RNAse_Pc	2	3.076923077	0.074970396	ANG4, ANG	34	25	10615	24.97647059	0.976260568	1
94	GOTERM_BP_DIRECT	GO:0030500~regulation of bone mineralization	2	3.076923077	0.076371641	BGLAP3, BGLAP2	60	27	20094	24.80740741	1	1
95	GOTERM_BP_DIRECT	GO:0009887~animal organ morphogenesis	3	4.615384615	0.077759296	WNT10A, LAMA3, TRP63	60	157	20094	6.399363057	1	1
96	GOTERM_MF_DIRECT	GO:0016620~oxidoreductase activity, acting on the aldehyde or oxo group of donors, NAD or NADP as acceptor	2	3.076923077	0.079016939	ALDH3B2, ALDH1A7	54	29	18713	23.899106	0.999998737	0.854562111
97	INTERPRO	IPR008952:Tetraspanin, EC2 domain	2	3.076923077	0.080012604	UPK1B, UPK1A	59	30	20908	23.62485876	0.999998851	0.771886295
98	INTERPRO	IPR018499:Tetraspanin/Peripherin	2	3.076923077	0.080012604	UPK1B, UPK1A	59	30	20908	23.62485876	0.999998851	0.771886295
99	GOTERM_BP_DIRECT	GO:0032148~activation of protein kinase B activity	2	3.076923077	0.084494935	ANG4, ANG	60	30	20094	22.32666667	1	1
100	GOTERM_CC_DIRECT	GO:0031528~microvillus membrane	2	3.076923077	0.085592412	PDZK1, PROM2	62	31	21179	22.03850156	0.999881116	0.960537063

Table S12. Functional annotation by DAVID for genes with decreased expression in E14.5 *Smad4cKO(UE)* ureters.

		Intensities				fold changes (FC)		
Rank	**Gene**	**control 1**	**mutant 1**	**control 2**	**mutant 2**	**FC1**	**FC2**	**avgFC**
1	*Myh11*	871	187	1326	182	-4.7	-7.3	-6.0
2	*Cnn1*	2474	783	3241	670	-3.2	-4.8	-4.0
3	*Sct*	7560	1573	6407	2092	-4.8	-3.1	-3.9
4	*Actg2*	1925	705	2640	585	-2.7	-4.5	-3.6
5	*Acta2*	7002	3485	10522	2308	-2.0	-4.6	-3.3
6	*Mrap2*	797	188	435	188	-4.2	-2.3	-3.3
7	*Smad9*	627	203	643	195	-3.1	-3.3	-3.2
8	*Car3*	41916	14122	24984	7723	-3.0	-3.2	-3.1
9	*Hpgd*	2820	875	2923	1006	-3.2	-2.9	-3.1
10	*Irf5*	368	119	335	123	-3.1	-2.7	-2.9
11	*Syt1*	3962	1087	2596	1258	-3.6	-2.1	-2.9
12	*Myocd*	366	174	560	157	-2.1	-3.6	-2.8
13	*Mansc4*	1313	453	1080	565	-2.9	-1.9	-2.4
14	*Maob*	2505	941	2466	1154	-2.7	-2.1	-2.4
15	*Id2*	22836	12088	18492	6473	-1.9	-2.9	-2.4
16	*Epha5*	581	255	677	284	-2.3	-2.4	-2.3
17	*Slitrk5*	855	320	630	332	-2.7	-1.9	-2.3
18	*Id1*	11291	5366	9950	4113	-2.1	-2.4	-2.3
19	*Bmp5*	1996	926	2061	880	-2.2	-2.3	-2.2
20	*A_55_P2041693*	417	217	516	204	-1.9	-2.5	-2.2
21	*Pcdh9*	323	139	341	168	-2.3	-2.0	-2.2
22	*Cfh*	4955	2598	5154	2117	-1.9	-2.4	-2.2
23	*Mylk*	234	116	285	124	-2.0	-2.3	-2.2
24	*Cfhr2*	1439	728	1596	696	-2.0	-2.3	-2.1
25	*Cox8b*	320	138	324	170	-2.3	-1.9	-2.1
26	*Srprb*	3640	1819	4499	2081	-2.0	-2.2	-2.1
27	*Id3*	80422	32033	40501	25098	-2.5	-1.6	-2.1
28	*Lhfpl3*	307	152	335	159	-2.0	-2.1	-2.1
29	*Alpl*	578	328	631	273	-1.8	-2.3	-2.0
30	*Asic1*	258	135	276	130	-1.9	-2.1	-2.0
31	*Sned1*	9858	4857	8190	4075	-2.0	-2.0	-2.0
32	*6720482D04*	589	307	617	299	-1.9	-2.1	-2.0
33	*Olfm1*	2219	1105	2464	1288	-2.0	-1.9	-2.0
34	*Lactb*	2833	1448	2714	1401	-2.0	-1.9	-1.9
35	*A_55_P2175050*	343	160	281	161	-2.1	-1.7	-1.9
36	*Actc1*	4203	2601	4630	2055	-1.6	-2.3	-1.9
37	*Sfrp2*	23604	14355	20265	9110	-1.6	-2.2	-1.9
38	*Slc38a5*	937	407	701	449	-2.3	-1.6	-1.9
39	*Sdpr*	4933	2437	4741	2589	-2.0	-1.8	-1.9
40	*Enpp2*	14584	7801	12288	6259	-1.9	-2.0	-1.9
41	*Ecm1*	489	278	557	275	-1.8	-2.0	-1.9
42	*9630023C09Rik*	254	118	214	133	-2.1	-1.6	-1.9
43	*F830014O18Rik*	276	142	320	180	-1.9	-1.8	-1.9
44	*Otop2*	450	248	486	255	-1.8	-1.9	-1.9
45	*Tmeff2*	1148	586	1055	601	-2.0	-1.8	-1.9

46	*Baiap2l2*	1376	716	1434	801	-1.9	-1.8	-1.9
47	*Tspan1*	536	251	668	425	-2.1	-1.6	-1.9
48	*Hapln1*	797	407	803	473	-2.0	-1.7	-1.8
49	*Srrm3*	293	169	299	155	-1.7	-1.9	-1.8
50	*Rbp4*	838	428	812	479	-2.0	-1.7	-1.8
51	*Efhd1*	175	101	235	123	-1.7	-1.9	-1.8
52	*Ppfia2*	174	102	191	102	-1.7	-1.9	-1.8
53	*Lmcd1*	2675	1672	2702	1367	-1.6	-2.0	-1.8
54	*Pde11a*	289	144	237	152	-2.0	-1.6	-1.8
55	*Tmem37*	5753	2910	5047	3208	-2.0	-1.6	-1.8
56	*Hmgcs2*	223	114	238	151	-2.0	-1.6	-1.8
57	*Nrg1*	1256	670	1121	676	-1.9	-1.7	-1.8
58	*Smad6*	1719	1075	1892	983	-1.6	-1.9	-1.8
59	*Pxylp1*	181	104	179	100	-1.7	-1.8	-1.8
60	*Smoc1*	1367	766	1315	757	-1.8	-1.7	-1.8
61	*Hspb6*	3559	1863	3608	2296	-1.9	-1.6	-1.7
62	*Akr1c14*	312	193	352	191	-1.6	-1.8	-1.7
63	*Itih5*	756	456	840	467	-1.7	-1.8	-1.7
64	*Trim9*	373	229	402	220	-1.6	-1.8	-1.7
65	*Des*	534	305	556	329	-1.7	-1.7	-1.7
66	*Gnao1*	2616	1637	2722	1485	-1.6	-1.8	-1.7
67	*Kcnt2*	420	225	374	243	-1.9	-1.5	-1.7
68	*Galm*	1428	815	1366	840	-1.8	-1.6	-1.7
69	*Abhd14b*	1168	642	1024	658	-1.8	-1.6	-1.7
70	*Fgfr4*	919	600	941	511	-1.5	-1.8	-1.7
71	*Lrfn5*	1484	808	1398	920	-1.8	-1.5	-1.7
72	*Sh3gl2*	261	149	246	155	-1.7	-1.6	-1.7
73	*Vstm4*	248	150	244	145	-1.7	-1.7	-1.7
74	*Pfkp*	396	217	382	254	-1.8	-1.5	-1.7
75	*Ebf1*	809	521	846	484	-1.6	-1.7	-1.6
76	*Pgbd5*	413	267	431	248	-1.5	-1.7	-1.6
77	*Fgfr3*	811	483	893	558	-1.7	-1.6	-1.6
78	*Hopx*	4143	2606	4165	2473	-1.6	-1.7	-1.6
79	*Dlgap3*	442	277	476	285	-1.6	-1.7	-1.6
80	*S100b*	813	483	890	576	-1.7	-1.5	-1.6
81	*Mdga1*	360	238	436	258	-1.5	-1.7	-1.6
82	*Btbd17*	829	516	917	576	-1.6	-1.6	-1.6
83	*Ifitm5*	703	433	756	483	-1.6	-1.6	-1.6
84	*Cav1*	6970	4492	6856	4271	-1.6	-1.6	-1.6
85	*Fam46a*	1855	1145	1738	1132	-1.6	-1.5	-1.6
86	*Lrrn2*	947	607	964	618	-1.6	-1.6	-1.6
87	*Sp7*	350	229	390	247	-1.5	-1.6	-1.6
88	*Il27ra*	311	200	334	215	-1.6	-1.5	-1.6
89	*Edil3*	1022	658	999	653	-1.6	-1.5	-1.5
90	*Abca9*	160	106	183	122	-1.5	-1.5	-1.5

Table S13. List of genes with decreased expression in microarrays of E14.5 *Smad4cKO(UM)* ureters. Shown are the gene names, the intensity of the two control and mutant ureter samples, the individual and the average (avg) fold change (FC).

Rank	Category	Term	Count	%	PValue	Genes	List Total	Pop Hits	Pop Total	Fold Enrichment	Bonferroni	Benjamini	FDR
1	UP_SEQ_FEATURE	CARBOHYD:N-linked (GlcNAc...) asparagine	29	34.11764706	4.29E-05	ITIH5, SNED1, ECM1, CFH, HAPLN1, IL27RA, ENPP2, SLITRK5, VSTM4, EDIL3, TSPAN1, SLC38A5, ASIC1, EPHA5, BTBD17, SYT1, ABCA9, BMP5, OLFM1, TMEFF2, LRFN5, SMOC1, MANSC4, PXYLP1, ALPL, FGFR4, MDGA1, MRAP2, FGFR3	81	3706	22511	2.17471501	0.017296073	0.01010561	0.01010561
2	KEGG_PATHWAY	mmu04350:TGF-beta signaling pathway	6	7.058823529	5.81E-05	ID2, ID1, SMAD9, ID3, SMAD6, BMP5	41	95	8992	13.85160462	0.006376125	0.006396353	0.006396353
3	UP_SEQ_FEATURE	DOMAIN:Fibronectin type-III	7	8.235294118	5.98E-05	EPHA5, SNED1, TRIM9, LRFN5, MDGA1, IL27RA, MYLK	81	190	22511	10.23892138	0.024039541	0.01010561	0.01010561
4	GOTERM_BP_DIRECT	GO:0007275~multicellular organism development	15	17.64705882	7.28E-05	EPHA5, EBF1, HOPX, BMP5, OLFM1, SFRP2, SMOC1, ID2, ID1, ID3, FGFR4, FGFR3, MDGA1, EDIL3, IFITM5	79	1095	20094	3.484307265	0.061659004	0.032257955	0.032036504
5	UP_SEQ_FEATURE	REGION:Interaction with IFI204	3	3.529411765	7.45E-05	ID2, ID1, ID3	81	4	22511	208.4351852	0.029862979	0.01010561	0.01010561
6	GOTERM_BP_DIRECT	GO:0010628~positive regulation of gene expression	11	12.94117647	8.36E-05	ACTA2, OLFM1, MYOCD, ACTC1, CAV1, ID2, ID1, ID3, NRG1, FGFR4, ACTG2	79	583	20094	4.799140196	0.07046287	0.032257955	0.032036504
7	INTERPRO	IPR026052:DNA-binding protein inhibitor	3	3.529411765	8.42E-05	ID2, ID1, ID3	80	4	20908	196.0125	0.017520185	0.014388419	0.013977321
8	UP_KW_MOLECULAR_FUNCTION	KW-0514~Muscle protein	5	5.882352941	1.32E-04	ACTA2, DES, ACTC1, MYH11, ACTG2	55	59	12158	18.73343606	0.004872161	0.004883747	0.004883747
9	INTERPRO	IPR003961:Fibronectin, type III	7	8.235294118	1.37E-04	EPHA5, SNED1, TRIM9, LRRN2, MDGA1, IL27RA, MYLK	80	208	20908	8.795432692	0.028368644	0.014388419	0.013977321
10	GOTERM_BP_DIRECT	GO:0030154~cell differentiation	14	16.47058824	1.43E-04	SYT1, CAV1, SMAD9, NRG1, SMAD6, HOPX, BMP5, SFRP2, SMOC1, ID2, ID1, ID3, FGFR3, MDGA1	79	1022	20094	3.484307265	0.117809345	0.032257955	0.032036504
11	GOTERM_BP_DIRECT	GO:0090131~mesenchyme migration	3	3.529411765	1.48E-04	ACTA2, ACTC1, ACTG2	79	5	20094	152.6126582	0.121062375	0.032257955	0.032036504
12	INTERPRO	IPR013098:Immunoglobulin I-set	6	7.058823529	2.61E-04	LRFN5, LRRN2, NRG1, FGFR4, FGFR3, MYLK	80	150	20908	10.454	0.053424838	0.015934609	0.015479334
13	INTERPRO	IPR003598:Immunoglobulin subtype 2	7	8.235294118	3.04E-04	LRFN5, LRRN2, NRG1, FGFR4, FGFR3, MDGA1, MYLK	80	241	20908	7.591078838	0.061758697	0.015934609	0.015479334
14	GOTERM_MF_DIRECT	GO:0005515~protein binding	36	42.35294118	3.34E-04	ECM1, CFH, MYLK, IL27RA, TRIM9, VSTM4, LMCD1, SH3GL2, PPFIA2, ASIC1, EPHA5, MYOCD, PCDH9, SYT1, CAV1, EBF1, SMAD9, SMAD6, HOPX, BMP5, ACTA2, GNAO1, OLFM1, RBP4, LRFN5, ACTC1, SFRP2, DES, ID2, ID1, ID3, ALPL, IRF5, SP7, FGFR4, FGFR3	74	5338	18713	1.705436797	0.080204832	0.083590299	0.083590299
15	KEGG_PATHWAY	mmu04550:Signaling pathways regulating pluripotency of stem cells	6	7.058823529	3.62E-04	ID2, ID1, SMAD9, ID3, FGFR4, FGFR3	41	140	8992	9.399303136	0.038995233	0.019884359	0.019884359
16	GOTERM_BP_DIRECT	GO:0010667~negative regulation of cardiac muscle cell apoptotic process	4	4.705882353	4.30E-04	MYOCD, SFRP2, HSPB6, NRG1	79	38	20094	26.77415057	0.313581647	0.066003385	0.065550272
17	GOTERM_BP_DIRECT	GO:0051216~cartilage development	5	5.882352941	4.53E-04	SFRP2, CFH, SMAD9, FGFR3, BMP5	79	92	20094	13.82361035	0.327067368	0.066003385	0.065550272
18	GOTERM_CC_DIRECT	GO:0005576~extracellular region	18	21.17647059	5.70E-04	ITIH5, SNED1, ECM1, HSPB6, BTBD17, CFH, SCT, S100B, HAPLN1, BMP5, IL27RA, OLFM1, RBP4, SFRP2, SMOC1, ENPP2, VSTM4, EDIL3	82	1859	21179	2.500833126	0.080867273	0.084300724	0.082591925
19	GOTERM_BP_DIRECT	GO:0010629~negative regulation of gene expression	8	9.411764706	7.60E-04	OLFM1, SFRP2, ID2, ID1, ID3, FGFR4, FGFR3, SH3GL2	79	387	20094	5.257972721	0.485547871	0.094914302	0.094262716
20	GOTERM_BP_DIRECT	GO:0030509~BMP signaling pathway	5	5.882352941	8.88E-04	SFRP2, ID1, SMAD9, SMAD6, BMP5	79	110	20094	11.56156502	0.540034008	0.097032224	0.096366099
21	INTERPRO	IPR004001:Actin, conserved site	3	3.529411765	9.08E-04	ACTA2, ACTC1, ACTG2	80	12	20908	65.3375	0.17364254	0.034881589	0.033884972
22	GOTERM_BP_DIRECT	GO:0007507~heart development	7	8.235294118	0.001062099	MYOCD, RBP4, ID2, ID1, ID3, NRG1, HOPX	79	298	20094	5.974768499	0.604959991	0.103141658	0.102433592
23	INTERPRO	IPR020902:Actin/actin-like conserved site	3	3.529411765	0.001070246	ACTA2, ACTC1, ACTG2	80	13	20908	60.31153846	0.201381521	0.034881589	0.033884972
24	INTERPRO	IPR013783:Immunoglobulin-like fold	14	16.47058824	0.00116272	EPHA5, SNED1, LRRN2, EBF1, NRG1, HAPLN1, MYLK, IL27RA, TRIM9, LRFN5, VSTM4, FGFR4, FGFR3, MDGA1	80	1307	20908	2.799464422	0.216757703	0.034881589	0.033884972
25	INTERPRO	IPR017855:SMAD domain-like	3	3.529411765	0.001433671	SMAD9, IRF5, SMAD6	80	15	20908	52.27	0.260134549	0.037633863	0.03655861
26	SMART	SM00408:IGc2	7	8.235294118	0.001471314	LRFN5, LRRN2, NRG1, FGFR4, FGFR3, MDGA1, MYLK	56	241	10615	5.505705394	0.089929714	0.094164104	0.094164104
27	GOTERM_CC_DIRECT	GO:0005869~dynactin complex	3	3.529411765	0.001674377	ACTA2, ACTC1, ACTG2	82	16	21179	48.42759146	0.219652128	0.105829934	0.103684733
28	UP_KW_DOMAIN	KW-0393~Immunoglobulin domain	8	9.411764706	0.002135633	LRFN5, LRRN2, VSTM4, FGFR4, FGFR3, MDGA1, HAPLN1, MYLK	65	434	15344	4.351364764	0.031560004	0.032034498	0.025627598
29	GOTERM_CC_DIRECT	GO:0045202~synapse	11	12.94117647	0.002145201	OLFM1, TRIM9, ACTC1, SYT1, SLITRK5, NRG1, DLGAP3, SH3GL2, HAPLN1, PPFIA2, ASIC1	82	895	21179	3.174397057	0.272274112	0.105829934	0.103684733
30	GOTERM_BP_DIRECT	GO:0045668~negative regulation of osteoblast differentiation	4	4.705882353	0.002452318	ID2, ID1, ID3, SMAD6	79	69	20094	14.74518437	0.883044069	0.214332571	0.212861181
31	GOTERM_MF_DIRECT	GO:0042802~identical protein binding	17	20	0.00320965	MAOB, SYT1, CFH, HPGD, CAV1, SMAD6, S100B, LACTB, BAIAP2L2, DES, ID1, IRF5, HMGCS2, FGFR3, MRAP2, PFKP, SH3GL2	74	1962	18713	2.19109706	0.552331809	0.401206236	0.401206236
32	GOTERM_BP_DIRECT	GO:0008284~positive regulation of cell proliferation	9	10.58823529	0.003349169	MYOCD, SFRP2, ID2, ENPP2, NRG1, FGFR4, S100B, FGFR3, BMP5	79	640	20094	3.576859177	0.946714251	0.266106689	0.26427987
33	GOTERM_CC_DIRECT	GO:0098978~glutamatergic synapse	8	9.411764706	0.003834404	OLFM1, LRFN5, ACTC1, SYT1, NRG1, DLGAP3, SH3GL2, PPFIA2	82	522	21179	3.958321652	0.433672434	0.121171611	0.11871543
34	GOTERM_CC_DIRECT	GO:0099523~presynaptic cytosol	3	3.529411765	0.004093636	TRIM9, SH3GL2, PPFIA2	82	25	21179	30.99365854	0.455071961	0.121171611	0.11871543
35	GOTERM_BP_DIRECT	GO:0048708~astrocyte differentiation	3	3.529411765	0.004211651	ID2, S100B, FGFR3	79	25	20094	30.52253165	0.974996927	0.3067486	0.304642775
36	INTERPRO	IPR004000:Actin-related protein	3	3.529411765	0.004653931	ACTA2, ACTC1, ACTG2	80	27	20908	29.03888889	0.624541298	0.108591724	0.105489103
37	UP_KW_MOLECULAR_FUNCTION	KW-9996~Developmental protein	12	14.11764706	0.005459597	OLFM1, SFRP2, SMOC1, ID2, ID1, EBF1, ID3, MDGA1, EDIL3, IFITM5, HOPX, BMP5	55	1044	12158	2.540856844	0.18336132	0.067335028	0.067335028
38	UP_KW_MOLECULAR_FUNCTION	KW-0217~Developmental protein	12	14.11764706	0.005459597	OLFM1, SFRP2, SMOC1, ID2, ID1, EBF1, ID3, MDGA1, EDIL3, IFITM5, HOPX, BMP5	55	1044	12158	2.540856844	0.18336132	0.067335028	0.067335028
39	GOTERM_BP_DIRECT	GO:0001935~endothelial cell proliferation	3	3.529411765	0.005642885	CAV1, VSTM4, FGFR3	79	29	20094	26.31252728	0.992887128	0.376495349	0.373910713
40	GOTERM_BP_DIRECT	GO:0048738~cardiac muscle tissue development	3	3.529411765	0.006030818	RBP4, NRG1, BMP5	79	30	20094	25.43544304	0.994942551	0.376495349	0.373910713

41	UP_KW_CELLULAR_COMPONENT	KW-0964~Secreted	16	18.82352941	0.006200262	ITIH5, SNED1, ECM1, HSPB6, BTBD17, CFH, SCT, HAPLN1, BMP5, OLFM1, RBP4, SFRP2, SMOC1, ENPP2, VSTM4, EDIL3	79	1709	17960	2.128419166	0.122440772	0.130205499	0.130205499
42	GOTERM_MF_DIRECT	GO:0005509~calcium ion binding	9	10.58823529	0.007429059	SNED1, PCDH9, SYT1, SMOC1, ENPP2, EFHD1, ALPL, S100B, EDIL3	74	730	18713	3.117678638	0.844979509	0.619088248	0.619088248
43	GOTERM_BP_DIRECT	GO:0031032~actomyosin structure organization	3	3.529411765	0.007700166	CNN1, ACTC1, MYH11	79	34	20094	22.44303797	0.998836113	0.420621574	0.417734011
44	GOTERM_BP_DIRECT	GO:1904706~negative regulation of vascular smooth muscle cell proliferation	3	3.529411765	0.007700166	CNN1, MYOCD, CAV1	79	34	20094	22.44303797	0.998836113	0.420621574	0.417734011
45	SMART	SM00060:FN3	5	5.882352941	0.008005636	EPHA5, SNED1, TRIM9, IL27RA, MYLK	56	153	10615	6.194561158	0.40215432	0.181663801	0.181663801
46	INTERPRO	IPR003599:Immunoglobulin subtype	8	9.411764706	0.008157232	LRFN5, LRRN2, NRG1, FGFR4, FGFR3, MDGA1, HAPLN1, MYLK	80	609	20908	3.43316913	0.82094167	0.171301868	0.166407529
47	SMART	SM00268:ACTIN	3	3.529411765	0.008515491	ACTA2, ACTC1, ACTG2	56	27	10615	21.06150794	0.421504838	0.181663801	0.181663801
48	GOTERM_BP_DIRECT	GO:1905606~regulation of presynapse assembly	3	3.529411765	0.008604087	LRFN5, SLITRK5, MDGA1	79	36	20094	21.19620253	0.999475209	0.442351299	0.439314563
49	UP_KW_DOMAIN	KW-0677~Repeat	29	34.11764706	0.009400479	SNED1, ECM1, CFH, HAPLN1, MYLK, IL27RA, TRIM9, CNN1, PDE11A, ENPP2, SLITRK5, EFHD1, LMCD1, EDIL3, PPFIA2, EPHA5, MYOCD, PCDH9, SYT1, LRRN2, ABCA9, S100B, TMEFF2, LRFN5, SMOC1, SP7, FGFR4, MDGA1, FGFR3	65	4487	15344	1.525693028	0.132095972	0.070503593	0.056402875
50	GOTERM_BP_DIRECT	GO:0060349~bone morphogenesis	3	3.529411765	0.010044431	SFRP2, FGFR3, IFITM5	79	39	20094	19.56572541	0.999852726	0.487712915	0.484364771
51	UP_KW_PTM	KW-0558~Oxidation	3	3.529411765	0.010422459	ACTA2, ACTC1, ACTG2	72	28	12816	19.07142857	0.154337085	0.177181796	0.177181796
52	UP_KW_BIOLOGICAL_PROCESS	KW-0495~Mineral balance	2	2.352941176	0.010596778	ECM1, IFITM5	40	3	11003	183.3833333	0.367511287	0.45566144	0.45566144
53	GOTERM_BP_DIRECT	GO:0007169~transmembrane receptor protein tyrosine kinase signaling pathway	4	4.705882353	0.010910282	EPHA5, NRG1, FGFR4, FGFR3	79	118	20094	8.622184081	0.999931453	0.501872949	0.498427597
54	GOTERM_CC_DIRECT	GO:0043235~receptor complex	5	5.882352941	0.011409378	EPHA5, SLITRK5, FGFR4, FGFR3, IL27RA	82	228	21179	5.664045785	0.817004684	0.276179766	0.270581528
55	GOTERM_BP_DIRECT	GO:0061144~alveolar secondary septum development	2	2.352941176	0.011600697	FGFR4, FGFR3	79	3	20094	169.5696203	0.999962766	0.504369221	0.500906732
56	GOTERM_BP_DIRECT	GO:0019216~regulation of lipid metabolic process	3	3.529411765	0.012118711	LACTB, ID2, FGFR4	79	43	20094	17.74565793	0.999976452	0.504369221	0.500906732
57	GOTERM_CC_DIRECT	GO:0044297~cell body	4	4.705882353	0.013062557	ACTA2, GNAO1, ACTC1, ACTG2	82	128	21179	8.071265244	0.857155129	0.276179766	0.270581528
58	UP_SEQ_FEATURE	BINDING:Substrate	7	8.235294118	0.013231746	RBP4, HPGD, AKR1C14, ENPP2, GALM, HMGCS2, PFKP	81	547	22511	3.556480917	0.995578457	1	1
59	GOTERM_BP_DIRECT	GO:0045471~response to ethanol	4	4.705882353	0.014148733	CAR3, RBP4, ACTC1, HPGD	79	130	20094	7.826290166	0.999996099	0.562090581	0.558231835
60	UP_KW_LIGAND	KW-0106~Calcium	11	12.94117647	0.014432807	TMEM37, SNED1, SYT1, SMOC1, ENPP2, EFHD1, ALPL, S100B, EDIL3, MYLK, ASIC1	38	836	6582	2.279085873	0.241355112	0.274223324	0.274223324
61	GOTERM_BP_DIRECT	GO:0055074~calcium ion homeostasis	3	3.529411765	0.014950711	CAV1, ALPL, FGFR3	79	48	20094	15.8971519	0.999998085	0.562200293	0.558340795
62	INTERPRO	IPR016248:Tyrosine-protein kinase, fibroblast growth factor receptor	2	2.352941176	0.015029459	FGFR4, FGFR3	80	4	20908	130.675	0.958420362	0.286926041	0.278728155
63	PIR_SUPERFAMILY	PIRSF000628:fibroblast growth factor receptor	2	2.352941176	0.015151247	FGFR4, FGFR3	8	4	1839	114.9375	0.114973418	0.121209975	0.121209975
64	GOTERM_BP_DIRECT	GO:0060157~urinary bladder development	2	2.352941176	0.015437994	MYOCD, RBP4	79	4	20094	127.1772152	0.999998757	0.562200293	0.558340795
65	UP_SEQ_FEATURE	DOMAIN:Sushi	3	3.529411765	0.015837984	SNED1, CFH, CFHR2	81	54	22511	15.43964335	0.998493025	1	1
66	GOTERM_CC_DIRECT	GO:0005615~extracellular space	15	17.64705882	0.016634827	ECM1, CFH, HPGD, LRRN2, SCT, NRG1, S100B, BMP5, OLFM1, RBP4, SFRP2, CFHR2, SMOC1, ENPP2, ALPL	82	1969	21179	1.967601481	0.916479362	0.307744308	0.301506247
67	GOTERM_BP_DIRECT	GO:0043065~positive regulation of apoptotic process	6	7.058823529	0.016639682	OLFM1, SFRP2, HPGD, ID3, IRF5, S100B	79	383	20094	3.984664706	0.999999573	0.58172328	0.577729757
68	INTERPRO	IPR008984:SMAD/FHA domain	3	3.529411765	0.017150995	SMAD9, IRF5, SMAD6	80	53	20908	14.79339623	0.973562006	0.300142409	0.291566912
69	GOTERM_CC_DIRECT	GO:0030485~smooth muscle contractile fiber	2	2.352941176	0.018978782	ACTA2, MYH11	82	5	21179	103.3121951	0.941331725	0.312095519	0.305769258
70	GOTERM_MF_DIRECT	GO:0005007~fibroblast growth factor-activated receptor activity	2	2.352941176	0.019355622	FGFR4, FGFR3	74	5	18713	101.1513514	0.992451064	1	1
71	INTERPRO	IPR000436:Sushi/SCR/CCP	3	3.529411765	0.020326049	SNED1, CFH, CFHR2	80	58	20908	13.51810345	0.986599293	0.328343867	0.318962613
72	GOTERM_BP_DIRECT	GO:0030514~negative regulation of BMP signaling pathway	3	3.529411765	0.020685065	SFRP2, CAV1, SMAD6	79	57	20094	13.38707528	0.999999988	0.6953364	0.690562924
73	GOTERM_BP_DIRECT	GO:0030282~bone mineralization	3	3.529411765	0.022065591	ALPL, FGFR3, IFITM5	79	59	20094	12.93327612	0.999999997	0.71427134	0.709367875
74	UP_KW_DOMAIN	KW-0768~Sushi	3	3.529411765	0.022825326	SNED1, CFH, CFHR2	65	56	15344	12.64615385	0.29273358	0.11412663	0.091301304
75	GOTERM_BP_DIRECT	GO:0097070~ductus arteriosus closure	2	2.352941176	0.023068523	MYOCD, HPGD	79	6	20094	84.78481013	0.999999999	0.720067464	0.715124209
76	KEGG_PATHWAY	mmu04270:Vascular smooth muscle contraction	4	4.705882353	0.025803792	ACTA2, MYH11, ACTG2, MYLK	41	144	8992	6.092140921	0.943622241	0.94613905	0.94613905
77	GOTERM_BP_DIRECT	GO:0008285~negative regulation of cell proliferation	6	7.058823529	0.026127285	MYOCD, SFRP2, CAV1, SMAD6, FGFR3, BMP5	79	431	20094	3.540896943	1	0.733664686	0.728628087
78	GOTERM_BP_DIRECT	GO:0055012~ventricular cardiac muscle cell differentiation	2	2.352941176	0.026861865	MYOCD, NRG1	79	7	20094	72.67269439	1	0.733664686	0.728628087
79	GOTERM_BP_DIRECT	GO:0071529~cementum mineralization	2	2.352941176	0.026861865	ALPL, SP7	79	7	20094	72.67269439	1	0.733664686	0.728628087
80	GOTERM_BP_DIRECT	GO:1903598~positive regulation of gap junction assembly	2	2.352941176	0.026861865	CAV1, HOPX	79	7	20094	72.67269439	1	0.733664686	0.728628087
81	UP_SEQ_FEATURE	DOMAIN:Ig-like	8	9.411764706	0.027448463	LRFN5, LRRN2, NRG1, VSTM4, FGFR4, FGFR3, MDGA1, MYLK	81	826	22511	2.691656952	0.999987965	1	1
82	UP_SEQ_FEATURE	DOMAIN:MH1	2	2.352941176	0.02808373	SMAD9, SMAD6	81	8	22511	69.47839506	0.999990776	1	1
83	UP_SEQ_FEATURE	DOMAIN:MH2	2	2.352941176	0.02808373	SMAD9, SMAD6	81	8	22511	69.47839506	0.999990776	1	1
84	UP_SEQ_FEATURE	MOTIF:Nuclear export signal	3	3.529411765	0.029280064	ID2, ID1, IRF5	81	75	22511	11.11654321	0.999994412	1	1
85	GOTERM_BP_DIRECT	GO:0033674~positive regulation of kinase activity	3	3.529411765	0.029513485	EPHA5, FGFR4, FGFR3	79	69	20094	11.05888828	1	0.753941022	0.748765226
86	INTERPRO	IPR013019:MAD homology, MH1	2	2.352941176	0.029835851	SMAD9, SMAD6	80	8	20908	65.3375	0.998272187	0.391595542	0.380407098
87	INTERPRO	IPR001132:SMAD domain, Dwarfin-type	2	2.352941176	0.029835851	SMAD9, SMAD6	80	8	20908	65.3375	0.998272187	0.391595542	0.380407098

88	INTERPRO	IPR013790:Dwarfin	2	2.352941176	0.029835851	SMAD9, SMAD6	80	8	20908	65.33375	0.998272187	0.391595542	0.380407098
89	GOTERM_MF_DIRECT	GO:0008201~heparin binding	4	4.705882353	0.030144716	CFH, CFHR2, SMOC1, FGFR4	74	173	18713	5.846898922	0.999524956	1	1
90	GOTERM_CC_DIRECT	GO:0071144~SMAD2-SMAD3 protein complex	2	2.352941176	0.030194827	SMAD9, SMAD6	82	8	21179	64.57012195	0.98930193	0.431054989	0.422317388
91	GOTERM_BP_DIRECT	GO:0001960~negative regulation of cytokine-mediated signaling pathway	2	2.352941176	0.030640666	ECM1, CAV1	79	8	20094	63.58860759	1	0.753941022	0.748765226
92	GOTERM_BP_DIRECT	GO:0051155~positive regulation of striated muscle cell differentiation	2	2.352941176	0.030640666	NRG1, HOPX	79	8	20094	63.58860759	1	0.753941022	0.748765226
93	GOTERM_BP_DIRECT	GO:0007517~muscle organ development	3	3.529411765	0.031917412	DES, ID3, NRG1	79	72	20094	10.59810127	1	0.753941022	0.748765226
94	GOTERM_BP_DIRECT	GO:0032922~circadian regulation of gene expression	3	3.529411765	0.031917412	ID2, ID1, ID3	79	72	20094	10.59810127	1	0.753941022	0.748765226
95	UP_KW_PTM	KW-0325~Glycoprotein	31	36.47058824	0.032809287	ITIH5, SNED1, ECM1, CFH, HAPLN1, IL27RA, KCNT2, ENPP2, SLITRK5, VSTM4, EDIL3, TSPAN1, SLC38A5, ASIC1, EPHA5, BTBD17, SYT1, ABCA9, BMP5, OLFM1, TMEFF2, LRFN5, SMOC1, MANSC4, PXYLP1, ALPL, FGFR4, MDGA1, MRAP2, FGFR3, PFKP	72	4008	12816	1.376746507	0.413600109	0.278878943	0.278878943
96	SMART	SM00032:CCP	3	3.529411765	0.033962959	SNED1, CFH, CFHR2	56	56	10615	10.15465561	0.890452655	0.434346708	0.434346708
97	GOTERM_MF_DIRECT	GO:0001851~complement component C3b binding	2	2.352941176	0.034573666	CFH, CFHR2	74	9	18713	56.19519952	0.999848719	1	1
98	GOTERM_MF_DIRECT	GO:0000149~SNARE binding	3	3.529411765	0.034687187	TRIM9, SYT1, CAV1	74	75	18713	10.11513514	0.999853101	1	1
99	INTERPRO	IPR007110:Immunoglobulin-like domain	9	10.58823529	0.035560001	LRFN5, LRRN2, NRG1, VSTM4, FGFR4, FGFR3, MDGA1, HAPLN1, MYLK	80	1004	20908	2.342778884	0.999501351	0.439270597	0.426720008
100	UP_SEQ_FEATURE	DOMAIN:BHLH	3	3.529411765	0.036039555	ID2, ID1, ID3	81	84	22511	9.925485009	0.999999675	1	1

Table S14. Functional annotation by DAVID for genes with decreased expression in E14.5 *Smad4cKO(UM)* ureters.

Concluding remarks

Ureter development is controlled by a complex interplay of different signaling pathways and TF genes

The functional relevance of signaling pathways during ureter development has been described in various studies. SHH and WNT signals released from the UE and BMP4 from the UM promote ureteric proliferation and cyto-differentiation while RA signaling maintains the epithelial and mesenchymal precursor populations (Bohnenpoll et al., 2017b, Bohnenpoll et al., 2017c, Mamo et al., 2017, Trowe et al., 2012). In contrast to the advances made in characterizing the function of individual signaling pathways, it remained poorly understood how these signaling pathways interact with each other and which TF genes mediate the patterning and cyto-differentiation program in the ureter. This thesis provided novel insight into these urgent questions by three independent experimental project lines concerning the role of FGF and BMP4 signaling in early ureter development.

In a first project, the relevance of epithelial FGFR signaling was characterized to increase the SHH-FOXF1-BMP4 signaling axis thereby ensuring the temporally precise onset of SMC differentiation as well as LP formation in the UM on one hand, and directing the patterning, stratification and cyto-differentiation of all three cell types within the urothelium on the other hand. In a second project, evidence was provided that mesenchymal FGFRs act as a sink to prevent overactivation of epithelial FGFR signaling, a state which leads to increased and premature development of the LP at the expense of SMC. Finally in a third project, BMP4 signaling was characterized as an important inhibitor of *Aldh1a2* expression and thereby RA signaling and LP formation. Moreover, a set of BMP4-dependent TFs was identified that mediates the cyto-differentiation in the UE and the UM (for graphical summary see Figure 8).

Patterning of the UM occurs as a consequence of cells differently responding to SHH and BMP4 signaling within the SM layer and the *lamina propria*

This thesis uncovered that patterning of the UM depends on the differential activity and levels of signaling pathways. *Shh* released from the UE is a crucial inducer of *Aldh1a2* expression in the UM and therefore for LP development. This is in good agreement with earlier studies reporting that LP development depends on high levels of SHH (Ikeda et al., 2017, Yu et al., 2002). However, one of these studies suggested that high levels of SHH inhibit SMC formation at the same time (Yu et al., 2002). Here, we suggested a different concept of LP formation and *Aldh1a2* expression. The first two projects of this thesis provided compelling evidence, that SHH acts as the main inducer for *Aldh1a2* expression and for LP formation. However, the second project suggests that high levels of SHH do not inhibit SMC development but promote

LP and SMC formation at the same time, speaking for additional regulatory mechanisms separately controlling the development of both cell layers. In this context we described BMP4 signaling in the second and third project as in important inhibitor for *Aldh1a2* expression and LP formation. Hence, the development of both mesenchymal compartments depends indeed on the same signals, but cells within the LP respond differentially to these signals than cells within the SMC layer.

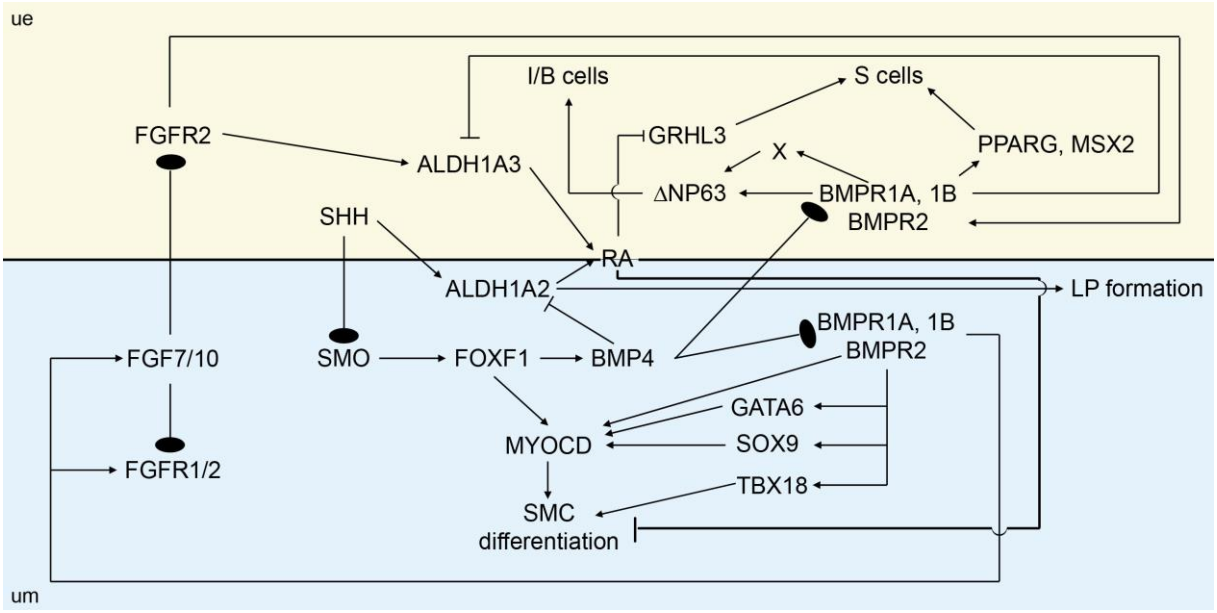

Figure 8: Network of signaling pathways and TF genes that direct early ureter development in the mouse. ue, ureteric epithelium; um, ureteric mesenchyme.

FGF signaling regulates SHH and BMP4 signaling to ensure correct patterning and cyto-differentiation in the murine ureter

The importance of SHH and BMP4 signaling for ureteric cyto-differentiation was shown before. Conditional inactivation of both pathways resulted in a complete loss of ureteric cyto-differentiation in both compartments (Bohnenpoll et al., 2017c, Mamo et al., 2017, Yu et al., 2002). The first two projects of this study highlighted the importance of the tight regulation of SHH and BMP4 signaling activity. Both projects determined that already minor changes in the activity of these signaling pathways impairs cyto-differentiation and leads to functional insufficiency of the ureter. We showed that mice lacking epithelial *Fgfr2* presented a mono-layered epithelium consisting of S cells, featured a reduced SMC layer and lacked the LP while mice with conditional inactivation of *Fgfr1/2* in the UM presented a widened LP at the expense of the SMC layer at the end of embryonic development. We have shown that FGF signaling in the UE is required to increase *Shh* expression, thereby promoting the differentiation of LP cells and SMC. We also determined mesenchymal *Fgfr1/2* to prevent overactivation of this signaling

axis and to tightly balance BMP4 signaling activity by controlling on the one hand *Bmp4* expression downstream of the FGFR2-SHH-signaling axis and on the other hand the expression of BMP receptors in the ureter. Notably, the third project identified BMP4 signaling as a regulator for mesenchymal expression of both, *Fgf7/10* and *Fgfr1/2*, indicating a complex feed-back activation loop between SHH, BMP4 and FGFR2 signaling.
We have provided compelling evidence, that correct cyto-differentiation in both ureter compartments depends on the tight regulation of the SHH-BMP4-signaling axis by FGFR2 signaling.

Precise onset of *Myocd* expression is of utmost relevance for ureter function and integrity

The importance of *Myocd* for the differentiation of SMCs in various cell types was known for long, as was its relevance for the differentiation of SMC in the context of ureter development (Kurz et al., 2022, Wang et al., 2003). Here, we provided additional evidence for the importance to precisely activate *Myocd* expression to ensure unopposed urine transport from the renal pelvis to the bladder. Conditional inactivation of *Fgfr2* in the UE and *Fgfr1/2* in the UM both resulted in a one-day delay in the onset of *Myocd* expression and/or SMC differentiation. Both mutants presented hydroureters at the end of embryonic development. Although *Fgfr2cKO-UE* embryos additionally suffered from physical obstruction, most likely aggravating hydroureter formation, we did not observe physical obstruction in *Fgfr1/2cDKO-UM* embryos. Thus, hydroureter formation in these mutants must be a consequence of delayed SMC development. Moreover, we showed that a one-day delay in the onset of *Myocd* expression already interferes with the functional integrity of the ureter. Delayed *Myocd* expression subsequently resulted in delayed expression of structural SM genes leading to delayed peristaltic activity and hydroureter formation after onset of urine production in the fetal kidney.
The importance of timely activating *Myocd* expression was further highlighted in the third subproject of this thesis. We did not only confirm the importance of BMP4 signaling for *Myocd* expression (Mamo et al., 2017) but we also found that regulation takes place by different mechanisms. Our model suggests that *Bmp4* regulates *Myocd* expression directly and additionally indirectly by controlling the expression of various TF genes that, in turn, control *Myocd* expression. This highlights the importance of strict regulation of *Myocd* in the context of ureter development to ensure ureter function and integrity.

Epithelial development and S cell differentiation in the murine ureter may depend on antagonism of BMP4 and RA signaling

The importance of BMP4 signaling for urothelial development in the murine ureter was previously revealed by targeted genetic inactivation of *Bmp4* in the UM (Mamo et al., 2017).

Moreover, our earlier study has shown that reinstallation of BMP4 downstream of SHH and FOXF1 is sufficient to rescue epithelial but not mesenchymal differentiation (Bohnenpoll et al., 2017c). But how exactly BMP4 drives the cyto-differentiation of three different cell types from a homogenous, uncommitted precursor cell population remained elusive. In the third sub-project of this thesis, we defined a set of TF genes (*Pparg, Msx2*) expressed in the UE that directly depends on *Bmp4* and controls S cell differentiation in other developmental contexts (Weiss et al., 2013, Liu et al., 2019, Yin et al., 2006). Moreover, we identified additional TF genes important for S cell differentiation that indirectly depend on *Bmp4* and are negatively influenced by RA signaling, most notably *Grhl3*. Combined with the observed phenotypes in *Fgfr2cKO-UE* and *Fgfr1/2cDKO-UM* ureters there are two possible mechanisms by which BMP4 signaling drives development of different cell types in the UE. First, it is possible that low doses of BMP4 may suffice to induce S cell fate, whereas higher doses are necessary to induce I/B cell differentiation. This notion is supported by ureter culture experiments, in which I cells are reduced upon low NOG concentrations while S cells are only reduced upon high NOG concentrations. Moreover, *Fgfr2cKO-UE* ureters suffered from a lack of I and B cells leaving a monolayered epithelium consisting only of S cells in agreement with a dose-depended function of BMP4 signaling in the UE. However, this hypothesis neglects the influence of reduced RA signaling activity in these mutant ureters as indicated by reduced expression of the RA synthesizing enzymes *Aldh1a2* and *Aldh1a3* and reduced target gene expression. As mentioned above, RA signaling represses TF genes important for S cell differentiation. Shortly before the onset of *Trp63*/ΔNP63 expression in the UE, *Aldh1a2* and *Aldh1a3* are expressed in the UM and UE, respectively, possibly inhibiting S cell differentiation from epithelial progenitors. With the onset of stratification and of S and B cell differentiation in the ureter around E16.5, a new source for RA is established: the *lamina propria*. Again, given the cyto-architecture of the ureter, luminal S cells are furthest away to the new RA source, supporting the theory that high levels of RA inhibit S cell differentiation from urothelial progenitor cells. This is further supported by the phenotypes of *Fgfr1/2cDKO-UM* ureters. Although at that time we did not pay much attention to it, mutant ureters did not only show increased and premature LP formation but additionally exhibited decreased expression of *Grhl3* and of *Upks.* This is in line with our findings in the third project, that *Grhl3* is negatively regulated by RA signaling. In summary, our studies suggest that epithelial development and S cell differentiation is antagonistically controlled by BMP4 and RA signaling.

Taken together, the characterization of FGFR1/FGFR2 and BMP4 signaling increased our knowledge of the molecular control mechanisms of patterning and differentiation in the development of a critical tubular organ, the murine ureter.

References

ACHARYA, P., BECKEL, J., RUIZ, W. G., WANG, E., ROJAS, R., BIRDER, L. & APODACA, G. 2004. Distribution of the tight junction proteins ZO-1, occludin, and claudin-4, -8, and -12 in bladder epithelium. *Am J Physiol Renal Physiol,* 287**,** 6.

AIRIK, R., BUSSEN, M., SINGH, M. K., PETRY, M. & KISPERT, A. 2006. Tbx18 regulates the development of the ureteral mesenchyme. *J Clin Invest,* 116**,** 663-74.

AIRIK, R. & KISPERT, A. 2007. Down the tube of obstructive nephropathies: the importance of tissue interactions during ureter development. *Kidney Int,* 72**,** 1459-67.

AIRIK, R., TROWE, M. O., FOIK, A., FARIN, H. F., PETRY, M., SCHUSTER-GOSSLER, K., SCHWEIZER, M., SCHERER, G., KIST, R. & KISPERT, A. 2010. Hydroureternephrosis due to loss of Sox9-regulated smooth muscle cell differentiation of the ureteric mesenchyme. *Hum Mol Genet,* 19**,** 4918-29.

AOKI, Y., MORI, S., KITAJIMA, K., YOKOYAMA, O., KANAMARU, H., OKADA, K. & YOKOTA, Y. 2004. Id2 haploinsufficiency in mice leads to congenital hydronephrosis resembling that in humans. *Genes Cells,* 9**,** 1287-96.

AYDOĞDU, N., RUDAT, C., TROWE, M. O., KAISER, M., LÜDTKE, T. H., TAKETO, M. M., CHRISTOFFELS, V. M., MOON, A. & KISPERT, A. 2018. TBX2 and TBX3 act downstream of canonical WNT signaling in patterning and differentiation of the mouse ureteric mesenchyme. *Development,* 145**,** 171827.

BARASCH, J., QIAO, J., MCWILLIAMS, G., CHEN, D., OLIVER, J. A. & HERZLINGER, D. 1997. Ureteric bud cells secrete multiple factors, including bFGF, which rescue renal progenitors from apoptosis. *Am J Physiol,* 273.

BELL, S. M., ZHANG, L., MENDELL, A., XU, Y., HAITCHI, H. M., LESSARD, J. L. & WHITSETT, J. A. 2011. Kruppel-like factor 5 is required for formation and differentiation of the bladder urothelium. *Dev Biol,* 358**,** 79-90.

BÖCK, M., HINLEY, J., SCHMITT, C., WAHLICHT, T., KRAMER, S. & SOUTHGATE, J. 2014. Identification of ELF3 as an early transcriptional regulator of human urothelium. *Dev Biol,* 386**,** 321-30.

BOHNENPOLL, T., BETTENHAUSEN, E., WEISS, A. C., FOIK, A. B., TROWE, M. O., BLANK, P., AIRIK, R. & KISPERT, A. 2013. Tbx18 expression demarcates multipotent precursor populations in the developing urogenital system but is exclusively required within the ureteric mesenchymal lineage to suppress a renal stromal fate. *Dev Biol,* 380**,** 25-36.

BOHNENPOLL, T., FERARIC, S., NATTKEMPER, M., WEISS, A. C., RUDAT, C., MEUSER, M., TROWE, M. O. & KISPERT, A. 2017a. Diversification of Cell Lineages in Ureter Development. *J Am Soc Nephrol,* 28**,** 1792-1801.

BOHNENPOLL, T. & KISPERT, A. 2014. Ureter growth and differentiation. *Semin Cell Dev Biol,* 36**,** 21-30.

BOHNENPOLL, T., WEISS, A. C., LABUHN, M., LÜDTKE, T. H., TROWE, M. O. & KISPERT, A. 2017b. Retinoic acid signaling maintains epithelial and mesenchymal progenitors in the developing mouse ureter. *Sci Rep,* 7**,** 017-14790.

BOHNENPOLL, T., WITTERN, A. B., MAMO, T. M., WEISS, A. C., RUDAT, C., KLEPPA, M. J., SCHUSTER-GOSSLER, K., WOJAHN, I., LUDTKE, T. H., TROWE, M. O. & KISPERT, A. 2017c. A SHH-FOXF1-BMP4 signaling axis regulating growth and differentiation of epithelial and mesenchymal tissues in ureter development. *PLoS Genet,* 13**,** 1006951.

BOHNENPOLL, T., WITTERN, A. B., MAMO, T. M., WEISS, A. C., RUDAT, C., KLEPPA, M. J., SCHUSTER-GOSSLER, K., WOJAHN, I., LÜDTKE, T. H., TROWE, M. O. & KISPERT, A. 2017d. A SHH-FOXF1-BMP4 signaling axis regulating growth and differentiation of epithelial and mesenchymal tissues in ureter development. *PLoS Genet,* 13.

BOUCHARD, M., SOUABNI, A., MANDLER, M., NEUBÜSER, A. & BUSSLINGER, M. 2002. Nephric lineage specification by Pax2 and Pax8. *Genes Dev,* 16**,** 2958-70.

BRENNER-ANANTHARAM, A., CEBRIAN, C., GUILLAUME, R., HURTADO, R., SUN, T. T. & HERZLINGER, D. 2007. Tailbud-derived mesenchyme promotes urinary tract segmentation via BMP4 signaling. *Development,* 134**,** 1967-75.

CARPENTER, A. R., BECKNELL, M. B., CHING, C. B., CUARESMA, E. J., CHEN, X., HAINS, D. S. & MCHUGH, K. M. 2016. Uroplakin 1b is critical in urinary tract development and urothelial differentiation and homeostasis. *Kidney Int,* 89**,** 612-24.

CARPENTER, A. R. & MCHUGH, K. M. 2017. Role of renal urothelium in the development and progression of kidney disease. *Pediatr Nephrol,* 32**,** 557-564.

CAUBIT, X., LYE, C. M., MARTIN, E., CORE, N., LONG, D. A., VOLA, C., JENKINS, D., GARRATT, A. N., SKAER, H., WOOLF, A. S. & FASANO, L. 2008. Teashirt 3 is necessary for ureteral smooth muscle differentiation downstream of SHH and BMP4. *Development,* 135**,** 3301-10.

CHANG, C. P., MCDILL, B. W., NEILSON, J. R., JOIST, H. E., EPSTEIN, J. A., CRABTREE, G. R. & CHEN, F. 2004. Calcineurin is required in urinary tract mesenchyme for the development of the pyeloureteral peristaltic machinery. *J Clin Invest,* 113**,** 1051-8.

CHEN, H., XU, C. F., MA, J., ELISEENKOVA, A. V., LI, W., POLLOCK, P. M., PITTELOUD, N., MILLER, W. T., NEUBERT, T. A. & MOHAMMADI, M. 2008. A crystallographic snapshot of tyrosine trans-phosphorylation in action. *Proc Natl Acad Sci U S A,* 105**,** 19660-5.

CHENG, W., JACOBS, W. B., ZHANG, J. J., MORO, A., PARK, J. H., KUSHIDA, M., QIU, W., MILLS, A. A. & KIM, P. C. 2006. DeltaNp63 plays an anti-apoptotic role in ventral bladder development. *Development,* 133**,** 4783-92.

CHEVALIER, R. L. 2015. Congenital urinary tract obstruction: the long view. *Adv Chronic Kidney Dis,* 22**,** 312-9.

CHING, B. J., WITTLER, L., PROSKE, J., YAGNIK, G., QI, L., DRAAKEN, M., REUTTER, H., GEARHART, J. P., LUDWIG, M. & BOYADJIEV, S. A. 2010. p63 (TP73L) a key player in embryonic urogenital development with significant dysregulation in human bladder exstrophy tissue. *Int J Mol Med,* 26**,** 861-7.

CHU, G. C., DUNN, N. R., ANDERSON, D. C., OXBURGH, L. & ROBERTSON, E. J. 2004. Differential requirements for Smad4 in TGFbeta-dependent patterning of the early mouse embryo. *Development,* 131**,** 3501-12.

COSTANTINI, F. & KOPAN, R. 2010. Patterning a complex organ: branching morphogenesis and nephron segmentation in kidney development. *Dev Cell,* 18**,** 698-712.

COSTANTINI, F. & SHAKYA, R. 2006. GDNF/Ret signaling and the development of the kidney. *Bioessays,* 28**,** 117-27.

DALGHI, M. G., MONTALBETTI, N., CARATTINO, M. D. & APODACA, G. 2020. The Urothelium: Life in a Liquid Environment. *Physiol Rev,* 100**,** 1621-1705.

DEUPER, L., MEUSER, M., THIESLER, H., JANY, U. W. H., RUDAT, C., HILDEBRANDT, H., TROWE, M. O. & KISPERT, A. 2022. Mesenchymal FGFR1 and FGFR2 control patterning of the ureteric mesenchyme by balancing SHH and BMP4 signaling. *Development,* 149**,** 12.

DIAMOND, J. R., VAN GOOR, H., DING, G. & ENGELMYER, E. 1995. Myofibroblasts in experimental hydronephrosis. *Am J Pathol,* 146**,** 121-9.

DUDKA, A. A., SWEET, S. M. & HEATH, J. K. 2010. Signal transducers and activators of transcription-3 binding to the fibroblast growth factor receptor is activated by receptor amplification. *Cancer Res,* 70**,** 3391-401.

FORBES, M. S., THORNHILL, B. A., MINOR, J. J., GORDON, K. A., GALARRETA, C. I. & CHEVALIER, R. L. 2012. Fight-or-flight: murine unilateral ureteral obstruction causes extensive proximal tubular degeneration, collecting duct dilatation, and minimal fibrosis. *Am J Physiol Renal Physiol,* 303**,** 25.

FRIEDMAN, C. E., NGUYEN, Q., LUKOWSKI, S. W., HELFER, A., CHIU, H. S., MIKLAS, J., LEVY, S., SUO, S., HAN, J. J., OSTEIL, P., PENG, G., JING, N., BAILLIE, G. J., SENABOUTH, A., CHRIST, A. N., BRUXNER, T. J., MURRY, C. E., WONG, E. S., DING, J., WANG, Y., HUDSON, J., RUOHOLA-BAKER, H., BAR-JOSEPH, Z., TAM, P. P. L., POWELL, J. E. & PALPANT, N. J. 2018. Single-Cell Transcriptomic Analysis

of Cardiac Differentiation from Human PSCs Reveals HOPX-Dependent Cardiomyocyte Maturation. *Cell Stem Cell,* 23**,** 586-598.

GOMEZ-PUERTO, M. C., IYENGAR, P. V., GARCÍA DE VINUESA, A., TEN DIJKE, P. & SANCHEZ-DUFFHUES, G. 2019. Bone morphogenetic protein receptor signal transduction in human disease. *J Pathol,* 247**,** 9-20.

GOTOH, N. 2008. Regulation of growth factor signaling by FRS2 family docking/scaffold adaptor proteins. *Cancer Sci,* 99**,** 1319-25.

GROTE, D., SOUABNI, A., BUSSLINGER, M. & BOUCHARD, M. 2006. Pax 2/8-regulated Gata 3 expression is necessary for morphogenesis and guidance of the nephric duct in the developing kidney. *Development,* 133**,** 53-61.

HAINS, D., SIMS-LUCAS, S., KISH, K., SAHA, M., MCHUGH, K. & BATES, C. M. 2008. Role of fibroblast growth factor receptor 2 in kidney mesenchyme. *Pediatr Res,* 64**,** 592-8.

HAINS, D. S., SIMS-LUCAS, S., CARPENTER, A., SAHA, M., MURAWSKI, I., KISH, K., GUPTA, I., MCHUGH, K. & BATES, C. M. 2010. High incidence of vesicoureteral reflux in mice with Fgfr2 deletion in kidney mesenchyma. *J Urol,* 183**,** 2077-84.

HARAGUCHI, R., MATSUMARU, D., NAKAGATA, N., MIYAGAWA, S., SUZUKI, K., KITAZAWA, S. & YAMADA, G. 2012. The hedgehog signal induced modulation of bone morphogenetic protein signaling: an essential signaling relay for urinary tract morphogenesis. *PLoS One,* 7**,** 30.

HARAMBAT, J., VAN STRALEN, K. J., KIM, J. J. & TIZARD, E. J. 2012. Epidemiology of chronic kidney disease in children. *Pediatr Nephrol,* 27**,** 363-73.

HARTWIG, J. H., THELEN, M., ROSEN, A., JANMEY, P. A., NAIRN, A. C. & ADEREM, A. 1992. MARCKS is an actin filament crosslinking protein regulated by protein kinase C and calcium-calmodulin. *Nature,* 356**,** 618-22.

HICKS, R. M. 1965. The fine structure of the transitional epithelium of rat ureter. *J Cell Biol,* 26**,** 25-48.

HICKS, R. M. 1966. *THE PERMEABILITY OF RAT TRANSITIONAL EPITHELIUM : Keratinization and the Barrier to Water*, J Cell Biol. 1966 Jan 1;28(1):21-31.

HOGAN, B. L. M. 1995. The TGF-β-related signalling system in mouse development. *Seminars in Developmental Biology,* 6**,** 257-265.

HOLLNAGEL, A., OEHLMANN, V., HEYMER, J., RUTHER, U. & NORDHEIM, A. 1999. Id genes are direct targets of bone morphogenetic protein induction in embryonic stem cells. *J Biol Chem,* 274**,** 19838-45.

HU, C. C., LIANG, F. X., ZHOU, G., TU, L., TANG, C. H., ZHOU, J., KREIBICH, G. & SUN, T. T. 2005. Assembly of urothelial plaques: tetraspanin function in membrane protein trafficking. *Mol Biol Cell,* 16**,** 3937-50.

HU, P., DENG, F. M., LIANG, F. X., HU, C. M., AUERBACH, A. B., SHAPIRO, E., WU, X. R., KACHAR, B. & SUN, T. T. 2000. Ablation of uroplakin III gene results in small urothelial plaques, urothelial leakage, and vesicoureteral reflux. *J Cell Biol,* 151**,** 961-72.

HU, P., MEYERS, S., LIANG, F. X., DENG, F. M., KACHAR, B., ZEIDEL, M. L. & SUN, T. T. 2002. Role of membrane proteins in permeability barrier function: uroplakin ablation elevates urothelial permeability. *Am J Physiol Renal Physiol,* 283**,** 30.

IKEDA, Y., ZABBAROVA, I., SCHAEFER, C. M., BUSHNELL, D., DE GROAT, W. C., KANAI, A. & BATES, C. M. 2017. Fgfr2 is integral for bladder mesenchyme patterning and function. *Am J Physiol Renal Physiol,* 312**,** F607-F618.

JACKSON, A. R., CHING, C. B., MCHUGH, K. M. & BECKNELL, B. 2020. Roles for urothelium in normal and aberrant urinary tract development. *Nat Rev Urol,* 17**,** 459-468.

JASLOVE, J. M. & NELSON, C. M. 2018. Smooth muscle: a stiff sculptor of epithelial shapes. *Philos Trans R Soc Lond B Biol Sci,* 373.

JENKINS, D., BITNER-GLINDZICZ, M., MALCOLM, S., ALLISON, J., DE BRUYN, R., FLANAGAN, S., THOMAS, D. F., BELK, R. A., FEATHER, S. A., BINGHAM, C., SOUTHGATE, J. & WOOLF, A. S. 2006. Mutation analyses of Uroplakin II in children with renal tract malformations. *Nephrol Dial Transplant,* 21**,** 3415-21.

JENKINS, D., BITNER-GLINDZICZ, M., MALCOLM, S., HU, C. C., ALLISON, J., WINYARD, P. J., GULLETT, A. M., THOMAS, D. F., BELK, R. A., FEATHER, S. A., SUN, T. T. &

WOOLF, A. S. 2005. De novo Uroplakin IIIa heterozygous mutations cause human renal adysplasia leading to severe kidney failure. *J Am Soc Nephrol,* 16**,** 2141-9.

JOHNSON, D. E., LU, J., CHEN, H., WERNER, S. & WILLIAMS, L. T. 1991. The human fibroblast growth factor receptor genes: a common structural arrangement underlies the mechanisms for generating receptor forms that differ in their third immunoglobulin domain. *Mol Cell Biol,* 11**,** 4627-34.

KAGAN, M., PLENICEANU, O. & VIVANTE, A. 2022. The genetic basis of congenital anomalies of the kidney and urinary tract. *Pediatr Nephrol,* 37**,** 2231-2243.

KAWABATA, M., IMAMURA, T. & MIYAZONO, K. 1998. Signal transduction by bone morphogenetic proteins. *Cytokine Growth Factor Rev,* 9**,** 49-61.

KHAN, K., AHRAM, D. F., LIU, Y. P., WESTLAND, R., SAMPOGNA, R. V., KATSANIS, N., DAVIS, E. E. & SANNA-CHERCHI, S. 2022. Multidisciplinary approaches for elucidating genetics and molecular pathogenesis of urinary tract malformations. *Kidney Int,* 101**,** 473-484.

KONG, X. T., DENG, F. M., HU, P., LIANG, F. X., ZHOU, G., AUERBACH, A. B., GENIESER, N., NELSON, P. K., ROBBINS, E. S., SHAPIRO, E., KACHAR, B. & SUN, T. T. 2004. Roles of uroplakins in plaque formation, umbrella cell enlargement, and urinary tract diseases. *J Cell Biol,* 167**,** 1195-204.

KOUHARA, H., HADARI, Y. R., SPIVAK-KROIZMAN, T., SCHILLING, J., BAR-SAGI, D., LAX, I. & SCHLESSINGER, J. 1997. A lipid-anchored Grb2-binding protein that links FGF-receptor activation to the Ras/MAPK signaling pathway. *Cell,* 89**,** 693-702.

KULESSA, H. & HOGAN, B. L. 2002. Generation of a loxP flanked bmp4loxP-lacZ allele marked by conditional lacZ expression. *Genesis,* 32**,** 66-8.

KURZ, J., WEISS, A. C., LÜDTKE, T. H., DEUPER, L., TROWE, M. O., THIESLER, H., HILDEBRANDT, H., HEINEKE, J., DUNCAN, S. A. & KISPERT, A. 2022. GATA6 is a crucial factor for Myocd expression in the visceral smooth muscle cell differentiation program of the murine ureter. *Development,* 149**,** 29.

KUSCHERT, S., ROWITCH, D. H., HAENIG, B., MCMAHON, A. P. & KISPERT, A. 2001. Characterization of Pax-2 regulatory sequences that direct transgene expression in the Wolffian duct and its derivatives. *Dev Biol,* 229**,** 128-40.

LANGBEIN, L., GRUND, C., KUHN, C., PRAETZEL, S., KARTENBECK, J., BRANDNER, J. M., MOLL, I. & FRANKE, W. W. 2002. Tight junctions and compositionally related junctional structures in mammalian stratified epithelia and cell cultures derived therefrom. *Eur J Cell Biol,* 81**,** 419-35.

LARONDA, M. M., UNNO, K., ISHI, K., SERNA, V. A., BUTLER, L. M., MILLS, A. A., ORVIS, G. D., BEHRINGER, R. R., DENG, C., SINHA, S. & KURITA, T. 2013. Diethylstilbestrol induces vaginal adenosis by disrupting SMAD/RUNX1-mediated cell fate decision in the Müllerian duct epithelium. *Dev Biol,* 381**,** 5-16.

LAWSON, K. A., DUNN, N. R., ROELEN, B. A., ZEINSTRA, L. M., DAVIS, A. M., WRIGHT, C. V., KORVING, J. P. & HOGAN, B. L. 1999. Bmp4 is required for the generation of primordial germ cells in the mouse embryo. *Genes Dev,* 13**,** 424-36.

LEE, P. L., JOHNSON, D. E., COUSENS, L. S., FRIED, V. A. & WILLIAMS, L. T. 1989. Purification and complementary DNA cloning of a receptor for basic fibroblast growth factor. *Science,* 245**,** 57-60.

LEWANDOSKI, M., MEYERS, E. N. & MARTIN, G. R. 1997. Analysis of Fgf8 gene function in vertebrate development. *Cold Spring Harb Symp Quant Biol,* 62**,** 159-68.

LIU, C., TATE, T., BATOURINA, E., TRUSCHEL, S. T., POTTER, S., ADAM, M., XIANG, T., PICARD, M., REILEY, M., SCHNEIDER, K., TAMARGO, M., LU, C., CHEN, X., HE, J., KIM, H. & MENDELSOHN, C. L. 2019. Pparg promotes differentiation and regulates mitochondrial gene expression in bladder epithelial cells. *Nat Commun,* 10**,** 019-12332.

LIVNAH, O., STURA, E. A., MIDDLETON, S. A., JOHNSON, D. L., JOLLIFFE, L. K. & WILSON, I. A. 1999. Crystallographic evidence for preformed dimers of erythropoietin receptor before ligand activation. *Science,* 283**,** 987-90.

LOWENSTEIN, E. J., DALY, R. J., BATZER, A. G., LI, W., MARGOLIS, B., LAMMERS, R., ULLRICH, A., SKOLNIK, E. Y., BAR-SAGI, D. & SCHLESSINGER, J. 1992. The SH2

and SH3 domain-containing protein GRB2 links receptor tyrosine kinases to ras signaling. *Cell,* 70**,** 431-42.

MAMO, T. M., WITTERN, A. B., KLEPPA, M. J., BOHNENPOLL, T., WEISS, A. C. & KISPERT, A. 2017. BMP4 uses several different effector pathways to regulate proliferation and differentiation in the epithelial and mesenchymal tissue compartments of the developing mouse ureter. *Hum Mol Genet,* 26.

MARTIN, E., CAUBIT, X., AIRIK, R., VOLA, C., FATMI, A., KISPERT, A. & FASANO, L. 2013. TSHZ3 and SOX9 regulate the timing of smooth muscle cell differentiation in the ureter by reducing myocardin activity. *PLoS One,* 8.

MEUSER, M., DEUPER, L., RUDAT, C., AYDOĞDU, N., THIESLER, H., ZARNOVICAN, P., HILDEBRANDT, H., TROWE, M. O. & KISPERT, A. 2022. FGFR2 signaling enhances the SHH-BMP4 signaling axis in early ureter development. *Development,* 149**,** 12.

MICHOS, O., GONÇALVES, A., LOPEZ-RIOS, J., TIECKE, E., NAILLAT, F., BEIER, K., GALLI, A., VAINIO, S. & ZELLER, R. 2007. Reduction of BMP4 activity by gremlin 1 enables ureteric bud outgrowth and GDNF/WNT11 feedback signalling during kidney branching morphogenesis. *Development,* 134**,** 2397-405.

MIYAZAKI, Y., OSHIMA, K., FOGO, A., HOGAN, B. L. & ICHIKAWA, I. 2000. Bone morphogenetic protein 4 regulates the budding site and elongation of the mouse ureter. *J Clin Invest,* 105**,** 863-73.

MIYAZAKI, Y., OSHIMA, K., FOGO, A. & ICHIKAWA, I. 2003. Evidence that bone morphogenetic protein 4 has multiple biological functions during kidney and urinary tract development. *Kidney Int,* 63**,** 835-44.

MIYAZONO, K., MAEDA, S. & IMAMURA, T. 2005. BMP receptor signaling: transcriptional targets, regulation of signals, and signaling cross-talk. *Cytokine Growth Factor Rev,* 16**,** 251-63.

MOHAMMADI, M., HONEGGER, A. M., ROTIN, D., FISCHER, R., BELLOT, F., LI, W., DIONNE, C. A., JAYE, M., RUBINSTEIN, M. & SCHLESSINGER, J. 1991. A tyrosine-phosphorylated carboxy-terminal peptide of the fibroblast growth factor receptor (Flg) is a binding site for the SH2 domain of phospholipase C-gamma 1. *Mol Cell Biol,* 11**,** 5068-78.

MOORMAN, A. F., HOUWELING, A. C., DE BOER, P. A. & CHRISTOFFELS, V. M. 2001. Sensitive nonradioactive detection of mRNA in tissue sections: novel application of the whole-mount in situ hybridization protocol. *J Histochem Cytochem,* 49**,** 1-8.

MURONE, M., ROSENTHAL, A. & DE SAUVAGE, F. J. 1999. Sonic hedgehog signaling by the patched-smoothened receptor complex. *Curr Biol,* 9**,** 76-84.

NAKAHIRO, T., KUROOKA, H., MORI, K., SANO, K. & YOKOTA, Y. 2010. Identification of BMP-responsive elements in the mouse Id2 gene. *Biochem Biophys Res Commun,* 399**,** 416-21.

OHUCHI, H., HORI, Y., YAMASAKI, M., HARADA, H., SEKINE, K., KATO, S. & ITOH, N. 2000. FGF10 acts as a major ligand for FGF receptor 2 IIIb in mouse multi-organ development. *Biochem Biophys Res Commun,* 277**,** 643-9.

OHYAMA, T. & GROVES, A. K. 2004. Generation of Pax2-Cre mice by modification of a Pax2 bacterial artificial chromosome. *Genesis,* 38**,** 195-9.

ONG, S. H., HADARI, Y. R., GOTOH, N., GUY, G. R., SCHLESSINGER, J. & LAX, I. 2001. Stimulation of phosphatidylinositol 3-kinase by fibroblast growth factor receptors is mediated by coordinated recruitment of multiple docking proteins. *Proc Natl Acad Sci U S A,* 98**,** 6074-9.

ORNITZ, D. M. & ITOH, N. 2015. The Fibroblast Growth Factor signaling pathway. *Wiley Interdiscip Rev Dev Biol,* 4**,** 215-66.

ORR-URTREGER, A., BEDFORD, M. T., BURAKOVA, T., ARMAN, E., ZIMMER, Y., YAYON, A., GIVOL, D. & LONAI, P. 1993. Developmental localization of the splicing alternatives of fibroblast growth factor receptor-2 (FGFR2). *Dev Biol,* 158**,** 475-86.

PEDERSEN, A., SKJONG, C. & SHAWLOT, W. 2005. Lim 1 is required for nephric duct extension and ureteric bud morphogenesis. *Dev Biol,* 288**,** 571-81.

PERANTONI, A. O., DOVE, L. F. & KARAVANOVA, I. 1995. Basic fibroblast growth factor can mediate the early inductive events in renal development. *Proc Natl Acad Sci U S A,* 92**,** 4696-700.

PETERS, C. A. 1995. Urinary tract obstruction in children. *J Urol,* 154**,** 1874-83.

PIGNON, J. C., GRISANZIO, C., GENG, Y., SONG, J., SHIVDASANI, R. A. & SIGNORETTI, S. 2013. p63-expressing cells are the stem cells of developing prostate, bladder, and colorectal epithelia. *Proc Natl Acad Sci U S A,* 110**,** 8105-10.

POLADIA, D. P., KISH, K., KUTAY, B., HAINS, D., KEGG, H., ZHAO, H. & BATES, C. M. 2006. Role of fibroblast growth factor receptors 1 and 2 in the metanephric mesenchyme. *Dev Biol,* 291**,** 325-39.

POSTOEV, V. A., GRJIBOVSKI, A. M., KOVALENKO, A. A., ANDA, E. E., NIEBOER, E. & ODLAND, J. 2016. Congenital anomalies of the kidney and the urinary tract: A murmansk county birth registry study. *Birth Defects Res A Clin Mol Teratol,* 106**,** 185-93.

QASRAWI, F., MEUSER, M., LEHNHOFF, F., SCHULTE, M. & KISPERT, A. 2022. S100A1 expression characterizes terminally differentiated superficial cells in the urothelium of the murine bladder and ureter. *Histochem Cell Biol,* 1**,** 022-02120.

QIAO, J., UZZO, R., OBARA-ISHIHARA, T., DEGENSTEIN, L., FUCHS, E. & HERZLINGER, D. 1999. FGF-7 modulates ureteric bud growth and nephron number in the developing kidney. *Development,* 126**,** 547-54.

RAATIKAINEN-AHOKAS, A., HYTÖNEN, M., TENHUNEN, A., SAINIO, K. & SARIOLA, H. 2000. BMP-4 affects the differentiation of metanephric mesenchyme and reveals an early anterior-posterior axis of the embryonic kidney. *Dev Dyn,* 217**,** 146-58.

REVEST, J. M., SPENCER-DENE, B., KERR, K., DE MOERLOOZE, L., ROSEWELL, I. & DICKSON, C. 2001. Fibroblast growth factor receptor 2-IIIb acts upstream of Shh and Fgf4 and is required for limb bud maintenance but not for the induction of Fgf8, Fgf10, Msx1, or Bmp4. *Dev Biol,* 231**,** 47-62.

SAHNI, M., AMBROSETTI, D. C., MANSUKHANI, A., GERTNER, R., LEVY, D. & BASILICO, C. 1999. FGF signaling inhibits chondrocyte proliferation and regulates bone development through the STAT-1 pathway. *Genes Dev,* 13**,** 1361-6.

SANCHEZ-DUFFHUES, G., WILLIAMS, E., GOUMANS, M. J., HELDIN, C. H. & TEN DIJKE, P. 2020. Bone morphogenetic protein receptors: Structure, function and targeting by selective small molecule kinase inhibitors. *Bone,* 138**,** 6.

SAXEN, L. & SARIOLA, H. 1987. Early organogenesis of the kidney. *Pediatr Nephrol,* 1**,** 385-92.

SCHLESSINGER, J., PLOTNIKOV, A. N., IBRAHIMI, O. A., ELISEENKOVA, A. V., YEH, B. K., YAYON, A., LINHARDT, R. J. & MOHAMMADI, M. 2000. Crystal structure of a ternary FGF-FGFR-heparin complex reveals a dual role for heparin in FGFR binding and dimerization. *Mol Cell,* 6**,** 743-50.

SCHLESSINGER, J., SHECHTER, Y., CUATRECASAS, P., WILLINGHAM, M. C. & PASTAN, I. 1978. Quantitative determination of the lateral diffusion coefficients of the hormone-receptor complexes of insulin and epidermal growth factor on the plasma membrane of cultured fibroblasts. *Proc Natl Acad Sci U S A,* 75**,** 5353-7.

SCHÖNFELDER, E. M., KNÜPPEL, T., TASIC, V., MILJKOVIC, P., KONRAD, M., WÜHL, E., ANTIGNAC, C., BAKKALOGLU, A., SCHAEFER, F. & WEBER, S. 2006. Mutations in Uroplakin IIIA are a rare cause of renal hypodysplasia in humans. *Am J Kidney Dis,* 47**,** 1004-12.

SCHULTHEISS, T. M., BURCH, J. B. & LASSAR, A. B. 1997. A role for bone morphogenetic proteins in the induction of cardiac myogenesis. *Genes Dev,* 11**,** 451-62.

SIGAFOOS, A. N., PARADISE, B. D. & FERNANDEZ-ZAPICO, M. E. 2021. Hedgehog/GLI Signaling Pathway: Transduction, Regulation, and Implications for Disease. *Cancers,* 13.

SIMON-TILLAUX, N. & HERTIG, A. 2017. Snail and kidney fibrosis. *Nephrol Dial Transplant,* 32**,** 224-233.

SIOW, R. C., MALLAWAARACHCHI, C. M. & WEISSBERG, P. L. 2003. Migration of adventitial myofibroblasts following vascular balloon injury: insights from in vivo gene transfer to rat carotid arteries. *Cardiovasc Res,* 59**,** 212-21.

SONGYANG, Z., SHOELSON, S. E., CHAUDHURI, M., GISH, G., PAWSON, T., HASER, W. G., KING, F., ROBERTS, T., RATNOFSKY, S., LECHLEIDER, R. J. & ET AL. 1993. SH2 domains recognize specific phosphopeptide sequences. *Cell,* 72**,** 767-78.

STONE, D. M., HYNES, M., ARMANINI, M., SWANSON, T. A., GU, Q., JOHNSON, R. L., SCOTT, M. P., PENNICA, D., GODDARD, A., PHILLIPS, H., NOLL, M., HOOPER, J. E., DE SAUVAGE, F. & ROSENTHAL, A. 1996. The tumour-suppressor gene patched encodes a candidate receptor for Sonic hedgehog. *Nature,* 384**,** 129-34.

SUN, T. T., ZHAO, H., PROVET, J., AEBI, U. & WU, X. R. 1996. Formation of asymmetric unit membrane during urothelial differentiation. *Mol Biol Rep,* 23**,** 3-11.

TANAKA, S. T., ISHII, K., DEMARCO, R. T., POPE, J. C. T., BROCK, J. W., 3RD & HAYWARD, S. W. 2010. Endodermal origin of bladder trigone inferred from mesenchymal-epithelial interaction. *J Urol,* 183**,** 386-91.

TRIPATHI, P., WANG, Y., CASEY, A. M. & CHEN, F. 2012. Absence of canonical Smad signaling in ureteral and bladder mesenchyme causes ureteropelvic junction obstruction. *J Am Soc Nephrol,* 23**,** 618-28.

TROWE, M. O., AIRIK, R., WEISS, A. C., FARIN, H. F., FOIK, A. B., BETTENHAUSEN, E., SCHUSTER-GOSSLER, K., TAKETO, M. M. & KISPERT, A. 2012. Canonical Wnt signaling regulates smooth muscle precursor development in the mouse ureter. *Development,* 139**,** 3099-108.

TROWE, M. O., MAIER, H., PETRY, M., SCHWEIZER, M., SCHUSTER-GOSSLER, K. & KISPERT, A. 2011. Impaired stria vascularis integrity upon loss of E-cadherin in basal cells. *Dev Biol,* 359**,** 95-107.

TSUKAMOTO, S., MIZUTA, T., FUJIMOTO, M., OHTE, S., OSAWA, K., MIYAMOTO, A., YONEYAMA, K., MURATA, E., MACHIYA, A., JIMI, E., KOKABU, S. & KATAGIRI, T. 2014. Smad9 is a new type of transcriptional regulator in bone morphogenetic protein signaling. *Sci Rep,* 4.

UETANI, N. & BOUCHARD, M. 2009. Plumbing in the embryo: developmental defects of the urinary tracts. *Clin Genet,* 75**,** 307-17.

VARLEY, C. L., BACON, E. J., HOLDER, J. C. & SOUTHGATE, J. 2009. FOXA1 and IRF-1 intermediary transcriptional regulators of PPARgamma-induced urothelial cytodifferentiation. *Cell Death Differ,* 16**,** 103-14.

VARLEY, C. L., GARTHWAITE, M. A., CROSS, W., HINLEY, J., TREJDOSIEWICZ, L. K. & SOUTHGATE, J. 2006. PPARgamma-regulated tight junction development during human urothelial cytodifferentiation. *J Cell Physiol,* 208**,** 407-17.

VARLEY, C. L., STAHLSCHMIDT, J., LEE, W. C., HOLDER, J., DIGGLE, C., SELBY, P. J., TREJDOSIEWICZ, L. K. & SOUTHGATE, J. 2004. Role of PPARgamma and EGFR signalling in the urothelial terminal differentiation programme. *J Cell Sci,* 117**,** 2029-36.

VELARDO, J. 1981. Histology of the ureter. In: *The ureter,* 2nd Ed., edited by Bergman H. *New York, Springer-Verlag*.

WALKER, K. A., SIMS-LUCAS, S., DI GIOVANNI, V. E., SCHAEFER, C., SUNSERI, W. M., NOVITSKAYA, T., DE CAESTECKER, M. P., CHEN, F. & BATES, C. M. 2013. Deletion of fibroblast growth factor receptor 2 from the peri-wolffian duct stroma leads to ureteric induction abnormalities and vesicoureteral reflux. *PLoS One,* 8**,** 7.

WALLACE, M. A. 1998. Anatomy and physiology of the kidney. *Aorn J,* 68**,** 803-16.

WANG, F., KAN, M., YAN, G., XU, J. & MCKEEHAN, W. L. 1995. Alternately spliced NH2-terminal immunoglobulin-like Loop I in the ectodomain of the fibroblast growth factor (FGF) receptor 1 lowers affinity for both heparin and FGF-1. *J Biol Chem,* 270**,** 10231-5.

WANG, G. J., BRENNER-ANANTHARAM, A., VAUGHAN, E. D. & HERZLINGER, D. 2009. Antagonism of BMP4 signaling disrupts smooth muscle investment of the ureter and ureteropelvic junction. *J Urol,* 181**,** 401-7.

WANG, Z., WANG, D. Z., PIPES, G. C. & OLSON, E. N. 2003. Myocardin is a master regulator of smooth muscle gene expression. *Proc Natl Acad Sci U S A,* 100**,** 7129-34.

WEBER, S., TAYLOR, J. C., WINYARD, P., BAKER, K. F., SULLIVAN-BROWN, J., SCHILD, R., KNÜPPEL, T., ZUROWSKA, A. M., CALDAS-ALFONSO, A., LITWIN, M., EMRE, S., GHIGGERI, G. M., BAKKALOGLU, A., MEHLS, O., ANTIGNAC, C., NETWORK, E., SCHAEFER, F. & BURDINE, R. D. 2008. SIX2 and BMP4 mutations associate with anomalous kidney development. *J Am Soc Nephrol,* 19**,** 891-903.

WEISS, A. C., BOHNENPOLL, T., KURZ, J., BLANK, P., AIRIK, R., LÜDTKE, T. H., KLEPPA, M. J., DEUPER, L., KAISER, M., MAMO, T. M., COSTA, R., VON HAHN, T., TROWE, M. O. & KISPERT, A. 2019. Delayed onset of smooth muscle cell differentiation leads to hydroureter formation in mice with conditional loss of the zinc finger transcription factor gene Gata2 in the ureteric mesenchyme. *J Pathol,* 248**,** 452-463.

WEISS, R. M., GUO, S., SHAN, A., SHI, H., ROMANO, R. A., SINHA, S., CANTLEY, L. G. & GUO, J. K. 2013. Brg1 determines urothelial cell fate during ureter development. *J Am Soc Nephrol,* 24**,** 618-26.

WERNER, S., DUAN, D. S., DE VRIES, C., PETERS, K. G., JOHNSON, D. E. & WILLIAMS, L. T. 1992. Differential splicing in the extracellular region of fibroblast growth factor receptor 1 generates receptor variants with different ligand-binding specificities. *Mol Cell Biol,* 12**,** 82-8.

WILKINS, S., ZHANG, K. W., MAHFUZ, I., QUANTIN, R., D'CRUZ, N., HUTSON, J., EE, M., BAGLI, D., AITKEN, K., FONG, F. N., NG, P. K., TSUI, S. K., FUNG, W. Y., BANU, T., THAKRE, A., JOHAR, K., JAUREGUIZAR, E., LI, L. & CHENG, W. 2012. Insertion/deletion polymorphisms in the ΔNp63 promoter are a risk factor for bladder exstrophy epispadias complex. *PLoS Genet,* 8**,** 20.

WILKINSON, D. G. & NIETO, M. A. 1993. Detection of messenger RNA by in situ hybridization to tissue sections and whole mounts. *Methods Enzymol,* 225**,** 361-73.

WINNIER, G., BLESSING, M., LABOSKY, P. A. & HOGAN, B. L. 1995. Bone morphogenetic protein-4 is required for mesoderm formation and patterning in the mouse. *Genes Dev,* 9**,** 2105-16.

WOOLF, A. S. & DAVIES, J. A. 2013. Cell biology of ureter development. *J Am Soc Nephrol,* 24**,** 19-25.

WOZNEY, J. M., ROSEN, V., CELESTE, A. J., MITSOCK, L. M., WHITTERS, M. J., KRIZ, R. W., HEWICK, R. M. & WANG, E. A. 1988. Novel regulators of bone formation: molecular clones and activities. *Science,* 242**,** 1528-34.

XU, X., HAN, J., ITO, Y., BRINGAS, P., JR., DENG, C. & CHAI, Y. 2008. Ectodermal Smad4 and p38 MAPK are functionally redundant in mediating TGF-beta/BMP signaling during tooth and palate development. *Dev Cell,* 15**,** 322-9.

YANG, X., LI, C., HERRERA, P. L. & DENG, C. X. 2002. Generation of Smad4/Dpc4 conditional knockout mice. *Genesis,* 32**,** 80-1.

YAO, J., ZHOU, J., LIU, Q., LU, D., WANG, L., QIAO, X. & JIA, W. 2010. Atoh8, a bHLH transcription factor, is required for the development of retina and skeletal muscle in zebrafish. *PLoS One,* 5**,** 0010945.

YEH, B. K., IGARASHI, M., ELISEENKOVA, A. V., PLOTNIKOV, A. N., SHER, I., RON, D., AARONSON, S. A. & MOHAMMADI, M. 2003. Structural basis by which alternative splicing confers specificity in fibroblast growth factor receptors. *Proc Natl Acad Sci U S A,* 100**,** 2266-71.

YIN, Y., LIN, C. & MA, L. 2006. MSX2 promotes vaginal epithelial differentiation and wolffian duct regression and dampens the vaginal response to diethylstilbestrol. *Mol Endocrinol,* 20**,** 1535-46.

YOSYPIV, I. V. 2012. Congenital anomalies of the kidney and urinary tract: a genetic disorder? *Int J Nephrol,* 909083**,** 20.

YU, J., CARROLL, T. J. & MCMAHON, A. P. 2002. Sonic hedgehog regulates proliferation and differentiation of mesenchymal cells in the mouse metanephric kidney. *Development,* 129**,** 5301-12.

YU, Z., MANNIK, J., SOTO, A., LIN, K. K. & ANDERSEN, B. 2009. The epidermal differentiation-associated Grainyhead gene Get1/Grhl3 also regulates urothelial differentiation. *Embo J,* 28**,** 1890-903.

ZHANG, Y. E. 2017. Non-Smad Signaling Pathways of the TGF-β Family. *Cold Spring Harb Perspect Biol,* 9.

ZHAO, H., KEGG, H., GRADY, S., TRUONG, H. T., ROBINSON, M. L., BAUM, M. & BATES, C. M. 2004. Role of fibroblast growth factor receptors 1 and 2 in the ureteric bud. *Dev Biol,* 276**,** 403-15.

ZIMMERMAN, L. B., DE JESÚS-ESCOBAR, J. M. & HARLAND, R. M. 1996. The Spemann organizer signal noggin binds and inactivates bone morphogenetic protein 4. *Cell,* 86**,** 599-606.

Acknowledgements

First of all, I want to thank Prof. Dr. Andreas Kispert for giving me the opportunity to work on these challenging projects and to perform my PhD thesis in his lab. I also want to thank him for all the helpful discussions, for his expertise, for taking care of the funding and for the support and the help in writing the manuscripts.

I also want to thank Prof. Dr. Rita Gerardy-Schahn for kindly accepting to be the second examiner of my thesis. I additionally want to thank her for providing me with a lab space and a kind working atmosphere after the water breakdown in our building. I want to thank Prof. Dr. Thomas Hollemann for accepting to be my third examiner at a short notice. Furthermore, I would like to thank Prof. Dr. Anaclet Ngezahayo for taking over the duty as chair of my disputation.

I would like to thank Prof. Dr. Achim Gosslar, the head of the IFM, for creating a nice environment in the institute, and for his support and his countenance after the water breakdown.

I want to thank Dr. Max Meuser for supervising me at the beginning of my thesis and for teaching me all the lab techniques. I want to thank Dr. Hauke Thiesler and Patricia Zarnovican for all the help with the qRT-PCRs. Furthermore, I want to thank all current and former colleagues of the IFM for support, helpful discussions and fun times in- and outside the lab.

Last but not least I want to thank my family. First and foremost, I want to thank my parents, Monika and Joerg, and also my sisters, Hannah and Laura, for all the constant support, not only during the last five years, but throughout my whole life. Not only for the financial support, but also for always being there for me, listening to my sorrows, constantly encouraging me and most importantly for the unconditional love. I also want to thank my friends, particularly Marie and Alexandra, for being my best friends since childhood, for crying and laughing with me, being there for me during tough times and for the constant support. Finally, I want to thank the best roommates anybody could ever wish for, Hannah and Lena. Without all of you this would not have been possible.

THANK YOU VERY MUCH!

Appendix

Curriculum vitae

Personal Information

Name:	Lena Deuper
Date of birth:	02.01.1993

University studies

2017-present	Hannover Medical School, Hannover, Germany PhD student in Developmental and Molecular Biology
2015-2017	Hannover Medical School, Hannover, Germany Master of Science (M.Sc.)
2011-2015	University of Applied Science Emden/ Leer, Emden, Germany Bachelor of Science (B.Sc.) in Biotechnology/ Bioinformatics
2004-2011	Gymnasium Bad Iburg (Abitur)

List of publications

Deuper L, Meuser M, Thiesler H, Jany UWH, Rudat C, Hildebrandt H, Trowe MO, Kispert A. (2022). Mesenchymal FGFR1 and FGFR2 control patterning of the ureteric mesenchyme by balancing SHH and BMP4 signaling. *Development* 149(17):dev200767.
https://doi.org/10.1242/dev.200767

Kurz J, Weiss AC, Lüdtke TH, **Deuper L**, Trowe MO, Thiesler H, Hildebrandt H, Heineke J, Duncan SA, Kispert A. (2022). GATA6 is a crucial factor for Myocd expression in the visceral smooth muscle cell differentiation program of the murine ureter. *Development* 149(15):dev200522.
https://doi.org/10.1242/dev.200522

Kurz J, Weiss AC, Thiesler H, Qasrawi F, **Deuper L**, Kaur J, Rudat C, Lüdtke TH, Wojahn I, Hildebrandt H, Trowe MO, Kispert A. (2022). Notch signaling is a novel regulator of visceral smooth muscle cell differentiation in the murine ureter. *Development* 149(4):dev199735.
https://doi.org/10.1242/dev.199735

Meuser M, **Deuper L**, Rudat C, Aydoğdu N, Thiesler H, Zarnovican P, Hildebrandt H, Trowe MO, Kispert A. (2022). FGFR2 signaling enhances the SHH-BMP4 signaling axis in early ureter development. *Development* 149(1):dev200021.
https://doi.org/10.1242/dev.200021

Becker S, Kiecke C, Schäfer E, Sinzig U, **Deuper L**, Trigo-Mourino P, Griesinger C, Koch R, Rydzynska Z, Chapuy B, von Bonin F, Kube D, Venkataramani V, Bohnenberger H, Leha A, Flach J, Dierks S, Bastians H, Maruschak B, Bojarczuk K, Taveira MO, Trümper L, Wulf GM, Wulf GG. (2020). Destruction of a Microtubule-Bound MYC Reservoir during Mitosis Contributes to Vincristine's Anticancer Activity. *Mol Cancer Res*. 18(6):859-872.
https://doi.org/10.1158/1541-7786.MCR-19-1203

Weiss AC, Bohnenpoll T, Kurz J, Blank P, Airik R, Lüdtke TH, Kleppa MJ, **Deuper L**, Kaiser M, Mamo TM, Costa R, von Hahn T, Trowe MO, Kispert A. (2019). Delayed onset of smooth muscle cell differentiation leads to hydroureter formation in mice with conditional loss of the zinc finger transcription factor gene Gata2 in the ureteric mesenchyme. *J Pathol*. 248(4):452-463.
https://doi.org/10.1002/path.5270